DTIC FILE COPY

(2)

FTD-ID(RS)T-0767-88

AD-A206 768

FOREIGN TECHNOLOGY DIVISION

AIR FORCE SYSTEMS COMMAND

NANOSECOND PULSE TECHNIQUE

by

L.A. Morugin, G.V. Glebovich

FOREIGN TECHNOLOGY DIVISION

Approved for public release;
Distribution unlimited.

89 4 06 021

PARTIALLY EDITED MACHINE TRANSLATION

FTD-ID(RS)T-0767-88 17 March 1989

MICROFICHE NR: FTD-89-C-000145

NANOSECOND PULSE TECHNIQUE

By: L.A. Morugin, G.V. Glebovich

English pages: 1018

Source: Nanosekundnaya Impul'snaya Tekhnika,
Publishing House "Sovetskoye Radio",
Moscow, 1964, pp. 1-623

Country of origin: USSR
This document is a machine translation.
Input by: David Servis, Inc.
F33657-87-D-0096
Merged by: Ruth A. Bennette, Nancy L. Burns, Donna L. Goode,
Charles W. Guerrant, Eva R. Johnson
Requester: Director, USAMSIC/AIAMS-DBL
Approved for public release; Distribution unlimited.

THIS TRANSLATION IS A RENDITION OF THE ORIGINAL FOREIGN TEXT WITHOUT ANY ANALYTICAL OR EDITORIAL COMMENT. STATEMENTS OR THEORIES ADVOCATED OR IMPLIED ARE THOSE OF THE SOURCE AND DO NOT NECESSARILY REFLECT THE POSITION OR OPINION OF THE FOREIGN TECHNOLOGY DIVISION.	PREPARED BY: TRANSLATION DIVISION FOREIGN TECHNOLOGY DIVISION WPAFB, OHIO.

TABLE OF CONTENTS

U. S. BOARD ON GEOGRAPHIC NAMES TRANSLITERATION SYSTEM

Block	Italic	Transliteration	Block	Italic	Transliteration
А а	*А а*	A, a	Р р	*Р р*	R, r
Б б	*Б б*	B, b	С с	*С с*	S, s
В в	*В в*	V, v	Т т	*Т т*	T, t
Г г	*Г г*	G, g	У у	*У у*	U, u
Д д	*Д д*	D, d	Ф ф	*Ф ф*	F, f
Е е	*Е е*	Ye, ye; E, e*	Х х	*Х х*	Kh, kh
Ж ж	*Ж ж*	Zh, zh	Ц ц	*Ц ц*	Ts, ts
З з	*З з*	Z, z	Ч ч	*Ч ч*	Ch, ch
И и	*И и*	I, i	Ш ш	*Ш ш*	Sh, sh
Й й	*Й й*	Y, y	Щ щ	*Щ щ*	Shch, shch
К к	*К к*	K, k	Ъ ъ	*Ъ ъ*	"
Л л	*Л л*	L, l	Ы ы	*Ы ы*	Y, y
М м	*М м*	M, m	Ь ь	*Ь ь*	'
Н н	*Н н*	N, n	Э э	*Э э*	E, e
О о	*О о*	O, o	Ю ю	*Ю ю*	Yu, yu
П п	*П п*	P, p	Я я	*Я я*	Ya, ya

*ye initially, after vowels, and after ъ, ь; e elsewhere.
When written as ё in Russian, transliterate as yё or ё.

RUSSIAN AND ENGLISH TRIGONOMETRIC FUNCTIONS

Russian	English	Russian	English	Russian	English
sin	sin	sh	sinh	arc sh	$\sinh^{-1}$
cos	cos	ch	cosh	arc ch	$\cosh^{-1}$
tg	tan	th	tanh	arc th	$\tanh^{-1}$
ctg	cot	cth	coth	arc cth	$\coth^{-1}$
sec	sec	sch	sech	arc sch	sech^{-1}
cosec	csc	csch	csch	arc csch	csch^{-1}

Russian	English
rot	curl
lg	log

GRAPHICS DISCLAIMER

All figures, graphics, tables, equations, etc. merged into this translation were extracted from the best quality copy available.

NANOSECOND PULSE TECHNIQUE.

L. A. Morugin, G. V. Glebovich.

Page 2.

Book is dedicated to presentation of fundamental questions of nanosecond pulse technique: to transient processes in distributed systems, generation and impulse shaping, to their conversion, amplification and recording.

Bases of theory, methods and principles of nanosecond pulse technique are examined, physical processes are illuminated, calculations of specific diagrams and elements are presented, technical characteristics of devices/equipment are given.

Book is intended for engineers, who work in region of radio electronics and who carry out development, by design and by application of pulse equipment, instructors and students of VUZ [- Institute of Higher Education].

Page 3.

PREFACE.

Present monograph is attempt at systematic presentation of new scientific discipline, which arose and which developed in last ten years - nanosecond pulse technique. In the book the work of the authors (in chapters 1, 2, 3, 5, 6, 9 and 10) are presented, and are also used other materials, published in the Soviet and foreign press. Chapters 1, 3, 4, 10, 11 and S 1, 4, 5 chapters 8 are written by G. V. Glebovich, while chapters 2, 5, 6, 7, 9 and S 2, 3 chapters 8 - by L. A. Morugin.

Authors express gratitude to professor, to Dr. of Technical Sciences Ya. S. Itskhoki, to docent, Cand. of tech. sciences N. I. Ovchinnikov and to docent, Cand. of tech. sciences T. M. Agakhanyan for the valuable observations, made by them during reading of the book.

Page 4.

INTRODUCTION.

Development of pulse technology in recent years follows path of mastery/adoption of range of pulses of short duration. Not more than ten years ago the fundamental range of the pulse durations was microsecond range; at the present time it arose area of technology, that is occupied by obtaining and using the pulses, into thousands of times of of shorter, nanosecond pulse technique. This direction reflects the changes, which occurred recently in the development of technology as a whole: transition/junction to the increased speeds, use of the quick-flowing reactions, increase in the accuracy of measurements. Investigations into the field of nuclear physics, ferrites, semiconductors, the new works in the technology of shf/SVCh, etc. required the creation of the equipment, capable of recording the processes, which last the billionth fractions of a second and even shorter intervals of time. The methods of nanosecond pulse technique found use in the radar, the radio gage technology, communication equipment and some other regions. The resolution of the problem of an increase in the operating speed of electronic computers depends substantially on the successes of nanosecond pulse technique. All these facts defined the position of nanosecond pulse technique as one of the most promising branches of radio engineering.

Problem of nanosecond pulse technique is generation, conversion

and recording pulse oscillations/vibrations, i.e., the same problem, which stands also before pulse technique in usual understanding of this term, i.e., before microsecond pulse technique. However, essential difference in the objects of conversion leads to the fundamental difference in the methods of the solution.

Page 5.

The width of the pulse spectrum of nanosecond duration is into thousands of times more than the width of the pulse spectrum of microsecond duration; the spectrum of nanosecond pulses stretches from the relatively low frequencies to the frequencies, which correspond to the oscillations/vibrations of shf/SVCh. In accordance with this all devices/equipment, utilized in the nanosecond pulse technique, must work in the range, in thousands of times which exceeds the range, in which work the devices/equipment in the "classical" pulse technique.

Extremely wide pulse spectrum of nanosecond duration does not make it possible effectively to utilize as linear elements of circuit diagrams with lumped parameters. This fact led to the general/universal application in the nanosecond pulse technique of distributed circuits. It is necessary to keep in mind which during the use of the distributed systems in the nanosecond range is necessary to consider the series/row of the specific phenomena, which they usually disregard in the microsecond range (loss in the dielectrics, the distortion of pulses on small heterogeneities, etc.).

As is known, effectiveness of work of tubes in pulsed operations is determined in essence by its quality. In the last decade the duration of operating pulses decreased to thousands of times, whereas the quality of tubes increased only several times. Because of this the effectiveness of the work of vacuum-tube circuits in the nanosecond pulse technique proved to be immeasurably lower than in the microsecond pulse technique. It is obvious that in proportion to further development of nanosecond pulse technology to the side of the shortening of the pulse duration the disruption between increase in the quality of tubes and width of oscillation spectrum will become more perceived. Deficiency in vacuum-tube circuits noted above leads to the need for transition/junction to other active elements (for example, to tunnel diodes, to ferrites, etc.) and to the need for the review of the methods of formation and converting the pulses; to a considerable degree transferred into the nanosecond pulse technique from the pulses technique of larger duration.

Thus, from point of view of obtaining pulses of short duration fundamental question in work of vacuum-tube circuits is question about steepness of edges of pulses generated by them.

Page 6.

The need of increasing the steepness of the pulse edges led to the development of new oscillator circuits, in particular the diagrams, in which are utilized the tubes with the secondary emission, the phenomenon of the recirculation of pulses, etc. However, these

measures do not make it possible to obtain pulses with the slope/transconductance of front of more than 10^{10} v/sec. The considerably greater possibilities in this respect possess the diagrams of formation with the commutating elements (steepness of front of approximately 10^{13} V/sec). The radical solution of obtaining the periodic steep-sided pulses was the use of shock electromagnetic waves in the distributed nonlinear systems, with the aid of which it is possible to form pulses with the steepness of front of approximately 10^{14} V/sec. The new possibilities of generation and amplifying the pulses of short duration open/disclose transition/junction from the vacuum-tube circuits to the solid-state element circuits, in particular on the tunnel diodes.

Great difficulties appear during recording and in measuring parameters of nanosecond pulses, especially when their duration less than nanosecond. At present high-quality transmission and oscillography of such pulses noticeably lag behind the methods of their formation. Appearance of the tunnel diodes and other high speed semiconductor devices, which make it possible to obtain the pulses of very short duration on the low stress level, raised requirements for the oscillographs. The requirement of the high sensitivity of oscillograph with the high time resolution is very difficult to fulfill. During recording of the repeating pulses this difficulty is overcome by using the stroboscopic method of oscillography.

In spite of ever larger need for use of nanosecond pulses and

increasing number of investigations in area of nanosecond pulse technology, still is perceived deficiency both in development of series/row of important questions of theory and in conducting of experimental investigations. Therefore it is advisable to dedicate present monograph to both the solution of the series/row of the urgent problems of nanosecond pulse technique and to systematic presentation of its contemporary state.

Page 7.

CHAPTER ONE.

TRANSIENT PROCESSES IN TRANSMISSION LINES.

Active width of spectrum of video pulses stretches by duration of order of 10^{-9}-10^{-10} s to frequencies of order of several gigahertz. Therefore very wide-band circuits are required for the formation, the transmission and converting such pulses.

In technology of microsecond pulses operations above pulses indicated successfully are realized in circuits with lumped parameters and only sometimes distributed systems are utilized [1, 2].

In nanosecond pulse technique application of circuits with lumped parameters is very limited [3]. Even with the perfection of the constructions/designs of circuits with the lumped parameters the unavoidable presence of stray inductances and capacities/capacitances does not make it possible to obtain the time constants of circuit considerably less than 0.1 ns. Therefore formation and conversion of pulses with the duration are less than one nanosecond, and that more their transmission with the aid of the circuits with the lumped parameters they prove to be impossible.

In connection with this in nanosecond pulse technique distributed systems increasingly more widely are utilized. The miniaturization of

different parts, electronic and especially semiconductor devices makes it possible to create the construction/design of devices/equipment for the generation, amplifications, conversions and recordings of nanosecond pulses with the coaxial and strip lines. The application of non-uniforms circuit permits implemention of a transformation of pulses, amplitude control and correction of their form.

Page 8.

Thus, distributed systems in the form of lines of transmission of different types compose base of many devices/equipment. For the evaluation/estimate of the quality of such devices/equipment and their calculation it is necessary to know frequency properties and transient responses of lines.

In nanosecond range of pulse durations in examination of transient processes in transmission lines it is necessary to consider some properties of lines (loss in dielectrics, small heterogeneities), which were not essential for microsecond pulse technique and therefore usually they were not considered.

1.1. COAXIAL LINES AND THEIR TRANSIENT RESPONSES.

Most widely used by line transmission, utilized in nanosecond pulse technique, is coaxial uniform line. This two-wire circuit consists of the continuous internal and hollow external of cylindrical conductors. Space between the conductors in the majority of the cases

is filled with high-frequency dielectric. If the diameters of conductors are constant/invariable along the line, then this line is uniform.

Fundamental type of electromagnetic wave, which is propagated along line, is wave of type TEM, whose electrical and magnetic fields are mutually perpendicular and arranged/located at right angle to direction of propagation of wave.

Besides rigid constructions/designs of coaxial lines radio-frequency coaxial cables most frequently are utilized.

Frequency properties of cable upon consideration of losses and conductors and dielectrics.

Primary parameters of coaxial line are effective resistance R, inductance L, capacity/capacitance of C and shunt conductance G. The secondary parameters of line are the functions of primary. They include wave impedance ρ and propagation constant $\overline{\gamma}=\beta+j\alpha$, where β - decay constant and α - constant of phase displacement.

Page 9.

The primary parameters of line and the propagation constant usually are determined per unit of the length of line.

In region of high frequencies interesting us secondary parameters

of line are defined through primary by following expressions [4]:

- wave impedance

$$\bar{\rho}=\sqrt{\frac{R+j\omega L}{G+j\omega C}}\approx\sqrt{\frac{L}{C}}; \qquad (1.1)$$

- propagation constant

$$\bar{\gamma}=\sqrt{(R+j\omega L)(G+j\omega C)}=\beta+j\alpha=\beta_{п}+\beta_{д}+j\alpha=$$
$$=\frac{R}{2}\sqrt{\frac{C}{L}}+\frac{G}{2}\sqrt{\frac{L}{C}}+$$
$$+j\sqrt{\omega^{2}LC+\left(\frac{R}{2}\sqrt{\frac{C}{L}}+\frac{G}{2}\sqrt{\frac{L}{C}}\right)^{2}}, \qquad (1.2)$$

where $\beta_{п}$, $\beta_{д}$ - respectively attenuation per unit length, caused by losses only in conductors, and attenuation per unit length, caused by losses only in dielectric of line;

α - phase constant, defined both by values of reactive/jet, and effective resistance of line taking into account lead loss and dielectric.

Primary parameters are determined from following formulas:

- effective resistance of line

$$R=\frac{1}{2\pi}\sqrt{\mu_{п}\rho_{п}\omega/2}\left(\frac{1}{r_1}+\frac{1}{r_2}\right)\left[\frac{Ом}{м}\right]; \qquad (1.3)$$

- inductance

$$L=L_{в}+L_{вн}=\frac{\sqrt{2\mu_{п}\rho_{п}}}{4\pi\sqrt{\omega}}\left(\frac{1}{r_1}+\frac{1}{r_2}\right)+\frac{\mu_{д}}{2\pi}\ln\frac{r_2}{r_1}\left[\frac{Гн}{м}\right]; \qquad (1.4)$$

- dielectric conductance

$$G = \omega C \operatorname{tg} \delta \left[\frac{1}{ом \cdot м} \right]. \qquad (1.5)$$

Page 10.

Here $L_в$ - internal inductance of cable (total inductance of conductors, found taking into account surface effect in them);

$L_{вн}$ - external (interconductor) inductance of line;

$\mu_п$ and $\mu_д$ - respectively magnetic permeability of the material of conductors and material of the dielectric between the conductors;

$\rho_э$ - specific strength of materials of conductors, $\Omega \cdot mm^2/m$;

r_1 and r_2 - radii of internal continuous and external is gentle conductors, m;

tg δ - dielectric power factor of the material of dielectric.

All enumerated parameters are related to unit of length of line.

Besides parameters indicated is of interest wave propagation velocity along line

$$v = \frac{1}{\sqrt{LC}} \overset{(1)}{[м/сек]} \qquad (1.6)$$

Key: (1). m/s.

and the transit time of the wave front on the section of line with a length of one meter, which is otherwise called delay time per unit of the length

$$t_{зо}=\sqrt{LC}. \qquad (1.7)$$

If line uniform and is loaded to the effective resistance, equal to its wave impedance, then the complex transmission factor of the line

$$\overline{K}=|\overline{K}|\,e^{-j\varphi(\omega)}=e^{-\overline{\gamma}l}, \qquad (1.8)$$

where l - length of line.

If we do not consider lead loss and dielectric, then modulus of transmission factor will be constant value, but phase response will be determined by expression

$$\varphi(\omega)=\omega\sqrt{LC}\,l=\omega t_{зо}l=\omega t_{з}.$$

Page 11.

This line would possess ideal characteristics and it would not introduce distortions into transmitted by it pulses.

In real cases of transmission of nanosecond pulses, active width of spectrum of which is very considerable and stretches to frequency on the order of 10 GHz, it is necessary to consider losses both in conductors and in dielectric. In connection with this are of considerable interest the frequency properties of the real coaxial transmission lines, and first of all of coaxial cable.

As show measurements of losses in coaxial cable with uniform polyethylene filling, lead loss have prevailing value at relatively

low frequencies. Losses in the dielectric become commensurate in the value with the lead loss at frequencies of 1.5-3 GHz, and at the higher frequencies losses in the dielectric have prevailing value. Fig. 1.1 for cable RK-6 gives the graph/diagrams of the frequency dependence of attenuation in conductors $\beta_{\text{п}}$ and in dielectric $\beta_{\text{д}}$ [5].

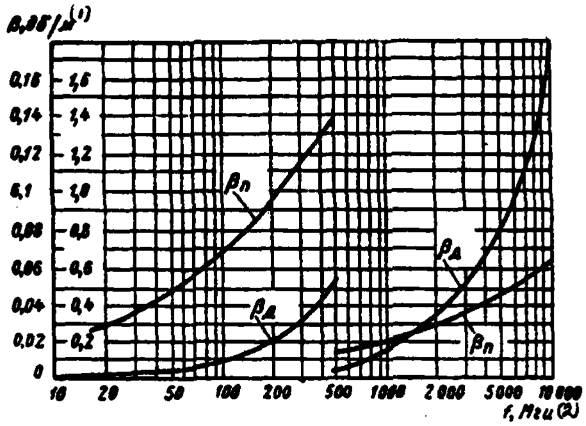

Fig. 1.1. Dependence of components of attenuation β_n and $\beta_д$ cable RK-6 on frequency.

Key: (1). dB/m. (2). MHz.

Page 12.

For evaluation/estimate of distortions of pulses of microsecond duration during their propagation according to cable it suffices it was sufficient to know frequency properties and transient responses of cable taking into account losses only in conductors [6]. During the investigation of transient processes in the cable during the transmission of nanosecond pulses it is necessary to know frequency properties and transient responses of cable taking into account lead loss and dielectric.

Let us examine general expression for propagation factor (1.2). The complete inductance of coaxial cable $L=L_в+L_{вн}$, but, as can be seen from (1.4), at the high frequencies occurs inequality $L_в \ll L_{вн}$. Therefore it is possible to record

$$\omega\sqrt{LC}=\omega\sqrt{(L_{\text{в}}+L_{\text{вн}})C}\approx\omega\sqrt{L_{\text{вн}}C}\left(1+\frac{1}{2}\frac{L_{\text{в}}}{L_{\text{вн}}}\right)$$

or, using expression (1.4),

$$\omega\sqrt{LC}\approx\omega\sqrt{L_{\text{вн}}C}+b_1\sqrt{\omega},$$

where

$$b_1=\frac{1}{4\pi}\sqrt{\frac{C}{L}}\sqrt{\mu_{\text{п}}\rho_{\text{э}}/2}\left(\frac{1}{r_1}+\frac{1}{r_2}\right)\left[\frac{\overset{(1)}{\text{сек}^{1/2}}}{\text{м}}\right]. \quad (1.9)$$

Key: (1). s

Then for decay constant and phase constant according to expressions (1.2), (1.3) and (1.9) we find

$$\beta=\beta_{\text{п}}+\beta_{\text{д}}=b_1\sqrt{\omega}+\frac{G}{2}\sqrt{\frac{L}{C}}\left[\frac{\overset{(1)}{\text{нп}}}{\text{м}}\right], \quad (1.10)$$

$$\alpha=\omega\sqrt{L_{\text{вн}}C}\mp b_1\sqrt{\omega}+\frac{(\beta_{\text{п}}-\beta_{\text{д}})^2}{2\omega\sqrt{L_{\text{вн}}C}}\left[\frac{\overset{(2)}{\text{рад}}}{\text{м}}\right]. \quad (1.11)$$

Key: (1). NP. (2). rad.

For determining attenuation due to losses in dielectric it is necessary to know value tg δ. Losses in the dielectric depend on frequency; however, analytical expression for this dependence is not known. In the case of polyethylene filling are known the experimental data for the attenuation in the cable both due to the lead loss and due to the losses in the dielectric, obtained as a result of special measurements over a wide range of frequencies. Is known also the graph/curve, which determines the character of the dependence of the loss tangent in cable polyethylene on frequency [4].

Page 13.

On the basis of experimental data is located formula, with the aid of which it is possible to approximate dependence of loss tangent in polyethylene on frequency. Since losses in the dielectric sense has to consider only at the high frequencies, beginning from several hundred megahertz, then the approximation of the graph/diagram of the frequency dependence of the loss tangent in the frequency region from hundreds of megahertz to 10 GHz is of greatest interest. In this frequency region dependence tg δ on the frequency can be approximated by formula [5]

$$\operatorname{tg}\delta=\frac{a_1\sqrt{\omega}}{1+m\omega}, \qquad (1.12)$$

where constant $a_1=1.2\cdot10^{-8}$ $\sec^{1/2}/\mathrm{rad}^{1/2}$ and $m=2\cdot10^{-11}$ sec/rad.

Conductivity of cable G at high frequencies according to formulas (1.5) and (1.12) is determined by expression

$$G=\frac{a_1\omega^{3/2}C}{1+m\omega}. \qquad (1.13)$$

Using this formula and expression for the losses in dielectric $\beta_д$, we find attenuation in the cable due to the dielectric. The results of calculation satisfactorily coincide with experimental data [5].

On the basis of expressions (1.10), (1.11), (1.13) and (1.2) for propagation constant we will obtain

$$\bar{\gamma} = b_1\sqrt{\bar{\omega}} + \frac{a\omega^{3/2}}{1+m\omega} +$$

$$+j\left[\omega\sqrt{L_{\text{вн}}C} + b_1\sqrt{\bar{\omega}} + \frac{\left(b_1\sqrt{\bar{\omega}} - \frac{a\omega^{3/2}}{1+m\omega}\right)^2}{2\omega\sqrt{L_{\text{вн}}C}}\right], \quad (1.14)$$

where

$$a = \sqrt{L_{\text{вн}}C}\,\frac{a_1}{2}.$$

Page 14.

Then transmission factor of coaxial cable according to (1.8) will take form

$$\bar{K}=e^{-\bar{\gamma}l}=\left\{\exp\left[l\left(b_1\sqrt{\omega}+\frac{a\omega^{3/2}}{1+m\omega}\right)+jl\left(\omega\sqrt{L_{\text{вн}}C}+\right.\right.\right.$$
$$\left.\left.\left.+b_1\sqrt{\omega}+\frac{\left(b_1\sqrt{\omega}-\frac{a\omega^{3/2}}{1+m\omega}\right)^2}{2\omega\sqrt{L_{\text{вн}}C}}\right)\right]\right\}^{-1}. \qquad (1.15)$$

Passband of cable can be found, if we use expression for modulus of transmission factor, which on the basis (1.15) will be recorded as follows:

$$|\bar{K}|=\exp\left[-l\left(b_1\sqrt{\omega}+\frac{a\omega^{3/2}}{1+m\omega}\right)\right]=e^{-l(\beta_{\text{м}}+\beta_{\text{д}})}. \quad (1.16)$$

Cut-off frequency of passband is equal to frequency with which transmission factor it decreases on 3 dB relative to its value at low frequencies. For the evaluation/estimate of the modulus of the transmission factor of the most frequently utilized in the nanosecond pulse technique cables it is necessary to know the values of coefficients b_1 and a, given in Table 1.1. Coefficient b_1 is calculated according to formula (1.9) taking into account correction for the fact that the internal conductor in some cables multiple, and external conductor is carried out in the form of braid/cover.

Fig. 1.2 gives dependences of cut-off frequency of passband of

cables on their length. Cut-off frequency f_{rp} was calculated from formula (1.16) when $|\bar{K}|=0.707$.

Table 1.1.

(1) Тип кабеля	(2) Значения коэффициентов	
	(3) b_1[10[illegible] сек$^{1/2}$/м]	(4) a[10[illegible] сек$^{3/2}$/м·рад$^{1/2}$]
РК-100-7-13	3,25	3,0
РК-75-4-15	4,35	3,0
РК-75-4-16	5,3	3,3
РК-3	2,15	3,2
РК-6	2,14	3,0
РК-50-11-13	2,16	3 1

Key: (1). Type of cable. (2). Values of coefficients. (3). ... sec$^{1/2}$/m. (4). ... sec$^{3/2}$/m·rad^{12}.

Page 15.

From the figure one can see that the frequency grows/rises at a small length of cable and it becomes almost identical for all cables. With an increase in the length of cable the frequency is reduced for the different cables differently. At a small length of cable (1-3 m) its broad-band character is more than 3 GHz and losses in the dielectric have prevailing value. The values of these losses for the cables of different brand are almost identical, since constant a, which determines attenuation $\beta_{д}$, for these cables is almost identical. At the large length of cable the lead loss have prevailing value. Since the value of constant b_1, entering the expression for attenuation $\beta_{п}$, is different for the cables of different brand (Table 1.1), the difference in the broad-band character of cables at their larger length is more noticeable.

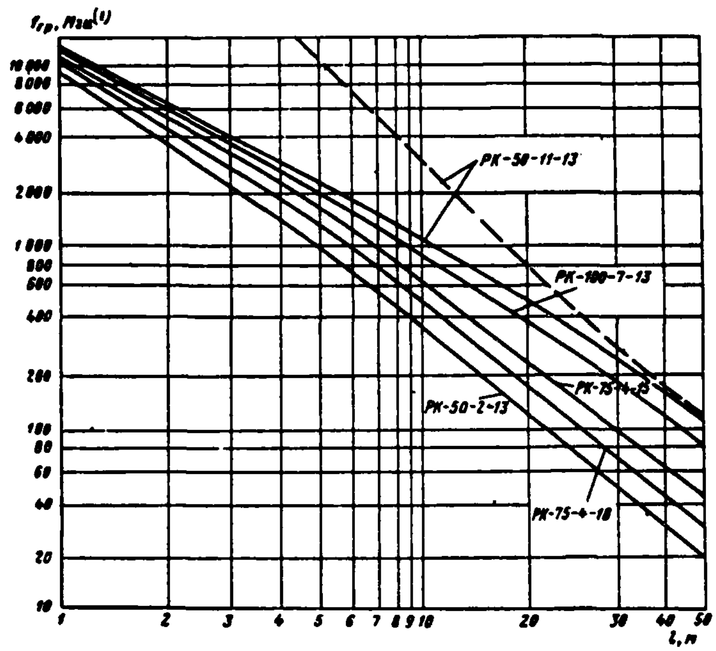

Fig. 1.2. Dependence of cut-off frequency of passband of cables on their length: —— taking into account losses in dielectric and in conductors; ---- taking into account losses only in conductors.
Key: (1). MHz.

Page 16.

Let us note that the curves virtually coincide for the cables of the type RK-3, RK-6 and RK-50-11-13.

In the same figure dotted line gave cut-off frequency of cable RK-50-11-13, obtained without taking into account losses in dielectric. As is evident, the disagreement by continuous and dotted curve is very considerable at a small length of cable, which indicates the need for the account of dielectric losses at a small length of

cables.

Transient responses of coaxial cables.

Knowing formula (1.15) for transmission factor, it is possible to obtain expression for transient response of cable:

$$A(t_1, l) = \frac{1}{2\pi} \int_{-\infty}^{\infty} \frac{1}{j\omega} e^{j\omega t - \bar{\gamma} l} d\omega, \qquad (1.17)$$

where $t_1 = t - l\sqrt{L_{\text{вн}} C} = t - t_з$; $t_з$ - delay time of cable by length l. The determination of the resultant expression of the transient response of cable by the Fourier integral method or with operating method is connected with the great difficulties due to the complexity of expression for the transmission factor (1.15). Even approximate solution of problem for the low values of t_1 and l leads to the very awkward expressions. Therefore transient response can be either found with grapho-analytic method from the real frequency characteristic of coaxial cable or it is calculated on the electronic computer.

Page 17.

Real part of transmission factor on the basis (1.15) has expression

$$\mathrm{Re}(\bar{K}) = P(\omega) = e^{-l\left(b_1\sqrt{\omega} + \frac{a\omega^{3/2}}{1+m\omega}\right)} \cos(l b_1 \sqrt{\omega}), \qquad (1.18)$$

where it is taken into consideration, that for real cables in interesting us frequency region occurs inequality

$$\frac{\left(b_1\sqrt{\omega}-\frac{a\omega^{3/2}}{1+m\omega}\right)^2}{2\omega\sqrt{L_{\text{вн}}C}}\ll b_1\sqrt{\omega};$$

furthermore, in value of argument of cosine is rejected/thrown term $l\omega\sqrt{L_{\text{вн}}C}$, since it determines linear increase of phase shift during emission of the signal along line, i.e., is of interest only during evaluation of signal delay.

Grapho-analytically transient response is found in the form of sum:

$$A(t)=\sum_{i=1}^{k}A_i(t),$$

where

$$A_i(t)=\frac{2}{\pi}\int_0^\infty\frac{P_i(\omega)}{\omega}\sin\omega t\,d\omega.$$

Function P(ω) is represented in the form of finite number of terms:

$$P(\omega)=\sum_{i=1}^{n}p_i(\omega).$$

Triangles are taken as elementary functions $p_i(\omega)$. For this dependence P(ω) is approximated by the sum of triangles, and then transient response is calculated with the aid of the appropriate formulas and tables [7].

Grapho-analytically calculated transient responses for set of

cables at their different length. Then transient responses were calculated with the aid of computer BESM-2. The results of calculations, obtained by both methods, gave satisfactory coincidence [8].

As example Fig. 1.3 gives transient responses of cable RK-50-11-13 for sections/segments length 1, 5, 10 and 30 m. The same figure gives the transient responses of this cable, calculated taking into account losses only in the conductors (dotted curves). Cable RK-50-11-13 has the transient responses, very close to the characteristics of cables RK-3 and RK-6 [9].

Page 18.

Fig. 1.4 gives transient responses of cable RK-75-4-15 with length of 5, 10 and 20 m, obtained in the case of account of lead loss and dielectric. Due to the lead loss dielectric are weakened/attenuated the high-frequency components of signal, which leads to the decrease of the slope/transconductance of the frontal part of transient response. This slope/transconductance is proportional to cut-off frequency $f_{\text{гр}}$ of the passband of line and is approximately equal to $S_A = (12 \div 13) f_{\text{гр}}$ [9].

Transient response of cable (Fig. 1.4) can be divided in two sections: rapid build-up/growth of function $A(t_1)$ and its slow build-up. Comparing continuous and dotted curves (Fig. 1.3), it is easy to see that the slope/transconductance of the first section of

transient response upon consideration of losses only in the conductors is noticeably more than mutual conductance, obtained taking into account lead loss and dielectric. The difference in the slope/transconductance is more noticeable, the less the length of cable, i.e., when the specific significance of losses in the dielectric is more.

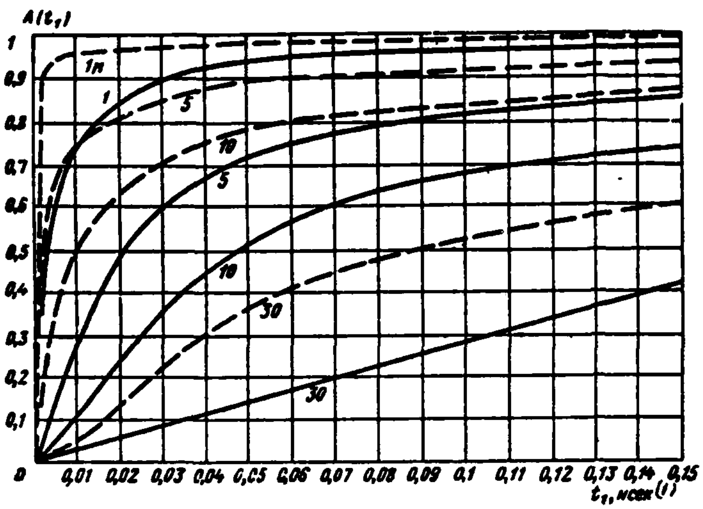

Fig. 1.3. Transient responses of cable RK-50-11-13 of length 1, 5, 10 and 30 m: —— taking into account losses only in conductors; ---- taking into account lead loss and dielectric.

Key: (1). ns.

Page 19.

Actually, the less the length l, the greater the cut-off frequency of passband (Fig. 1.2), and losses in the dielectric already predominate at frequencies of more than 3 GHz.

Transient responses of coaxial cable are characterized by fact that time of establishment of transient processes, determined usually at level 0.1 and 0.9 from steady-state value, proves to be very great and does not reflect value of time of establishment t_y, which determines distortions of edge of pulse transmitted through cable. This is explained by the slow build-up of the second section of

transient response (Fig. 1.4). As is evident, value $A(t_1)=0.9$ proves to be not characteristic. Therefore the evaluation of the transient response of cable according to the determination of the time of establishment accepted is unsuitable.

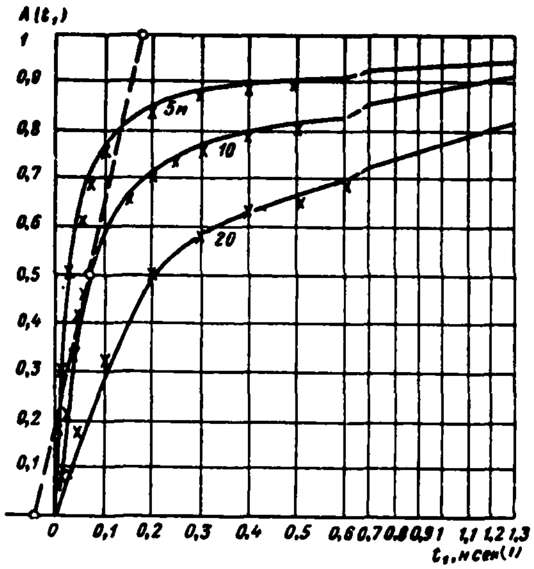

Fig. 1.4. Transient responses of cable RK-75-4-15 with length of 5, 10 and 20 m, obtained taking into account lead loss and dielectric. Key: (1). ns.

Page 20.

For calculating duration of edge of pulse $t_{\Phi 2}$ at output of linear network we will use known relationship/ratio

$$t_{\Phi 2}=\sqrt{t_{\Phi 1}^2+t_y^2},$$

where $t_{\Phi 1}$ - duration of pulse edge at input,

t_y - time of establishment of transient response of line.

Knowing $t_{\Phi 1}$ and $t_{\Phi 2}$ (they are measured at level 0.1 0.9 from amplitude value of pulse), it is easy to find value t_y, which can be approximately accepted for time of establishment of transient response of coaxial cable. The calculations of the shape of pulse at the

output of cable according to the assigned shape of pulse at the input and the known transient response, carried out in electronic computer [10], make it possible to determine t_{Φ_2} and then t_y. It proves to be that the time of the establishment of transient response can be rated/estimated on the time interval, included between the points of intersection with tangent to the transient response (at point $A(t_1)=0.5$) with the axis of abscissas and the line, which corresponds to $A(t_1)=1$. In Fig. 1.4 tangent is carried out to the transient response of cable RK-75-4-15 with a length of 10 m.

For analysis of transient processes in cable under influence of nanosecond pulses it is desirable to have resultant expression for transient response, and not to resort to grapho-analytic calculations.

In the case of account of losses only in conductors of cable in expression (1.15) one should assume a=0, and then integral (1.17) easily is calculated, and transient response is expressed by known dependence [6].

$$A(t_1, l)=1-\Phi\left(\frac{bl}{2\sqrt{t_1}}\right), \tag{1.19}$$

where $\Phi\left(\frac{bl}{2\sqrt{t_1}}\right)$ - function of Kramp [transliterated]; $b=b_1\sqrt{2}$.

Numerical calculations of transient responses of coaxial cables taking into account lead loss and dielectric show that for transient response of coaxial cable with polyethylene filling can be proposed expression, obtained as a result of changing formula (1.19):

$$A(t_1, l) = 1 - \Phi\left(\frac{\beta_{rp} l}{2\sqrt{\pi f_{rp} t_1}}\right). \quad (1.20)$$

Page 21.

Here β_{rp} - attenuation of cable, determined taking into account lead loss and dielectric at the cut-off frequency of passband f_{rp}, i.e. according to (1.16)

$$\beta_{rp} = \beta_{\pi\,rp} + \beta_{\text{д}\,rp} = b_1 \sqrt{2\pi f_{rp}} + \frac{a\,(2\pi f_{rp})^{3/2}}{1 + 2\pi m f_{rp}}. \quad (1.21)$$

Cut-off frequency for different cables by length l is determined on curves $f_{rp}=F(l)$ (Fig. 1.2). In Fig. 1.4 crosses noted the values of transient responses, obtained according to approximation formula (1.20), and unbroken curves correspond to the characteristics, designed on the basis (1.17) with the aid of the electronic computer. As is evident, approximate values are close to the calculated.

1.2. Distortions of nanosecond pulses about to transmission on coaxial cable.

Using approximation for transient response of cable (1.20) and Duhamel integral, it is possible to find shape of pulse at output of cable $u_2(t)$ from known shape of pulse at input $u_1(t)$:

$$u_2(t_1) = u_1(t)\,A(0) + \int_0^{t_1} u_1(t_1 - \xi)\,A'(\xi)\,d\xi.$$

If to input of cable is given linearly increasing voltage/stress $u_1(t)=kt$, then output potential of cable by length l with $u_1(t)=0$, where $t\leq 0$, will be

$$u_2(t_1)=\frac{k\beta_{rp}^2 l^2}{\omega_{rp}}\left\{\left(1+\frac{\omega_{rp}t_1}{\beta_{rp}^2 l^2}\right)\left[1-\Phi\left(\frac{bl}{2\sqrt{\pi f_{rp}t_1}}\right)\right]-\right.$$

$$\left.-\frac{2}{\beta_{rp}}\sqrt{f_{rp}t_1}\,e^{-\frac{\beta_{rp}^2 l^2}{2\omega_{rp}t_1}}\right\}. \qquad (1.22)$$

Using method of imposition, on the basis of expression (1.22) it is possible to find distortions of video pulse of triangular, trapezoidal form or drop/jump in voltage/stress with final duration of front.

Page 22.

Fig. 1.5a shows the form of output potential of cable RK-75-4-15 with a length of 5 m (unbroken curves), if to its input drops/jumps in the voltage/stress with the amplitude, equal to one, are given and by the duration of front with respect 0.01, 0.05 and 0.1 ns (dotted lines). As is evident, the pulse edge at the output has considerably smaller slope/transconductance, than at the input. Fig. 1.5b shows a change in the form of the initial video pulse, described by function $u(t)=\sin^2 kt$, during its transmission through the segment of cable RK-50-11-13 with a length of 5 m. The shape of pulse at the output is designed according to the transient response, obtained taking into account losses in dielectric (1.20), also, without taking into account

losses in dielectric (1.19). As is evident, for the pulse duration, considerably by smaller 1 ns, and the account of losses in the dielectric is necessary at the small length of cable.

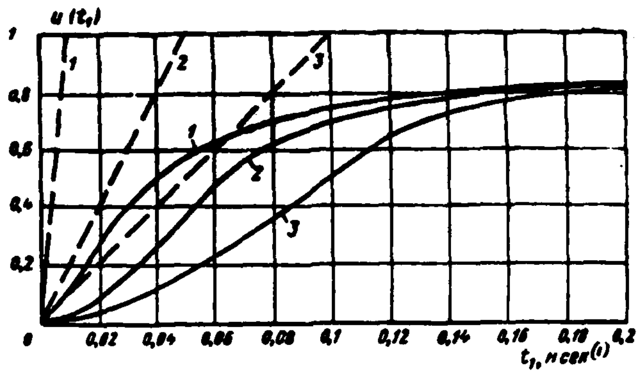

Fig. 1.5a. Output potential of cable RK-75-4-15 with a length of 5 m (unbroken curves) during the supplying to its input of a drop/jump in the voltage/stress with a duration of the front of 0.01 ns (1); 0.05 ns (2) and 0.1 ns (3).

Key: (1). ns.

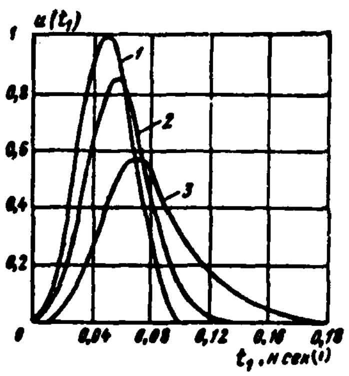

Fig. 1.5b. Output potential of cable RK-50-11-13 with a length of 5 m during the supplying to the input of the cable of the pulse of form $u(t)= \sin^2 kt$ (1), designed according to the transient response of cable without taking into account losses in dielectric (2) and taking into account losses in dielectric (3).

Key: (1). ns.

Page 23.

Let us examine distortions of nanosecond radio pulses during their transmission along cable. Let the input of cable the radio pulse

$$u_1(t) = F(t)\, e^{j\omega_0 t},$$

where F(t) - function, which presents pulse envelope, enter;

ω_0 - carrier frequency.

Transient response of cable [see formula (1.20)] let us record in the form

$$A(t_1, l) = \operatorname{erfc}\left(\frac{Ml}{2\sqrt{t_1}}\right),$$

where

$$M = \frac{\beta_{\text{гр}}}{\sqrt{\pi f_{\text{гр}}}}.$$

Assuming that $u_1(t)=0$ with $t \leq 0$, and using Duhamel integral, for pulse at output of line by length l we will obtain

$$u_2(t_1, l) = \int_0^{t_1} F(t_1 - \xi)\, e^{j\omega_0 (t_1 - \xi)} \frac{d}{d\xi} \operatorname{erfc}\left(\frac{Ml}{2\sqrt{\xi}}\right) d\xi =$$

$$= \int_0^{t_1} F(t_1 - \xi)\, e^{j\omega_0 (t_1 - \xi)} \frac{Ml}{2\sqrt{\pi}}\, \xi^{-3/2} e^{-\frac{M^2 l^2}{4\xi}} d\xi. \qquad (1.23)$$

If pulse envelope is rectilinear (for example, pulse edge), i.e., F(t)=kt, where k=const, then from preceding/previous expression we

will obtain

$$u_s(t_1, l) = \frac{Ml}{2\sqrt{\pi}} e^{j\omega_0 t_1} k \left[t_1 \int_0^{t_1} e^{-j\omega_0 \xi} \xi^{-3/2} e^{-\frac{M^2 l^2}{4\xi}} d\xi - \right.$$
$$\left. - \int_0^{t_1} e^{-j\omega_0 \xi} \xi^{-1/2} e^{-\frac{M^2 l^2}{4\xi}} d\xi \right]. \qquad (1.24)$$

Integrals in this expression can be calculated by asymptotic method.

Page 24.

Using expression (1.24) and superposition principle, it is possible to find output signal, if at the input of cable operates nanosecond radio pulse from the enveloping triangular or trapezoidal form.

Calculation of distortions of nanosecond pulses, connected with their transmission through coaxial cable, and also experimental check [8, 9] of given above formulas they indicate need for account of losses both in conductors and in dielectric of cable. The account of losses in the dielectric is especially necessary during the transmission of pulses with the duration of less than 1 ns through the segments of the cable of small length. When pulses are transmitted through the cable by the length of more than 40-50 m, the account of losses in the dielectric on is so/such essential.

In the case of application for delay and transmission of nanosecond pulses of coaxial cables with length of more than 1-2 m it

is expedient to utilize cables with large diameters of internal and external conductors as a result of the fact that losses in such conductors of cable are less. The possibility of the existence in them of the oscillations/vibrations of the highest types is eliminated, since due to the total losses the passband of the cables with a length of 1.5-2 m is limited by frequency 5-10 GHz which lower than the critical frequencies the dog.

1.3. Coaxial delay lines.

Selection of coaxial cables.

Coaxial cables with polyethylene filling as delay line of nanosecond pulses to admissibly use only with small delay time. In the case of pulse delay by the duration of less than 1 ns it is expedient to utilize the cables with the filling of their teflon, which have loss in the dielectric somewhat less. Cables with an air-plastic insulation have even smaller losses, but they are characterized by discontinuity, which leads to the distortions of the pulses of short duration.

Table 1.2 gives data of Soviet coaxial cables, which are most adequate/approach for transmission and delay of nanosecond pulses [4].

Page 25.

First five cable make-ups have as dielectric continuous polyethylene filling, and latter/last four cables have continuous

filling from teflon. Dielectric losses in teflon are almost two times less than in polyethylene (at frequencies from hundreds of megahertz to 10 GHz); therefore the resulting attenuation in latter/last cables is less than in five preceding/previous (Table 1.2).

Special delay lines.

For delay of nanosecond pulses are developed miniature coaxial delay lines, in which is utilized property of superconductivity of materials at very low frequencies [11]. This delay line with a wave impedance of 50 ohms has a small cross section of conductors. Center conductor is fulfilled from niobium with a diameter of 0.25 mm, and external - from lead with a diameter of 0.86 mm. In this case critical frequency for the oscillations/vibrations of the highest types is equal to 100 GHz. For purposes of reduction in the losses to the minimum entire system is at a temperature 4°K, for which the cable, wound around the drum, is placed into the container with liquid helium. At this temperature the losses in the dielectric (teflon) of cable vanish, and conductivity, for example in lead, it increases 10^{17} times in comparison with the conductivity at 0°C.

Thus, line is very wide-band both with small and at its large length.

Table 1.2.

(1) Тип кабеля	(2) Волновое сопротивление, ом	(3) Емкость, пф/м	(4) Затухание на частоте 10 Ггц, дб/м	(5) Испытательное напряжение, кв
РК-50-11-13	50	106	2,4	12
РК-50-7-16	50	102	2,6	9
РК-75-7-16	75	69	2,7	7
РК-75-7-11	75	75	2,7	6
РК-100-7-13	100	57	2,6	10
РК-50-11-21	50	106	1,7	12
РК-75-7-21	75	71	1,7	12
РК-75-7-22	75	69	1,9	7
РК-100-7-21	100	57	1,9	10

Key: (1). Type of cable. (2). Wave impedance, ohm. (3). Capacity/capacitance, pF/m. (4). Attenuation at frequency of 10 GHz, dB/m. (5). Testing voltage, kV.

Page 26.

However, during the use of this zero-loss circuit difficulties appear. If coaxial pairs are carried out not very accurately, then in the places for heterogeneity (just as in the case of heterogeneity in line itself) appear the waves reflected. During the transmission of pulses the appearing echo pulses by the force of the absence of line loss will be for long propagated from the end/lead of the line at the beginning and vice versa. As a result the considerable distortions of main impulses can arise. Therefore the special constructions/designs of small/miniature coaxial pairs of high quality are necessary for similar lines. The experimental studies of this superconducting line showed [11] that during the transmission of pulses with the front with the duration of 0.4 ns along the line with the length of 30 m the steepness of their front does not change.

Extension (telescopic) lines with air filling can be used if necessary for small continuously adjustable delay of nanosecond pulses. In their construction/design must be provided the constancy of wave impedance, the high accuracy of the fulfillment of transitions from one section of line to another is required for which and the proper quality of sliding contacts. Such lines successfully are used in the very high speed oscillographs for calibrating the duration of the observed pulses. For obtaining the delay 1-2 ns the length of line must be equal to 30-60 cm. The measurement of the time interval is made with an accuracy to 10^{-11} s and is limited to the resolution of the electronic part of the oscillograph. The distortions of the shape of pulse in the line are small and are affected the quality of coaxial pairs at its ends/leads.

1.4. Strip transmission lines and their transient responses.

With formation of low-power nanosecond pulses with duration of order of nanosecond and less, for example, with the aid of tunnel diodes and other semiconductor devices, are used diagrams, carried out by means of printed wiring. In this way it is possible to considerably reduce the parasitic circuit parameters.

Page 27.

In these cases it is convenient for the delay, the transmission of pulses and as the forming lines to use the strip transmission lines. In connection with this it is necessary to know the characteristics of

strip lines as the lines of transmission of nanosecond pulses.

Parameters of strip line.

For transmission of nanosecond pulses strip line (Fig. 1.6), which is called symmetrical strip line, is of interest. Line consists of two grounded external metallic bands and metallic strip, situated between them at a distance of h (from each external band). Space between them is usually filled with dielectric. Symmetrical strip line is the shielded system. Exemplary/approximate field distribution in this system is shown in Fig. 1.6b. Entire electric field is concentrated in the region of cavity, and since there are no between the external bands of potential difference, then the plane of central strip (beyond the limits of strip), actually, is the region, free from the field.

Strip, as coaxial line, works in mode of fundamental oscillations of form of TEM. The most important parameters of strip line include the capacitance per unit length C, wave impedance ρ and wave propagation velocity v.

Wave impedance and wave propagation velocity are respectively determined by formulas

$$\rho = \sqrt{\frac{L}{C}}, \quad (1.25)$$

$$v = 1/\sqrt{LC}, \quad (1.26)$$

whence we will obtain

$$\rho = \frac{1}{vC}. \quad (1.27)$$

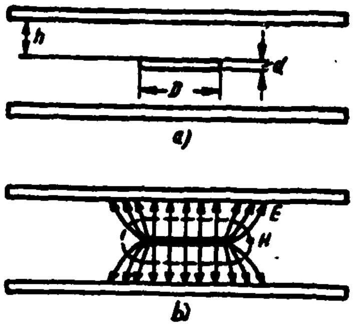

Fig. 1.6. Strip line of transmission (a) and field distribution in it (b).

Page 28.

Since wave propagation velocity can be recorded

$$v=\frac{3\cdot 10^8}{\sqrt{\epsilon_r\mu_r}}\left[\frac{м}{^{(1)}сек}\right], \qquad (1.28)$$

Key: (1). s.

where ϵ_r and μ_r - relative dielectric and magnetic constants of the material of line, the wave impedance·

$$\rho=\frac{\sqrt{\mu_r\epsilon_r}}{3\cdot 10^8 C}\ [ом]. \qquad (1.29)$$

In the case of absolutely conducting strips zero thickness following precise formula for wave impedance of strip line [12] is valid:

$$\rho=\frac{30\pi K(k)}{K(k')}, \qquad (1.30)$$

where K(k) and K(k') - complete elliptical integrals of the first

kind, expressed through

$$k = \mathrm{sch}\,(\pi D/4h),$$
$$k' = \mathrm{th}\,(\pi D/4h).$$

In real construction/design of line thickness of strip is final and exerts a substantial influence on wave impedance (Very approximate value of wave impedance can be) obtained on the basis (1.29), if capacity/capacitance of line is calculated from formula for capacity/capacitance of parallel-plate capacitor

$$C_{\text{п}} = 35{,}4\,\frac{\varepsilon D/2h}{1 + d/2h}. \qquad (1.31)$$

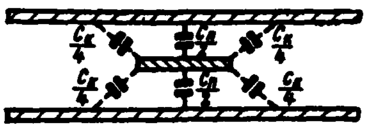

Fig. 1.7. Distribution of capacities/capacitances in strip line.

Page 29.

Use of expression (1.31) is admissible during very approximate calculations of wave impedance, whose value is less than 25 ohms, and with high values ρ capacity/capacitance of fringing field composes noticeable part of total capacitance (Fig. 1.7). General/common capacitance per unit length then will be

$$C = C_{п} + C_{к}. \qquad (1.32)$$

Capacity/capacitance of fringing field $C_{к} = f\left(D, \frac{d}{h}\right)$ is determined by sizes/dimensions of line and by dielectric constant ϵ. A precise formula, found with the aid of conformal mapping, is given in [12]. In view of the unwieldiness of the expressions, which are obtained for the wave impedance, to more conveniently use the graph/curve of the line characteristics, given in Fig. 1.8. Size/dimension change makes it possible to obtain lines with the very different wave impedance. Lines with the low wave impedance have wider strip, i.e., the larger value of D/(2h+d).

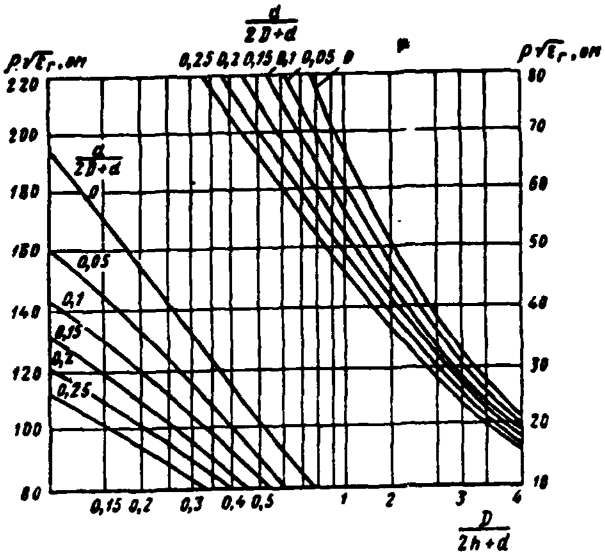

Fig. 1.8. Graph/curve for calculating wave impedance of strip line.

Page 30.

Lines with very low wave impedance are necessary for some schematics of nanosecond generators, and in these cases it is possible to utilize strip lines. During the selection of the geometric dimensions of line it is necessary to have in mind that the transverse sizes/dimensions of line must be small for the avoidance of the possibility of the onset of the waves of the highest types. Thus, the distance between the external bands must be less λ/2, where λ - maximum critical wavelength of highest type oscillations. The width of strip also must not substantially exceed this value.

Attenuation is important parameter of strip line. Just as in the coaxial line, here energy losses depend on lead loss, mainly due to the surface effect, and by losses in the dielectric, which fills line. Total attenuation is caused by lead loss $\beta_п$ and losses in dielectric $\beta_д$:

$$\beta = \beta_п + \beta_д. \qquad (1.33)$$

Attenuation constant in conductors is determined by ratio of power of losses $P_п$ to transmitted power P:

$$\beta_п = \frac{P_п}{2P}.$$

Power of losses is found from expression

$$P_{п} = \frac{\eta^2}{2\mu} \int |E|^2 \, ds,$$

where $\eta = \sqrt{\pi f \mu / \sigma}$. - value, which determines surface strength of materials of conductors;

σ - conductivity of material of strips;

E - electric intensity;

s - no-flow length of way of integration, which is conducted on boundaries of all conductors.

Page 31.

Rate of flow of energy, which takes place in line, is equal to

$$P = \frac{U^2}{2\rho},$$

where U - maximum instantaneous value of voltage/stress in line.

Approximate computation of attenuation in conductors of line when central strip is sufficiently wide (D/2h≥0.35), should be performed according to expression [12]

$$\beta_{п} = \frac{2\sqrt{\omega\mu_{п}/2\sigma}\,\rho\varepsilon_{д}}{\mu_{д} h}\left[1 + D/h + \frac{1}{\pi}(1 + d/2h)\ln(1 + 4h/d)\right], \tag{1.34}$$

where $\mu_{д}$ and $\mu_{п}$ - respectively magnetic permeability of dielectric medium and material of conductors, H/m;

$\varepsilon_{д}$ - dielectric constant of dielectric medium, F/m;

σ - conductivity, 1/ohm·m.

Geometric dimensions are expressed in meters.

In the case of copper conductors we will obtain

$$\beta_{\text{п}} \approx \frac{2{,}55\cdot 10^{-11}\rho\varepsilon_r \sqrt{\omega}}{\mu_r h}\left[1 + D/h + \frac{1}{\pi}(1 + d/2h) \times \times \ln(1 + 4h/d)\right] [\overset{(1)}{\text{дб}}/\text{м}];$$

Key: (1). dB/m.

here ε_r and μ_r - relative values of the dielectric and magnetic constant of dielectric medium.

Instead of (1.34) let us record

$$\beta_{\text{п}} = B_1 \sqrt{\omega}, \qquad (1.35)$$

where

$$B_1 = \frac{2\sqrt{\mu_{\text{п}}/2\sigma}\rho\varepsilon_{\text{д}}}{\mu_{\text{д}} h}\left[1 + D/h + \frac{1}{\pi}(1 + d/2h) \times \times \ln(1 + 4h/d)\right] [\overset{(1)}{\text{сек}}{}^{1/2}/\text{м}]. \qquad (1.36)$$

Key: (1). $\sec^{1/2}$/m.

Expression for attenuation in the case of very narrow central strip give we will not be, since this corresponds to case of high wave impedance, which are not here of interest.

Page 32.

It is evident from expression (1.34) that attenuation $\beta_{\text{п}}$ in conductors decreases with increase in distance between strips, and also with decrease of wave impedance ρ, whose value in turn decreases with increase in ratio D/h.

Attenuation $\beta_д$ due to losses in dielectric, which fills evenly space between strips, can be calculated, knowing power losses in dielectric $P_д$ and rate of flow of energy, transmitted by line P. Power losses in the dielectric per unit of the length of the line

$$P_д = \frac{\sigma_д}{2} \int |E|^2 dS,$$

where $\sigma_д$ - dielectric conductance, which is determined from the complex dielectric constant;

dS - element of area of dielectric.

Attenuation in dielectric is determined by relation of power:

$$\beta_д = \frac{P_д}{2P}.$$

Since in expressions for $P_д$ and P range of integration one and the same, then for $\beta_д$ is obtained expression, which does not depend on sizes/dimensions of conductors. Attenuation per unit length [12] is equal

$$\beta_д = \frac{\omega \sqrt{\varepsilon_r}\, \mathrm{tg}\,\delta}{2c} = \frac{\omega \sqrt{\varepsilon_r}}{6 \cdot 10^8} \; \overset{(1)}{[нп/м]}, \qquad (1.37)$$

Key: (1). np/m.

where ε_r - relative dielectric constant;

c - wave propagation velocity in the free space;

tg δ - loss tangent in the dielectric.

Attenuation in dielectric can be recorded otherwise:

$$\beta_{д}=A_{1}\omega \operatorname{tg}\delta \ \overset{(1)}{[нп/м]}, \qquad (1.38)$$

Key: (1). np/m.

where

$$A_{1}=\frac{\sqrt{\varepsilon_{r}}}{6\cdot 10^{8}}=1{,}66\cdot 10^{-9}\sqrt{\varepsilon_{r}}\ \overset{(1)}{[сек/м]}. \qquad (1.39)$$

Key: (1). s/m.

For determining phase constant strip line it is necessary to consider internal inductance $L_{в}$ of conductors, which appears due to surface effect.

Page 33.

The modulus of resistance of this inductance is equal to the value of the effective resistance of lead loss. Therefore, as in the case of coaxial line, propagation constant $\bar{\gamma}$ in general form will be expressed:

$$\bar{\gamma}=\beta_{п}+\beta_{д}+j\alpha=\beta_{п}+\beta_{д}+j\left[\omega\sqrt{L_{вн}C}+\beta_{п}+\frac{(\beta_{п}-\beta_{д})^{2}}{2\omega\sqrt{L_{вн}C}}\right].$$

Using expressions (1.35) and (1.38), we will obtain

$$\bar{\gamma}=B_{1}\sqrt{\omega}+A_{1}\omega \operatorname{tg}\delta+j\left[\omega\sqrt{L_{вн}C}+B_{1}\sqrt{\omega}+\frac{(B_{1}\sqrt{\omega}-A_{1}\omega \operatorname{tg}\delta)^{2}}{2\omega\sqrt{L_{вн}C}}\right], \qquad (1.40)$$

where external inductance of line L_{BH} is determined according to (1.25) in terms of known values of wave impedance ρ and capacity/capacitance of C [formula (1.32)].

For real constructions/designs of strip lines in interesting us frequency region (to 10 GHz) are always fulfilled following inequalities [13]:

$$\frac{(B_1\sqrt{\omega}-A_1\omega\,\mathrm{tg}\,\delta)^2}{2\omega\sqrt{L_{BH}C}} \ll B_1\sqrt{\omega},$$

$$\frac{(B_1\sqrt{\omega}-A_1\omega\,\mathrm{tg}\,\delta)^2}{2\omega\sqrt{L_{BH}C}} \ll \omega\sqrt{L_{BH}C}.$$

Then for transmission factor of uniform strip line, continuously filled with dielectric, we obtain expression

$$\bar{K}=\left\{\exp l\left[B_1\sqrt{\omega}+A_1\omega\,\mathrm{tg}\,\delta+j\left(\frac{\omega}{v}+B_1\sqrt{\omega}\right)\right]\right\}^{-1}. \tag{1.41}$$

Transient responses of strip lines. Distortions of pulses.

Transient response of strip line with continuous dielectric filling between bands must be obtained taking into account lead loss and dielectric.

Page 34.

For the transmission of nanosecond pulses the line must be residual/remanent wide-band, and therefore the region of the

frequencies interesting us includes high frequencies to value on the order of 10 GHz. Just as in coaxial cable, at frequencies on the order of 1-3 GHz losses in the dielectric prove to be commensurate with the lead loss, and at the higher frequencies they considerably exceed them.

Using expression for transmission factor (1.41), we will obtain following formula for computing transient response of strip line:

$$A(t_1, l) = \frac{1}{2\pi}\int_{-\infty}^{\infty}\frac{1}{j\omega}\overline{K}e^{j\omega t}d\omega =$$

$$= \frac{1}{2\pi}\int_{-\infty}^{\infty}\frac{1}{j\omega}\,\frac{e^{j\omega t}d\omega}{\exp\,[B_1\sqrt{\omega} + A_1\omega\,\mathrm{tg}\,\delta + jB_1\sqrt{\omega}]l}, \quad (1.42)$$

where $t_1 = t - \frac{l}{v} = t - t_3$; t_3 - delay time of pulse with passage along line.

However, loss tangent in dielectric tg δ usually depends on frequency, which complicates expression (1.42).

Let us examine first transient response of strip line without taking into account losses in dielectric. This case is of interest when space between the bands is filled with air.

For considerable reduction in line losses it is expedient to utilize strip line, whose central strip is arranged/located on thin sheet of dielectric, fastened/strengthened along edges between external bands with the aid of rigid supports (Fig. 1.9). Here central strip consists of the metallic coatings, plotted/applied from both sides of dielectric sheet.

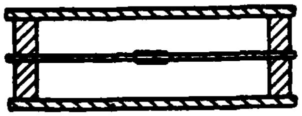

Fig. 1.9. Strip line with central strip on dielectric sheet.

Page 35.

If both central strips are connected in parallel at input and output of line, then electric field will exist only in the air gaps between each central strip and corresponding external grounded band. In this case only the small part of the dielectric sheet will be in the fringing field of central strip. In the case of applying the low-loss dielectric (polystyrene, Teflon glass, etc.) of loss in it due to the edge effect they will be small and the resulting line losses will be in essence determined by lead loss.

In this case for transmission factor of line instead of (1.41) we will obtain approximation

$$\overline{K}=e^{-l\left(j\frac{\omega}{v}+B\sqrt{j\omega}\right)}, \qquad (1.43)$$

where $B=B_1\sqrt{2}$.

Let us record transmission factor in operational form:

$$\hat{K}(p)=e^{-l\left(\frac{p}{v}+B\sqrt{p}\right)}.$$

Transient response of line in this case is found from following

converted through Laplace function:

$$\frac{1}{p}\hat{K}(p)=\frac{1}{p}\,e^{-l(p/v+B/\sqrt{p})},$$

original of which is expression

$$A(t_1, l)=1-\Phi\left(\frac{Bl}{2\sqrt{t_1}}\right), \qquad (1.44)$$

where $\Phi\left(\frac{Bl}{2\sqrt{t_1}}\right)$ - function of Kramp [transliterated]; $t_1=t-\frac{l}{v}$.

Fig. 1.10 gives transient responses of strip lines length of 1 m, made from copper strips with thickness of central strip 0.1 mm. Unbroken curves represent the transient responses of lines with a wave impedance of 50 ohms with the values of the transverse size/dimension of h=1; 2.5 and 5 mm. The transient responses of lines with a wave impedance of 75 ohms with the same values of h are represented by dotted curves.

Page 36.

As can be seen from this figure, slope/transconductance of initial section of transient response of strip line depends substantially on distance between central and external strips h. With an increase in this distance mutual conductance grows/rises, since lead loss decrease and the broad-band character of line increases. Line with a wave impedance of 75 ohms has high losses, and the slope/transconductance of its transient response is less than in line with a wave impedance of 50 ohms.

Fig. 1.11 gives transient responses of strip lines with wave impedance of 50 ohms with length of 10 m with values of h=1; 2.5 and 5 mm. In the same figure of dotted curve is represented the transient response of cable RK-50-11-13, which has the wave impedance of 50 ohms. The diameter of the external conductor (braid/cover) of this cable is equal to 11 mm. As is evident, the slope/transconductance of the transient response of cable is considerably less than the slope/transconductance of the transient response of strip line approximately with the same transverse size/dimension (curve for h=5 mm Fig. 1.11).

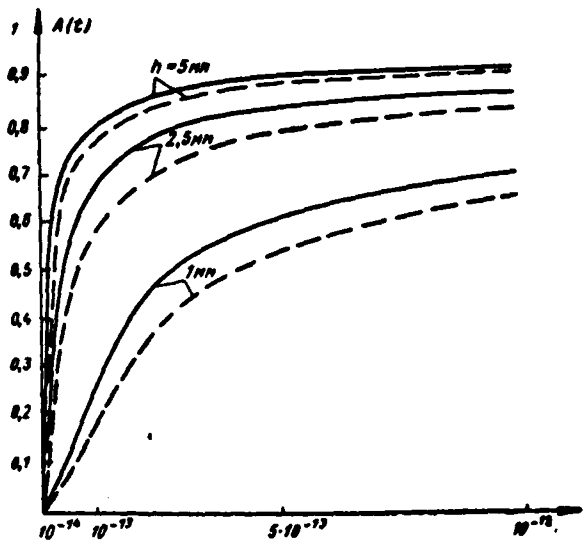

Fig. 1.10. Transient responses of strip line with length of 1 m with wave impedance: —— 50 ohms, ---- 75 ohms.

Page 37.

It is necessary to note that the transient response of cable is constructed taking into account lead loss and dielectric.

With increase in distance between central and external strip h for retaining/maintaining constancy of assigned wave impedance it is necessary to increase width of central strip D. This fact leads to the need for increasing the width of external strips $D_{вн}$, which must be equal to $D_{вн} \approx D + 4h$.

Thus, if we consider losses only in conductors of strip line, then its transient response will have considerable

slope/transconductance. At the length of line 1 m and is less it is possible to transmit by it without the distortion pulses with duration about 0.1 ns.

If would be required even wider-band line for transmission of low-power pulses, then for this it is possible to utilize strip line with strips in the form of thin metallic films. Thus, in the line, whose construction/design is given to Fig. 1.9, central strip and external bands it is possible to fulfill in the form of the finest metallic films, whose thickness is equal to the depth of penetration of electromagnetic waves into the metal at the greatest frequency of the region of the frequency spectrum interesting us.

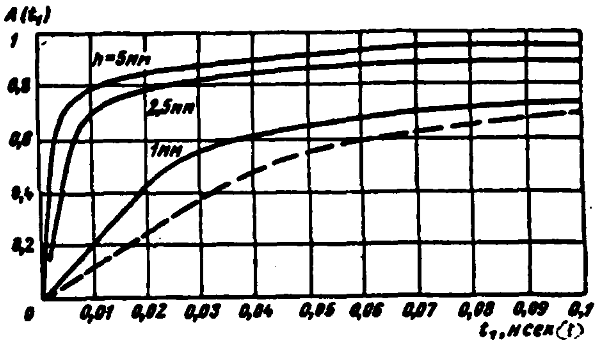

Fig. 1.11. Transient responses of strip lines with length of 10 m with wave impedance of 50 ohms and transverse sizes/dimensions h=1; 2.5 and 5 mm (solid lines) and cable RK-50-11-13 (dotted line) the same length.

Key: (1). ns.

Page 38.

Then in this band of frequencies of the loss in the metal will not depend on frequency, i.e., $\beta_{\text{п}}=\text{const}$.

Attenuation of wave amplitude during its penetration into metal up to distance of d will be determined by exponential function $e^{-\xi d}$, where

$$\xi=\sqrt{\frac{\omega\sigma\mu}{2}}.$$

With attenuation of wave amplitude on 3 dB wave will cover a distance

$$d_{э}=\frac{0,35}{\xi}\approx\frac{180}{\sqrt{f_{макс}\sigma\mu_r}},$$

where $f_{макс}$ - maximum frequency of interesting us spectrum;

σ - conductivity;

μ_r - relative magnetic permeability.

For copper conductors at maximum frequency of spectrum $f_{макс}=10$ GHz depth of penetration is approximately equal to 0.25 μ. This strip line would have ideal frequency and phase responses in the frequency region indicated and would be the wide-band attenuator, which weakens equally all components of pulse spectrum.

However, in the case of transmission of comparatively powerful nanosecond pulses constructions/designs examined can prove to be unacceptable. Furthermore, line with the rigidly fixed dielectric sheet in the center at its comparatively large length will be inconvenient. Therefore strip line with the continuous filling with elastic dielectric is more convenient and more universal construction/design. This line, as coaxial cable, can be if necessary convoluted into the bay and designed for the transmission of the pulses of a comparatively large power.

For computing transient response of this line it is necessary to turn to expression (1.42).

Page 39.

If line has continuous polyethylene filling, then according to (1.12)

we have

$$\operatorname{tg}\delta=\frac{a_1\sqrt{\omega}}{1+m\omega},$$

and then instead of (1.42) we will obtain the expression

$$A(t_1,l)=\frac{1}{2\pi}\int_{-\infty}^{\infty}\frac{1}{j\omega}\frac{e^{j\omega t}d\omega}{\exp\left[l\left(B_1\sqrt{\omega}+\frac{A_0\omega^{3/2}}{1+m\omega}+jB_1\sqrt{\omega}\right)\right]},\tag{1.45}$$

where $A_0=A_1a_1=3\cdot10^{-17}$ $\sec^{3/2}/\mathrm{rad}^{1/2}\cdot\mathrm{m}$.

Since direct computation of transient response according to formula (1.45) causes considerable difficulties, then computation, as in the case of coaxial cable, they are conducted by grapho-analytic method (see § 1.1).

Fig. 1.12 gives graphs/curves of transient responses of strip line from copper strips with thickness of central strip 0.1 mm with continuous polyethylene filling. Line has a wave impedance of 50 ohms and sizes/dimensions of D=3.5 mm, h=2.5 mm. Calculations are carried out for the line by length 1; 5 and 10 m.

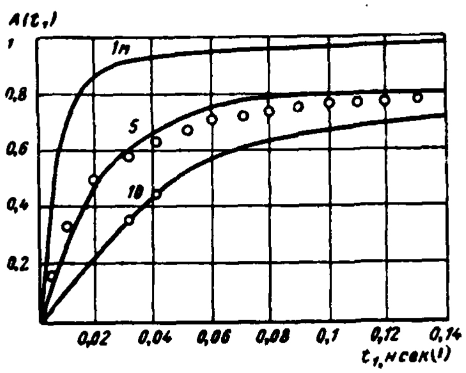

Fig. 1.12. Transient responses of strip lines with dielectric filling from polyethylene.

Key: (1). ns.

Page 40.

If we compare these transient responses with the transient responses of line (with the same sizes/dimensions of d, D, h and l), given in Fig. 1.11 (curve for h=2.5 mm), then it is easy to note the large difference in the slope/transconductance of transient responses. The presence of dielectric filling leads to a considerable increase of the total line losses, which decreases its broad-band character.

Just as in the case of coaxial cable, it is possible to construct graph/diagram of dependence of bandwidth of strip lines on its length for different values of transverse size/dimension of h. Using expression for the transmission factor (1.41), we find its modulus/module $|\vec{K}|$ and expression for dependence of phase shift on frequency $\Delta\varphi(\omega)$:

$$|\bar{K}|=\left[\exp\left(B_1\sqrt{\omega}+\frac{A_1\omega^{3/2}}{1+m\omega}\right)l\right]^{-1}, \qquad (1.46)$$

$$\Delta\varphi(\omega)=lB_1\sqrt{\omega}. \qquad (1.47)$$

Fig. 1.13 gives dependences of bandwidth of strip lines with wave impedance of 50 ohms on their lengths l, calculated according to formula (1.46). The cut-off frequency of passband corresponds to the frequency, at which the modulus of transmission factor decreases on 3 dB relative to values at the low frequencies. Its broad-band character grows/rises at a small length of line and the specific significance of the losses in the dielectric, whose value does not depend on the transverse size/dimension of line h, becomes more, but it grows/rises with an increase in the frequency. Therefore with the low values l curves are arranged/located more closely than at the large length of line.

Calculation of transient responses on the basis of expression (1.45) is connected with cumbersome calculations, and, furthermore, absence of their resultant analytical expression does not make it possible to record shape of pulse at output of line with assigned expression for input pulse. Therefore, as in the examination of the characteristics of coaxial cable, it is expedient to introduce the approximate analytical expression of the transient response of strip line, which considers losses both in the conductors, and in the dielectric.

Page 41.

Similar to formula (1.22) for the transient response of strip line it is possible to record the following expression:

$$A(t_1, l) = 1 - \Phi\left(\frac{B_{rp} l}{2\sqrt{t_1}}\right). \qquad (1.48)$$

Here coefficient B_{rp} is located through the resulting line loss at the cut-off frequency of passband f_{rp} at the assigned length of line and transverse size/dimension h:

$$B_{rp} = B_{1rp}\sqrt{2} = \frac{\beta_{rp}\sqrt{2}}{\sqrt{\omega_{rp}}} = \frac{\beta_{rp}}{\sqrt{\pi f_{rp}}}. \qquad (1.49)$$

Attenuation β_{rp} is determined by sum of attenuations β_{urp} and $\beta_{\pi rp}$, which are located at frequency f_{rp} according to expressions (1.34) and (1.38).

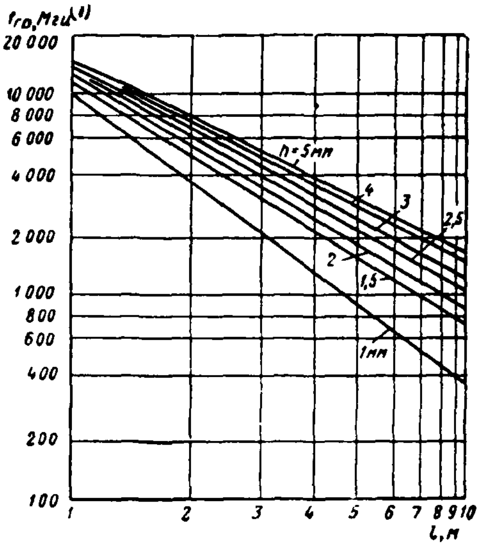

Fig. 1.13. Dependences of cut-off frequency of passband of strip lines with wave impedance of 50 ohms on length of line with its different transverse sizes/dimensions.

Key: (1). MHz.

Page 42.

In Fig. 1.12 small circles noted values of transient response of strip line with length of 5 m, calculated by approximation formula (1.48). As is evident, this transient response differs little (especially in its initial part) from the transient response, obtained by grapho-analytic method on the basis of expression (1.45). It follows from the verifying calculations that at the length of line 2-10 m it is possible to use formula (1.48).

If analytical expression of transient response of line with

continuous dielectric filling is known, then it is possible to rate/estimate distortion of shape of nanosecond pulses during their transmission along this line. Using the method of imposition, on the basis of expression (1.48) it is easy to find the distortion of square pulse by duration $t_{и}$. Expression for the pulse, which passed distance l along the line, in this case can be represented in the form

$$u_{вых}(t_1, l, t_и) = A(t_1, l) - A(t_1 + t_и, l). \qquad (1.50)$$

If pulse edge has final duration and increases according to linear law, then distortion of front can be determined on form of output voltage/stress, obtained with the aid of Duhamel integral and formula (1.48) with input voltage, assigned in the form $u_{вх}(t) = kt$, where k=const.

Output voltage/stress is determined by expression

$$u_{вых}(t_1, l) = u_{вх}(t) A(0) + \int_0^t u_{вх}(t-\xi) A'(\xi)\, d\xi =$$
$$= k\frac{(B_{rp} l)^2}{2}\left\{\left(1 - \frac{2t_1}{B_{rp}^2 l^2}\right)\left[1 - \Phi\left(\frac{B_{rp} l}{2\sqrt{t_1}}\right)\right] - \right.$$
$$\left. - \frac{2}{B_{rp} l}\sqrt{\frac{t_1}{\pi}}\, e^{-\frac{B_{rp}^2 l^2}{4t_1}}\right\}. \qquad (1.51)$$

Thus, with the aid of formulas (1.48), (1.51) and method of imposition it is possible to determine distortions of shape of pulse, transmitted by strip line.

Page 43.

1.5. EFFECT OF HETEROGENEITIES ON THE CHARACTERISTICS OF LINE.

Examining characteristics of lines, we assumed lines uniform and those ideally coordinated with resistor/resistance of generator at input of line and with load at output. However, during the transmission of the nanosecond pulses (especially with the duration of the order of nanosecond and less) are manifested the relatively small heterogeneities of the transmitting circuit. In the circuit of transmission, besides strictly line, are usually included also input and output couplings, different terminations and matching transitions.

Real uniform line has some heterogeneities, which can be named/called internal heterogeneities. Thus, in the case of coaxial cable its wave impedance in the individual sections somewhat changes in view of insignificant changes in the transverse sizes/dimensions of conductors. In the cable changes in the form of conductors or heterogeneity of dielectric filling can be observed. Just as in the technology of shf/SVCh, in the nanosecond technology it is necessary to consider the possibility of the onset in the two-wire circuit of the waves of the highest types, whose appearance is connected with the presence in it of heterogeneities.

As is known, for oscillations of highest types lines of force of electrical and magnetic fields are not perpendicular to direction of propagation of waves, but phase speed depends on frequency. For each

type of oscillations there is a specific critical frequency. The transmission of vibrational energy of highest type with the frequency below critical proves to be impossible, since fields rapidly attenuate. The waves of the highest types can exist in the line during the transmission of such high frequencies, when wavelength the line commensurate with the transverse sizes/dimensions becomes.

Page 44.

Thus, for coaxial cable critical frequency for the waves of the type TE those is determined by formula [4]:

$$f_{\text{к1}} = \frac{2c}{\pi(D+d)\sqrt{\varepsilon_r}},$$

but for the waves of the type TM

$$f_{\text{к2}} = \frac{c}{(D-d)\sqrt{\varepsilon_r}},$$

where $c=3\cdot10^8$ m/s - speed of light;

D and d - diameters of external and internal conductors;

ε_r - relative dielectric constant of dielectric.

If in line is certain heterogeneity, for example stepped variation in sizes/dimensions of conductors (Fig. 1.14a), then in area of heterogeneity distortion of field occurs and oscillations of highest types are possible. This phenomenon is most noticeable at the high frequencies. The part of the energy of high-frequency pulse component is expended on the oscillations of the highest types. As a result the shape of the pulse, transmitted by the line with the

heterogeneity, will be distorted. The greater the sections of heterogeneity, the greater the distortion of pulse. If it is necessary to pass from the sections of coaxial line with some transverse sizes/dimensions to the sections with other sizes/dimensions, after preserving in this case the constancy of wave impedance, then this transition is fulfilled by smooth, and the length of transition must be several times of more than the diameter of external conductor.

If in line is heterogeneity in the form of stepped variation in transverse sizes/dimensions, for example, in strip line or line, formed by parallel plates (Fig. 1.14b), then its action on shape of transmitted pulse can be represented by action of certain shunt capacitance $C_э$ (Fig. 1.14c), switched on in that place, where heterogeneity of line is located. The value of this capacity/capacitance depends from the relation of the transverse sizes/dimensions of line to heterogeneity h_1 and in the place for heterogeneity h_2, i.e., $C_э=f\left(\frac{h_1}{h_2}\right)$ [14, 15]. Dependence $C_э=f\left(\frac{h_1}{h_2}\right)$ is given in Fig. 1.15.

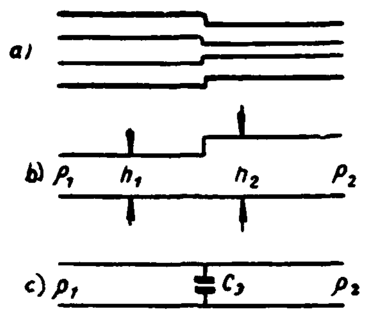

Fig. 1.14. Transmission line with stepped heterogeneity (a, b) and with equivalent capacity/capacitance (c).

Page 45.

If line is filled with uniform dielectric, then the value of capacity/capacitance must be multiplied by the value of the relative dielectric constant of dielectric.

In the case of coaxial line value of equivalent capacity/capacitance can be determined by expression [14, 15]

$$C_{эк} = 2\pi r C_{эо}. \tag{1.52}$$

Here capacity/capacitance $C_{эо}$ is the function of the ratio of a difference in the radii of conductors to heterogeneity h_1 to a difference in the radii of conductors in the place for heterogeneity h_2 and is determined on the curve, given in Fig. 1.15. The value of radius r depends on the form of stepped heterogeneity.

If stepped heterogeneity appears only due to change in diameter of external conductor, then $r=r_1$, where r_1 - radius of internal conductor of line.

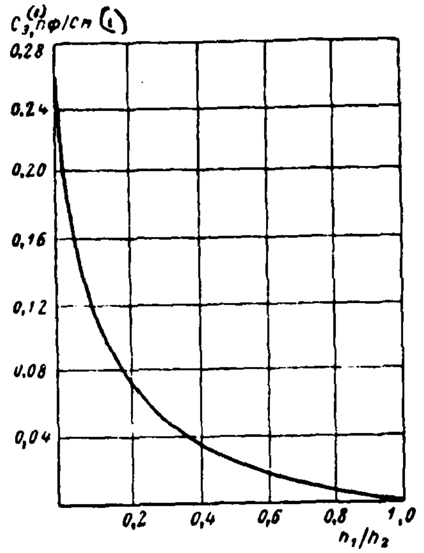

Fig. 1.15. Dependence of equivalent capacity/capacitance on transverse sizes/dimensions of line.

Key: (1). pF/cm.

Page 46.

If heterogeneity is formed only due to a change in the diameter of internal conductor, then $r=r_2$, r_2 - radius of external conductor. With a simultaneous change in diameters of both conductors the capacity/capacitance is calculated from the formula

$$C_{эк} = 2\pi r'_2 C_э\left(\frac{h_2}{h_1}\right) + 2\pi r''_1 C_э\left(\frac{h_3}{h_2}\right), \qquad (1.52a)$$

where value r'_2, r''_2, h_1, h_2, h_3 are shown in Fig. 1.16.

Knowing equivalent capacity/capacitance $C_э$ (or $C_{эк}$) and effective resistance R of line in place for heterogeneity, it is possible to

approximately rate/estimate distortion of transmitted pulse due to heterogeneity. In this case is examined the distortion due to the equivalent $RC_э$-circuit. Effective resistance in the place for heterogeneity R is the resistor/resistance of the parallel-connected resistors/resistances ρ_1 and ρ_2, where ρ_1 - output resistance of the section of line to the heterogeneity, ρ_2 - input resistance of the section of line after the heterogeneity. Thus, the time constant of the circuit

$$\tau = \frac{\rho_1 \rho_2}{\rho_1 + \rho_2} C_э.$$

This simplified evaluation of effect of heterogeneity on shape of pulse occurs in the range of high frequencies, when wavelength still is somewhat more than greatest transverse size/dimension of line, and also, if distance between heterogeneities is not too small, i.e., in the absence of mutual interaction between heterogeneities [16].

Sometimes heterogeneities in lines (random or specially formed) present for waves propagated in cable effective resistance.

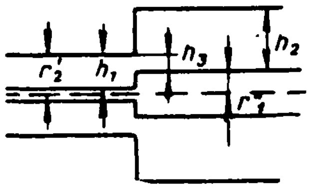

Fig. 1.16. Line with stepped heterogeneity.

Page 47.

In these cases in the area of heterogeneity although occurs the wave reflection, reflection coefficient does not depend on frequency and therefore the shape of the transmitted pulse is not distorted, but is observed only a change in its amplitude.

Besides internal heterogeneities of line usually are heterogeneities at input and output of line. In the real constructions/designs of couplings, for example for coaxial cables, already at frequencies of 1-3 GHz the standing-wave ratio in the voltage/stress noticeably differs from one. If the heterogeneity introduced at the ends/leads of the line has reactive/jet or complex character, then the coefficient of reflection of waves depends on frequency, which leads to the distortion of the shape of the pulse transmitted by the circuit.

Important value for undistorted transmission of pulses has quality of agreement of line with resistance/resistor of load and generator. During the transmission of the pulses of nanosecond

duration the effect even of the low parasitic reactance, which occur in the simplest constructions/designs of resistive loads, is noticeable. The most successful simple construction/design is washer effective resistance. In this case washer load must be assembled at the end/lead of the coaxial line strictly perpendicular to its axis. In the nanosecond technology, just as in the technology of shf/SVCh, find use conical type load resistors/resistances with the special coating.

During evaluation/estimate qualities of line, intended for transmission of long pulses and following with high frequency, usually are turned to frequency characteristics of steady state. During the evaluation/estimate of the distortions of nanosecond pulses, produced according to the frequency characteristic line with the heterogeneities, which is found in steady state, it is possible to obtain inaccurate results. It is here necessary to consider that the duration of nanosecond pulse can be much less than the transit time of pulse along the line and much less than the spacing between pulses.

Actually, in the case, when pulse duration is less than time of its transmission along line, pulse is propagated in the absence of waves, which appear with multiple reflection from end/lead of line or from internal heterogeneities.

Page 48.

The transmission lines, which have heterogeneities at the ends/leads

and internal heterogeneities, are characterized by the specific phenomena, called "counterflow" and "wake current". These phenomena consist in the fact that after pulse advancing in the line (from its end/lead at the beginning and in the opposite direction) the parasitic oscillations, which are the sum of the pulses, repeatedly reflected from the heterogeneities, are propagated. Parasitic pulse streams manage to attenuate with the large porosity of main impulses, without causing the distortions of the transmitted pulses.

In connection with this quality of line of transmission of nanosecond pulses, which contain heterogeneities, is expedient to evaluate according to pulse transient responses, obtained experimentally on oscillographic installations with the aid of sounding pulse of very short duration (Chapter 11). This installation makes it possible to observe and to measure the pulses echo from the heterogeneities, that gives the possibility to determine also character and the value of heterogeneity and, consequently, also the reflection coefficient. Thus are located the fundamental characteristics of line, according to which it is possible to correctly rate/estimate the distortions of nanosecond pulses.

1.6. THE HELIXES OF TRANSMISSION.

Coaxial and strip transmission lines are sufficiently wide-band systems, since constraint of their passband is associated only with lead loss and dielectrics. However, these lines under the condition

of the absence of the oscillations of the highest types have low wave impedance. Furthermore, delay per unit of length in them is small. Therefore, if the high line characteristic of transmission is required and considerable pulse delay, it is expedient in a number of cases to utilize helixes of transmission.

Most widely used construction/design of helix is spiral conductor that placed within cylindrical screen/shield. Fig. 1.17 shows the cable of delay with the spiral internal conductor.

Page 49.

The distinctive special feature of helix is its considerable linear inductance, which reaches sometimes several millihenry to the meter, which exceeds the inductance of usual coaxial cable into thousands of times.

Presence of spiral causes appearance of longitudinal magnetic field, directed along axis of line; therefore sharply grows/rises overall magnetic field and respectively increases inductance per unit of length. In view of this the helix possesses high wave impedance and large linear delay. Furthermore, changing along the line spiral pitch, it is easy to obtain non-uniform circuit of transmission, which is conveniently utilized for impedance matching at output and input of line, for the transformation of the voltage/stress of pulses.

From theoretical studies of helixes are known expressions for

determining of inductance, capacity/capacitance of line, and also specific phase distortions of line [4, 17-20].

Fundamental parameters and characteristics of helix.

For evaluation/estimate of properties of helixes as transmission systems and delay of nanosecond pulses let us examine their fundamental parameters and characteristics.

Internal spiral conductor can be circular or flat/plane (strip/tape). High-frequency dielectric usually is placed between the spiral and the cylindrical screen/shield. Fig. 1.18 depicts the turn of flat/plane spiral in the expanded/scanned form.

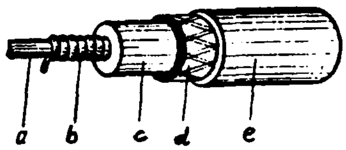

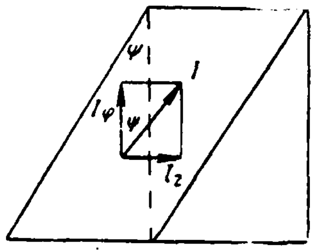

Fig. 1.17. Fig. 1.18.

Fig. 1.17. Cable of delay with internal conductor in the form of spiral: a) central rod; b) internal conductor; c) dielectric; d) external conductor (braid/cover); e) external insulation.

Fig. 1.18. Turn of flat/plane spiral.

Page 50.

Total current of internal wiring I can be decomposed on two components: I_z - axial, directed in parallel to the axis of line, and I_φ - tangential, directed in parallel to tangent toward the circle/circumference of cross section of internal wiring. Component I_z creates transverse magnetic field H_φ, while component I_φ creates longitudinal field H_z. Due to longitudinal field H_z is reached the necessary effect of loading of cable; however, simultaneously occurs an increase in the effective resistance of cable due to the eddy current losses, created in the conductors of cable by field H_z. This increase in the losses, as is known, leads to reduction in the slope/transconductance of the transient response of line and it is a deficiency in the line of transmission of nanosecond pulses.

Total value of linear effective resistance of R, inductance L, of capacity/capacitance of C and conductivities G of helix are determined according to approximations [4]:

$$R = 8{,}35 \cdot 10^{-6} \frac{\sqrt{f}}{d} \left[\frac{\left(\frac{D^2}{d^2} - 1\right)^2 + 0{,}93 d\, D}{(D/d)^2} \right] \mathrm{ctg}^2 \psi \left[\overset{(1)}{\frac{\text{ом}}{\text{м}}} \right], \quad (1.53)$$

$$L = 10^{-7} \frac{(D/d)^2 - 1}{(D/d)^2} \mathrm{ctg}^2 \psi \left[\overset{(2)}{\frac{\text{гн}}{\text{м}}} \right], \quad (1.54)$$

$$C = \frac{10^{-9} \varepsilon}{41{,}4 \lg D/d} \; \overset{(3)}{[\text{ф}/\text{м}]}, \quad (1.55)$$

$$G = \omega C \,\mathrm{tg}\, \delta \left[\overset{(4)}{\frac{1}{\text{ом} \cdot \text{м}}} \right], \quad (1.56)$$

Key: (1). ohm. (2). H. (3). F/M. (4). Ω·m.

where D and d - diameters of external and internal conductors, cm;

φ - angle of ascent of spiral, deg.

Wave impedance of helix is determined by expression

$$\rho = \sqrt{\frac{L}{C}} = \frac{60}{\sqrt{\varepsilon}} \sqrt{\frac{(D/d)^2 - 1}{2\,(D/d)^2} \ln \frac{D}{d} \,\mathrm{ctg}^2 \psi} \; [\text{ом}], \quad (1.57)$$

and delay time per unit of length is equal

$$t_{з0} = \sqrt{LC} = \frac{\sqrt{\varepsilon}}{3 \cdot 10^8} \sqrt{\frac{(D/d)^2 - 1}{2\,(D/d)^2 \ln D/d} \,\mathrm{ctg}^2 \psi}. \quad (1.58)$$

Attenuation of line, as usual, is determined by expression

$$\beta = \beta_п + \beta_д = \frac{R}{2} \sqrt{\frac{C}{L}} + \frac{G}{2} \sqrt{\frac{L}{C}}.$$

Page 51.

Attenuation of cable due to lead loss strongly grows/rises with decrease of helix angle φ. At the preset angle φ attenuation length β_{II} has a minimum with specific relationship D/d. If it is necessary to obtain line with the maximum value of delay t_{30}, then minimum attenuation β_{II} will occur when $\frac{D}{d}=1{,}8$, while if it is necessary to obtain line with the maximum wave impedance, then minimum attenuation will begin when $\frac{D}{d}=2{,}7$.

In the case of applying as internal conductor round conductor attenuation β_{II} will prove to be more than in the case of replacing conductor by flat wire, approximately to 15-25%.

Distortions of pulses during the transmission along the helix.

In helix besides ohmic losses phase distortions, which substantially determine resulting broad-band character of line, have most important value. Phase distortions appear at the high frequencies as a result of change in the inductance with the frequency and effect of distributed capacitance between adjacent turns.

Above were given relationships/ratios, obtained on the assumption that current strength along axis of spiral remains constant/invariable. However, if frequency is so/such high, that the wavelength in the spiral in the axial direction is commensurate with the diameter of spiral, then the value of inductance noticeably decreases. At such current frequencies in different turns of spiral

differ in the phase, total magnetic flux decreases in consequence of which. The mutual inductance of two turns with an increase in the frequency can even change sign. The dependence of inductance on the frequency can be expressed by formula [18]

$$\frac{L}{L_{n}}=2J_{1}\left(\frac{\pi d}{\lambda}\right)K_{1}\left(\frac{\pi d}{\lambda}\right), \qquad (1.59)$$

where L_{n} - inductance at the low frequencies;

$J_1(x)$ and $K_1(x)$ - modified functions of Bessel of the first and second orders;

d - diameter of spiral;

λ - wavelength in the spiral along its axis.

Page 52.

Under condition $\pi d/\lambda<1$ it is possible to write [19]

$$\frac{L}{L_{\text{н}}} \approx 1-25\left(\frac{d}{2\lambda}\right)^2. \qquad (1.60)$$

Delay time of line $t_з$ will also decrease with increase in frequency. Fig. 1.19 for the helix of delay gives the dependence of delay time on the frequency in the form of relation $t_з/t_{зн}$, where $t_{зн}$ - delay time at the low frequencies. Along the axis of abscissas is plotted product $t_з df/l_0$, where l_0 - distance between the turns of the spiral (scale it is obtained in the relative units).

With pulse advancing along helix of delay their form at output of line is determined to larger degree by presence of phase distortions, than amplitude (caused by dependence of attenuation on frequency). Phase distortions are the factor, which limits the transmission of narrow pulses along the line, and can serve as criterion in the evaluation/estimate of the quality of the helix of delay.

It is possible to consider that those high-frequency components are boundary, which cause phase divergence (at given length of line) of 1/2 rad larger than phase divergence, which is obtained from condition of linear phase response [20].

Let us assume that delay time per unit of length $t_{зо}$ at high frequency ω differs from delay time $t_{зн}$ at low frequency. Phase error at the frequency ω at the output of line by length l must not exceed 1/2 it is glad in such a case, when this frequency does not exceed the permissible cut-off frequency. Then, disregarding losses in the effective resistance of line, it is possible to record the equality

$$\omega_{макс} l (t_{зо} - t_{зон}) = \pm 1/2. \qquad (1.61)$$

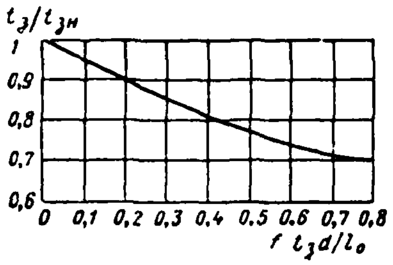

Fig. 1.19. Dependence of delay time on frequency.

Page 53.

Let us assume that capacity/capacitance of C does not depend on frequency, but inductance L in a specific manner depends on frequency and, if one considers that $t_{зо}=\sqrt{LC}$, then expression (1.61) is reduced to the form

$$\omega_{макс} l t_{зон} \left(\sqrt{\frac{L}{L_н}} - 1\right) = \pm 1/2. \qquad (1.62)$$

If change in inductance of line is connected with phenomenon described above, then in formula (1.62) relation $L/L_н$ can be replaced with expression (1.60); then

$$\omega_{макс} t_{зон} \left(\frac{ld^2}{4}\right)^{1/3} \approx 3$$

when

$$\omega_{макс} t_{зон} \frac{d}{2} < 1/2.$$

Hence for frequency $\omega_{макс}$ we obtain following expression:

$$\omega_{\text{макс}} \approx \frac{3}{t_{\text{зон}} l} \left(\frac{2l}{d}\right)^{2/3}. \qquad (1.63)$$

With the aid of formula (1.63) is determined greatest permissible signal frequency during its transmission along line with delay $t_з = t_{з0} l$ with given one to ratios of length of spiral to its diameter. During the transmission of right-angled pulses with a duration of front on the order 30 ns the distortion of front in the form of rounding in the upper part in the case of the delay is observed, beginning with 0.6 μs, which corresponds to the length of line of approximately 3 m.

Use of helixes for pulse delay of nanosecond duration requires improvement in their characteristics. One of the methods of the correction of phase responses is based on the application of series capacitor, which shunts spiral. As a result of correction the effective inductance of line grows/rises with an increase in the frequency.

Line with corrective capacity/capacitance is arranged as follows. Internal insulating rod is covered/coated with the thin conducting layer. This layer is cut along the line by several identical bands. All bands, except one, are grounded.

Page 54.

The ungrounded band is divided into the series/row of plates with the specific gap. Entire conducting layer is covered/coated with the thin

layer of insulation, and then spiral is coiled.

Capacity/capacitance is formed between grounded and ungrounded corrective plates. The value of this shunt capacitance can change via the appropriate selection of width and length of the corrective plates, and also the thickness of insulation. The form of the phase response of delay line can to the known degree be modified in accordance with this. At the high frequencies the delay time increases with the increase of shunt capacitance.

With specific values of frequency is observed mutual compensation for potentials, induced on corrective plate by current, flowing in different turns of spiral. This leads to the appearance of maximums on the frequency characteristic of delay line. The application of the considerable number of corrective plates is necessary for the smoothing of the form of frequency characteristic. The smallest number of plates is determined by expression [2]

$$N = 2t_{30}f_{\text{макс}},$$

where $f_{\text{макс}}$ - maximum frequency, to value of which frequency characteristic is uniform.

Fig. 1.20 gives characteristics of helix of delay ($t_з$=0.9 μs) without correction and with correction (48 corrective plates [21].

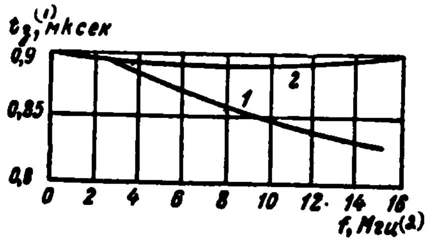

Fig. 1.20. Dependence of delay time on frequency for line: 1 - without correction; 2 - with correction.

Key: (1). μs. (2). MHz.

Page 55.

In general theory of helix of delay with shunt capacitances relationships/ratios for determining optimum values of shunt capacitances and corresponding sizes/dimensions of plates are given.

Let there be between two turns of spiral, which are located at a distance of x from each other, shunt capacitance C'(x). Let us introduce the capacity/capacitance of line per unit of length relative to earth/ground C_0 and we will further examine dependence $C(x)=C'(x)/C_0$. The problem of transit time correction is reduced to the selection of function C(x), which corresponds to the condition of the constancy of the phase speed into Lynn for different frequencies.

Investigations showed that their arrangement, depicted in Fig. 1.21 [21], is one of advisable distributions of plates of shunt capacitance along turns of spiral. For this case function C(x) will be recorded as follows:

$$C(x)=\frac{aC_n}{l_0^2C_0}\left[1-\frac{x}{l_n}\right]=\frac{g}{l_n}\left[1-\frac{x}{l_n}\right], \qquad (1.64)$$

where a - width of the shunting plate;

g - ratio of the total capacitance of spiral relative to the shunting plates to the capacity/capacitance of spiral relative to the earth/ground at the length of spiral, equal to its diameter;

C_n - capacity/capacitance between one turn of spiral and plate;

l_n - length of the shunting plate;

l_0 - spiral pitch.

Controlled parameters of shunting plate are g and l_n.

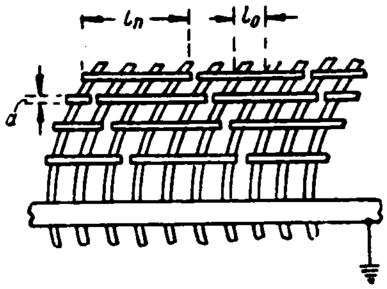

Fig. 1.21. Distribution of shunting plates along spiral.

Page 56.

For the selection of these values it is possible to use plotted function F(z) (Fig. 1.22), which is Fourier transform function C(x). For the selected dependence this function takes the form

$$F(z)=g\left[1-\frac{\sin^2\frac{l_n z}{a}}{(l_n z/a)^2}\right], \tag{1.65}$$

where $z=\frac{\pi f d}{v}$ - phase delay for the section of line by the length, equal to a radius of spiral;

v - phase speed in the line at frequency f.

Change of parameters g and l_n in expression (1.65) scale plotted function F(z) along axis of ordinates and axis of abscissas, where along coordinate axes are plotted values on logarithmic scale [21].

By approaching function F(z) to graph/curve, which corresponds to ideal phase of corrections ($\Delta\varphi_1$=0), are determined parameters of shunting plates at this band of frequencies of transmission of line:

$$f_{\text{макс}} = \frac{z_{\text{макс}}}{\pi d \sqrt{L_{\text{н}} C}}, \qquad (1.66)$$

where $L_{\text{н}}$ - inductance of line per unit of length at low frequency;

$z_{\text{макс}}$ - phase delay at frequency $f_{\text{макс}}$.

With permissible value of phase distortions $\Delta\varphi_1$=0.05 rad ($\Delta\varphi_1$ - phase distortions of section of line by length, equal to its radius) optimum will be values g and $\frac{l_{\text{п}}}{a}$ with their following values:

$$g = 3{,}5 \overset{(1)}{\text{и}} \frac{l_{\text{п}}}{a} = 0{,}55.$$

Key: (1). and.

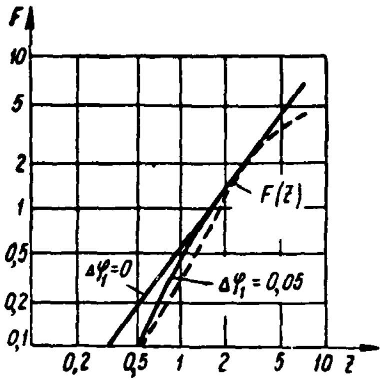

Fig. 1.22. Plotted function F(z).

Page 57.

During calculations of line it is necessary to consider fundamental characteristic of line - product of delay time to bandwidth of line. The delay time of line by length l at low frequencies $t_{зн}=l\sqrt{L_н C}$, and passband is determined by expression (1.66); consequently, the product of delay time to the bandwidth will take form

$$\frac{z_{макс}\Delta\varphi}{2\pi\Delta\varphi_1}. \tag{1.67}$$

Using given formulas and graphs/curves, it is possible to calculate helix of delay for this passband of frequencies when arrangement of shunting plates corresponds to that given in Fig. 1.21.

Studies of helixes of transmission, utilized as lines of delay and transformers of nanosecond pulses [22, 23], show that helixes noticeably distort edge of nanosecond pulse and it is insignificant its apex/vertex. An increase in the duration of the pulse edge is caused by high-frequency distortions, and decay in the apex/vertex -

low-frequency. With an increase in the delay time of line low-frequency distortions decrease, and high-frequency increase. The low-frequency distortions of the shape of pulse are explained by the fact that are transmitted only those components, the wavelength of which is more than the "electrical" length of line. For the pulse duration into several nanoseconds and less decay in the pulse apex proves to be insignificant. Ohmic losses and phase distortions grow/rise with an increase in the frequency. It follows from the experiments that the lead loss of line and dielectric are noticeable for the short duration of the front (order of one nanosecond and less), while phase distortions they are developed also for the duration more than 1 ns.

If for retention/maintaining of edge of pulse of stringent requirements it is not presented, then as line of pulse delay with duration of front in several nanoseconds can be used standard spiral radio-frequency cables of delays, whose data are cited in table 1.3 [4].

Helix of delay usually works in conditions of matched load.

Page 58.

Sometimes at the output helix must be coordinated with usual coaxial cable. A precise agreement of the helix of delay at its output presents definite difficulty. Inductance per unit of length in the helix with the insufficiently good correction falls in the direction

of the end/lead of the line. If reflections are not admitted, then the heterogeneities of circuit must be removed throughout its entire length. For this purpose it is necessary to use special transitions between the helix and the line of another type. In the technology of the electronic devices of shf/SVCh, which use circuits in the form of helix, the constructions/designs of transitions from the helix to usual coaxial cable and to the load are developed. These constructions/designs can be used also in the devices/equipment of nanosecond technology, which use helixes of delay.

1.7. Transient processes in the waveguides during the transmission of nanosecond radio pulses.

At present in series/row of regions of radio electronics radio pulses of nanosecond duration increasingly more are utilized. In waveguide trunk lines of communications, in the ultra-high-speed electronic computers, in the radio systems with the large resolution the nanosecond radio pulses of different duration are used. Radio pulses are very successfully utilized by a duration of 1-5 ns for the investigation of the heterogeneities of different waveguide systems. In connection with this the attention to the study of transient processes in the waveguides for the evaluation/estimate of the distortions of nanosecond radio pulses during their propagation along the waveguides is recently turned.

Table 1.3.

(1) Параметры кабеля	(2) Марка кабеля	
	РК3-400	РК3-401
(3) Волновое сопротивление, ом	350—500	350—500
(4) Затухание, нп/м (при частоте)	0,125 (5) (1 Мгц)	0,5 (5) (10 Мгц)
(6) Время задержки, мксек/м	0,1	0,5

Key: (1). Parameters of cable. (2). Cable make-up. (3). Wave impedance, ohm. (4). Attenuation, np/m (at frequency). (5). ... MHz. (6). Delay time, μs/m.

Page 59.

Specific character of transient processes in waveguides. Distortions of right-angled radio pulses.

Rate of establishment of transient processes, or slope/transconductance of transient response of waveguides as other lines of transmission of nanosecond pulses, is determined by character of frequency dependence of propagation constant $\bar{\gamma}$. But this means that the character of transient processes is defined by both the frequency dependence of attenuation in the waveguide and by its dispersive characteristic. Even in the ideal waveguide the most essential possible distortion of radio pulses due to the specific dispersive properties of waveguide.

Let us examine uniform waveguide, input of which pulse

$$u_1(t) = F_1(t)e^{j\omega_0 t}, \qquad (1.68)$$

where $F_1(t)$ - function, which presents pulse envelope, enters; ω_0 - carrier frequency.

Pulse, which passed along waveguide distance l, is expressed by function $u_2(l, t)$.

If transmission factor of waveguide is determined by expression

$$\overline{K} = e^{-\bar{\gamma} l} = e^{-l(\beta + j\alpha)}, \qquad (1.69)$$

that function $u_2(l, t)$ can be found with the aid of Fourier integral:

$$u_2(l, t) = \frac{1}{2\pi}\int_{-\infty}^{\infty} \overline{S}_1(\omega)e^{j(\omega_0+\omega)t - l\bar{\gamma}}d\omega, \qquad (1.70)$$

where $\overline{S}_1(\omega)$ - spectral function of envelope of launched pulse $u_1(t)$.

In contrast to cases of transmission of video pulses along line examined above, during transmission of radio pulse with carrier frequency ω_0 expressions for components of propagation constant $\bar{\gamma}$, i.e., for β and α, it is possible to approximate by finite number of members of Taylor series.

Page 60.

These values in the frequency region in question vary monotonically and insignificantly, and therefore it is possible to be restricted to the first three terms of the expansion:

$$\beta(\omega_0 + \omega) = \beta_0 + \beta_1\omega + \beta_2\omega^2, \qquad (1.71)$$
$$\alpha(\omega_0 + \omega) = \alpha_0 + \alpha_1\omega + \alpha_2\omega^2, \qquad (1.72)$$

where β_0 and α_0 - values of the decay constant and phase at the carrier frequency ω_0; β_1 α_1 correspond to coefficients in a linear change in the values with the frequency, the derivative $\partial x/\partial\omega$ in particular gives the signal velocity. Coefficients with the quadratic terms will be:

$$\beta_2 = \frac{1}{2}\frac{\partial^2\beta}{\partial\omega^2}\bigg|_{\omega_0},$$

$$\alpha_2 = \frac{1}{2}\frac{\partial^2\alpha}{\partial\omega^2}\bigg|_{\omega_0}.$$

Derivatives of second and higher order must determine signal distortions. Sometimes the above-indicated coefficients can be determined with the approximation of graphs/curves for $\beta(\omega)$ and $\alpha(\omega)$, constructed according to the experimental data.

Let us first examine transmission of carrying oscillation, modulated by function $F_1(t)$, which is single drop/jump in voltage/stress 1(t). Let us record transmission factor in the form of the function of the complex frequency $p=j\omega$, then

$$\hat{K}(p) = e^{-\gamma(p)l} = e^{-l[\beta(p)-j\alpha(p)]}.$$

Let waveguide be ideal (β=0), which has propagation constant, expressed in the form [24]

$$\hat{\gamma}(p) = j\alpha(p) = \frac{1}{c}\sqrt{p^2+\omega_\kappa^2},$$

where ω_κ - critical frequency of waveguide.

Page 61.

For determining signal $u_2(l, t)$ at certain point of waveguide with modulating function in the form of single drop/jump in voltage/stress instead of expression (1.70) it is possible to use integral of Carson [24], who in this case is written/recorded in the form

$$u_2(l,\ t)=\frac{1}{2\pi j}\int\limits_{c_p}\frac{\exp\left[pt-\frac{l}{c}\sqrt{p^2+\omega_\kappa^2}\right]}{p-j\omega_0}\,dp. \qquad (1.73)$$

Here the duct/contour of integration c_p, as it is usually accepted, is passed from $\sigma-j\infty$ to $\sigma+j\infty$, where σ is selected from the conditions of integration on the complex plane; c - wave propagation velocity in the vacuum.

Without bringing asymptotic method of computing integral (1.73), presented into [24], let us record immediately expression for basic part of signal, which proved to be at moment/torque t at a distance l from beginning of waveguide:

$$u_2(l,\ t)\approx\frac{1}{\sqrt{\pi}}\operatorname{erfc}(jb\sqrt{t}), \qquad (1.74)$$

where

$$\operatorname{erfc}(x)=\int\limits_x^\infty e^{-\xi^2}\,d\xi.$$

Here value b is determined by the expression

$$b^2=j\left[-\omega_0+\frac{l}{ct}(\omega_0^2-\omega_\kappa^2)^{1/2}+\omega_\kappa\left(1-\frac{l^2}{c^2t^2}\right)^{1/2}\right]. \qquad (1.75)$$

For high values of argument it is possible to use approximation for erfc(x). Thus, if $b\sqrt{t}$ high value and b (value, which determines the position of the pole of the integrated function on the complex plane) lies/rests above real axis, then

$$u_2(l,\ t)\sim\left(1-\frac{1}{\sqrt{\pi}}\frac{e^{b^2t}}{2jb\sqrt{t}}\right), \qquad (1.76)$$

and if b lies/rests below real axis, then

$$u_2(l,\ t)\sim\frac{1}{\sqrt{\pi}}\frac{e^{-b^2t}}{2b\sqrt{t}}. \qquad (1.77)$$

Page 62.

It follows with modulating function in the form of single drop/jump in voltage/stress from expressions (1.74)- 1.77) that at point of waveguide at a distance l from it it began signal it is absent to moment of time $t_0=\frac{l}{c}$, to arrival of initial slowly increasing part of function $u_2(l,\ t)$. At the moment of time $t_r=\frac{l}{v_r}$, where v_r - the group velocity, signal reaches half of statiorary amplitude, and then it approaches its steady-state value, completing oscillations about this value. The steepness of the front of signal when $t=t_r$ is determined by formula [24]

$$S_{\text{н}}=\sqrt{\frac{\omega_0 c}{2l}}\frac{\omega_0}{\omega}\left[1-\left(\frac{\omega_{\text{к}}}{\omega_0}\right)^2\right]. \qquad (1.78)$$

In particular it is apparent that slope/transconductance $S_{\text{н}}$ is

inversely proportional to square root of length of waveguide.

Fig. 1.23 shows signal amplitude envelope $U_2(l, t)$, constructed depending on product $S_n t_1$, where $t_1 = t - t_r$. It is expedient along the axis of abscissas to plot/deposit product $S_n t_1$, but not value t_1, since graph/curve is universal, suitable for the different waveguides (having different S_n).

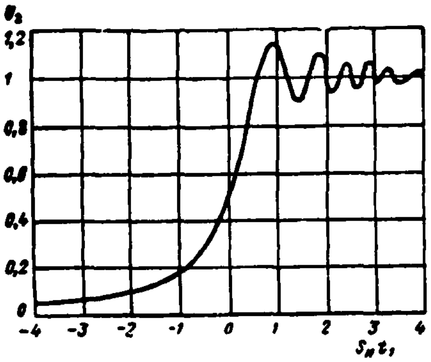

Fig. 1.23. Pulse envelope at waveguide output.

Page 63.

Thus, from case of transmission of signal on ideal waveguide examined it follows that waveform is substantially distorted only due to dispersive properties of waveguide. The steepness of the front of signal decreases, and oscillations are observed at the apex/vertex.

For real waveguide propagation constant $\bar{\gamma}$ is expressed by more complicated dependence and depends on form of waveguide, type of propagated waves, and also on surface impedance of walls $Z_n = R_n + jX_n$, which is function of frequency. In this case the transmitted signal is distorted to a great degree, but general/common waveform $u_2(l, t)$ is close to that shown in Fig. 1.23.

Knowing reaction of waveguide to signal with envelope in the form of function of single drop/jump in voltage/stress (1.74) and using superposition principle, it is possible to find reaction of waveguide

to square pulse by duration $t_и$:

$$u_{t_и}(l,\ t,\ t_и)=u_2(l,\ t)-u_2(l,\ t+t_и). \qquad (1.79)$$

If we use concept of slope/transconductance $S_и$ according to (1.78), then formula (1.74) becomes standardized/normalized complex range of Fresnel from $S_и$ and $t_1=t-t_г$. If at moment/torque t=0 to the input of waveguide (l=0) is given radio pulse with an enveloping in the form of ideal rectangular video pulse duration of $t_и$, and to moment/torque $t_1= l/v_г$ it is observed the front of the radio pulse, which passed distance l along the waveguide, then the envelope of output pulse can be determined by function [24]

$$U_{\text{вых}}(t,\ l,\ t_и)=U_{\text{вых}1}(S_и t,\ S_и t_и).$$

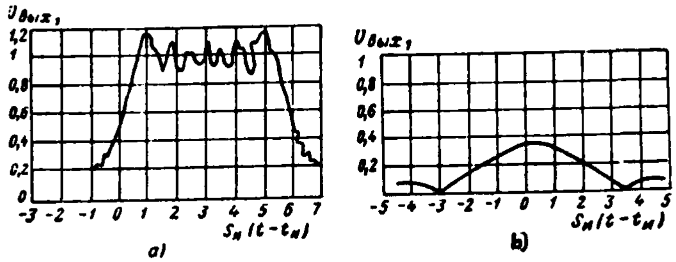

Fig. 1.24. oscillogram of envelope of rectangular radio pulse at waveguide output: a) with $S_н t_н=6$; b) when $S_н t_н=0.4$.

Page 64.

Fig. 1.24 depicts values of function $U_{вых1}$ in dependence on product $S_н(t-t_н)$ for two values of parameter $S_н t_н$, equal to 6 and 0.4. For longer durations of pulses (higher value $S_н t_н$) they to a certain extent retain their initial form, but the slope/transconductance of front and shear/section decreases, and oscillations are observed at the pulse apex. With decrease $S_н t_н$ the pulse noticeably is dilated/extended in the time, testing/experiencing ever larger distortions, approaching in the form a pulse of bell-shaped form with the ghost pulses.

Distortions of the radio pulses of bell-shaped form.

During generation of radio pulses with duration several nanoseconds their real form is close in form to bell-shaped. Therefore is of interest the investigation of transmission on the waveguide of nanosecond radio pulses from the enveloping $F_1(t)$

bell-shaped form. The problem of the determination of the form of output pulse here is solved simpler than [25]. For the pulse of bell-shaped form we have

$$F_1(t)=e^{-nt^2},$$
$$\overline{S}_1(\omega)=\sqrt{\pi/n}\,e^{-\frac{\omega^2}{4n}}. \qquad (1.80)$$

Duration of Gaussian pulse $t_и$ will be further determined at level 0.1 of its amplitude value. Substituting (1.71), (1.72) and (1.80) into formula (1.70), we will obtain initial expression for the form of the output pulse

$$u_2(l,\ t)=\frac{1}{2\sqrt{\pi n}}\int\limits_{-\infty}^{\infty}e^{-\frac{\omega^2}{4n}}e^{j(\omega_0+\omega)t}\times$$
$$\times\{\exp[\beta_0+\beta_1\omega+\beta_2\omega^2+j(\alpha_0+\alpha_1\omega+\alpha_2\omega^2)]\,l\}^{-1}\,d\omega. \quad (1.81)$$

Condition of integrability (1.81) can be recorded as $\beta_2 l$+1/4n>0.

Page 65.

It sets limitation on the maximum value of length l, if β_2 it is negative, expression (1.71) must be correctly only in the specific frequency region, in which must be satisfied the condition

$$\left\{\exp\left[\left(\beta_2 l+\frac{1}{4n}\right)\omega^2+\beta_1\omega l\right]\right\}^{-1}\ll 1.$$

Out of this frequency region components of signal must have very low values. Then integral (1.81) can be calculated [25]. The real part of the obtained expression gives the shape of the unknown pulse:

$$\mathrm{Re}\, u_2(l,\ t_1) = U_2(l,\ t_1)\cos(\Omega t_1 + \xi t_1^2 + \eta), \qquad (1.82)$$

where $t_1 = t - \alpha_1 l = t - \frac{l}{v_{\text{гр}}} = t - t_3$; here t_3 - delay time of pulse, determined by the length of waveguide and by group velocity $v_{\text{гр}}$;

$$U_2(l,\ t_1) = \frac{\exp\left\{\frac{-\beta_0 l + n(1 + 4n\beta_2 l)[\beta_1^2 l^2 - t_1^2] - 8n^2\beta_1\alpha_2 l^2 t_1}{(1 + 4n\beta_2 l)^2 + (4n\alpha_2 l)^2}\right\}}{[(1 + 4n\beta_2 l)^2 + (4n\alpha_2 l)^2]^{1/4}}; \qquad (1.83)$$

$$\Omega = \omega_0 - \frac{2n\beta_1 l(1 + 4n\beta_2 l)}{(1 + 4n\beta_2 l)^2 + (4n\alpha_2 l)^2}; \qquad (1.84)$$

$$\xi = \frac{4n^2\alpha_2 l}{(1 + 4n\beta_2 l)^2 + (4n\alpha_2 l)^2}; \qquad (1.85)$$

$$\eta \approx (\omega_0\alpha_1 - \alpha_0) l - \frac{4n^2\alpha_2\beta_1^2 l^3}{(1 + 4n\beta_2 l)^2 + (4n\alpha_2 l)^2} - \arg[1 + 4n\beta_2 l + j4n\alpha_2 l]. \qquad (1.86)$$

In the case of absence of dispersion and losses in waveguide solution of equation for $u_2(l,\ t)$ give undistorted form of launched pulse:

$$\mathrm{Re}\, u_2(l,\ t_1) = \mathrm{Re}\, u_1(t).$$

It follows from solution (1.82) and expressions (1.83)- (1.86) that pulse $u_2(l,\ t_1)$ has bell-shaped form, but are somewhat sealed, and its maximum is displaced relative to $t_1=0$ (Fig. 1.24b). Furthermore, occurs the frequency modulation of the carrying oscillation, since the instantaneous value of frequency according to (1.82)

$$\omega_0(t_1) = \frac{\partial}{\partial t_1}(\Omega t_1 + \xi t_1^2 + \eta) = \Omega + 2\xi t_1.$$

Page 66.

Although in real waveguide usually occurs simultaneously attenuation and dispersion, during analysis more conveniently to nevertheless examine separately cases of presence only of dispersion (β=0) and only attenuation (α=0).

In first case with β=0 expression (1.82) is simplified and takes form

$$\operatorname{Re} u_2(l, t_1) = \frac{\left[\exp\frac{nt_1^2}{1+(4n\alpha_2 l)^2}\right]^{-1}}{\sqrt[4]{1+(4n\alpha_2 l)^2}} \cos\left[\omega_0 t_1 + \frac{4n^2\alpha_2 l t_1^2}{1+(4n\alpha_2 l)^2} + \right.$$
$$\left. + (\omega_0\alpha_1 - \alpha_0)\, l - \frac{1}{2}\operatorname{arctg}(4n\alpha_2 l)\right]. \qquad (1.87)$$

Value of duration of pulse $t_{\text{н вых}}$ and value of frequency modulation of carrying oscillation is located from this expression. For the Gaussian pulse its duration at level 0.1 of amplitude is determined by the expression

$$t_{\text{н}} = 2\sqrt{\frac{\ln 10}{n}} = 2\sqrt{\frac{2,3}{n}}.$$

Then on the basis of expression (1.87), substituting for n value

$$\frac{n}{1+(4n\alpha_2 l)^2},$$

we obtain expression for duration of pulse, which passed in waveguide distance l:

$$t_{\text{и вых}} = 2\sqrt{\frac{2.3}{n}\left[1+(4n\alpha_2 l)^2\right]} = t_{\text{и}}\sqrt{1+(4n\alpha_2 l)^2}. \quad (1.88)$$

Change in carrier frequency is rated/estimated by expression

$$\frac{\partial\omega_0(t_1)}{\partial t_1} = 2\xi = \frac{8n^2\alpha_2 l}{1+(4n\alpha_2 l)^2}.$$

For case of normal dispersion $\alpha_2<0$, i.e., group velocity increases with increase in frequency. Therefore at the point of reception/procedure the high-frequency components of signal will prove to be earlier than low-frequency constituting.

Fig. 1.25 gives dependences of pulse duration with carrier frequency of 10 GHz from length of waveguide l for different duration of launched pulse $t_{\text{и}}$.

Page 67.

From the figure one can see that most of all changes the pulse duration with an initial duration of $t_{\text{и}}=1$ ns. This pulse to the larger degree is subjected to the frequency modulation of the carrying oscillation, than the pulse of larger duration.

Distortion of pulse can be reduced due to decrease of value α_2. This is achieved, however, by a simultaneous increase in the frequency ω_0, which is limited to the permissible frequency for this waveguide.

In the case of account only of losses, in waveguide (α=0) solution (1.82) takes form

$$\operatorname{Re} u_2(l,\ t_1) = \frac{\exp\left\{\left[\frac{n(\beta_1^2 l^2 - t_1^2)}{1+4n\beta_2 l}\right](-\beta_0 l)\right\}}{\sqrt{1+4n\beta_2 l}} \times$$
$$\times \cos\left[\left(\omega_0 - \frac{2n\beta_1 l}{1+4n\beta_2 l}\right) t_1 + (\omega_0\alpha_1 - \beta_0)\, l\right]. \qquad (1.89)$$

Then for duration of pulse, which passed distance l in waveguide, we obtain expression

$$t_{\text{и вых}} = 2\sqrt{\frac{2,3}{n}(1+4n\beta_2 l)} = t_{\text{и}}\sqrt{1+4n\beta_2 l}. \qquad (1.90)$$

Deviation of carrier frequency will take form

$$\Delta\omega = -\frac{2n\beta_1 l}{1+4n\beta_2 l}.$$

Increase in attenuation with increase in frequency, thus, leads to decrease of carrier frequency and increase in pulse duration.

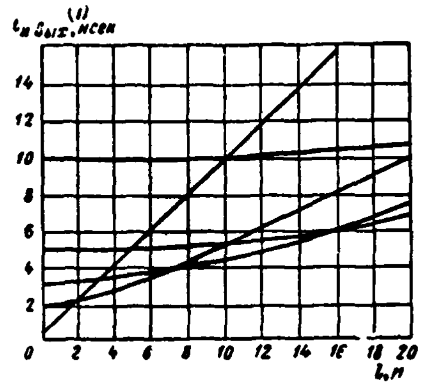

Fig. 1.25. Change of duration of radio pulses in dependence on length of waveguide (carrier frequency of 10 GHz).

Key: (1). ns.

Page 68.

Distortions of radio pulses by line with the transmission factor, determined by the function of Gauss.

Expressions given here make it possible to examine question of distortion of nanosecond pulses of bell-shaped form with passage concerning line, which has transmission factor, determined by expression

$$K(\omega_0+\omega)=e^{-a\omega^2}. \qquad (1.91)$$

This case can occur, for example, during transmission of radio pulse along strip line with very thin metallic strips with continuous dielectric filling. Only the frequency dependence of attenuation in the dielectric here has a value. The value of this attenuation is proportional to the square of frequency, since the loss tangent in dielectric tg δ in the small region high frequencies $\omega_0 \pm \Delta\omega$ grows/rises approximately proportional to frequency, i.e., according to expression (1.38) we will obtain

$$\beta_д = A_1\omega\,\mathrm{tg}\,\delta = A_1\omega a_2\omega = A_2\omega^2,$$

where A_2=const.

Then in expression (1.91) coefficient $a=A_2 l$, where l - length of line.

In this case expression for output pulse $u_2(l, t_1)$ is found from expression (1.89), where it is necessary to assume/set $\beta_0=\beta_1=0$, and $\beta_2 l=a$, i.e., we have

$$\operatorname{Re} u_2(l, t_1)=\frac{\left[\exp\frac{nt_1^2}{1+4na}\right]^{-1}}{\sqrt{1+4na}}\cos\omega_0 t. \qquad (1.92)$$

From (1.92) we find expression for the pulse duration:

$$t_{\text{и вых}}=t_{\text{и}}\sqrt{1+4nA_2 l}. \qquad (1.93)$$

Page 69.

Fig. 1.26 gives dependence of duration of bell-shaped radio pulse from passband of line (band at level 3 dB) in the case of different duration of launched pulse $t_{\text{и}}$.

1.8. NON-UNIFORM CIRCUITS OF TRANSMISSION.

During formation and transformation of nanosecond pulses is found use of line with changing along the length linear parameters. Such non-uniforms circuit can be used also for the transmission of pulses, if it is necessary to simultaneously carry out a correction of their form. For the assigned duration of pulse and degree of a change in its form the necessary length of non-uniform circuit is determined by the special features of its transient response and by the time of the emission of the signal along the line. To different transient

responses of such lines correspond different laws of a change in their wave impedance $\rho_1(X)$. Therefore during the calculation during calculation and use of non-uniforms circuit of transmission it is necessary to know their transient responses under different laws of a change in the wave impedance along the line.

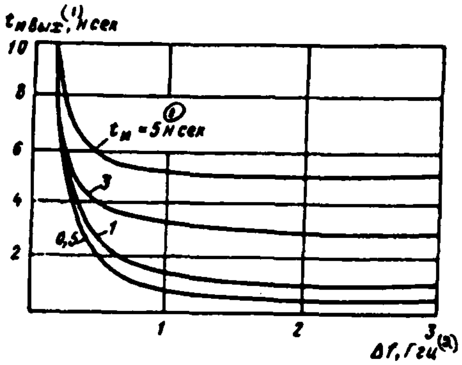

Fig. 126. Change of duration of bell-shaped radio pulse in dependence on passband of strip line.
Key: (1). ns. (2). GHz.

Page 70.

Equations of non-uniform circuit. Undistorted transmission of pulses.

For investigation of transient processes in non-uniform circuit let us examine first equations of heterogeneous zero-loss circuit [26, 27, 28]:

$$-\frac{\partial u}{\partial x}=L(x)\frac{\partial i}{\partial t}, \quad (1.94)$$

$$-\frac{\partial i}{\partial x}=C(x)\frac{\partial u}{\partial t}, \quad (1.94a)$$

where u(x, t) and i(x, t) - instantaneous values of voltage/stress and current,

L(x) and C(x) - linear parameters of line, which are changed with distance of x, calculated off beginning of line.

Wave impedance $\rho_1(x)$ and wave propagation velocity $v(x)$ depend on

coordinate x:

$$\rho_1(x)=\sqrt{\frac{L(x)}{C(x)}},$$
$$v(x)=\frac{1}{\sqrt{L(x)C(x)}}.$$

Let us introduce into equations (1.94) and (1.94a) value $\rho_1(x)$ and $v(x)$, then we obtain equations for voltage/stress and current [28]:

$$\frac{\partial^2 u}{\partial x^2}+\left(\frac{1}{v(x)}\frac{\partial u}{\partial x}-\frac{1}{\rho_1(x)}\frac{\partial \rho_1(x)}{\partial x}\right)\frac{\partial u}{\partial x}-\frac{1}{[v(x)]^2}\frac{\partial^2 u}{\partial t^2}=0, \quad (1.95)$$
$$\frac{\partial^2 i}{\partial x^2}+\left(\frac{1}{v(x)}\frac{\partial i}{\partial x}-\frac{1}{\rho_1(x)}\frac{\partial \rho_1(x)}{\partial x}\right)\frac{\partial i}{\partial x}-\frac{1}{[v(x)]^2}\frac{\partial^2 i}{\partial t^2}=0. \quad (1.95a)$$

Let us introduce delay factor of line

$$\tau=\int_0^x \sqrt{L(\xi)\cdot C(\xi)}\,d\xi \qquad (1.96)$$

and let us designate line characteristic in function τ through ;pю(τ). Then, after using to (1.95) and (1.95a) the Laplace transform, we obtain equations in the operational form:

$$\frac{d^2\hat{u}(p)}{d\tau^2}-\frac{1}{\rho(\tau)}\frac{d\rho(\tau)}{d\tau}\frac{d\hat{u}(p)}{d\tau}-p^2\hat{u}(p)=0, \qquad (1.97)$$
$$\frac{d^2\hat{i}(p)}{d\tau^2}-\frac{1}{\rho(\tau)}\frac{d\rho(\tau)}{d\tau}\frac{d\hat{i}(p)}{d\tau}-p^2\hat{i}(p)=0. \qquad (1.97a)$$

Page 71.

For convenience we further use recording

$$\rho(\tau)=\rho,\ U_н=\frac{u}{\sqrt{\rho(\tau)/\rho(0)}},\ U_н(p)=\hat{U}_н,$$
$$I_н=\sqrt{\rho(\tau)/\rho(0)}\,i,\ I_н(p)=\hat{I}_н,$$

where $\hat{U}_\kappa$ and $\hat{I}_\kappa$ - normalized values u and i.

Then equations are reduced to the form:

$$\frac{d^2\hat{U}_\kappa}{d\tau^2}-p^2\hat{U}_\kappa=\varphi\hat{U}_\kappa, \qquad (1.98)$$

$$\frac{d^2\hat{I}_\kappa}{d\tau^2}-p^2\hat{I}_\kappa=\psi\hat{I}_\kappa, \qquad (1.98a)$$

where

$$\varphi(\tau)=\left(\frac{1}{2\rho}\frac{d\rho}{d\tau}\right)^2-\frac{d}{d\tau}\left(\frac{1}{2\rho}\frac{d\rho}{d\tau}\right)=N^2-\frac{dN}{d\tau}, \qquad (1.99)$$

$$\psi(\tau)=\left(\frac{1}{2\rho}\frac{d\rho}{d\tau}\right)^2+\frac{d}{d\tau}\left(\frac{1}{2\rho}\frac{d\rho}{d\tau}\right)=N^2+\frac{dN}{d\tau}. \qquad (1.99a)$$

Here value N is called function of drop/jump [28] and characterizes rate of change of transformation ratio of wave front along line.

Equations (1.98) and (1.98a) with arbitrary φ (τ) and ψ (τ) are not integrated in final form and can be solved by approximation methods. Only in the case of the exponential law of a change of parameters L(x) and C(x), when N=const, is located a strict solution of the equations [29] indicated.

Let us examine first equation (1.98) for case φ=0. Its solution in this case takes the form

$$\hat{U}_\kappa=A_1e^{-p\tau}+A_2e^{p\tau},$$

where A_1 and A_2 - integration constant.

In the case of infinitely long line $A_2=0$. If at the input of line operates the pulse of the voltage, whose operational image $\hat{U}_1(p)$, and internal resistor/resistance of pulse generator is equal to zero, then

$$\hat{U} = \hat{U}_1(p)\,e^{-p\tau}.$$

Page 72.

In this case during propagation of pulse along line form of its initial voltage/stress is retained. From the condition $\varphi=0$ we have

$$\left(\frac{1}{2\rho}\frac{d\rho}{d\tau}\right)^2 - \frac{d}{d\tau}\left(\frac{1}{2\rho}\frac{d\rho}{d\tau}\right) = 0,$$

whence we find the law of a change in the wave impedance of this nondistorting line [28]:

$$\rho(\tau) = \rho(0)\frac{B^2}{(B+\tau)^2}. \qquad (1.100)$$

Integration constant B here characterizes rate of change in line characteristic along its length. The line, whose wave impedance changes according to formula (1.100), is called hyperbole trace. With any positive and final B with an increase in the delay τ wave impedance decreases, and consequently, decreases the voltage/stress of output pulse.

Supplying on input of this line single drop/jump in voltage/stress $u_1(t)=1(t)$, it is easy to find its transient response:

$$u=\frac{B}{B+\tau}1(t-\tau). \qquad (1.101)$$

If we take hyperbole trace of finite length l_1, loaded to resistor/resistance, equal to input resistance of missing part of line ($l \geq l_1$), then this line also must be nondistorting. For this let us find current in hyperbole trace of infinite length under the influence on its input of a single drop/jump in the voltage/stress. According to (1.94) and (1.94a) for the present instance it is possible to find

$$i=\frac{B+t}{\rho(0)B}1(t-\tau).$$

Then line impedance for any value τ_1 (i.e. for any length of line l_1) is determined by expression

$$\hat{Z}_{вх}(\tau_1)=\frac{\rho(\tau_1)(B+\tau_1)\rho(\tau_1)p}{\rho(\tau_1)+p(B+\tau_1)\rho(\tau_1)}. \qquad (1.102)$$

Page 73.

This input resistance can be represented as parallel connection of active $\rho(\tau_1)$ and inductive $p(B+\tau_1)\rho(\tau_1)$ resistors/resistances.

Thus, if line with length l_1 is loaded to this resistor/resistance, then pulse of voltage $u_1(t)$ will be transmitted

along line without distortion of its form, but with reduced amplitude. Analogously it is possible to show [29] that the line of infinite length with the parabolic law of a change in the wave impedance ρ (τ) does not distort the form of the current pulse, transmitted along this line.

Nondistorting non-uniform circuit examined has such properties when pulse generator, connected at input of line, has internal resistor/resistance, equal to zero.

Non-uniform circuits with the smoothly changing parameters. The transient responses of lines.

As noted above, non-uniforms circuit are utilized for formation and transformation of nanosecond pulses. In connection with this appears the task of determining the law of a change in the line characteristic with the given ones the internal resistor/resistance of generator and the load resistance/resistor, and also the task of determining the transient response of line. In the general case this task is complicated, and therefore is proposed the series/row of the approximation methods of the study of non-uniforms circuit, and also their synthesis [27, 30].

If parameters of line change copper-feudatory with increase in its length, then for solving equation (1.98) it can be, in particular, is used small parameter method. Equation (1.98) in this case is

written/recorded in the form

$$\frac{d^2\hat{U}_\kappa}{d\tau^2} - p^2\hat{U}_\kappa = \mu\varphi\hat{U}_\kappa, \qquad (1.103)$$

where when φ is a factor - low parameter μ.

Let us represent solution of this equation in the form of series/row from low parameter μ:

$$\hat{U}_\kappa = \hat{U}_{0\kappa} + \mu\hat{U}_{1\kappa} + \mu^2\hat{U}_{2\kappa} + \dots$$

Page 74.

After substituting this expression in (1.103), we will obtain system of differential equations:

$$\begin{aligned}
&\frac{d^2\hat{U}_{0\kappa}}{d\tau^2} - p^2\hat{U}_{0\kappa} = 0,\\
&\frac{d^2\hat{U}_{1\kappa}}{d\tau^2} - p^2\hat{U}_{1\kappa} = \varphi\hat{U}_{0\kappa},\\
&\dots\dots\dots\dots\\
&\dots\dots\dots\dots\\
&\frac{d^2\hat{U}_{n\kappa}}{d\tau^2} - p^2\frac{d\hat{U}_{n\kappa}}{d\tau} = \varphi\hat{U}_{n-1,\kappa}.
\end{aligned}$$

Solution of these equations can be represented in the form

$$\begin{aligned}
&\hat{U}_{0\kappa} = A_0 e^{-p\tau} + A_0 e^{p\tau},\\
&\hat{U}_{n\kappa} = \frac{e^{-p\tau}}{2p}\int_\tau^\infty \varphi(y)\hat{U}_{n-1}(y)e^{py}dy -\\
&- \frac{e^{p\tau}}{2p}\int_\tau^\infty \varphi(y)\hat{U}_{n-1,\kappa}(y)e^{-py}dy + A_n e^{-p\tau} + A_{nn}e^{py},\\
&\dots\dots\dots\dots\dots\dots\dots\dots
\end{aligned}$$

Here integration constant are determined from boundary conditions. On the basis of the obtained solution it is possible to find the transient response of the infinitely long line, when the internal resistor/resistance of pulse generator is equal to zero. Here they will be boundary conditions

$$\hat{U}_{\kappa}(0)=1, \quad \hat{U}_{\kappa}(\infty)=0.$$

After determining integration constant, after conversions and transition from image of function to its original it is possible to obtain [28]

$$U_{\kappa} \approx 1-\int_0^t \int_0^{\tau} \varphi(y+\xi)\, dy d\xi. \qquad (1.104)$$

Page 75.

On the basis of expression for transient response of heterogeneous infinitely long line (1.104) it is possible to determine function $\varphi(\tau)$, with which voltage/stress changes according to assigned law. Let the delay of line be equal to one ($\tau=1$). As a result of differentiation of expression (1.104) twice on t is obtained difference equation relative to $\varphi(t)$:

$$\varphi(t)-\varphi(1+t)=\frac{d^2U_{\kappa}(t)}{dt^2},$$

solution of which takes the form

$$\varphi(t)=-\sum_{n=0}^{\infty}\frac{B_n}{n!}U_{\kappa}^{n+1}(t), \qquad (1.105)$$

where B_n - Bernoulli number.

If it is necessary to obtain non-uniform circuit with desired transient response, assigned by law of change in voltage/stress $U_n(t)$, then from (1.105) it is necessary to find function φ(t), and from it according to (1.99) - law of change in line characteristic $\rho(\tau)$.

Let it be, for example, desirable to have transient response of line, when voltage/stress $u_1(t)$ changes according to the law

$$u_1(t) = 1 + kt,$$

where k=const. This line is necessary for the correction of the flat/plane part of the input pulse, which is changed exponentially, i.e., when

$$u(t) = E\,e^{-kt}.$$

It is possible to ascertain that with the aid of Duhamel integral output potential of this line will be actually constant value:

$$u_{\text{вых}}(t) = u_1(0)\,u(t) + \int_0^t \frac{d}{dt}[u_1(t-\xi)]\,u(\xi)\,d\xi =$$

$$= E\,e^{-kt} + \int_0^t kE\,e^{-k\xi}\,d\xi = E.$$

According to (1.105) we determine φ=-k, or on the basis (1.99) we have

$$\left(\frac{1}{2\rho}\frac{d\rho}{d\tau}\right)^2 - \frac{d}{d\tau}\left(\frac{1}{2\rho}\frac{d\rho}{d\tau}\right) = -k.$$

Page 76.

Assume as second example it is required to obtain line, which possesses characteristic $u_1(t)=1(t)$, i.e., not distorting transmitted signals. From (1.105) we determine $\varphi(t)=0$ and according to (1.99) we find

$$\rho(\tau)=\rho(0)\frac{B^2}{(B+\tau)^2},$$

i.e. we obtain expression (1.100) for hyperbole trace.

Is of considerable practical interest determination of form of non-uniform circuit, which works under matching condition at input with internal resistor/resistance of generator $R_i=\rho(0)$ and at output with resistance/resistor of load of $R_u=\rho(\tau_3)$. The optimum law of a change in the wave impedance is determined from the solution of variational problem relative to the function of drop/jump N, i.e., rate of change in the heterogeneity along the line. As is known [28], the solution of problem proves to be condition $N=k_1=\text{const}$.

Hence it follows that line characteristic changes exponentially

$$\rho=\rho(0)e^{k_1\tau}. \qquad (1.106)$$

After determining values N and ρ, it is possible then on the

basis (1.104) to find expression for transient response of infinitely long exponential line:

$$u_1 = 1 - \frac{1}{2}\left(k_1 + \frac{k_1^2}{2}\right)t + \frac{k_1^2 t^2}{8}. \qquad (1.107)$$

Transient response of exponential line is given in Fig. 1.27.

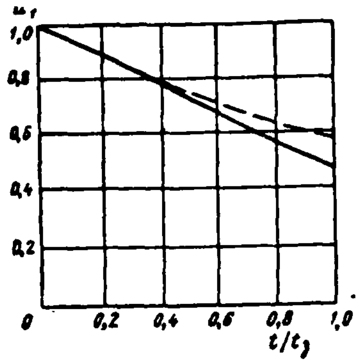

Fig. 1.27. Transient response of exponential transmission line in dependence on delay time of line, calculated: ---- according to precise formulas; —— according to approximations.

Page 77.

Dotted line showed the course of the transient response, expression for which is obtained as a result of the exact solution of the equation of exponential line [29].

Exponential line.

Exponential lines find wide application in nanosecond pulse technique as equalizers and distributed transformers. This line has an inductance and a capacitance per unit length, which change along the line according to the law

$$L(x)=L_0e^{kx},\ C(x)=C_0e^{-kx},$$

where k - positive or negative constant.

Line characteristic can be recorded in the form

$$\rho=\sqrt{\frac{L_0}{C_0}}\,e^{kx}=\rho(0)\,e^{kx}.$$

Delay time per unit of length of line remains constant/invariable and is determined by expression

$$t_{30}=\sqrt{L(x)C(x)}=\sqrt{L_0C_0}. \qquad (1.108)$$

Consequently, expression for wave impedance can be recorded thus:

$$\rho=\rho(0)\,e^{\frac{k\tau}{t_{30}}}, \qquad (1.109)$$

where τ is determined by expression (1.96).

We will obtain equations of exponential line, if into equations (1.97) and (1.97a) we substitute value ρ from (1.109). Then

$$\frac{1}{p^2}\frac{d^2\hat{u}}{d\tau^2}-\frac{k}{p^2t_{30}}\frac{d\hat{u}}{d\tau}-\hat{u}=0, \qquad (1.110)$$

$$\frac{1}{p^2}\frac{d^2\hat{i}}{d\tau^2}-\frac{k}{p^2t_{30}}\frac{d\hat{i}}{d\tau}-\hat{i}=0. \qquad (1.110a)$$

Solution of equation (1.110) in general form can be recorded as sum of waves: wave $\hat{u}_a(\tau)$, propagated from beginning line (x=0) to its end/lead, and wave $\hat{u}_b(\tau)$, which is propagated in opposite direction, i.e., we have

$$\hat{u}(\tau)=\hat{u}_a(\tau)+\hat{u}_b(\tau).$$

Page 78.

Expressions for these take form

$$\hat{u}_a(\tau) = \hat{u}_a(0)\exp\left[\frac{\tau}{t_{30}}(k/2-q)\right], \qquad (1.111)$$

$$\hat{u}_b(\tau) = \hat{u}_b(0)\exp\left[\frac{\tau}{t_{30}}\left(\frac{k}{2}+q\right)\right], \qquad (1.111a)$$

where $u_a(0)$ and $u_b(0)$ - integration constant, and q is determined by expression

$$q = +\sqrt{p^2t_{30}^2 + \frac{k^2}{4}} \approx pt_{30} + \frac{k^2}{8pt_{30}}.$$

Hence expressions (1.111) and (1.111a) approximately will be recorded in the form

$$\hat{u}_a(\tau) = \hat{u}_a(0)\ e^{\frac{k\tau}{2t_{30}}}\ e^{-p\tau}\left(1 - \frac{k^2\tau}{8pt_{30}^2}\right), \qquad (1.112)$$

$$\hat{u}_b(\tau) = \hat{u}_b(0)\ e^{\frac{k\tau}{2t_{30}}}\ e^{p\tau}\left(1 + \frac{k^2\tau}{8pt_{30}^2}\right), \qquad (1.112a)$$

where by members of higher order relative to 1/p how the first, we here disregard.

It is evident from expression (1.112) that constant $u_a(0)$ (i.e. $u_a(\tau)$ with $x=\tau=0$) is amplitude of voltage/stress in the beginning of line. Factor $e^{-p\tau}$ indicates the motion of wave along the line with the delay τ. The second member of expression (1.112) determines the distortion of pulse due to the reduction of his amplitude on the value, proportional to integral on the time of input pulse $\hat{u}(0)$.

If to input of line is given single square pulse by duration $t_и$, then with its passage along line pulse apex will change according to linear law on value, determined by term $k^2 t_и / 8 t_{з0}$.

Exact expression of solution (1.111) shows that change in pulse apex during its propagation along line differs somewhat from linear dependence, which follows from Fig. 1.27.

Page 79.

Transient response of line with the losses.

Losses in non-uniform circuit were not considered in all cases examined above. However, in the nanosecond range for the evaluation/estimate of the distortions of pulses (especially their front and of shear/section) it is desirable to consider losses.

Effect of total losses in non-uniform circuit to its transient response to consider difficultly. This problem is approximately solved only for the case of losses only in the conductors of line [31]. For the determination of transient response in this case it is necessary to solve the generalized equation of non-uniform circuit taking into account the impedance, caused by surface effect in the conductors. This resistor/resistance is represented in the same form, as in the case of uniform line; however, here its value per unit of length depends on distance along the line.

Transient response of non-uniform circuit with losses differs from characteristic of zero-loss circuit by fact that frontal part of characteristic increases according to the law, determined by function

$$A(t_1, l) = 1 - \Phi\left(\frac{\xi}{2\sqrt{t_1}}\right),$$

where $\Phi(\xi/2\sqrt{t_1})$ - function of Kramp;

$$\xi = -\frac{1}{2}\int_0^{x_2} \eta(x)\sqrt{\frac{C(x)}{L(x)}}\,dx,$$

where $\eta(x)$ - coefficient of surface effect in conductors;

C(x) and L(x) - linear capacity/capacitance and inductance;

x_2 - distance at point of line in question, calculated off its beginning;

$t_1 = t - \frac{x_2}{v} = t - t_3$; t_3 - delay time.

Furthermore, decay in flat/plane part of characteristic occurs on somewhat different law, than in characteristic of zero-loss circuit. During the transmission of pulses with duration about 1 ns decay in its apex/vertex, as in the case of zero-loss circuit, it is insignificant. However, the distortions of the edge of pulse (decrease of its slope/transconductance) in non-uniform circuit it is just as noticeable as in the uniform line of transmission, upon consideration of losses only into the conductor.

Page 80.

CHAPTER TWO.

TRANSIENT PROCESSES IN TRANSMISSION LINES WITH THE DISCRETE/DIGITAL HETEROGENEITIES. TRANSFORMATION OF PULSES.

2.1. SPECIAL FEATURES OF TRANSMISSION OF PULSES IN DISTRIBUTED SYSTEMS WITH DISCRETE/DIGITAL HETEROGENEITIES.

In first chapter was examined question about transmission of pulses of nanosecond duration along such distributed systems as coaxial cables, strip lines, etc. It was shown that unavoidable losses in the metal and the dielectric it leads to the distortion of the shape of pulses. However, the source of the distortions of pulses in the transmission lines can be heterogeneities at the ends/leads of the line or at any point of it. These heterogeneities are caused by the insufficiently good agreement of line with the load or with other lines. Furthermore, in a number of cases of line they are specially made by heterogeneous, since heterogeneities in them it is in principle necessary for the normal functioning of system (stepped transformers, traveling-wave amplifiers, etc.). Heterogeneities in the transmission line do not always lead to the distortions of the shape of pulses. In order to explain this fact, let us examine the condition for the undistorted transmission of pulses.

It is known from theory of transmission of signals that undistorted transmission is possible when modulus of complex transmission factor of system is equal to constant value, and argument is linear function of frequency:

$$K(\omega) = K_0,$$
$$\varphi(\omega) = -t_3\omega. \qquad (2.1)$$

Page 81.

In temporary/time aspect condition for undistorted transmission is formulated as follows: transient response of nondistorting system must take form of unit function, multiplied by value K_0 and displaced to the right to period t_3, which represents delay time of oscillation with passage along system:

$$A(t) = K_0 1(t - t_3). \qquad (2.2)$$

We will consider it that very transmission lines are ideal, i.e., not contributing distortions, and that all distortions of pulses are caused by presence of discrete/digital heterogeneities. In this case it is possible to show that for the pulses, the repetition period of which is much more than their duration $(T \gg t_u)$, the conditions for the undistorted transmission, formulated above, are sufficient, but not necessary.

Pulse signal is function of limited extent. This means that conditions (2.1) or (2.2) must be fulfilled only in the limited

period, equal to the duration of the converted oscillation, and can not be fulfilled at the later moments of time. Thus, the condition for the undistorted transmission can be formulated in the form

$$A(t)=K_{0}1(t-t_{3}) \quad t_{3}\leqslant t\leqslant t_{3}+t_{\text{и}}. \tag{2.3}$$

It is not difficult to see that facilitation of conditions for undistorted transmission significantly expands class of linear systems, suitable for converting oscillations without change in their form. For example, the linear network, which satisfies condition (2.2), is the uniform long line, loaded to the wave impedance. The realization of this system meets large difficulties due to the need of guaranteeing the constancy of the load resistance/resistor in the very wide frequency band, which stretches to ones and even to tens of gigahertz.

Account of final and, more precise speaking, for very short pulse duration makes it possible in many instances to forego agreement of line with load.

Page 82.

For the pulse with duration $t_{\text{и}}$ even the mismatched line is ideal, i.e., not distorting, by quadrupole, if only travel time along the line is not less than half of the pulse duration.

In microsecond range of pulse durations satisfaction of condition $t_{\text{и}}\leqslant t_{3}$ (t_{3} - doubled time of landing run of pulse along line) is

hindered/hampered by fact that it requires application of lines of large length. In the nanosecond range the necessary lengths of lines are structurally acceptable. (For example, during the use of cable PK-75-4-15 with the delay 5 ns/m the required length of cable for the undistorted transmission of pulses by the duration of 1 ns is approximately 10 cm.) The account of the final pulse duration makes it possible not only to facilitate the task of the agreement of lines, but also opens/discloses the possibilities of designing of systems with the discrete/digital heterogeneities, in which precisely the presence of heterogeneities creates the desired effect of conversion (transformation, inversion, amplification, etc.) and at the same time does not lead to the distortions of the shape of pulse.

2.2. CONCEPT ABOUT LOOP CIRCUITS.

Any radio engineering device/equipment can be considered as certain set, elements of which are its blocks, either assemblies or parts, or even infinitesimal sections/segments of conductors. The elements of the construction/design of device/equipment not necessarily must be elements of set; the voltages/stresses between any points or currents in the separate branches can be also them. All elements of the set, which composes radio engineering device/equipment, are located between themselves in the specific connections/communications. These connections/communications are created from the set of the elements of the system of elements.

As a rule, any two elements of system are connected with bilateral internal connection. A change in the value of the first element (as which it can be accepted, for example, input voltage) produces a change in the value of the second element (for example, output voltage/stress); in turn, a change in the size of the second element produces a change in the value of the first element, etc.

Page 83.

Together with the elements, which are found in the two-way communication, are elements, connected with one-way communication (this connection/communication it is called also directed). Following M. S. Neumann [32], we will call the system of elements, which are found in the two-way communication, ring, and the system of elements, which are located in one-way communication, by the broken circuit or simply by circuit.

In present section are examined some properties of rings, whose knowledge is necessary for understanding of work of distributed systems with discrete/digital heterogeneities, such, as stepped transformers, transformers and inverters, formed by cable segments, traveling-wave amplifiers and other devices/equipment. All distributed systems with the discrete/digital heterogeneities are rings. Simple ring forms the uniform line, not matched in the beginning and at the end/lead. The connection/communication between the voltages/stresses on its input and output appears due to the reflection of waves from the beginning and the end/lead of the line.

The lines, which have heterogeneities halfway, such, as stepped transformer, the traveling-wave amplifier, etc., are the complex system of the intersected rings, called subsequently in abbreviated form loop circuit.

In subsequent chapters it will be shown also, that rings are all devices/equipment with feedback; circular mechanism is inherent in elements with negative resistance. Therefore the examination of the general/common properties of loop circuits is of considerable interest for the nanosecond pulse technique.

Let us pause first at processes, which occur in single ring, i.e., ring, formed by two elements. In it there are two communication channels: by the straight line, by which is transmitted the effect of the first element on the second, and the reverse/inverse, on which gives self up the effect of the second element on the first. Ring differs from the broken circuit in terms of the fact that in it is certain locked internal circuit, formed by the series-connected channels of straight line and reverse/inverse supply. The characteristics of the rings, which define its behavior in external circuit, in which it is included, they depend substantially on the processes, which occur in its internal circuit, and appear as the reflection of these processes.

In present section we will assume that channels of straight line and reverse/inverse supply are characterized by linear integral

operators A_K and A_B respectively.

Page 84.

The integral character of linear operators is caused by the limitedness of the bandwidth of communications. When the bandwidth of communications can be considered unlimited, linear transformations no longer carry integral character.

Second special feature of communication channels consists in the fact that effect of one element on another is transmitted by them not instantly, but for a certain period of time called time lag. In the systems with the distributed constants this time lag is caused by the final velocity of propagation of oscillations, while in the systems with the concentrated constants, in which there is no true time lag of oscillations, by the specific distortions of the shape of the transmitted pulses, which create the effect, which reminds the effect of time lag.

We will call process of converting oscillation loop circuit by circular process of conversion. In general form the circular process of conversion consists of the following. The converted voltage/stress u_0 enters the input of system. With the aid of the connection/communication, which exists between the input of system A and its output B, the voltage/stress indicated is transmitted from A to B, undergoing a certain conversion in the channel of direct feed. Output potential of system B changes; this change is characterized by

value $A_K u_0$, where A_K - operator, who presents the process of conversion, which is realized above the input voltage in the channel of direct feed. The presence of feedback - from B to A - leads to the fact that the voltage/stress at point A again changes and this change is characterized by value $A_K A_B u_0$, where A_B - operator, who presents the process of conversion, completed above the oscillation during the transmission from B to A. input oscillation completed complete cycle on locked internal circuit of ring.

Process of circular conversion is theoretically process with infinite number of repetition of operations. After completing one cycle on internal circuit of ring, input oscillation completes then the second cycle, the third, the fourth, etc. With respect to this a change in the voltage/stress at point A is characterized consecutively/serially by values u_0; $A_K A_B u_0$; $A_K^2 A_B^2 u_0$; ..., where the degree of operator shows the number of repetitions of the operation of conversion.

Page 85.

In exactly the same manner voltage/stress at point B equal to the sum of disturbances/perturbations $A_K u_0$; $A_K^2 A_B u_0$; $A_K^3 A_B^2 u_0$; ..., so that total variation in the voltage/stress at point B

$$u_B = \sum_{n=1}^{\infty} A_K^n A_B^{n-1} u_0,$$

moreover A_B^0 is an operator of multiplication by one.

It is easy to see that u_B is solution of operational equation

$$u_B - A_K A_B u_B = A_K u_0. \tag{2.4}$$

Since A_K and A_B is linear integral operators, (2.4) - linear integral equation of Volterra of 2nd order. The solution of equation is convenient to represent in the form

$$u_B = A_K u_0 + \sum_{n=1}^{\infty} A_K^{n+1} A_B^n u_0. \tag{2.5}$$

First member of expression (2.5) is fundamental oscillation, i.e., oscillation, devoted from input of ring to his output and converted in channel of direct feed. For the majority of the systems, intended for the undistorted conversion of oscillations, precisely, this term in (2.5) gives the efficiency of conversion. Second term, which is the sum of the infinite series of components, is caused by the presence of feedback in the system. This oscillation accompanies fundamental oscillation and in communication equipment are called "wake current" [33].

Special feature of distributed systems with discrete/digital heterogeneities is the fact that they possess true time lag. Because of this all components of series/row (2.5) prove to be displaced along the time axis. If the duration of converted oscillation $A_K u_0$ is sufficiently short, i.e., it is less than the time by which lag the components of series/row (2.5), then the action of wake current will be begun after the passage of fundamental oscillation and system will

prove to be satisfying condition undistorted transmission (2.3). It must be noted that wake current is not always undesirable phenomenon.

Page 86.

In the series/row of devices/equipment it is utilized for an increase in the amplitude of oscillations, for converting of the oscillations and other targets.

Linear ring can be represented by functional diagram, shown in Fig. 2.1. This diagram consists of four blocks. In block 1 with the positive sign of feedback is conducted the addition of input voltage and recurrent, that enters from the channel of feedback, and their subtraction occurs with the negative sign of feedback. Block 2 is the unipolar or directed element with the transmission factor m(m<1). This element does not introduce distortions into the form of the transmitted oscillation and does not change its polarity. The directed element does not pass oscillations from the output of system to the input besides the channel of reverse/inverse supply. The transmission factor of this element is a modulus of the complex transmission gain on internal circuit of ring on the medium frequencies, which does not affect the action of the reactive/jet network elements. Block 3 is filter. It is assumed that it considers the action of all reactive/jet circuit parameters, including delay line, that limit the passband of device/equipment. Ideal delay line (block 4) possesses delay time $t_з$. Its idealization lies in the fact that it possesses neither attenuation nor dispersion.

Systems with distributed parameters can be represented by the same functional diagram. As noted, the first node of functional diagram determines the sign of feedback.

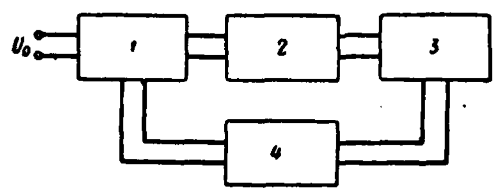

Fig. 2.1. Functional diagram of single ring: 1 - summator; 2 - directed element; 3 - filter; 4 - delay line.

Page 87.

In the system with the distributed parameters, not matched on the ends/leads and presenting single ring, sign of feedback it is determined by the sign of the product of reflection coefficients from the ends/leads of the line at the medium frequencies, which does not affect the action of the reactances of loads. Feedback will be positive, if reflection coefficients will have identical signs, and negative, if the signs of reflection coefficients will be different. The directed element of functional diagram determines the value of feedback. In the distributed system without the losses the factor of feedback is equal to the product of the moduli of complex reflection coefficients from the ends/leads of the line at the medium frequencies. The complex transmission factor of filter for the distributed systems is equal to the product of complex reflection coefficients from the ends/leads of the line, divided into the factor of feedback. Delay time in the delay line is equal to doubled time of landing run of oscillation along the distributed system.

Let us examine transient processes, which occur in single ring during the supplying to its input of single drop/jump in voltage/stress. For this we will use formula (2.5), which let us rewrite in the form

$$u_B = A_K \sum_{n=1}^{\infty} R^{n-1} u_0, \qquad (2.6)$$

where $R = A_K A_B$ - operator of internal circuit of ring.

Let us assume that u_0 is harmonic oscillation, then R will be complex transmission factor of internal circuit of ring, and A_K - complex coefficient of channel of direct feed. It is easy to see that

$$A_K = (1+\bar{p}_2)\, e^{-\frac{1}{2} j\omega t_s}, \qquad (2.7)$$

$$R = \bar{p}_1 \bar{p}_2\, e^{-j\omega t_s}, \qquad (2.8)$$

where $\bar{p}_1$ - complex reflection coefficient from the left end/lead of the line;

$\bar{p}_2$ - from right end of line.

Substituting expression (2.7) and (2.8) in (2.6), we will obtain

$$u_B = (1+\bar{p}_2) \sum_{n=1}^{\infty} (\bar{p}_1 \bar{p}_2)^{n-1}\, e^{-j\omega (n-1/2) t_s}\, u_0.$$

Page 88.

Let us turn first to case, when reflection coefficients are real. Then

$$u_B = K_0 \sum_{n=1}^{\infty} m^{n-1} e^{-j\omega (n-1/2) t_3} u_0, \qquad (2.9)$$

where $K_0=1+p_2$, $m=p_1p_2$.

If we assume that u_0 is spectral function of single drop/jump in voltage/stress, then u_B will be spectral function of transient response of ring. Using to expression (2.9) inverse transformation of Fourier, we will obtain the equation of the transient response of the ring

$$A(t) = K_0 \sum_{n=1}^{\infty} m^{n-1} 1 [t-(n-1/2) t_3]. \qquad (2.10)$$

Example of transient response for case, when m>0, is given in Fig. 2.2. it is step function. From the figure one can see that in section/segment $\frac{1}{2} t_3 < t < \frac{3}{2} t_3$ the system, whose transient response is described by equation (2.10), satisfies the condition for undistorted transmission (2.3).

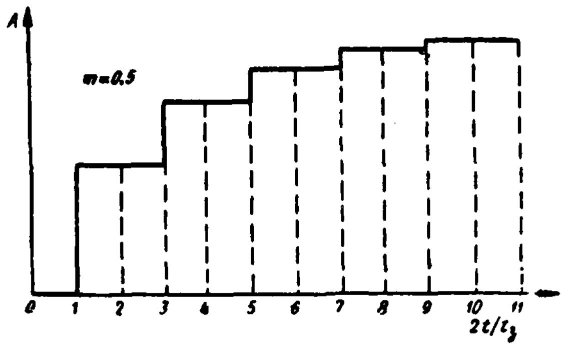

Fig. 2.2. Transient response of single ring with unlimited passband of internal circuit.

Page 89.

Let us note that the equation of the enveloping transient response is the exponential function

$$P(n)=K_0\sum_{\nu=1}^{n} m^{\nu-1}=\frac{K_0}{1-m}(1-e^{n\ln m}).$$

With m<1 and $n\to\infty$ the envelope approaches the steady-state value

$$P_{\text{ст}}=\frac{K_0}{1-m}.$$

Fig. 2.3 presents processes, which occur during the supplying to input of ring of single pulse. Output potential of ring in this case is the sum of fundamental (first) pulse and series of the decreasing in the amplitude pulses, which were being formed with the reflection from the ends/leads of the line. These supplementary pulses are wake current, which was discussed above.

Let us assume now that passband of internal circuit is limited and complex transmission factor of internal circuit

$$R=\frac{m}{1+j\omega\tau}e^{-j\omega t_3},$$

where τ - certain equivalent time constant.

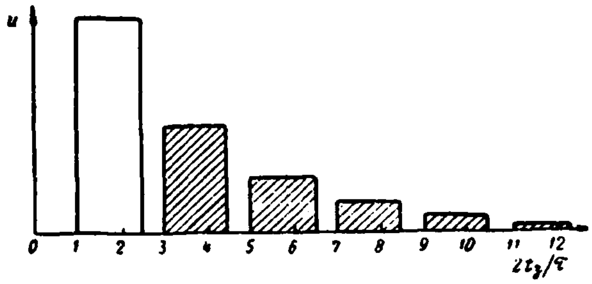

Fig. 2.3. Passage of single pulse through loop circuit. The shaded pulses are wake current.

Page 90.

In this case

$$u_B = K_0 \sum_{n=1}^{\infty} \left(\frac{m}{1 + j\omega\tau} \right)^{n-1} e^{-j\omega (n-1/2) t_3} u_0.$$

Using to this expression inversion formula, we will obtain [34]

$$A(t) = K_0 \sum_{n=1}^{\infty} m^{n-1} \frac{\Gamma[n-1,\ x-(n-1/2)x_3]}{(n-2)!}, \quad (2.11)$$

where Γ(n, x) - incomplete gamma function; $x = \frac{t}{\tau}$; $x_3 = \frac{t_3}{\tau}$.

According to equation (2.11) in Fig. 2.4 is constructed transient response of ring for case of m>0. It differs from the transient response of ring with the unlimited passband in terms of the fact that the steps of characteristic are rounded off. System is distorting; however, the distortions of different sections of curve are different.

In interval of time $[{}^1/_2 t_3, {}^3/_2 t_3]$ transient response is to exponent, time constant of which is equal to τ. If the pulse duration is less than t_3, then the distortions of its front can be evaluated by the time of establishment $t_y = 2{,}2\tau$.

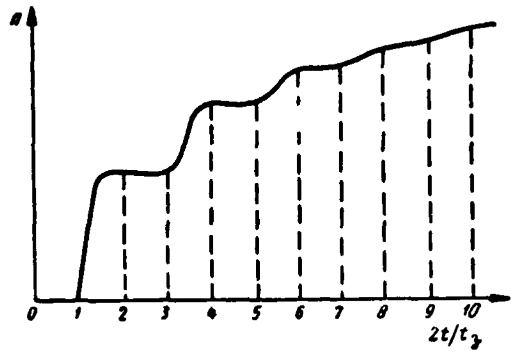

Fig. 2.4. Transient response of single ring, passband of internal circuit of which is limited in region of higher frequencies.

Page 91.

In the large pulse duration the distortion of their form will be more essential; however, their amplitude due to wake current will increase in 1/(1-m) times.

In order to rate/estimate distortions of pulses, whose duration much more t_3, let us introduce concept of generalized envelope. The concept of envelope for the piecewise-smooth function is characterized by known arbitrariness. We will understand under generalized envelope such flat approximating function, which in a sense presents well transient response. In this case the envelope, understood in a broader sense, must: a) in the process of the transition of characteristic from the piecewise-smooth function to the stepped present known envelope of step function and b) in the process of transition from the piecewise-smooth function into the flat function represent function itself.

Approximating function of form

$$P(t)=\frac{K_0}{1-m}(1-e^{-t/\theta}), \qquad (2.12)$$

where equivalent time constant

$$\theta=\frac{\tau}{1-m}-\frac{t_3}{\ln m}.$$

satisfies these conditions.

When $\tau=0$ $\theta=-\frac{t_3}{\ln m}$ AND envelope coincides from enveloping step function. When $t_3=0$ $\theta=\frac{\tau}{1-m}$ AND the envelope coincides with function itself. According to expression (2.12), the time of the establishment of the pulse of large duration $t_y=2{,}2\theta$ is always more than the time of the establishment of the pulse, whose duration is less than t_3. With the high values of t_3 these times can be incommensurable.

Very frequently, however, values τ and t_3 have identical order (for example, in traveling-wave amplifiers). Above has already been indicated that for the pulses of large duration is observed an increase of the amplitude of oscillations in 1/(1-m) times due to the use of wake current. This fact cannot, however, compensate for an increase in the time of establishment.

Page 92.

Let us introduce a certain value (equivalent to the area of amplification), which is the ratio of gain in the amplitude of oscillation due to the use of wake current to the time of the establishment:

$$\Delta=\frac{1}{2,2(1-m)\left(\frac{\tau}{1-m}-\frac{t_3}{\ln m}\right)}. \qquad (2.13)$$

For pulses of short duration this value is equal to $\frac{1}{2,2\tau}$. Let us assume in formula (2.13) t_3=0, then value $\frac{2,2\tau}{1-m}$ will be the time of the establishment of pulse in the re-generative amplifier without the time lag. It is obvious that in this case Δ=1/2.2τ, i.e., no gain in the area of amplification it is obtained. With any t_3, different from zero, value Δ is still less, i.e., the introduction of time lag only increases the distortions of pulse, evaluated on generalized envelope.

Let us turn now to spectral characteristics of ring. Let us assume for simplicity that K_0=1, and let us drop/omit the time lag of pulse in transit through the channel of direct feed, i.e., will accept expression for the complex transmission factor in the form

$$\overline{K}(\omega)=\sum_{n=1}^{\infty} m^{n-1}e^{-j\omega(n-1)t_3}. \qquad (2.14)$$

Since m<1, then series/row (2.14) converges and

$$\overline{K}(\omega)=\frac{1}{1-me^{-j\omega t_3}}.$$

Modulus of this expression, i.e., amplitude-frequency characteristic of ring

$$K(\omega)=\frac{1}{\sqrt{1+m^2-2m\cos\omega t_3}}, \qquad (2.15)$$

is periodic function of frequency.

Page 93.

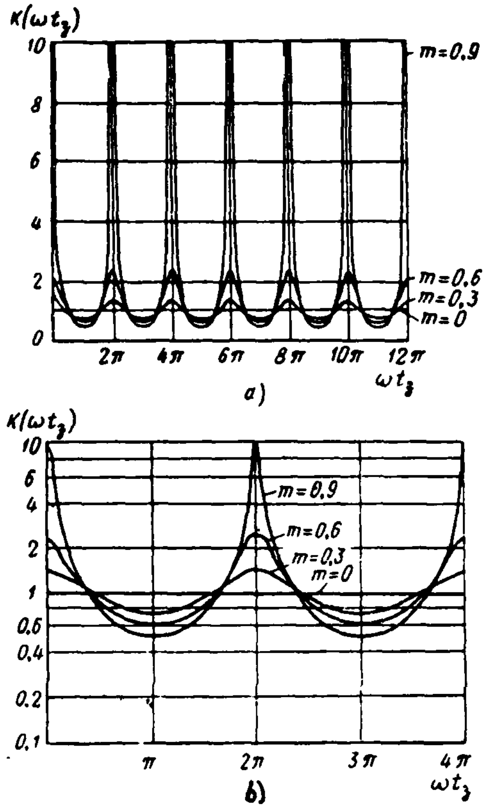

Fig. 2.5. Amplitude-frequency characteristics of single ring with unlimited passband of internal circuit: a) in usual and b) in logarithmic scales.

Page 94.

With m>0 at frequencies $\frac{2k\pi}{t_з}$ this characteristic passes through maximums,

$$K_{макс}=\frac{1}{1-m},$$

but at frequencies $\frac{2k-1}{t_з}\pi$ - through the minimums

$$K_{мин}=\frac{1}{1+m}.$$

Example of amplitude-frequency characteristic of ring, which possesses unlimited passband of internal circuit, is given in Fig. 2.5. It takes the characteristic comb form.

Phase-frequency characteristic of ring can be found from (2.14) and is represented in the form

$$\varphi(\omega) = -\operatorname{arc\,tg} \frac{m \sin \omega t_3}{1 - m \cos \omega t_3}. \qquad (2.16)$$

Phase-frequency characteristic of ring for case of m>0 is shown in Fig. 2.6.

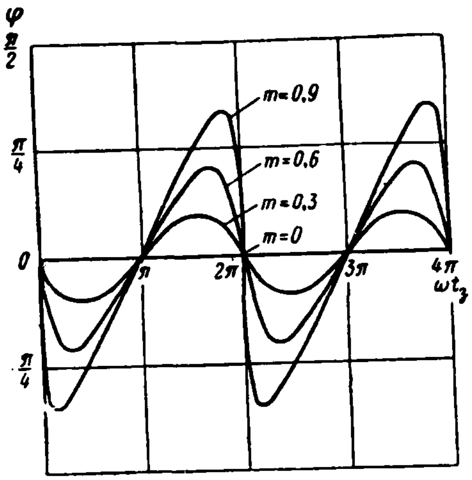

Fig. 2.6. Phase-frequency characteristics of single ring with unlimited passband of internal circuit.

Page 95.

Graphs/curves given in Fig. 2.5 and 2.6 do not make it possible to judge that, are suitable data of system for distorted transmission of pulses. In Fig 2.5 amplitude-frequency characteristics of ring are given for several values of the factor of feedback m.

With small m amplitude-frequency characteristic is more smoothed. Decrease m in connection with the ring, formed by the section of long line, indicates an improvement in the agreement of line with the load. However, the examination of the transient responses of ring, given earlier, shows that the conditions for the transmission of the pulses, whose duration is less than t_3, do not change from that, the value of the factor of feedback more or less is undertaken.

Spectral characteristics of ring, given in mentioned above Fig. 2.5 and 2.6, are static characteristics. In order to be introduced to its dynamic characteristics and to explain the process of the formation of static characteristics, let us turn to the diagram of the substitution of ring. In order to construct this diagram, we will use expression (2.6). According to this expression the oscillation at the output of ring is the infinite sequence of pulses. The first pulse is formed by the input pulse, which passed only along the channel of direct feed, the second - by pulse, which passed from the input to the output along the channel of direct feed and which completed one additional cycle of rotation/access on the closed loop of feedback, the third - by pulse, which completed two cycles of rotation/access and, etc.

On the basis of mechanism of work of ring described above, it is possible to represent its equivalent circuit in the form, shown in Fig. 2.7. This diagram consists of quadrupole K, which replaces the channel of direct feed, and the infinite series of the circuits, which replace the channel of the reverse/inverse supply B. Let us write expression for the complex transmission factor of the equivalent circuit, which consists of the N branches:

$$\overline{K}(N, \omega) = \frac{1 - m^N e^{-jN\omega t_3}}{1 - m e^{-j\omega t_3}}.$$

Page 96.

Modulus of this expression, i.e., equation of amplitude-frequency characteristic, takes form

$$\bar{K}(N,\ \omega)=\sqrt{\frac{1+m^{2N}-2m^{N}\cos N\omega t_3}{1+m^{2}-2m\cos\omega t_3}}$$

Form of amplitude-frequency characteristic of equivalent circuit depends on N; with N→∞, as it is not difficult to see, K(N, ω) accepts form (2.15) ($m^N \to 0$ with N→∞.

In Fig 2.8. amplitude-frequency characteristics of equivalent circuit, which contain one, two, are shown, three and more than branches. It is possible to examine these curves just as separate stages of the formation of the stationary amplitude-frequency characteristic of ring. In the period, which does not exceed t_3, amplitude-frequency characteristic is the straight/direct, parallel axes of abscissas, i.e., system is nondistorting. To its output the oscillations/vibration/oscillations, which completed one, two, begin to come in proportion to, three and more than cycles on the internal loop of feedback, the form of amplitude-frequency characteristic changes. The maximums and the minimums appear at the characteristic; in the course of time the maximums increase, and failures/dips/troughs between them become deeper. With the unlimited increase of time amplitude-frequency characteristic how conveniently closely approaches the characteristic of steady state. From the graphs/curves given the role of the dynamic characteristics of the systems, which actually

determine the distortions of the pulses of different duration, here becomes clear.

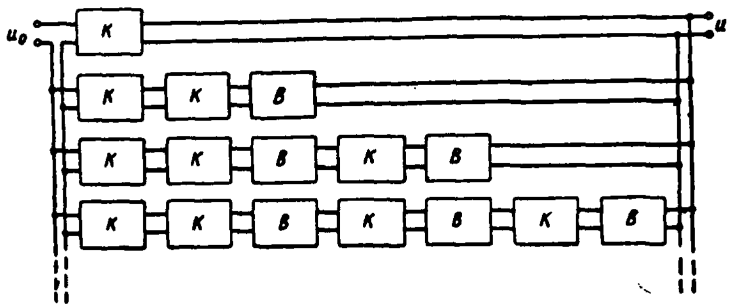

Fig. 2.7. Diagram of substitution of single ring by broken circuits.

Page 97.

Let us turn now to case, when ring has limited passband, so that transmission factor of internal circuit

$$\bar{R}(\omega)=me^{-j\omega t_з}\frac{1}{1+j\omega\tau}.$$

After using known formula for complex transmission factor of device/equipment with feedback

$$\bar{K}(\omega)=\frac{1}{1-\bar{R}(\omega)},$$

it is possible to obtain

$$\bar{K}(\omega)=\frac{1}{1+j\omega\tau-me^{-j\omega t_з}}.$$

Modulus of transmission factor

$$K(y)=\frac{1}{\sqrt{1+m^2+y^2-2m\sqrt{1+y^2}\cos\theta(y)}}, \qquad (2.17)$$

where

$$y=\omega\tau;\ x_з=\frac{t_з}{\tau};\ \theta(y)=-(\mathrm{arc\,tg}\,y+x_з y).$$

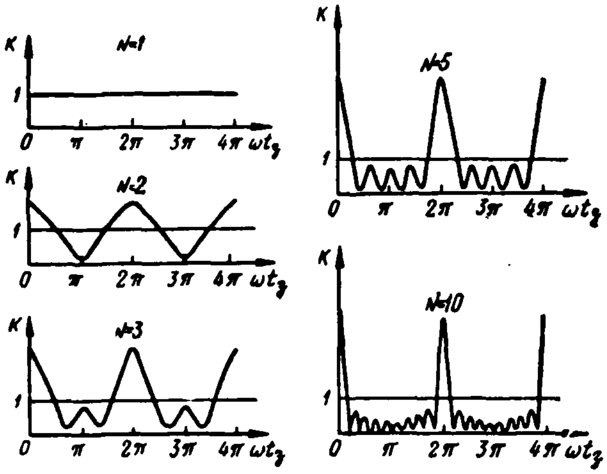

Fig. 2.8. Process of formation of amplitude-frequency characteristics of single ring.

Page 98.

When in ring layout of integrating component/link is present, its amplitude-frequency characteristic will no longer be periodic function of frequency. The maximums of characteristic are arranged/located not at equidistance, but their value decreases with an increase in the frequency. The frequencies, at which occur the maximums, can be determined from the equation

$$\operatorname{arc\,tg} y + x_s y = 2k\pi.$$

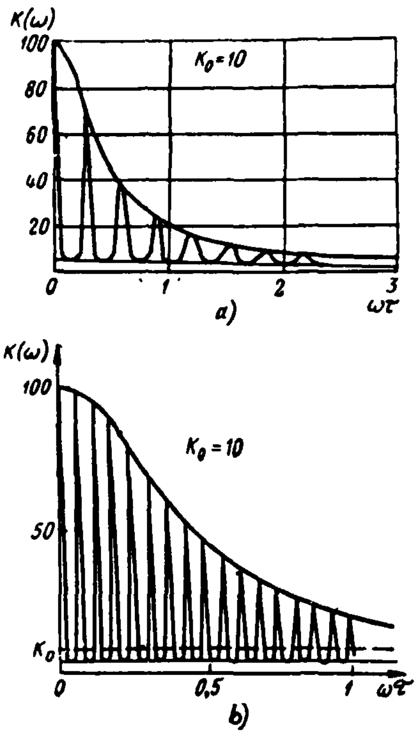

Fig. 2.9. Amplitude-frequency characteristics of single ring, passband of internal circuit of which is limited in region of higher frequencies: a) for $t_3/\tau=20$; b) for $t_3/\tau=100$.

Page 99.

Envelope of maximums of characteristic

$$K(y)=\frac{1}{\sqrt{1+y^2}-m}.$$

It is easy to see that envelope of maximums decreases with increase in frequency more rapidly than transmission factor of filter. This is explained by the fact that at frequencies, which correspond to

maximum values, in the ring operates purely the positive feedback, which amplifies the nonuniformity of characteristic.

Fig. 2.9 gives amplitude-frequency characteristics of ring with positive delayed feedback, which contains low-pass filter. Fig. 2.9a corresponds to the case, when $t_з/\tau=20$, while Fig. 2.9b - when $t_з/\tau=100$. In both cases of m=0.9. The disturbance/breakdown of the equidistance of the maximums and minimums is developed the stronger, the less $x_з$.

Let us determine passband of ring on enveloping amplitude-frequency characteristic. After assuming

$$\frac{1}{\sqrt{1+y_{rp}^2}-m}=\frac{1}{\sqrt{2}}\frac{1}{1-m},$$

let us find that

$$y_{rp}=\sqrt{[\sqrt{2}-m(\sqrt{2}-1)]^2-1}$$

or approximately

$$\Omega_{rp}=\omega_{rp}\sqrt{1-1{,}17m+0{,}17m^2}, \tag{2.18}$$

where ω_{rp} - the cut-off frequency of filter.

Dependence of relation Ω_{rp}/ω_{rp} on m is given in Fig. 2.10. It follows from the graph/curve that the passband of ring is the less, the nearer m to one, and it becomes zero with m=1.

For practice there is great interest in possibility of

evaluation/estimate of distortions of shape of pulse according to static amplitude-frequency characteristics. In the general case the solution of this problem is very complicated, but some recommendations can be expressed for the example of single ring in question. Formula (2.18) makes it possible to rate/estimate the filter pass band, which stands in internal circuit of ring $\omega_{гр}$, if are known $\Omega_{гр}$ and m.

Page 100.

Value $\Omega_{гр}$ can be determined on the enveloping stationary amplitude-frequency characteristic of ring, and m - through the relation of the first maximums and minimums of characteristic according to the formula

$$m=\frac{K_{макс}-K_{мин}}{K_{макс}+K_{мин}}.$$

After determining value $\omega_{гр}$, let us find time of establishment of pulse, whose duration is less $t_з$; $t_у=2,2/\omega_{гр}$.

2.3. DISTORTIONS OF THE SHAPE OF PULSES WITH THE PASSAGE ALONG THE TRANSMISSION LINES WITH THE THE DISCRETE/DIGITAL TO IRREGULARITIES ENDTITLE.

In preceding/previous sections of present chapter were examined conditions, with which was possible undistorted transmission of pulses through transmission lines with discrete/digital heterogeneities, and general/common properties of loop circuits are also analyzed.

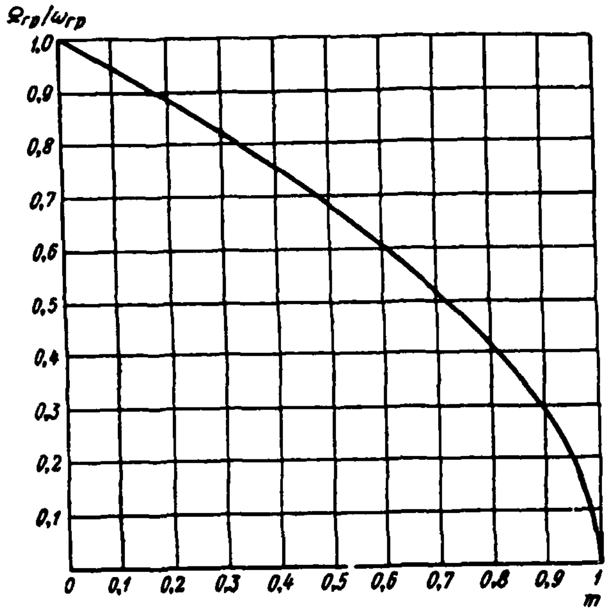

Fig. 2.10. Dependence of relative passband of ring on value of factor of feedback.

Page 101.

Let us pause now at a question about the distortions of pulses, during their propagation concerning the transmission lines due to the discrete/digital heterogeneities in the lines. Such heterogeneities can be formed as a result of a change in the distance between the conductors of the line, presence of the insulating washers and other reasons.

Let us examine first simple case, when heterogeneity in line is caused by change in its wave impedance. Let the line characteristic in section/segment $[0, x_1]$ be equal ρ_0, in the section/segment $[x_1,$

x_2] is equal to ρ and with $x>x_2$ is again equal ρ_0. Value ρ can be both more and it is less ρ_0.

Fig. 2.11 shows law of change in line characteristic for case $\rho>\rho_0$. The section of line [x_1, x_2] is single ring. It is easy to see that for the wave, which is propagated from left to right, the reflection coefficients at points x_1 and x_2 are equal in magnitude and are reverse/inverse on the sign, and therefore

$$A_K=(1-p^2)e^{-1/2j\omega t_3}. \qquad (2.19)$$

Here in A_K are taken into consideration two passages of signal through heterogeneity in contrast to formula (2.7). Time of landing run along the line in the section [x_1, x_2] is marked through $^1/_2t_3$. For the waves reflected, which circulate within the ring, the reflection coefficients at points x_1 and x_2 are identical, and therefore

$$R=p^2e^{-j\omega t_3}.$$

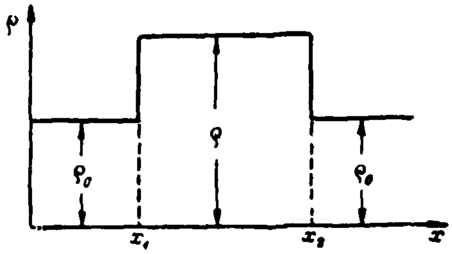

Fig. 2.11. Example of abrupt change in line characteristic of transmission.

Page 102.

On the basis of formula (2.19) it is possible to write following expression for transient response of line, which contains heterogeneity:

$$A(t)=(1-p^2)\sum_{n=1}^{\infty} p^{2(n-1)}\, 1\left[t-\left(n-\frac{1}{2}\right)t_3\right].$$

With passage of square pulse through heterogeneity, frontal part of pulse is distorted, taking stepped form, as it was shown in Fig. 2.2. The pulse amplitude in this case does not change, since the steady-state value of transient response is equal to one, since

$$\sum_{n=1}^{\infty} p^{2(n-1)}=\frac{1}{1-p^2}.$$

Step function approximately it can replace with exponential, after defining latter/last as envelope

$$P(n)=(1-p^2)\sum_{\nu=1}^{n} p^{2(\nu-1)}=1-p^{2n}=1-e^{2n\ln|p|}.$$

This expression can be rewritten in the form

or

$$P(t)=1-e^{\frac{2t}{t_s}\ln|p|}$$

$$P(t)=1-e^{-t/\tau_{oe}},$$

where

$$\tau_{oe}=-\frac{t_s}{2\ln|p|}. \quad (2.20)$$

Thus, if we judge by envelope, square pulse will be distorted then, as if into transmission line was included/switched on certain capacity/capacitance C_{oe}. Time constant of capacity/capacitance $\tau=\frac{1}{2}\rho_0 C_{oe}$. Equalizing values τ and τ_{oe}, it is possible to find the value of the equivalent capacity/capacitance:

$$C_{oe}=-\frac{t_s}{\rho_0\ln|p|}.$$

Page 103.

Time of establishment of pulse after passage of heterogeneity $t_y=2,2\tau_{oe}$.

For determining value τ_{oe} it is possible to use graph/curve,

given in Fig. 2.12, in which is given dependence $\tau_{oe}=f(\rho/\rho_0)$ for different values of t_3 [16]. It is evident from the graph/curve that the equivalent time constant depends substantially on the ratio ρ/ρ_0.

If heterogeneity is caused by presence in line of insulating washer with dielectric constant ϵ and by length l, then

$$\tau_{oe}=\frac{l\sqrt{\epsilon}}{2c\ln\left|\frac{1-\sqrt{\epsilon}}{1+\sqrt{\epsilon}}\right|}.$$

It is taken into consideration during derivation of this formula that $\rho=\frac{\rho_0}{\sqrt{\epsilon}}$, a $t_3=\frac{2l\sqrt{\epsilon}}{c}$, where c=3·10¹⁰ cm/s. Calculation shows that with l=5 mm and $\epsilon=2\div2,5$ $\tau_{oe}=13,4\cdot10^{-12}\div18\times10^{-12}$ s.

Jump of wave impedance appears with curvature of strip transmission lines.

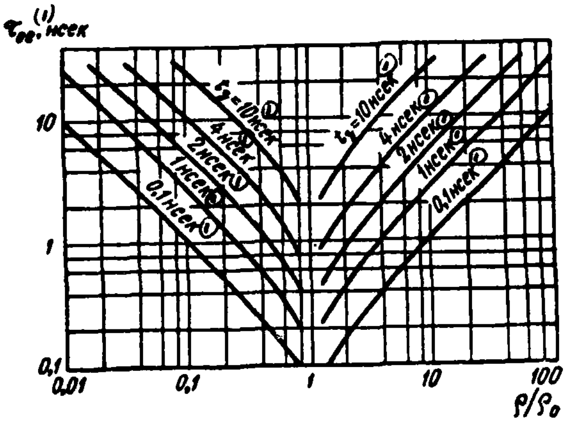

Fig. 2.12. Dependence of equivalent time constant on relation of wave impedance of adjacent sections of line for different values of time lag.

Key: (1). ... ns.

Page 104.

Fig. 2.13 show two cases of the curvature of line. The wave impedance of the bent part of the line

$$\rho=\rho_0\left[1\pm\frac{1}{6}\left(\frac{a}{R_1+R_2}\right)^2\right],$$

where ρ_0 - wave impedance of straight line;

a - width of ribbon conductors;

R_1 and R_2 - bending radii.

Positive sign in formula corresponds to Fig. 2.13a, and negative - Fig. 2.13b. Substituting this expression into the formula for determining the time constant, let us find that

$$\frac{\tau_{oe}}{t_3}=\frac{1}{\ln\left[48\left(\frac{R}{a}\right)^2\pm1\right]},$$

where $R=\frac{1}{2}(R_1+R_2)$.

For determining time lag it is necessary to know average/mean length of curvature of line $l_{cp}=\frac{\pi}{2}R$ and wave propagation velocity in line v. Then $t_3=l_{cp}/v$. The dependence of value τ_{oe}/t_3 from ratio R/a is given in Fig. 2.14. Knowing this value and delay time t_3, it is possible to find equivalent time constant. For example, with R=2 cm and $\varepsilon=2$ $t_3=1{,}5\cdot10^{-10}$ s. If R/a varies from 0.5 to 5, then $\tau_{oe}=50\cdot10^{-12}\div21\cdot10^{-12}$ s.

Analogous phenomenon occurs, also, with curvature of coaxial cable. The wave impedance of the bent part of the cable

$$\rho=\rho_0\left[1-\left(\frac{D}{8R}\right)^2\right],$$

where D - diameter of external conductor;

R - bending radius.

Relation τ_{oe}/t_3 will take form:

$$\frac{\tau_{oe}}{t_3}=\frac{1}{\ln\left[128\left(\frac{R}{D}\right)^2-1\right]}.$$

After accepting R/D=5, we obtain $\frac{\tau_{oe}}{t_3}=0{,}12$, approximately the same value, as for strip line.

Page 105.

Formulas given in present section and graphs/curves make it possible to rate/estimate effect of discrete/digital heterogeneities on transmission of nanosecond pulses.

Action only of single heterogeneity above was examined; in many cases of such heterogeneities there can be sufficiently much.

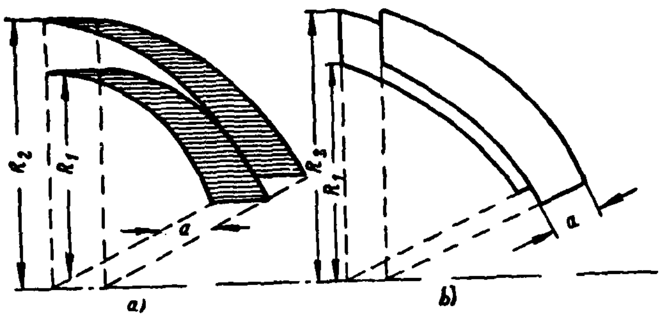

Fig. 2.13. Forms of curvature of strip transmission line.

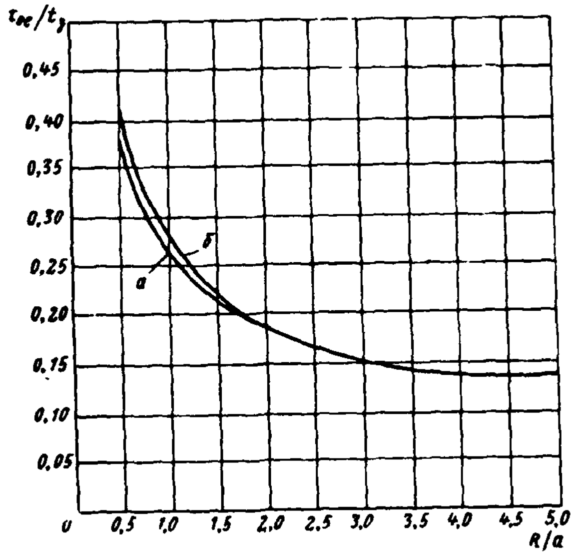

Fig. 2.14. Dependence of value τ_{0e}/t_3 from ratio R/a. The curves a and b correspond to strip lines with the different curvature (Fig. 2.13a and b).

Page 106.

In this more complicated case they proceed from the following considerations. Fundamental oscillation and wake current is obtained with the passage of the pulse oscillation through the distributed

system with the discrete/digital heterogeneities at its output. If wake current is not superimposed on the fundamental oscillation, which occurs when the pulse duration is less than doubled time of landing run between the nearest heterogeneities, then time constant

$$\tau_{oe}=\sqrt{\tau_{oe1}^{2}+\tau_{oe2}^{2}+\tau_{oe3}^{2}+\cdots+\tau_{oeN}^{2}},$$

where τ_{oe1}, τ_{oe2}, τ_{oe3}, ... - time constants of individual heterogeneities.

Present formula is consequence of fundamental limit theorem of probability theory and assumes independence of action of heterogeneities.

But if wake current is superimposed on fundamental oscillation, then calculation of distortions of pulses becomes considerable more complicated. In this case it follows to first calculate fundamental oscillation and wake current on the assumption that they are spread on the time, and then to use the principle of superposition. It is necessary to keep in mind that component/term of wake current, which arrive at the later moments of time, are usually strongly they are weakened, which simplifies the calculation of distortions. The calculation of the distortions of the shape of pulse due to the action of wake current is examined in chapter 9 in connection with traveling-wave amplifier. The more general case is analyzed into [35], where the method of calculation of the effect of heterogeneities, convenient for using the digital computer, is presented.

2.4. TRANSFORMATION OF PULSES.

One of most widely used forms of conversion of pulse oscillations is conversion, which consists in multiplication of oscillation by constant value K_0 and bias/displacement along time axis to the right on t_3. This form of conversions includes the transformation of oscillations, inversion, weakening, amplification, the time lag, transmission along the channels of communication, etc.

Page 107.

All enumerated conversions of oscillations occur without a change (or without the distortion) in their form.

In series/row of similtude one of first places occupies transformation. It is used for impedance matching, increase or decrease in the voltage/stress of pulse oscillations, inversion of the pulses and other targets [36]. In the low-voltage devices/equipment of nanosecond range (blocking oscillators, amplifier-limiters on transformers, etc.) miniature peak transformers on the ferrites are utilized. These transformers have the very small inductance of magnetization and small geometric dimensions, in consequence of which their parasitic parameters (self-capacitance and leakage inductance) are also very small, and passband - sufficient for the undistorted transmission of pulses nanosecond duration. To deficiencies in such transformers should be related their inadequacy for the transformation of high-amplitude pulses. (Similar transformers are examined further

in Chapter. 6).

Widest use in nanosecond pulse technique received transformers with distributed parameters. These transformers make it possible to transform high voltages and high currents, they possess sufficiently wide passband. By the advantage of transformers with the distributed parameters is the fact that their geometric dimensions decrease in proportion to the decrease of the duration of the transformed pulses. Simplest of the transformers with the distributed parameters is the section of the long line, whose parameters change along the length according to any law. Examples of such devices/equipment were already examined earlier in the first chapter. Non-uniforms circuit as transformers are inconvenient in a number of cases due to their large geometric dimensions. Therefore such transformers for decreasing the overall dimensions frequently are manufactured in the form of spiral with the variable step/pitch (the so-called spiral transformers).

For transformation of pulses can be utilized also distributed systems, in which parameters are changed not continuously, but it is abrupt.

Page 108.

An example of transformer in the form of the distributed system with the discrete/digital heterogeneities is the stepped transformer, which is the line, whose wave impedance is changed abruptly, for example being raised from the beginning of line toward the end. In this

system output potential is raised with respect to the voltage on the input. Stepped and spiral transformers have the deficiency, that they cannot realize an inversion of the phase of pulse oscillations. The inverters and the transformers, formed by the sections/segments of coaxial cable, are used for this purpose. A change in the order of the connection of the central core of cable and braid/cover at the output in comparison with the order of their connection at the input makes it possible to carry out a change in the pulse polarity. But if to connect two or is more than cables at the input in parallel, and at the output consecutively/serially, then it is possible to obtain the step-up peak transformer, the transformation ratio of which is equal to the number of connected cable segments.

2.5. SPIRAL TRANSFORMER.

Spiral transformers (Fig. 2.15) in structural/design sense are tube from insulation 1, which possesses low losses, to which is plotted/applied spiral with variable step/pitch of 2. Spiral is surrounded by metal screen/shield 3, which the external conductor forms. Both spiral and screen/shield must be made from material with the low ohmic resistance in order as far as possible to decrease the transformer losses.

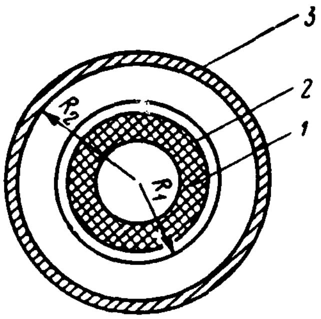

Fig. 2.15. Section of spiral transformer: 1 - dielectric tube; 2 - spiral; 3 - screen/shield.

Page 109.

It is possible to consider during production of transformer from materials with low losses that properties of transformer are characterized only by linear capacity/capacitance and linear inductance, which determine wave impedance of spiral. The wave impedance of spiral can be determined according to following formula [37]:

$$\rho = \alpha \frac{R_1}{\tau} \sqrt{\frac{1}{2}\left[1-\left(\frac{R_1}{R_2}\right)^2\right] \ln \frac{R_2}{R_1}},$$

where

$$\alpha = \sqrt{\frac{\mu_0}{\epsilon_0 k}};$$

μ_0 and ϵ_0 - magnetic and dielectric constants of free space;

k - relative dielectric constant of the dielectric, which fills space between the spiral and the screen/shield;

τ - spiral pitch ($1/\tau$ - number of turns per unit of length);

R_1 - radius of spiral;

R_2 - radius of screen/shield.

Optimum value of ratio of radius of screen/shield to radius of spiral is equal to 2.06. Thus, in the optimum version

$$\rho = 0,44\alpha \frac{R_1}{\tau}.$$

After assigning a value of input resistance $\rho_{вх}$ and a radius of spiral R_1, it is possible from the preceding/previous formula to find spiral pitch on the input of the transformer:

$$\tau_{вх} = 0,44\alpha \frac{R_1}{\rho_{вх}}.$$

Spiral pitch at the output of the transformer

$$\tau_{вых} = 0,44\alpha \frac{R_1}{\rho_{вых}},$$

where

$$\rho_{вых} = n^2 \rho_{вх},$$

but n - transformation ratio.

Change in level of wave impedance to turn γ determines value of distortions of pulse apex. Usually they are assigned by this value in the limits from 1 to 5%. Knowing total variation in the resistor/resistance along the length of spiral, equal to the square of transformation ratio, is easy to find the number of turns N.

Page 110.

The axial length of exponential helix from the N turns is found by the

formula

$$l_0 = \tau_{\text{вх}} \frac{1 - e^{-2\pi R_1 \gamma N}}{e^{2\pi R_1 \gamma} - 1}.$$

Formulas given above make it possible to conduct engineering of transformer with distributed constants.

In work [37] constructions/designs of two spiral transformers are described. One of them had a spiral, prepared from the wire, and another - from the tape of variable width. Transformers were structurally connected with hydrogen thyratron. Data of these transformers are visible from Table 2.1.

In table they are given: d - diameter of wire, h - thickness are flight, δ - clearance of strip/tape spiral, m - ratio of axial length of spiral to length of wire, γ - change in level impedance to turn.

Fig. 2.16 depicts oscillograms of pulses at input and output of transformer, which testify about its broad-band character. At the input of transformer the pulse duration in foundation is equal to approximately 14 ns, while at the output - about 19 ns. The spread/scope of positive pulse at the input is 3500 V, and at the output 8600 V. As can be seen from Table 2.1, wire and strip/tape transformers have approximately identical indices.

Table 2.1.

(1) Параметры трансформатора	(2) Проволочная спираль	(3) Ленточная спираль
R_1, мм	19,45	22,30
R_2, мм	37,23	37,23
d, мм	1,62	—
h, мм	—	0,07
δ, мм	—	0,25
l_0, м	1,74	2,22
m	1/14,4	1/14,2
N	210	230
γ %	1	0,9
$\rho_{вх}$, ом	290	145
$\rho_{вых}$, ом	1590	1070

Key: (1). Parameters of transformer. (2). Wire helix. (3). Strip/tape spiral.

Page 111.

Difference lies in the fact that the transformers with the strip/tape spirals are more convenient for low-level obtaining of resistor/resistance.

Yu. S. Belozerov [22] carried out investigation of distortions of shape of pulses, and also analysis of amplitude-frequency and dispersive characteristics of spiral transformers of round and rectangular cross sections (Fig. 2.17). Calculation data of transformers are given in Table 2.2. In the circular transformers the law of a change of spiral pitch is accepted by such, with which the wave impedance of spiral changes exponentially. The law of a change of spiral pitch in the rectangular transformers is shown in Fig. 2.18.

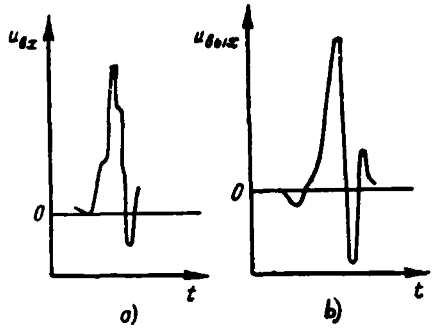

Fig. 2.16. Oscillograms of pulses at input (a) and output (b) of spiral transformer.

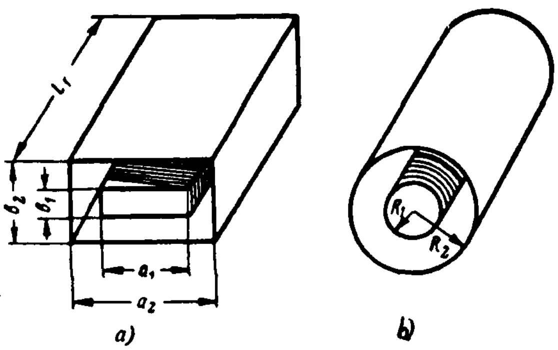

Fig. 2.17. Constructions/designs of spiral transformers: a) rectangular and b) circular of sections.

Page 112.

The number of transformer according to Table 2.2 indicates number under the curve. Air was insulation in transformer No 1, and in the rest - polyethylene. Spirals were coiled from the copper wire, and screen/shield was manufactured from brass.

Measured values of resistors/resistances and transformation ratio are given in Table 2.3.

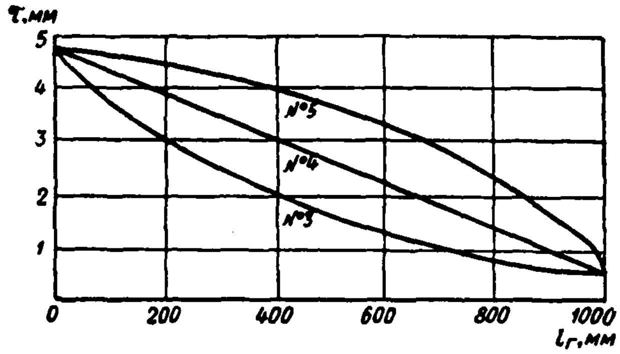

Fig. 2.18. Dependence of step/pitch of coil/winding on axial length of spiral for different types of transformers.

Table 2.2.

(1) Параметры трансформатора	(2) Круглые трансформаторы		(3) Прямоугольные трансформаторы		
	№ 1	№ 2	№ 3	№ 4	№ 5
n	2	2,3	—	—	—
$\rho_{вх}$, ом	240	145	—	—	—
$\rho_{вых}$, ом	960	765	—	—	—
R_1, мм	5	4,75	—	—	—
R_2, мм	10	6,9	—	—	—
l_1, мм	1100	1000	1000	1000	1000
T_0, нсек(4)	40	60	160	214	284
$\tau_{вх}$, мм	5	4,75	4,8	4,8	4,8
$\tau_{вых}$, мм	1	0,5	0,35	0,35	0,35
N	375	390	453	611	810
K	1	2,25	2,25	2,25	2,25
τ	0,5	0,25	0,15	0,15	0,15
a_1	—	—	30	30	30
a_2	—	—	35	35	35
b_1	—	—	4	4	4
b_2	—	—	9	9	9

Key: (1). Parameters of transformer. (2). Circular transformers. (3). Rectangular transformers. (4). ns.

Page 113.

With the aid of rectangular transformers, which have identical transformation ratio, but different delay, were investigated

distortions of shape of rectangular pulse depending on electrical length of transformer. The pulse, supplied to the input of transformer, had flat/plane apex/vertex; the pulse duration was 60 ns for the duration of front 8.5 ns. The results of measurements are given in Table 2.4.

In Table 2.4 T_0 indicates delay time, g - decay in flat/plane part of pulse.

It follows from Table 2.4 that with an increase in electrical length of transformer, which is characterized by delay factor T_0, it begins to transform lower-frequency components of pulse spectrum, which leads to decrease of decay in pulse apex g. The high-frequency distortions, connected with an increase in the losses and an increase of phase distortions with an increase in the electrical length of transformer at the same time grow/rise.

For evaluation of effect of ohmic losses and phase distortions amplitude-frequency and dispersive characteristics of transformers were plotted. Measurements showed that the delay time of transformers barely depends on frequency, i.e., dispersion virtually is absent. The same result is obtained also from the theoretical calculations. The measurements of the passband of transformers showed that it has value on the order of 250 MHz.

Distortions of pulse edge transformer No 2 are given in Table 2.5.

Table 2.3.

(1) Номер трансформатора	$\rho_{вых}$, ом	$\rho_{вх}$, ом	n
1	850	220	1,97
2	650	120	2,08
3	1300	150	2,92
4	1300	150	2,92
5	1300	150	2,92

Key: (1). Number of transformer.

Table 2.4.

(1) Параметры трансформатора	(2) Номер трансформатора		
	3	4	5
T_ϕ, (3) нсек	160	216	284
g, %	20	12	6
t_ϕ, нсек (3)	13	14	15,5

Key: (1). Parameters of transformer. (2). Number of transformer. (3). ns.

Table 2.5.

$t_{\phi\ вх}$, (1) нсек	2	4	6
$t_{\phi\ вых}$, (1) нсек	3	4,7	6,7

Key: (1). ns.

Page 114.

Of aforesaid it above follows that spiral transformers successfully can be used for transformation of nanosecond pulses.

2.6. STEPPED TRANSFORMER.

Together with simplest single rings, whose analysis was carried out in second section, in pulse technique are utilized systems with distributed parameters with large number of heterogeneities. For example, such systems stepped transformer and traveling-wave amplifier are. Stepped transformer is the line, whose wave impedance abruptly changes at points x_1, x_2, x_3 .... Traveling-wave amplifier is fulfilled in the section of the line, in which at points x_1, x_2, x_3 ... are connected the tubes. Such devices/equipment are the system or the intersected rings, schematically shown in Fig. 2.19. System consists of Q components/links K, included by P by feedback loops B. The number of channels of feedback and, therefore, the number of rings is equal to sum of Q of the first members of the natural series of the numbers:

$$P=\frac{1}{2}Q(Q+1).$$

Let us assume for simplicity of analysis that all components/links of channel of direct feed are identical and are rated/estimated by complex transmission factors $\overline{K}$.

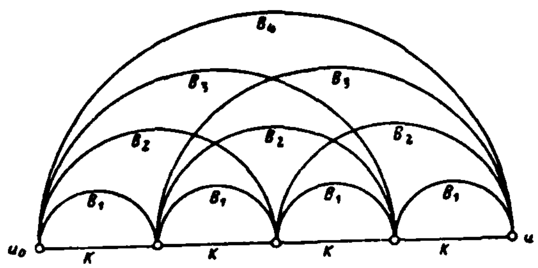

Fig. 2.19. Diagrammatic representation of system of intersected rings.

Page 115.

The feedback loops, which encompass the identical number of components/links, let us also place by their identical and we will rate/estimate complex transmission factors $\overline{B}_1$, $\overline{B}_2$, $\overline{B}_3$, where the index indicates the number of included by this circuit components/links.

Voltage on input of system of intersected rings

$$\overline{U}_{BX}=\overline{U}_0+\sum_{q=1}^{Q}\overline{U}_q \qquad (2.21)$$

is composed of voltage/stress $\overline{U}_0$ and voltages/stresses, which enter from output of the first, the second, the third and so forth of components/links. In turn,

$$\overline{U}_q=\overline{R}_q\overline{U}_{BX}=\overline{K}\overline{A}_{q-1}\overline{B}_q\overline{U}_{BX}, \qquad (2.22)$$

where $\overline{A}_{q-1}$ - complex transmission factor of loop circuit, which contains (q-1) component/link in the channel of direct feed;

$\overline{R}_q$ - transmission factor of internal circuit of system from q components/links.

Substituting expression (2.20) in (2.9) we obtain

$$\bar{U}_{\text{вх}} - \left\{ \sum_{q=1}^{Q} \bar{K} \bar{A}_{q-1} \bar{B}_q \right\} \bar{U}_{\text{вх}} = \bar{U}_0, \qquad (2.23)$$

whence

$$\bar{U}_{\text{вх}} = \frac{\bar{U}_0}{1 - \sum_{q=1}^{Q} \bar{K} \bar{A}_{q-1} \bar{B}_q}$$

and

$$\bar{U}_{\text{вых}} = \frac{\bar{K} \bar{A}_{Q-1} \bar{U}_0}{1 - \sum_{q=1}^{Q} \bar{K} \bar{A}_{q-1} \bar{B}_q} = \bar{U}_0 \bar{A}_Q, \qquad (2.24)$$

where

$$\bar{A}_Q = \frac{\bar{K} \bar{A}_{Q-1}}{1 - \sum_{q=1}^{Q} \bar{K} \bar{A}_{q-1} \bar{B}_q}$$

or

$$A_Q = K \bar{A}_{Q-1} \sum_{n=1}^{\infty} \left\{ \sum_{q=1}^{Q} \bar{K} \bar{A}_{q-1} \bar{B}_q \right\}^{n-1}.$$

Page 116.

Passing from complex transmission factors to transient responses, we will have

$$A_Q = K * A_{Q-1} * \sum_{n=1}^{\infty} \left\{ \sum_{q=1}^{Q} K * A_{q-1} * B_q \right\}^{[n-1]}, \qquad (2.25)$$

where sign # — symbol of fold of Stieltjes [38], and [n-1] indicates multiplicity of repetition of operation of fold.

Expression (2.25) is recursion formula for transient response of system of intersected rings. In order to determine the shape of pulses at the output of stepped transformer or traveling-wave amplifier, expression (2.25) can be substantially simplified. If device/equipment works under these conditions, during which the pulse duration is less than doubled time of landing run along one section, then for such pulses the equation of transient response will be

$$A_Q = K^{[Q+1]},$$

where K - the transient response of one component/link.

Without concerning thus far question about effect of wake current, let us examine passage of main impulse. Stepped transformer is schematically depicted on Fig 2.20. It is the line, which has N of heterogeneities (jump of wave impedance). Let us designate reflection coefficient from the heterogeneity with the passage of wave from left to right through ρ_n, where n - number of heterogeneity. In the first

approximation, we will consider reflection coefficient from the heterogeneity real.

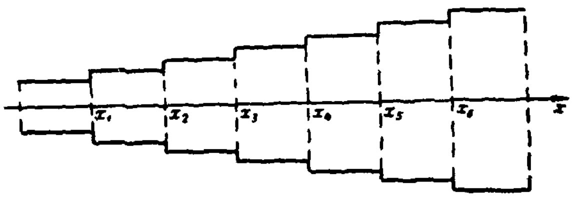

Fig. 2.20. Diagrammatic representation of stepped transformer.

Page 117.

Let us designate through u_n wave of voltage/stress, which passed through the n-th heterogeneity;, while is known,

$$u_n = u_{n-1}(1 + p_n).$$

It is obvious that if $p_n > 0$, then $u_n > u_{n-1}$; and if p<0, then $u_n < u_{n-1}$. The value of voltage/stress in the first case of its transformation on the heterogeneity is raised, and in the second case it is reduced. Thereby heterogeneity in the line can play the role of transformer with the transformation ratio

$$W_n = 1 + p_n.$$

After traversing N of heterogeneities, pulse will N of times transform itself; resulting transformation ratio in this case

$$W_T = W_N = \prod_{n=1}^{N} (1 + p_n).$$

Since p cannot be more than one, then W_n there cannot be more

than two and resulting transformation ratio will not exceed 2^N.

In order to determine transformation ratio of stepped transformer in diagram, it is necessary to consider its input and output circuits. Input circuit of transformer is shown in Fig. 2.21a. As can be seen from this diagram, the amplitude of voltage on the input of the transformer

$$U_0 = B\frac{\rho_1}{R_i+\rho_1}.$$

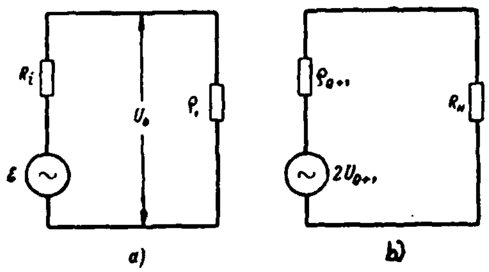

Fig. 2.21. Input (a) and output (b) circuits of stepped transformer.

Page 118.

Schematic of output circuit of transformer is shown in Fig. 2.21b. It consists of equivalent generator, emf. which is equal to $2U_{Q+1}$, and output resistance, equal to ρ_{Q+1}. Let us note relative to value $2U_{Q+1}$ that when the traveling wave of voltage/stress, which has amplitude U_{Q+1}, reaches the extended end/lead of the line, then receiving-end voltage becomes equal to $2U_{Q+1}$. This value is to emf of equivalent generator. Voltage/stress on the load

$$U_н = 2U_{Q+1}\frac{R_н}{R_н + \rho_{Q+1}}.$$

It is easy to see that when $R_н > \rho_{Q+1}$ voltage/stress on load can be more than U_Q, and when $R_н = \rho_{Q+1}$, with matched load, $U_н = U_{Q+1}$.

Taking into account input and output circuits transmission factor of stepped transformer will take form

$$W_{T\,общ} = K_{вх} W_T K_{вых},$$

where

$$K_{вх}=\frac{\rho_1}{\rho_1+R_г},$$
$$K_{вых}=\frac{2R_н}{R_н+\rho_{Q+1}}.$$

Let us determine, according to what law should be changed line characteristic in dependence on number of transition so that transformation ratio W_T would have maximum value. The number of sections of transformer Q+2(Q=N-1) and the relation of the wave impedance of extreme sections $\frac{\rho_{Q+1}}{\rho_1}=\theta$ we will assume/set by the given ones. Thus, it is necessary to find the condition, under which the product

$$\prod_{n=1}^{N}(1+p[n])$$

has maximum value. $\rho[n]$ here means that p is step function n.

Page 119.

It is possible to show that product will be maximally when all terms are equal to each other, i.e., when $p[1]=p[2]=p[3]=\ldots=p[N]$. In other words, maximum transformation ratio in the stepped transformer occurs in the case, when reflection coefficient is constant for each heterogeneity.

Since

$$p[n]=\frac{\rho[n+1]-\rho[n]}{\rho[n+1]+\rho[n]},$$

the increment in step function

$$\Delta\rho[n] = \mathrm{const}\,\{\rho[n] + \rho[n+1]\} \sim \mathrm{const}\,\rho[n]$$

is proportional to value of function itself. Hence it follows that $\rho[n]$ is the step function, formed from the exponential function

$$\rho[n] = Ae^{\alpha[n]}. \qquad (2.26)$$

Let us assume for convenience $\rho_1=1$, then $\rho_{N+1}=\theta$. For determining of A and α we have: when $n=1$ $Ae^{\alpha}=1$, and when $n=N+1$ $Ae^{\alpha[N+1]}=\theta$, whence

$$\alpha = \frac{\ln\theta}{N}, \quad A = e^{-\frac{\ln\theta}{N}}.$$

Finally we obtain, substituting α and A in (2.26),

$$\rho[n] = e^{\frac{\ln\theta}{N}[n-1]}. \qquad (2.27)$$

Let us find expression for maximum transformation ratio

$$W_{T\,\text{макс}} = \prod_{n=1}^{N}(1+\rho[n]) = \prod_{n=1}^{N}\frac{2\rho[n+1]}{\rho[n+1]+\rho[n]} = \prod_{n=1}^{N}\frac{2}{1+e^{-\frac{\ln\theta}{N}}} = \frac{2^N}{\left(1+e^{-\frac{\ln\theta}{N}}\right)^N}.$$

Page 120.

It follows of reasonings given above that stepped transformer, which possesses maximum transformation ratio, is system of intersected

rings, in which all components/links are indent, and also rings, which consist of identical number of components/links. Therefore the formulas, derived above for the system of the intersected rings, can be used for the analysis of this transformer.

Let us turn now to calculation of wake current. Let us take account of the fact that the coefficients of reflection are assumed to be real and that reflection coefficient with the passage of wave from right to left has opposite sign in comparison with the coefficient of reflection of wave with the passage of it from left to right. Let us take also into consideration the fact that the reflection coefficients from all heterogeneities are equal. In this case transient response for the main impulse

$$A_Q(t)=(1+p)^{Q+1}1(t-Qt_3)\quad (t<Qt_3).$$

Main impulse will appear at output after time Qt_3 in comparison with onset of pulse at input [1].

FOOTNOTE [1]. Here is not taken into consideration the time lag of pulse in the line to the first heterogeneity and after latter/last heterogeneity, since these sections of lines do not enter into loop circuit. ENDFOOTNOTE.

The first echo pulse will arrive more lately to period $2t_3$, and in order to determine its value, it is necessary in expression (2.25) to select the terms, which operate in the interval of time $[Qt_3(Q+2)t_3]$.

After conducting this operation, we will obtain that the transient response is determined by the expression

$$A_Q(t)=(1+p)^{Q+1}\{1(t-Qt_3)-Qp^2 1[t-(Q+2)t_3]\}$$
$$[t<(Q+2)t_3].$$

Analogously can be found transient response for greater moments of time, for example,

$$A_Q(t)=(1+p)^{Q+1}\Big\{1(t-Qt_3)-Qp^2 1[t-(Q+2)t_3]+$$
$$+\Big[\Big(Q+\frac{1}{2}Q(Q-1)\Big)p^4-(Q-1)(1+p)^2p^2\Big]\times$$
$$\times 1[t-(Q+4)t_3]\Big\}\quad [t<(Q+4)t_3]$$

and so forth.

Page 121.

For normal functioning of device/equipment, which stands after transformer (for example, magnetron generator), greatest danger they are first and second pulses, which follow after main impulse. On the basis of the expressions for the transient response of stepped transformer given above it is possible to write formulas for the values of the first and second pulses, in reference to the amplitude of main impulse, namely

$$\alpha_1=-Qp^2, \qquad (2.28)$$
$$\alpha_2=\Big[Q+\frac{Q(Q+1)}{2!}\Big]p^4-(Q+1)p^2. \qquad (2.29)$$

Coefficients $\alpha_{1,2}$ are function of number of rings Q=N-1 (where N - number of heterogeneities) and of coefficient of reflection p. As it follows from the formulas, coefficient α_1 is always negative, and

coefficient α_2 can be both the positive and negative. With the assigned magnitude θ of the relation of the wave impedance of extreme sections the greater the number of heterogeneities N or the number of rings Q, the less p. Therefore with increase in N coefficients α_1 and α_2 decrease; furthermore, coefficient α_2 becomes negative.

As already mentioned in Chapter 1, presence of heterogeneities in the form of change in geometric dimensions of line leads to distortion of field distribution in vicinities of heterogeneities and to appearance of waves of highest types. Weakening oscillation, which is realized due to the appearance of waves of the highest types, it is possible to consider certain shunt capacitance C_n after introducing in the place of transition. Taking into account this capacity/capacitance the equivalent diagram of junction can be represented in the form, shown in Fig. 2.22a. In this figure $2U_{n-1}$ — equivalent emf of the generator, which replaces the left side of the line; ρ_{n-1} — its output resistance, equal to the wave impedance of left (n-1)-1 section; ρ_n - wave impedance of the n section; C_n - transition capacitance. This equivalent diagram can be given to the diagram of the integrating component/link with resistor/resistance $R=\frac{\rho_{n-1}\rho_n}{\rho_{n-1}+\rho_n}$ and capacity/capacitance C_n; to the component/link applied voltage/stress $2U'_{n-1}=2U_{n-1}\frac{\rho_n}{\rho_n+\rho_{n-1}}$ (Fig. 2.22b).

Page 122.

Time constant of component/link $\tau_n=C_nR$. Square pulse is distorted in transit through this heterogeneity. Time of its establishment

$t_y = 2{,}2\tau_n$. If the pulse duration is less than doubled time of landing run of its along the section of transformer, then the time of the establishment of the edge of the pulse, which passed N of heterogeneities,

$$t_y = 2{,}2\sqrt{\tau_{n1}^2 + \tau_{n2}^2 + \ldots + \tau_{nN}^2}.$$

In the particular case all time constants of transitions/junctions can prove to be approximately identical and then $t_y = 2{,}2\tau_n\sqrt{N}$. It should be noted that usually capacity/capacitance C_n is very small, and if the wave impedance of the sections of transformer is sufficiently low, then the effect of transition capacitance is virtually imperceptible.

Relation of wave impedance of extreme sections, determined by design considerations, can serve for calculating stepped transformer by initial value. Stepped transformer is conveniently performed in the form of strip line. The value of transformation ratio W_T depends on value θ and number of transitions/junctions. For determining the number of transitions/junctions it is possible to use tables 2.6.

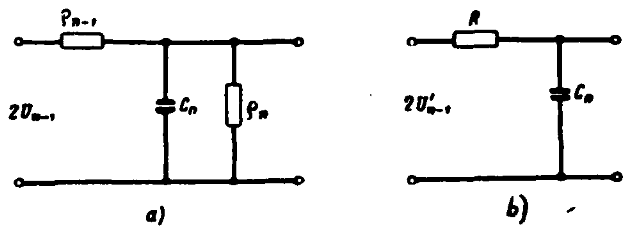

Fig. 2.22. equivalent schematic of the section of transformer with the heterogeneity: a) initial; b) converted.

Table 2.6.

θ	(1) Коэффициент трансформации W_τ			
	N=1	N=2	N=3	N=4
2	1,33	1,36	1,38	1,39
4	1,60	1,76	1,84	1,88
6	1,71	2,00	2,15	2,20
8	1,78	2,20	2,35	2,50
10	1,82	2,28	2,55	2,70

Key: (1). Transformation ratio ....

Page 123.

Knowing number of transitions/junctions, we are assigned by wave impedance of first transition/junction and find wave impedance of subsequent sections through formula (2.27). The length of each section is determined from condition $l = \frac{15 t_n}{\sqrt{\varepsilon}}$ [cm] (t_n expressed in the nanoseconds). Transition capacitance usually is very small and it is possible not to consider it. For calculating vake current it is possible to utilize formulas (2.28), (2.29).

Stepped transformers can be fulfilled not only in the form of

distributed circuits. For the sufficiently long pulses (on the order of hundreds of nanoseconds) and in the case, when to their form it is not presented especially stringent requirements, the sections of stepped transformer can be manufactured from the equivalents of long lines, i.e., be fulfilled in the form of the chains/networks of filters. Such transformers are used, in particular, in the pulse-shaping circuits of pedestal in the powerful/thick pulse modulators of magnetron generators [39]. The number of components/links in the section and the value of their parameters are selected on the basis of the condition for the permissible distortions of pulses, i.e., the guarantee of the necessary for broad-band character diagram, while the number of sections - on the basis of the guarantee of the assigned transformation ratio, which usually is determined by the values of the resistance/resistor of load (for example, with the resistor/resistance of magnetron in the pulsed operation) and by output resistance of pulsed source.

2.7. Inverters of pulses and the transformers, formed by the cable segments.

Lines with variable/alternating section, just as spiral transformers, do not change polarity of transformed pulses. Therefore frequently it is necessary to supplement such transformers by inverters.

As inverter can be used section/segment of coaxial cable with

wave impedance ρ, at the beginning of which is connected source of voltage $2\mathcal{E}$ with internal resistor/resistance ρ (Fig. 2.23). The external facing of cable is everywhere, besides initial point, isolated/insulated from the earth/ground. At the end/lead of the cable is included/switched on the potentiometer, whose resistor/resistance is equal to ρ.

Page 124.

If the wiper is located in position Q, then between point P and earth/ground operates the pulse of the same polarity, as at the input. If the wiper is supplied in position P, then the pulse of the reversed polarity will operate between point Q and earth/ground. When slide/wiper is located halfway, symmetrical output is obtained. It is not difficult to see that this phase inverter can work only at the high frequencies, since in the position of slide/wiper at point P generator at the low frequencies proves to be short-circuited.

Work of this phase inverter occurs as follows. The traveling wave of voltage/stress u appears with the connection to the input of the cable of voltage/stress in it. This wave of voltage/stress causes current wave i, which flows along the internal conductor of cable. This current, flowing/occurring over the resistance/resistor of load ρ, creates on it the voltage drop, which is removed/taken at points P or Q in the positive or negative polarities with respect to the earth/ground.

Since point Q of outer covering of cable is located under specific voltage/stress with respect to earth/ground, over external braid/cover of cable flows/occurs certain current i_1. The resistor/resistance of the external braid/cover of cable is connected in parallel to the resistance/resistor of load (in the position of slide/wiper at point P) and shunts it. It is obvious that by-passing of this resistor/resistance is the greater, the lower the frequency of the transformed vibrations. For the direct current this resistor/resistance is in effect equal to zero.

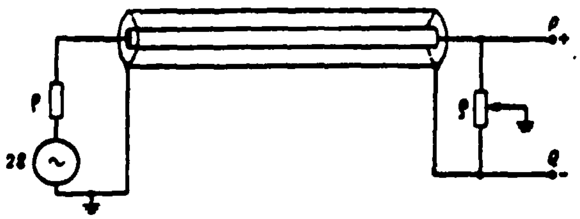

Fig. 2.23. Diagram of inverter, assembled in cable segment.

Page 125.

In order to increase inductive reactance of outer covering of cable, it they displace into coil in such a way that its self-capacitance would be minimum. In this case in parallel to the resistance/resistor of load ρ proves to be connected inductive reactance $j\omega L_K$, where L_K - inductance of the convoluted into the coil cable, as can be seen from the equivalent diagram, given in Fig. 2.24a. On this diagram of severings of cable it is replaced with the voltage source with emf $2U_n$ (where U_n - voltage/stress of the traveling wave in the line) and with internal resistor/resistance ρ. According to the theorem of Tevenen [transliterated] the resistance/resistor of load ρ can be converted in the internal resistor/resistance of source, and then diagram will take the form, shown in Fig. 2.24b. It is the inductive differentiating circuit, the time constant of which $\tau_K = \frac{2L_K}{\rho}$.

During the supplying to input of inverter of single drop/jump in voltage/stress, voltage/stress on its output, i.e., transient response of inverter, takes form

$$A(t) = e^{-t/\tau_{\text{н}}}.$$

In this expression, written on the basis of equivalent diagram, given in Fig. 2.24b, is not taken into consideration influence of circuit parameters, which block undistorted transmission of edge of pulses (this it is examined further).

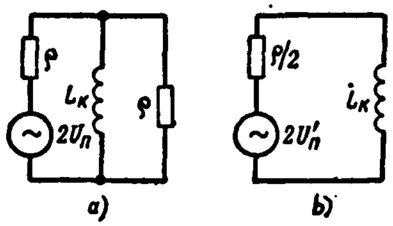

Fig. 2.24. Equivalent diagram of inverter: a) initial; b) converted.

Page 126.

Knowing the equation of transient response, it is easy to find the value of the distortions of pulse apex due to the differentiation. Decay in the pulse apex by duration $t_и$ will be determined from the formula

$$g=\frac{\Delta\mathscr{E}}{\mathscr{E}}=1-e^{-\frac{t_и}{\tau_K}},$$

where $\Delta\mathscr{E}$ - absolute decay in the apex/vertex;

$\mathscr{E}$ - pulse amplitude.

If $t_и \ll \tau_K$, then

$$g\approx\frac{t_и}{\tau_K}.$$

Knowing duration of pulses $t_и$ and being assigned by permissible value of decay in apex/vertex g, it is easy to find time constant τ_K. Since value ρ usually is assigned or selected previously, then through known τ_K and g is found the value of inductance L_K, necessary for the transmission of the flat/plane part of the pulses without the distortions. It follows of the formulas given above that the less the

duration of the inverted pulse, the less the required value $L_к$ and therefore inverter is obtained simpler in structural/design sense. This fact makes the inverters (and transformers), carried out in the cable segments, promising from the point of view of transition/junction to the pulses of smaller duration. Let us note also that with the decrease of the length of cable, caused by the decrease of desired value $L_к$, decrease the distortions of the pulse edge due to the losses in the cable. For loading $L_к$ they coil cable around the annular cores from the ferromagnetic materials. Similar constructions/designs are described below.

Distortion of edge of transmitted pulses occurs, in the first place, due to losses in metal and dielectric of cable. This question was examined in Chapter 1.

Presence of output capacitance in source of surge voltage and input capacitance of load is second reason for distortion of pulse edge. These capacities/capacitances together with input and output resistance of diagram form the integrating chains/networks, which lead to the decrease of the slope/transconductance of the build-up/growth of the pulse edges.

Page 127.

Time constant of output chain/network $\tau_{вых}=\frac{1}{2}\rho C_{вх}$; with $\rho=150$ Ohm and $C_{вх}=10$ pF $\tau_{вых}=0,75$ ns and $t_у=2,2\tau_{вых}=1,65$ ns. If the time constant of input circuit has the same value, then the time of establishment

increases $\sqrt{2}$ once. Therefore during the construction of inverters and transformers it is necessary as far as possible to decrease the parasitic circuit parameters. By advantage to decrease the parasitic circuit parameters. The advantage of inverters and similar type transformers are their linearity, simplicity of construction/design in comparison with the transformers of other types, to transmissivity large power. The deficiencies include large overall dimensions and large signal delay.

In inverter, described into [40], cable with length of 8 m with wave impedance of 72 ohms (diameter of 4.8 mm) was wound in coil and included into housing by length about 140 mm and by diameter of 190 mm. The time of the establishment of the transient response of this inverter was 2 ns; time constant τ_K was equal to 0.8 μs. Instead of the potentiometer at the end/lead of the cable were utilized two plugs, to which were connected internal conductor and screen/shield. Grounding points P or Q was realized with the aid of the special short-circuiting plug.

Another construction/design of inverter is described into [41]. The inverting transformer was connected in parallel to the plate load of tube, and therefore the inductance of the coil, formed by the external braid/cover of cable, was selected from the condition

$$L_K > \frac{t_u}{g} \frac{R_a R_i}{R_a + R_i},$$

where t_u - maximum pulse duration;

g - permissible relative decay in the apex/vertex;

$R_н$ - load resistance/resistor;

R_i - anode resistance in the pulsed operation.

For loading of external braid/cover of cable latter uncoiled itself into coil, into which was introduced ferrite core. For decreasing the interturn capacity/capacitance of this coil, it was made in the form of two sections. The first section consisted of 7 turns of cable PK-50-2-13, wound to the ferrite toroid by the diameter of 30 mm and by the section 6×6 of mm^2, forming inductance 30 μH. This section was connected directly to the anode of tube.

Page 128.

The second, main section consisted of 17 turns of the same cable, wound to the ferrite ring with an outside diameter of 56 mm and with a cross-section of 11×12 mm^2. The total inductance of this coil was approximately 400 μH and it was sufficient for pulse advancing with duration to 400 ns with the decrease of voltage/stress on the pulse apex not more than on 10%. The length of coaxial cable was 2 m, which created the time delay of pulse of approximately 10 ns. The duration of the pulse edge at the output was approximately 3 ns.

In this case, when grounding facings of cable is impossible, for realization of inversion of pulses should be included cable segments in the manner that it is shown in Fig. 2.25. The switching on/inclusion of cables with a wave impedance of $\rho/2$ shown in the figure provides input and output resistance, equal to ρ. The

inversion of pulses is realized here due to a change in the order of the connection of the supplying and load cables to inverter [42].

Constructions/designs of inverters described above have the deficiency, that for higher frequencies of pulse spectrum cable convoluted into coil is not inductance, but it presents certain distributed system. Therefore are used such constructions/designs, in which the cable is coiled around the cylinder so that the external braid/cover of cable forms the internal conductor of the helix of transmission. The external conductor of helix is formed by the screen/shield, inside which consists the cable (Fig. 2.26) [40]. A similar construction/design differs from preceding/previous in terms of the fact that here in parallel to the load resistance/resistor stands the input resistance of helix. This resistor/resistance is sufficiently to large, since helix has large linear inductance.

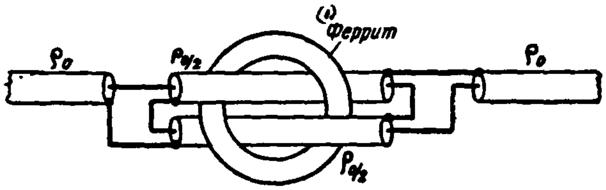

Fig. 2.25. Inverter, which does not have grounded points.

Key: (1). Ferrite.

Page 129.

Equivalent diagram of an inverter of such type will differ from the equivalent diagram of inverter with the cable, wound by coil, fact that inductance L_K will be in it replaced with input resistance to helix R_{BX}. If the pulse duration is such, that the signal reflected from the end/lead of helix will not have time to return conversely, i.e., if the pulse duration is less than doubled time of landing run of signal along the helix, then line impedance there will be to its purely active and equal wave impedance. In this case the pulse will traverse the inverting device/equipment without the distortions of flat/plane part. But if the pulse duration is more than doubled time of landing run, then pulse apex will be distorted due to the reflections in the helix.

Fig. 2.27 shows diagrams/curves of emf on input of inverter, equal to $2\mathscr{E}$, and modulus/module of voltage/stress on its output. It follows from the figure that the pulse at the output delays in comparison with the pulse at the input to period t, (delay time in coaxial cable). The amplitude of this pulse $U=k\mathscr{E}$, where k -

coefficient, which characterizes the reduction of the amplitude of output voltage/stress due to by-passing of the wave impedance of helix ρ_c; $k = \frac{\rho_c}{\rho_c + \frac{1}{2}\rho}$.

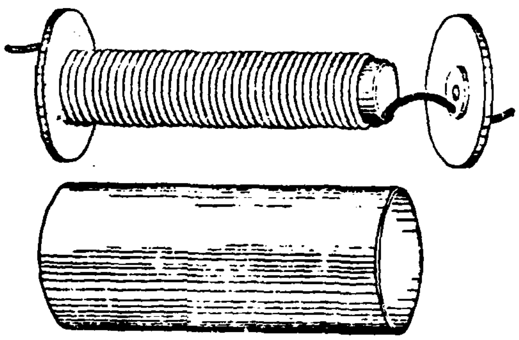

Fig. 2.26. Form of inverter with helix.

Page 130.

After time $2t_{3c}$ (doubled time of landing run of ol along the helix) to the output comes the echo pulse of negative polarity $\mathcal{E}'$, and the amplitude of output voltage/stress decreases. After another time $2t_{3c}$ to the output again comes the echo pulse, on already smaller amplitude and so on, as a result of which the apex/vertex of output pulse is collapsible/dropped. After using the formulas, given in § 2.2, it is easy to find expression for the signal reflected. Since $\rho_c > \rho$, then reflection coefficients from both ends/leads of helix are negative; their product has positive sign, and therefore inverse cyclic bond, formed by the mismatched helix, is positive. Omitting intermediate linings/calculations, it is possible to show that the envelope of output voltage/stress, given in Fig. 2.27b dotted line, is the exponential function

$$P(t) = ke^{-t/\tau_{oe}},$$

where

$$\tau_{oe} = t_{3c} \ln \frac{2\rho_c + \rho}{2\rho}.$$

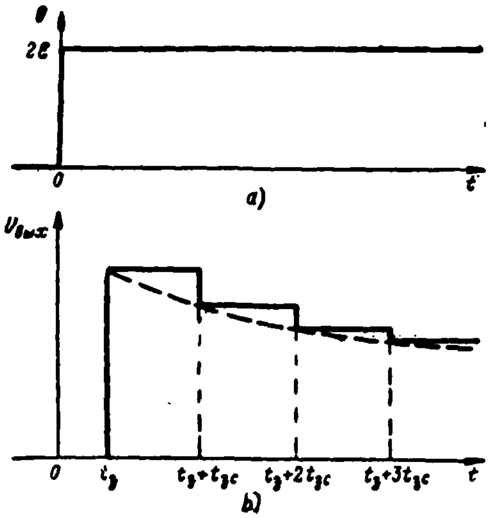

Fig. 2.27. Voltages on input (a) and output (b) of inverter with helix.

Page 131.

Principle of construction of phase inverter in section/segment of coaxial cable can be used also for construction of transformers. Fig. 2.28 schematically shows the simplest transformer with the transformation ratio, equal to two. It consists of two sections/segments of coaxial cable of the equal length, whose center conductors are connected to the center conductor of the supplying cable. Thereby with respect to it they prove to be switched on in parallel, so that the input resistance of transformer $Z_{вх}=\rho/2$. At the output severings of cable are connected in series, and output resistance of transformer $Z_{вых}=2\rho$. Transformation ratio of this transformer $n=\sqrt{\frac{Z_{вых}}{Z_{вх}}}=2$.

In order to clarify mechanism of action of this transformer, let us turn to its equivalent diagram, given in Fig. 2.29. On this diagram the lower cable segment is represented in the form of equivalent generator with emf, equal to $2\mathcal{E}$, and by internal resistor/resistance ρ. The output of this cable, as can easily be seen, is shunted by resistor/resistance Z_{κ}.

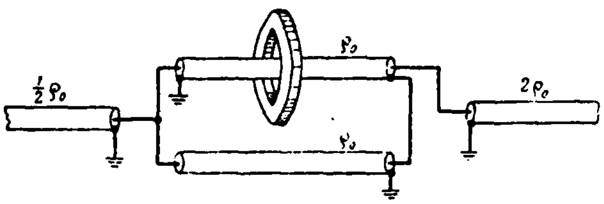

Fig. 2.28. Schematic of transformer in cable segments.

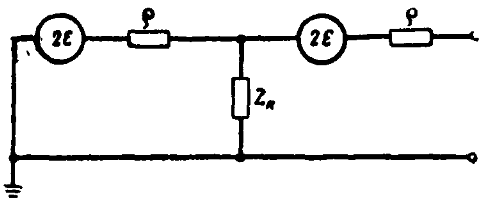

Fig. 2.29. Equivalent schematic of transformer.

Page 132.

If resistor/resistance of facing of cable Z_K is sufficiently great, then it can be excluded from equivalent diagram and entire device/equipment will be certain equivalent generator with emf $4\mathcal{E}$ and internal resistor/resistance of 2ρ. The input resistance of this transformer, as can be seen from diagram, it is equal $\rho/2$, whence the transformation ratio of transformer on the voltage/stress is equal to two.

Similar to transformer with two cable segments transformers in n cable segments can be constructed. Since the input terminals of all cables are connected in parallel, the input resistance of transformer from the N sections/segments will be equally ρ/N; whereas output resistor/resistance equally ρN since the output terminals of the cable

segments are connected in series.

One of samples of matching transformers was described into [42]. Transformer consisted of ferrite toroid with a cross section of $\frac{1}{4''}\times\frac{1}{4''}$ and an outer diameter 1". In the transformer the sections/segments of miniature coaxial cable with a length of 30 cm with a wave impedance of 100 ohms were utilized. Cable (6 turns) was packed on the toroid. Testing this transformer showed that the distortions of the pulse edge were negligible and are determined only by distortions in the cable (duration of the pulse edge it was approximately 1 ns).

Page 133.

CHAPTER THREE.

IMPULSE SHAPING IN LINEAR DISTRIBUTED CIRCUITS.

Different shapers are utilized together with relaxation oscillators in pulse technique for obtaining pulses. The forming circuits contain usually linear and nonlinear elements. When fundamental network elements of formation are linear, it is possible to speak about the linear shapers.

By linear method of formation is understood, in particular, method, based on conversion of voltage/stress, applied to input of linear network, and also method of obtaining pulses on certain load element by its connection/attachment to linear network, which contains statically stored energy. Thus, as a result of changing the energy, stored up in the reactive/jet elements of the linear network, caused by the commutation of equivalent components, appears the transient process, which is utilized for the impulse shaping.

If method of formation is connected with need to preliminarily have initial drop/jump in voltage/stress, which is supplied to linear forming circuit, then in this case is excluded from examination method of obtaining steep edge in voltage/stress.

Page 134.

Both process of impulse shaping of one or the other form from drop/jump in voltage/stress or current and method of obtaining very steep edges is very important for nanosecond pulse technique, since minimum duration of formed/shaped pulse is limited to finite time of initial drop/jump in voltage/stress or current.

In relaxation oscillators of nanosecond pulses, described in subsequent chapters, it is difficult to obtain pulses by duration of order of nanosecond with their considerable amplitude (to ones and tens of kilovolts). In the difference that relaxation oscillators different pulse-shaping circuits make it possible to obtain nanosecond pulses with the large amplitude. For guaranteeing a sufficient broad-band character of diagrams of formation it is expedient to utilize as fundamental network elements of system with the distributed constants. Using the diagrams of formation with the transmission lines as the fundamental elements, it is possible to obtain the pulses of short duration, in the form very close to the rectangular. Is substantial the fact that the duration of the formed/shaped pulses is determined here only by the parameters of circuits and does not depend on the mode of feeding of the corresponding devices/equipment.

In this chapter are examined fundamental questions of obtaining nanosecond pulses, mainly, with the aid of linear forming lines of transmission and corresponding switching devices/equipment.

3.1. Methods of impulse shaping in the uniform lines from drops/jumps in the voltage/stress or current.

Impulse shaping can be realized with the aid of initial drop/jump in voltage/stress or current. In this case to the forming circuit from the primary source a drop/jump in the voltage/stress or current is supplied.

In the case of presence of initial drop/jump in voltage/stress simplest of pulse (Fig. 3.1) is series connection of source of drop/jump in voltage/stress $U_{вх}(t)$, certain two-terminal network $Z_д$ and resistance/resistor of load $Z_н$. The two-terminal network, which ensures impulse shaping to this diagram, is usually called the two-terminal network of the first hearth. It must possess such characteristics that under the effect of an initial drop/jump in the voltage in the circuit (Fig. 3.1) would be the pulse of the assigned form.

Page 135.

If current taper is initial, then diagram of formation (Fig. 3.2) is parallel connection of source of current taper $I_{вх}$, forming two-terminal network $Z_д$, second kind called two-terminal network, and resistance/resistor of load $Z_н$.

Characteristics of forming two-terminal networks can be in general case determined on base of synthesis of forming circuits [1].

Examining the schematic of the formation Fig. 3.1, it is necessary to assign the required form of the output pulse of voltage/stress $u_{вых}(t)$, obtained from initial voltage/stress $u_{вх}(t)$. With assigned load $Z_н$ it remains to determine character two-terminal networks $Z_д$. Let us pass to the operational form of recording, in this case we will consider it known of the image of input and output voltages $\hat{u}_{вх}(p)$ and $\hat{u}_{вых}(p)$. Transmission factor of the diagram

$$\hat{K}(p)=\frac{\hat{u}_{вых}(p)}{\hat{u}_{вх}(p)}.$$

Then for image $\hat{Z}_д(p)$ we obtain

$$\hat{Z}_д(p)=\hat{Z}_н(p)\left(\frac{1}{\hat{K}(p)}-1\right). \qquad (3.1)$$

Second aspect of task of synthesis of forming circuit consists of construction of circuit according to obtained expressions for $\hat{K}(p)$ and $\hat{Z}_д(p)$. Two-terminal network $\hat{Z}_д(p)$ is sometimes located through its transient response that it requires the determination of original A(t)1 of image $1/p\hat{Z}_д(p)$.

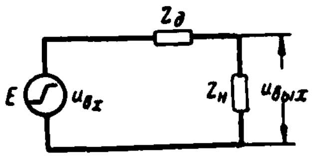

Fig. 3.1.

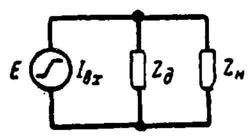

Fig. 3.2.

Fig. 3.1. Pulse-shaping circuit from drop/jump in voltage/stress.

Fig. 3.2. Pulse-shaping circuit from current taper.

Page 136.

Let at input of circuit (Fig. 3.1), which has as load effective resistance $\hat{Z}_{н}(p)=R_{н}$, operate drop/jump in voltage/stress $u_{вх}(t)=U_{вх}\cdot 1$, whose image $U_{вх}/p$. On the load it is necessary to obtain current pulse of right-angled with an amplitude of I and durations of $t_{н}$, i.e.,

$$\hat{u}_{вых}(p)=\frac{IR_{н}}{p}\left(1-e^{-pt_{н}}\right).$$

Transmission factor

$$\hat{K}(p)=\frac{IR_{н}\left(1-e^{-pt_{н}}\right)}{U_{вх}}.$$

Image of expression for the resistor/resistance of two-terminal network according to (3.1):

$$\hat{Z}_{д}(p)=R_{н}\left(\frac{1}{\hat{K}(p)}-1\right)=R_{н}\frac{U_{вх}-IR_{н}+IR_{н}e^{-pt_{н}}}{IR_{н}\left(1-e^{-pt_{н}}\right)}.$$

If we for simplification in obtained expression assume $2R_{н}I=U_{вх}$, then, multiplying numerator and denominator of fraction by $\exp(pt_{н}/2)$, we have

$$\hat{Z}_{\text{д}}(p) = R_{\text{н}} \frac{e^{p\frac{t_{\text{н}}}{2}} + e^{-p\frac{t_{\text{н}}}{2}}}{e^{pt_{\text{н}}/2} - e^{-pt_{\text{н}}/2}} = R_{\text{н}} \operatorname{cth} \frac{pt_{\text{н}}}{2}. \qquad (3.2)$$

Obtained expression coincides with image of input resistance of section of uniform line of transmission without losses, extended on end/lead and having wave impedance $\rho = R_{\text{н}}$, if length of line is equal to $l = 0{,}5\ vt_{\text{н}}$, where to v - wave propagation velocity in line, and $t_{\text{н}}$ - duration of formed/shaped pulse.

Actually, in this case line impedance is equal

$$Z_{\text{вх}}(j\omega) = -j\rho \operatorname{ctg} \frac{2\pi}{\lambda} l = R_{\text{н}} \operatorname{cth} j \frac{\omega t_{\text{н}}}{2}. \qquad (3.3)$$

Thus, two-terminal network of first hearth can be section of uniform line, extended at end/lead.

Page 137.

Analogous with this it is possible to show that for formation of square pulse on load $R_{\text{н}}$ from initial current taper (Fig. 3.2) as two-terminal network of second hearth section of uniform long zero-loss circuit, short-circuited at its end/lead can be utilized. The length of section/segment must be $l = \frac{vt_{\text{н}}}{2}$. In this case the line impedance is equal

$$Z_{\text{вх}}(j\omega) = j\rho \operatorname{tg} \frac{2\pi}{\lambda} l = R_{\text{н}} \operatorname{th} j \frac{\omega t_{\text{н}}}{2}. \qquad (3.4)$$

As in the preceding case, amplitude of current pulse I in load will be in this case equal to half of value of initial drop/jump.

In connection with the fact that duration of nanosecond pulses is short, then length of sections of forming lines proves to be small. With the impulse shaping of microsecond duration by the methods indicated the required length of line proves to be excessively large that it leads to the need of applying the artificial transmission lines, which possess considerably smaller broad-band character.

In both diagrams (Fig. 3.1 and 3.2) internal resistor/resistance of generator of drop/jump in voltage/stress is not shown (current). In the devices/equipment of the impulse shaping of nanosecond duration during the use of such diagrams usually the internal resistor/resistance of generator is commensurate with the load resistance/resistor.

For formation of square pulses from initial drop/jump in voltage/stress it is most expedient to use diagram, shown in Fig. 3.2. Here as the forming two-terminal network is conveniently used the section/segment of coaxial cable or entire diagram performed in the form of a coaxial system of the type of tee. The schematic diagram of this system is given in Fig. 3.3.

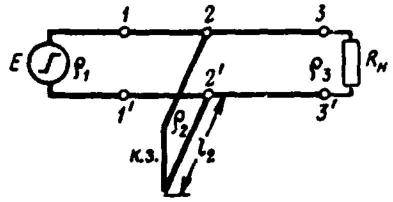

Fig. 3.3. Pulse-shaping circuit with the aid of line and short-circuited stub.

Page 138.

Here the line, which supplies from the generator a drop/jump in the voltage, has the wave impedance ρ_1, equal to the wave impedance of tee on its input part (point 1-1'). In section 2-2' is connected short-circuited stub by the length l_2 with a wave impedance of ρ_2. The output part of the tee (point 3-3'), loaded to effective resistance $R_{н}$, has wave impedance $\rho_3 = R_{н}$.

Process of impulse shaping is explained by Fig. 3.4, where is shown wave allocation of voltage/stress in different sections of tee at different moments of time $t_1<t_2<t_3<t_4$. At moment/torque t_1 the initial wave of voltage/stress yet did not achieve the points of 2-2' tees. Moment/torque t_2 corresponds to the time, when wave, after achieving points 2-2', underwent changes. The part of the energy formed the wave, which passed to the load (to points 3-3'), part formed the wave, which is propagated to the short-circuited end of the loop, and part - the wave in the supplying line reflected. The wave, reflected from the short-circuited end of the loop, has a polarity

opposite to initial wave. As a result of the superposition of three waves the shear/section of output pulse is formed/shaped (Fig. 3.5). It is evident from Fig. 3.4 that the square pulse will be formed on the load (at points 3-3') and repeated pulses will be absent, if there are no wave reflections at points 2-2', which is propagated from the short-circuited end of the loop, i.e., it is necessary to satisfy the condition

$$\rho_2 = \frac{\rho_1 \rho_3}{\rho_1 + \rho_3}. \qquad (3.5)$$

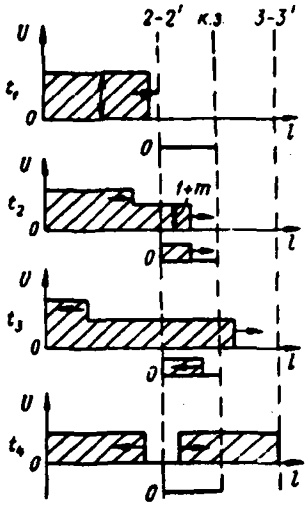

Fig. 3.4. Wave allocation of voltage/stress in sections of line with impulse shaping.

Page 139.

This condition defines both the relative values of wave impedance of sections/segments of tee and magnitude of losses of amplitude of initial drop/jump with impulse shaping, since value of coefficient of reflection of wave at input of tee is equal to

$$m = \frac{\frac{\rho_2\rho_3}{\rho_2+\rho_3} - \rho_1}{\frac{\rho_2\rho_3}{\rho_2+\rho_3} + \rho_1}. \tag{3.6}$$

Transmission factor of diagram is equal to

$$K = \frac{U_н}{U_{вх}} = 1 + m = \frac{1}{1 + \rho_1/R_н}. \tag{3.7}$$

Duration of formed/shaped pulse, equal to doubled delay time of

loop, it is determined by expression

$$t_{и} = \frac{2l_{з}}{v}, \qquad (3.8)$$

where $l_{з}$ - length of loop;

v - wave propagation velocity in it.

Using method of imposition, we will obtain for output potential of diagram, taking into account (3.7),

$$U_{вых}(t) = (1+m)\,[U_{вх}(t) - U_{вх}(t - t_{и})]. \qquad (3.9)$$

In real cases initial drop/jump in voltage/stress has finite time of build-up/growth and, consequently, also process of impulse shaping proceeds somewhat differently from for case of ideal drop/jump. Now instead of Fig. 3.5 let us examine Fig. 3.6.

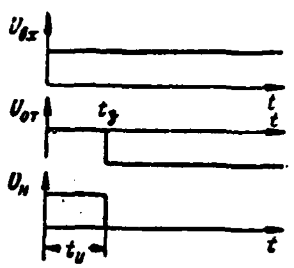

Fig. 3.5. Voltage oscillograms with impulse shaping with the aid of short-circuited section of line.

Page 140.

As can be seen from figure, the duration of shaped pulse (measured on the foundation) depends on the doubled delay time of short-circuited stub $t_з = 2l/v$ and on the duration of the front of initial drop/jump, i.e., $t_и = t_з + t_{ф0}$.

Pulse amplitude at output

$$U_{вых} = K \frac{t_з}{t_{ф0}} U_{вх}, \qquad (3.10)$$

where K - transmission factor of diagram, determined according to formula (3.7).

Minimum duration of shaped pulse in this case cannot be less than duration of front of initial drop/jump. It is easy to see from Fig. 3.6 that with $t_з$, that vanishes, the pulse duration approaches the duration of the front of initial drop/jump $t_и \to t_{ф0}$, however, the pulse amplitude in this case according to (3.10) vanishes. Actually, if we

examine the shortening (differentiating) RC network, to input of which is supplied a drop/jump in the voltage/stress of the exponential form:

$$U_{\text{вх}} = U_{\text{вх}}\left(1 - e^{-\frac{t}{\Delta}}\right),$$

the duration of front of which (measured at level 0.1 and 0.9 of amplitude) $t_{\Phi 0} = 2{,}2\Delta$, then the output voltage/stress, determined with the aid of the Duhamel integral, will be

$$U_{\text{вых}} = \int_0^t \frac{U_{\text{вх}}}{\Delta} e^{-\xi/\Delta} e^{-\frac{t-\xi}{\tau}} d\xi.$$

When time constant of circuit is equal to $\tau=\Delta$, output voltage/stress

$$U_{\text{вых}} = U_{\text{вх}} \frac{t}{\Delta} e^{-t/\Delta}.$$

Active duration of output pulse (measured at level 0.5 of amplitude) in this case is equal to 2.5Δ, i.e., it is approximately equal to duration of front of initial drop/jump. Now, if we decrease the time constant of circuit ($\tau<\Delta$), drawing it nearer zero, and to calculate $U_{\text{вых}}$, then it appears that the pulse amplitude rapidly decreases, while its duration remains virtually constant/invariable.

Page 141.

Thus, action of short-circuited stub in this respect is analogous with action of differentiating circuit with lumped parameters. Therefore the shortening of the pulse duration with the aid of the

short-circuited section of line is occasionally referred to as differentiation of the pulse of nanosecond duration.

When it is necessary to form pulse, whose duration (on foundation) must be less than duration of front of initial drop/jump in voltage/stress, it is expedient to use dual impulse shaping with the aid of two short-circuited sections of line (double differentiation). Fig. 3.7 shows the diagram of the dual shortening of the pulse duration. Here with the aid of the first tee it is necessary to form the pulse, whose duration (on the foundation) will be somewhat more than the duration of the front of initial drop/jump $t_{ф0}$, but the duration of its front $t_{ф1}$ is less $t_{ф0}$. After the second shortening tee it is possible to obtain the pulse, whose duration will prove to be somewhat more than $t_{ф1}$, but is considerably less the duration of the front of initial drop/jump.

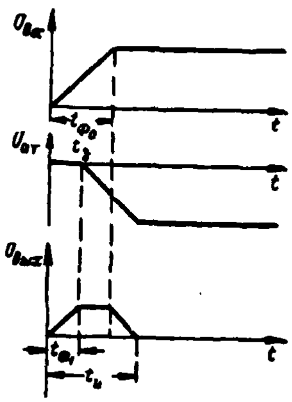

Fig. 3.6. Voltage oscillograms with impulse shaping from drop/jump in voltage/stress with final duration of front.

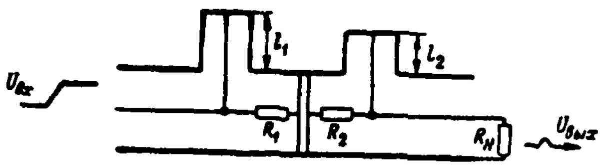

Fig. 3.7. Schematic of dual coaxial tee for pulse shortening.

Page 142.

The duration of the output pulse

$$t_{и}=t_{з1}+t_{з2}, \qquad (3.11)$$

where $t_{з1}$ and $t_{з2}$ - respectively doubled delays of the first and second loops, moreover $t_{з2}<t_{з1}$.

Amplitude of output pulse

$$U_{вых}=U_{вх}K_1K_2K_0\frac{t_{з2}}{t_{ф0}}, \qquad (3.12)$$

where $U_{вх}$ - amplitude of initial drop/jump in voltage/stress;

K_1 and K_2 - respectively transmission factors of the first and the second it is branch;

K_0 - transmission factor of attenuator.

Attenuator is placed between tees for eliminating noticeable effect of second tee on the first, which occurs due to presence of waves reflected, which appear in place for heterogeneity. Attenuator decreases the amplitude of the nearest echo pulse, which must traverse the attenuator 3 times, in $K^2{}_0$ once relative to the pulse, passing through the attenuator one time.

Methods of impulse shaping from drop/jump in voltage/stress (current) examined commonly are used for obtaining pulses of fixed period of time, and sometimes also for variable/alternating duration, if length of short-circuited stub can be regulated.

For impulse shaping with smoothly changing duration method, based on use of forming line and two initial drops/jumps in voltage/stress finds use (current). In this case the generator, which develops initial drops/jumps in the voltage/stress, puts out them with the specific temporary displacement, whose value smoothly changes, by changing the electrical mode of generator.

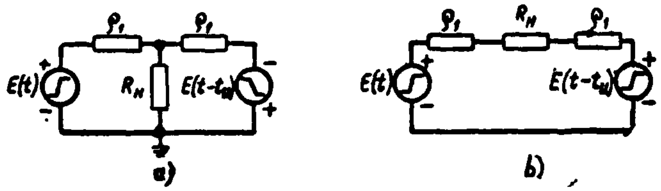

Fig. 3.8. Parallel (a) and consecutive (b) pulse-shaping circuits with adjustable duration.

Page 143.

Such diagrams can have in parallel series-connected load or (Fig. 3.8). In the case of series circuit (Fig. 3.8b) is hindered/hampered obtaining the point of zero potential in load or in one of the generators. In this respect is more convenient the diagram in Fig. 3.8a. Here the generator of a positive drop/jump in the voltage/stress with shaping of front and pulse apex is loaded both on the resistor/resistance $R_н$ and on output resistance of the generator, which creates the second drop/jump in the voltage/stress (negative). Therefore the transmission factor of diagram is equal to

$$K = \frac{2}{2 + \rho/R_н}. \qquad (3.13)$$

Deficiency in method of impulse shaping with the aid of two drops/jumps in voltage/stress is presence of waves reflected. propagating in the circuit of generator, which can lead to the onset of spurious pulses. Furthermore, the presence of two drops/jumps, shifted on the time, requires the high stability of the value of this

shift, since with the impulse shaping of nanosecond duration even the insignificant instability of this shift can substantially influence the stability of the pulse duration.

3.2. Methods of impulse shaping in the diagrams with the uniform discharge lines.

Methods of impulse shaping examined are connected with need for presence of initial drop/jump in voltage/stress or current. For the formation of square pulse this drop/jump must be ideal, i.e. have infinite steepness of front.

Method of impulse shaping, when drop/jump in voltage/stress is formed directly in squaring circuit, is of interest. Squaring circuit with the aid of the section of the extended line (Fig. 3.1) can be equivalent to shaping circuit with the charged/loaded to voltage/stress $E=U_{вх}=2IR_{н}$ section of the same line, locked at one end/lead to resistor/resistance $R_{н}$ (Fig. 3.9). This diagram is occasionally referred to as diagram with the discharge line.

Page 144.

In it is utilized the alternating discharge of line through effective resistance $R_{н}$, equal to line characteristic [1].

Energy of dc power supply E is utilized for charge of line through resistor/resistance of R_1, while electrical or mechanical

commutators are used for alternating discharge. The current pulse, which appears during the discharge of the section of uniform zero-loss circuit through the effective resistance, equal to wave impedance, and through the ideal commutator, has rectangular form. The duration of pulse $t_и$ is determined by the time of the dual passage of the wave of discharge current along the line

$$t_и = \frac{2l}{v} = \frac{2l}{c}\sqrt{\varepsilon\mu}, \qquad (3.14)$$

where l - length of line;

v - wave propagation velocity in it;

c - wave propagation velocity in the vacuum;

μ and ϵ - with respect the magnetic and dielectric constants of the material of line.

Since current wave in process of discharge of line has amplitude

$$I = \frac{E}{R_н + \rho} = \frac{E}{2R_н},$$

that on load resistance/resistor voltage pulse with amplitude of $U_{вых} = E/2$ is formed/shaped.

In actuality with impulse shaping of nanosecond duration is necessary to consider quality of agreement of line with load resistance/resistor, value and character of change in time of resistor/resistance of commutating element and presence of losses in forming line.

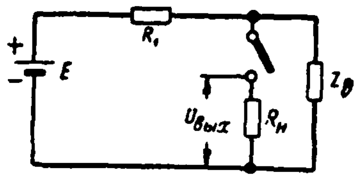

Fig. 3.9. Pulse-shaping circuit with discharge line.

Page 145.

In oscillator circuit condition of equality of load $R_н$ and line characteristic ρ always cannot be strictly carried out. In the process of operating the generator relation $R_н/\rho$ can prove to be somewhat more or less than one. The divergence of this relation from one affects the process of impulse shaping and it leads to the disturbance/breakdown of its form. In these cases due to the appearing partial reflections of waves (point or of voltage/stress) from the loaded end/lead of the line the process of its discharge lasts longer than in the case of the matched load. The shape of pulse on the load takes the form, shown in Fig. 3.10a and b, depending on that $R_н/\rho < 1$ or $R_н/\rho > 1$.

On the basis of expressions (3.3) and (3.2) for image of input resistance of forming line it is possible tc record

$$\hat{Z}_л(p) = \frac{1 + e^{-pt_н}}{1 - e^{-pt_н}}.$$

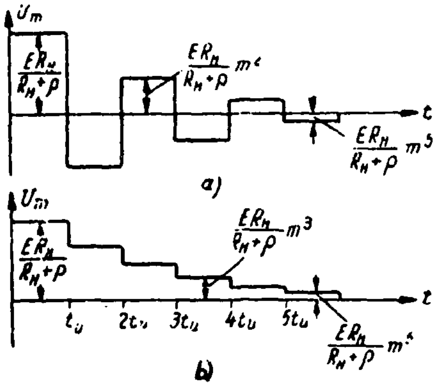

Fig. 3.10. Shape of pulse on load: a) when $\frac{R_н}{\rho}<1$; b) when $\frac{R_н}{\rho}>1$.

Page 146.

After finding then image for current in load, it is possible to obtain expression for voltage/stress on load, represented in the form of right-angled pulses by duration $t_и$, that appear consecutively/serially through gaps/intervals $t_и$. Expression for the amplitude of k pulse takes form [1]

$$U_к = E\frac{R_н}{R_н+\rho}m^{k-1}, \qquad (3.15)$$

where k=1, 2, 3, ...; m - coefficient of reflection of the waves:

$$m=\frac{R_н-\rho}{R_н+\rho}.$$

Expression for amplitude of voltage/stress makes it possible to determine permissible value of relation $R_н/\rho$ according to assigned ratio U_2/U_1, where U_1 - amplitude of the first, and U_2 - amplitude of second pulse (Fig. 3.10). So if it is assigned, which U_2 must comprise to

more than 5% of value U_1, then the value of relation $R_н/\rho$ takes values of 0.90 or 1.102. The load resistance/resistor in this case must be in limits $0{,}9\rho < R_н < 1{,}1\rho$.

Real forming lines with losses have transient responses with finite time of build-up/growth of their front. Therefore the shape of the obtained pulses into the reality differs from rectangular. The steepness of the front of transient response is determined by magnitude of losses in the line (coaxial cable, band line) and by its length. Therefore depending on the pulse duration the slope/transconductance of its shear/section changes, since required length of the forming line will be different.

In pulse generators of nanosecond duration of such type as discharge lines coaxial cables are utilized, or strip lines, slope/transconductance of frontal part of transient responses of which can be evaluated according to formulas, obtained in chapter 1.

Properties of commutating element affect besides line losses to shape of pulse. The commutating elements have a resistor/resistance, to equal to zero and changing in the time in the process of commutation. Therefore voltage/stress on the commutating element also varies for the time of commutation (Fig. 3.11) from certain value $U'_к$ to $U''_к$. This fact can lead to the noticeable divergence of the shape of the obtained pulse from the rectangular.

Page 147.

Essential is time $t_{\text{к}}$ for which is realized commutation, and also stability of commutation. The law of a change in the resistor/resistance of the commutating element, thus, determines the form of front and, consequently, also the shear/section of pulse. Fig. 3.12 shows the process of the discharge of the line, when the time of commutation is final. The duration of front and the cutter of the formed/shaped pulse can to a greater degree be determined by the characteristics of the commutating element, than by the special features of the transient response of line.

Therefore it is desirable so that resistor/resistance of commutating element (contact resistance) would be constant and it is close to zero. The contact of commutator must if necessary provide sufficiently high current. The instability of the time of commutation (with the formation of periodic pulses) must be considerably less than the assigned duration of the edge and o' pulse. The frequency of the formed/shaped pulses in this case is determined, as a rule, by the frequency of commutation. Therefore it is desirable so that the commutator would be controlled by external trigger pulse.

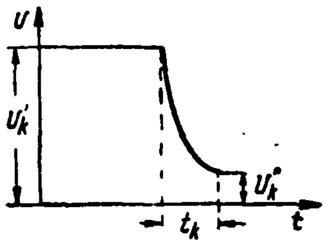

Fig. 3.11. Voltage oscillogram on commutating element.

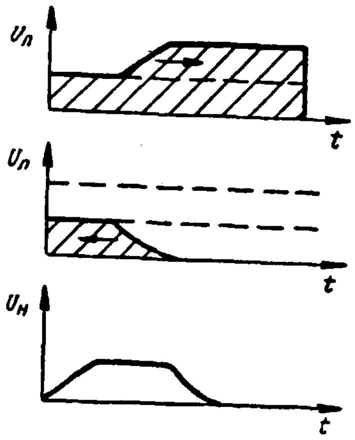

Fig. 3.12. Voltage oscillograms impulse shaping in diagram with commutator, which has finite time of commutation: $U_л$ - voltage/stress on line, $U_н$- voltage/stress on load.

Page 148.

In generators of nanosecond pulses find use switching devices/equipment, which use thyratrons, mechanical relay, electron tubes and and gap arrestors.

Output pulse in in practice utilized devices/equipment is transmitted through high-frequency cable, which is coordinated with

load resistance/resistor. If necessary for observation on the oscillograph of the formed/shaped pulse for guaranteeing the required synchronization it is desirable to provide in the diagram the output, from which it is possible to obtain the trigger pulse of scanning/sweep of oscillograph. For the same purpose the main impulse must be delayed on the period, required for functioning of sweep circuits. In these cases load resistor/resistance is made in the form of the voltage divider with several outputs, each of which is connected with the high-frequency cable, which has the necessary delay time of the pulse, transmitted through it. The input resistance of divider will be coordinated with the wave impedance forming lines taking into account the contact resistance of commutator.

During proper selection of forming line and commutating element for guaranteeing shape of pulse, close to rectangular (front and shear/section of order of ones or portions of nanosecond and absence of distortions on apex/vertex), it is necessary also to care about decrease of parasitic circuit parameters. The latter fact causes high requirements for the mounting of diagram.

With impulse shaping (Fig. 3.9) output pulse is removed/taken from load, whose resistor/resistance is equal to wave impedance of forming line.

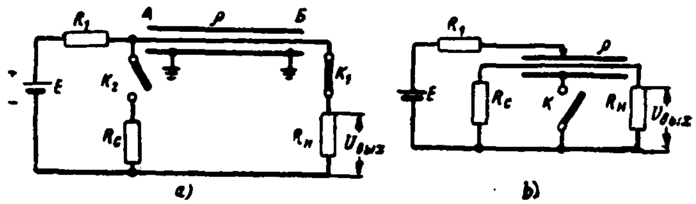

Fig. 3.13. Pulse-shaping circuit with line, loaded at both ends/leads: a) with two commutators; b) with one.

Page 149.

As the load usually are utilized coaxial cables, whose wave impedance has the small number of different nominal values.

This essential deficiency in diagrams to a considerable degree described earlier is removed in method of formation with discharge line, loaded to effective resistance at both ends/leads. Fig. 3.13a gives the diagram of formation, proposed by Yu. V. Vvedenskiy [43, 44], in which instead of the discharge line, extended at one end/lead, is used the line (coaxial cable), loaded at one end/lead for certain load $R_{н}$ (required on the working conditions) and on matched impedance $R_{с}$ at other end/lead.

Is here preliminarily charged/loaded through resistor/resistance of R_1 line at moment of closing/shorting key/wrench K_1 begins to be discharged. Let from the end/lead B along the line begin to be propagated the wave of voltage/stress U_1 less than E/2, since $R_{н} > \rho$ (Fig. 3.14).

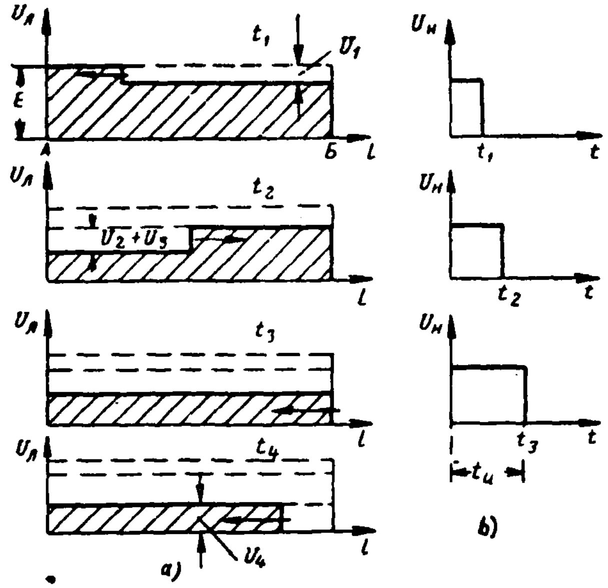

Fig. 3.14. Wave allocation of voltage/stress along line (a) and on load (b).

Page 150.

At the moment of the arrival of wave toward the end A of line is closed key/wrench K_2 the forming line it proves to be loaded to resistor/resistance R_c. Because of this conversely to load $R_н$ will go sum wave U_2+U_3, whose value is determined by the relationship/ratio between the wave impedance of cable ρ and by resistor/resistance R_c. Here U_2 - wave, reflected from end/lead A of line; U_3 - wave, caused during closing/shorting of key/wrench K_2. The relationship/ratio between the resistors/resistances ρ and R_c is selected in such a way that backward wave after reflection from load (at the end/lead B) would completely remove/take from it voltage/stress.

Since voltage/stress on load at moment/torque $t=t_{и}$ must be turned into zero, i.e.,

$$U_1+U_2+U_3+U_4+E=0, \tag{3.16}$$

it is possible to find from this condition value of matching impedance R_c. The amplitudes of the propagated waves will be respectively equal to:

$$\left.\begin{aligned}
U_1&=-E\frac{\rho}{\rho+R_{н}},\\
U_2&=-E\frac{\rho}{\rho+R_{н}}\frac{R_c-\rho}{R_c+\rho},\\
U_3&=-E\left(1-\frac{\rho}{\rho+R_{н}}-\frac{\rho}{\rho+R_{н}}\frac{R_c-\rho}{R_c+\rho}\right)\frac{\rho}{\rho+R_c},\\
U_4&=(U_2+U_3)\frac{R_{н}-\rho}{R_{н}+\rho}.
\end{aligned}\right\} \tag{3.17}$$

In resulting expressions final duration of wave front is not considered, but charging resistor R_1 is considered as the very large. If inequality $\rho\ll R_{н}$, occurs then matched impedance differs little from the wave impedance.

With change in value of load from $R_{н}=\rho$ to value $R_{н}\gg\rho$ value of matched impedance virtually on is changed. If the forming line has the low wave impedance (for example, it is used the corresponding strip transmission line), then the value of load can vary from ten of ohms to megohm with constant quantity of resistor/resistance R_c, and the shape of pulse remains rectangular.

Page 151.

As can be seen from operating principle of diagram, between moments/torques of closing/shorting keys/wrenches K_1 and K_2 is passed time, equal to half of duration of formed/shaped pulse. Changing the

time of closing key/wrench K_2, it is possible to regulate the pulse duration in the limits from the dual delay of the forming line to the doubled duration of the wave front, which is determined by the time of the commutation of key/wrench.

If time interval between closing/shorting of keys/wrenches K_1 and K_2 will be considerably more than delay time of formed/shaped pulse, then steps, explained by presence of wave reflection from extended end/lead A of line, will appear at apex/vertex of this pulse.

In real cases usually $R_c \approx 0.1 R_н$. With load change the amplitude of formed/shaped pulse, which is here greater than E/2, changes insignificantly. This change can be rated/estimated with use of the expression

$$\Delta U_{вых} \leqslant \left(1 - \frac{1}{1+\frac{R_c}{R_н}}\right) = \frac{\frac{R_c}{R_н}}{1+\frac{R_c}{R_н}}. \qquad (3.18)$$

Efficiency of this diagram is less than diagram with matched load (Fig. 3.9).

To deficiencies in method of formation in question can be attributed requirement for two keys/wrenches. Therefore, if there is no need for continuously variable control of the pulse duration, diagram can be altered, as this is shown in Fig. 3.13b [44]. In this case both waves of the voltage/stress of the discharge of line begin to be propagated from the ends/leads of the line during

closing/shorting of key/wrench simultaneously. The pulse duration is obtained here two times less, since it is determined now by the propagation of wave only in one direction.

Page 152.

3.3. Impulse shaping in non-uniforms circuit.

In some practical cases of impulse shaping of nanosecond duration of small and large power difficulties, connected with need for impedance matching of load with wave impedance of forming lines with the aid of special matching systems, are encountered, while in number of cases load contains except active even and reactance. In the case of pulsing of high voltage it is necessary to use the forming lines, designed for high voltages or large workers after all. This substantially complicates the construction/design of generators, it makes with its bulkier, which leads to an increase in the circuit parameters, which affect the duration of front and shear/section of the formed/shaped pulse.

Noted difficulty in number of cases succeeds in decreasing or completely removing during use those of heterogeneous forming lines.

Decrease in charging voltage (current) in the diagrams with non-uniforms circuit.

With impulse shaping of nanosecond duration of high voltage in

diagram with discharge line for reduction in voltage/stress on line it is possible to use method, proposed by O. N. Litvinenko, by V. A. Il'in, by V. I. Soshnikov [1, 45]. High charging voltage on the usual uniform forming lines depends on the fact that entire/all that energy, which during the pulse duration is realized on the load resistor/resistance, reserves itself in a comparatively small static capacity/capacitance of line. An increase in this capacitance for the assigned pulse duration is connected with a change in the line characteristic; in view of the fixed/recorded value of load, coordinated with the line characteristic, its change proves to be impossible.

Charging voltage of line can be reduced, if supplementary accumulator/storage, which accumulates part of energy, reserved by device/equipment will be included in oscillator circuit. Lumped capacitance can perform the role of this accumulator/storage (Fig. 3.15). However, in this case it is not possible to use the uniform forming line, since the inclusion in the diagram of lumped capacitance will change the resistor/resistance of circuit and generator it will lose its forming properties.

Page 153.

Input resistance of diagram with capacitance and non-uniform circuit, measured between points a-a' with off voltage source and resistor/resistance $R_{\text{н}}$ must be determined by expression (3.2)

$$\hat{Z}_{вх}(p) = R_н \operatorname{cth} \frac{pt_и}{2}.$$

For determination of necessary law of change in wave impedance of non-uniform circuit it is possible to examine equivalent diagram (Fig. 3.16), comprised for determining voltage/stress on resistor/resistance $R_н$. Charged/loaded to voltage/stress E the section of line is here represented in the form of the dc power supply E and resistor/resistance $Z_{вх}$, measured between points b-b'. The pulse on load $R_н$, which appears after closing/shorting of key/wrench K, will have rectangular form in such a case, when the current, flowing through this resistor/resistance for time $t_и$, will not change its value. This is possible in such a case, when the source of voltage E it is loaded the resistor/resistance, which has purely active character. In other words, resistor/resistance $Z_{вх}$ must be the series connection of effective resistance and negative capacitance, which on the modulus/module must be equal to capacitance of C.

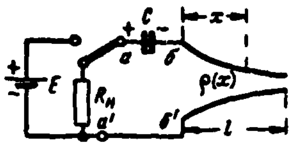

Fig. 3.15.

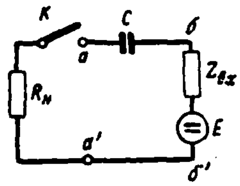

Fig. 3.16.

Fig. 3.15. Diagram of generation of pulse with non-uniform circuit and supplementary capacitor/condenser.

Fig. 3.16. Equivalent schematic of shaper.

Page 154.

It is possible to show that in this case it is necessary to use parabolic type non-uniform circuit, whose wave impedance along the axis of line changes according to the law of [45]

$$\rho(x)=\rho_0\left(1-\frac{x}{N}\right)^2, \qquad (3.19)$$

where x - coordinate, calculated off the beginning of line along its longitudinal axis;

N - parameter of line, which characterizes rate of change of its wave impedance;

ρ_0 — wave impedance in the beginning of line.

Input resistance of this line (extended at end/lead) is expressed

$$\hat{Z}_{вх}(p)=\rho_0\left(\mathrm{cth}\frac{pt_и}{2}-\frac{1}{pC_1}\right), \qquad (3.20)$$

where C_1 - capacitance, whose value is determined by

relationship/ratio

$$C_1=\frac{N}{v\rho_0};\qquad(3.21)$$

v - wave propagation velocity along line.

As is evident, input resistance of parabolic line differs from input resistance of usual uniform forming line only by presence of term - $1/pC_1$, that is operational image of resistor/resistance of certain negative capacitance. Thus, the actually consecutive compound of this line with capacitance C, in the absolute value of the equal capacitor C_1, forms circuit with an input resistance of

$$\hat{Z}(p)=\rho_0 \operatorname{cth}\frac{pt_u}{2},$$

which coincides with the image of the resistor/resistance of the usual forming two-terminal network.

Thus, circuit in the form of series connection of line, whose wave impedance changes according to parabolic law, and lumped capacitances can serve as discharge line in squaring circuit.

Presence in this generator of supplementary capacitance of C makes it possible to substantially lower working voltage/stress on line. Actually, in the process of the charge of diagram supply voltage proves to be applied to the circuit, formed by the consecutive connection of capacitance of C and static capacitance of line, and after the termination of charge it is divided between the elements indicated inversely proportional to the values of their capacitance.

Page 155.

Selecting capacitance value C, it is possible to ensure decrease in charging voltage to a certain degree directly on line.

It is considered during selection of capacitance value C that it determines required rate of decrease of wave impedance along axis of non-uniform circuit, i.e., determines parameter N. Virtually capacitance of C can be equal to the static capacitance of line. In this case it is possible to use voltage-doubling circuit, in which during the charge of circuit capacitanc of C, connected in parallel with the line, is connected to the source of voltage E and is charged up to the value of this voltage/stress.

These elements prove to be those switched on between themselves consecutively/serially during discharge of circuit (with impulse shaping), in view of which general/common equivalent emf, which operates in discharge circuit, is equal to doubled supply voltage. This fact allows approximately doubly (with an accuracy to a voltage drop across commutator) to reduce the value of supply voltage.

If for impulse shaping is utilized diagram with second-order two-terminal network (with short-circuited line), then it is possible to lower charging current by inclusion in forming circuit of supplementary inductance L (Fig. 3.17). Inductance here plays the same role, as capacitance in the diagram in Fig. 3.15.

For impulse shaping of right-angled in this diagram it is necessary to utilize non-uniform circuit, whose wave impedance changes according to hyperbolic law

$$\rho(x)=\frac{\rho_0}{(1-x/N)^2}. \qquad (3.22)$$

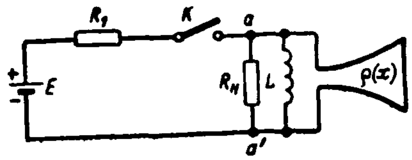

Fig. 3.17. Pulse-shaping circuit with non-uniform circuit and supplementary inductance.

Page 156.

In this case value of inductance must be undertaken equal to

$$L = N\rho_0/v, \tag{3.23}$$

where, as before, N - parameter of line, which characterizes rate of change of its wave impedance; ρ_0 - wave impedance in the beginning of line; v - wave propagation velocity.

Correction of the shape of pulse with the aid of non-uniform circuit.

Besides diagrams of decrease in charging voltage (current) in lines, which it is expedient to use with formation of powerful pulses, non-uniforms circuit can be successfully used for correction of shape of pulses. In the real diagrams sometimes it is impossible to avoid the parasitic parameters. So load instead of the purely active proves to be complex.

If, for example, for formation of square pulse it is utilized with uniform discharge line, extended at one end/lead and loaded to effective resistance $R_н$ on other, then presence of stray inductance $L_н$, back-out resistor $R_н$ leads to distortion of shape of pulse.

Let line with wave impedance ρ be preliminarily charged/loaded to voltage/stress E. Then during the discharge of line on load $Z_н$, which presents the parallel connection of resistor/resistance $R_н$ and

inductance $L_н$, voltage/stress on the load will be $u_н$. It is easy to show that the operational expression for this voltage/stress will be

$$\hat{u}_н(p)=\frac{E}{R_н+\frac{L_н pR_н}{pL_н+R_н}}\frac{pL_н R_н}{pL_н+R_н}=\frac{E}{2}\frac{p}{p+R_н/2L_н}$$

or, passing to the original

$$u_н=\frac{E}{2}e^{-\frac{R_н t}{2L_н}}. \qquad (3.24)$$

As is evident, shaped pulse of voltage/stress decreases exponentially.

Page 157.

Relative value of decay in the pulse apex is determined by the expression

$$\frac{u(0)-u(t_и)}{u(0)}=1-e^{-\frac{R_н t}{2L_н}}.$$

For retention/maintaining under these conditions of rectangular shape of pulse, as O. N. Litvinenko [1, 45] showed, it is possible instead of uniform line to use heterogeneous forming line, whose wave impedance $\rho(x)$ changes according to hyperbolic law.

In this case diagram of formation (Fig. 3.18a) with non-uniform circuit of finite length, charged/loaded in initial state to voltage/stress E, can be enticed by equivalent diagram (Fig. 3.18b), where line is undertaken infinite length. This is correct only for

the range of time from t=0 to $t=t_{u}$. i.e. for the doubled delay time of the section of the line, when the form of voltage/stress on resistor/resistance Z_{u} does not depend on conditions at the end/lead of the line.

If input resistance of infinitely long non-uniform circuit $Z_{\text{вх}}$, then voltage/stress on resistor/resistance Z_{u} will be equally

$$u_{u} = \frac{EZ_{u}}{Z_{\text{вх}} + Z_{u}}. \quad (3.25)$$

If on load pulse is formed/shaped right-angled, then voltage/stress u_{u} for period $0 \leqslant t \leqslant t_{u}$ is constant value. At the moment of closing/shorting the key/wrench voltage/stress on the load

$$u_{u} = \frac{ER_{u}}{R_{u} + \rho_{0}}, \quad (3.26)$$

where ρ_{0} - wave impedance in the beginning of line.

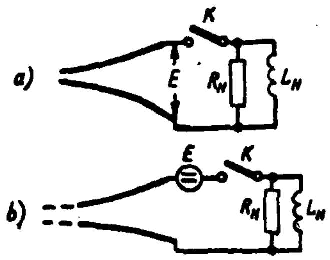

Fig. 3.18. Pulse-shaping circuit with corrective non-uniform circuit (a) and its equivalent diagram (b).

Page 158.

Since $u_н = \text{const}$, then the same value $u_н$ will be supported during entire period in question. Thus, for the input resistance of non-uniform circuit we will obtain from (3.25) taking into account (3.26) the operational expression

$$\hat{Z}_{вх}(p) = Z_н(p)\frac{\rho_0}{R_н} = \frac{pL_н\rho_0}{pL_н + \rho_0} = \frac{\rho_0}{1 + R_н/pL_н}. \quad (3.27)$$

Knowing input resistance, it is possible to find law of change in wave impedance along line (along x axis).

As shown into S 1.8, processes in non-uniform circuit are described by equations:

$$-\frac{\partial u}{\partial x} = L(x)\frac{\partial i}{\partial t},$$
$$-\frac{\partial i}{\partial x} = C(x)\frac{\partial u}{\partial t},$$

where L(x) and C(x) - linear parameters of line;

x - distance from beginning of line.

Converting these equations and deciding by their path, analogous how this is made into S 1.8, it is possible to show that expression for wave impedance will take form

$$\rho(x)=\frac{\rho_0}{\left(1+\frac{R_н}{L_н}\frac{x}{v}\right)^2}, \qquad (3.28)$$

where v - wave propagation velocity along line.

Thus, wave impedance changes according to hyperbolic law.

Resistor/resistance ρ_0 is found from condition of minimum remainder/residue of energy in line after its discharge and is equal to $\rho_0=R_н$. Insignificant energy (about 1%) remains during the discharge of line in it, but the apex/vertex of the formed/shaped pulse becomes flat/plane. However, over the load energy in turn is distributed between payload $R_н$ and stray inductance $L_н$.

Page 159.

Since in the shapers the energy, stored up in the inductance, is not utilized, then it must be scattered on the supplementary elements, specially introduced into the diagram (diodes, thyratrons), which leads to the complication of diagram and decreases its efficiency. The greater the decay in the pulse apex it is corrected by hyperbole trace, the greater the energy reserves itself in inductance $L_н$.

Diagram of formation with matching non-uniform circuit.

In certain cases during use of diagram with discharge line effective resistance of load cannot be undertaken by equal to wave impedance of forming line. Then agreements use non-uniform circuit, which performs the role of transformer. However, as it was shown into § 1.8, non-uniform circuit distorts the flat/plane part of the pulse. So that the pulse on the load would be rectangular, discharge line also must be heterogeneous.

Fig. 3.19a gives diagram, where between discharge exponential line 1 and load $R_н$ after key/wrench K is included/switched on matching transformer 2 in the form of exponential line of transmission [46]. Fig. 3.19b gives the equivalent schematic of this device/equipment. Load resistor/resistance is selected by the equal to the resistor/resistance of transformer in output terminals. It is evident from the equivalent diagram that the voltage on the input of transformer (point C) will be

$$U_C = \frac{Z_2 E}{Z_1 + Z_2},$$

where Z_1 - input resistance of the forming line (from the side of commutator);

Z_2 - input resistance of transformer.

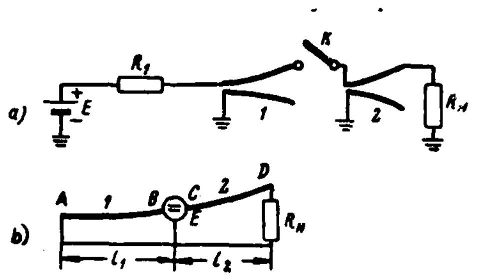

Fig. 3.19. Diagram of formation with matching non-uniform circuit (a) and its equivalent diagram (b).

Page 160.

From theory of exponential line, which is used as forming two-terminal network and transformer, are known expressions for input resistances [40, 46, 47]. The wave impedance of exponential line according to (1.109) is equal

$$\rho(x) = \rho_0 e^{kx} = \sqrt{\frac{L_0}{C_0}}\, e^{kx}.$$

input resistance of exponential forming line has following operational expression:

$$\hat{Z}_1(p) = \rho_0 \left[1 + \frac{k_1}{2pt_{з0}} + 2e^{-2pt_{з1}}\left(1 - \frac{k_1^2 t_{з1}}{4pt_{з0}^2}\right)\right], \quad (3.29)$$

where $t_{з1}$ - delay time, which corresponds to overall length of line l_1.

Input resistance of transformer, coordinated with termination,

$$\hat{Z}_2(p)=\rho_{02}\left[1+\frac{k_2}{2pt_{30}}(1-e^{-2pt_{32}})\right]. \qquad (3.30)$$

It is here assumed that both lines have identical delay per unit of length t_{30}=const, and exponents k_1 and k_2 are different.

After substituting values of resistors/resistances of $Z_1(p)$ and $Z_2(p)$ into expression for U_C, we will obtain for image of voltage on input of transformer (at point C in Fig. 3.19b) following expression:

$$\hat{U}_C(p)=\left[1-\frac{k_1}{4pt_{30}}-e^{-2pt_{31}}\left(1-\frac{k_1}{2pt_{30}}-\frac{k_1^2t_{31}}{4pt_{30}^2}\right)+\right.$$
$$\left.+\frac{k_2}{4pt_{30}}(1-e^{-2pt_{32}})\right]\frac{E}{2}. \qquad (3.31)$$

As positive direction of motion of wave is accepted motion to the left for forming line and from left to right for transformer, and are also taken into consideration corresponding signs in coefficients of K_1 and K_2.

Page 161.

Exponential term with index $2pt_{32}$ considers the presence of reflections from the outlet end of the transformer.

Voltage/stress $U_н$ in terminals of termination (at point D in Fig. 3.19b) can be found, if we use solution of equation for exponential line [46], after using it in this case to exponential transformer. Output voltage/stress $U_н$ will be composed from direct wave, which is propagated from point C to D ($U'_н$), and reflected, passing from point D

to $C(U''_{\text{н}})$, i.e.

$$U_{\text{н}} = U'_{\text{н}} + U''_{\text{н}} = U'_{\text{н}}(1 + m_{\text{н}}),$$

where $m_{\text{н}}$ - reflection coefficient on the voltage from the outlet end of the transformer:

$$m_{\text{н}} = -\frac{k_2}{4pt_{30}}.$$

Image for voltage/stress $U'_{\text{н}}$ will take the form

$$\hat{U}'_{\text{н}}(p) = \hat{U}'_0(p) e^{\frac{k_2 t_{32}}{2t_{30}}} e^{-pt_{32}} \left(1 - \frac{k_2 t_{32}}{8pt_{30}^2}\right),$$

where value $\hat{U}'_0(p)$ in the case in question is equal to value $\hat{U}_C(p)$. Then the output voltage/stress

$$\hat{U}_{\text{н}}(p) \sim \left[1 - \frac{k_1}{4pt_{30}} - \frac{k_2^2 t_{32}}{8pt_{30}^2} - \right.$$
$$\left. - e^{-2pt_{31}}\left(1 - \frac{k_1}{2pt_{30}} - \frac{k_2}{4pt_{30}} - \frac{k_1^2 t_{31}}{4pt_{30}^2} - \frac{k_2^2 t_{32}}{8pt_{30}^2}\right)\right] \frac{E}{2}. \quad (3.32)$$

Factors, which determine value of transformation ratio of voltage and delay time in transformer are here omitted. In the forming system the divergence of the pulse amplitude from the constant value is determined by the second and third members of expression (3.32). These terms are reduced, if the condition

$$k_1 = -\frac{k_2^2 t_{32}}{2t_{30}}$$

is satisfied.

Page 162.

Condition, necessary for compensation for decay ("avalanche") in pulse apex, thus, can be recorded in the following form:

$$-\frac{k_1}{k_2}=\frac{k_2 t_{32}}{2t_{30}}. \qquad (3.33)$$

Let us recall that for forming line and transformer is accepted equality of delay times per unit of length, i.e., $t_{301}=t_{302}=t_{30}$.

Transformer must be designed so that pulse amplitude would be reduced not more than to 10% in the case of its connection/attachment to usual forming line (to uniform). Then, assuming/setting in expression (3.32) $K_1=0$ and producing integration for the time from t=0 to $t=2t_{31}$, we obtain

$$\frac{k_2^2 t_{32} t_{31}}{4t_{30}^2}=0,1. \qquad (3.34)$$

Thus, using known values R_{11}, ρ_0, t_{30} and duration of pulse $t_{11}=2t_{31}$, from expression (3.34) we find k_2, and values of t_{32} and k_1 - from expression (3.33).

If forming line and transformer have identical delay per unit of length, then necessary lengths of lines are assigned by relationships/ratios

$$\frac{t_{31}}{t_{30}},\ \frac{t_{32}}{t_{30}}. \qquad (3.35)$$

System examined, which consists of exponential forming line and

transformer, makes it possible to obtain on termination pulse, very close in form to rectangular, although resistance/resistor of load $R_н$ can considerably differ from wave impedance of forming line.

Diagrams of formation with uniform and non-uniforms circuit examined it requires application of lines, whose sizes/dimensions become large, if pulse duration is more than 5-10 ns.

Page 163.

Thus, in the case of using coaxial cable in the diagram with the discharge line its length is equal to 1 m for the duration of pulse 10 ns. Therefore they are of interest of the forming lines with the long delay time per unit of length.

Ya. S. Itskhoki [1] has proposed special construction/design of magnetodielectric line for impulse shaping of short duration. Line has the sufficiently long delay time and the significant magnitude of wave impedance. This is achieved/reached by loading during the special construction/design of the cable, distinctive features of which is the special method of introduction inside the cable of magnetic dielectric.

Idea of construction/design of cable is illustrated by Fig. 3.20. Central current-conducting rod (1) is surrounded by ferromagnetic cylinder (2), which is assembled from the thin plates of ferromagnetic material, isolated from each other by the insulating layers.

Ferromagnetic cylinder is surrounded by the concentric "dielectric cylinder" (3), which fits closely by external surface to external conducting cable sheathing (4).

In cable of described construction/design magnetic field is concentrated, in essence, in ferromagnetic cylinder, and electric field - in dielectric cylinder. Ferromagnetic cylinder does not block the course of permittance current in the radial direction of cable, but it blocks (due to the presence of those insulating interlayer) the course of conduction current lengthwise of cable. Due to this into dozens of times it is possible to raise both the linear inductance of cable and linear capacity/capacitance. Therefore it is possible to construct this cable with the wave impedance into several hundred ohms with the long delay time per unit of length (order of several ten nanoseconds to the meter).

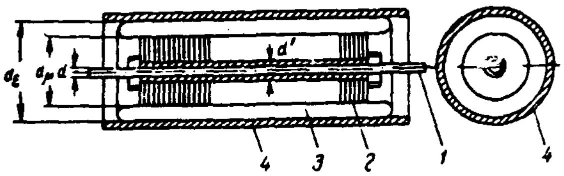

Fig. 3.20. Diagrammatic representation of construction/design of magnetodielectric forming line.

Page 164.

Linear parameters of cable are determined by relationship/ratio [1]:

$$L=\frac{\delta_\mu \mu_\Delta \cdot 10^{-3}}{2\pi(\delta_\mu+\delta_\varepsilon)}\ln\frac{d_\mu}{d'}\left[\frac{\text{мкгн}^{(1)}}{\text{см}}\right],$$

$$C=\frac{2.22\pi}{\frac{1}{\varepsilon_1}\ln\frac{d_\varepsilon}{d_\mu}+\frac{1}{\varepsilon_2}\ln\frac{d'}{d}}\left[\frac{\text{пф}^{(2)}}{\text{см}}\right],$$

Key: (1). μH. (2). pF.

where μ_Δ – operating in the pulsed operation magnetic permeability of ferromagnetic washers (by thickness δ_μ);

ε_1 and ε_2 - with respect the dielectric constants of dielectric cylinder and insulating layer of internal wiring of cable;

δ_ε - thickness of the insulating layer between the ferromagnetic washers.

[1] Show experimental investigations that with the aid of this magnetodielectric forming line it is possible to obtain to pulse by duration several ten nanoseconds during relatively steep front and shear/section. For the formation of such pulses can be also used

spiral coaxial cables of the delays, whose data are cited in Table 1.3.

3.4. PROPERTIES OF THYRATRON AS THE COMMUTATING ELEMENT OF THE NETWORKS OF THE FORMATION OF NANOSECOND PULSES.

As commutating element in pulse-shaping circuits of nanosecond duration thyratrons find wide application. The advantages of thyratrons as commutators include their following properties:

- control capability of the moment/torque of commutation, also, within certain limits of frequent commutation;
- low value of a voltage drop across commutator;
- the significant magnitude of the permissible discharge current with the relatively low voltages/stresses;
- possibility of work in the sufficiently broad band of anode voltages.

Page 165.

With impulse shaping of nanosecond duration to thyratron as commutator are presented stringent requirements relative to speed of response. Time the course of this time determine the form of front and partially pulse apices. The stability of the moment/torque of commutation and the frequency of commutation are other important requirements.

Depending on character of processes of ionization and

deionization in thyratron it to a certain degree can satisfy requirements indicated. The considerable number of investigations is devoted to the processes of deionization and ionization in the thyratrons. To questions of deionization time was initially given more than attention, since the process of deionization limits the operating frequency of thyratron. The duration of the ionization of thyratron was counted very small in comparison with the deionization time and the pulse duration, and therefore they frequently disregarded it.

Process of deionization depends on internal factors, such, as character of gas filling, construction/design of electrodes of thyratron, and from external - circuit diagrams of thyratron and mode of its operation [48, 49, 50].

It is known that in period of deionization instantaneous value of breakdown strength of thyratron depends on value of pulse of anode current, grid bias and resistor/resistance passed through thyratron. With a change in the value of anode voltage or duration of the formed/shaped pulse the process of deionization in the time will flow/occur somewhat differently.

Sometimes for evaluation/estimate of limiting frequency of separate thyratrons they use relationship/ratio

$$U_a i_a F = \text{const},$$

where U_a - anode voltage;

i_a - anode current of thyratron;

F - pulse repetition rate. The value of constant is different for different thyratrons.

Page 166.

With work of thyratron in oscillator circuit at the beginning of ignition of thyratrons at different moments of time (from one pulse to the next) state of the gas in it can differ somewhat, i.e., process of deionization proceeds somewhat differently. This fact leads to a change in the firing point of thyratron during the supplying to its grid of identical and strictly stable in the time trigger pulse, i.e., causes the instability of commutation, what is an essential deficiency in the thyratron.

Application of thyratron in pulse generators of nanosecond duration led to need for more detailed study not only of process of deionization, but also process of ionization, or stability of ignition of thyratron. In the works, dedicated to the studies of deionization and ionization of thyratrons, some authors expressed considerations relative to the reasons, which cause ionization time [48, 49, 50].

They sometimes divide ionization time into two intervals. During the first interval, called delay time, the anode current of thyratron changes very slowly, for the time of the second interval, called the time of commutation, anode current changes sharply. Duration of both periods is connected with the special features of ionization and is

different for different thyratrons.

Absence at present of sufficient theoretical data of those making it possible to accurately determine time of commutation of thyratron, is completed by experimental investigations of commutation properties of thyratrons, which became possible with development of high-speed/high-velocity oscillography.

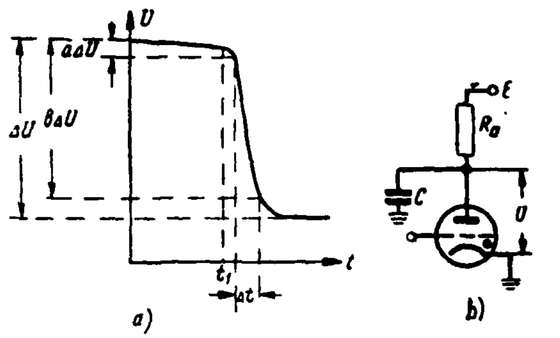

Fig. 3.21. Characteristic of ionization of thyratron (a); diagram of its switching on/inclusion (b).

Page 167.

For evaluation/estimate of commutation properties of thyratron are examined its characteristics of ionization, which present dependence of change in voltage on anode of thyratrons from time in process of its ignition (Fig. 3.21a). The time of commutation can be defined as interval of Δt, in which the anode voltage will fall from value of $E-a|\Delta U|$ to $E-b|\Delta U|$, where E - supply voltage (Fig. 3.21b); ΔU - total variation in the anode voltage. Coefficients a and b are usually taken as equal to with respect 0.1 and 0.9. Moment of time t_1 characterizes the time lag of the ignition of thyratrons. For obtaining the characteristic of ionization it is necessary to remove/take the oscillogram of anode voltage U(t) (Fig. 3.21a) or voltages/stresses $U_{н}(t)$ on known resistive load $R_{н}$ (Fig. 3.22), connected in series with the thyratron, to which is given the voltage/stress from the dc power supply with the zero resistor/resistance. In this case a change in the voltage/stress on

the load uniquely determines voltage/stress on the thyratron:

$$U_{\text{т}}(t) = E - U_{\text{н}}(t),$$

the current through the thyratron

$$I_{\text{т}}(t) = \frac{U_{\text{н}}(t)}{R_{\text{н}}}$$

and, therefore, the resistor/resistance of thyratron as the function of the time

$$R_{\text{т}}(t) = \left(\frac{E}{U_{\text{н}}(t)} - 1\right) R_{\text{н}}.$$

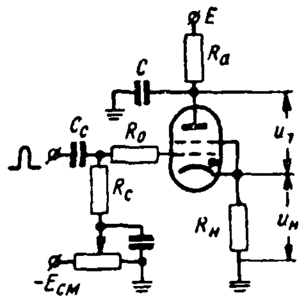

Fig. 3.22. Circuit diagram of cathode-loaded thyratron for plotting curve/characteristic of ionization.

Page 168.

Voltage source with zero resistor/resistance is capacitor/condenser C, whose value is selected so that time constant of its discharge

$$\tau_{p} = C\,(R_{\text{н}} + R_{\text{т0}})$$

would be at least ten times more than duration of process being investigated. Here $R_{\text{т0}}$ - steady-state value of the internal resistor/resistance of thyratron.

Value of resistor/resistance in circuit of anode R_a is taken by such that within period of trigger pulses capacitor/condenser C would manage to virtually completely be loaded to supply voltage E. It is possible to consider during this identification of the parameters of diagram that during the process being investigated the potential of the anode of thyratron remains constant.

In diagram for plotting curves/characteristics of ionization (Fig. 3.22) virtually excluded effect parasite ache plate capacitance - earth/ground. Other parasitic circuit parameters must have low value, such, that the time constant of the circuits, which are formed due to the parasitic parameters, would be small in comparison with the ionization time of thyratron. Fig. 3.23 gives the equivalent diagram, which corresponds to diagram in Fig. 3.22 for plotting the curves/characteristics of the ionization of thyratron taking into account the possible parasitic parameters of real installation. In the diagram are shown the self-capacitances of thyratron $C_{\text{аз0}}$ (anode - earth/ground), $C_{\text{ак0}}$ (anode - cathode), $C_{\text{кз0}}$ (cathode - earth/ground), the wiring capacitance $C_{\text{аз}}$, $C_{\text{кз}}$, $C_{\text{ак}}$ and inductance of the anodic and cathode introductions/inputs of thyratron $L_{\text{а}}$ and $L_{\text{к}}$.

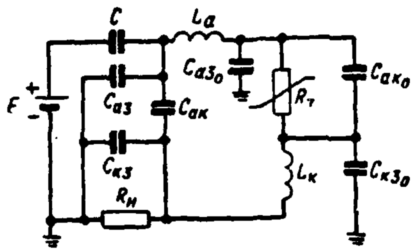

Fig. 3.23. Equivalent diagram of thyratron diagram for plotting curve/characteristic of ionization (Fig. 3.22).

Page 169.

As commutating element of pulse-shaping circuits of nanosecond duration of small power had extensive application finger pulse thyratron of type TGI1-31/1, and in pulse-shaping circuits of high voltage are successfully utilized pulse hydrogen thyratron of type TGI1-35/3, TGI1-50-5, of TGI1-130/10 and other more powerful/thicker thyratrons [50, 51, 52].

Table 3.1 gives average/mean values of stray capacitances of some thyratrons, and also value taking into account mounting of real diagram [64, 65].

As show research on the schemes with thyratrons [51, 52] application of finger thyratron TGI1-3/1 makes it possible to carry out diagram, whose parasitic parameters are so/such low, that they do not affect work of diagram and characteristic of ionization can be obtained without distortion by its external circuits.

In order to have picture of ionization of thyratron with different values of supply of power, characteristic of ionization it is expedient to examine in the form of dependence $U_{u}=u_{u}(E, t)$. In fig. 3.24 are given the characteristics of the ionization of a finger pulse thyratron of the type TGI1-3/1 with the screen grid, connected to cathode [51].

Voltage/stress $u_{u}(t)$ increases to its steady-state value for time for time t_2 called total ionization time.

Table 3.1.

(1) Паразитные емкости, пф	ТГИ1-3/1		ТГИ1-35/3		ТГИ1-50/5		ТГИ1-130/10	
	(2) Лампы	(3) Лампы и монтажа	(2) Лампы	(3) Лампы и монтажа	(2) Лампы	(3) Лампы и монтажа	(2) Лампы	(3) Лампы и монтажа
$C_{ак}$	1,65	5,2	1,7	3,15	4,2	6,4	8,9	11,6
$C_{кз}$		7,8		12,5		16,4		21,0
$C_{аз}$		5,2		3,1		6,2		11,6

Key: (1). Stray capacitances. (2). Tubes. (3). Tubes and mounting.

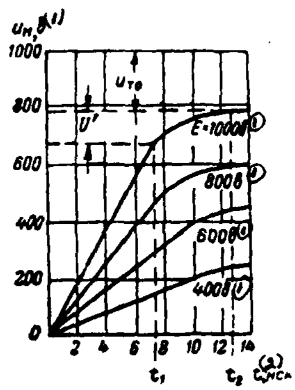

Fig. 3.24. Characteristics of ionization of finger thyratron TGI1-3/1.

Key: (1). IN. (2). NSK.

Page 170.

With the voltage error of the incandescence/filament of thyratron from the nominal value the ionization time changes. An increase in the filament voltage decreases the ionization time.

Ionization time of thyratron can be broken into two gaps/intervals. The first gap/interval corresponds to the interval of

time t_1, during which occurs the rapid increase of voltage/stress $u_n(t)$ according to the law, close to the linear. During gap/interval t_1 in the oscillator circuits occurs, in essence, the formation of the pulse edge. The first gap/interval subsequently will be called simply ionization time.

Second gap/interval corresponds to interval of time t_2-t_1, when voltage/stress $u_n(t)$ increases slowly. This time interval affects shaping of flat/plane pulse apex. As can be seen from characteristics (Fig. 3.24), ionization time decreases with an increase in voltage/stress E. An increment in voltage/stress U' for time t_2-t_1 remains with the different values of voltage/stress E approximately identical.

General view of characteristics of ionization for different values of resistance/resistor of load R_n is not changed, changes only value of steady-state value of voltage/stress on thyratron u_{Tn} and, therefore, voltage/stress on load.

For high-voltage pulse hydrogen thyratron TGI1-35/3, TGI1-50/5, TGI1-130/10 value of capacity/capacitance C_{K3}, shunting cathode load in diagram in Fig. 3.22, is more than in finger thyratron, and time constant of circuit of charge of this capacity/capacitance $\tau_1=R_n C_{K3}$ is equal to 1-2 ns (when $R_n=75$ ohm), and ionization time of thyratrons of approximately 11-14 ns. Thus, and for these thyratrons the effect of stray capacitance also can be disregarded/neglected. It should be

noted that to the filament circuit of powerful/thick thyratron it is necessary to connect high-frequency choke, since cathode and heater of thyratrons frequently have common point and cathode load can prove to be the shunted capacity/capacitance of the filament wires (or with the capacity/capacitance of the winding of filament transformer) relative to the earth/ground.

Stray inductance of diagram $L_{п}$, determined by inductance of introductions/inputs of high-voltage thyratrons, proves to be equal to approximately 0.15-0.2 μH.

Page 171.

Therefore in the equivalent diagram in Fig. 3.23 it is expedient to leave inductance $L_{а}$ and $L_{к}$, been connected in series with the resistance/resistor of load $R_{н}$ and the resistor/resistance of thyratron $R_{т0}$, and stray capacitances in the first approximation, can be disregarded/neglected. The time constant of circuit, which affects the period of the establishment of process during plotting of the curves/characteristics of the ionization of thyratron, thus, is determined by expression $\tau = L_{п}/R$, where R - the total resistance of circuit, and $L_{п}$- total inductance of the introductions/inputs of thyratron.

Presence of parasitic parameters of thyratron, strictly speaking, does not make it possible to obtain actual value of ionization time of thyratron. In the case of the finger pulse thyratron TGI1-3/1 the

time constant of circuit, caused by the parasitic parameters of thyratron, is considerably lower than the ionization time of gas in the thyratron, and therefore the ionization time observed on the oscillograph corresponds to actual value. However, in the case of high-voltage pulse thyratrons it is necessary to consider stray inductance $L_{\text{п}}$, and consequently, it is impossible to observe the actual value of ionization time. This is explained by the fact that during the ionization of thyratron as a result of the rapid build-up/growth of current grows/rises the voltage/stress on the inductance of introductions/inputs and, therefore, decreases voltage/stress on the thyratron, which affects the rate of the process of the ionization of gas in it.

However, experimental investigations of high-voltage thyratrons, given in Table 3.1, showed that effect of this factor on period of commutation of thyratrons is considerably less than integrating action of circuit $L_{\text{п}}R_{\text{н}}$, by formed inductance of introductions/inputs and with load resistance/resistor. Therefore in the first approximation, i.e., without taking into account the dependence of the ionization time of thyratron on the stray inductance, the time of the establishment of process (measured at level 0.1 and 0.9 from the steady-state value) during plotting of the curve/characteristic of the ionization of thyratron can be rated/estimated by the expression

$$t_{\text{у}} = \sqrt{t^2_{\text{ион}} + \left(2{,}2\frac{L_{\text{п}}}{R_{\text{н}}}\right)^2}. \qquad (3.36)$$

Page 172.

Knowing characteristic of ionization of thyratron, it is possible to determine possible duration of pulse edge, formed/shaped in diagram with thyratron as commutating element. Using diagram of formation with discharge line examined above (Fig. 3.9) and by thyratron commutator, it is possible to obtain on cathode load $R_н$ the pulse, whose frontal part according to the form corresponds to the characteristic of the ionization of the thyratron used in the diagram, and the shear/section of pulse repeats correspondingly the form of front (Fig. 3.25), if we do not consider an insignificant change of shearing/sectioning the pulse in its foundation due to the current of the deionization of thyratron.

With impulse shaping of nanosecond duration stringent requirements on stability of moment/torque of onset of pulses are imposed. In the generators, which use a thyratron as commutator, this stability is determined by the stability of functioning thyratron.

Investigations of stability of ignition of thyratron [51, 52] showed that periodic instability of ignition of thyratron or "chattering" of starting/launching of oscillator circuit changes within large limits, but in best cases it can be lowered to tenths of nanosecond.

Should be distinguished two forms of factors, which affect moment/torque of opening of thyratron, and also to stability of

starting/launching of diagram - external and internal.

Internal factors depend on construction/design of thyratron, i.e. on character of gas filling and construction/design and arrangement/position of electrodes. For many low-power thyratrons the absolute value of the temporary/time instability of that caused by internal factors, has very low value in comparison with the ionization time and therefore high value they acquire environmental factors.

Environmental factors include stability of supplies of power, value of parameters of trigger pulse and their constancy in time. The sources of the grid-bias voltage, anode voltage and filament voltage of thyratron must be stable.

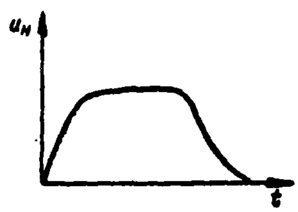

Fig. 3.25. Shape of pulse, obtained in thyratron diagram.

Page 173.

Special attention must be focused on high quality of voltage regulation of bias/displacement. The selection of the value of this voltage/stress also plays the significant role. Bias voltage must provide the reliable closing of thyratron, but not be too great, since the large amplitude of trigger pulses will be required and the delay time of the starting/launching of thyratron can prove to be large.

Starting/launching of thyratron proves to be more stable, if it occurs at that moment/torque, when frontal part of trigger pulse operates on grid of thyratron. In this case the stability of starting/launching is above with the large steepness of the front of trigger pulse. As show investigations [51, 52], in the case of applying the finger pulse thyratron TGI1-3/1 the trigger pulse must have an amplitude of approximately 200 V, a duration of 2-3 μs for the duration of front not more than 0.1 μs. With such parameters of stable trigger pulse and power supplies stabilized to a sufficient degree the instability of the starting/launching of this thyratron does not exceed the tenths of nanosecond, i.e., it proves to be order

10^{-10} s.

For stable starting/launching of high-voltage pulse hydrogen thyratron amplitude of trigger pulses must be 300-400 V, and steepness of their front - about 4 kV/μs.

With ignition of thyratrons besides phenomenon of instability of starting/launching it is necessary to consider time lag of starting/launching, caused by time lag of firing point of thyratron relative to moment of supplying trigger pulse. This time lag, which depends on the character of the gas filling of thyratron and mode of operation of diagram (value of anode voltage, amplitude and the steepness of the front of trigger pulse, grid-bias voltage, etc.), has a value of the order of the tenths of microsecond and can be or more depending on mode and parameters of grid circuit.

Delay factor of starting/launching of diagrams with thyratrons, which has important value in series/row of schematics of nanosecond pulse technique, can smoothly be regulated. The adjustment of the delay of starting/launching is realized by changing the value of bias voltage on the grid of thyratron.

Page 174.

However, this adjustment is possible only in the permissible limits, when the stable starting/launching of thyratron still is provided. Virtually this adjustment proves to be possible in the limits from

50-80 to 600 ns for the finger thyratron and in the limits of 150-500 ns for the high-voltage thyratrons. The delay time of starting/launching decreases with an increase in the steepness of the front of trigger pulse (with the fixed/recorded grid-bias voltage).

Comparatively low permissible frequency of commutation is one of deficiencies in thyratron as commutator. As noted, this frequency depends on the duration of the process of the deionization of thyratron, which determines recovery time of the controllability of thyratron. Recovery time of the controllability of thyratron is the less, is the greater the negative grid-bias voltage, the less the grid leak and the less the duration of the formed/shaped pulse. Furthermore, recovery time of thyratron depends also on the internal factors, determined by type and gas pressure and by construction/design of electrodes.

In pulse hydrogen thyratron TGI1-35/3, TGI1-50/5, TGI1-130/10 recovery time of controllability is 3-5 times less than in finger thyratron TGI1-3/1, and this makes it possible with high-voltage hydrogen thyratron to obtain frequency of commutation to 30-40 kHz, and with finger thyratron to 10 kHz.

Operating frequency of thyratron TGI1-3/1 can be increased by effect on it of magnetic field [53]. Placing the thyratron into the permanent magnetic field of the necessary value, oriented correspondingly relative to the electrodes of thyratron, it is

possible to decrease the deionization time of thyratron by the effect of this field to the processes in the plasma, which will lead to an increase in the operating frequency.

3.5. PULSE-SHAPING CIRCUITS WITH THE THYRATRONS.

Simplest pulse-shaping circuits.

For impulse shaping of nanosecond duration are used diagrams with thyratron commutators, in which as accumulator/storage of energy are utilized sections/segments of coaxial cables or capacity/capacitance.

Page 175.

The application of a capacity/capacitance instead of the cable is expedient when the duration of the formed/shaped pulse is commensurate with the ionization time of thyratron. If it is necessary to form the pulse, whose duration is commensurate with the ionization time of thyratron, and it is not presented to its form of stringent requirements, then the diagram, which completely coincides with the diagram Fig. 3.22 can be used. In this case capacitance value of capacitor/condenser C is selected from condition of its complete discharge approximately for ionization time. During the capacitor discharge on the cathode load the voltage pulse, in the form which differs from the rectangular is formed (Fig. 3.26). With the decrease of value C the pulse duration is shortened, but in this case it decreases and to amplitude. In this case the pulse duration can be less than the ionization time. Knowing the characteristic of the

ionization of thyratron, it is possible to find the parameters of pulse. In the interval of time $0 \le t \le t_2$ (where t_1 - first interval of ionization time) the set of characteristics of ionization it is possible to approximate by the linearly increasing function

$$u_{\text{и}} = (E - U_0) kt, \quad (3.37)$$

where k - coefficient, which characterizes the rate of the increase of process;

U_0 - averaged value of voltage/stress $U_{\text{T0}} + U'$ (for the differ it values of voltage/stress E), and values U_{T0} and U' are shown in fig. 3.24.

Values k and U_0 are determined from solution of system of equations

$$U'_{\text{и}} = (E' - U_0) kt',$$
$$U''_{\text{и}} = (E'' - U_0) kt''.$$

Values $U'_{\text{и}}, U''_{\text{и}}, t', t'', E'$ and E" can be found from characteristics of ionization graphically of [54].

Fig. 3.26. Pulse, formed/shaped in thyratron diagram with small storage capacity/capacitance.

Page 176.

From equivalent diagram in Fig. 3.27, appropriate thyratron diagram, it follows that voltage/stress on load $R_{н}$ can be recorded thus:

$$u_{н}(t) = [u(t) - U_0]\, kt, \quad (3.38)$$

Voltage across capacitor u(t) can be determined through capacity/capacitance of C and resistor/resistance of thyratron $R_{т}(t)$, which, however, depends on voltage/stress. Therefore equation proves to be nonlinear and its numerical solution can be obtained, after assigning the approximation of the characteristic of ionization. The parameters of the formed/shaped pulses are determined usually experimentally.

If we in diagram in question use finger thyratron TGI1-3/1 and to fulfill mounting, without introducing essential parasitic parameters (value of which does not exceed values, given in Table 3.1), then it is possible to form pulses by duration (at level 0.5 of amplitude) of 2.5-3 ns with amplitude 30-50 V.

Squaring circuit, where as accumulator/storage of energy serves segment of cable (Fig. 3.28), i.e., diagram of type fig, is propagated version of diagram with thyratron. 3.9. Generator, assembled according to diagram in Fig. 3.28a, is fulfilled in the form of

coaxial line, which provides agreement of forming cable with load and it makes it possible to reduce to minimum parasitic circuit parameters. In the places of the disruption of the center conductor inside of it is placed the thyratron, moreover for the realization of agreement $R_{\text{к}}+R_{\text{т0}}=\rho$ in the connection point of thyratron line is fulfilled so as to ensure the jump of wave impedance to value $R_{\text{т0}}$ due to the different diameter of center conductor. Here $R_{\text{к}}$ - resistance/resistor of cathode load; $R_{\text{т0}}$ - the steady-state value of the resistor/resistance of thyratron; ρ - wave impedance of the forming line. For obtaining the pulse of negative polarity is utilized the diagram in Fig. 3.28b.

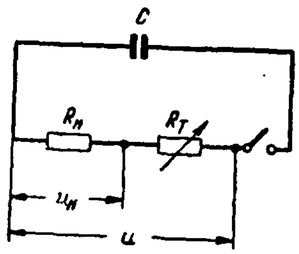

Fig. 3.27. Equivalent diagram, which corresponds to thyratron diagram.

Page 177.

For interval of time $0 \leq t \leq 2t_3$, where t_3 - delay time of forming line, equivalent oscillator circuit without taking into account parasitic parameters (which is easy to ensure with finger thyratron) is represented in Fig. 3.28c. This diagram when $R_н = R_к + \rho$ proves to be the completely identical equivalent to diagram installation, with the aid of which is plotted the characteristic of ionization (Fig. 3.22). Therefore it is possible to assert that for time $0 \leq t \leq 2t_3$ pulse, created on the load, repeats the characteristic of ionization for this value of supply voltage E, but on other scale:

$$u_к = u_н(t) \frac{R_к}{\rho + R_к}.$$

Without taking into account small effect of current of deionization, noticeable after discharge of line, shear/section of pulse must be on form the same as front (Fig. 3.25).

Duration of formed/shaped pulse in its foundation exceeds doubled delay time of line 2t, to ionization time of thyratron. The shape of pulse is close to the rectangular, if the doubled delay time of line noticeably exceeds ionization time.

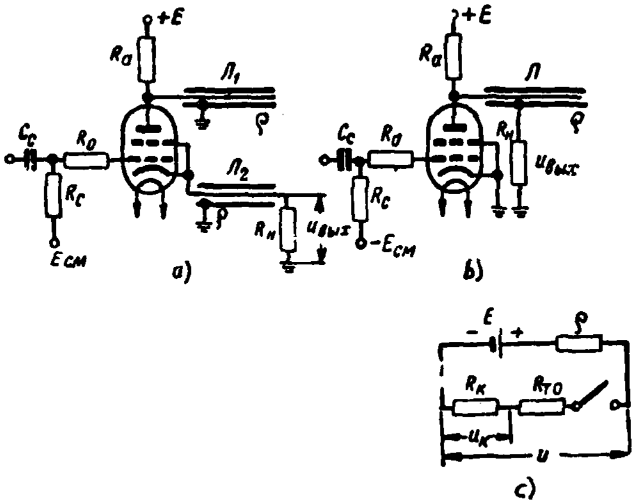

Fig. 3.28. Thyratron pulse-shaping circuits: a) diagram of formation of positive pulse; b) diagram of formation of negative pulse; c) equivalent diagram.

Page 178.

Pulse apex, however, has in the beginning smoothly increasing section, caused by the presence of the interval of the slowly increasing voltage/stress of the characteristic of ionization. The effect of this section is especially noticeable with low supply voltages.

Depending on length of line in diagram, which works on thyratron TGI1-3/1, are formed/shaped pulses with amplitude of up to 500 V and duration of from 15 ns and more for duration of front of approximately 6 ns.

If length of segment of forming cable is such, that doubled time

of its delay of the same order as as ionization time, then obtained pulse noticeably differs in form from rectangular, approaching pulse, obtained during capacitor discharge in diagram in Fig. 3.22, whose oscillogram is given in Fig. 3.26.

In diagrams described parasitic parameters here were not considered. However, with the formation of the powerful pulses of nanosecond duration in the diagrams with the high-voltage thyratrons, which have relatively larger overall dimensions, the presence of the parasitic parameters is possible. In the preceding/previous paragraph it is indicated, that in such thyratrons it is necessary first of all to consider the inductance of introductions/inputs.

Diagram with forming cable and load in cathode of thyratron (Fig. 3.28a) can be replaced with equivalent diagram, where inductance of introductions/inputs and stray inductance of mounting are taken into consideration (Fig. 3.29). The resulting duration of the edge of the formed/shaped pulse, thus, is determined by the ionization time of thyratron and by the parasitic parameters of circuit.

Duration of front can be approximately rated/estimated on the basis (3.36) by expression

$$t_{ф} = \sqrt{t^2_{ион} + (2{,}2L_{н}/R)^2},$$

where $R = R_{н} + R_{io} + \rho.$

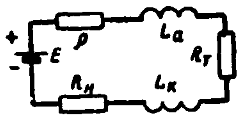

Fig. 3.29. Equivalent diagram, which corresponds to thyratron diagram taking into account stray inductances.

Page 179.

Account only of inductance of introductions/inputs of thyratron introduces insignificant correction in duration of edge of pulse (5-10%). During the insufficiently good mounting of the real diagram, when total stray inductance reaches 0.5 μH and more, this correction becomes essential.

During use in diagram of high-voltage pulse thyratrons, indicated in Table 3.1, it is possible to form pulses, duration of front of which 11-14 ns.

Diagrams, noncritical k to the value of load.

Pulse-shaping circuits with discharge line (of type of that given in Fig. 3.9) work under matching condition of line characteristic with load resistance/resistor. Since the sections/segments of coaxial cables, which have small set of the ratings of wave impedance (50, 75, 100 150 ohms), usually are utilized as the forming line, then the value of the load resistance/resistors is limited. Therefore far from

always it is possible to coordinate load with the cable, furthermore diagram cannot successfully work on the nonlinear load.

Advantage considerable in this respect possesses pulse-shaping circuit of nanosecond duration, in which is utilized discharge line, loaded from one end/lead and locked to matched impedance from another. The principle of the operation of this diagram (Fig. 3.13) is described into S 3.2.

Diagrams of such type with thyratrons as commutating elements are given in Fig. 3.30 [44]. In the diagram with two thyratrons (Fig. 3.30a) is possible continuously variable control of the pulse duration by changing the delay time of the starting/launching of one thyratron relative to the moment/torque of the starting/launching of another $t_p = t_2 - t_1$. For obtaining the pulse duration, equal to the doubled delay of cable, it is necessary that the forming thyratron L_1 would operate/actuate earlier than matching L_2 to the period, equal to the delay of cable ($t_3 = t_{3,0} l$).

$$t_p = t_2 - t_1 = t_3,$$
$$t_u = 2t_3.$$

Page 180.

If thyratrons operate/actuate simultaneously, i.e., $t_p = 0$, Then pulse duration will be equal to delay of cable $t_u = t_3$. If the matching thyratron operates/actuates earlier than forming to the period, equal

to the delay of cable, then it will not be on the load of pulse, since the wave of voltage/stress from the end/lead of the cable reflected, to which is connected the forming thyratron (Fig. 3.14), will have time to go away.

Thus, it is possible to say that pulse duration is linear function of delay factor of starting/launching of one thyratron relative to another

$$t_{и}=t_{з}\pm t_{р}.$$

Minimum pulse duration without reduction of its amplitude is determined by expression

$$t_{и\,мин}=t_{ф}+t_{с},$$

where $t_{ф}$ and $t_{с}$ - duration of front and shear/section of pulse, determined, in essence, by ionization time of thyratron. In this case the pulse has a form, close to the triangular.

If they take place of inequality $t_{р}>t_{з}$ and $R_{н}\gg\rho$, then duration of formed/shaped pulse will be more than time of dual delay of forming cable as a result of possibility of multiple reflection of waves of voltage/stress from ends/leads of cable (one of which proves to be extended). The shape of pulse is shown in Fig. 3.31.

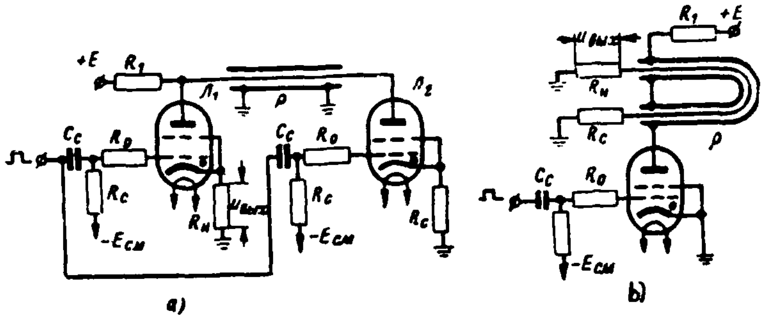

Fig. 3.30. Thyratron diagrams, noncritical to value of load: a) with two thyratrons; b) with one thyratron.

Page 181.

The form of pulse apex proves to be stepped. The duration of each step (except the latter) - constant value is equal to the doubled delay of cable $2t_з$. The duration of latter/last step can be less than $2t_з$, since it changes with change $t_р$.

During external starting/launching of generators delay time of their starting/launching is of interest. In this diagram it proves to be possible to realize an adjustment of the delay of starting/launching for the constant/invariable duration of the formed/shaped pulse. The delay of starting/launching is determined by triggering time of the thyratron of formation L_1 and does not depend on triggering time of the second thyratron.

Pulse duration depends on triggering time of both thyratrons, since $t_и = t_2 - t_1$. Consequently, to smoothly change pulse delay without a

change in its duration is possible when time difference of functioning t_p remains constant value, i.e., with change t_1 on $\pm\Delta t$, t_2 must change to the same value $\pm\Delta t$. This is possible, if within the limits of the necessary delay of the forming line t_3 the front of trigger pulse will be linear. Then a change in the delay of the formed/shaped pulse can be obtained with the aid of a change in the bias voltage on grids of both thyratrons simultaneously.

Actually, if front of trigger pulse is linear and has slope/transconductance S_n, then moment/torque of triggering/opening of first thyratron t_1 corresponds to voltage/stress of trigger pulse U_{n1}, i.e.

$$t_1 = \frac{U_{n1}}{S_n}.$$

Respectively moment/torque of starting/launching of second thyratron

$$t_2 = \frac{U_{n2}}{S_n}.$$

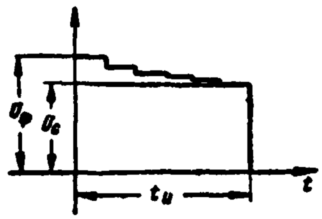

Fig. 3.31. Shape of pulse of considerable duration.

Page 182.

Since in limits of linear sector of the front of trigger pulse $S_п = \text{const}$, then range of adjustment of moment/torque of starting/launching of thyratrons is equal to

$$t_p = t_2 - t_1 = \frac{U_{п2} - U_{п1}}{S_п}.$$

For obtaining pulse by duration, equal to $t_и = 0 \div 2t_з$, it is necessary to have linear sector of the front with duration $t_{ф_и} \geqslant 2t_з$. In this case range of adjustment of the delay of the formed/shaped pulse will be equal to

$$t_и = \frac{U_{п2} - U_{п1}}{S_п} - 2t_з.$$

Designating.

$$\frac{U_{п2} - U_{п1}}{S_п} = t_{ф_и}, \quad t_н = 2t_з,$$

we obtain

$$t_п = t_{ф_п} - t_н.$$

This is correct, if duration of formed/shaped pulse $t_{и} \leqslant 2t_{з}$.

With

$$\frac{U_{п2} - U_{п1}}{S_{п}} \leqslant 2t_{з}$$

adjustment of delay of formed/shaped pulse without change in its duration is impossible. In this case it is necessary to increase the duration of the front of trigger pulse and its amplitude.

It is necessary to consider that

$$U_{п1} \geqslant U_{п\,мин} - E_{см\,мин},$$

where $U_{п\,мин}$ - minimum starting voltage with steepness of front of trigger pulse $S_{п}$;

$E_{см\,мин}$ - smallest allowable voltage of bias/displacement on grid of thyratron.

For obtaining pulse by duration, equal to $t_{и} = 2t_{з}n$, it is necessary to have linear sector of the front of trigger pulse with duration

$$t_{ф_{п}} = t_{з}(n + 1).$$

Page 183.

General formula for determining range of adjustment of delay of formed/shaped pulse will be

$$t_{\text{и}} = t_{\text{ф}_{\text{п}}} - (t_{\text{и}} + t_{\text{з}}).$$

Exception/elimination is case, when both thyratrons operate/wear simultaneously, i.e., $t_{\text{р}}=0$ and $t_{\text{и}}=t_{\text{з}}$. For this case the requirement for the linearity of the front of trigger pulse becomes meaningless and range of adjustment of the delay

$$t_{\text{и}} = t_{\text{ф}} - t_{\text{ф1}},$$

where $t_{\text{ф1}}$ - rise time of trigger pulse to the firing point of the thyratron of formation (L_1).

Range of adjustment of grid-bias voltage will be

$$E_{\text{см}_1} = U_{\text{и мин}} - U_{\text{п}_1},$$
$$E_{\text{см}_2} = U_{\text{и мин}} - U_{\text{п}_2}.$$

Adjustment of delay of formed/shaped pulse can be realized by adjustment of conjugated/combined potentiometers, circuitals of bias/displacement of thyratrons.

In the case of impulse shaping with duration up to $2t_з$, its amplitude is equal to

$$U = E\frac{R_{\text{н}}}{R_{\text{н}} + R_{\text{т}} + \rho}.$$

With formation of long pulse, when $t_{\text{и}} > 2t_{\text{з}}$ and at pulse apex appears n of steps, amplitude of shear/section of pulse is equal to

$$U_{\text{с}} = E\frac{R_{\text{н}}m^{n-1}}{R_{\text{н}} + R_{\text{т}} + \rho},$$

where

$$m = \frac{R_н + R_т - \rho}{R_н + R_т + \rho}.$$

With high resistance/resistors of load $R_н$ ($R_н \gg \rho$) difference in amplitudes of adjacent steps is very small and actually is observed smooth decay in apex/vertex, which is determined by relationship/ratio

$$\xi = \frac{U_ф - U_c}{U_ф} = \frac{\Delta U}{U} = 1 - m^{n-1}.$$

Page 184.

Value ξ characterizes form of pulse apex, it is possible to use it during calculations, determining number of steps, maximum pulse duration and value $t_р$.

Thus, this diagram (Fig. 3.30a) makes it possible to form/shape square pulses with duration up to $t_и = 2t_з$ with value of load, which is changed within large limits (from $R_н = \rho$ to hundred of kilohms), and with constant quantity of matched impedance R_c.

If load large, $R_н \geqslant 100$ kilohms, and time difference of starting/launching of thyratrons exceeds 2t₃, then it is possible to form/shape pulses with duration to 1-2 µs. This gives the large universality to diagram, which can be utilized both in the nanosecond range and for the impulse shaping of the beginning of microsecond range. However, its main advantage is noncriticality to the value of

resistive load and, therefore, the possibility of its application in the devices/equipment with the nonlinear and changing in the time load.

Diagram in Fig. 3.30b, assembled on one thyratron, possesses the same properties, but it does not permit implemention of continuously variable control of pulse duration, which is equal to delay time of cable.

Fig. 3.32 gives oscillator circuit of pulses of nanosecond duration, assembled according to diagram in Fig. 3.30a, with cascades/stages of starting/launching. The trigger circuit of generator consists of the assigning blocking oscillator ($L_{1,2}$), amplifier (L_2) and cathode followers ($L_{3,1}$ and $L_{3,2}$). Blocking oscillator works both in the mode of auto-oscillations and in the mode of synchronization by the external trigger pulses, which enter through the phase inverter in the amplifier of starting/launching (half of tube $L_{1,1}$).

Pulse forming unit consists of cascade/stage of formation (L_5) and cascade/stage of agreement (L_4), assembled on finger thyratrons TGI1-3/1. The first them them is intended for the impulse shaping on the load, connected to the discharge circuit of thyratron, the second - for obtaining shearing/sectioning of pulse and change in its duration.

Pulse, generated by blocking oscillator, has duration of 3 μs with amplitude of 150 V.

Page 185.

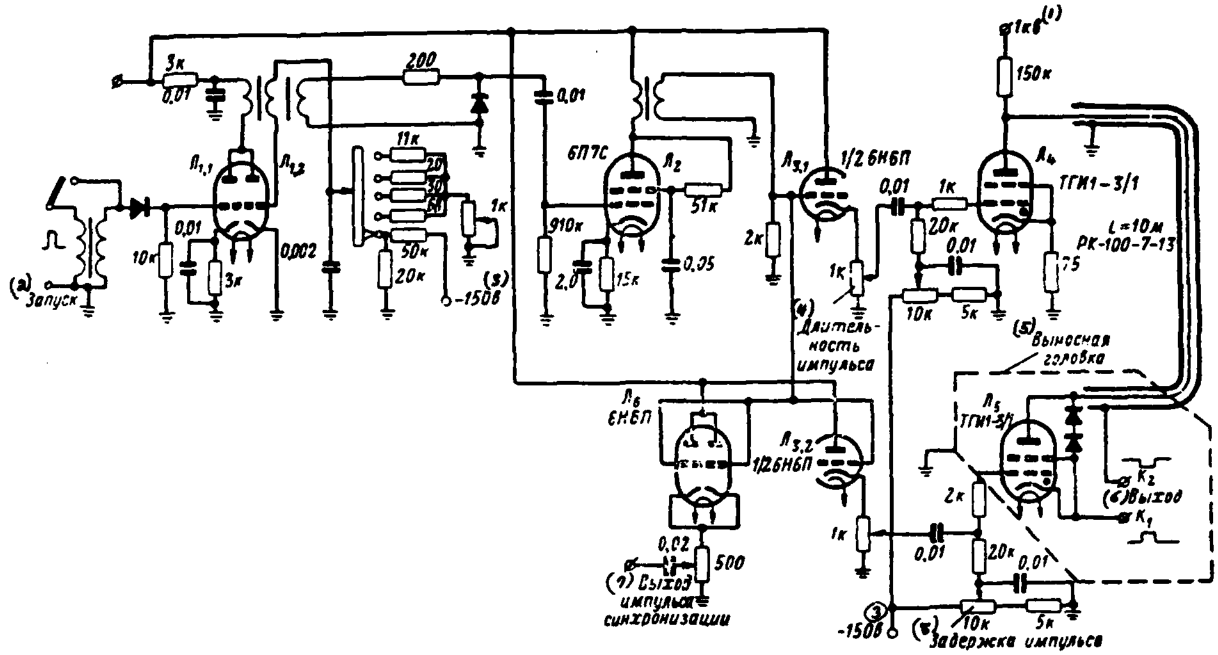

Fig. 3.32. Simplified circuit of thyratron generator, noncritical to value of load.

Key: (1). kV. (2). Starting/launching. (3). in. (4). Pulse duration. (5). Extension cap. (6). output. (7). output of synchronizing pulse. (8). Pulse delay.

Page 186.

It is removed/taken from the third winding of the transformer of blocking oscillator and enters the input of amplifier. The pulse with an amplitude of 300 V is removed/taken from the output of amplifier and it is supplied simultaneously to the grids of the cathode followers, assembled on two halves of tube 6N6P ($L_{3.1}$ and $L_{3.2}$) and to the cathode follower (L_4). The first two cathode followers serve for the starting/launching of the thyratrons of shaping unit, and the

latter (L_6) is the output stage of pulse for the synchronization of the external diagrams, when blocking oscillator works in the auto-oscillating mode.

For obtaining pulses of different duration on cascade/stage of agreement pulse with delay t_p relative to admission on cascade/stage of formation comes. Delay factor is regulated by changing the load of cathode follower ($L_{3,1}$). Ranges of adjustment of delay from 15 to 100 ns. Maximum pulse repetition rate 10 kHz. With the formation of square pulses with the strictly flat/plane apex/vertex the load of the thyratron of the forming cascade/stage, i.e., termination of generator can vary within the range of 75 ohms to 100 kilohms. With the very large load (from 100 kilohms to 1 MΩ) it is possible to form/shape long pulses with a small decay in the apex/vertex.

With impulse shaping in the range 15-100 ns, pulse amplitude grows/rises with increase in load from 450 V when $R_н=75$ ohm to 900 V with $R_н=750$ kilohms. Smooth of a change in the pulse amplitude relative to its maximum value can be obtained by a change in the value of the anode voltage of the feed of thyratron.

As forming line is used segment of cable RK-100-7-13 with length of 10 m. With the impulse shaping of positive polarity, the load is switched on in the cathode circuit of thyratron L_8, and in the case of negative polarity - between the external braid/cover of cable and the earth/ground. In the second case the pulse current of the discharge

can pass not through the load, but on the braid/cover from the opposite end/lead of the cable. To avoid this cable it is coagulated into the bay, and then its braid/cover forms the inductance coil, which presents high resistor/resistance for the current pulse.

Switched on thyratron (L_2) semiconductor diodes in parallel serve for correction of shear/section of output pulse with high load resistance/resistors.

Page 187.

Diodes make it possible to rapidly carry out a discharge of stray capacitance in the cathode circuit of thyratron, which noticeably is charged with the large load (shunting this capacity/capacitance) for the pulse action time.

For convenience in supply of output pulse into any diagram being investigated forming thyratron L_2 is installed into extension cap. Extension cap is connected with basic part of the generator by the hose, which supplies the forming cable, wire of the grid of thyratron and wire of incandescence/filament.

Described generator, which is characterized by noncriticality to value of load, is used as signal generator. With the aid of similar generator it is possible to produce testing the impulse circuits, whose input resistances have values from tens of ohms to hundreds of kilohms.

Version of diagram without continuously variable control of duration of output pulses (with one thyratron) finds use as modulator of shf/SVCh generators, which are time-varying load (in process of modulation, for example, of magnetrons and other shf/SVCh instruments). This diagram is utilized just as the generator of an initial drop/jump in the voltage/stress or current (especially if diagram on the powerful/thick thyratrons), necessary for the impulse shaping in the nonlinear lines (Chapter 4), where it is difficult to coordinate the input resistance of nonlinear line with the resistor/resistance of generator.

Pulse-shaping circuits of high voltage.

If it is necessary to form nanosecond pulses of high voltage, then it is necessary to utilize high-voltage thyratrons. However, how for more high voltage is designed thyratron, than more the time of its ionization. Therefore in the presence of the thyratrons, which have good commutation properties, but designed for the work with insufficiently high voltage, can be used the diagrams, in which the commutating element are two series-connected thyratrons (Fig. 3.33) [3].

Page 188.

The series connection of thyratrons makes it possible to utilize power supplies with the voltage/stress, two times which exceeds working the

anode voltage of one thyratron.

In this diagram trigger pulse is supplied through transformer to grids of thyratrons. It is possible to obtain three operating modes by the adjustment of bias voltage in the circuit of the grid of thyratrons: first operates/wears the first thyratron, both thyratrons operate/wear it simultaneously and anticipates/leads the second thyratron. During the starting/launching of the first thyratron L_1 at the output of diagram together with the main impulse can be observed the supplementary pulse, which anticipates/leads basis. The onset of supplementary pulse is connected with the discharge of stray capacitances in the circuit of the anode of thyratron L_1.

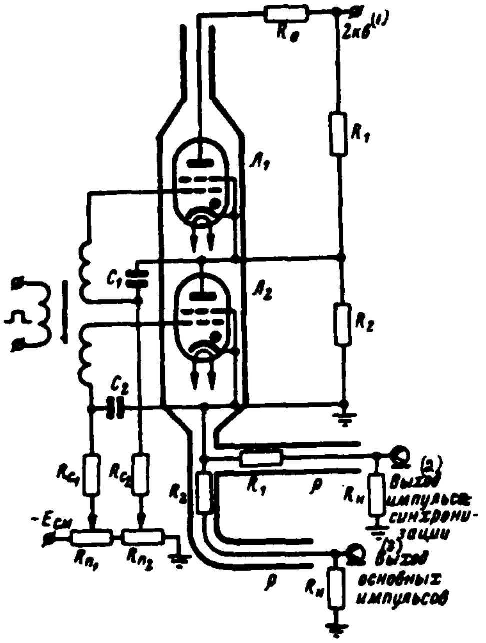

Fig. 3.33. Pulse-shaping circuit of high voltage with two thyratrons. Key: (1). kV. (2). output of synchronizing pulse. (3). output of main impulses.

Page 189.

The mode of the coincidence of the ignition of thyratrons makes it possible to obtain the pulse of the same form, as in the case of diagram with one thyratron, but with the doubled amplitude. True, in this case it is necessary to ensure the rigid synchronization of ignition of both thyratrons, what is sufficiently difficult problem and requires the high stability of the supplies of power and large steepness of the front of trigger pulse with a sufficient stability of its parameters. The mode of operation of the diagram, when first ignites thyratron L_1, makes it possible to obtain the edge of the

pulse of noticeably smaller duration, than in the diagram with one thyratron. This occurs because the ionization of thyratron L_1 occurs with the increased voltage/stress not its anode, since upper half of the voltage divider proves to be that shunted by thyratron L_2, which conduct current.

Structurally generators are fulfilled in the form of coaxial system, which is special container with thyratrons and built in coaxial cables (Fig. 3.33).

Frequently together with main impulse it is necessary to have another pulse, displaced in time relative to the first, at separate output. In such cases at the output of generator the splitters of pulses, which represent the dividers with several outputs (Fig. 3.33), matched with the forming line are used. For displacing the pulses in the time at the output the segments of the cables of different length are used.

However, other recently appearing methods of impulse shaping of high voltage with very short duration of front, make it possible to use one high-voltage thyratron and nonlinear forming distributed circuits (see Chapter 4).

3.6. CORRECTION OF THE SHAPE OF PULSE.

Characteristic deficiency in shape of pulse, obtained in diagram

with discharge line and thyratron, is smoothly increasing section in the beginning of pulse apex (Fig. 3.25), caused by retarding/deceleration of change in conductivity of thyratron up to moment/torque of total ionization of gas, and also slow decay in apex/vertex at the end of pulse.

Page 190.

The presence of such sections more noticeably expressed in the pulses, formed/shaped in the diagrams with the high-voltage thyratrons. So that the shape of pulse would be more rectangular, it is possible to use the methods of correction.

Correction of apex/vertex at its beginning, and also partial decrease of duration of pulse edge it is possible to achieve by inclusion of supplementary anodic capacity/capacitance C_a in parallel to forming line (Fig. 3.34a). The current through the thyratron with shaping of the initial section of pulse apex grows/rises due to the discharge of this capacity/capacitance. As a result to a considerable degree the form of flat/plane pulse apex is improved and the steepness of front in the upper part of the pulse (Fig. 3.35) somewhat is raised [3, 51]. With excessive capacitance value C_a is observed overcorrection, which is evinced by the appearance of an overshoot in the beginning of apex/vertex.

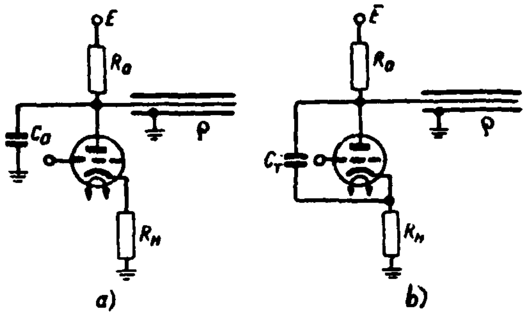

Fig. 3.34. Thyratron diagrams with corrective capacitors, capacitors, switched on: a) in parallel to cable; b) in parallel to thyratron.

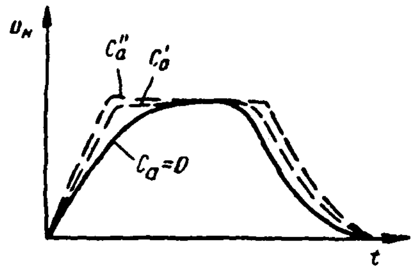

Fig. 3.35. Shape of pulse with different value of corrective capacity/capacitance $(C''_a > C'_a)$.

Page 191.

For finger thyratron TGI1-3/1 capacity/capacitance $C_{a\,опт} = 15 \div 20$ pF, while for high-voltage thyratrons $C_{a\,опт} = 35 \div 50$ pF. The application of the corrective capacity/capacitance makes it possible in the case of finger thyratron to decrease the duration of front on 1 ns, and in the case of high-voltage thyratrons - on 2 ns.

Application of corrective capacity/capacitance C_a in diagram in Fig. 3.28a makes it possible also to a considerable degree to weaken/attenuate integrating effect of shunt capacitance $C_ш$, which

sometimes proves to be to shunt resistance to loadings $R_н$. The discharge of the corrective capacity/capacitance creates the conditions of the more rapid charge of shunt capacitance, the steepness of the pulse edge increases in consequence of which and the nonuniformity of its apex/vertex decreases.

Presence of capacity/capacitance, which shunts load, and also application for correction of capacity/capacitance, switched on in parallel to forming cable, leads, however, to increase in time of shear/section of pulse. This is caused by the process of the discharge of the indicated capacities/capacitances through the load after time t=2t,.

Time constant of discharge of capacity/capacitance C_a is determined by internal resistor/resistance of open thyratron $R_{т0}$ and by resistance/resistor of load $R_н$. it is equal to

$$\tau_k = C_a (R_{т0} + R_н).$$

Occurring due to discharge of this capacity/capacitance increase in pulse duration, measured at level 0.5 of amplitude, will be equally

$$t_k \approx 0{,}35 \frac{E}{U_н} R_н C_a,$$

where $U_н$ - amplitude of formed/shaped pulse.

Increase in pulse duration, caused by discharge of capacity/capacitance $C_ш$.

$$t_{ш} \approx 0{,}7C_{ш}R_{н}.$$

Method of correction with the aid of capacity/capacitance $C_{т}$, connected in parallel to thyratron, does not have this deficiency (Fig. 3.34b). The current of discharge $C_{т}$ contributes to the more rapid process of the ionization of gas in its final phase.

Page 192.

If the value of this capacity/capacitance is not very great and it manages rapidly to be discharged at the moment of the complete triggering/opening of thyratron, then its presence does not cause an increase in the duration of the pulse edge, but slows down the displacement of operating point from the characteristic of ionization, which corresponds to voltage/stress U=E, to the characteristic, which corresponds to $U=\frac{E}{2}$ (Fig. 3.36). Curves 1 and 2 characterize a change in the voltage on the load of generator taking into account the decrease of voltage/stress in the forming line with E of up to E/2 and can be named the dynamic characteristics: curve 1 in the presence of capacity/capacitance $C_{т\ опт}$ and curve 2 when $C_{т}=0$.

Capacity/capacitance $C_{т}$, corrects form of dynamic characteristic in its upper part, which leads to correction of apex/vertex and pulse edge on load $R_{н}$. The discharge current of this capacity/capacitance does not pass through the load resistance/resistor, and therefore the duration of the shear/section of pulse does not grow/rise and is equal to the duration of front. Optimum capacitance value $C_{т}$ for the finger

thyratron of approximately 20 pF and for the high-voltage thyratrons of approximately 30 pF.

However, connection of capacitor C_T to high-voltage thyratrons can cause appearance of stray inductance due to jumpers, since distance between anodic and cathode outputs in series/row of thyratrons is not very small.

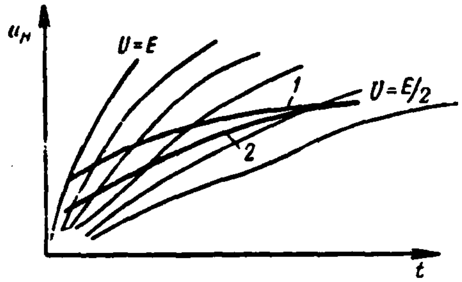

Fig. 3.36. Dynamic characteristics of ionization of thyratron: 1 - in presence of capacity/capacitance with $C_{a\ опт}$; 2 - when $C_a=0$.

Page 193.

As noted earlier, presence in diagram of capacity/capacitance $C_ш$ which shunts cathode load, and also application of corrective capacity/capacitance C_a, increase in duration of shear/section of pulse is caused. For decreasing the duration of shear/section it is possible to use the special circuits of correction [3, 52].

Fig. 3.37 gives diagram, which corrects simultaneously as shear/section of pulse, so to a certain extent and its apex/vertex. Capacitor $C_к$ with a capacity/capacitance of hundreds of picofarads, connected consecutively/serially with the load resistance/resistor, transmits the pulse edge without the distortions. The capacitor partially is charged for the pulse action time and voltage/stress on the resistance/resistor of load $R_н$ during the formation of the shear/section of pulse will be determined by value $U_{Rк}-U_c$, which leads to the decrease of the duration of shear/section.
Resistors/resistances R_1 and $R_к$ serve for the capacitor discharge

after the termination of pulse.

Circuit of correction must not introduce disagreement/mismatch into forming line with load. The time constant of equalizer must be such that to ensure the undistorted transmission of the pulse edge and to at the same time ensure charge of capacitor $C_к$ to voltage/stress $\Delta U_{макс}$ (Fig. 3.38), a sufficient for the correction shear/section of pulse.

Matching condition of forming line is given by expression

$$\rho = R_1 + R_{т0} + \frac{R_к R_н}{R_к + R_н}. \qquad (3.39)$$

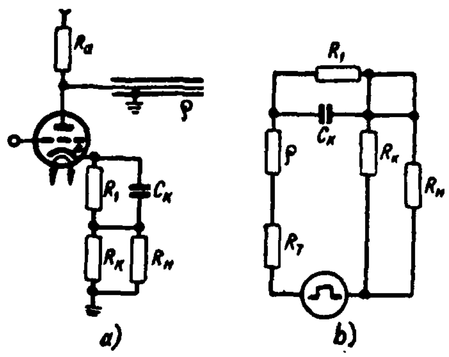

Fig. 3.37. Corrector of shear/section of pulse (a) and its equivalent diagram (b).

Page 194.

Time constant of capacitor charging circuit $C_{к}$ under effect of pulse edge must satisfy condition

$$\tau_{з} = R_{э} C_{к} \geqslant 5 t_{ф}. \qquad (3.40)$$

Time constant of capacitor charging circuit for pulse action time must be

$$\tau'_{з} = R_{э} C_{к} = \frac{t_{и}}{\ln \frac{U_{макс}}{U_{макс} - \Delta U_{макс}}}, \qquad (3.41)$$

where

$$R_{э} = R_{1}\left(1 - \frac{R_{1}}{2\rho}\right).$$

Value of resistor/resistance of R_{1} is selected from condition of permissible decay in apex/vertex:

$$\frac{\Delta U_{макс}}{U_{макс}} = \frac{R_{1}}{R_{1} + \frac{R_{к} R_{н}}{R_{к} + R_{н}}} = \frac{R_{1}(R_{к} + R_{н})}{R_{1} R_{к} + R_{1} R_{н} + R_{к} R_{н}}. \qquad (3.42)$$

Capacitance of capacitor $C_{к}$ is determined from conditions (3.40) and (3.41), which can be recorded in the form

$$\frac{t_{и\,мин}}{\ln \frac{U_{макс}}{U_{макс} - \Delta U_{макс}}} \geqslant \tau'_{з} \geqslant 5 t_{ф},$$

where $t_{и\,мин}$ - minimum pulse duration.

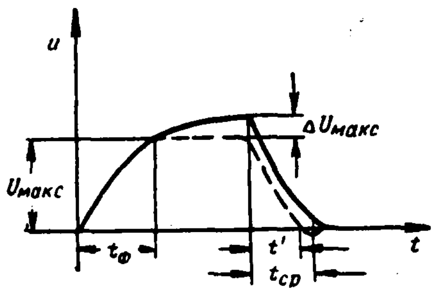

Fig. 3.38. Oscillogram of pulse, obtained in diagram with correction.

Page 195.

With realization of correction of shape of pulses with the aid of diagram in Fig. 3.37 it is possible to decrease duration of front and shear/section of pulse on 1-1.5 ns with retention/maintaining of flat/plane pulse apex.

Application of circuits of correction is expedient in diagrams with thyratrons, when forming cascade/stage, which is located on output of device/equipment, is basic. In these cases there is a possibility to consider the special features of load, on which works the pulse generator. When the forming cascade/stage on the thyratron is not output, but it is utilized as the generator of current taper or voltage/stress, which enters others the those forming value, then, naturally, to complicate diagrams by network elements of correction does not have a sense. For example, this position place during the use of the nonlinear forming circuits or lines has (chapter 4 and 8).

3.7. PULSE-SHAPING CIRCUITS WITH RELAYS.

In pulse-shaping circuits with thyratrons it is possible to obtain pulses, duration of front of which lies/rests within limits of 5-15 ns, which depends on type of thyratron. The ionization time of thyratron sets limitation on the rate of the commutation of thyratron. Application instead of the thyratron of electron tube (corresponding power) makes it possible to obtain the pulses, the duration of front of which the order of the units of nanoseconds. If necessary for the impulse shaping of a small power for the duration of front for less than the nanosecond it is possible to use a commutator of another type. The electromechanical relay of special construction/design is such commutator.

Commutation properties of relay.

Electromechanical relay has very short time of commutation and insignificant and sufficiently fixed resistor of contact. It finds use as the commutating element in the pulse-shaping circuits of nanosecond duration.

Page 196.

In diagrams of formation it is possible to utilize usual electromagnetic relays, which are used in automation and equipment of communication (open type polarized relays and vacuum) [55]. However, for the diagrams of nanosecond range special relays are developed [56, 57].

Time of commutation of relay is considerably less than in thyratrons. Relay realizes a commutation via the periodic contact of armature and fixed contact. The motions of armature occur under the action of the alternating magnetic field, created by coil current, connected with the power supply by relay (usually with the voltage generator of low frequency). Therefore the stable work of electromechanical relay is defined by both the construction/design of mechanical system and by special features of electrical circuit. Some relays stably work in the very limited frequency region, others - in the wider region. The operating frequency of relay is caused by the resonance frequency of its mechanical oscillatory system.

Resistor/resistance of commutation and constancy of its value are caused by construction/design of contacts of relay. The strength of current, switched in the contacts of relay, in the majority of the cases is considerably lower than the current strength in the thyratron of average/mean or even small power.

Rate of commutation of relay is determined by construction/design of movable system of relay and by special features of contacts themselves. However, for the time of commutation they can noticeable effect exert the parasitic parameters of the circuit, formed by conclusions from the contacts. In the usual electromagnetic relays, not designed specially for the work in the diagrams of the formation of nanosecond pulses, stray inductance and capacity/capacitance is

very noticeable. During the application of such relays the certain possible change in the mounting of relay.

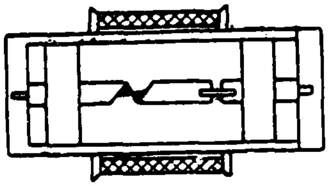

Fig. 3.39. Diagrammatic representation of construction/design of relay for coaxial system.

Page 197.

For eliminating parasitic parameters of mounting relays, specially designed for diagrams of formation of nanosecond pulses [40] against those fitted out for mounting in coaxial system are used (Fig. 3.39). This relay is fulfilled in the form of the copper cylinder, which serves as the external conductor of coaxial system, within which is fastened to the insulators the internal conductor (from the elastic material, covered with silver), that consists of two parts - with motionless and movable. Both parts of the internal conductor have the platinum contacts, designed for the transmission of the current of the significant magnitude. Slide contact is set in motion and completes oscillations/vibrations at its resonance frequency, equal to 100-150 Hz, under the action of the magnetic field of the coil, arranged/located on the external conductor of relay.

Sizes/dimensions of external and internal conductors are selected so that wave impedance of system of relay corresponds to wave impedance of forming cable, which is connected up to one end/lead of

relay, and also cable of output, which is connected up to another end/lead of relay.

Some constructions/designs of relay have essential deficiency, which is expressed in the fact that at moment of closing of contacts their repeated contacts appear ("chattering"). As a result the shape of the obtained pulse sharply is distorted. Since in the relays, which have mechanical solid contacts, such repeated contacts of contacts during their closing/shorting are very probable, then for eliminating this essential deficiency are proposed relay with the hydrophilic contacts. In such relays the commutation is realized via the contact of two hydrophilic contacts or one solid nonwettable contact with liquid conducting medium, as which is utilized mercury [56, 57].

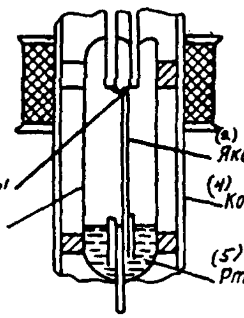

Fig. 3.40. Diagrammatic representation of construction/design of relay with hydrophilic contacts.

Key: (1). Contacts. (2). armature. (3). Capsule. (4). Housing. (5). Mercury.

Page 198.

Relays with contacts moistened by mercury, found use in series/row of generators of nanosecond pulses, is represented in Fig. 3.40 [56]. In glass bulb, whose lower part is filled with mercury, are installed contacts. One contact in the form of the long springy armature, made from the ferromagnetic material, has capillaries, using which rises mercury. The second contact is motionless and made in the form of the platinum ball/sphere, attached to the small pole piece, sealed in in the upper part of the flask/bulb.

Proceeding to junction mercury wets both contacts and during closing/shorting reliable compound is formed. Armature touches the contact at the point, close to the center of system, which limits the force of the jerk/impulse, which throws/rejects armature to this value

of the amplitude, whose value is insufficient for the disturbance/breakdown of the mercury bridge, which is formed during the closing of contacts. Thus, completely is removed bouncing of contacts during closing/shorting of relay.

For increasing reliability of work of relay space within flask/bulb is filled with hydrogen under pressure in 10 atm. Relay is included in oscillator circuit as the part of the coaxial system.

In generator with such relay it is possible to obtain pulses with amplitude of up to 50 V for duration of front 0.2 ns. Further increase in the pulse amplitude can lead to the disruption of the work of relay as a result of possible evaporation of mercury in the place of contact.

Fig. 3.41 gives construction/design of relay with one rigid [57]. In glass bulb 1 is an armature 2 in the form of the jarring steel plate. Flat/plane platinum contact 3 is fastened/strengthened to the free end/lead of the plate. In the lower part the flask/bulb has a contraction. It together with glass small tube 4, mixed at the end/lead of the lower molybdenum conclusion/output, forms capillary. As a result of this mercury, which fills the lower part of the flask/bulb, is held in the capillary on the same level and counterbalances mercury column in the central tube.

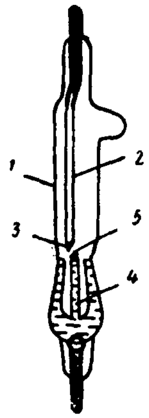

Fig. 3.41. Flask/bulb of relay with one solid contact and mercury drop.

Page 199.

At the end/lead of this tube mercury forms convex meniscus 5, which is the second contact of relay. With the vibration of armature platinum contact each period, concerning the drop of mercury, cuts its and, thus, is realized commutation without the supplementary contacts of contacts. The drop of mercury then is restored due to mercury, which enters from the tube. The space of intra-flask/intra-bulb is filled with hydrogen under the pressure approximately 10 atm. In the upper and lower parts of the flask/bulb are conclusions, connected in accordance with armature and mercury. Flask/bulb is placed into the copper cylinder, on which is arranged/located the coil of relay. For the preliminary magnetic biasing of armature outside the coil permanent magnet is placed.

Relay of such type is used in series pulse generator of

nanosecond duration G5-12. The formed/shaped pulses have a duration of front of approximately 0.4 ns and an amplitude, adjusted in the limits from 10 mV to 100 V. The pulse repetition frequency is determined by the resonance frequency of the oscillations of armature and is equal to 200 Hz.

For formation in diagram with relay of pulses with duration of less than nanosecond it is necessary to have relay with time of commutation of less than 10^{-10} s, and also to considerably decrease length of forming line. L. N. Tyul'nikov [58] proposed the generator, which contains the electromechanical relay, in which the element, which accumulates energy, simultaneously fulfills Paul interrupter. Schematically the *construction/design of generator* is depicted in Fig. 3.42.

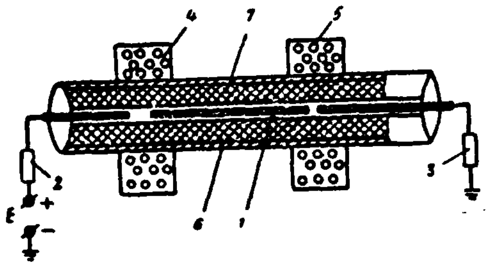

Fig. 3.42. Diagrammatic representation of device/equipment of generator with relay, which have movable section/segment of center conductor of coaxial line.

Page 200.

Here coaxial line contains central conductor 1, which is cut in two places. Middle section/segment freely is moved in axial direction, alternately oscillating by the ends/faces of left and right of the attached sections/segments of center conductor. Left section is connected through resistor 2 to the dc power supply, right to matched load 3.

In process of moving middle section/segment along axis of coaxial line with its contact of left section/segment charge of line occurs, and discharge of line for matched load is realized with contact of right section/segment of conductor. The motion of middle section/segment occurs due to the energy of the alternating magnetic field of coils 4 and 5, arranged/located out of the coaxial line.

Generator, thus, is carried out as single coaxial line.

Dielectric 7 is placed between the center conductor and external conductor 6. The gap between the center conductor and the internal cylindrical surface of dielectric is led to the tenths of millimeter, which comprises less than 1% of the diameter of external surface. Therefore a change in the line characteristic due to the gap is less than 1%. The reciprocating motions of the section/segment of center conductor without the axial bias/displacement do not introduce noticeable heterogeneity into the line.

Generator can work stably even during repeated collision of contacts in process of their closing/shorting. This is admissible, since charging circuit is extended during the discharge of coaxial line for the load, and the discharge time of line, which determines the pulse duration, is considerably less than the time of the first contact of the sections/segments of center conductor.

Possibility of shortening duration of formed/shaped pulse up to limit, which is generally feasible in generators with relay, is one of fundamental advantages of this generator. Thus, at the length of the middle section/segment of center conductor, by wound 1 cm, the pulse duration is close to 0.08 ns. With the considerable decrease of the length of the movable section/segment it is already necessary to consider of it as the lumped element of diagram.

Limiting case of impulse shaping of very short duration will be during discharge of ball/sphere, into which degenerates movable

section/segment of center conductor with decrease of its length.

Page 201.

Its ability to work in frequency band relatively wide for usual relays is special feature of generator with movable section/segment of center conductor. The middle section/segment of center conductor is analogous to the loose beam/gully, which can freely be moved in the axial direction. This beam/gully under the influence of periodic force can complete motions out of the resonance of system up to the natural vibration frequencies of rod. Upper working oscillator frequency, however, can be limited due to finite time of the magnetic reversal of the ends/leads of the rod upon the replacement of the direction of the manager of the magnetic field of coils. In this case essential is the material, from which is prepared the center conductor, and also the form of external the control voltage, supplied to the coils. The maximum operating frequency of this generator can reach several kilohertz.

Oscillator circuits with the relay.

Oscillator circuits with relay are sufficiently simple. Fig. 3.43 gives the oscillator circuit from the relays, which makes it possible to obtain at the output simultaneously three pulses, shifted in the time relative to each other.

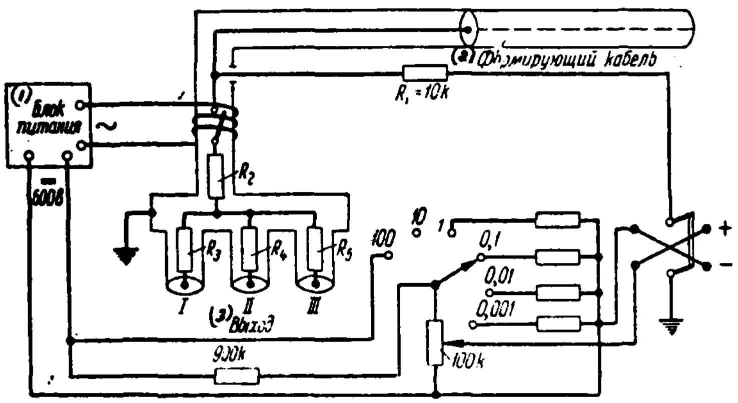

Fig. 3.43. Oscillator circuit with relay.

Key: (1). Power supply unit. (2). Forming cable. (3). output.

Page 202.

With extended relay forming cable is charged through resistor/resistance of R_1, and from moment/torque of closing/shorting relay it is discharged for matched load. Load is composed from resistors/resistances of R_2, R_3, R_4, R_5 and the resistors/resistances of the output cables, locked for the resistive loads, equal to their wave impedance. In this diagram the matching condition of the forming cable with the load is satisfied, if the resistor/resistance of divider has a value $R_2=R_3=R_4=R_5=\rho/2$, where ρ - wave impedance of cable. In this case the amplitude of output pulses is equal to $U_1=U_2=U_3=E/6$, where E - supply voltage.

Is possible application of matched divider, at output of which pulses have different amplitude. If one of the outputs is not utilized, then it must remain loaded to the resistor/resistance, equal

to the wave impedance of the cable of this output.

Pulse amplitude in diagrams with relay is very stable in value, in this case its stability is determined by stability of supply voltage, connected to forming line for its charge. In the diagram in question the amplitude of output pulses is regulated by changing supply voltage, which is conducted with the aid of switching of the divider of voltage and continuously variable control by potentiometer. The range of a change in the pulse amplitudes is virtually feasible from the millivolts to tens of volts. The duration of front and shear/section of pulse is the less, the more qualitatively the mounting of the diagram of formation is carried out.

Generators with relay possess that advantage that in them easily can be obtained pulses both positive and negative polarity, which is determined by polarity of switching on/inclusion of source of power. The replacement of the pulse polarity is realized with the aid of the switch.

Described oscillator circuit with relay as similar simplest diagrams with relay, has, however, number of deficiencies. Many relays work stably only at the specific frequency, equal or to very close to the resonance frequency of armature. For the same reason it is difficult to carry out synchronization of the work of generator by external trigger pulses. Generators with the relay have low pulse repetition rate.

Page 203.

3.8.

PULSE-SHAPING CIRCUITS WITH THE ELECTRON TUBES.

Examined diagrams of formation with thyratrons either relay as forming element contain first-order two-terminal network in the form of section/segment of coaxial cable, extended at one end/lead, or special two-terminal network in the form of cable segment, connected at ends/leads with load and matched impedance.

With impulse shaping is found also use of diagrams, whose work is based on properties of second kind forming two-terminal network. In such diagrams frequently as the source of current taper are utilized the cascades/stages on the electron tubes. The diagrams, which have electron tubes as the commutator, make it possible to obtain pulses with the repetition frequency, considerably larger than in the diagrams with the thyratrons and the relay.

Fig. 3.44 gives diagram with forming line and pentode, which ensures required current taper [59]. In initial state both tubes are closed and current in load R_2 is absent.

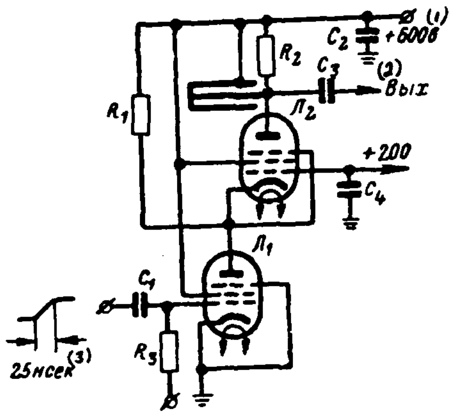

Fig. 3.44. Diagram with forming line on pentodes.

Key: (1). V. (2). ~~VYKh~~ input. (3). ns.

Page 204.

The trigger pulse of positive polarity with the steep front, obtained from the blocking oscillator, is supplied to the grid of the first pentode. For the time, during which the current in the tube L_1 reaches maximum, stray capacitances, available in the circuit of the anode of tube L_1 and cathode of tube L_2 manage to be discharged from 600 V approximately to 200 V, which corresponds to positive voltage/stress on control electrode of the second tube.

As a result of negative drop/jump in voltage/stress, which is created on cathode of second tube L_2, it is opened/disclosed also through resistor/resistance of R_2 flows/occurs current of constant value. The negative drop/jump in the voltage/stress, which appears in this case on the anode of tube L_2, is transmitted along the cable segment, short-circuited at the end/lead. After reflection from the

end/lead of the line this drop/jump in the voltage/stress returns with opposite phase, as a result of which the shear/section of pulse is formed/shaped. Thus, on the anode of tube L_1 is created the pulse, whose duration is determined by the doubled delay of the forming line. The duration of front and shear/section of pulse in this diagram depends on the duration of the front of the drop/jump in the voltage/stress, supplied to the line, which is determined by triggering time of diagram on the pentode L_2.

Duration of front of output pulse here succeeds in obtaining equal to several nanoseconds. Pulse repetition rate reaches hundreds of kilohertz.

Forming properties of second-order two-terminal network are utilized also in pulse-generating circuit of triangular form, proposed by Yu. N. Prozorovskiy [60]. Diagram consists of the forming two-terminal network, the cascade/stage, which creates current taper, and limiter. In the simplified form the diagram is given in Fig. 3.45.

In the case of applying pentode as current generator front of current taper is linear in its middle part, and beginning and end/lead are distorted due to effect of stray capacitances. The distortion of front at the pulse apex in this diagram is eliminated, since the forming line has a delay time less than the duration of the front of current taper. However, the application of limitation from below

makes it possible to remove the distortions of front in its initial part.

Page 205.

As a result in the diagram the pulses of sufficiently correct triangular form are formed/shaped.

Trigger pulse of positive polarity is supplied to input of blocking oscillator (to tube L_1), which generates steep-sided pulses approximately 4 kV/μs. This pulse is fed/conducted to control electrode of tube L_2, which works in the mode of the generator of current taper. The anode current of tube in the pulse is equal to 2 a, which makes it possible to obtain the sufficiently powerful pulse of nanosecond duration.

Plate load of tube L_2 is cable segment and ohmic resistance. In the anode circuit of tube L_2 are formed/shaped two triangular pulses of negative and positive polarity, that correspond to front and shear/section of the pulse, which triggers tube. Negative and the lower part of positive pulses are intercepted/detached in the cascade/stage limitations L_3. The upper part of positive pulse in this case is additionally amplified by the tube of limiter.

Output pulse of negative polarity has correct triangular form and rate of build-up of front on the order of 30 kV/μs. The pulse duration can be regulated by bias/displacement change on the grid of

tube L, from 3 to 19 ns. The pulse amplitude on the load of 150 ohms in this case varies respectively from 50 to 600 V. The pulse repetition frequency reaches several hundred kilohertz.

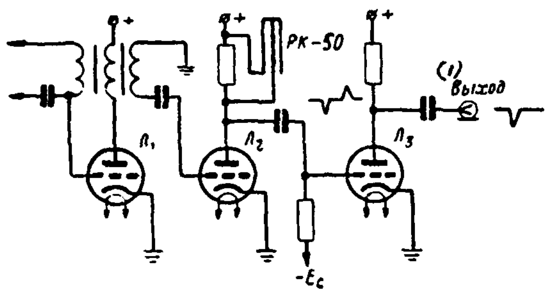

Fig. 3.45. Pulse-shaping circuit of triangular form.

Key: (1). output.

Page 206.

Diagram can be altered for obtaining pulses of positive polarity. In this case limiting cascade/stage must be transferred into the mode of cathode follower; however, the steepness of the front of output pulse in this case falls to 4 kV/μs.

Application in this schematic of low-power electron tubes (receiver-amplifier) makes it possible to form/shape pulses with amplitude of up to 50 V.

For all pulse-shaping circuits with nanosecond duration with electron tubes as commutating element, is essential form of trigger pulse. If in the diagrams with the thyratrons trigger pulse defines the operational stability of diagram, but not the form of the formed/shaped pulse, then in the diagrams with the electron tubes it defines both the stability of starting/launching and form of output pulse. Here the steepness of the front of trigger pulse must be

considerable, since it determines the jump steepness in the current, and consequently, front and the shear/section of the formed/shaped pulse. Only with the considerable slope/transconductance of trigger pulse stray capacitances of the diagrams, which also determine the shape of pulse, begin to play noticeable role. If the slope/transconductance of trigger pulse is insufficiently great, then in essence trigger pulse determines the form of the frontal part of output pulse. In the diagrams, where limiters are not used, the nonlinearity of the initial section of trigger pulse can affect the form of output pulse.

However, possibility of obtaining high pulse repetition rate in diagrams with electron tubes is their essential advantage.

3.9. Pulse-shaping circuits with the spark dischargers.

In pulse-shaping circuits with relay is possible obtaining pulses, duration of front of which about 0.1-0.4 ns, but their amplitude is limited virtually by value 100 V. However, in the diagrams with the thyratrons it is possible to obtain the pulses of high voltage, but the duration of their front is considerably more than formed/shaped in the diagrams with the relay.

Page 207.

However, in number of cases it is necessary to have pulses of high voltage, duration of front of which is less than nanosecond.

Such pulses can be formed in the diagrams with the discharge lines, in which as the commutator are utilized the spark dischargers.

COMMUTATION PROPERTIES OF SPARK DISCHARGERS.

by experiments [61, 62] established that rate of breakdown of discharger at atmospheric pressure grows/rises with increase in voltage/stress applied to electrodes. If the applied voltage/stress considerably exceeds breakdown (it occurs overvoltage), then the time of fundamental breakdown, i.e., the time of the commutation of gap/interval, can be less than one nanosecond.

Valuable property of spark discharger consists in possibility of transmission by it very high currents. However, application in the discharger/gap of supplementary third electrode makes it possible to create the commutator, controlled by trigger pulse.

However, spark discharger as commutator of pulse-shaping circuit of nanosecond duration has considerable deficiency. This deficiency consists in the large instability of the moment/torque of the fundamental prebreakdown of discharger/gap. Therefore the use of a spark discharger in the diagrams of the formation of periodic pulses is virtually excluded. However, with the formation of the single pulses of large power the dischargers/gaps find wide application.

Time of commutation of spark discharger and duration of pulse

edge determined by it can be evaluated by expression [63, 64]

$$t_{\phi} = k\frac{s^2}{U^2} + 2{,}2\frac{L}{R},$$

where k - constant, which depends on form and gas pressure in spark discharger;

s - spark-gap length;

U - voltage on discharger/gap;

L - stray inductance of circuit;

R - load resistance/resistor.

Page 208.

If parasitic parameters of mounting are low, then duration of front is determined by properties of commutator, i.e., by parameters k and s, and also with value of voltage/stress. The greater the applied voltage/stress, and consequently, the greater the amplitude of formed/shaped pulses, the less the duration of front. However, in the real cases with the high value of voltage/stress U and the small gaps/intervals s value t_{ϕ} does not depend on s and is determined by the time constant of the circuit, formed due to the parasitic parameters. This position occurs, when the duration of front approaches a value of order 10^{-10} s.

Value of time lag of breakdown relative to moment/torque of arrival of igniting pulse or applied voltage/stress is important characteristic of discharger. In many instances during the investigations with the aid of the high-voltage pulses, obtained in the diagrams with the spark dischargers, to undesirably have long time

lag.

Time of statistical time lag of breakdown succeeds in descending with work in mode of considerable overvoltage. Large overvoltage can be obtained in the special constructions/designs, so-called series spark gaps [65, 66].

SCHEMATICS OF DEVICES/EQUIPMENT WITH THE SPARK DISCHARGERS.

Fig. 3.46a gives diagram of installation for formation of nanosecond pulses of high voltage, with the aid of which it is possible to obtain pulses of high voltage with duration of front of 0.3 ns [67].

Forming cable L_1 is charged through resistor/resistance of R_1 from source with voltage/stress of E, equal to 20 kV. The center conductor of cable is connected with one of the electrodes of the starter gap, which consists of two sections. The first section by length l is formed by left and average/mean electrodes in the form of the spheres, placed accurately in the direction of center conductor. The second section with a length of $l/4$ is formed by average/mean and right electrodes.

Voltage/stress E, applied to first section of starter gap, is lower than breakdown voltage.

Page 209.

Therefore the breakdown of the first section begins only during the supplying to the average/mean electrode of the negative trigger pulse, as a result of which average/mean electrode is charged up to voltage/stress E. The second section, which has smaller length, proves to be under the voltage/stress, which exceeds breakdown voltage approximately 4 times, which leads to the rapid breakdown of this section.

Pulse formed/shaped in starter gap enters cable L_2. Duration of the edge of this pulse of approximately 20 ns. This duration is not connected with the properties of the second section of starter gap, it depends on the fact that in the beginning of breakdown the current in the first section cannot achieve the necessary value due to the high resistor/resistance of the trigger generator, on which falls the significant part of the voltage/stress. After the breakdown of the second section the resistor/resistance of gap/interval is determined by the low value of the wave impedance of cables L_1 and L_2 and current reaches value 200 a.

For peaking is used second discharger, so-called peaker, which is isolated from starter gap by cable L_2.

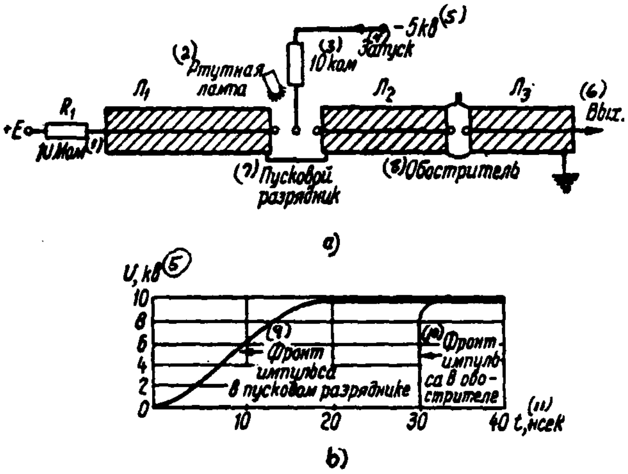

Fig. 3.46. Oscillator circuit with spark dischargers (a); oscillogram of formation of edge of pulse (b).

Key: (1). Megohm (2). Mercury-vapor lamp. (3). kilohms. (4). Starting/launching. (5). kV. (6). Output. (7). starting/launching discharger/gap. (8). Peaker. (9). Pulse edge in starting/launching discharger/gap. (10). leading edge of pulse in peaker. (11). ns.

Page 210.

The pulse through the separating cable emergent in the starter gap proceeds to discharger/gap with the very short gap/interval, which proves to be under the voltage/stress, which considerably exceeds breakdown. Breakdown flows/occurs very rapidly, but on the time it delays relative to the moment/torque of the arrival of pulse. If time lag lasts more than 20 ns, then the flat initial part of the pulse, which enters the peaker, manages to pass (Fig. 3.46b) and then the edge of the pulse, formed/shaped in the peaker, is determined by the rate of breakdown in it. For obtaining the necessary value of the

time lag of breakdown in the peaker the space is filled with nitrogen under the high pressure. For decreasing the time of commutation the length of gap/interval is small and equal to 0.025 mm.

Formed/shaped pulses have amplitude of 10 kV for duration of front 0.3 ns. Since the time lag of breakdown is unstable, then it is difficult to ensure assigned delays of breakdown, equal to 20 ns.

Another oscillator circuit is free from some deficiencies in preceding/previous diagram. Generator has one discharger, whose space is filled with nitrogen under the high pressure. The peaking of the formed/shaped pulse occurs in the same gap/interval with the aid of the high-frequency corrective capacitor, connected to the electrodes of discharger/gap (Fig. 3.47). Here ρ - wave impedance of cables.

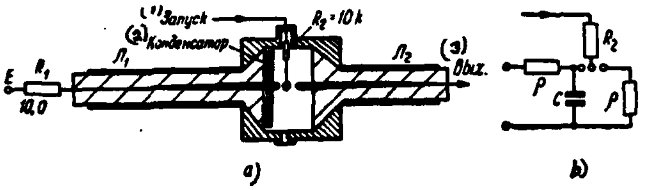

Fig. 3.47. Oscillator circuit with spark discharger (a); its equivalent diagram (b).

Key: (1). Starting/launching. (2). Capacitor. (3). Output

Page 211.

If discharger/gap would be ignited instantly, then the voltage/stress, which enters the output cable, would be equally to $\frac{E}{2}(1+e^{2t/RC})$ and it caused the surge, which dropped with the time constant $\rho C/2$. If this time constant of the order of the pulse rise-time in the discharger/gap without peaking circuit, then in the case of discharger/gap with peaking circuit it is possible to obtain steep-sided pulses without the distortions. After the selection of the value of the peaking capacity/capacitance and fine adjustment of length of both sections of discharger the diagram works reliably.

Diagram of formation of nanosecond pulses of high voltage, which uses series spark gap [66], sufficiently simply is regulated and reliably works. Fig. 3.48 gives oscillator circuit with series spark gap and peaker. This diagram makes it possible to obtain large overvoltage on the discharger/gap which leads to the short duration of the pulse edge and the small delay of starting/launching. Discharger/gap is carried out in the form of coaxial system. From the

dc power supply 30 kV is charged the segment of cable L_1. After functioning consecutive discharger p_1 in the line L_2 appears the pulse by the voltage/stress of 15 kV and by duration about 40 ns with a duration of the front of 5 ns. After the breakdown of the latter/last discharger/gap p_3 the current reaches 200 a.

For shortening of duration of pulse edge is used corrective capacity/capacitance $C_к$, switched on in parallel to line L_1. Fig. 3.48b gives the equivalent diagram of the discharge circuit.

Let us record characteristic of commutation of discharger/gap in the form [66]

$$u_p = Ue^{-at},$$

where a - constant, and assuming/setting U=1, for change in voltage/stress with time we will obtain expression

$$u(at) = \frac{1}{2}\left[1 - \frac{1 - aC_к}{2 - a\rho C_к} e^{-at} - \frac{a\rho C_к}{2 - a\rho C_к} e^{-\frac{2t}{\rho C_к}}\right].$$

It follows from this expression that with increase in capacitance $C_к$ pulse edge decreases with constant amplitude.

Page 212.

However, with excessively high value $C_к$ is observed overcorrection of pulse, which is evinced by the appearance of an overshoot for its apex/vertex. When $C_к = 1{,}4/a\rho$ the value of overshoot composes 5%. Since $a = 2{,}2/t_к$, then the optimum value of capacitance $C_к$ will be value

$$C_{\text{к}} = 0{,}63 \frac{t_{\text{к}}}{\rho},$$

where $t_{\text{к}}$ - time of the commutation of discharger/gap.

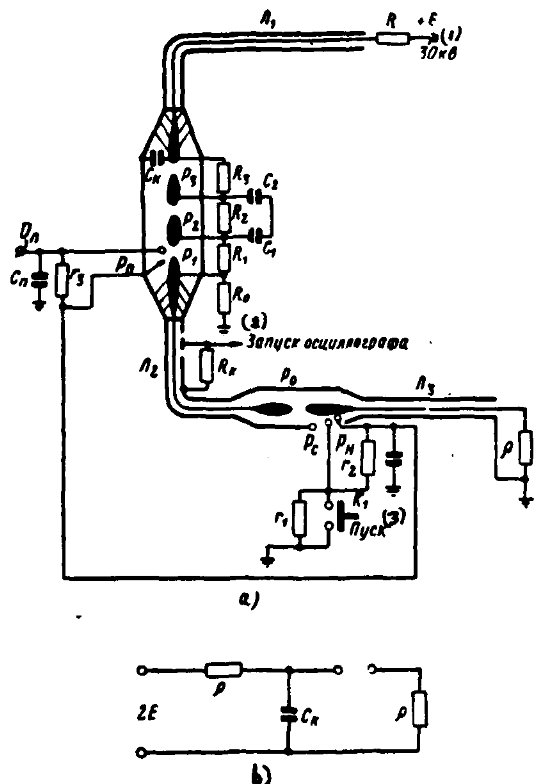

Fig. 3.48.

Fig. 3.48. Oscillator circuit with series spark gap and peaker (a); equivalent schematic of discharge line (b).
Key: (1). kV. (2). Starting/launching of oscillograph. (3). Launching/starting.

Page 213.

With this value $C_{к}$ the duration of the pulse edge is determined by the expression

$$t_{ф} \approx 1,1 \frac{l}{a} = \frac{t_{и}}{2}.$$

With the aid of corrective capacitance succeed in obtaining duration of front of approximately 2.5 ns.

For further decrease of duration of pulse edge is used peaking discharger/gap p_{o}. The length of the gap/interval of this discharger/gap is selected by such that its breakdown would occur on

the upper part of the edge of the pulse (s_0≈3 mm entering). In this case occurs maximum overvoltage in the gap/interval and, therefore, the minimum time of commutation. The duration of the front of output pulse proves to be equal to approximately 0.6 ns.

For formation of shear/section of pulse in diagram is provided special discharger/gap p_c, built in chamber/camera of discharger/gap p_0. The moments/torques of breakdown across gap p_H and p_Π are synchronized by the special circuit, connected with the key/wrench o. launching/starting generator K_1. The pulse duration is regulated by the length of the gap/interval of discharger/gap p_c. The cathode of discharger/gap p_c is irradiated by ultraviolet rays from special gap/interval p_H. The moment/torque of the breakdown of this gap/interval must be synchronized with the starting/launching of the coaxial commutator, which is ionized by spark in gap/interval p_H.

All generators of high-voltage pulses examined are intended for formation of single pulses.

Such generators are used during diverse physical investigations and during different tests [66]. Usually during the supplying of high-voltage nanosecond pulse on the object being investigated is realized the starting/launching of scanning/sweep of the oscillograph, with the aid of which is observed the studied phenomenon. Therefore in the generators the output of the trigger pulse of oscillograph must be provided. So in Fig. 3.48 is shown the output of this pulse, R_B.

removed from resistor/resistance

Page 214.

Pulse-shaping circuit with discharge line, noncritical to value of load (Fig. 3.13), it can be used also with construction of generators of nanosecond pulses of high voltage with spark dischargers. This diagram, used for the impulse shaping of microsecond duration in the installation with spark dischargers [68], proved to be very advisable with the work with the mismatched load or time-varying load. Besides noncriticality to the value of load this diagram and in the case of applying the spark dischargers makes it possible to obtain the pulses, whose duration easily is regulated in the considerable limits with the aid of a change in time difference between the moments/torques of the breakdown of two dischargers/gaps.

Page 215.

CHAPTER FOUR

Impulse shaping from the shock electromagnetic waves, which are propagated in the lines of transmission.

In contemporary physics and technology there is need for application of electric pulses of high voltage with duration on the order of 10-' s. Obtaining such pulses with the aid of the thyratron diagrams without their subsequent conversion is impossible, since the ionization time of high-voltage thyratrons is considerably more than one nanosecond. The application of diagrams with the accumulators/storage and the spark dischargers is possible only in obtaining of single pulses, because in the case of the formation of repetitive pulses is manifested the considerable instability of triggering time of spark discharger. The use of the simplest circuits with the nonlinear inductance contributes to the solution of this problem, but to the insufficient degree.

Obtaining such pulses became possible with the aid of forming lines with nonlinear parameters. Initially by I. G. Katayev [69] was expressed the possibility of the formation of very steep edges in the current (voltage/stress) by the transmission of the pulse through the

artificial delay line with the nonlinear parameters, in which the delay time decreases with an increase in the instantaneous values of current and voltage/stress.

Pulse edge at output of this line increases with considerably larger rate, than at input.

Page 216.

In contrast to many other methods of impulse shaping in this case with an increase in the amplitude of initial current taper (voltage/stress) the duration of front at the output decreases, what is the very valuable advantage of the method in question.

Theoretical studies of physical phenomena, which lie at basis of this method of formation of steep edges in current, they showed possibility of presence of impact electromagnetic of will and explained mechanism of their formation in media and transmission lines with nonlinear parameters [70-77].

Phenomenon of impact of will in nonlinear media is known in hydrodynamics and gas dynamics. Thus, for instance, velocity of propagation of the sonic of will in the nonlinear media depends on sound intensity and shock acoustic waves are formed under specific conditions in this medium.

Shock electromagnetic waves in nonlinear transmission lines with

ferrites, ferroelectrics and semiconductors made it possible to obtain drops/jumps in voltage/stress (current) with slope/transconductance to 10^{12}-10^{14} V/s. This, in turn, it made it possible with the aid of the subsequent conversion to form/shape pulses with the duration of less than the nanosecond with amplitudes of from tens of volts to tens of kilovolts.

Are described below processes of formation of shock electromagnetic waves in transmission lines, methods of calculating such lines are given and methods of impulse shaping with the aid of devices/equipment, which use nonlinear lines, are examined. In this case primary attention is given to the forming lines with the ferrite, which found the widest use in the nanosecond technology, especially with the impulse shaping of considerable amplitude.

4.1. Formation of shock electromagnetic waves in the nonlinear transmission lines.

In nonlinear media during propagation of electromagnetic waves two mechanisms of formation of shock electromagnetic waves are observed in essence. These mechanisms, connected with the dependence of the rate of propagation of waves on their amplitude and with the phenomenon of the dissipation of energy at the wave front, can be under specific conditions examined separately. In connection with this let us first examine the case relative to a slow drop/jump in the field.

Page 217.

Formation of shock waves at the relatively low speed of field change.

In the case of unbounded nonlinear nonconducting medium propagation of plane uniform linearly polarized electromagnetic waves $E=E_x(z, t), H=H_y(z, t)$ is described by Maxwell's equations, which in this case are reduced to two differential equations in partial first-order derivatives [70]

$$\begin{aligned} \frac{\partial H}{\partial z} &= -\frac{1}{c}\frac{\partial D}{\partial t}, \quad B = B(H), \\ \frac{\partial E}{\partial z} &= -\frac{1}{c}\frac{\partial B}{\partial t}, \quad D = \varepsilon E. \end{aligned} \tag{4.1}$$

Case of space, filled with ferrite, where connection/communication between vectors of electric field D and E is taken by linear is here undertaken, and connection/communication between vectors of magnetic field B and H - nonlinear. For sufficiently slow quasi-statices process the value of induction B at any point of space is uniquely determined by the strength of field H at this point at the same moment of time.

In the case of limited space, for example line of transmission, whose transverse sizes/dimensions are small, equations can be recorded in the form of two first-order equations (telegraph equations) [70, 71]

$$\frac{\partial i}{\partial z} = -\frac{\partial Q}{\partial t},$$
$$\frac{\partial u}{\partial z} = -\frac{\partial \Phi}{\partial t}, \qquad (4.2)$$

where u(z, t) - voltage/stress between wires in section Z (two-wire circuit);

i(z, t) - current in one of wires in the same section;

Q - charge per unit of length of line;

Φ - electric flux per unit of length of line.

For sufficiently slow processes flow Φ is considered only function of current

$$\Phi = \Phi(i). \qquad (4.3)$$

Page 218.

Charge Q is linearly connected with the voltage/stress

$$Q = Cu, \qquad (4.4)$$

where C - capacitance per unit length of line.

Equations (4.2) are suitable for case of heterogeneous and artificial lines, if values, entering these equations, are are replaced with their average/mean values, when temporary/time and three-dimensional/space scales i(z, t) and u(z, t) are much more than appropriate scales of separate component/link of line.

Nonlinear equations (4.2)- 4.4) in general case are not solved. However, are known their particular solutions for the case of the so-called simple waves, when one of the unknown values is the

single-valued function of another value. Assuming/setting u=u(i), it is possible to find

$$u = \pm \int \sqrt{\frac{L(i)}{C}}\, di \qquad (4.5)$$

and then equations (4.2) will have solution recorded in the form [70, 71]

$$z = \pm v(i)t + F(i), \qquad (4.6)$$

$$i = F_1\left(z \pm \frac{t}{\sqrt{L(i)C}}\right), \qquad (4.7)$$

where F and F_1 - arbitrary functions, determined from the boundary and initial conditions, and L(i)=dΦ/di - inductance per unit of the length of line.

Solution (4.6) takes form of traveling wave (simple wave). In simple wave each point of its front moves at a velocity, which depends on the value of current at this point. If inductance L(i) of line is monotonically decreasing function of the absolute value of current, then with the larger rate those points of the front, where the current is more, will be propagated. Consequently, in the case of the transmission of pulse, the steepness of its front along the line grows/rises, and the shear/section of pulse becomes flatter Fig. 4.1. Solution (4.7) assumes that at some moments of time the isolated points at the wave front "will pass" points with the smaller value of current. Solution (4.7) in this case becomes ambiguous (with $t=t_3$ in Fig. 4.1).

Page 219.

In actuality this is impossible and the ambiguity of solution (4.7) means that the solution became disruptive, moreover in this case gap is formed at the wave front.

After formation of flow separation wave ceases to be simple - shock electromagnetic wave appears. Place and interrupting time is determined from solutions (4.6) and (4.7). The moment/torque of gap t^* and coordinate the points of discontinuity are determined by the equations

$$\left(\frac{\partial z}{\partial i}\right)_{t^*}=0, \quad \left(\frac{\partial^2 z}{\partial i^2}\right)_{t^*}=0, \qquad (4.8)$$

where z(i, t) takes form (4.6).

If L(i) - nonmonotonic function, i.e., if magnetic permeability of ferrite μ(H) - nonmonotonic (single-valued or ambiguous) function, then velocity of propagation of different points of pulse depends on state of ferrite at preceding/previous moments of time. In other words, the character of impulse shaping with its passage along the line will to a considerable degree depend on the selection of initial operating point in the curve of magnetization (Fig. 4.2) [71, 73]. By the figure the hysteresis loop is displaced to the right, since the reference point of coordinates is displaced to the constant value field of magnetic biasing. If the pulse amplitude is so considerable that field H takes the values more than value H_1, then shock waves can arise both at the front and in the shear/section of launched pulse.

Actually, steepnesses of pulse edge according to (4.6) and (4.7)

it grows/rises for its those sections, where for ferrite $d\mu/dH<0$, and cutoff attenuation rate of pulse will increase, when $d\mu/dH>0$.

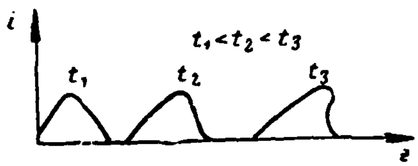

Fig. 4.1. Strain of pulse during its propagation along line.

Page 220.

Consequently, at the pulse edge with the larger rate will be propagated points in which current more, and in the shear/section of pulse, on the contrary, more rapid will be propagated points with the smaller value of current.

Thus, if we with the aid of constant magnetic biasing of ferrite fit such mode, during which in operating range of strength of field H dependence of magnetic permeability on field strength will have maximum, then it is possible to form wave with steep front and shear/section (Fig. 4.3).

However, it is necessary to have in mind that phenomenon in question occurs until is retained quasi-static dependence B(H), which is characteristic for microsecond range of change in durations of front and shear/section of pulse, i.e., as long as rate of change in magnetic field H at front (shear/section) of wave does not exceed value of 10^7-10^8 Oe/s [76].

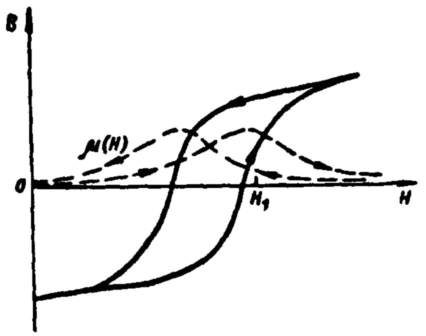

Fig. 4.2. Dependence B(H) and μ(H) for ferrite.

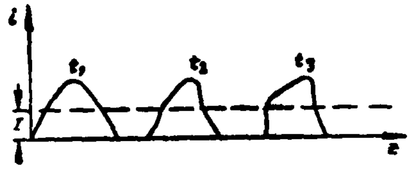

Fig. 4.3. Strain of pulse during propagation along line.

Page 221.

Mechanism of formation of shock electromagnetic waves due to phenomenon of "raid" of parts of front examined, which correspond to greater instantaneous values of current (voltage/stress), and, by such, by shape, increase in steepness of front occurs, also, in other media. The phenomenon of the formation of shock electromagnetic waves is observed, in particular, in the nonlinear transmission lines with the ferroelectrics and the semiconductors. Nonlinear element in the semiconductors is capacitance of p-n junction.

Formation of shock electromagnetic waves at high rates of change in the field.

In the case of high rate of build-up (more than 10^{8}-10^{9} Oe/s) of magnetic field with shaping of front is disrupted quasi-static dependence B(H) and need for considering dynamic process with magnetic reversal of ferrite appears. Large Paul begins to play magnetic viscosity of ferrite, which leads to energy losses at the front of wave [71, 72, 73]. Therefore with rapid changes in the magnetic field it is possible to speak about the dissipative mechanism of the formation of shock electromagnetic waves.

Dissipation of energy at wave front to certain degree occurs, also, with shaping of shock wave due to mechanism of raid at those moments/torques, when steepness of front noticeably grows/rises. However, the phenomenon of the dissipation of energy in this case will not be fundamental. At high rates of change in the magnetic field the phenomenon of dissipation already plays essential role.

In this case process of rapid magnetic reversal of ferrite is considered. The connection/communication between the vector magnetization of ferrite M and the operating intensity/strength of magnetic field $H_{д}$ is assigned by the equation of precession in the form of the equation of Landau and Lifschitz [70]:

$$\frac{\partial M}{\partial t} = -\gamma [MH_{д}] - \frac{\lambda}{M^2} [M[MH_{д}]], \qquad (4.9)$$

where γ - absolute value of gyromagnetic ratio; or in the form, which considers viscous friction, i.e., in the form of the equation of Gilbert/Hilbert [70, 71]:

$$\frac{\partial \mathbf{M}}{\partial t} = -\gamma\,[\mathbf{MH}] - \frac{\alpha}{M}\left[\frac{\partial \mathbf{M}}{\partial t}\,\mathbf{M}\right]. \qquad (4.10)$$

Page 222.

Here the coefficient of dissipation α and relaxation frequency λ are connected with the relationship/ratio

$$\lambda = \frac{\alpha}{1+\alpha^2}\gamma M$$

or with the low values α

$$\alpha \approx \frac{\lambda}{\gamma M}.$$

In the case of transmission lines with toroidal or cylindrical ferrite cores process of magnetic reversal of ferrite at high rates of change in field is most correctly described by model of heterogeneous precession [73]. In this case the equation of relation takes form [70, 73]

$$\frac{\partial M_h}{\partial t} = \frac{\alpha\gamma M}{1+\alpha^2}\left(1 - \frac{M_h^2}{M^2}\right)H, \qquad (4.9a)$$

where M_h - projection of vector magnetization on the direction of field of action H:

$$H = qI, \qquad (4.11)$$

where q-const.

Electric flux per unit of length of line is equal to

$$\Phi = L_0\left(I + \frac{4\pi M_h \eta}{q}\right), \qquad (4.12)$$

where L_0 - linear inductance of line without ferrite;

η - duty factor of line with ferrite ($0<\eta<1$).

Using telegraph equations (4.2), and also by equation (4.9a) and by relationships/ratios (4.11) and (4.12), it is possible to find approximate solution of equations for nonlinear line [73].

Physical picture of formation of shock electromagnetic waves with rapid magnetic reversal of ferrite approximately can be represented as follows.

Page 223.

During the propagation of pulse along the nonlinear line in connection with the rapid magnetic reversal of ferrite occurs dissipation of energy at the front (energy losses to heating of ferrite with the magnetic reversal), whose relative value changes with a change in the current strength. In this case with the increase of the amplitude of current in proportion to the saturation of ferrite the relative energy losses decrease also they can already be absent at the pulse apex. As a result of this one part of the edge of pulse (in its foundation) as "is absorbed" more noticeably than another part (at the apex/vertex), and, thus, front becomes steeper/more abrupt. The picture of a change in the pulse during its transmission along the line is shown in Fig. 4.4.

If duration of sector of the front, at which occurs magnetic reversal of ferrite, is short in comparison with duration of initial pulse edge, then this section can be considered as "gap", i.e., as shock wave, before front of which current i is equal to zero, and its ferrite is already completely saturated behind front.

Beginning from certain time dissipation of energy at wave front it is kept constant, and form of front remains constant/invariable. In this case wave can be considered as stationary. The expressions, which describe stationary shock wave, which follow:

$$i(\xi) = i(v_p t - z),$$
$$u(\xi) = u(v_p t - z),$$

where v_p - rate of shock wave, which is constant and determined by the values of field on both sides of gap.

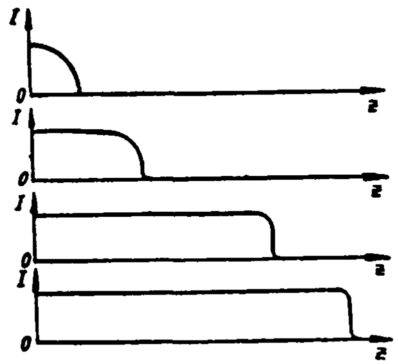

Fig. 4.4. Strain of wave front due to losses in ferrite during its propagation along line.

Page 224.

Dispersive mechanism of formation of shock electromagnetic waves is of essential interest for nanosecond pulse technique as phenomenon, with the aid of which it is possible in nonlinear forming lines to obtain very steep edges in current and voltage/stress.

It is necessary to note value of initial intensity of magnetization of ferrite with formation of shock wave front. Changing value and sign of the field of magnetic biasing, it is possible to affect, to the process of the formation of shcck wave, in particular, to change the duration of its front.

In the case of propagation of strong shock wave (with which $H_{макс}>H_0, M$) duration of front of stationary shock wave $t_{ф2}$ is proportional to value of magnetic moment of ferrite M and it is

inversely proportional to amplitude of magnetic field $H_{макс}$ and to relaxation frequency of ferrite (to constant λ) [70, 72]:

$$t_{\Phi 2} \sim \frac{M}{\lambda H}. \quad (4.13)$$

Thus, the greater pulse amplitude at input of forming line, i.e., is the greater field $H_{макс}$, the less duration of front can be obtained at output of line. This property of the forming lines, which use a phenomenon of shock electromagnetic waves, is very valuable for the nanosecond technology. Usually with an increase in the pulse amplitude the duration of its front also increases with other methods of the formation of nanosecond pulses in the majority of the cases.

4.2. Shock electromagnetic waves in the transmission lines with the lumped parameters.

Since time, for which is formed/shaped in line shock wave, cannot be less than initial duration of pulse edge, then for this time considerable distance passes pulse to transmission line. For reduction in the strength of current and shortening of the overall dimensions of line it is expedient to utilize artificial transmission lines, for example, in the form of nonlinear delay line with the lumped parameters. The wave propagation velocity in such lines can be relatively small; therefore the formation of shock waves in the line with the small sizes/dimensions is provided.

Page 225.

As the artificial delay line can be undertaken multilink chain/network with LC by components/links of the type of the constant k (Fig. 4.5).

Here capacitance of C - constant value, and inductance is nonlinear and is carried out in the form of inductance coils on ferrite rings. This line possesses the dispersion, connected with the dependence of the parameters of separate components/links on the frequency (frequency dispersion) and with the periodic character of a change in the properties of system along the direction of propagation of pulse (spatial dispersion).

Dispersion begins to be manifested, when during transmission of pulse steepness of its front grows/rises and it becomes sufficient large. If the slope/transconductance of launched pulse at the input of line is relatively small ($dH/dt<10^{7}$ Oe/s), then dispersion in the line can be manifested even before will be destroyed assumption about the uniqueness of dependence $\Phi=\Phi(i)$, i.e., the form of the usual static hysteresis loop of ferrite is disrupted before.

But if steepness of front of input pulse is great, and consequently, required time constants of components/links of line are very low, then static curve of hysteresis loop no longer occurs and it is necessary in this case to consider switching time of ferrite. The analysis of processes in the nonlinear artificial transmission line is various for these two cases.

Stationary shock electromagnetic waves in a line with the small steepness of the front of initial current taper.

Processes, which occur in nonlinear discrete/digital line during transmission of pulse, are described by nonlinear differential-difference equations, whose general/common investigation is hindered/hampered. However, the stationary shock electromagnetic waves, which occur in this line [74], can be examined.

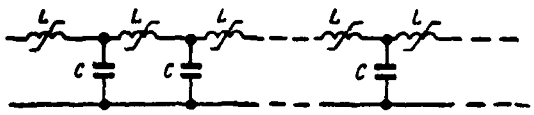

Fig. 4.5. Artificial delay line with inductance coils on ferrite cores.

Page 226.

The equivalent schematic of line is represented in Fig. 4.6a The equation of the circuit in question takes following form [74]:

$$\int (i_{n+1} - 2i_n + i_{n-1})\,dt + CR(i_{n+1} - 2i_n + i_{n-1}) +$$
$$+ CR\frac{d}{dt}(\Phi_{n+1} - 2\Phi_n + \Phi_{n-1}) + \frac{1}{r}(\Phi_{n+1} - 2\Phi_n + \Phi_{n-1}) =$$
$$= C\frac{d\Phi_n}{dt}, \qquad (4.14)$$

where i_n and Φ_n - respectively current and magnetic flux in the n component/link of line;

C - capacitance of component/link;

R - resistor/resistance.

Since line uniform, then $C_n = C$, $R_n = R$ and $r_n = r$. The investigation of the steady-state solution of the form

$$i_{n-1}(t) = i_n(t + \Delta t)$$

(where Δt - delay time of wave in one component/link of line) shows that formed/shaped current taper is the function, given in Fig. 4.6b.

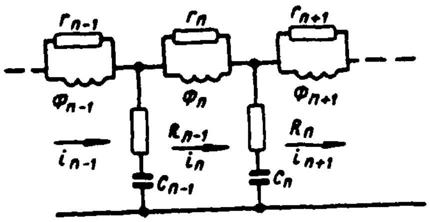

Fig. 4.6a. Equivalent schematic of artificial delay line.

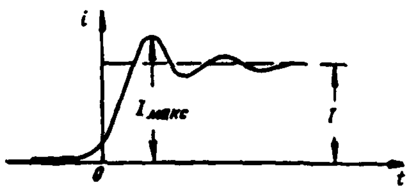

Fig. 4.6b. Oscillogram of shock wave front.

Page 227.

The current strength in the line increases exponentially in initial sectors of the front of shock wave, while in the subsequent sections oscillating it approaches steady-state value I. With the high attenuation instead of the oscillations there can be the aperiodic process of approaching the current to value I. If dependence Φ and) is approximated by function $\Phi(i)=\beta i-\delta i^3$, where β and δ - constant positive coefficients, then it is possible to obtain approximations for the evaluation/estimate of initial sector of the front and frequency of oscillations [74]. Initial sector of the front, defined as the time interval, which corresponds to the values of current from 0.1 I to 0.9 I, is rated/estimated with the aid of formula [74]

$$t_н=0{,}7\frac{(\Delta l)^2}{\sqrt{\delta C}}\frac{1}{I}=0{,}7(\beta-\delta I^2)\sqrt{C/\delta}\,1/I. \qquad (4.15)$$

Frequency of oscillations

$$f = \frac{\sqrt{\delta C}}{(\Delta t)^2} I = \frac{1}{\beta - \delta I^2} \sqrt{\delta C} I \qquad (4.16)$$

and amplitude of oscillations

$$I_k \approx \frac{I}{2} \left[\exp\left(\frac{12R}{\beta - \delta I^2} \right) \right]^{-1}.$$

It follows from these formulas that with decrease of parameters of component/link of line (by decrease of value Δt) steepness of shock wave front and frequency of oscillations grow/rise.

Thus, with relatively small steepness of front of current taper at output of line, when is valid static dependence Φ(i) of curve of magnetization of ferrite, significant role plays spatial dispersion of artificial transmission line. However, the time of the magnetic reversal of ferrite still sufficiently little and does not determine the duration of the front of formed/shaped current taper.

Shock waves in a line with the considerable slope/transconductance of initial current taper.

Page 228.

For nanosecond pulse technique are of greatest interest shock electromagnetic waves, which are formed in line under influence of current pulses with large steepness of front, when rate of magnetic

reversal of ferrite exceeds 10^{8}-10^{9} Oe/s.

In this case in examination of processes in line it is necessary to use dynamic equations of relation, which consider that value of vector magnetization M at certain moment of time is not determined, generally speaking, by intensity/strength of magnetic field H at this moment. In this case, when in the process of magnetic reversal is changed only the value (but not direction) of magnetic field, i.e., when ferrite it is not possible to consider saturated, the projection of vector M on direction H is satisfactorily described by equation [73, 75]

$$\frac{dm_{n}}{dt}=\frac{\alpha}{1+\alpha^{2}}\gamma|M|(1-m_{n}^{2})qI, \tag{4.17}$$

where $m_{n}=\frac{|M_{n}|}{|M|}$, $|M_{n}|$ - projection of vector magnetization on the direction of the magnetic field;

α - coefficient of the dissipation of ferrite;

γ - absolute value of gyromagnetic ratio;

$$q=\frac{H}{I}.$$

Magnetic flux is connected with current in this case with expression

$$\Phi_{n}=L_{0}\left(I_{n}+\frac{4\pi M\eta m_{n}}{q}\right), \tag{4.18}$$

where η - duty factor of coil with ferrite.

For determining stationary shock wave it is necessary to find

solution of differential equation of transmission line, obtained from equation (4.14), taking into account equations (4.17) and (4.18) [75]. Therefore the solution in the general case must give the dependence of shock wave front both on the parameters of ferrite (α, M) and state of its intensity of magnetization $\left(m_0 = \frac{M_0}{|M|}\right)$, and on the parameters of the component/link of line $\tau_0 = \sqrt{L_0 C}$(L_0 - the inductance of the component/link of line at the saturated ferrite).

Let us give first solutions for case, when constant of component/link of line is very low $\tau_0 \sim 0$.

Page 229.

In this case the line is distributed, since its discreteness is not expressed. In the particular case the front of shock electromagnetic wave will be by pillar determined by the properties of ferrite [73]

$$t_{\phi 0} = \frac{1+\alpha^2}{2\alpha\gamma I} f(m_0), \tag{4.19}$$

where

$$f(m_0) = \frac{1}{1-m_0}\left[2,2(3+m_0) - (1-m_0)\ln\frac{1,9+0,1m_0}{1,1+0,9m_0}\right]. \tag{4.20}$$

Plotted function $F=f(m_0)$ is given in Fig. 4.7.

With assigned current I minimum duration of front is determined by properties of ferrite. Decreasing the value of the ratio of remanence to the saturization magnetization of ferrite $m_0 = \frac{B_r}{B_s}$, it is possible to decrease the duration of front. The duration of front

proves to be smallest in ferrites, which have a constant $\alpha=1$. The coefficient α, which has value from 0.3 to 1, is measured experimentally and it can be calculated from the expression for the switching coefficient of ferrite S_w, which is determined from formula [73]

$$S_w = \frac{1+\alpha^2}{2\alpha\gamma} f(m_0) \; [^{(1)}Э. \, сек], \qquad (4.21)$$

Key: (1). Oe·sec.

where $\gamma = \mathrm{const} = 1{,}76 \cdot 10^7 \frac{1}{Oe \cdot sec}$.

Thus, function $f(m_0)$ determines dependence of rate of process of magnetic reversal on initial conditions. Actually, switching time will depend on the mobility of vector magnetization and on the angle, to which it must additionally turn itself in order to prove to be parallel to the affecting field H. Thus, in the ferrites with the right-angle hysteresis loop in the absence of the applied field of magnetic biasing value m_0 is close to one, since vector magnetization is already in the initial state little deflected from the direction, which it accepts upon the saturation of ferrite. With the high squareness ratio of hysteresis loop it is possible to consider value $f(m_0)$ of constant for all ferrites, which have right-angle hysteresis loop, which work in the presence of the zero magnetic biasing, and equal to 4.5.

Page 230.

But if ferrite with the flat hysteresis loop is utilized or magnetic

biasing is used, then value $f(m_0)$ can be determined from the graph/curve (Fig. 4.7). In the case of magnetic biasing, changing value m_0 (from -1 to +1), it is possible to change the duration of shock wave front $t_{\phi 2}$ almost three times.

In actuality in line lumped parameters it is necessary to consider not only parameters of ferrite, but also with parameters of components/links of line (τ_0 and η). Already it cannot be considered that $\tau_0 \ll t_{\phi 2}$, since the duration of formed/shaped front $t_{\phi 2}$ and value τ_0 it is approximately equal with the high currents in the line (with the large steepness of the pulse edge).

In this case solution of initial equations of line very complicatedly and can be realized either by grapho-analytic method or numerical calculation. Fig. 4.8 gives graph/curve $\frac{\tau_0}{\tau_n} = f(k)$, constructed on the basis of the approximate equation, which occurs in the case of [75] in question:

$$\mathrm{sh}^2\left(\frac{\tau_0}{2\tau_n}\sqrt{1+\frac{1}{k}}\right) = \left(\frac{\tau_0}{2\tau_n}\right)^2 + \frac{\eta}{4}\frac{\tau_0}{\tau_n}. \qquad (4.22)$$

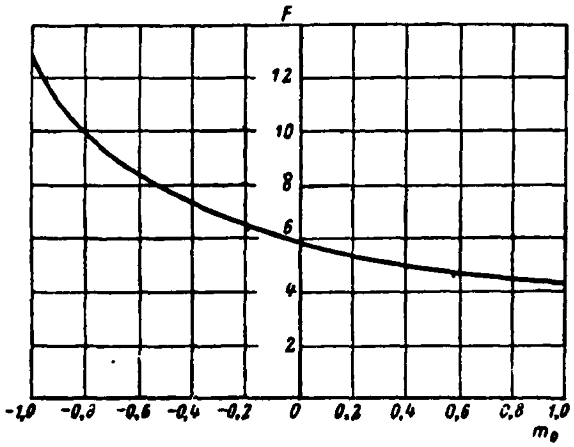

Fig. 4.7. Plotted function $f(m_0)$.

Page 231.

Here

$$\vartheta = 4\pi M_s \gamma_1 \frac{\alpha\gamma}{1+\alpha^2}(1-m_0^2)\tau_0; \qquad (4.23)$$

$$k = \frac{0,1qI}{M_s\gamma_1(1-m_0)}; \qquad (4.24)$$

value $\tau_{н} = (0,4 \div 0,33)\, t_{\phi_2}$ characterizes rise time of front; M_s - intensity of magnetization of the saturated ferrite. The parameter ϑ determines value τ_0, when straight line $\frac{\tau_0}{\tau_{н}} \approx (2,3 \div 3)\frac{\tau_0}{t_{\phi_2}}$ interesects the curve f(k) (Fig. 4.8).

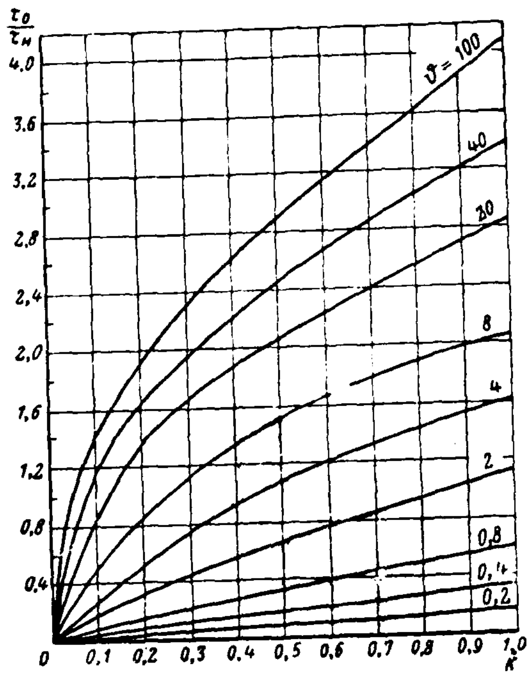

Fig. 4.8. Dependence $\tau_0/\tau_H = f(k)$.

Page 232.

Thus, with selected value τ_0 from graphs/curves it is possible to find value of duration of pulse edge, formed in line. This duration is here the function of the value of field (qI), parameters of ferrite (M_s, m_0) and parameters of line (τ_0, η).

When duration of front, formed/shaped with line, becomes close to value τ_0, oscillation appears at apex/vertex of formed/shaped drop/jump. The period of these oscillations T approximately can be evaluated according to the expression

$$\sin\left(\pi \frac{\tau_0}{T} \sqrt{1+\frac{1}{k}}\right) = \pi \frac{\tau_0}{T}. \qquad (4.25)$$

For reduction in amplitude of oscillations it is possible consecutively/serially with capacitance of component/link of line to include resistor/resistance (Fig. 4.6). However, in the nanosecond range of durations this is difficult to carry out, without introducing the parasitic reactive/jet parameters. Therefore the duration of the formed/shaped front is actually limited to value $t_{\phi 2} \geqslant (3 \div 5)\tau_0$. when the value of oscillation is still low.

As already mentioned, for formation of stationary wave is required length of line, which ensures pulse delay, not less than duration of front of input pulse. If the length of line is small, then shock electromagnetic wave is formed not on entire current taper (Fig. 4.9a). At a certain optimum length of line shock wave is formed/shaped on entire current taper (Fig. 4.9b). The rate of the formation of shock wave is determined by the parameters of ferrite and components/links of line. The rate of formation is more, if ferrite has the larger value of magnetic moment $|M|$ and smaller value of m_0.

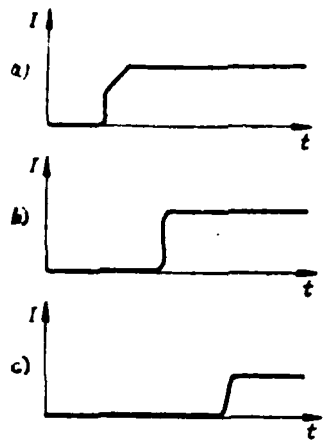

Fig. 4.9. Oscillograms of pulse edge, formed/shaped in line: a) in the case of insufficient quantity of components/links of line: b) with optimum number of components/links; c) in the case of excessive quantity of components/links.

Page 233.

Optimum number of components/links of line can be determined according to formula [73]

$$n_{\text{опт}} = k\frac{t_{\phi 1}}{\tau_0} = \frac{0{,}1 q l}{M_s \gamma_1 (1 - m_0)} \frac{t_{\phi 1}}{\tau_0}. \qquad (4.26)$$

Here $t_{\phi 1}$ and τ_0 - respectively the duration of the front of the drop/jump at the input of line and the time constant of component/link with the saturated ferrite.

If number of components/links is great, i.e., line has excessively large length $(n > n_{\text{опт}})$, then current strength decreases due to energy losses in process of passage of will along line, and this

leads to increase in duration of shock wave front (Fig. 4.9c). In this case it is possible to indicate that the front of drop/jump is re-formed.

For accelerating formation of shock wave front non-uniforms circuit with ferrite can be utilized. In this case the line is fulfilled in the form of components/links with different values of the parameters τ_0 (stepped line). The first components/links have high value τ_0, and the subsequent finer/smaller components/links have all decreasing values τ_0 .

During propagation along line of formed shock wave it is possible to introduce concept of resistor/resistance of line to shock electromagnetic wave:

$$Z_y = \frac{U_y}{I_y} = \rho\left[1 + \frac{4\pi M\eta}{H}(1 - m_0)\right]^{1/2}. \qquad (4.27)$$

With $\eta M \to 0$ resistor/resistance of line to shock wave passes into usual wave impedance of linear line of transmission ρ. The nonlinear forming line, in which is propagated shock wave, strictly speaking, can be coordinated with the load only on the resistor/resistance to shock wave. Therefore the same nonlinear line can be the best load. With the usual linear load nonlinear line will prove to be mismatched and the part of the energy of the end/lead of the line will be reflected and to be propagated to it they began. With the considerable porosity of the pulses supplied to the line the waves

reflected manage completely to damp during the period between them.

Page 234.

The presence of the echo pulses, just as the oscillations, which occur after the shear/section of pulse with its large slope/transconductance, determines the magnetic state of ferrites, i.e., to the arrival of next pulse ferrite has the specific initial state. The presence of the damped oscillation in the period between the pulses can lead to the fact that a ferrite it will not have initial constant magnetic biasing.

Described phenomena with formation of steep edges in current with the aid of nonlinear forming line on ferrites, and also given fundamental principles make it possible to express considerations about selection of ferrite for such lines.

For evaluation/estimate of ferrite it is necessary to know saturation induction B_s $\left(M_s=\frac{B_s}{4\pi}\right)$, remanent induction B_r $(M_r 4\pi=B_r)$ and coefficient of dissipation α.

With α=1 duration of front $t_{ф2}$ and optimum number of components/links of line $n_{опт}$ are minimum. The greater the saturation induction B_s (or M_s), the less the optimum number of components/links of line. With decrease $m_0=B_r/B_s$ the duration of formed front $t_{ф2}$ and the wave impedance of nonlinear line in other constant parameters of ferrite and parameters of component/link, and also with the assigned

amplitude of current increase. However, with the the small m_0 the optimum number of components/links $n_{опт}$ is less than with the the large m_0, but the duration of front $t_{ф2}$ changes insignificantly; therefore it is expedient to have values of $m_0 \geq 0$.

Consequently, ferrites adequate/approaching for use in nonlinear forming lines it is possible to consider such, which have coefficient $\alpha \approx 1$, high value of saturation flux density B_s and small remanent induction B_r. forming line can be heterogeneous, when at first line contains one type components/links, and at the end - another. In this case in the first components/links is desirable to use ferrites with the high B_s and average value m_0, while in the latter/last (fine/small) components/links to use ferrite with average value B_s, on with the squareness ratio, close to one.

Enumerated characteristics of ferrite must be stable.

Page 235.

Otherwise with the formation of repetitive pulses with the large steepness of front, for example, for the signal generators or the very high speed oscillographs will appear the noticeable in the nanosecond range instability of functioning the corresponding diagrams. In connection with this the operating temperature of the forming nonlinear line has high value.

If temperature of ferrite is close to Curie point, then

insignificant temperature fluctuations can cause instability of delay time of line, since in this case value of magnetic saturation of ferrite changes.

Power, scattered in line in the form of heat, can be rated/estimated with the aid of formula [78, 79]

$$P_{\text{и}} = I^2 F\left(\frac{\rho_0 t_{\text{ф}2}}{3} + R t_{\text{и}}\right)\ \overset{(1)}{[\text{вт}]}, \qquad (4.28)$$

Key: (1). W.

where F - pulse repetition rate, Hz;

R - resistor/resistance of the wires of the inductance coils, ohms;

ρ_0 - line characteristic with the saturated ferrite.

First member of expression (4.28) determines power, spent on magnetic reversal of ferrite and then scattered in the form of heat, and second term - losses to Joule heat.

4.3. Calculation of those forming lines with the ferrite filling.

On the basis of expressions, given in preceding/previous paragraph, and description of phenomena, which occur in forming lines, filled with ferrite, it is possible to present order of calculation of such lines. Let us examine one of the possible versions of the calculation of the forming line with the ferrite, proposed by A. M. Belyantsev and Yu. K. Bogatyrev [80, 81].

Initial values for calculating line are usually duration of front of current taper (or voltage/stress) $t_{\phi 1}$ at input of line and duration of front $t_{\phi 2}$, which is required to obtain at output, I - amplitude of current of input drop/jump, $R_{\text{н}}$ -- load resistance/resistor, brand and sizes/dimensions of ferrite ($d_{\text{ср}}$ - mean diameter of ring and S - its section). Sometimes the parameters and the sizes/dimensions of ferrite filling are already known, i.e., there are standard ferrite rings, for example, used in the electronic computers.

Page 236.

In other case the sizes/dimensions of rings must be calculated according to their obtained space. The usually following values are determined: τ_0 - time constant of component/link, ρ_0 - line characteristic with the ferrite magnetized before the saturation, q - number of turns per unit of the average/mean length of ferrite ring, η - duty factor, m_0 - initial intensity of magnetization of ferrite, $n_{\text{опт}}$ - optimum number of components/links of line; $t_з$ - delay time of line.

Case of the relatively small steepness of the front of drop/jump.

Let us examine first case, when duration of formed front is noticeably more than time constant of component/link τ_0. Minimum value τ_0, in turn, is always limited by the finite dimensions of ferrite rings and by the parasitic parameters of the mounting of line.

In the case in question occurs inequality $\tau_0 \leq 0.2\ t_{\phi 2}$. The dispersive properties of line, connected with the discreteness of its structure, can be disregarded/neglected, in other words, considered under this condition that the artificial line is distributed-parameter line.

A. Let us begin calculation for line on the assumption that sizes/dimensions of ferrite ring are not yet selected. Then order of calculation is the following.

1. Let us determine time constant of cell τ from condition

$$\tau_0 = \sqrt{L_0 C_0} \leq 0{,}2 t_{\phi 2}, \qquad (4.29)$$

where L_0 - inductance of component/link of line without ferrite, H;

C_0 - capacitance of capacitor of component/link, φ.

2. We find number of turns per unit of average/mean length of core

$$q = \frac{10}{4\pi} \frac{S_w}{t_{\phi 2} l} \left[\frac{\overset{(1)}{\text{вит}}}{\text{см}}\right], \qquad (4.30)$$

Key: (1). turns/cm

where S_w - switching coefficient of ferrite, Oe.s, [see (4.21)], whose value usually lies/rests within the limits (0.3-0.5) $\cdot 10^{-6}$ Oe.s.

On the basis of expressions (4.20) and (4.21) it is possible approximately to record

$$q \approx (5 \div 8) \cdot 10^{-6} \frac{f(m_0)}{t_{\phi 2} l} \left[\frac{\overset{(1)}{\text{вит}}}{\text{см}}\right]. \qquad (4.31)$$

Key: (1). turns/cm

3. Let us calculate space of doughnut coil, i.e., size/dimension of ferrite core (taking into account agreement of line with load $R_{\text{н}}$):

$$d_{\text{ср}}S = \frac{\tau_0 R_{\text{н}}}{4\pi^2 q^2} \frac{10^9}{\sqrt{1+\frac{1}{k}}} \ [\text{см}^3], \qquad (4.32)$$

where parameter k according to (4.24) is equal to

$$k = \frac{0.1 q l}{M_s \eta (1 - m_0)}.$$

Here duty factor with the dense single-layer coil/winding of coil is close to one, and with a small quantity of turns η=0.3-0.6.

Approximately value η is rated/estimated with the aid of expression

$$\eta = \frac{L_{\text{н}} - (L_1 + L_2 + L_3)}{L_{\text{н}}}, \qquad (4.33)$$

where L_1 - inductance of neutral conductor (grounding/ground);

$L_{\text{н}}$ - complete inductance of component/link of line;

L_2 - inductance of supplying ends/leads of coil;

L_3 - leakage inductance, in particular, if ferrite partially fills coil $L_3 = L_0(S - S_0)/S_0$;

S_0 - cross-sectional area of coil. Since the sizes/dimensions of coil are not yet known, then value η is taken very approximately.

4. Let us determine inductance of doughnut coil without ferrite core

$$L_0 = 4\pi^2 q^2 d_{0\text{ср}} S_0 10^{-9} \ [\text{гн}]^{(1)}, \qquad (4.34)$$

Key: (1). H.

where $d_{0\text{ср}}$ - the mean diameter of coil, cm;

S_0 - area of its cross section, cm^2.

Knowing inductance, with the aid of (4.33) it is possible to refine value η. If disagreement proved to be more than 20-25% should be introduced correction and anew calculated the space of ferrite core (d_{cp}, S).

Page 238.

5. We find capacitance of capacitor in component/link of line and line characteristic without ferrite:

$$C_0 = \frac{\tau_0^2}{L_0} \ [\phi]^{(1)}, \qquad (4.35)$$

$$\rho_0 = \frac{L_0}{\tau_0} \ [o\text{м}]^{(2)}. \qquad (4.36)$$

Key: (1). f. (2). ohm.

6. Let us calculate optimum number of components/links of line

$$n_{\text{опт}} = k\frac{t_{\phi 1}}{\tau_0} = \frac{0,1ql}{\eta M_s(1-m_0)}\frac{t_{\phi 1}}{\tau_0}. \qquad (4.37)$$

7. Delay time of line let us determine according to expression

$$t_з = (1 \div 1,3)\, n_{\text{опт}}\tau_0 \sqrt{1+\frac{\eta M_s(1-m_0)}{0,1ql}} = (1 \div 1,3)\, n_{\text{опт}}\tau_0 \sqrt{1+\frac{1}{k}} \ [\text{сек}]^{(1)}. \qquad (4.38)$$

Key: (1). s.

8. We find line characteristic with ferrite

$$\rho = \rho_0 \sqrt{1+\frac{1}{k}} \ [o\text{м}]^{(1)}. \qquad (4.39)$$

Key: (1). ohm.

B. Teper' let us calculate line on the assumption that ferrite core is assigned, i.e., type and sizes/dimensions of ferrite ring are given. In this case the sequence of calculation is the following.

1. Let us determine number of turns per unit of average/mean length of ferrite core (4.31)

$$q = \frac{10}{4\pi}\frac{S_w}{t_{\phi 2} l} \approx (5 \div 8)\frac{10^{-6} f(m_0)}{t_{\phi 2} l}\left[\frac{^{(1)}\text{вит}}{\text{см}}\right].$$

Key: (1). turns/cm

2. We find inductance of coil without core (4.34)

$$L_0 = 4\pi^2 d_{0cp} S_0 q^2 10^{-9} \; [\overset{(1)}{\text{гн}}],$$

Key: (1). H.

where d_{0cp} and S_0 are approximately taken equal to d_{cp} and S, which are given for the ferrite; we rate/estimate duty factor

$$\eta = \frac{L_n - (L_1 + L_2 + L_3)}{L_n}.$$

Page 239.

3. Let us calculate time constant of component/link of line without ferrite

$$\tau_0 = \frac{4\pi^2 q^2 d_{cp} S}{R_n 10^9}\sqrt{1 + \frac{1}{k}}, \qquad (4.40)$$

where parameter k according to (4.24) is equal to

$$k = \frac{0,1 q l}{M_s \eta (1 - m_0)}.$$

The obtained value τ_0 must be not more than $0,2\, t_{\phi 2}$, it is otherwise necessary to select another core (smaller size/dimension).

4. Let us determine capacitance of component/link and line characteristic without ferrite:

$$C_0 = \frac{\tau_0^2}{L_0}, \quad \rho_0 = \frac{L_0}{\tau_0}.$$

5. We will obtain optimum number of components/links in line (4.37)

$$n_{\text{опт}} = kt_{\text{ф}1}/\tau_0.$$

6. We find delay time of line (4.38)

$$t_{з} = (1 \div 1{,}3)\, n\tau_0 \left[1 + \frac{10 M_s \eta (1 - m_0)}{ql}\right]^{1/2} \ [\overset{(1)}{сек}]$$

Key: (1). s.

and it is checked line characteristic with ferrite (4.39)

$$\rho = \frac{\rho_0}{\tau_0} \frac{t_{з}}{n_{\text{опт}}} = R_{н}.$$

In the case of ferrites with right-angle hysteresis loop another procedure of calculation [72] can be used. However, the method in this case examined is applicable. Here during calculations it is necessary to propose $f(m_0)=4.5$ what is real for the majority of the ferrites, which have right-angle hysteresis loop.

Example of calculation of forming line with ferrite. It is

necessary to design the forming line for obtaining for its output of current taper (voltage/stress), whose front must have a duration of 2 ns in the absence of oscillations on the apex/vertex.

Page 240.

Initial current taper by value 10 a has a duration of front 40 ns. Line must be loaded to the resistor/resistance of 75 ohms.

Let there be ferrite rings of type VT-7 with outer diameter of 3 mm. This ferrite has data $\alpha\approx 1,\ m_0\approx 0{,}9,\ M_s\approx 170$ and $f(m_0)$ it is possible to take as equal to 4.5. Ferrite ring with an outer diameter of 3 mm and an inside diameter of 2 mm has $d_{cp}=0{,}25$ cm and $S=10^{-2}$ cm^2.

Since sizes/dimensions of ferrite are already given, then calculation must be conducted accordingly version, presented in section "B".

1. We find number of turns per unit of average/mean length of coil q through formula (4.31)

$$q=8\,\frac{10^{-8}\cdot 4{,}5}{2\cdot 10^{-9}\cdot 10}=18\ \overset{(1)}{\text{вит/см}},$$

Key: (1). turns/cm.

then in all turns on the core

$$N=q\pi d_{cp}=18\cdot 3{,}14\cdot 0{,}25=14\ \overset{(1)}{\text{вит.}}$$

Key: (1). turns.

2. We find inductance of coil L_0 let us calculate from formula (4.34):

$$L_0 = 40 \cdot 0{,}25 \cdot 10^{-2} \cdot 3{,}25 \cdot 10^{2} \cdot 10^{-9} = 32{,}5 \cdot 10^{-9} \text{ гн.}^{(1)}$$

Key: (1). H.

Since core is tightly filled with turns, then it is possible to place duty factor with equal to η=0.8.

3. Let us determine parameter k according to formula (4.24) and time constant of component/link of line without ferrite (4.40):

$$k = \frac{0{,}1 \cdot 18 \cdot 10}{170 \cdot 0{,}9 \cdot 0{,}2} = 0{,}59.$$

$$\tau_0 = \frac{32{,}5}{75 \cdot 10^{9}} \sqrt{1 + \frac{1}{0{,}59}} = 6{,}7 \cdot 10^{-10} \text{ сек.}^{(1)}$$

Key: (1). s.

Since it proves to be that $\tau_0 \approx 0{,}2 t_{\Phi_2}$, then calculation is continued.

4. We find capacitance of component/link C_0 and line characteristic without ferrite ρ_0 through formulas (4.35) and (4.36):

$$C_0 = \frac{45 \cdot 10^{-20}}{32{,}5 \cdot 10^{-9}} = 14 \text{ пф,}^{(1)}$$

$$\rho_0 = \frac{32{,}5 \cdot 10^{-9}}{6{,}7 \cdot 10^{-10}} = 48{,}5 \text{ ом.}^{(2)}$$

Key: (1). pF. (2). ohm.

Page 241.

5. Let us determine number of components/links in line according to formula (4.37)

$$n = 0{,}59\,\frac{40\cdot 10^{-9}}{6{,}7\cdot 10^{-10}} = 35.$$

6. Delay time of line $t_з$ we will obtain according to formula (4.38)

$$t_з = 1{,}2\cdot 35\cdot 6{,}7\cdot 10^{-10}\cdot\sqrt{1+\frac{1}{0{,}59}} = 43 \text{ }^{(1)}\text{нсек}.$$

Key: (1). ns.

7. It is checked value of line characteristic with ferrite according to formula (4.39)

$$\rho = 48{,}5\cdot\sqrt{1+\frac{1}{0{,}59}} = 75{,}2 \text{ }^{(1)}\text{ом}.$$

Key: (1). ohm.

Case of the large steepness of front.

When duration of formed front is approximately equal to smallest possible time constant of component/link τ_0 it is necessary to consider discrete/digital structure of line. This case occurs with shaping of the drop/jump with the minimum duration of front, i.e., with its maximum slope/transconductance. If the switch time of ferrite makes it possible to obtain the required steepness of front, it is necessary to select the time constant of the component/link τ_0 of minimum. For this it is necessary to take ferrite rings with the minimal sizes, and the mounting of line must be carried out with the smallest parasitic parameters. In these cases it is possible to

obtain the smallest constant value of time τ_0, which proves to be order 0.1 ns.

In this case calculation of line can be conducted as follows [81]. First with the aid of the curve of Fig. 4.10b we select the constant value of the time of component/link τ_0, on the basis of the assigned to duration of front at output of line $t_{\Phi 2}$ and of permissible nonuniformity of apex/vertex (value of oscillations) of shaped pulse, characterized by relation $\frac{I_{макс}}{I}$, where $I_{макс}$ - amplitude of oscillations.

Page 242.

The duty factor η of coil with ferrite is selected tentatively and we more precisely formulate subsequently. We further determine the dimensionless parameter ϑ

$$\vartheta = 4\pi M_s \eta \frac{\alpha\gamma}{1+\alpha^2}(1-m_0^2)\tau_0 = 2\pi M_s \eta (1-m_0^2) \times \times f(m_0)\frac{\tau_0}{S_w} \quad (4.41)$$

and the value of relation $\tau_0/\tau_{\text{н}}$, where $\tau_{\text{н}} = t_{\Phi 2}/2{,}5 + t_{\Phi 2}/3$.

Then with the aid of curves $\tau_0/\tau_{\text{н}} = f(k)$ (Fig. 4.8) we find parameter k, which corresponds to point of intersection with straight line $\tau_0/\tau_{\text{н}} = \text{const}$ with dependence $\tau_0/\tau_{\text{н}} = f(k)$, constructed for this value ϑ. Knowing k, it is possible to determine then a quantity of turns per unit of the average/mean length of the coil

$$q = \frac{M_s \eta (1-m_0) k}{0{,}1 I} \left[\frac{\overset{(1)}{вит}}{см}\right]. \quad (4.42)$$

Key: (1). turns/cm.

We further determine sizes/dimensions of core (coil) and inductance of coil according to formulas (4.32) and (4.34)

$$d_{\text{cp}}S = \frac{\tau_0 R_{\text{н}}}{4\pi^2 q^2} \frac{10^9}{\sqrt{1+\frac{1}{k}}} \, [\text{см}^3],$$
$$L_0 = 4\pi^2 q^2 d_{\text{cp}} S 10^{-9} \, [\overset{(1)}{\text{гн}}].$$

Key: (1). H.

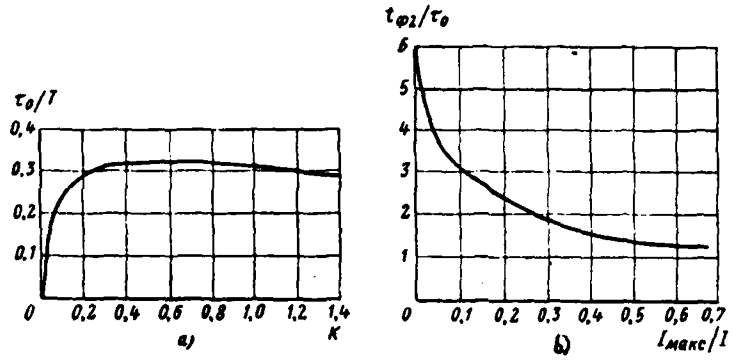

Fig. 4.10. Dependences $\frac{\tau_0}{T}=f(k)$ (a) and $\tau_{\phi 2}/\tau_0=\varphi(I_m/I)$ (b).

Page 243.

Then, as during calculation of line, given for case of "A" of this paragraph, we find following values:

$$C_0=\frac{\tau_0^2}{L_0},$$
$$\rho_0=\frac{L_0}{\tau_0},$$
$$n_{опт}=k\frac{t_{\phi 1}}{\tau_0},$$
$$t_3=2n_{опт}\tau_0\sqrt{1+1/k},$$
$$\rho=\rho_0\sqrt{1+1/k}.$$

Period of available on apex/vertex oscillations of oscillations can be found from expression (4.25). Fig. 4.10a gives graph/curve $\tau_0/T=f(k)$, with the aid of which can be found period of oscillations T from the already known τ_0 and k. Fig. 4.10b gives graph/curve $t_{\phi 2}/\tau_0=f(I_{макс}/I)$, where $I_{макс}$ - maximum amplitude of oscillation.

Let us examine calculation of forming line when type and sizes/dimensions of ferrite ring are already assigned. In this case

it is first necessary to assign an exemplary/approximate quantity of turns per unit of the average/mean length of coil, on the basis of the formula

$$q \approx 1,5 \frac{10}{4\pi} \frac{S_w}{t_{\phi 2} I}$$

and to further determine the inductance of coil L_0 according to formula (4.34). On the basis of the sizes/dimensions of core and number of turns of coil $N = q\pi d_{cp}$, we are assigned by value η and find parameter k

$$k = \frac{0,1 q I}{M_s \eta (1 - m_0)}.$$

Then we determine parameter

$$A = 4\pi M_s \eta \gamma \frac{\alpha}{1 + \alpha^2} (1 - m_0^2).$$

In assigned duration of front of drop/jump on output of line we find

$$\tau_H = t_{\phi 2}/3.$$

Page 244.

It is further necessary to fit constant value of time of component/link τ_0. For this, using graph/curve $\tau_0/\tau_H = f(k)$ and straight line $\tau_0/\tau_H = \text{const}$ (Fig. 4.8), we find this value of the parameter $\Phi = A\tau_0$, in which straight/direct $\tau_0/\tau_H = \text{const}$ and curved graph/curve $\tau_0/\tau_H = f(k)$ they will be crossed at the point, which corresponds to value of k

obtained earlier. The matching condition of line with the load

$$L_0/\tau_0 = R_н(1+1/k)^{-1/2}$$

is checked after this.

Then according to formulas given above are determined values C_0, ρ_0, $n_{опт}$ and $t_з$.

Let us examine example of calculation of line, intended for obtaining on its output of current taper with large steepness of front, when duration of front $t_{ф2}$ is commensurate with time constant of component/link τ_0.

Assume drop/jump in voltage/stress with front with duration of 0.4 ns is required to obtain 50 ohms on load. The nonuniformity of apex/vertex must not exceed 10%, i.e., $I_{макс}/I=0{,}1$. At the input current taper is assigned by value 30 a for the duration of front $t_{ф1}=15$ ns. A ferrite core of the type F-600 has $m_0=0{,}57$, $M_s=280$ G, $S_w=3\cdot10^{-7}$ Oe·sec.

1. Through curve of Fig. 4.10b we find time constant $\tau_0=1{,}3\cdot10^{-10}$ s.

2. Assuming/setting η=0.8, we determine according to (4.41) parameter

$$\vartheta = 6{,}28\cdot280\cdot0{,}8\cdot5\cdot(1-0{,}32)\cdot\frac{1{,}3\cdot10^{-10}}{3\cdot10^{-7}} = 2{,}1.$$

3. We obtain value of relation $\tau_0/\tau_н$, where $\tau_н = t_{ф2}/2{,}5$:

$$\frac{\tau_0}{\tau_{\text{н}}}=\frac{1{,}3\cdot 10^{-10}\cdot 2{,}5}{4\cdot 10^{-10}}=0{,}82.$$

4. With the aid of curves of Fig. 4.8 on ϑ and $\tau_0/\tau_{\text{н}}$ we find k=0.65.

5. We determine number of turns per unit of average/mean length of coil according to formula (4.42)

$$q=\frac{280\cdot 0{,}8\cdot 0{,}43\cdot 0{,}65}{0{,}1\cdot 30}=2{,}1\ \frac{^{(1)}\text{вит}}{\text{см}}.$$

Key: (1). turns/cm

Page 245.

6. We design size/dimension of core

$$d_{\text{ср}}S=\frac{1{,}3\cdot 10^{-10}\cdot 50\cdot 10^{9}}{40\cdot 4{,}4}\sqrt{1+\frac{1}{0{,}65}}\approx 0{,}055\ \text{см}^3,$$

whence it follows that it is possible to take standard core with mean diameter of ring $d_{\text{ср}}=6$ мм Then the number of turns in the coil

$$N=q\cdot\pi d_{\text{ср}}=2{,}1\cdot 3{,}14\cdot 0{,}6\simeq 4\ ^{(1)}\text{вит}.$$

Key: (1). turns/cm

7. We further determine values L_0, C_0, ρ_0, ρ, $n_{\text{опт}}$, t_3 according to formulas, given above:

$$L_0=40\cdot 4{,}4\cdot 0{,}6\cdot 0{,}04\cdot 10^{-9}=4{,}2\cdot 10^{-9}\ ^{(1)}\text{гн},$$

$$C_0=\frac{1{,}7\cdot 10^{-20}}{4{,}2\cdot 10^{-9}}=4\ ^{(2)}\text{пф},$$

$$\rho_0=\frac{4{,}2\cdot 10^{-9}}{1{,}3\cdot 10^{-10}}=32,$$

$$\rho=32\cdot\sqrt{1+\frac{1}{0{,}65}}=50{,}5\simeq R_{\text{н}}=50\ ^{(3)}\text{ом},$$

$$n_{\text{опт}}=0{,}65\cdot\frac{15\cdot 10^{-9}}{1{,}3\cdot 10^{-10}}=75\ ^{(4)}\text{звеньев},$$

$$t_3=150\cdot 1{,}3\cdot 10^{-10}\cdot 1{,}58=30\ ^{(5)}\text{нсек}.$$

Key: (1). H. (2). pF. (3). ohm. (4). components/links. (5). ns.

8. Period of oscillations at apex/vertex is determined on curve Fig. 4.10a and by already found τ_0 and k; we find $T=4.3\cdot10^{-10}$ s.

4.4. COAXIAL FORMING LINE WITH THE FERRITE FILLING.

If we conduct calculations for different types of ferrites, then it follows of them that in forming lines in the form of multilink artificial line it is possible to form/shape current tapers from ones to thousands of amperes. In this case the duration of the front of the formed drop/jump can be from the units of nanoseconds to 0.1 ns. Further decrease of the duration of front is hindered/hampered due to the discrete/digital properties of this line.

Drops/jumps in voltage/stress (current) with large steepness of front in the absence of oscillations on apex/vertex can be obtained in distributed forming lines.

Page 246.

Construction/design of coaxial line with ferrite filling is most advisable construction/design. Fig. 4.11 gives diagrammatic representation of the coaxial forming line with the ferrite filling. Are here ferrite rings arranged/located on the center conductor. The

external surface of rings is isolated by dielectric (teflon, polyethylene) from the external cylindrical conductor (copper braid/cover of the type of the external braid/cover of coaxial cables).

Since standard ferrite rings encompass only one center conductor with current I, then for creation of necessary value of field H high current, which reaches hundred amperes, is required. Furthermore, in contrast to the artificial forming lines the geometric length of coaxial line proves to be very considerable (from several meters to several ten meters).

Since between rings of ferrite is air gap, then ionization of air is created with high voltages and to insulation of line considerable voltage/stress proves to be applied that it is possible to lead to breakdown of line. Therefore the actual limitation of the maximum steepness of the front of the formed/shaped drop/jump in the voltage/stress (current) can begin not due to the properties of ferrite, the switching time of which decreases with an increase in magnetic field H, but due to the disturbance/breakdown of dielectric strength of system. Therefore coaxial line sometimes is immersed in the container with the transformer oil.

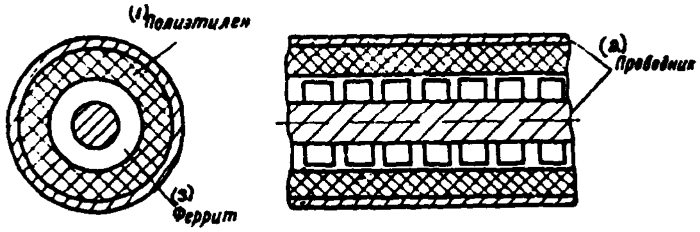

Fig. 4.11. Diagrammatic representation of construction/design of coaxial forming line with filling from ferrite rings.

Key: (1). Polyethylene. (2). Conductor. (3). Ferrite.

Page 247.

Duration of front of drop/jump, formed/shaped in coaxial line with thin layer of ferrite, in essence will be determined by magnetic field strength, created by initial current taper, and by relaxation properties of ferrite [78]. This duration can be evaluated with the aid of expression (4.19):

$$t_{\Phi 2} = \frac{1+\alpha^2}{2\alpha\gamma H} f(m_0).$$

Therefore during calculation of coaxial forming line first according to assigned duration of front $t_{\Phi 2}$ and current I it is expedient to determine sizes/dimensions of ferrite ring [80]

$$d_1 + d_2 = 0,8\frac{t_{\Phi 2} I}{S_w} = 0,8 t_{\Phi 2} I \frac{2\gamma}{1+\alpha^2} f(m_0), \qquad (4.43)$$

where d_2 and d_1 - outside and inside diameters of ferrite ring.

Considering that value α for most adequate/approaching ferrites

lies/rests within limits of 0.3-1, it is possible to record

$$d_1 + d_2 \approx (0{,}9 \div 1{,}4) \cdot 10^7 \frac{t_{\phi 2} l}{f(m_0)} \; [cm].$$

Knowing sizes/dimensions of ring (d_1 and d_2), we determine diameter of external wire

$$d_3 = d_2 + 2h \; [cm],$$

where h - thickness of the layer of insulation between ferrite and external conductor of line, which is found from condition of dielectric strength of dielectric

$$h \approx \frac{I R_n}{E_n} \; [cm],$$

where E_n - voltage of dielectric breakdown.

Page 248.

Matching condition of forming line with load is determined by expression

$$\frac{R_n^2}{1+\eta_i \pi \mu (1-m_0)(d_1+d_2)\, 0{,}2l} =$$
$$= \frac{3600}{\varepsilon_1 \varepsilon_2} \left[\ln \frac{d_3}{d_1} \left(\varepsilon_2 \ln \frac{d_3}{d_2} + \varepsilon_1 \ln \frac{d_2}{d_1} \right) \right], \qquad (4.44)$$

where ε_1 and ε_2 - respectively relative dielectric constant of insulating layer and ferrite; η - duty factor, which characterizes leakage flux, whose value is approximately equal to

$$\eta \approx \frac{d_2 - d_1}{d_3 - d_1}.$$

If left side of equality (4.44) differs from right not more than by 10-15%, then with accuracy sufficient for practice matching condition of line with load is considered carried out. In the case of large disagreement it is necessary to assign to new values d_2 and d_3, when equality (4.43) remains valid and to again conduct calculations.

After ensuring equality (4.44), we determine length of forming line

$$l = \frac{0,2I}{\pi\eta M(1-m_0)(d_1+d_2)} \frac{t_{\phi 1}}{\sqrt{LC}}, \qquad (4.45)$$

where L and C - respectively inductance and capacitance of coaxial line per unit of lengths in the absence of ferrite, which are connected with dependence

$$\frac{1}{\sqrt{LC}} = \frac{3\cdot 10^{10}}{\sqrt{\varepsilon_1\varepsilon_2}}\left(\frac{\varepsilon_2 \ln\frac{d_3}{d_2} + \varepsilon_1 \ln\frac{d_2}{d_1}}{\ln d_3/d_1}\right)^{1/2}.$$

Calculations show that for impulse shaping of voltage/stress with amplitude of 5 kV (on load of 50 ohms) and duration of front of about 1 ns with initial current taper I=100 a with duration of front of 50 ns line with rings of ferrite of type Ф-1000 has length of approximately 10 m [79].

Low permissible repetition frequency of formed/shaped pulses is deficiency in all forming lines with ferrite (to 100 kHz). At the high repetition frequency in the ferrite is isolated the considerable heat, which raises its temperature, which deranges of line.

Table 4.1 gives averaged parameters of ferrites: H_c - coercive force, B_r - remanent induction, relation $m_0=\frac{B_r}{B_s}$, M_s - magnetic moment of saturation, S_w - switching coefficient, T_h - values of Curie points [82].

Page 249.

4.5. SPECIFIC CHARACTER OF OBTAINING SHOCK ELECTROMAGNETIC WAVES IN THE LINES WITH THE FERROELECTRICS AND THE SEMICONDUCTORS.

It was above noted that mechanism of formation of shock electromagnetic waves in lines with ferrite filling was valid and in the case of formation of shock waves in lines with ferroelectrics and semiconductors.

In the case of forming lines with ferrite it is possible to obtain drops/jumps in voltage/stress with steep front and considerable amplitude on low-resistance load. Obtaining steep edges in the voltage/stress on the high-impedance load proves to be possible with the aid of the shock electromagnetic waves, which are formed in the lines with the ferroelectrics.

Table 4.1.

(1) Тип феррита	(2) H_c, э	(3) B_r, гс	α_0	M_s	(4) S_w, э·мксек	T_k, °C
ВТ-1	1,25	2 350	0,9	210	0,57	280
ВТ-2	0,7	2 450	0,91	215	0,59	270
ВТ-5	0,16	2 000	0,85	193	0,40	150
ВТ-6	4,0	1 800	0,81	176	0,46	320
ВТ-7	2,0	1 850	0,88	166	0,46	300
К-28	1,4	2 200	0,92	190	0,52	—
К-65	0,45	2 300	0,93	205	0,56	—
Ф-100	3,5	3 000	0,75	316	0,32	—
Ф-400	1,0	1 400	0,56	200	0,36	—
Ф-600	0,65	2 000	0,57	280	0,30	—
Ф-1000	0,35	1 300	0,44	235	0,40	—

Key: (1). Type of ferrate. (2). ...Oe. (3). ... G. (4). ...Oe.μs.

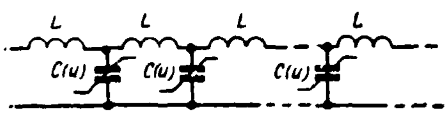

Fig. 4.12. Artificial delay line on capacitors with ferroelectric.

Page 250.

Here as forming line is utilized artificial delay line, which consists of components/links, which contain coil of constant inductance L and nonlinear capacitance C(u), in the form of capacitors with ferroelectric (Fig. 4.12). The dependence of capacitance value of these capacitors from the voltage/stress is connected with the fact that the dielectric constant of ferroelectric is the function of electric intensity $\epsilon = f(E)$ (such capacitors are called variconds).

During transmission of wave along this line its propagation velocity grows/rises with increase in wave amplitude, since value of dielectric constant falls from increase in modulus/module of strength

of field E. Therefore just as in the line with the ferrite, during the propagation of pulse along the line with the ferroelectric the steepness of the pulse edge grows/rises also under specific conditions can arise shock wave.

Steepness of edge of formed/shaped pulse is limited both due to finite time of relaxation processes in ferroelectric (finite time of switching) and due to dispersive properties of multilink transmission line, i.e., due to finite value of time constant τ_{0}.

Relaxation time for some ferroelectrics proves to be order of nanosecond with strength of field E of approximately hundred of kilovolts to centimeter. This fact impedes the application of lines with the ferroelectrics for the formation of nanosecond pulses. With the work with very high voltage usually the breakdown in the line begins earlier than it is possible to form the pulse edge by the duration of the order of nanosecond. However, location line into the container with the transformer oil at a high hydrostatic pressure complicates the construction/design of system. However, under the usual conditions it is possible to obtain drops/jumps in the voltage/stress with the front by duration into several nanoseconds. The permissible pulse repetition rate in this line reaches tens of kilohertz.

Application of forming lines with semiconductors is more promising. This line is fulfilled in the form of the artificial delay

line, which consists of the components/links with the constant inductance L and a nonlinear capacitance of C(u) in the form of semiconductor diodes (Fig. 4.13) [83].

Page 251.

It is known that in transition layers of semiconductors static differential capacitance changes with change in value of applied external voltage. Therefore in each component/link of line is included/switched on semiconductor diode with the expressed nonlinear capacitance (such diodes are occasionally referred to as varicaps). The existing at present semiconductor diodes with the noticeable nonlinear capacitance make it possible to obtain in the line shock electromagnetic waves with a duration of front of approximately one nanosecond with the voltage/stress of the transmitted pulses in all into 10-30 V. In the case of applying the semiconductor materials with the appropriate admixtures/impurities is possible obtaining the diodes, which make it possible to form/shape in the line shock waves with the front with duration into the hundredths of nanosecond. Lines with the semiconductors make it possible to transmit pulses with the repetition frequency to 10 MHz (but in the lines with the ferrite approximately to 100 kHz).

If we compare method of formation of steep edges in current and voltage/stress with the aid of shock electromagnetic waves with other known methods (in diagrams with vacuum lamps, thyratrons and in simplest circuits with nonlinear parameters), then it is possible to

note that with the aid of shock waves are obtained drops/jumps with slope/transconductance, greater approximately to two orders, than with other methods.

4.6. METHODS OF OBTAINING THE PULSES FROM STEEP EDGES IN THE CURRENT AND VOLTAGE/STRESS.

After obtaining with the aid of nonlinear line steep edges in current (voltage/stress), it is possible then by usual methods to form pulse with very steep front and shear/section. The minimum duration of this pulse (at level 0.5 of amplitude) proves to be equal to the duration of shock wave front.

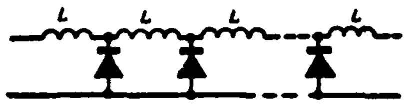

Fig. 4.13. Artificial delay line on semiconductors.

Page 252.

Since duration of drop/jump, obtained at output of nonlinear line, is always final, but its apex/vertex is not flat/plane, but it is characterized by certain decay, then it is necessary to examine drop/jump in voltage/stress in the form of pulse, whose form is depicted in Fig. 4.14a.

As it was already examined in Chapter 3, for formation of nanosecond pulse with very steep front it is possible to accumulate two comparatively prolonged steep-sided pulses, but with voltages/stresses of different polarity (Fig. 4.14b). For obtaining the pulse with the form, close to the rectangular, it is necessary to utilize a small initial part of launched pulses. Then decay in the apex/vertex of shaped pulse is very small, i.e. $\frac{\Delta U}{U} \ll 1$.

For formation of nanosecond steep-sided pulse and by shear/section it is possible to utilize short-circuited section of coaxial line. Then one nonlinear line, which creates drop/jump with the steep front, is required.

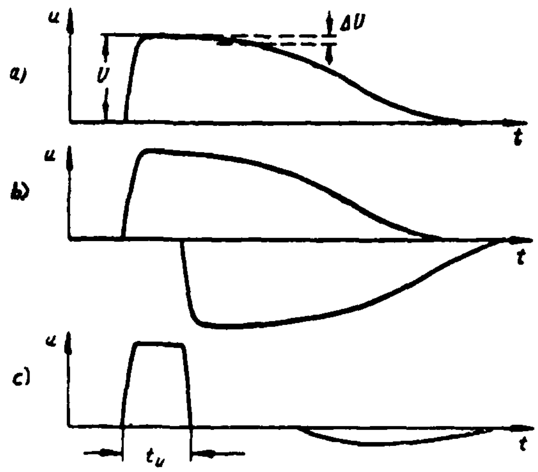

Fig. 4.14. Oscillograms of waves with impulse shaping from shock electromagnetic waves: a) pulse from one line; b) pulses from two lines; c) resulting pulse.

Page 253.

In the case of two identical nonlinear lines the required pulse can be obtained by addition on the total load of two steep edges, mixed in the time relative to each other to the duration of formed/shaped pulse t_u. In the second case it is possible to form the pulse of any polarity.

Application of line with the short-circuited section.

In the case of use for impulse shaping of short-circuited section of line T-shaped coupling of coaxial lines of transmission is used (tee). In this case it is necessary to fit the wave impedance of its separate sections (Fig. 4.15). Let the shock wave enter arm A, whose

wave impedance ρ_A. Arm B is the short-circuited section with a resistor/resistance of ρ_B, arm B - output section of tee, its wave impedance ρ_B. It is necessary so to fit the wave impedance of sections so that the wave reflected from the short circuit would compensate wave in section B, i.e.

$$\rho_B = \frac{\rho_A \rho_B}{\rho_A + \rho_B}.$$

On input of section A drop/jump in voltage/stress is supplied from load of nonlinear forming line (for example, artificial line from L, C of components/links). This load, coordinated with the wave impedance to nonlinear line with the ferrite, can be the wave impedance of section A. In another version very section A of tee can it is the nonlinear coaxial forming line, filled with ferrite.

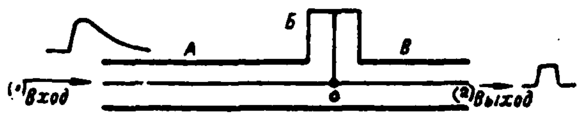

Fig. 4.15. Forming line in the form of coaxial tee.

Key: (1). input. (2). output.

Page 254.

Then, if pulse duration at input of tee (in section A) is more than doubled electrical length of short-circuited section $t_и$, then at output of section B is formed/shaped pulse with duration $t_и$, durations of front and shear/section of which are equal to duration of shock wave front.

Since input pulse has certain decay in apex/vertex, then small overshoot will appear after superposition in section B after shear/section of obtained pulse, since amplitudes of straight line and reflected of pulses are somewhat different. During the guarantee of condition $\frac{\Delta U}{U} \ll 1$ the amplitude of this overshoot is very small. The amplitude of output pulse is determined by the expression

$$U_{вых} = U_{вх} \frac{\rho_B}{\rho_A} \Big/ (1 + \rho_B/\rho_A),$$

where $U_{вх}$ - pulse amplitude at the input of section A.

It is necessary to have in mind that at point O of tee appears wave reflected, which is propagated in direction of input of tee. This wave, after proving to be in the nonlinear forming line, can

affect the value of the initial magnetic state of ferrite.

Application of two nonlinear forming lines.

It is sometimes necessary to obtain pulse of any polarity and continuously adjustable duration. In these cases it is expedient to utilize two nonlinear forming lines, in which are formed identical stationary shock waves. The pulse of different polarity from both lines comes the total load. Pulse initial for both nonlinear lines can be undertaken from one generator (Fig. 4.16), to which the lines are connected in parallel.

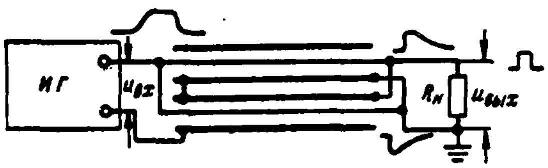

Fig. 4.16. Pulse-shaping circuit with the aid of two coaxial lines with ferrite filling.

Page 255.

In this case one of the line (for example, the coaxial line, convoluted into the spiral) is connected so that the pulse from its output has polarity opposite to the pulse, obtained from another line (Fig. 4.16).

Necessary in time shift/shear of pulses at outputs of nonlinear lines can be achieved/reached either via delay of launched pulse before it it will enter input of one of nonlinear lines or via constant magnetic biasing of ferrite, which fills line.

Delay time per unit of length of line with ferrite can be determined according to formula

$$t_{з0} = \sqrt{\mu_{cp} L_0 C_1} \qquad (4.46)$$

where μ_{cp} - average/mean magnetic permeability of ferrite, which is changed under different initial conditions of its intensity of magnetization.

Due to direct current of magnetic biasing changes value μ_{cp} and, therefore, delay time $t_{3,0}$. Depending on the length of line, using standard ferrite rings with the right-angle hysteresis loop, it is possible to change delay within considerable limits. Thus, in the coaxial line with the length of 20 m delay can smoothly change to the value to 100 ns.

However, application of magnetic biasing of ferrite can be reason for certain instability of temporary situation of front of one drop/jump relative to another, which will cause temporary/time instability of pulse. The position of initial operating point on the hysteresis loop of ferrite can fluctuate, and consequently, will fluctuate and the moment/torque of the formation of shock wave, and also to a certain extent and the steepness of its front.

Pulse-shaping circuit with two lines is generally to larger degree subjected to unstable in operating time, than diagram with short-circuited section. The fact is that the magnetic modes of ferrites in two lines can be at the separate moments of time somewhat different. As a result appears the fluctuation of the moment of operation (formation of the wave front) of diagram at front and shear/section of pulse. Instability in the case of applying the coaxial forming lines, which work with the high currents, which lead to an increase in the temperature of ferrite, is especially noticeable.

Page 256.

In all pulse-shaping circuits use of nonlinear lines it is necessary to consider with possibility of onset of waves in insufficiently matched sections of transmission lines reflected. Multiple traversal of the echo pulses along the nonlinear line, especially with their considerable amplitude, noticeably changes the initial magnetic state of ferrite, i.e., changes the time of its delay and increases the probability of the unstable work of the entire diagram of formation. Therefore to the quality of the agreement of nonlinear line it is necessary to focus proper attention.

Oscillator circuits with the nonlinear forming lines.

Fig. 4.17 gives one of possible schematics of construction of generator of nanosecond pulses with nonlinear forming line on ferrites [9]. Diagram contains start-up stages L_1, L_2, circuits for internal and external synchronization, the cascade/stage of the formation of initial current difference L_3 (on thyratron TGI1-35/3), the forming line with the ferrite, and dual coaxial tee.

Start-up stages shape trigger pulse of thyratron diagram. The steepness of front and the amplitude of trigger pulse must be sufficient for guaranteeing the stable starting/launching of thyratron. With the triggering/opening of thyratron reservoir capacitor C, charged/loaded to the voltage/stress 3 kV, is discharged through the thyratron and the circuit, which contains the forming line.

on the ferrites. The value of current pulse can be regulated with the aid of resistor/resistance of R_1.

Current pulse of discharge with initial duration of front of about 12 ns with passage along nonlinear forming line causes in it formation of shock wave, duration of front of which 0.8-1 ns (depending on strength of current of launched pulse).

Nonlinear line is carried out in the form of artificial delay line with constant capacitance of component/link, equal to 15 pF. Inductance coils are wound on the ferrite rings of the type VT-6 with an outside diameter of 1 mm. The number of turns of coil is equal to 12.

Page 257.

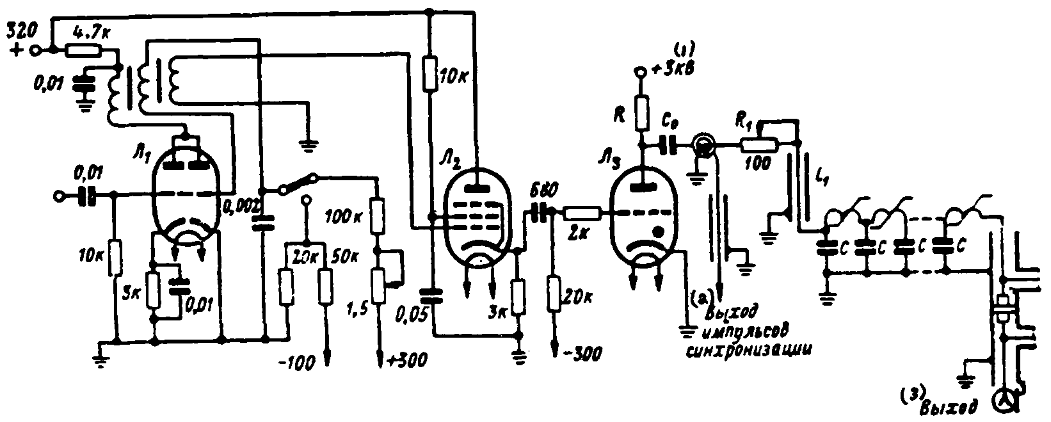

Fig. 4.17. Oscillator circuit of nanosecond pulses with nonlinear forming line.

Key: (1). kV. (2). Output of synchronizing pulses. (3). Output.

Page 258.

Line contains 50 components/links. Line characteristic with the ferrite equally to 75 ohms. On termination of line is formed voltage difference with an amplitude of 1-1.6 kV (depending on the strength of current of launched pulse) and the steepness of the front 10^{12}-$2.5 \cdot 10^{12}$ V/s.

With maximum current in forming line output drop/jump has at apex/vertex oscillation, which is about 15% of amplitude of drop/jump.

With reduction in current it is possible to decrease oscillation to the insignificant value. For decreasing the parasitic parameters of the components/links of its forming line they fulfill the form of brass (silver-plated) plate with the cylindrical openings/apertures and the thin gashes on the edges (Fig. 4.18). Cylindrical rods are placed in the openings/apertures, and between these rods and bore surfaces runs dielectric film made from polytetrafluoroethylene or polyethylene with a thickness of 0.1-0.2 mm. Cylindrical capacitors for the components/links of line are thus formed. Between each of the capacitors (distance between centers of which is 5 mm) coils are arranged/located on the ferrite rings. The length of the ends/leads of the coils, soldered to the rods of capacitors, is not more than 2 .mm. This construction/design makes it possible to obtain the time constant τ_0 of component/link without ferrite (or with the saturated ferrite) on the order of 0.1-0.2 ns. Coaxial pairs are assembled at the ends/leads of the line or coaxial cable is installed. With the work with the increased voltage/stress the line can be placed into the container with the transformer oil.

Voltage difference from forming line on ferrites enters through coaxial cable to coaxial tee.

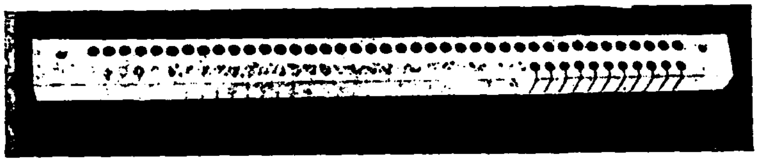

Fig. 4.18. Form of partially mounted forming line with ferrite VT-6.

Page 259.

In the case of using only one tee with short-circuited stub it is possible to form the pulse of the desired duration (not less than the duration of shock wave front) by changing the length of loop. If it is necessary to form the pulse, whose duration is less than the duration of shock wave front, then it is necessary to use two tees. The electrical length of the loop of the first tee must be less than half of the duration of shock wave front t_{ϕ}. But the electrical length of the second loop must be still less. Using two tees, it is possible in this diagram to obtain a bell-shaped pulse with a duration of 0.2-0.3 ns (at the level of 0.5 amplitude values) with the amplitude 200-300 V.

For guaranteeing stable starting/launching of other diagrams or high-speed/high-velocity oscillograph, with the aid of which is observed obtained pulse, in generator is provided output of synchronizing pulse. This pulse is removed/taken from the winding of the ferrite ring, within which will pass the wire, which passes current pulse from the thyratron diagram to the nonlinear forming line. In this way removed the effect of the possible instability of

functioning thyratron. Delay time of the forming line 25 ns. The stability of functioning the forming line (stability of delay time) is not worse than 0.01 ns [9].

Fig. 4.19 gives oscillator circuit, high-voltage nanosecond pulses, in which are used two nonlinear coaxial forming lines [72].

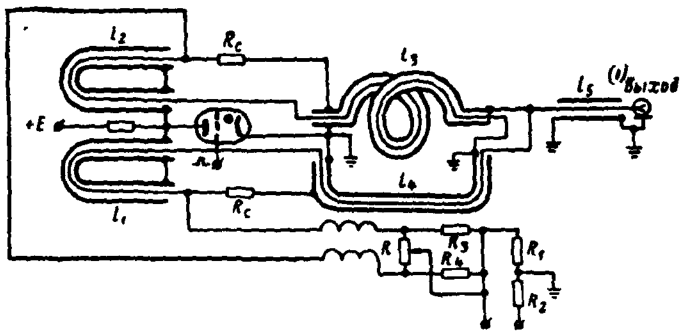

Fig. 4.19. Oscillator circuit with two nonlinear forming lines.
Key: (1). output.

Page 260.

Here initial current pulse is formed/shaped with the thyratron diagram, noncritical to the value of load, with two coaxial charge lines l_1 and l_2. With the triggering/opening of thyratron as a result of the discharge of lines l_1 and l_2 to the input of the forming coaxial lines with the ferrite filling l_3 and l_4 enters initial current taper. The nonlinear forming line l_3 (convoluted into the spiral) is simultaneously coaxial phase inverter.

At output of lines l_3 and l_4 are added two voltage gradients of different polarity. As a result of what on termination (cable l_5 with the matched load) is formed/shaped the voltage pulse with the steep front and the shear/section. The delay time of one of the lines is selected less to value t_u and shock wave from the output of this line enters the load earlier. The part of the current of this wave will be isolated on the load, while part will pass into the second line,

forming in the latter the shock wave, which is propagated towards the shock wave of the second line. In the second line the addition of these waves occurs. As a result through the time interval $t_{\text{и}}$ after pulse arrival on the load from the first line enters the pulse, also, from the second line of the same, the value, but the opposite polarity. The appearance of a pulse from the second line causes the formation of the shear/section of the output pulse, removed from the load.

For obtaining initial current taper application of diagram of formation, noncritical to value load (described in Chapter 3) provides the necessary agreement of the forming lines with the thyratron diagram. The wave impedance of the forming lines l_3 and l_4 in the absence of the intensity of magnetization of ferrite ρ_0 is selected equal to the wave impedance of the charge lines l_1 and l_2 of thyratron diagram. Therefore all waves reflected, which appear at the ends/leads of the forming lines in load, are passed into the charge lines and they are further extinguished by matched impedances $R_c=\rho_0$.

Continuously variable control of duration of output pulse is achieved by change in delay time of forming lines. For changing the delay time, the circuit of magnetic biasing is provided. The current of magnetic biasing from potentiometer R comes the input of lines.

Page 261.

The strength of current of the magnetic biasing of ferrites of one

line relative to current in another is changed by a change in the position of the wiper of potentiometer R to one side or the other. As a result change the delays of lines, and consequently, the pulse duration and its polarity on termination can be changed.

Coaxial forming line is filled with ferrite rings of type VT-6 with outside diameter of 1 mm. In each line a difference in the voltage of 5 kV for a duration of 1 ns is formed/shaped. The length of each line is 25 m. Changing the strength of current of magnetic biasing (from 0.5 to 1.4a), it is possible to ensure a change in the delay of line to ±50 ns. The duration of output pulse (at level 0.5 of amplitude) is regulated in the limits of 1-100 ns. Permissible pulse repetition rate to 1 kHz. The stability of the temporary situation of pulse is not worse than the tenths of nanosecond.

Page 262.

Chapter Five.

PULSING IN RC-CIRCUITS WITH FEEDBACK.

Formation of steep edges in voltage/stress is one of central problems of pulse technique. For the solution of this problem in the pulse technique of microsecond range are used relaxation oscillators: multivibrators, start-up circuits, blocking oscillators and other devices/equipment, which are positive-feedback circuits. In such diagrams two different electrical modes or two different states of equilibrium occur. Transition/junction from one state to another, caused by external forces or action of internal reasons, is completed in them so/such rapidly, that in the vibration theory these transitions/junctions were called jumps, and oscillations themselves - relaxation oscillations [84].

Concept of relaxation oscillations in connection with relaxation oscillators (subsequently those briefly called relaxation oscillators), fruitfully utilized in vibration theory, cannot be accepted in nanosecond pulse technique, since it does not answer most important for it question about transit time of relaxation oscillator from one state of equilibrium into another. In order to determine this time, called switch time, it is necessary to consider the effect of the low parameters of circuit of relaxation oscillator - stray capacitances, and sometimes also stray inductances, i.e. to consider

the effect of precisely those elements, which does not take into consideration the disruptive vibration theory.

Page 263.

It is natural that account of effect of low parameters substantially complicates determination of switch time of relaxation oscillators, and therefore for simplification in problem they assume that into switchings relaxation oscillator is linear amplifier, included by positive feedback. The account of the nonlinear properties of the tube of relaxation oscillator in the process of its switching does not give any new qualitative results; moreover, virtually the results of this investigation are depreciated by the unavoidable spread of the parameters of tubes and parts [2, 85-87].

These facts served as reason for fact that nonlinear by their nature pulse generators in nanosecond pulse technique are considered as piecewise-linear systems, i.e., systems, whose phase space consists of several fields; in each of such fields behavior of system it is described by linear equations. The problem of the formation of pulse oscillations in the nanosecond pulse technique is actually the problem of conversion. After considering that the relaxation oscillator is piecewise-linear system, it can consider the process of the formation of pulse oscillation as the totality of the linear transformations, completed above the input oscillation in the separate regions of phase space.

These conversions are linear integral transforms. The integral character of conversions is caused by the limitedness of the passband of the devices/equipment, which realize a conversion. Specifically, the limitation of the passband of linear system is the reason for the final duration of the process of the transition/junction of relaxation oscillator from one state to another. Because of this the avalanche-like process of switching relaxation oscillator is completed although sufficiently rapidly, not instantly. Since from the point of view of nanosecond pulse technique in the work of relaxation oscillator there is greatest interest in the precisely avalanche-like process of transition/junction from one state of equilibrium to another, it is expedient to begin the examination of the work of relaxation oscillator precisely from this question.

Page 264.

5.1. AVALANCHE-LIKE PROCESSES IN RELAXATION OSCILLATORS.

Let us define operator of conversion as linear integral operator

$$Au_0(t) = \int_0^t u_0(t-\xi)\, dK(\xi),$$

where A - symbol of operator;

$u_0(t)$ - converted oscillation;

K(t) - transient response of converter.

In contrast to generally accepted fold of Riemann, fold of Stieltjes is here used. The application of Stieltjes' integral frees

function K(t) from the need for being differentiated, which is very valuable when K(t) is discontinuous function. Another advantage of the fold of Stieltjes is the fact that it does not require the introduction of special conversion diagram - pulse transient function, being limited only to transient response.

Linearized relaxation oscillator is quadrupole with feedback, at input of which operates converted oscillation $u_0(t)$, and at output - converted oscillation u(t), as shown in Fig. 5.1. Voltage/stress u(t) is removed/taken from the output terminals and again is supplied to the input for the conversion.

Fig. 5.1 depicts consecutive application of voltage of feedback into input circuit of relaxation oscillator. In practice together with series circuit widely is used the parallel diagram of supply. It is easy to show that the parallel diagram of supply can be brought to the consecutive. For this purpose let us turn to Fig. 5.2. Fig. 5.2a depicts the parallel diagram of supply to feedback into input circuit, while in Fig. 5.2b - the equivalent diagram of input circuit. Here $\mathcal{E}_0$ - emf of the source of the converted oscillation; R_i - its internal resistor/resistance; $\mathcal{E}_K$ - equivalent emf. of K-circuit; R_K - its output resistance; R_{K0} - input resistance of K-circuit.

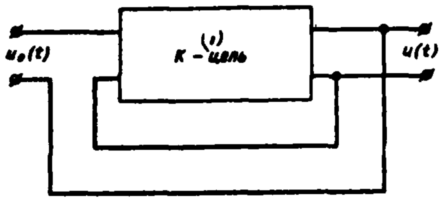

Fig. 5.1. Block diagram of relaxation oscillator with consecutive feedback.

Key: (1). K-circuit.

Page 265.

Since K-circuit is nonautonomous quadrupole, then its equivalent emf is caused by the action of voltage/stress on its input. In steady state of emf it is equal to the product of voltage on the input of K-circuit on its transmission factor.

Let us determine voltage/stress, which operates at input of K-circuit. This voltage/stress is equal to the sum of the currents, developed by electromotive forces $\mathcal{E}_0$ and $\mathcal{E}_K$ in resistor/resistance R_{K0}, multiplied by the value of this resistor/resistance. After producing the necessary computations, let us find that the voltage on the input of K-circuit will be determined as follows;

$$u_{вх} = \alpha\mathcal{E}_0 + \beta\mathcal{E}_K,$$

where

$$\alpha = \frac{R_K R_{K0}}{R_K R_i + R_K R_{K0} + R_i R_{K0}}; \quad \beta = \frac{R_i R_{K0}}{R_K R_i + R_K R_{K0} + R_i R_{K0}}.$$

Let us designate $u_0 = \alpha\mathcal{E}_0$, $u = \beta\mathcal{E}_K$.

Value u_0 is voltage/stress, which operates at input of K-circuit and developed by sour e $\mathcal{E}_0$, and u - voltage/stress of feedback, which operates in the same section.

Resulting voltage on input of K-circuit

$$u_{\text{вх}}(t)=u_0(t)+u(t), \tag{5.1}$$

where for parallel diagram $u_0(t)$ and u(t) they are defined in the manner that it was indicated earlier, and for consecutive - these voltages/stresses present converted oscillation and output oscillation.

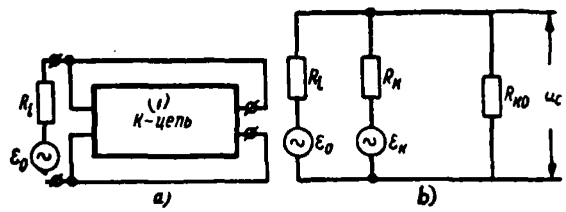

Fig 5.2. Block diagram of relaxation oscillator with parallel feedback (a) and equivalent diagram of input circuit (b).
Key: (1). K-circuit.

Page 266.

On the basis of expression (5.1) via simple translation the parallel diagram of application of voltage it is possible to lead to the consecutive.

Let us designate through K(t) transient response of K-circuit, then

$$u(t)=\int_0^t u_{\text{вх}}(t-\xi)\,dK(\xi). \tag{5.2}$$

Output voltage/stress is to roll of voltage/stress, which operates at input of K-circuit and transient response. Substituting (5.2) and (5.1), we obtain the integral equation of Volterra of the 2nd order:

$$u_{\text{вх}}(t)-\int_0^t u_{\text{вх}}(t-\xi)\,dK(\xi)=u_0(t), \tag{5.3}$$

solution of which let us record in the form of the series/row of

Neumann-Liouville:

$$u_{вх}(t)=\sum_{n=1}^{\infty} u_{n-1}(t),$$

where

$$u_{n-1}(t)=\int_0^t u_0(t-\xi)\,dK^{[n-1]}(\xi)$$

there is the oscillation, which completed (n-1)-th circulation on internal circuit of relaxation oscillator, and $K^{[n-1]}(t)$ - iterated transient response of K-circuit:

$$K^1(t)\equiv K(t),$$

$$K^{[n-1]}(t)=\int_0^t K^{[n-2]}(t-\xi)\,dK(\xi).$$

Subsequently we will write/record expression for transient response of K-circuit of relaxation oscillator in the form $K(t)=K_0M(t)$, where K_0 - maximum value, and $M(t)$ - standardized/normalized transient response, swing $M(t)=1$. In this case

$$K^{[n-1]}(t)=K_0^{n-1}M^{[n-1]}(t).$$

Page 267.

Solution of integral equation can be also represented in the form

$$u_{вх}(t)=\int_0^t u_0(t-\xi)\,d\Gamma_\Sigma(\xi), \qquad (5.4)$$

where $\Gamma_\Sigma(t)$ - resolvent [6], which let us record as

$$\Gamma_{\Sigma}(t)=\sum_{n=1}^{\infty} K_{\bullet}^{n-1} M^{[n-1]}(t). \quad (5.5)$$

Assuming/setting in (5.4) $u_{0}(t)=1(t)$, we obtain, that resolvent of integral equation is transient response of relaxation oscillator, in reference to its input, i.e. voltage/stress, which appears at input of relaxation oscillator in the case, when from without is supplied single voltage gradient:

$$A_{BX}(t)=\sum_{n=1}^{\infty} K_{\bullet}^{n-1} M^{[n-1]}(t). \quad (5.6)$$

As it follows from this expression, voltage on input of relaxation oscillator is composed from infinite number of components. First of them is a single voltage gradient, supplied to the input of relaxation oscillator [when $n=1$ $M^{[0]}(t)=1(t)$], and all subsequent are recurrent voltage/stress. In turn, recurrent voltage/stress consists of the infinite number of iterated transient responses of K-circuit.

It is known from theory of integral equations that series/row (5.6) converges regularly on t, if derivative M'(t) is final [88]. Let us assume that swing $K_{0}M'(t)=\nu$, then for the iterated transient responses of K-circuit we will have the following evaluations/estimates:

$$K_0 M^{[1]}(t) \leqslant \frac{\nu t}{1!},$$

$$K_0^2 M^{[2]}(t) \leqslant \int_0^t M^{[1]}(t-\xi) M'(\xi)\, d\xi \leqslant \frac{(\nu t)^2}{2!},$$

$$K_0^3 M^{[3]}(t) \leqslant \int_0^t M^{[2]}(t-\xi) M'(\xi)\, d\xi \leqslant \frac{(\nu t)^3}{3!},$$

. . . .

$$K_0^n M^{[n]}(t) \leqslant \int_0^t M^{[n-1]}(t-\xi) M'(\xi)\, d\xi \leqslant \frac{(\nu t)^n}{n!}.$$

Page 268.

These inequalities mean that iterated transient responses of K-circuit of relaxation oscillator not with what n and t will exceed in their change in value $(\nu t)^n/n!$

Let us name/call expressions, which are in right side of inequality, maximum iterated transient responses of K-circuit and will designate them through $\hat{K}_n(t)$, then

$$\hat{K}_n(t) = \frac{(\nu t)^n}{n!}.$$

Let us determine, with what values of effective time lag of oscillation $t_{\text{эн}}$ maximum transient responses reach single, level, for which let us solve equation

$$\frac{(\nu t_{\text{эн}})^n}{n!} = 1,$$

whence we will obtain

$$t_{\text{эн}} = \frac{1}{\nu} \sqrt[n]{n!}.$$

Let us assume that ν=10' Hz. (As it will be shown further, $\nu = \frac{S}{C_0}$ there is a quality of tube in the diagram). Then the time,

spent by the iterated transient response for achievement of single level, is 1.00 ns for n=1; 1.41 ns - for n=2; 1.82 ns - for n=3; 2.21 ns - for n=4; 2.63 ns - for n=5 and so forth.

Maximum iterated transient responses reach single level faster, the lower index of iteration.

As it follows of aforesaid earlier, $\hat{K}_1(t)$ is transient response of K-circuit of relaxation oscillator, $\hat{K}_2(t)$ - transient response of two series-connected K-circuits, $\hat{K}_3(t)$ - transient response of three series-connected circuits, etc.

Page 269.

Value $t_{зп}$ shows, to what period delays pulse right-angled oscillation with passage of one, two, three and more than once on K-circuit of relaxation oscillator. The greater the number of circulations oscillation completed, the later it reaches fixed level, in particular single level.

Effective time lag of oscillation, which passes to K-circuit, is caused by fact that reaction rate of K-circuit to effect of form of unit function is final on condition. The presence of this time lag is explained, why the sum of the infinite number of iterated transient responses of K-circuit, which generates the transient response of relaxation oscillator, in reference to its input circuit, is finite. Each subsequent component of voltage on the input of relaxation

oscillator appears somewhat later than preceding/previous; in this case at the initial moments of time the intensity of components with the large numbers immeasurably lower than intensity of components with the small numbers.

Obviously, this fact has vital importance during solution of question about rate of increase of transient response of relaxation oscillator and time of its switching. The greater the time of effective time lag, the more slowly the grid voltage of tube increases and the greater the switch time.

Let us introduce maximum transient response of relaxation oscillator

$$\hat{A}_{\text{вх}}(t)=\sum_{n=1}^{\infty}\hat{K}_n(t).$$

After substituting into this expression value $\hat{K}_n(t)$, we will obtain

$$\hat{A}_{\text{вх}}(t)=e^{\nu t}. \qquad (5.7)$$

Maximum transient response of relaxation oscillator, in reference to circuit of grid (5.7), makes following sense. This characteristic shows, how there can be the maximum value of grid voltage of the first tube of relaxation oscillator at any moment of time during the supplying to its input of a single voltage gradient in the linear system, the maximum speed of the reaction of internal circuit of which

is limited by value ν.

Page 270.

No real transient response of relaxation oscillator can increase more rapidly than maximum transient response.

As is known, process of transition/junction of relaxation oscillator from one state of equilibrium into another is avalanche-like [36]. Equation (5.7) expresses the maximum law of avalanche-like process. It is easy to see that in the limiting case in question the function and all its derivatives at any moment of time have identical sign. The process, described by function e^x in the natural science is called the process of organic increase/growth. The process of organic increase/growth - this is such process, during which rate of change in any value is proportional to the most changing value. At the initial moments of the time, when the changing value is low, its change is completed with the low speed; with an increase in the changing value grows/rises the rate, with which occurs this increase. This property of the processes of organic increase/growth has vital importance for the evaluation of the role of avalanche-like process in the formation of the front of the pulse oscillations, developed by relaxation oscillators.

Absolute value of voltage/stress, attained up to any moment of time on grid of tube of relaxation oscillator, depends on value of very moment of time and on value of quality of tube ν. In the last

decade the quality of tubes increased in all several times, whereas the duration of operating pulses decreased to more than thousands of times. After considering that value νt_1 (where t_1 - time, during which actively it is utilized avalanche-like process) for the relaxation oscillators of nanosecond range 1000 times less than for the relaxation oscillators of microsecond range, we will obtain that in the microsecond range the effectiveness of the use of an avalanche-like process is e^{1000} times more than in the nanosecond pulse technique. In the majority of the schematics of microsecond pulse generators the time, occupied by avalanche-like process, is so/such small, that it can be disregarded/neglected in comparison with the time of the charge of output capacitance, which determines the duration of the pulse edge. In other words, in many diagrams of microsecond range the switch time of current in the tube can be considered equal to zero.

Page 271.

In the diagrams of nanosecond range in view of the low effectiveness of avalanche-like process the switch time of relaxation oscillators is relatively more in the sense of its portion in entire time of shaping of the pulse edge.

In nanosecond relaxation oscillators use of avalanche- like processes is very frequently ineffective, and therefore in many instances for obtaining steep-sided pulses are used diagrams, in which avalanche-like processes are absent, for example amplifier-limiters

and recirculators. In order to determine the role of avalanche-like processes in the diagrams of nanosecond relaxation oscillators, let us produce the following calculations.

We will call relaxation oscillator I those relaxation oscillators, whose transient response takes form $e^{\nu t}$, and by relaxation oscillator II relaxation oscillators, which have unlimited transient response, for example characteristic of form ch νt. It is obvious that with any t $e^{\nu t} > \mathrm{ch}\,\nu t$. Then we record

(1)Релаксатор I	(2)Релаксатор II
$A_{\text{вх}}(t) = e^{\nu t}$	$A_{\text{вх}}(t) = \mathrm{ch}\,\nu t.$

Key: (1). Relaxation oscillator ....

Under actual conditions input voltage cannot take form of unit function. In the first approximation, it is possible to consider that the voltage on the input changes according to the linear law

$$u_0(t) = \alpha t.$$

In this case voltage on input of K-circuit taking into account action of feedback will be located with the aid of fold

$$u_{\text{вх}}(t) = \int_0^t u_0(t-\xi)\, dA_{\text{вх}}(\xi).$$

Substituting in this expression of value for $u_0(t)$ and $A_{\text{вх}}'(t)$ and producing necessary computations, we obtain

$$u_{\text{вх}}(t) = \frac{a}{\nu}\left(e^{\nu t} - 1\right) \quad \Big| \quad u_{\text{вх}}(t) = \frac{a}{\nu}\,\text{sh}\,\nu t. \qquad (5.8)$$

Page 272.

In order to rate/estimate gain, attained due to introduction to positive feedback, we will use value

$$\varphi(t) = \frac{u_{\text{вх}}(t)}{u_0(t)},$$

which can be represented in the form

$$\varphi_1(x) = \frac{e^x - 1}{x} \quad \Big| \quad \varphi_2(x) = \frac{\text{sh}\,x}{x},$$

where $x=\nu t$ - dimensionless time.

Plotted function $\varphi(x)$ is given in Fig. 5.3. Its examination makes it possible to draw a number of conclusions relative to the effectiveness of avalanche-like processes in the relaxation oscillators, which work in the nanosecond range.

It is obvious that application of positive feedback is little effective, if given by it gain in value of voltage on input of relaxation oscillator comprises less than 50%.

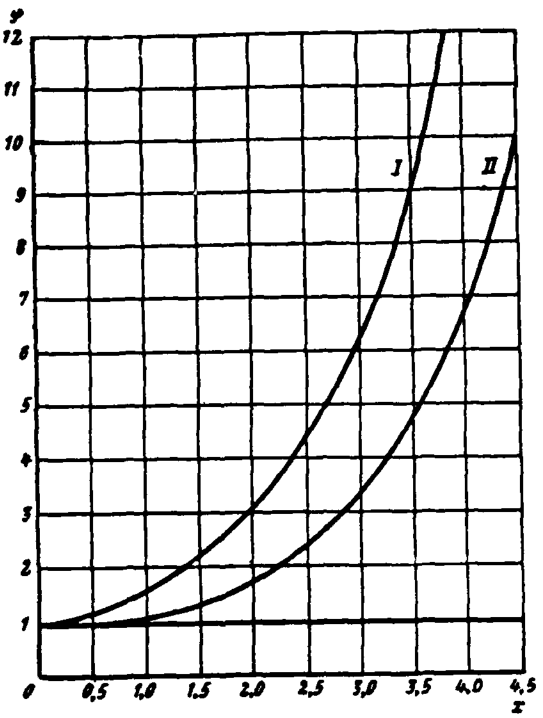

Fig. 5.3. Plotted function $\varphi(x)$.

Page 273.

(Let us note that with this increase in the grid voltage of tube the gain in the decrease of the duration of the pulse edge at the output will be considerably smaller percentage). For relaxation oscillator to this I section of curve corresponds $x \leq 0.85$. Let us accept value ν of the equal to 10^9 Hz. Then to the value x indicated will correspond time $t_1 \leq 0.85$ ns. This time can be named the time lag of feedback in the relaxation oscillator.

Gain, attained in increase in grid voltage of tube of relaxation oscillator at fixed/recorded t, is defined by value ν, which is, as it

was already said to re, by quality of tube in diagram of relaxation oscillator. With $\nu=10^{9}$ Hz and t=1 ns in an increase in the grid voltage for relaxation oscillator I will be 1.7, and at t=1 μs this gain reaches e^{113}. The character of the process of organic increase/growth in the nanosecond and microsecond ranges is this greatly distinguished.

5.2. SWITCHING TIME OF RELAXATION OSCILLATORS.

Let us turn now directly to determination of switch time of relaxation oscillators. By switch time of relaxation oscillator is understood the time, during which the relaxation oscillator passes of one state of electrical equilibrium into another, for example from the state, when tube is completely opened and through it flows current I_0, to the state, when tube is closed and the current through it is equal to zero. Let us assume that the drop/jump between the states indicated is realized when grid voltage of the first tube of relaxation oscillator changes to value E_0, called subsequently the solution/opening of grid characteristic. If in the diagram of relaxation oscillator feedback was absent, then during the supplying to its input of linearly increasing voltage/stress switch time would be equal to t_0 (Fig. 5.4). Under such conditions work, in particular, limiters. In the presence of feedback and caused by it avalanche-like increase of grid voltage of the first tube of relaxation oscillator, the switch time decreases to value t_n. The essential shortening of switch time, attained due to the introduction to feedback, served as

the reason for the wide use of such diagrams in the pulse technique of microsecond range.

Page 274.

Switch time can be found from relationship/ratio

$$u_{вх}(t_п)=E_0.$$

After using formulas (5.8), let us find that

(1)Релаксатор I	(2)Релаксатор II
$t_п=\frac{1}{\nu}\ln(1+\nu t_0)$	$t_п=\frac{1}{\nu}\operatorname{Arsh}\nu t_0,$

Key: (1). Relaxation oscillator.

where

$$t_0=\frac{E_0}{\alpha}$$

there is the time, during which the linearly increasing voltage/stress changes to value E_0. Let us rewrite the second formula in the more convenient for the calculations form. As is known,

$$\operatorname{Arsh}x=\ln(x+\sqrt{1+x^2}),$$

on the basis of what

$$t_п=\frac{1}{\nu}\ln\left[\nu t_0+\sqrt{1+(\nu t_0)^2}\right].$$

Let us introduce value

$$\theta=\frac{t_п}{t_0},$$

showing the ratio of the switch time of relaxation oscillator to time t_0:

$$\theta=\frac{\ln(1+x_0)}{x_0} \qquad \Bigg| \qquad \theta=\frac{\ln(x_0+\sqrt{1+x_0^2})}{x_0},$$

where $x_0=\nu t_0$.

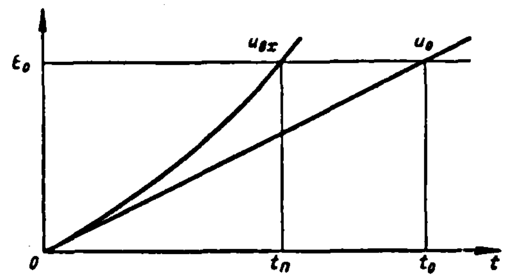

Fig. 5.4. Determination of switch time of relaxation oscillator.

Page 275.

Fig. 5.5 depicts plotted functions $\theta(x_0)$ for relaxation oscillators I and II. They show, as decreases the switch time of relaxation oscillator as a result of the introduction to positive feedback. Assuming/setting ν=const, it is possible to consider that along the axis of abscissas is plotted time t_0. In particular, in $\nu=10^9$ Hz to point $x_0=1$ correspond $t_0=1$ ns.

Graphs/curves show that effective decrease of switch time t_n occurs only if time t_0 is sufficiently great. However, gain in the switch time, attained due to the introduction to feedback, is small for the majority of the diagrams of nanosecond range of sizes. (This concerns only the latter/last cascodes of the diagrams, where to the conversion are subject the pulses of nanosecond duration).

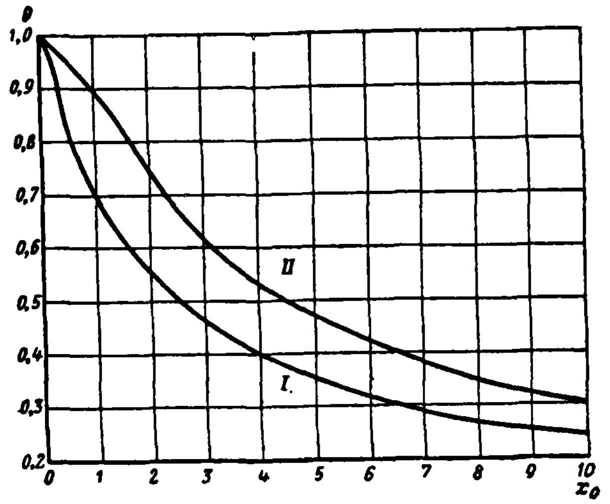

Fig. 5.5. Dependence of relative switch time t_n of relaxation oscillator on value t_0, which characterizes quality of tube.

Page 276.

It is possible to establish on the basis of given earlier (in Fig. 5.3) graph/curve that with positive feedback in a circuit made with a tube with $\nu=10^9$ Hz, grid voltage of tube of relaxation oscillator I increases up to moment of time t=3 ns 6 times. The graph/curve, given in Fig. 5.5, shows that the switch time in this case decreases a little larger than twice in comparison with the case, when feedback is absent.

5.3. DURATION OF PULSE EDGES AT OUTPUT OF RELAXATION OSCILLATORS.

Switch time of relaxation oscillator does not determine completely duration of pulse edge at its output. It determines only

the duration of the front of current, which takes place through the tube. However, as far as the duration of the front of voltage/stress on the load is concerned, it depends substantially on the properties of output circuit.

Let us assume that output circuit of relaxation oscillator is integrating component/link as this shown in Fig. 5.6a. The same figure depicts the equivalent diagram of output circuit. In order to find output potential of relaxation oscillator, we will use the fold

$$u(t) = -K_0 \int_0^t u_{\text{вх}}(t-\xi)\, dK_1(\xi). \qquad (5.9)$$

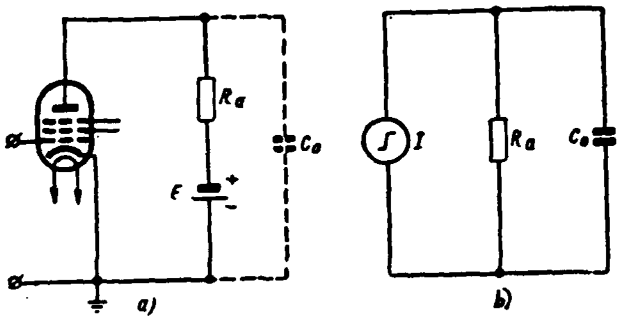

Fig. 5.6. Output circuit of relaxation oscillator (a) and its equivalent diagram (b).

Page 277.

Here transient response of output circuit

$$K_1(t) = 1 - e^{-\frac{t}{\tau}}, \qquad (5.10)$$

and $\tau = C_0 R_a$ - time constant of integrating circuit, where R_a - resistor/resistance of plate load, and C_0 - stray capacitance, which shunts load. Factor of amplification of K-circuit $K_0 = SR_a$ (S - mutual conductance of tube at the operating point).

For determining u(t) there is no need for using exact expression for $u_{\text{вх}}(t)$: it necessarily only for computing switch time. Further examination of process can be produced, assuming that the voltage on the input of relaxation oscillator changes according to the law, shown in Fig. 5.7. Analytically this law can be expressed as follows:

$$\begin{aligned} u_{\text{вх}}(t) &= \frac{E_0}{t_{\text{и}}} t \quad (0 \leq t \leq t_{\text{и}}), \\ u_{\text{вх}}(t) &= \frac{E_0}{t_{\text{и}}} t + \frac{E_0}{t_{\text{п}}} (t - t_{\text{и}}) \quad (t > t_{\text{и}}). \end{aligned} \qquad (5.11)$$

Latter/last expression indicates also that

$$u_{BX}(t) = -E_0.$$

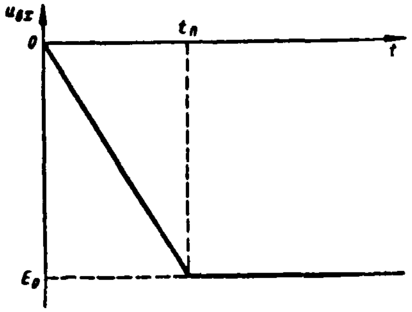

Fig. 5.7. Approximation of grid voltage of relaxation oscillator.

Page 278.

Substituting (5.11) and (5.10) in (5.9), we obtain after computation

$$u(t)=U_{\text{макс}}\left[\frac{t}{t_п}-\frac{1-e^{-t/\tau}}{\frac{t_п}{\tau}}\right] \quad (0\leqslant t\leqslant t_п), \quad (5.12а)$$

$$u(t)=U_{\text{макс}}\left[1-\frac{\left(e^{\frac{t_п}{\tau}}-1\right)e^{-\frac{t}{\tau}}}{\frac{t_п}{\tau}}\right] \quad (t>t_п), \quad (5.12б)$$

where amplitude of temporary voltage on anode of tube

$$U_{\text{макс}}=K_0E_0.$$

It follows from written expressions that up to moment/torque of end of process of switching output potential of relaxation oscillator attains value

$$u(x_п)=U_{\text{макс}}\left[1-\frac{1-e^{-x_п}}{x_п}\right],$$

where

$$x_п=\frac{t_п}{\tau},$$

and at $t \to \infty$ it approaches $U_{макс}$.

Graphs/curves of anode voltage are given on Fig. 5.8 for two cases: $x_n=0$ and $x_n=1$.

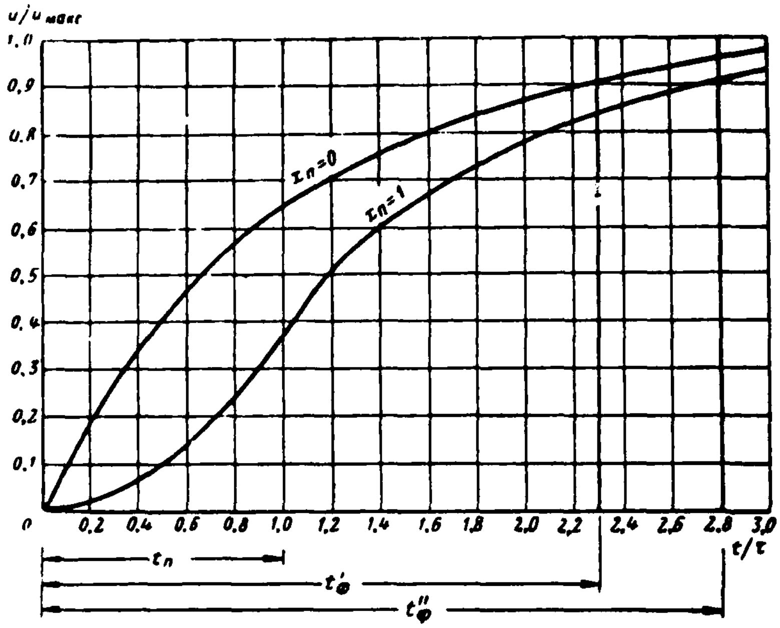

Fig. 5.8. Form of output potential of relaxation oscillator with different values of parameter

Page 279.

In the first case the value of the switch time of relaxation oscillator is negligible in comparison with the time constant of output circuit. Output potential in this case increases according to the law

$$u(t)=U_{\text{макс}}\left(1-e^{-\frac{t}{\tau}}\right),$$

reaching 90% of its steady-state value for the duration of front $t_{ф}=2{,}3\tau$. In the second case the switch time is equal to constant equal to the time constant of output circuit and output potential is described by formulas (5.12), in which one should assume $\frac{t_{п}}{\tau}=1$.

Duration of front t_Φ of output voltage/stress can be found from condition

$$U_{\text{макс}}\left[1-\frac{1}{x_п}(e^{x_п}-1)e^{-\frac{t_\Phi}{\tau}}\right]=0{,}9U_{\text{макс}},$$

whence

$$t_\Phi=\tau\left(\ln 10+\ln\frac{e^{x_п}-1}{x_п}\right)=\tau\left(2{,}3+\ln\frac{e^{x_п}-1}{x_п}\right).$$

First term in this formula is rise time of output potential of relaxation oscillator in the case, when switch time it is equal to zero, and second term - elongation of front due to finite time of switching. When $x_п=0$ we have $t_\Phi=2{,}3\tau$, while when $x_п=1$ we obtain $t_\Phi=2{,}8\tau$.

Fig. 5.9 gives dependence of relation $\frac{t_\Phi}{\tau}$ on $x_п$, with the aid of which it is possible to determine duration of front of output pulses with known values $t_п$ and τ. Graph/curve shows that the conventional approximation formula for the duration of the edges of pulses $t_\Phi=2{,}3\tau$ [89] is valid only when switch time is small in comparison with the time constant of output circuit.

In preceding/previous section it was established that presence of positive feedback in relaxation oscillator of I with quality tube 10' Hz decreases switch time of relaxation oscillator approximately two times (namely, 2.15 times).

Page 280.

Let the time constant of output circuit τ be equal to the switch time of diagram with the extended feedback loop, i.e. is equal to t_0. The duration of the pulse edge in this case, as soon as which was established, it composes 2.8 τ. If due to the introduction to positive feedback switch time decreased 2.15 times, then this will lead to the fact that the duration of front decreases to 2.5 τ, i.e., it will be lowered only by 11%. This gain will be still less at a larger value of the ratio of the time constant of output circuit to the switch time. The given numerals show that the action of feedback in the nanosecond range little effective, which more narrowly was discussed above. Therefore in the final stages of the conversion of the pulses, in which the pulse duration is short they usually place not relaxation oscillators, but amplifier-limiters.

Presence of positive feedback in final stages of peakers of pulses is undesirably also for following reasons. During the amplification of very narrow pulses in such diagrams the time lag of the voltage/stress, which enters from the feedback loop the grid of relaxation oscillator, is observed. The pulse, which arrives from the feedback loop, proves to be somewhat displaced with respect to the pulse, which entered the input of relaxation oscillator for the conversion.

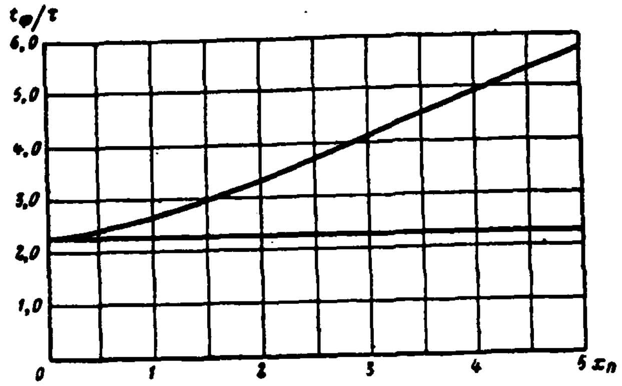

Fig. 5.9. Dependence of relativity of duration of front from parameter x_n.

Page 281.

As a result of this bias/displacement the resulting pulse on the grid of tube seemingly is expanded, what is negative moment/torque in the device/equipment, intended for pulse shortening.

All these deficiencies in positive-feedback circuits are greater, the shorter the duration of converted pulses. Therefore similar diagrams should be considered little promising for the work in the range of very narrow pulses.

5.4. CONSECUTIVE PEAKING IN RELAXATION OSCILLATOR CIRCUITS.

Shaping of very short pulses or pulses with very steep fronts in single-stage relaxation oscillators is not always attained. For example, at the rate of the starting voltage/stress, characterized by

value t_0=1 μs, even in the tube with the quality 10^9 Hz switch time will be 6.9 ns, and the duration of the pulse edge is still more. In order to obtain possible narrow pulses, relaxation oscillators frequently connect up consecutive chains/networks. Each subsequent relaxation oscillator is started in this case by pulses with the steeper front than preceding/previous. Because of this at the network output, the steepness of the pulse edges is more than at the input. It should be noted that the method of consecutive peaking gives improvement only when in the process of the consecutive starting/launching of relaxation oscillators switch time decreases.

Let us assume that at input of chain/network from Q of identical relaxation oscillators operates linearly increasing voltage/stress

$$u_0(t) = at.$$

Then, as it was shown in second section of present chapter, switch time of relaxation oscillator I (with chain connection, as a rule, are utilized relaxation oscillators I)

$$x_1 = \ln(1 + x_0),$$

where $x_0 = \nu t$; $x_1 = \nu t_{n_1}$.

Page 282.

For switch time output potential of first relaxation oscillator will change according to the law

$$u_1(t)=E_0K_0\left[\frac{t}{t_{n1}}-\frac{1-e^{-\frac{t}{\tau}}}{\frac{t_{n1}}{\tau}}\right],$$

reaching up to moment of time $t=t_{n_1}$ of value

$$U_1=E_0K_0\left[1-\frac{1-e^{-\frac{t_{n1}}{\tau}}}{\frac{t_{n1}}{\tau}}\right]=E_0K_0\left[1-\frac{1-e^{-\frac{x_1}{K_0}}}{\frac{x_1}{K_0}}\right],$$

since

$$\frac{x_1}{K_0}=\frac{\nu t_{n1}}{SR_a}=\frac{\frac{S}{C_0}t_{n1}}{SR_a}=\frac{t_{n1}}{C_0R_a}.$$

We linearize voltage/stress $u_1(t)$, after assuming

$$u_1(t)=a_1t,$$
$$a_1=\frac{U_1}{t_{n1}}.$$

Then switch time of second relaxation oscillator

$$x_2=\ln\left[1+\nu\frac{E_0}{a_1}\right]=\ln\left[1+\frac{x_1}{K_0}\psi\left(\frac{x_1}{K_0}\right)\right],$$

where

$$\psi\left(\frac{x}{K_0}\right)=\frac{1}{1-\frac{1-e^{(-x/K_0)}}{\frac{x}{K_0}}}.$$

Graph/curve of this function is shown in Fig. 5.10 $\psi\left(\frac{x}{K_0}\right)\to 1$ when $\frac{x}{K_0}\to\infty$; virtually this value can be considered close to one when $\frac{x}{K_0}\geqslant 10$.

Page 283.

During time $t_{\text{п}_1}$ output potential of second relaxation oscillator increases according to the law

$$U_2(t) = E_0 K_0 \left[\frac{t}{t_{\text{п}2}} - \frac{1 - e^{-t/\tau}}{t_{\text{п}2} \tau}\right],$$

reaching up to moment of time $t = t_{\text{п}_2}$ of value

$$U_2 = \frac{E_0 K_0}{\psi(x_2/K_0)}.$$

We linearize this voltage/stress, after assuming

$$u_2(t) = a_2 t.$$

In this case switch time of third relaxation oscillator

$$x_3 = \ln\left(1 + \nu \frac{E_0}{a_2}\right) = \ln\left[1 + \frac{x_2}{K_0} \psi\left(\frac{x_2}{K_0}\right)\right].$$

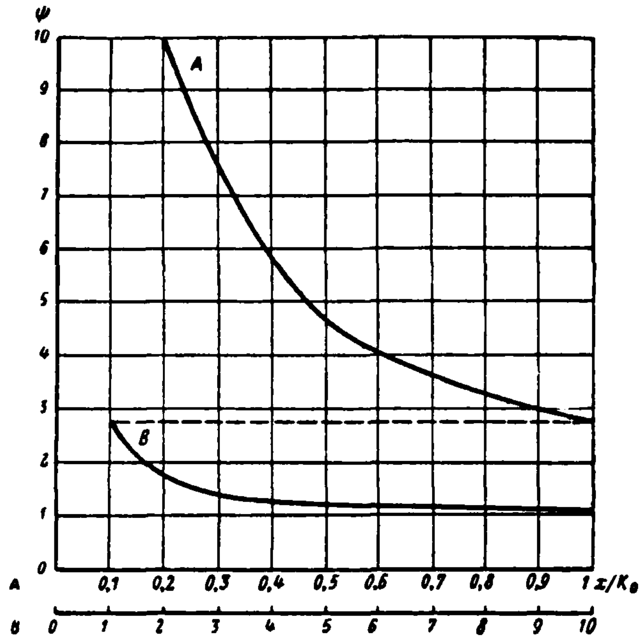

Fig. 5.10. Plotted function $\psi(x/K_0)$.

Page 284.

Continuing this operation further, we will obtain

$$x_Q = \ln\left[1 + \frac{x_{Q-1}}{K_0}\,\psi\left(\frac{x_{Q-1}}{K_0}\right)\right]. \qquad (5.13)$$

Fig. 5.11 gives dependences of dimensionless switch time on number of relaxation oscillators in chain/network, constructed for different values of factor of amplification K_0. The examination of these graphs/curves shows that with an increase in the number of relaxation oscillators the dimensionless switch time decreases, approaching a certain limit. Switch time reaches limiting value sooner, the greater the rate of the increase of the converted

voltage/stress and the greater the factor of amplification K_0.

It is physically easy to explain, why triggering time does not decrease unlimitedly with time of ripening of number of cascades/stages. Let us assume that the switch time in the q cascade/stage decreased to zero; then rise time of voltage on its output is 2.3 τ and, therefore, the switch time of the (q+1)-th cascade/stage will be certain. This means that in the presence of stray capacitance in output circuit the switch time not with what q can become zero.

In order to find steady-state value of switch time, i.e., value of switch time in q relaxation oscillator with $q_1 \to \infty$, let us enter as follows. In steady state

$$x_q = x_{q+1} = x^*,$$

where x^* indicates the stationary value x.

For determination x^* we will use formula (5.13), into which instead of x_{Q-1} let us substitute value x^*

$$x^* = \ln\left[1 + \frac{x^*}{K_0}\psi\left(\frac{x^*}{K_0}\right)\right]$$

mode this equation relatively x^*. Let us substitute in it value $\psi\left(\frac{x^*}{K_0}\right)$, we convert and will obtain

$$e^{x^*} = 1 + \frac{\left(\frac{x^*}{K_0}\right)^2}{\frac{x^*}{K_0} - 1 + e^{-\frac{x^*}{K_0}}}.$$

Page 285.

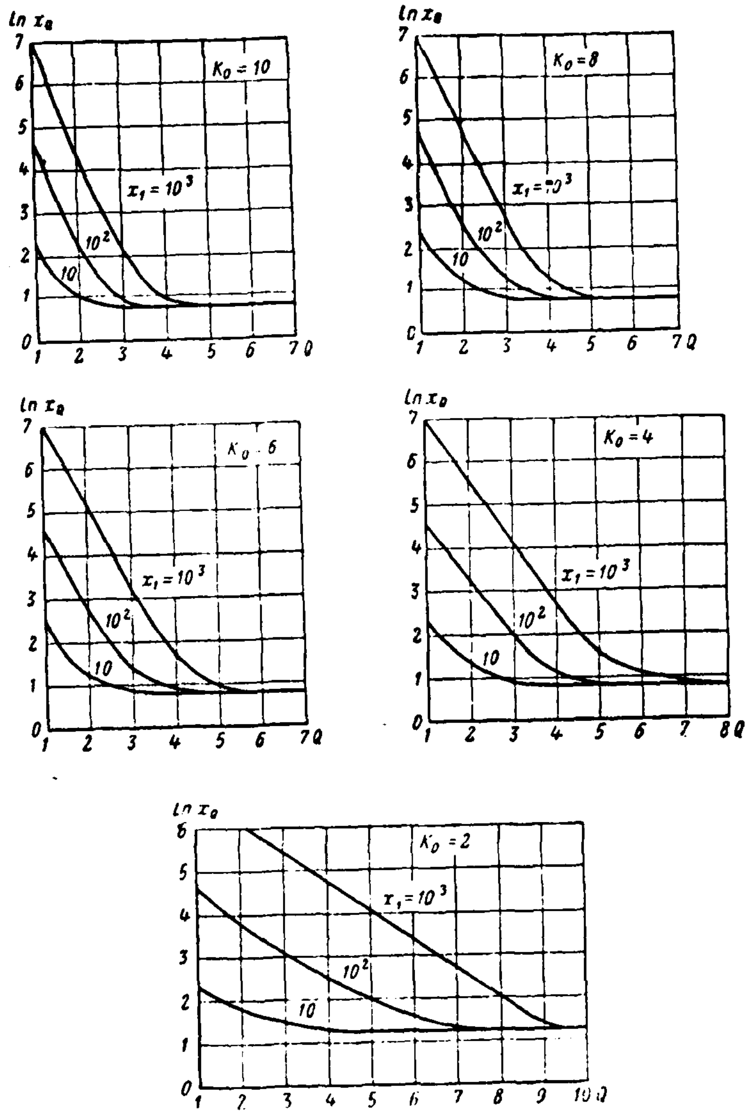

Fig. 5.11. Dependence of relative switch time on number of relaxation oscillators in chain/network with different values of K_0.

Page 286.

Numerical solution of this equation with respect to x^* is given in Table 5.1.

On the basis of this table it is possible to consider in the first approximation, that with sufficiently high amplification factor steady-state value of dimensionless switch time of relaxation oscillator $x^* \approx 1$

$$t^*_n \approx \frac{1}{\nu}.$$

Switch time cannot be less than value of reverse/inverse ν (i.e. value, reverse/inverse quality of tube). Thus, with γ=10' Hz $t^*_n = 1$ ns.

5.5. RELAXATION OSCILLATORS BUILT ON TUBES WITH SECONDARY EMISSION.

In preceding/previous sections of present chapter analysis of work of relaxation oscillators was conducted on the basis of known transient responses of these relaxation oscillators and volt-ampere characteristics of tubes irrespectively of concrete/specific diagrams of relaxation oscillators. Let us examine now the diagrams of relaxation oscillators, beginning from the single-tube diagrams, assembled on the tubes with the secondary emission.

As was shown earlier, switch time of relaxation oscillators and duration of pulse edges at their outputs depend substantially on quality of tubes utilized in relaxation oscillators. The problem of increasing the quality of tubes without a considerable increase in the current density on the cathode and a decrease of the distance between

the cathode and the grid proved to be resolvable under the condition for use in the tubes of the phenomenon of secondary emission. Furthermore, the presence in these tubes of the special electrode, which possesses the ability to emit secondary electrons, offers the new possibilities of the construction of the oscillator circuits of pulses.

Table 5.1.

K_0	2	4	6	8	10	12	∞
x^*	1,230	1,180	1,140	1,120	1,115	1,114	1,113

Page 287.

Diagrammatic representation of one of the types of tubes with the secondary emission is given in Fig. 5.12.

Work of tube with secondary emission occurs as follows. Electronic flux, being headed from the cathode toward the anode, falls on dynode, being under higher potential, and dislodges/chases from it the flow of the secondary electrons, which are fixed to the anode, which has an even larger potential. The internal surface of dynode is covered with the layer of the substance, which has secondary-emission coefficient $\sigma>1$. Because of this anode current is more than cathode σ once (if we do not consider the current of screen grid).

Tubes with secondary emission possess a series/row of special features in comparison with usual tubes. First of all, as already mentioned above, they they have high quality. For the tubes with the secondary emission the ratio of mutual conductance of tube to the grid capacitance - cathode $\sigma^{3/2}$ once is more than for the tubes, which do not use the phenomenon of secondary emission.

Second special feature of tubes with secondary emission consists in the fact that current of dynode has opposite direction in comparison with current of anode, i.e., in external current circuit flows from dynode. Because of this voltage/stress on the dynode and the grid they prove to be cophasal that it makes it possible to obtain positive feedback in single-tube track layout application of voltage from the dynode to the grid through isolating capacitor.

Third special feature of tubes with secondary emission lies in the fact that current of anode of these tubes can considerably exceed current of cathode. This fact makes it possible to obtain positive feedback by means of the connection of the anode with the cathode through the coupling capacitor.

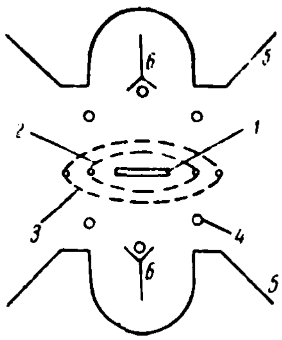

Fig. 5.12. Diagrammatic representation of tube with secondary emission: 1 - cathode; 2 - control electrode; 3 - screen grid; 4 - focusing electrode; 5 - dynode - electrode, which emits secondary electrons; 6 - anode.

Page 288.

Tubes with secondary emission can be used in most diverse oscillator circuits of pulses; however, most specific for them are single-tube transformerless diagrams which were discussed above. Two versions of the diagrams of relaxation oscillators on the tubes with the secondary emission are given in Fig. 5.13. The first diagram (Fig. 5.13a) is diagram with a dynode-grid connection/communication, and the second (Fig. 5.13b) - diagram with the anode-cathode connection/communication.

Let us examine work of diagram with dynode-grid connection/communication (work of second diagram and its advantage approximately the same as in the first).

Diagram of relaxation oscillator, given in Fig. 5.13a, can work both in mode of self-excitation and in mode of waiting relay in dependence on bias voltage, supplied to control electrode. From the point of view of obtaining possible narrow pulses, there is greatest interest in the second case, when relaxation oscillator works as peaker.

As can be seen from figure, positive voltage of source, which feeds dynode, is applied to it through resistor/resistance $R_д$.

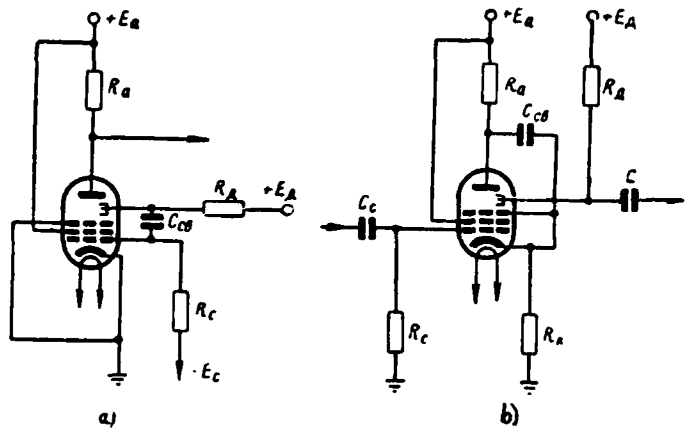

Fig. 5.13. Diagrams of relaxation oscillators on tubes with secondary emission: a) with dynode-grid connection; b) with anode-cathode connection.

Page 289.

This resistor/resistance is analogous with anodic resistor/resistance in the usual schematic of multivibrator. It is selected sufficiently high value so that the factor of amplification of dynode circuit would be more than one and diagram could be self-excited. Alternating voltage from the dynode through isolating capacitor $C_{cв}$ is supplied to control electrode of tube. Capacitance value of isolating capacitor defines the duration of the pulses generatable in the diagram similarly, as it takes place in the blocking oscillator. Leakage resistance of grid is large enough that it would not shunt the dynode resistor/resistance. The value of this resistor/resistance together with the capacitance of isolating capacitor determines the period of oscillations of generator in the mode of auto-oscillations.

Let us pause at some special features of tube in diagram of relaxation oscillator. The current of dynode is the difference between the currents of cathode and anode of the tube

$$i_{д} = i_{к} - i_{а},$$

and since the current of the anode as a result of the phenomenon of secondary emission is more than the current of cathode, then the current of dynode flows in the opposite direction in comparison with the current of the anode. If in external circuit anode current flows to the anode, then in the dynode circuit the current flows from the dynode. Voltage on the anode of tube when there is a load on the anode circuit is always lower than supply voltage by the value of the voltage drop across load. However, voltage on the dynode when there is a load on the dynode circuit is always greater than the voltage of the source which feeds this circuit. With an increase in the grid voltage, the dynode current grows/rises in absolute value and the voltage/stress on the dynode grows/rises because of this, i.e., voltages/stresses on the dynode and the grid prove to be cophasal.

For self-excitation of oscillations in the relaxation circuit based on a tube with secondary emission and a dynode-grid connection, besides cophasality of the voltages on the dynode and the grid, it is necessary for the transmission gain the closed feedback loop to be greater than one. This is accomplished, first of all, by having the value of resistor/resistance in the dynode circuit be great enough, which was already discussed above. Furthermore, in the diagram they try to obtain the coefficient of feedback, i.e., the transmission gain

from the dynode to the grid, close to one.

Page 290.

This is reached with the aid of the sufficiently great capacity of isolating capacitor (capacitance of isolating capacitor it must be much more than the input capacitance of tube).

For analysis of work of generator on tube with secondary emission we will use characteristic, which expresses dependence of voltage/stress on dynode from voltage/stress on control electrode (Fig. 5.14). Dynode voltage/stress is product of dynode current to load resistance/resistor and therefore reflects/represents shape of the curve of dynode current. Dynode current appears with a certain negative voltage/stress on control electrode - cutoff voltage on the dynode circuit. The build-up of dynode current occurs with an increase in the voltage on control electrode until the phenomenon of the redistribution of the cathode current between the dynode and control electrode sets in. With further increase in the grid voltage dynode current decreases due to the phenomenon indicated.

On the same graph/curve are given straight lines of feedback for two end positions, which correspond to moments/torques of "jumps" of current. The straight line of feedback is the dependence of voltage on control electrode on the voltage on the dynode. With the sufficiently great capacity of isolating capacitor when the coefficient of feedback can be considered equal to one, the straight

line of feedback will pass at angle of 45° (with the equality of scales along the coordinate axes).

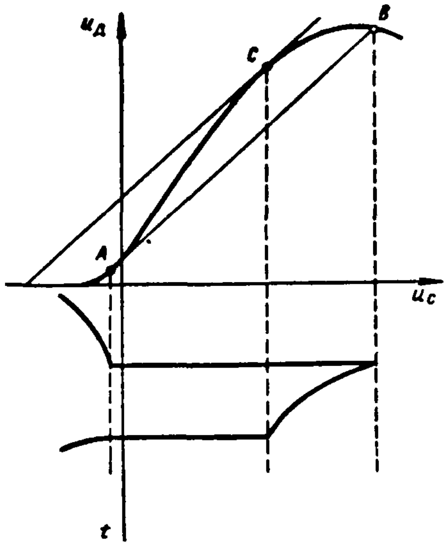

Fig. 5.14. Analysis of relaxation oscillator on tube with secondary emission.

Page 291.

Examination of work of relaxation oscillator let us begin from that moment/torque when tube it is closed and in diagram occurs capacitor discharge. The process of capacitor discharge lasts until tube is opened and operating point falls on that section of the dynode characteristic, where the slope/transconductance is sufficient so that in the diagram the condition of self-excitation would be satisfied. At this moment the transmission gain on the closed loop of feedback becomes equal to one and in the diagram appears avalanche-like process. Operating point abruptly passes from position A to position B. In actuality this process occurs during finite time due to the unavoidable parasitic circuit parameters.

After operating point falls into position B, in diagram process of charge of separating capacitance begins with grid current of tube. As a result of special feature of dynode current noted earlier, the voltage/stress on the dynode is more than supply voltage, so that with the charge of capacitor acquires the potential difference, which exceeds the voltage of source. As a result of charge of capacitor the grid voltage is gradually decreased, in consequence of which the operating point passes in the section of characteristic with the large slope/transconductance. At point C mutual conductance becomes sufficient so that the transmission factor on the closed loop of feedback would become more than one, and in the diagram appears the reverse avalanche-like process, which rapidly leads to the closing of tube. Thus, capacitance value of isolating capacitor determines time between the straight line and the reverse/inverse by avalanche-like processes, i.e., the pulse duration.

After closing of tube in circuit, which contains resistors/resistances R_c and $R_{л}$, begins capacitor discharge. Although in the discharge circuit of capacitor is contained the source of dynode voltage $E_{д}$, as has already been indicated, voltage across capacitor at the beginning of the process of discharge is more than supply voltage of dynode. Discharge time is determined by the time constant of this circuit, i.e. virtually with the value of the product of the capacitance of isolating capacitor to leakage resistance.

Page 292.

With a certain approximation/approach it is possible to consider that this time determines the period of oscillations of the relaxation oscillator (when the oscillatory period much more than the pulse duration).

Anode circuit of tube, as follows from description of work of diagram given above, does not participate in process of impulse shaping, but it is utilized only for their amplification.

5.6. ANALYSIS OF OPERATION OF RELAXATION OSCILLATOR BASED ON TUBE WITH SECONDARY EMISSION.

Let us now move on to analysis of work of relaxation oscillator on tube with secondary emission, beginning from investigation of process of switching. For this we linearize the characteristic of tube in section AC, after replacing with its line segment. Let us assume that the starting voltage on the grid of tube is given in the form of unit function. Then grid voltage

$$u_{\text{c}}(t) = 1(t) + u_{\text{д}}(t), \qquad (5.14)$$

where $u_{\text{д}}(t)$ - alternating voltage on the dynode.

In turn,

$$u_{\text{д}}(t) = \int_0^t u_{\text{c}}(t-\xi)\, dK(\xi), \qquad (5.15)$$

where K(t) - transient response of amplifier, formed by dynode part of

diagram:

$u_c(t)$ - voltage/stress on control electrode.

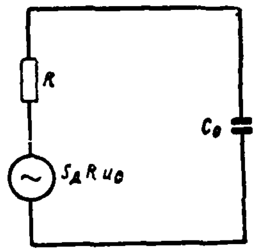

Fig. 5.15. Equivalent diagram of output circuit of relaxation oscillator.

Page 293

Equivalent diagram matic of this amplifier is shown in Fig. 5.15, where $S_Д$ - slope/transconductance of dynode characteristic; C_0 - stray capacitance, back-out resistor of R; R - resistance/resistor of load of dynode (taking into account by-passing of section grid - cathode of tube).

Substituting (5.15) in (5.14), we obtain integral equation of Volterra of 2nd order:

$$u_c(t) - \int_0^t u_c(t-\xi)\, dK(\xi) = 1(t),$$

solution of which takes form

$$u_c(t) = 1(t) + \sum_{n=1}^{\infty} K_n(t),$$

where $K_n(t)$ - transient response n of series-connected K-circuits.

According to equivalent diagram

$$K(t) = K_0(1 - e^{-t/\tau}),$$

where

$$K_0 = S_д R, \quad \tau = C_0 R.$$

In order to find transient response of n series- connected K-circuits, it is necessary to realize (n-1)-fold convolution of K(t). The result of this operation, as is known, can be represented in the form [90]

$$K_n(t) = K_0^n \left[1 - e^{-t/\tau} \sum_{k=0}^{n-1} \frac{1}{k!} \left(\frac{t}{\tau}\right)^k \right].$$

This formula is equation of transient response of n-stage resistance-coupled amplifier or result of n-fold passage of voltage/stress of stepped form through one amplifier stage. Substituting this expression into the solution of integral equation, we obtain

$$u_c(t) = 1(t) + \sum_{n=1}^{\infty} \left[1 - e^{-t/\tau} \sum_{k=0}^{n-1} \frac{1}{k!} \left(\frac{t}{\tau}\right)^k \right] =$$

$$= 1(t) + \frac{K_0}{1 - K_0} \left[1 - e^{-\frac{(1-K_0)t}{\tau}}\right].$$

Page 294.

Setting $K_0 \gg 1$, we will have

$$u_c(t) = e^{\nu t},$$

where

$$\nu = \frac{S_1}{C_0}. \qquad (5.16)$$

By definition, $u_c(t) = A_c(t)$ since at input of relaxation oscillator single voltage gradient acts. It follows from formula (5.16) that the pulse generator on the tube with secondary emission is relaxation oscillator I (when $K_0 \gg 1$).

Conclusions drawn above make it possible to use for timing of switching relaxation oscillator to tube with secondary emission and duration of pulse edges, generated by this relaxation oscillator, formulas, derived earlier in § 5.2 and 5.3.

Let us turn now to question about determination of duration of pulses, generated by single-tube diagrams on tubes with secondary emission. For this purpose will examine first the oscillograms of electrode voltages of tube in the diagram of relaxation oscillator. These oscillograms are given in Fig. 5.16. The first oscillogram (Fig. 5.16a) shows the law of a change in the grid voltage of tube.

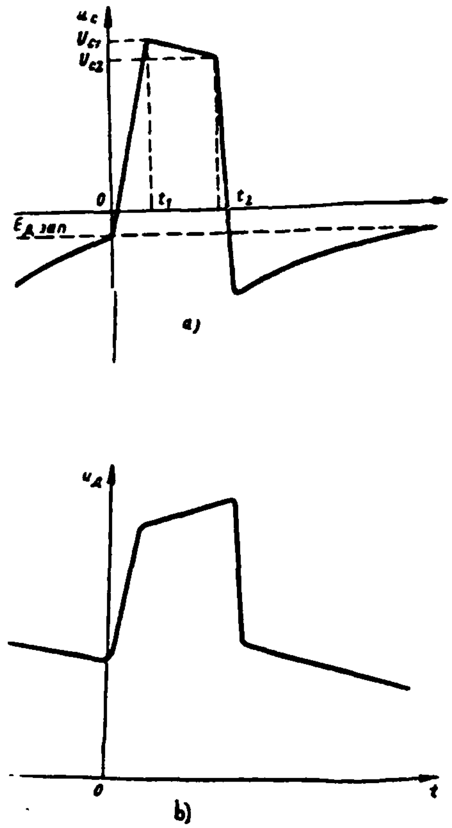

Fig. 5.16. Voltage oscillograms on elements of network of relaxation oscillator on tube with secondary emission: a) on grid; b) on dynode.

Page 295.

The grid voltage of tube is negative at point in time t=0 and it is less than the cutoff voltage $E_{д\,зап}$. At the moment of time t=0 in the diagram appears the avalanche-like process, as a result of which the grid voltage of tube during the small interval of time rises to value U_{c1}. At subsequent points in time shaping of pulse apex occurs. The pulse apex of grid voltage has a decay, which is obtained due to an increase in the voltage/stress on capacitance $C_{cп}$ with its charge by

grid currents. Up to the moment/torque of the termination of the flat/plane part of the pulse the grid voltage of tube falls to value U_{c2}.

Second oscillogram (Fig. 5.16b) presents dependence of dynode voltage/stress from time. It is characteristic for it that the pulse apex on the dynode has a lift. This lift is caused by the special feature of the work of tube with the secondary emission, which consists in the fact that the current of dynode in external circuit flows from the dynode, and therefore in the presence of load in the dynode branch circuit on the dynode grows/rises with an increase in the dynode current. The third oscillogram presents the law of a change in the voltage/stress on the coupling capacitor.

In order to determine duration of flat/plane part of pulse (knowing this, as well duration of front and shear/section of pulse, makes it possible to determine pulse duration at any level), let us allow some idealizations. Let us assume that the current of dynode does not depend on the value of dynode voltage/stress. Let us assume also that during shaping of pulse apex the current of dynode does not depend on voltage/stress on control electrode. The input resistance of section grid - cathode we will consider constant.

It is obvious that in this system in process of formation of flat/plane part of pulse grid voltage of tube will decrease exponentially:

$$u_c(t) = U_{c1} e^{-\frac{t}{\tau_з}},$$

where U_{c1} - maximum grid voltage, which occurs with $t=t_1$ (see Fig. 5.16);

$\tau_з$ - time constant of charge of capacitor.

Page 296.

Time constant $\tau_з$ is equal to product of capacitance of isolating capacitor to total resistance of circuit of charge, which consists of series-connected resistance/resistors of dynode load and resistor/resistance of section grid - cathode of conducting tube:

$$\tau_з = C_{ов} R_з,$$
$$R_з = R_д + r_c.$$

Time, required for decreasing grid voltage from value U_{c1} to value U_{c2}, let us find from condition

$$U_{c2} = U_{c1} e^{-\frac{t_и}{\tau_з}},$$

whence [1]

$$t_и = \tau_з \ln \frac{U_{c1}}{U_{c2}}.$$

Detailed study of generator on tube with secondary emission was carried out into [91], where was given following formula for determining pulse duration:

$$t_и = \tau_з \tau_w (\alpha, \beta), \tag{5.17}$$

where $\tau_w(\alpha, \beta)$ - certain function of parameters α and β, represented in Fig. 5.17.

In turn,

$$\alpha = 1 + 2\frac{E_{д\,зап}}{E_{д\,нас} - E_{д\,зап}},$$

$$\beta = R\frac{I_{д\,нас}}{E_{д\,нас} - E_{д\,зап}}.$$

Here $E_{д\,зап}$ - cutoff voltage of dynode current; $E_{д\,нас}$ - voltage/stress, with which dynode current achieves saturation $I_{д\,нас}$; $E_{д\,нас} - E_{д\,зап}$ - the absolute difference between the saturation voltages and cutoff. Relation $I_{д\,нас}/(E_{д\,нас} - E_{д\,зап})$ is equal to the averaged slope/transconductance of dynode characteristic $S_д$, so that the parameter β plays the role of the factor of amplification of dynode circuit.

Page 297.

(Value $R = \frac{R_д r_c}{R_д + r_c}$ - the resistance/resistor of the load of dynode circuit).

In [91] is given also formula for determining minimum duration of pulses (at level 0.5), which is determined by stray capacitances of diagram and by value of load resistance/resistor:

$$t_{и\,мин} = (2 \div 5{,}2)\,RC_0,$$

where $C_0 = C_{ск} + C_{дк}$ - sum of parasitic grid capacitances and dynode.

Different values of coefficient in formula are caused by varied conditions of starting/launching.

Analysis given above makes it possible to determine procedure of engineering of relaxation oscillators on tube with secondary emission. In the nanosecond pulse technique these generators, as a rule, work as the peakers of previously formed oscillations, i.e., are used for increasing the steepness of the pulse edges. In connection with this calculation let us begin from the determination of the duration of fronts and impulse steepness, developed by relaxation oscillators.

Let us accept as initial value for calculation steepness of front of starting voltage α. Then the switch time of tube with the extended loop of feedback $t_0=E_0/\alpha$, where E_0 - value of the opening of the idealized characteristic of tube $I_a=f(U_c)$. Let us find the switch time of relaxation oscillator taking into account the action of feedback from the formula

$$t_n=\frac{1}{\nu}\ln(1+t_0\nu),$$

where $\nu=\frac{S_a}{C}$.

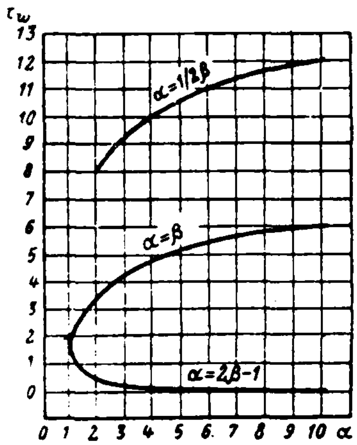

Fig. 5.17. Plotted function $\tau_w(\alpha, \beta)$.

Page 298.

Here $S_д$ - slope/transconductance of idealized characteristic $I_д=f(U_c)$, and C_0 - total stray capacitance, which shunts dynode resistor/resistance.

Duration of pulse edges at output of relaxation oscillator

$$t_\Phi=\tau\left(2{,}3+\ln\frac{e^{x_п}-1}{x_п}\right),$$

where $x_п=\frac{t_и}{\tau}$; $\tau=C_0R$.

After determining parameter $x_п$ in known values τ and $t_п$, let us find t_Φ.

Pulse amplitude at output of relaxation oscillator (considering that voltage/stress is removed/taken from dynode resistor/resistance)

$$U = I_{\text{д нас}} R_{\text{д}},$$

where $I_{\text{д нас}}$ - saturation current of diode, determined from idealized characteristic.

Here it is thought that characteristic is taken/removed in pulsed operation. Average/mean steepness of the edge of the pulses

$$S_{\Phi} = 0{,}9 \frac{U}{t_{\Phi}}.$$

Coefficient of 0.9 is undertaken here because for time t_{Φ} of output potential of relaxation oscillator it increases to value 0.9 U.

Pulse duration at output of relaxation oscillator can be determined according to formula (5.17). Since $E_{\text{д нас}} \approx 0$, then essentially it is possible to consider that α≈3. Knowing this value, according to the graph/curve, given on Fig. 5.17, it is possible to find that with β=6 (upper curve) $\tau_{u} = 9{,}4$, with β=3 (average/mean curve) $\tau_{u} = 4{,}4$ and with β=2 (lower curve) $\tau_{u} = 0{,}4$. The pulse duration obtained is greater, the greater the factor of amplification of diagram, well known property of all relaxation oscillators.

Period of oscillations of relaxation oscillator, which works in mode of peaking, is equal to period of converted oscillations. In the mode of auto-oscillations recovery time of relaxation oscillator can be calculated by the formulas, proposed by Ya. S. Itskhoki [1].

Page 299.

As has already been spoken, relaxation oscillators sometimes are connected up chains/networks for consecutive peaking. The calculation of similar chains/networks can be performed on the basis of the graphs/curves, given in Fig. 5.11. On these graphs/curves, constructed for different factors of amplification K_0, is shown the dependence of the logarithm of dimensionless switch time $x=t_n\nu$ on the number of relaxation oscillators in chain/network Q. As the parameter is accepted value x_1 - the dimensionless switch time of one relaxation oscillator. The series connection of relaxation oscillators is expedient only if in the process of consecutive peaking the decrease of the switch time of diagram occurs. It follows from the graphs/curves that with $K_0=10$ and $x_1=10^3$ is expedient to take the chain/network, which consists of four relaxation oscillators (counting the first, the switch time of which is equal x_1), when $x_1=10^2$ - chain/network of three relaxation oscillators and when $x_1=10$ - chain/network of two relaxation oscillators.

Order of calculation of chain/network of relaxation oscillators can be following. After accepting known value x_0 for the first relaxation oscillator, we find the time of its switching through the formula

$$t_{n1} = \frac{1}{\nu} \ln (1 + x_0),$$

and the switch time of the second and subsequent relaxation oscillators - according to formula (5.13), where $\psi(x/K_0)$ is given by

the graph/curve, given in Fig. 5.10.

If $t_{п2}$ is considerably less than $t_{п1}$, then should be determined switch time of third relaxation oscillator, the fourth, etc., until switch time ceases substantially to decrease. After determining thus tentatively the number of relaxation oscillators Q, should be found the duration of the pulse edges at the output of latter/last and next-to-last relaxation oscillators. If $t_{фQ}$ noticeably differs from $t_{фQ-1}$, then the number of relaxation oscillators is selected correctly, but if these values differ little from each other, then the number of relaxation oscillators in the chain/network must be decreased by one and repeated the same operation again until it is noticeable that the decrease of the number of relaxation oscillators by one leads to the considerable elongation of the pulse edge.

Page 300.

5.7. DIAGRAMS OF RELAXATION OSCILLATORS BUILT ON TUBES WITH SECONDARY EMISSION.

Diagram of relaxation oscillator on tube with secondary emission, whose analysis was given above, is experimentally investigated [92]. All data of the entering the diagram elements are cited in Fig. 5.18a. Diagram was assembled on tube EFP-60, which has the following parameters: $E_а=250$ V, $E_д=250$ V, $E_c=-2$ V, $I_а=20$ ма, $S_а=25$ mA/V, $S_д=17$ mA/V, $C_{вх}=9{,}2$ pF, $C_{вых\,а}=6$ pF, $C_{вых\,д}=11$ pF. Diagram worked in the stagnation mode, which was achieved by the supply of negative

voltage/stress on control electrode of tube. Diagram was started up by positive pulses with an amplitude of 6 V, supplied to the grid circuit through the small separating capacitance. The duration of the generatable pulses changed by changing capacitance value of block capacitor C. Output pulse was removed/taken from the load, connected to anode circuit. The load resistance/resistor composed only of 10 ohms, and the amplitude of the current, which flows through the load, reached 1a. The pulse rise-time was equal to 10 ns, i.e., the steepness of front composed 10' V/s. The maximum value of the pulse of dynode voltage was 200 V.

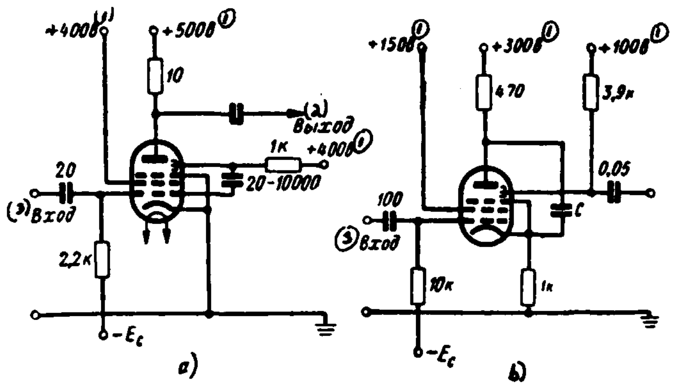

Fig. 5.18. Practical diagrams on tubes with secondary emission: a) with dynode-grid connection/communication; b) with anode-cathode connection/communication.

Key: (1). V. (2). Output. (3). Input.

Page 301.

Oscillator circuit of pulses on tube with secondary emission, which has connection/communication anode - cathode, is investigated into [93]. In the simplified form this relaxation oscillator is depicted in Fig. 1.18b; are there given the values of the entering the diagram elements. Generator was assembled on tube EFP-60.

Work of this generator occurs as follows. In the initial state the tube is closed on control electrode by the source of negative voltage. Trigger pulse of positive polarity with an amplitude of 5 V enters control electrode and is opened/disclosed tube. The absence of the connection of control electrode with the dynode is a difference in this oscillator circuit from preceding/previous. Consequently, to the

input capacitance of tube the output capacitance of dynode is not added. Thereby relaxation oscillator can be started from the pulsed source with high output resistance, than in the preceding case.

When tube is open due to presence of positive feedback, avalanche-like build-up/growth of anode current will be begun. Simultaneously a sharp drop in the anode voltage on the dynode occurs with this in the diagram. Rate of voltage rise on the dynode is determined by the quality of the dynode part of the tube and is of the order of 10' V/s. Output voltage/stress is removed/taken from the dynode and has the same polarity, as the starting voltage/stress. The build-up/growth of anode current, as in the preceding case, it is limited due to the redistribution of the cathode current between the anode and the grid.

Pulse generator on tubes with secondary emission was investigated into [91]. The schematic diagram of this generator is given in Fig. 5.19. Trigger pulses are fed/conducted to the grid of the first tube with the secondary emission, which works as amplifier. The intensive pulses of negative polarity enter the cathode of the second tube, which is strictly feedback oscillator dynode - grid. In initial state both tubes are closed by the bias voltage, introduced into the grid circuit.

Anode of first tube is connected with cathode of the second through capacitance so that when positive trigger pulse enters grid of

first tube, voltage on cathode of second tube will be negative.

Page 302.

In the cathode circuit of the second tube there is diode 1N98, designation/purpose of which is the maintenance of large cathode impedance until trigger pulse transfers tube from the closed state into open. The duration of the pulses, generated by diagram, is regulated by a change in the capacitance of the connection/communication between the dynode and the grid within the limits from 25 ns to 12.5 μs. Output pulse is removed/taken from the anode of the third tube. The pulse amplitude is equal to 17 V, and maximum repetition frequency 10 MHz.

L. S. Bartenev [94] proposed for decreasing time of formation of pulse edge to replace in diagrams by tubes with secondary emission linear coupling capacitor nonlinear (by varicond). Fig. 5.20 shows two oscillator circuits with a dynode-grid (a) and with the anode-cathode (b) connection/communication. The equivalent schematic of these generators is depicted in Fig. 5.21.

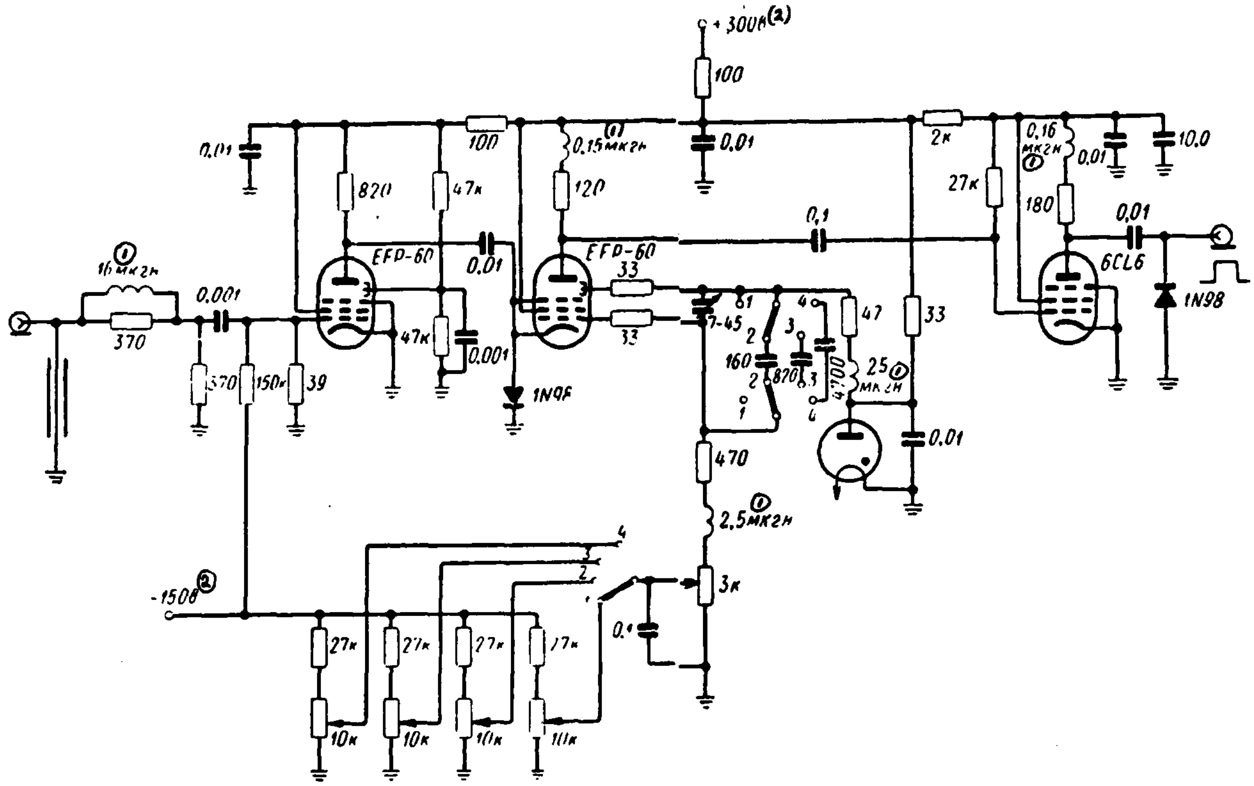

Fig. 5.19. Oscillator circuit of pulses on tubes EFP-60.

Key: (1). μH. (2). V.

Page 303.

On this diagram $R_{н}$ - the load resistance/resistor in the circuit of dynode (or the anode); $R_{с}$ - resistor/resistance of drain circuit, the considering resistor/resistance of section grid - cathode with the positive grid voltages in the diagram (Fig. 5.20a); for the diagram (Fig. 5.20b) $R_{с}$ there is input resistance of cathode circuit; C_{o1} - stray capacitance dynode - the earth/ground (or the anode - the earth/ground); C_{o2} - parasitic grid capacitance - earth/ground; R_{i} - anode resistance in the section dynode - cathode (or the anode -

cathode).

Coupling capacitor $C_{св}$ is delivered in such conditions, with which its capacitance sharply decreases in process of formation of pulse edge.

Page 304.

Because of this the effect of grid circuit on the dynode (Fig. 5.20a) substantially decreases, decreases the current strength, which is branched/shunted into the grid circuit and is accelerated the charge of stray capacitance C_{01}. The steepness of the edge of the pulse of dynode voltage/stress is more than in the diagrams with the constant capacitance of connection/communication. In the process of the formation of the shear/section of pulse capacitance $C_{св}$ increases, which leads to an increase in the duration of the shear/section of pulse. Since average/mean (for the time of the pulse duration) capacitance of nonlinear capacitor is lower than the capacitance capacitor constant (when $C_{пост}=C_{нср}$ with t=0), then the pulse duration in the diagrams with the nonlinear capacitors is obtained somewhat less than in the diagram with capacitor constant of connection/communication.

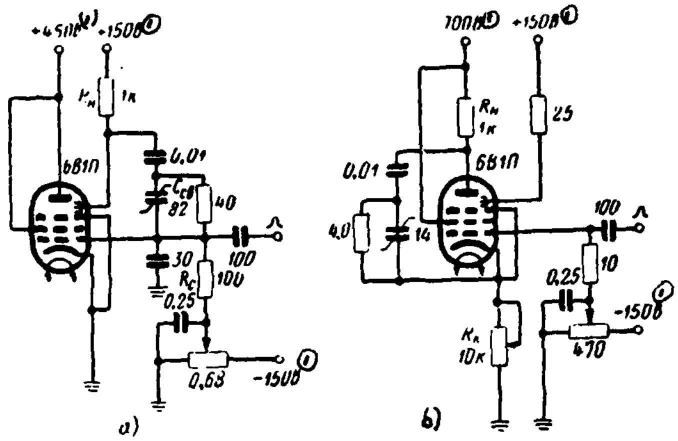

Fig. 5.20. Oscillator circuits with nonlinear capacitance: a) with dynode-grid connection; b) with anode-cathode connection;

Key: (1). V .

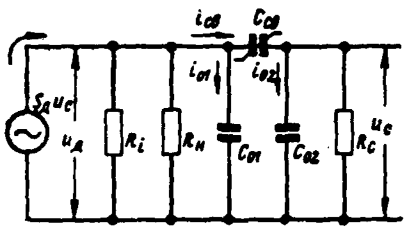

Fig. 5.21. Equivalent oscillator circuit with nonlinear capacitance.

Page 305.

Replacement capacitor constant of connection/communication by variable, without complicating substantially oscillator circuit, gives gain in the steepness of the front of output pulse on 20-25%, which was confirmed by experiment.

5.8. RELAXATION OSCILLATORS OF TYPE OF MULTIVIBRATOR.

By relaxation oscillators of type of multivibrator here are understood usual schematics of multivibrators, reactive/jet start-up circuits, diagrams, which contain supplementary tube, etc. Twin-tube rheostat re-generative amplifier is the basis of these diagrams. Relaxation oscillators of the type of multivibrator in the technology of nanosecond pulses are of interest mainly as the sources of voltage gradients with the steep fronts, which make it possible as a result of the subsequent conversions to obtain the pulses of short duration.

Let us examine processes, which occur in schematic of multivibrator during its switching. The designations, accepted subsequently, they are shown in Fig. 5.22. During the supplying to the grid of the first tube of the multivibrator of a single voltage gradient, the voltage on it will be

$$A_c(t) = 1(t) + \sum_{n=1}^{\infty} K_n(t), \tag{5.18}$$

where $K_n(t)$ - transient response n of the series-connected K-circuits.

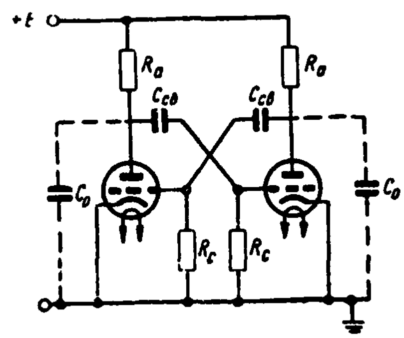

Fig. 5.22. Schematic diagram of multivibrator.

Page 306.

In case in question transient response of K-circuit is transient response of two-stage resistance-coupled amplifier

$$K(t) = K_0^2\left[1 - e^{-t/\tau}\left(1 + \frac{t}{\tau}\right)\right],$$

where $K_0 = SR_a$; $\tau = C_0R_a$.

Realizing (n-1)--fold fold, we will obtain

$$K_n(t) = K_0^{2n}\left[1 + e^{-t/\tau}\sum_{k=1}^{2n-1}\frac{1}{k!}\left(\frac{t}{\tau}\right)^k\right]. \qquad (5.19)$$

Substituting (5.19) in (5.18) and producing addition, we obtain

$$A_c(t) = 1(t) + \frac{K_0^2}{1 - K_0^2}\left[1 - e^{-\frac{t}{\tau}}\left(\operatorname{ch}\frac{K_0}{\tau}t + \frac{1}{K_0}\operatorname{sh}\frac{K_0}{\tau}t\right)\right].$$

With $K_0 \gg 1$ this expression takes form

$$A_c(t) = \operatorname{ch}\nu t.$$

Multivibrator and diagrams with K_0>>1 allied to it relate to relaxation oscillators II.

Calculation of duration of pulse edges, developed by relaxation oscillator II, can be performed in the same order, that also in the case of relaxation oscillator I, only switch time should be designed from formula

$$t_{п} = \frac{1}{\nu} \ln [\, \nu t_0 + \sqrt{1 + (\nu t_0)^2}\,].$$

Let us give example of calculation of duration of pulse edges at input of relaxation oscillator II on tubes 6Zh9P, for which S=18.5 mA/V, C_0=18 pF, so that $\nu=10^9$ Hz. Let us assume

t_0 [нсек] (1)	10^3	10^2	10,
$t_{п}$ [нсек] (1)	7,6	5,2	3,0.

then

Key: (1). ns.

We accept anodic resistor/resistance to equal to 100 ohms (condition of self-excitation in this case it is fulfilled), then $\tau_a = 1{,}8$ ns and auxiliary parameter

$x_{п}$	4,2	2,9	1,7.

Page 307.

To these values $x_п$ corresponds duration of front

$$t_ф\ [нсек]^{(1)} \mid 9{,}0 \mid 7{,}2 \mid 5{,}6.$$

Key: (1). ns.

When $E_a = E_э = 150$ V into current of anode of tube 6Zh9P it is 45 mA. The pulse amplitude on the load in this case there will be 4.5 V, and the steepness of the edges of the pulses

$$S_ф\ [в/сек]^{(1)} \mid 0{,}50 \cdot 10^9 \mid 0{,}62 \cdot 10^9 \mid 0{,}80 \cdot 10^9.$$

Key: (1). V/s.

Is increased load resistance/resistor to 1 kilohms, then $\tau_a = 18$ ns and parameter

$$x_п \mid 0{,}42 \mid 0{,}29 \mid 0{,}17.$$

In this case $t_ф = 2{,}3\tau = 42$ ns independent of $x_п$. The pulse amplitude at the output will be equal to 45 V, and the steepness of their fronts rises to 1.07•10' V/s.

As can be seen from this example, increase in pulse amplitude with increase in load occurs more rapidly than increase of duration of front. This phenomenon occurs only until the time constant of output circuit is low or one value with the switch time of relaxation oscillator. When $x_п$ it becomes less than one, the steepness of the pulse edges at the output in practice reaches its maximum value and

with further increase in the load resistance/resistor it does not grow/rise. With the short switch time the duration of the pulse edges at the output is determined in essence of the time constant of output circuit, namely $t_{\phi} \approx 2{,}3\tau$. However, the steepness of fronts in this case

$$S_{\phi} = 0{,}39\frac{I_{a0}R_{a}}{C_{0}R_{a}} = 0{,}39\frac{I_{a0}}{C_{0}}$$

depends only on the ratio of the anode current of tube (when $E_c=0$) to stray capacitance and it does not depend on the load resistance/resistor.

As it was said above, with short switch time duration of pulse edges is determined in essence of time constant of output circuit. In order to raise the steepness of the pulse edges at the output of schematics of the type of multivibrator, there was proposed [95] to carry out a charge of the output tube through the tube with the secondary emission.

Page 308.

For this purpose in parallel to output tube is connected tube with secondary emission in the manner that this is shown in Fig. 5.23. Dynode L_3 is connected to anode L_2, and the anode - to the power supply. Control grid of tube with secondary emission is grounded, and resistor/resistance is connected to cathode. The cathode of the third tube is connected with the anode of the first tube through the transient capacitance.

Work of this diagram occurs as follows. When the first tube opens, voltage on its anode falls. Negative drop in the voltage from the anode of the first tube falls on the grid of the second tube and cuts off it. Simultaneously the same voltage/stress enters the cathode of the third tube and opens this tube. In the circuit the stray capacitance which shunts the load of the second tube, begins to be charged. This capacitance is charged not only through the resistance/resistor of load R_{a2} from the power supply, but also through the resistor/resistance of section the anode - dynode of the third tube. Since the second resistor/resistance much less R_{a2}, capacitance is charged considerably more rapid than in the schematic of usual multivibrator despite the fact that the value of stray capacitance in the described diagram increases due to the capacitance of dynode.

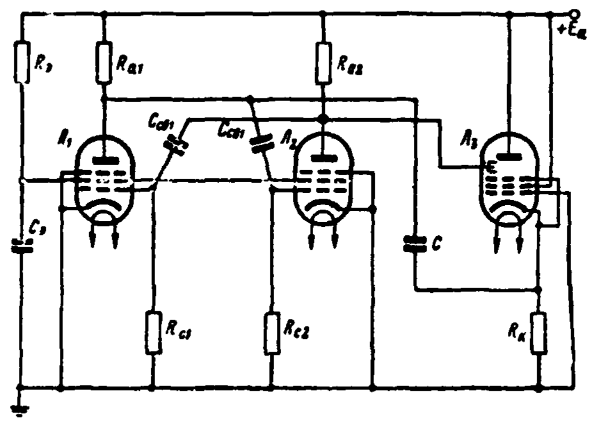

Fig. 5.23. Application of tube with secondary emission in schematic of multivibrator for accelerating charge of stray capacitances.

Page 309.

Since additional path besides path through load resistance/resistor is created for charging capacitance, this resistor/resistance can be made as large as desired without damage for duration of pulse edges. Therefore the schematics of the multivibrators, in which besides usual tubes are used the tubes with the secondary emission, make it possible to obtain pulses high-amplitude.

Triggering/opening of second tube occurs at moment of formation of shear/section of pulses in diagram. Voltage on its anode falls and its negative drop/jump cuts off the first of tube. In turn, the closing of the first tube leads to an increase in the voltage on its anode. A positive drop/jump in the anode voltage enters the cathode of the third tube and cuts off it. Thus, in the process of the

formation of the shear/section of pulse the third tube does not participate. The capacitance, which shunts the load of output (second) tube, is discharged through this tube. The pulse edge in this diagram is steeper/more abrupt than shear/section, since the time constant of the circuit of charge proves to be less than the time constant of discharge circuit.

Results of experimental study of series/row of schematics of multivibrators, which use tubes with secondary emission, are given in [96]. One of the diagrams is depicted in Fig. 5.24.

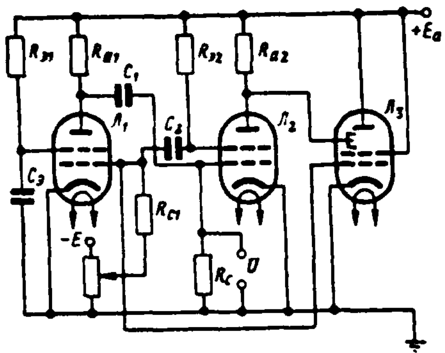

Fig. 5.24. Schematic of multivibrator, which contains tube with secondary emission.

Page 310.

It differs from the diagram, proposed by Craybill in that here the grid of tube with the secondary emission is directly connected to the grid of the first tube. The principle of the operation of diagram remains the same. The load resistance/resistor in the diagram was undertaken equal to 100 kilohms. Diagram worked at frequencies of pulse repetition to 30 kHz. In Table 5.2 are given the results of the experimental investigation of this diagram. Here $F_{ф}$ - time, necessary for the increase of voltage/stress to 1 V (value, inverse of impedance of the pulse edge). Since measuring meter introduced supplementary capacitance into the diagram, then data for $F_{ф.пл}$ were cited taking into account the effect only of the self-capacitance of the diagrams, i.e., data, which would be observed in the presence of ideal measuring meter.

Considerably best results were obtained upon start of tube with

secondary emission according to diagram, shown in Fig. 5.25. In this diagram is achieved/reached the decrease of stray capacitance, which shunts the plate load of output tube, fact that the anode of the second tube on is connected with the grid of the first tube. Thus, stray capacitance proved to be reduced by the value of input capacitance of the first tube. During the use of tubes EFP-60 in this diagram were obtained the results, given in Table 5.3.

Table 5.2.

(1) E_a, в	(1) U, в	(2) $t_ф$, нсек	(3) $F_ф$, $\frac{сек}{в}$ (1)	(3) $F_{ф\ пд}$, $\frac{сек}{в}$ (1)
400	160	175	$11 \cdot 10^{-10}$	$5{,}8 \cdot 10^{-10}$
470	225	147	$6{,}5 \cdot 10^{-10}$	$3{,}4 \cdot 10^{-10}$
540	260	118	$4{,}6 \cdot 10^{-10}$	$2{,}4 \cdot 10^{-10}$
615	330	118	$3{,}5 \cdot 10^{-10}$	$1{,}8 \cdot 10^{-10}$
690	370	118	$3{,}2 \cdot 10^{-10}$	$1{,}65 \cdot 10^{-10}$

Key: (1). ..., V. (2). ..., ns. (3). s.

Table 5.3.

(1) E_a, в	(1) U, в	(2) $t_ф$, нсек	(3) $F_ф$, $\frac{сек}{в}$ (1)	(3) $F_{ф\ пд}$, $\frac{сек}{в}$ (1)
400	250	145	$5{,}8 \cdot 10^{-10}$	$3 \cdot 10^{-10}$
470	340	120	$3{,}5 \cdot 10^{-10}$	$1{,}8 \cdot 10^{-10}$
540	375	86	$2{,}3 \cdot 10^{-10}$	$1{,}2 \cdot 10^{-10}$
615	445	78	$1{,}8 \cdot 10^{-10}$	$0{,}95 \cdot 10^{-10}$

Key: (1). ..., V. (2). ..., ns. (3). s.

Page 311.

Besides diagrams, in which tubes with secondary emission are utilized for accelerating charge of output capacitance, widely are used diagrams, in which such tubes serve for starting/launching of diagrams, assembled on usual tubes, for example for starting/launching of diagrams of multivibrators, blocking oscillators, etc. Application of tubes with the secondary emission for these purposes gives noticeable gain.

Fig. 5.26 and 5.27 give two schematics of multivibrators, investigated into [97]. Multivibrator is assembled on the tubes 6J6,

equivalent 6N15P. As separative element in the first diagram are utilized the batteries, and secondly - gas-filled diodes of the type 5651.

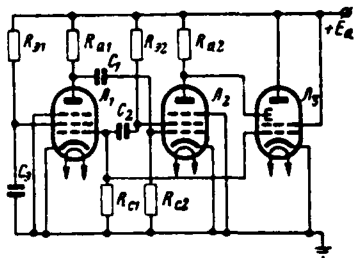

Fig. 5.25. Improved schematic of multivibrator, which contains tube with secondary emission.

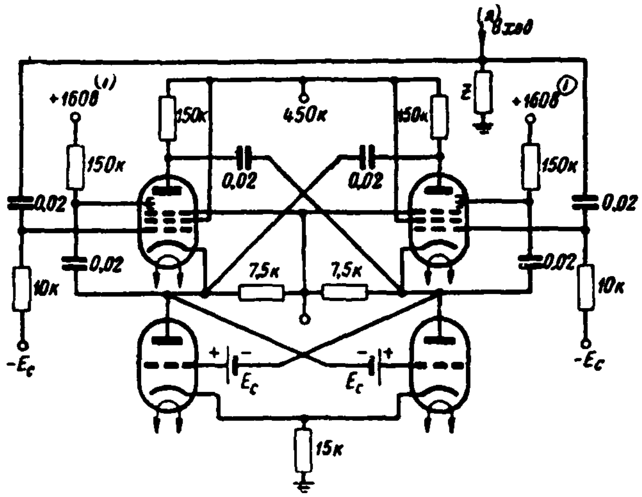

Fig. 5.26. First schematic of multivibrator with starting/launching from generator on tubes with secondary emission.

Key: (1). V. (2). Input.

Page 312.

For the starting/launching of diagram are utilized the tubes with secondary emission EFP-60. The absence of condensers as separative elements makes it possible to substantially reduce the duration of the generatable pulses. Thus, in the first diagram the duration of the generatable pulses is 5 ns, and in second 2 ns. The minimum time, which divides two pulses and characteristic triggering times of diagram, comprises for both diagrams 50 ns; therefore diagrams can work with the high repetition frequencies, which reach to 1 MHz and limited only by dissipated power on the electrodes of tubes. The amplitude of output pulses is obtained about 15 V.

It is indicated in [95], that in diagram, assembled on tube EL-41 and tube with secondary emission EFP-60 it is possible to obtain pulses with steepness of front of 10^{10} V/s. The pulse amplitudes in this case were limited to the permissible value of electrode voltage. In the described diagram with supply voltage of 700 V it is possible to obtain the amplitude of pulses of 400 V.

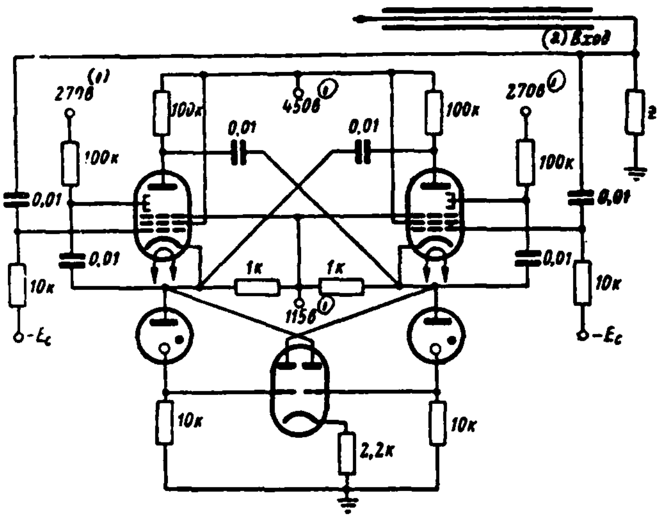

Fig. 5.27. Second schematic of multivibrator with starting/launching from generator on tubes with secondary emission.

Key: (1). V. (2). Input.

Page 313.

Let us conduct calculation of steepness of pulse edges at output of this diagram, assuming that first two tubes in it - 6Zh9P, and third tube - 6V1P. In the pulsed operation the current of the anode 6V1P is 1 a when $E_a=500$ V and $E_n=150$ V, which makes it possible to consider the resistor/resistance of section anode - dynode for the equal to 350 ohms. Stray capacitance, which shunts the load of output tube, is approximately equal to 18 pF. Then switch time at different starting velocities comprises, as this was calculated earlier,

$$t_n \text{ [(1) nsec]} \mid 7,6 \mid 5,2 \mid 3,0.$$

Key: (1). ns.

For τ=350 ohms $\times 18 \cdot 10^{-12}$ f =6.3 ns, the parameter

x_n | 1,2 | 0,83 | 0,48.

Whence duration of front

t_ϕ [(1) нсек] | 18 | 16 | 15.

Key: (1). ns.

Amplitude of output pulses is determined by permissible value of drop/jump in electrode voltage of tubes. Assuming that this drop/jump can be 200 V, we obtain, that the steepness of the pulse edges at the output of diagram will be 10^{10} V/s.

Schematic of multivibrator, which generates pulses of nanosecond duration, is given in [98].

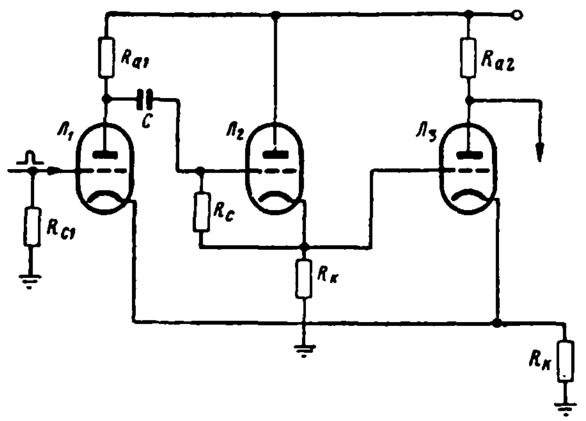

Fig. 5.28. Application of cathode follower in schematic of multivibrator.

Page 314.

With the best fulfillment of diagram and during the use of tubes with the high quality, the multivibrators make it possible to obtain pulses by duration to 100 ns. In order to decrease the pulse duration, it is proposed to supply the cathode follower in the coupling circuit (Fig. 5.28). In this case two advantages are obtained. First, the capacitance which shunts the resistor of the plate load of the first tube decreases, since cathode follower has considerably smaller input capacitance than the second tube of multivibrator, whose load is connected to the anode. In the second place, the grid circuit of the second tube is low-resistance, since leakage resistance of the grid of the second tube in this case is equal to the input resistance of cathode follower. The decrease of resistor/resistance is useful in that sense, that in this case decreases the ill effect of capacitance

C_{ac} of the second tube. The diagram of cathode follower can be improved by the installation of supplementary tube (Fig. 5.29). Anodes of both tubes cophasally are controlled by input voltage. Therefore besides the decrease of capacitance $C_{cк}$ of lower triode, which occurs in the usual diagram of cathode follower, decreases capacitance C_{ac} (also in lower triode), which also facilitates the work of the first tube of multivibrator.

To schematic of multivibrator must be premised forming cascade/stage, which develops trigger pulse. The oscillator circuit of pulses is given in Fig. 5.30. Trigger pulses are supplied to the grid $L_{1,1}$ and are amplified by this tube. Diode in the grid circuit $L_{1,1}$ serves in order to limit the pulse amplitude. In order to remove the effect of the start-up stage on the work of multivibrator, the capacitance of connection/communication must be very small (in the diagram 10 pF).

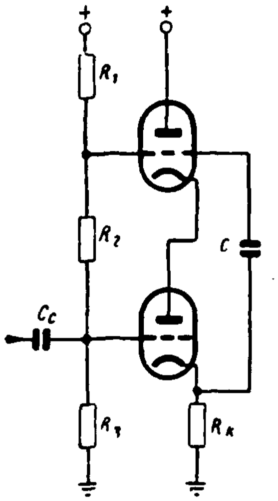

Fig. 5.29. Improved diagram for decoupling of input and output tubes in multivibrator.

Page 315.

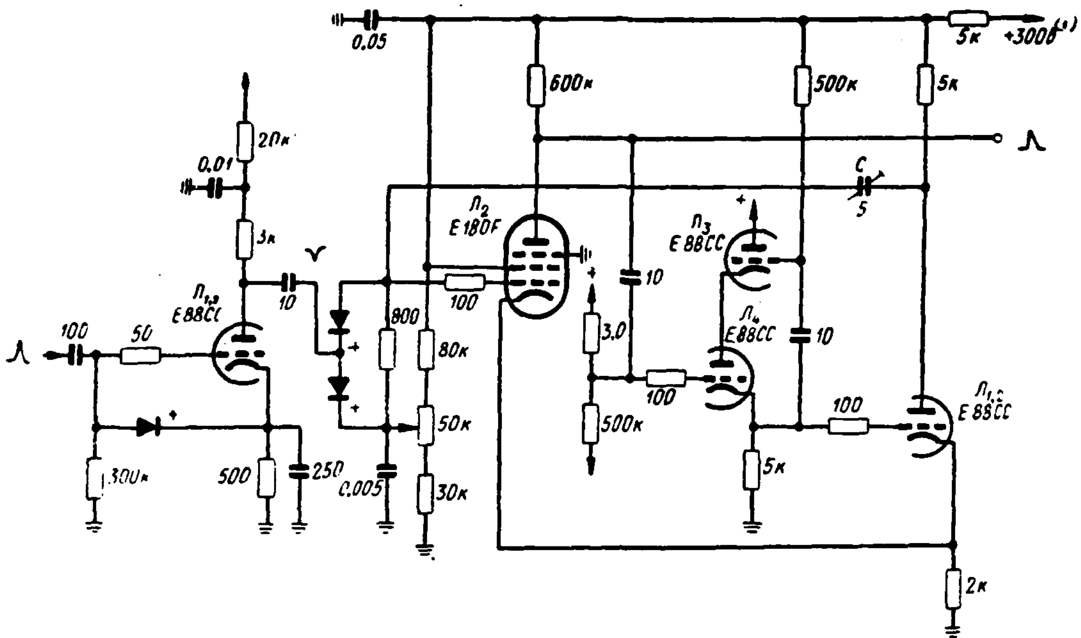

Fig. 5.30. Schematic of multivibrator, which generates nanosecond pulses.

Key: (1). V.

Page 316.

Diodes in the coupling circuit serve in order to have the capability to work by pulses of both polarities, and also for the fastest discharge of capacitance C, which connects the anode of the second tube of multivibrator $L_{1,2}$ with the grid L_2. This capacitance, equal to 5 pF, determines the pulse duration. The pulse, removed from the anode L_2, has bell-shaped form. The diagram, the data of which are cited in Fig. 5.30, generated pulses with a duration of 35 ns at the level of half of amplitude. The pulse amplitude was 9 V. The pulse repetition frequency was equal to 1 MHz, and in the auto-oscillating mode it reached several megahertz.

Page 317.

CHAPTER SIX.

PULSING IN CIRCUITS WITH INDUCTIVE FEEDBACK. RECIRCULATORS.

6.1. Pulsing in diagrams with inductive feedback (blocking oscillators).

Method, based on use of single-tube diagrams with inductive feedback, is one of most known and effective methods of pulsing of nanosecond duration. Such diagrams are called usually blocking oscillators. Blocking oscillators make it possible to obtain in the mode of auto-oscillations pulses with duration into tens of nanoseconds with an amplitude of about 100 V. The special diagrams of the blocking oscillators, in which is utilized consecutive peaking or starting/launching from the tubes with the secondary emission, make it possible to form/shape pulses with duration into the units of nanoseconds.

Process of impulse shaping diagrams with inductive feedback is analogous to process of impulse shaping in single-tube diagrams on tubes with secondary emission. The tube of blocking oscillator works under these conditions, in which at the moment of pulse advancing on its grid appears large positive voltage and in the tube occurs the redistribution of the cathode current between the anode and the grid. Another special feature of blocking oscillator is the presence in it of the transformer, whose parameters also affect the shape of pulses,

the duration of their fronts, etc.

Page 318.

Considerable role here play the processes, which occur in the transformer core: the process of the magnetization of core, phenomenon of eddy currents, etc. All these facts very complicate the analysis of the work of blocking oscillator, especially in the range, the nanosecond pulses, where the duration of pulses themselves is frequently determined by the duration of their front and shear/section.

Let us examine process of impulse shaping in blocking oscillator, whose schematic diagram is depicted in Fig. 6.1.

Description of work of blocking oscillator let us begin from moment of time t_1, when tube opens and voltage on its grid is equal to $E_{зап}$ (Fig. 6.2). At this moment the loop of feedback proves to be locked. Grid voltage of tube begins to increase more rapidly and, when the transmission gain on the closed loop of feedback becomes more than one, the increase of voltage acquires avalanche-like nature. Up to moment of time t_2 the grid voltage of tube attains maximum; it approximately at the same time reaches maximum and the pulse of anode current. For the time of the formation of the pulse edge the grid voltage of the tube of blocking oscillator varies from cutoff voltage to its maximum value.

Increase of grid voltage leads to sharp increase in current of control electrode, which becomes comparable with anode current. Since an increase in the current occurs due to the redistribution of the cathode current between the anode and the grid, the slope/transconductance of anode current and, therefore, the transmission gain along the closed loop of feedback fall and this incidence/drop occurs until in the diagram avalanche-like process is discontinued. Thus, the limitedness of the cathode current of tube blocks the infinite development of avalanche-like process.

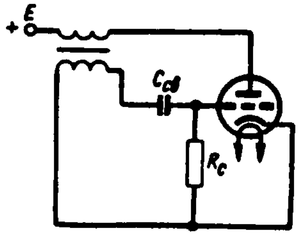

Fig. 6.1. Schematic diagram of blocking oscillator.

Page 319.

In blocking oscillator feedback loop remains locked during entire process of impulse shaping; however, after grid voltage achieved its maximum, parameters of tube so changed that slope/transconductance of plate characteristic proves to be insufficient for onset of avalanche-like process. The process of shaping of pulse apex occurs at this time in the diagram. As soon as grid current in the tube appeared, the charge of capacitance C_{cn} begins. The charge of this capacitance causes the decrease of grid voltage of tube and the displacement of operating point over the grid-plate characteristic. Since mutual conductance of tube in the region of redistributing the currents is small, the grid voltage of tube must change to the sufficiently high value so that the operating point would go down according to the characteristic of tube in the section with the large slope/transconductance, where the transmission factor on the closed loop of feedback again would become more than one. At point in time t_3 concludes the stage of shaping of apex/vertex and reverse avalanche-like process begins.

As a result of close coupling between anode and grid circuits decrease of anode current leads to appearance in grid circuit of emf of mutual induction, which has negative polarity. Anode current begins to decrease with the ever-growing rate and through the small time interval it drops to zero. Tube is closed also at the moment of time t_4 concludes the process of impulse shaping. Subsequently in the diagram occurs the discharge of capacitance C_{cB} through resistor/resistance R_c.

In Fig. 6.2 oscillograms of voltages and currents in blocking oscillator are given.

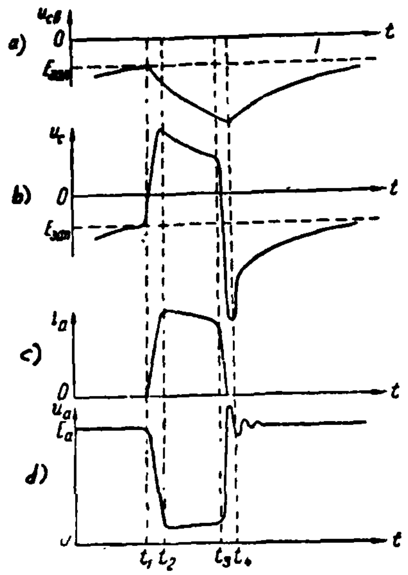

Fig. 6.2. Oscillograms of currents and voltages/stresses in blocking oscillator.

Page 320.

The curve a depicts a change in the voltage/stress on capacitance In the period of impulse shaping the capacitor is charged by the grid current of tube, while during the entire remaining part of the period it is discharged through resistor/resistance $C_{cп}$. The grid voltage of tube, shown curved b, is the algebraic sum of the anode voltage, transformed into the grid circuit, and voltage across capacitor R_c.

Grid voltage of tube, shown curved b, is algebraic sum of anode voltage, transformed into grid circuit, and voltage across capacitor $C_{cп}$. After the passage of the shear/section of pulse of the grid voltage becomes negative due to emf of mutual induction, induced from the anode circuit. Subsequently the grid voltage increases exponentially, trying to achieve the cutoff voltage of tube. The curve c presents the pulse of anode current, and curve d - pulse of anode voltage. The

oscillation of anode voltage after pulse advancing is caused by the collision excitation of parasitic oscillatory circuit.

From point of view of possibility of obtaining very narrow pulses in examination of process of work of blocking oscillator there is greatest interest in question about duration of generatable pulses and duration of their fronts. The duration of the pulses, generated by blocking oscillator, is determined by the time of the charge of capacitance C_{cn}. In the computations of this time, Ya. S. Itskhoki [36] it proceeded from the equivalent diagram of grid circuit, represented in Fig. 6.3. The grid voltage of tube is composed of voltage on the grid winding of transformer, which can be considered constant during the duration of the pulse (when the primary inductance of transformer is sufficiently great), and voltage/stress on capacitance C_{cB}.

Change in grid voltage is equal to force of constancy of voltage/stress on grid winding of transformer and it is opposite on sign to change in voltage across capacitor.

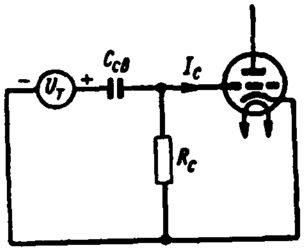

Fig. 6.3. Diagram of input circuit of blocking oscillator.

Page 321.

The grid voltage falls with the charge of capacitance; this decrease occurs until operating point passes in the section of characteristic with the slope/transconductance, sufficient for the onset of avalanche-like process. The less capacitance value $C_{cв}$ and the less the resistor/resistance of charging circuit, the more rapidly will fall the grid voltage of up to the value, which causes the onset of avalanche-like process and the shorter the pulse duration will be. Ya. S. Itskhoki gives the following approximation formula for determining the pulse duration in the blocking oscillator:

$$t_{и} \approx 2C_{cв}\frac{U_{c\,макс}}{I_{c\,макс}},$$

where $U_{c\,макс}$ - maximum grid voltage,

$I_{c\,макс}$ - maximum grid current.

However, as far as duration of edges of pulses generated by blocking oscillator is concerned, Ya. S. Itskhoki proposes to determine it according to formula $t_{ф} \approx 2C_0\frac{U_{c\,макс}}{I_{c\,макс}}$, where C_0 - stray capacitance of

diagram, in reference to grid circuit.

6.2. Duration of the pulse edges in the blocking oscillator.

For answering question about duration of pulse edges, developed by blocking oscillator, in the first approximation, following path can be accepted. We approximate the anodic and grid characteristics of tube in the manner that it is shown in Fig. 6.4. Let us accept further, that the transformer is ideal, i.e., affects neither the form of pulse apex nor the duration of its front. Then the equivalent diagram of the anode circuit of blocking oscillator can be represented in the form, depicted in Fig. 6.5.

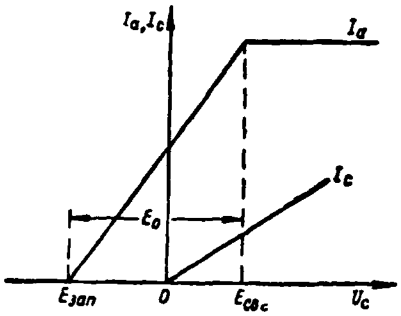

Fig. 6.4. Approximation of characteristics of tube of blocking oscillator.

Page 322.

On this diagram μ and R_i - parameters of tube, C_0 - total stray capacitance, in reference to anode circuit, R - converted into anode circuit resistor/resistance of section grid - cathode of tube.

We will consider that voltage/stress of synchronization is introduced into grid circuit of tube consecutively/serially and that resistor/resistance of source of signals of synchronization is negligibly small. In this case grid voltage of the tube of the blocking oscillator

$$u_c(t) = u_0(t) + u_{o6}(t), \qquad (6.1)$$

where $u_0(t)$ - input voltage;

$u_{o6}(t)$ - voltage/stress of feedback.

Voltage drop across capacitor $C_{cв}$ can be disregarded/neglected in form of short duration of pulse edge. Let us designate the

transformation ratio of the transformer

$$n=\frac{w_a}{w_c},$$

where w_a - number of turns of anodic winding;

w_c - number of turns of grid winding, and let us consider that

$$u_{o6}(t)=-\frac{1}{n}u_a(t).$$

In view of linearity of response of tube

$$u_a(t)=-\int_0^t u_c(t-\xi)\,dA_K(\xi), \qquad (6.2)$$

where $A_K(t)$ - transient response of circuit, depicted in Fig. 6.5.

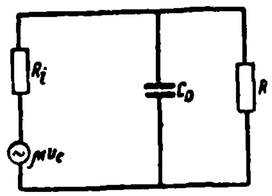

Fig. 6.5. Equivalent diagram of anode circuit of blocking oscillator.

Page 323.

It is easy to be convinced of the fact that

$$A_K(t) = K_0\left(1 - e^{-\frac{t}{\tau}}\right),$$

where

$$K_0 = \frac{\mu R}{R_i + R},$$

$$\tau = C_0 \frac{RR_i}{R + R_i}.$$

Substituting (6.2) in (6.1) on the basis of preceding/previous formula and assuming that $u_0(t)$ has form of unit function, we obtain integral equation of Volterra of 2nd order

$$u_c(t) - \frac{1}{n}\int_0^t u_c(t-\xi)\,dA_K(\xi) = 1(t).$$

Let us represent solution of this equation in the form

$$u_c(t) = A_c(t) = 1(t) + \sum_{k=1}^{\infty} \frac{A_{Kk}(t)}{n^k}, \qquad (6.3)$$

where $A_{Kk}(t)$ - transient response k of series-connected K-circuits:

$$A_{Kk}(t)=K_0^k\left[1-e^{-\frac{t}{\tau}}\sum_{j=0}^{k-1}\frac{1}{j!}\left(\frac{t}{\tau}\right)^j\right]. \quad (6.4)$$

Substituting (6.4) in (6.3) and fulfilling operation of addition, we obtain

$$A_c(t)=1(t)+\frac{K_0 n}{1-K_0 n}\left[1-e^{-\frac{(1-K_0/n)}{\tau}t}\right].$$

If $K_0/n\gg1$, then we obtain simpler expression

$$A_c(t)=e^{\frac{K_0 t}{\tau_n}}=e^{\frac{\nu t}{n}}.$$

Hence it follows that blocking oscillator under condition $K_0/n\gg1$ and in presence of ideal transformer is relaxation oscillator I.

Page 324.

Let us note that value ν/n is a quality of tube in the diagram and in the more demonstrative form can be expressed thus:

$$\frac{\nu}{n}=\frac{S}{nC_0}=\frac{nS}{C_2+n^2C_1}=\frac{S}{C_2}\,\frac{n}{1+n^2\eta},$$

where $\eta=\frac{C_1}{C_2}$; C_1 - capacitance of the anodic winding of transformer together with the output capacitance of tube and the wiring capacitance, and C_2 - capacitance of the grid winding of transformer together with the input capacitance of tube and the wiring capacitance.

Investigating expression for quality of tube to maximum as function of transformation ratio, let us find that its optimum value it will be:

$$n_{\text{опт}}=\frac{1}{\sqrt{\eta}},$$

$$\left.\frac{\nu}{n}\right|_{\text{макс}}=\frac{S}{C_0}\frac{1}{\sqrt{\eta}}.$$

For determining duration of pulse edges in blocking oscillator can be used the same method, as for diagrams on tubes with secondary emission. Since the equations of the transient responses of blocking oscillator and diagram on the tube with the secondary emission are analogous, the switch time of blocking oscillator can be recorded thus:

$$t_{\text{п}}=\frac{n}{\nu}\ln\left(1+\frac{\nu t_0}{n}\right),$$

where t_0 - time, during which the linearly increasing voltage/stress changes to value E_0 (Fig. 6.4).

If we consider (as this it was accepted in the beginning) that transformer of blocking oscillator has negligible leakage inductance, then duration of front of anode voltage can be determined according to formula

$$t_{\text{ф}}=\tau\left(2,3+\ln\frac{e^{x_{\text{п}}}-1}{x_{\text{п}}}\right).$$

where $x_{\text{п}}=t_{\text{п}}/\tau$; τ - time constant of anode circuit.

Page 325.

Time constant τ is equal to product of total stray capacitance, which shunts anode circuit of tube, to output resistance of diagram. Capacitance is composed of the output capacitance of tube and by that converted from the grid circuit into the anodic input capacitance of tube, and also from the capacitance of the windings of transformer. Output resistance of diagram is the parallel connection of anode resistance and converted into the anode circuit of resistor/resistance section grid - cathode of tube.

6.3. Impulse shaping of short duration.

In preceding/previous sections it was assumed that parameters of circuit of blocking oscillator can be divided into "small", that play significant role in process of formation of front and shear/section of pulse (leakage inductance of transformer, stray capacitances), and "large", that have vital importance with shaping of pulse apex (inductance of magnetization of transformer, working capacitance). This separation correctly when blocking oscillator is utilized for the impulse shaping of relatively larger duration, but having steep front and shear/section; the pulses of nanosecond duration they are obtained of them by the subsequent conversion. With the direct impulse shaping of short duration in the blocking oscillators this separation is impossible, since each parameters simultaneously affect both the processes of forming of front and shear/section and the process of forming the apex/vertex. Therefore during the analysis of nanosecond

blocking oscillators it is necessary to proceed from the equivalent diagram, which considers the "low" and "high" parameters.

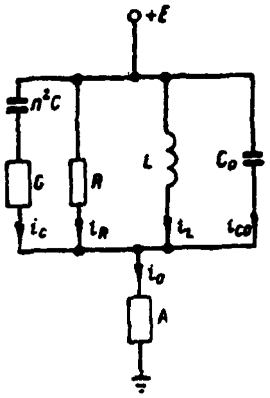

Fig. 6.6. Equivalent diagram of blocking oscillator, which forms pulses of nanosecond duration.

Page 326.

Yu. P. Mel'nikov and S. Ya. Shats [99, 100] conducted research of blocking oscillator in the mode of the impulse shaping of short duration, on the basis of the equivalent diagram, represented in Fig. 6.6. In this figure through A and G are designated the nonlinear two-terminal networks, whose properties are described by dynamic characteristics for anodic A and grid G of the circuits of tube. R indicates the resistance/resistor of the load, connected to the anode circuit of transformer, taking into account the resistor/resistance of core loss of transformer, L is inductance of the magnetization of transformer, $C_0 = C_1 + n^2 C_2$. - total stray capacitance of anode circuit, C_2 - grid circuit; C - working capacitance, $n = \frac{w_r}{w_a}$.

Using dog-leg approximation of dynamic characteristics of tube, authors compile differential equation for interval of time, during which is formed/shaped pulse edge:

$$C_0 \frac{du}{dt} + \frac{1}{L} \int_0^t u\,dt + nC \frac{du_k}{dt} = S_{a1} \left(u - \frac{1}{n} u_k \right) - \frac{u}{R},$$

where $u = \frac{1}{n} u_k + \frac{1}{n} \frac{C u_k}{S_{g1}},$

u_k - voltage/stress on capacitance,

S_{a1} - slope/transconductance of dynamic characteristic of anode current in section of understressed mode $(S_{a1} \approx n S_a$, where S_a - slope/transconductance of static plate characteristic for pulsed operation). S_{g1} has the same value for the grid circuit (Fig. 6.7).

Results of solving this equation during starting/launching of blocking oscillator linearly increasing voltage/stress are on Fig. 6.8, in which along axis of abscissas is plotted logarithm of ratio of voltage/stress u to $T_0 v_0$, where $T_0 = C_0/S_0$, $S_0 = S_{a1} - nS_{c1}$, v_0 - rate of increase of starting voltage/stress. Curves are constructed for the different values of parameters P and Q, where $P = L_\Phi/L$, a $Q = C_0/C$.

Page 327.

Value L_Φ is calculated from the formula

$$L_\Phi = \frac{1}{S_0}\left[\frac{S_0}{\omega_{rp}} + 2C_0 + 2\sqrt{C_0\left(\frac{S_0}{\omega_{rp}} + C_0\right)}\right],$$

where ω_{rp} - the cut-off frequency of ferrite, at which its magnetic permeability falls into $\sqrt{2}$ once in comparison with the permeability at the lower frequencies.

Graphs/curves, given in Fig. 6.8, show that decrease in the velocity of starting/launching, inductance of magnetization with working capacitance leads to decrease in the velocity of build-up/growth of front. The process of the formation of front concludes, when voltage/stress u attains value U_1 (Fig. 6.7).

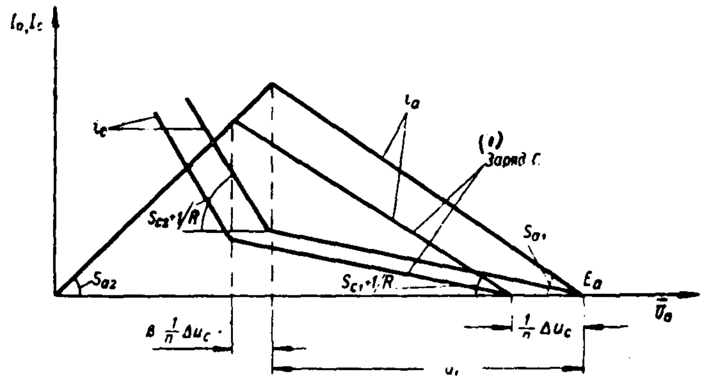

Fig. 6.7. Dynamic characteristics of tube.

Key: (1). Charge

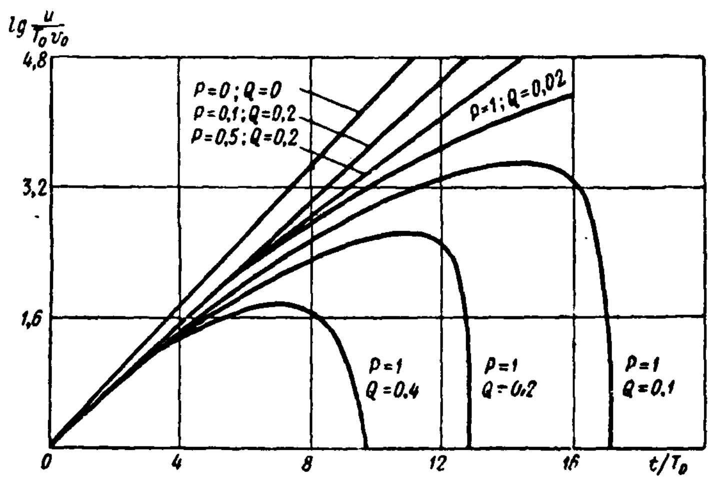

Fig. 6.8. Determination of output potential of blocking-generator.

Page 328.

Results of solving equation for apex/vertex taking into account initial conditions, determined from condition of solving equation for edge of pulse (I_1, $\dot{U}_{к1}$, U_1, where index "1" shows that these values are taken for moment/torque of termination of front), they are given in Fig. 6.9 and 6.10. Fig. 6.9 shows the form of pulse apex, while in

Fig. 6.10 is given the dependence of the duration of apex/vertex from parameter P at the different values of parameter Q.

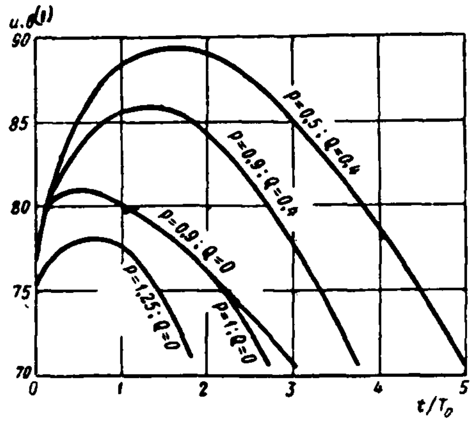

Fig. 6.9. Determination of form of pulse apex.

Key: (1). V.

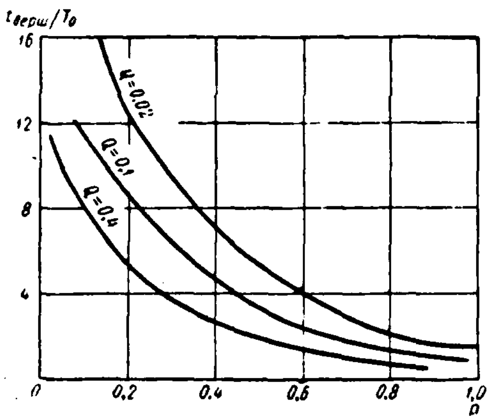

Fig. 6.10. Determination of the duration of pulse apex.

Page 329.

As can be seen from this graph/curve, decrease L and C leads to the decrease of the duration of apex/vertex. Fig. 6.11 shows the dependence of the duration of the shear/section of pulse from P for different Q.

Fig. 6.12 depicts dependence of general/common duration of pulse $t_{и}$ and parameter $\xi = U_{макс}/U_1$ from P and Q. Here $U_{макс}$ - maximum value of pulse, and U_1 - value of pulse up to the moment/torque of the termination of front. Dependence $t_{и}/T_0$ on P and Q in the range of values 0.1<P<1, 0.1<Q<1 is approximated by the expression

$$t_{и}/T_0 \approx 12e^{-2(P+Q)} + 6e^{-0,1P}.$$

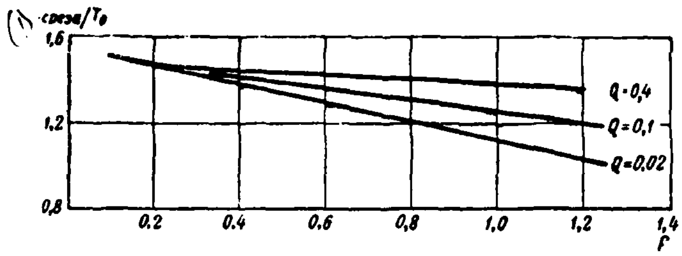

Fig. 6.11. Cetermination of duration of shear/section of pulse.
Key: (1). cross section.

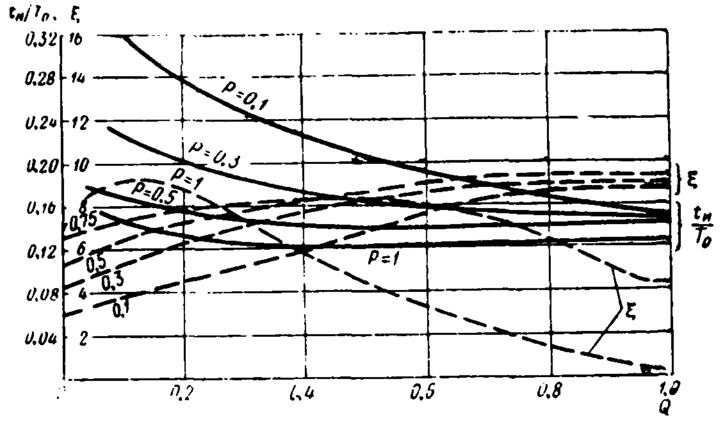

Fig. 6.12. Graph/curve for calculating pulse duration.

Page 330.

6.4. Special features of the work of tube and transformer in the diagram of blocking oscillator.

Tubes in blocking oscillator work in strongly overstressed mode, in which maximum grid voltage can considerably considerably exceed minimum voltage on anode. In connection with this there is a difference in the work of triodes and pentodes in the diagrams of blocking oscillators. Triodes have large power gain in the region of the positive values of grid voltage how pentodes and therefore they make it possible to obtain the surge voltages of larger value.

Increase of positive grid voltage of tube occurs approximately until operating point falls on section of characteristic of anode current with small slope/transconductance, which leads to

cessation/discontinuation of avalanche-like process. For different tubes, in particular for the triodes and the pentodes, the value of grid voltage, with which occurs the end of avalanche-like process, is different. This value is great enough for triodes (it equals tens of volts), whereas for the pentodes it a little differs from zero. Respectively currents in the pulsed operation are determined for the triodes with large positive grid voltage, and for the pentodes - with voltage close to zero. Triodes usually are utilized for these reasons in the diagrams of low-power blocking oscillators.

In blocking oscillators boosting mode of tubes frequently is used. It is necessary to keep in mind that the limit of boosting mode is frequently established/installed not by power capacity of plate dissipation and grid of the tube (with the sufficiently large porosity these values they can be not exceeded), but with the maximum permissible voltage/stress between the anode and the grid. The maximum voltage/stress between the anode and the grid is obtained at the moments of time, which directly follow after the termination of pulses. Voltage on the anode in this case is equal to supply voltage plus the voltage/stress of the overshoots, caused by the excitation of sneak circuits in the anode circuit. The voltage/stress of overshoots can sometimes comprise more than half of supply voltage.

Page 331.

Grid voltage at the same moments of time is equal to the voltage/stress of fixed bias plus the voltage/stress, induced from the

anode circuit due to the phenomenon of mutual induction. As a result a potential difference between the anode and the grid can several times exceed nominal voltage/stress and tube will malfunction.

Maximum pulse repetition frequency is determined by power capacity of scattering on electrodes of tube. However, with an increase in the repetition frequency by several times the scattered power is raised several times (for the constant pulse duration). In connection with this, other conditions being equal, for increasing the pulse repetition rate it is necessary to decrease either their amplitude or their duration. Virtually the blocking oscillators of nanosecond pulses, assembled on the finger triodes, stably generate pulse oscillations to the frequencies of 1 MHz.

Peak transformer is second critical node in diagram of blocking oscillator, it is intended for inversion of stage of pulse and replaces second tube in schematic of multivibrator. Providing maximum connection/communication between the anode and grid circuits in entire range of the generatable frequencies is fundamental requirement for the transformer of blocking oscillator (i.e. in entire frequency band of the pulse spectrum). The undistorted transmission of the pulse edge is possible only in such a case, when the parasitic parameters of transformer will be sufficiently small. However, as far as the requirement of the undistorted transmission of the flat/plane part of the pulse is concerned, it is fulfilled sufficiently easily for the very short pulse duration.

During design of transformers of blocking oscillators, intended for work in nanosecond range, it is necessary to focus attention on two fundamental points. First processes in the magnetic core of transformer are of them. The magnetic core must work at very high rates of change of the induction in the peak transformers, which work in the microsecond range. The second fact concerns the frequency properties of transformer as linear quadrupole. The need for the transmission of very rapid changes in the voltage/stress requires that the transmission factor of transformer would be constant up to the very high frequencies, measured by hundred megahertz.

Page 332.

Transformers of blocking oscillators are fulfilled with cores from ferromagnetic material. The application of a core provides the necessary value of primary inductance with least possible number of turns which in turn, is necessary for decreasing stray capacitance of transformer. The presence of core from the magnetic material indirectly decreases the leakage inductance of transformer. Both these of fact increase its broad-band character.

At the same time processes, which occur in core, significantly influence its properties and, consequently, also work of blocking oscillator. With the feed of the primary winding of transformer by periodic unipolar pulses the process of the magnetization of transformer core, as is known, differs from the process of

magnetization in terms of alternating current. This difference lies in the fact that the operating point in the magnetization curve moves not along the usual loop, but on a certain other curve, called maximum loop of specific cycle.

Magnetic permeability μ_Δ on particular cycle, which plays with work of peak transformers the same role, that also usual permeability μ with work of transformers on alternating current, is considerably less μ_0. In order to obtain high value μ_Δ, it is necessary to utilize for the cores magnetic materials with the high value of saturation induction B_S and small remanent induction B_r, with small relation B_r/B_S. For decreasing the value of remanent induction they sometimes supply magnetic circuit with air gap.

With work of peak transformers with high rates of change in induction eddy currents have vital importance. For decreasing harmful eddy-current effect the cores of peak transformers are manufactured from the very thin tape (0.08-0.02 mm). The decrease of the thickness of the sheets of iron significantly decreases the eddy current losses, since these losses are proportional to the square of thickness of sheet.

Page 333.

Furthermore, for producing the cores of peak transformers are used magnetic materials with the high specific resistor/resistance, which so leads to the decrease of eddy currents.

At present as ferrite rings are utilized as cores for peak transformers of blocking oscillators of nanosecond range. These cores are not inferior on their, to qualities to the cores, made from transformer steel of the highest brands. Table 6.1 gives the information about some types of ferrites [82].

Question about its broad-band character is second question, which appears during design of peak transformer. As has already been spoken, the passband of peak transformer must stretch to hundreds of megahertz. Therefore during the construction of peak transformer it is necessary to take measures to decrease its spurious parameters to the minimum. The very short duration of pulses, favors achieving this goal, in consequence of which the production of transformers with the low value of primary inductance is possible (measured by the units of microhenry). Thus, at the actually allowed values of coefficient of scattering the absolute value of leakage inductance is very small. Furthermore, as has already been indicated, the use of materials with the large magnetic permeability makes it possible to perform primary winding with the small number of turns, which leads to the decrease of stray capacitance of transformer.

Table 6.1

(1) Марка феррита	μ_0	(2) tg δ на 100 Кгц	$B_{макс}$, гс (3)	H_c, э (4)
$Ф_1$-2000	2 000	0,035	3000	0,16
$Ф_1$-1000	1 000	0,011	2 200	0,30
$Ф_2$-1000	1 000	0,032	2 100	0,35
$Ф_1$-600	600	0,009	3 000	0,65
$Ф_2$-600	600	0,032	2 300	0,58
$Ф_1$-400	400	0,008	2 500	1,00
$Ф_2$-400	400	0,008	4 200	0,60
$Ф_3$-400	400	0,027	2 700	0,79
$Ф_1$-100	100	0,004	3 800	2,00

Key: (1). Brand of ferrite (2). tg/δ per 100 kHz (3). ... G (4). ... Oe

Page 334.

Structurally peak transformers are made very simply. Onto the ferrite ring the windings, which for decreasing stray capacitance are made single-layer, are applied. Windings will be deposited or by one to another, the turns of one winding are arranged/located between the turns of another.

Frequently transformers are supplied with third (load) winding. Transformation ratio between the anodic and grid windings is taken by the usually equal to one. However, as far as transformation ratio between the load and grid windings is concerned, its value is determined by the load resistance/resistor.

6.5. Diagrams of blocking oscillators.

Blocking oscillators, utilized for impulse shaping of nanosecond

duration, work, as a rule, with external synchronization due to instability of frequency. In this case the work of blocking oscillators actually consists in the conversion of pulse oscillations with the large amplitude, but relative to low-ts by slope/transconductance, in the oscillations with the large slope/transconductance.

Ye. N. Butorin [3] produced research on the schemes of blocking oscillator on tubes of finger series. The data of diagram are cited in Fig. 6.13.

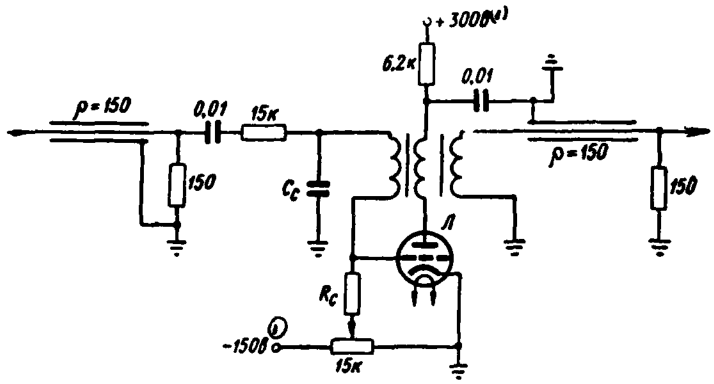

Fig. 6.13. Diagram for investigation of blocking oscillator.
Key: (1). V.

Page 335.

The transformer of blocking oscillator was made on the ferrite ring from the material Φ_1=2000with a diameter of 18 mm and with the number of turns in anodic winding 10, in grid 10 and in load 6. The primary inductance of transformer composed 37 μH, leakage inductance 0.63 μH and stray capacitance 7.2 pF. The described diagram on the tube 6N15P (S=11.2 mA/V, C_0=8 pF) with parallel connection of both of triodes and capacitance $C_{cn}=30$ pF generated pulses by duration 35 ns several with an amplitude of 60 V on the resistor/resistance of 150 ohms. Tube 6N6P (S=12 mA/V, C_0=9 pF) during the use of one triode under the same conditions made it possible to generate pulses by the duration of 35 ns with an amplitude of 125 V. Diagram on the tube 6SZP (S=19.5 mA/V, C_0=10 pF) generated pulses by the duration of 18 ns and by the amplitude of 90 V with $C_{cn}=10$ pF. Diagram on the tube 6S14P (S=45 mA/V, C_0=16.3 pF) with $C_{cn}=22$ pF, generated pulses 14 ns with an

amplitude of 80 V.

In [101] is described oscillator circuit of nanosecond pulses, capable of generating pulses with fixed period of time of 20, 50 and 100 ns with repetition frequency of from 10 kHz to 1.5 MHz. Blocking oscillator was assembled on the tube 6N6P with the transformer, made on the ferrite ring F-400 with an outside diameter of 18 mm. This type of ferrite is selected because it retains its initial permeability without the noticeable increase of losses to frequencies on the order of 5 MHz. Oscillator circuit is shown in Fig. 6.14a. In the load winding of transformer there is a diode for damping undershoot. The pulses, taken from the blocking oscillator, are supplied to the diagram, shown in Fig. 6.14b, the being diagram with the duct/contour of collision excitation. Tube in the initial state is closed with negative grid voltage; the arriving pulse triggers it. The duct/contour of collision excitation is made on the ferrite ring of the type F-400, the number of turns in primary and secondary windings with $t_{u}=20$ ns is equal to 4. For n improvement in the shape of pulse to secondary winding the diode is connected. Amplitude control of output pulse is realized with the aid of the potentiometer of 470 ohms, shunted by the corrective chain/network RC and diode. The amplitude of output voltage/stress is changed in the limits from 0 to 30 V.

Generator of groups of pulses of nanosecond duration, using blocking oscillator, are described into [102].

Page 336.

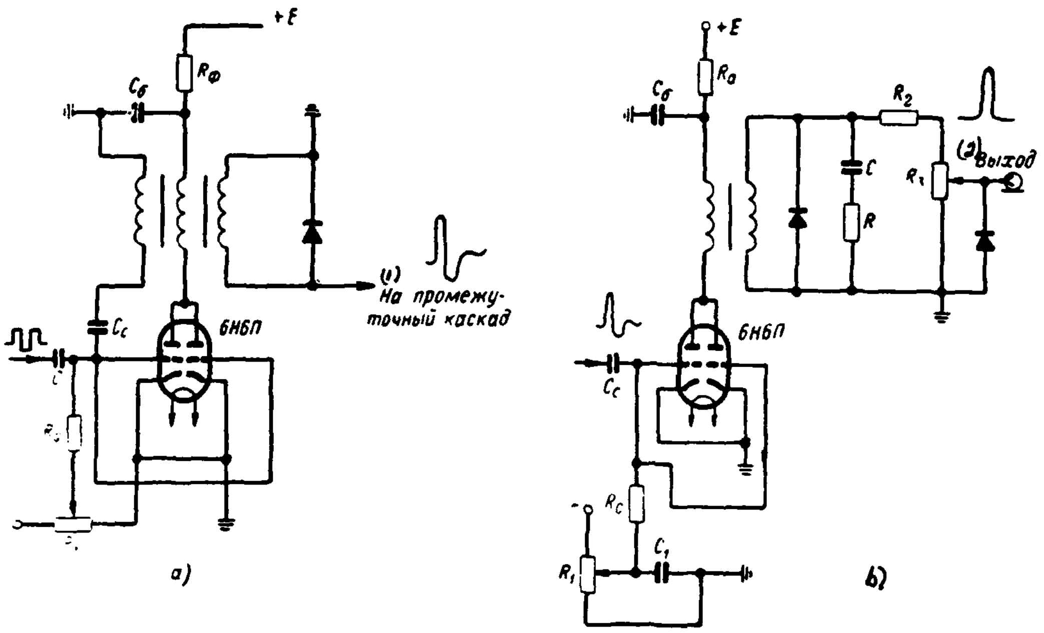

Fig. 6.14. Diagrams of assigning blocking oscillator (a) and output stage (b).

Key: (1). To the intermediate cascade/stage. (2). Output.

Page 337.

The schematic of the part of the generator is given in Fig. 6.15. Trigger pulses enter input of first blocking oscillator, which has duration of pulses 50 ns; pulses from the first blocking oscillator enter the second, which forms pulses with the duration of 20 ns. Finally pulses are formed/shaped in the output stage. Peak transformers are made on ferrite rings with an outside diameter of cores of 14 mm; data of windings Tp1: w_1=8 turns, w_2=4 turns; data of windings Tp2: w_1=6 turns, w_2=6 turns, w_3=3 turns; wire PEShO of 0.2 mm. Was tested the pulse generator, in which at the output was utilized the amplifier-limiter on the tube with the secondary emission, shown in Fig. 6.16.

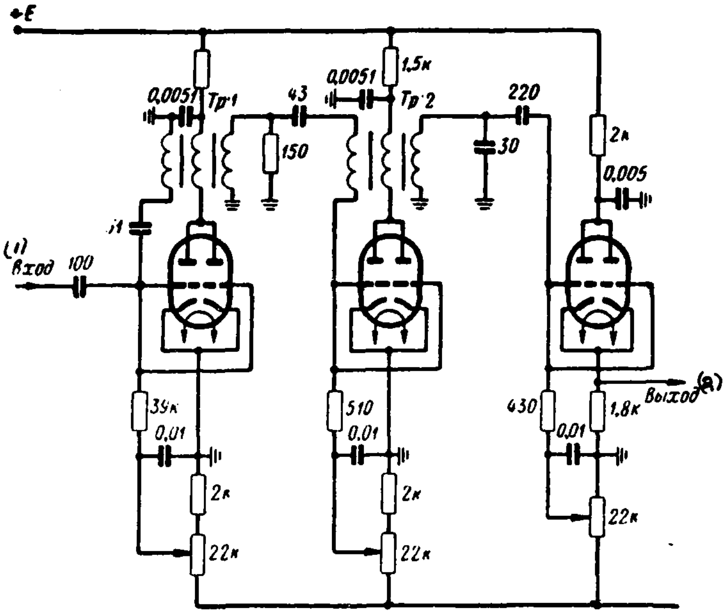

Fig. 6.15. Oscillator circuit of pulses, which uses blocking oscillators.

Key: (1). Input. (2). Output.

Page 338.

Are developed also diagrams of blocking oscillators, which make it possible to obtain durations of pulses of order of tens of nanoseconds with repetition frequencies of 400-500 kHz [103]. Fig. 6.17 gives the diagram of blocking oscillator on tube E182CC. The limitation of reverse/inverse overshoot and damping is conducted by chain/network D, R_5, where D - high-frequency silicon diode, R_5=100 ohm. Cathode follower is made on the same tube, as generator. Interstage connection is attained through the differentiating circuit R_7, C_4. Diodes D_2 and D_3 limit the reverse/inverse overshoot of

output voltage/stress, furthermore, stray capacitance of diode D_2 participates in the formation of the shortened pulse. With the pulse, removed from the blocking oscillator with an amplitude of U=75 V and $t_{и}=75$ ns, from the cathode resistor/resistance of $R_{10}=60$ ohms is removed/taken the pulse with an amplitude of 30 V and the duration on the foundation 45 ns. The steepness of the pulse edges composes 1.2·10' V/s. Data of transformer: $w_{I}=6$ turns, $w_{II}=5$ turns, $w_{III}=13$ turns, L_1=4.3 μH.

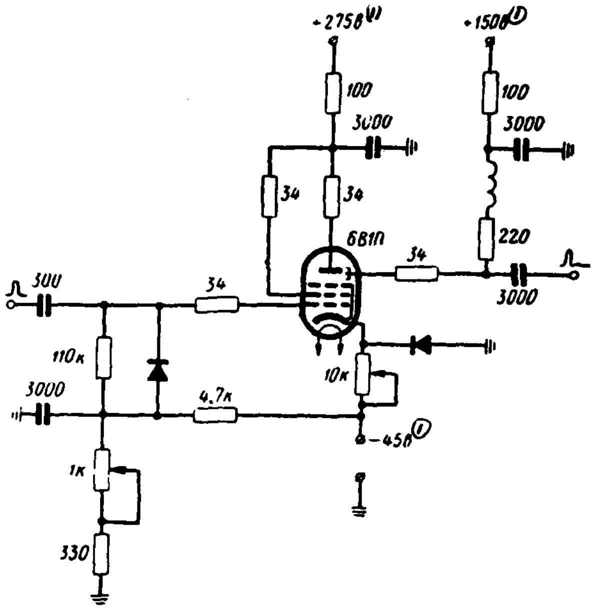

Fig. 6.16. Diagram of output amplifier-limiter.

Key: (1). V.

Page 339.

For obtaining more narrow pulses it is necessary to take measures for increase in steepness of pulse edges by changing trigger conditions. As it was shown earlier, rate of voltage rise on the input of blocking oscillator affects rate of voltage rise on its output. Therefore for obtaining the more narrow pulses the starting/launching of blocking oscillator from other pulse generators with the sufficiently steep fronts widely are utilized. In this case the blocking oscillator works not as self-contained system, and as nonlinear amplifier-limiter with the feedback. The purpose of blocking oscillator is an increase in the steepness of the edge of

subject by it pulse; the pulse amplitude at the output of blocking oscillator can be even less than the pulse amplitude at the input.

During use of blocking oscillators as peakers of pulses it is necessary to consider that each subsequent cascade/stage forms/shapes more narrow pulse.

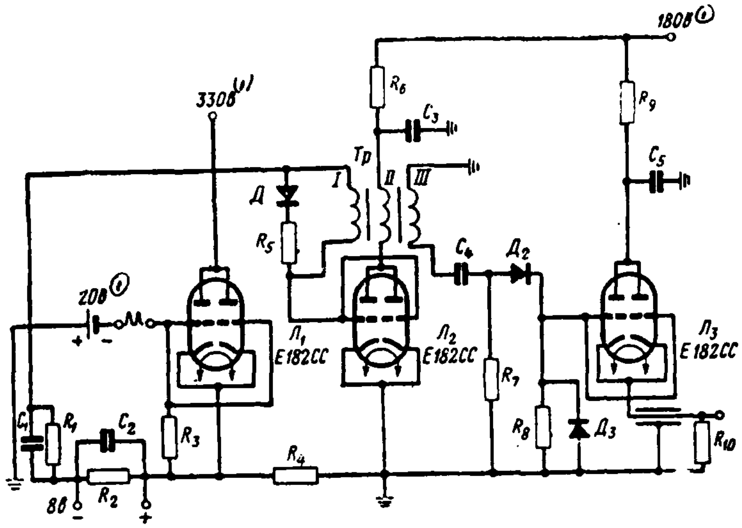

Fig. 6.17. Pulse generator circuit.

Key: (1). V.

Page 340.

Therefore the transient capacitance of each subsequent stage must be less than the transient capacitance of the preceding stages; this makes it possible to utilize the shortenings of the duration of fronts and shear/sections of pulses for further shortening of their duration occurred in the preceding stages. In connection with shortening of the pulse duration grow/rise the requirements also for the broad-band character of transformers. This requirement is comparatively easily satisfied by the decrease of the number of turns and overall dimensions of core. The decrease of the number of turns in the windings of transformers becomes possible because the pulse duration decreases and, therefore, the smaller value of primary inductance is necessary with the allowed value of decay in the apex/vertex.

Question about most advisable method of connecting separate stages into network is one of important questions. The series connection of generators causes greater difficulties than the series connection of amplifiers because between the anode and grid circuits of tube there is a connection/communication. The presence in generators of feedback, furthermore, is opened path to the direct passage of pulse oscillation from the preceding stage to the output of that following, passing/avoiding tube and thereby substantially changing the impulse steepness of output potential. One should in this case consider that the preceding stages can be even more powerful/thicker than following. However, the installation of any decoupling cascades/stages, i.e., through repeaters without the feedback, in the range of the pulses of nanosecond duration, is difficult.

Diagram, given in Fig. 6.18 [87], is most convenient trigger circuit. In this diagram the start-up voltage/stress is supplied through capacitor C_1 directly to the grid of tube following after the source of signal. So that on the capacitor C_1 it would not occur a considerable drop in the voltage of the transmitted oscillation, its value must be not too small.

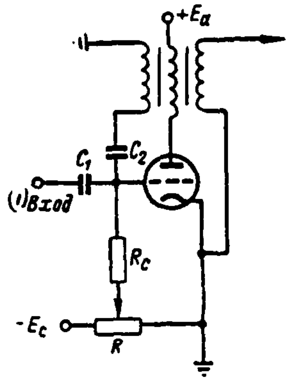

Fig. 6.18. Trigger circuit of blocking oscillator.

Key: (1). input

Page 341.

It cannot be at the same time taken and too great to avoid strong effect generator of the source of starting voltage. Usually capacitor C_1 is taken several times of more than capacitance of C_2.

Ye. N. Butorin [3] produced study of generator of short pulses on tubes 6S3P according to diagram, given in Fig. 6.19.

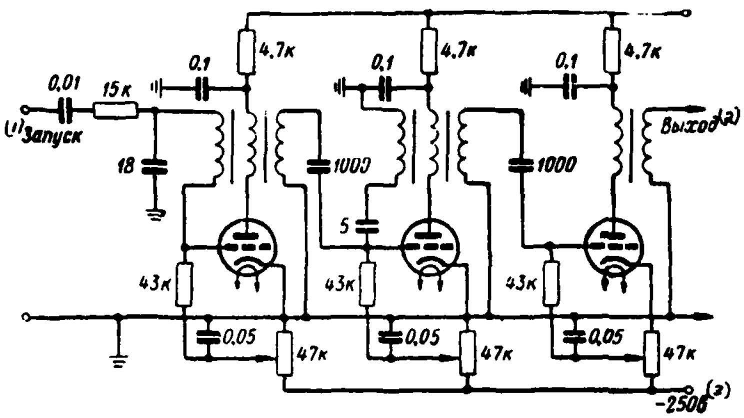

Fig. 6.19. Diagram of cascade blocking oscillator on tubes 6S3P.

Key: (1). Start-up. (2). Output. (3). V.

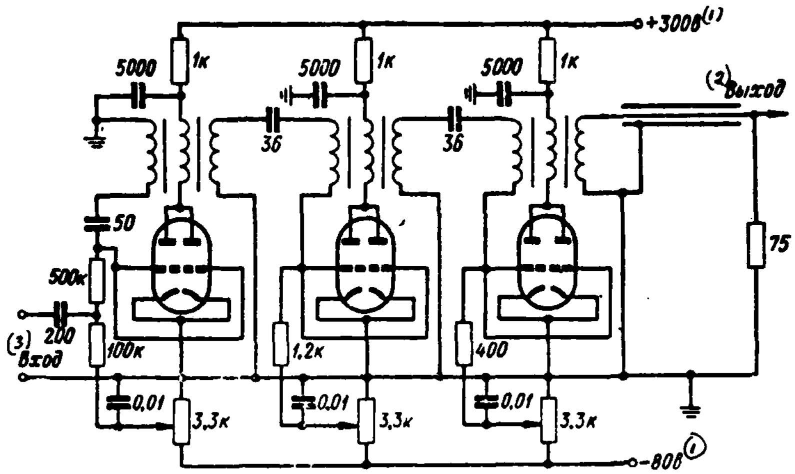

Fig. 6.20. Diagram of stage of blocking oscillator on tubes 6N15P.
Key: (1). V. (2). Output. (3). Input.

Page 342.

In this diagram at the output of the second cascade/stage were formed/shaped the pulses with duration from 5.5 to 8 ns with an amplitude of from 40 to 90 V respectively. At the output of the third cascade/stage the pulses had a duration from 4.5 to 6 ns with an amplitude of from 40 to 85 V. The load resistance was 75 ohms, and the pulse repetition frequency 10 kHz.

Generator of narrow pulses on tubes 6N15P is shown in Fig. 6.20. The triodes are connected in parallel in each tube. Diagram was started from the pulse generator with a frequency of 2 kHz. Transformers were assembled on the miniature cores made of steel of brand 80NKhS, the thickness of belt 0.02 mm.

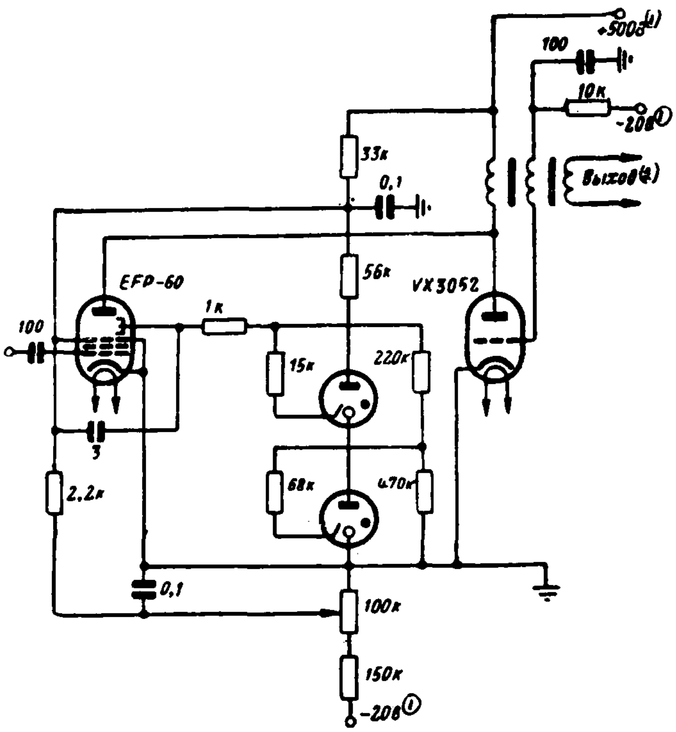

Fig. 6.21. Diagram of blocking oscillator with starting/launching from tube with secondary emission.

Key: (1). V. (2). output.

Page 343.

The transformer of the first cascade/stage contained in the anodic and grid windings with 8 turns, and in the load - 6 turns. The transformer of the second stage had respectively $\omega_a=\omega_c=5$ turns, $\omega_n=3$ turns, the transformer of third stage $\omega_a=\omega_c=3$ turns, $\omega_n=2$ turns. Diagram generated pulses with the duration of 6 ns with an amplitude of 100 V on the load of 75 ohms.

Blocking oscillator of nanosecond pulses on tube VX3052, started by pulse generator on tube with secondary emission, is described into [104]. Oscillator circuit is given in Fig. 6.21. Transformer had toroidal core. Wound from strip. As the magnetic material was utilized mu-metal (thickness of strip 0.0006"). The number of turns in the windings of transformer was varied from 2 to 10 with the transformation ratio n=1. Diagram made it possible to generate pulses from 20 to 100 ns with an amplitude of up to 200 V.

6.6. Pulse generators with delayed feedback.

In preceding/previous chapter, dedicated to analysis of RC-generators with feedback, it was shown that action of positive feedback in nanosecond range of pulse durations little is effective in comparison with its action microsecond range. Therefore in a number of cases the last stages of pulse generators are fulfilled not as relaxation oscillators, but as amplifier-limiters. At the same time for increasing the steepness of the pulse edges the series connection of amplifier-limiters is utilized. It is obvious that taking a sufficient quantity of series-connected amplifier-limiters, it is possible to obtain the same result, that in the chain/network of relaxation oscillators, without resorting in this case to the use of an avalanche-like process. It is easy to see also that there is no need to physically fulfill the chain/network of amplifier-limiters; the same result of repeated nonlinear conversion can be achieved/reached, also, with the consecutive transmission of the

converted pulse through one and the same amplifier-limiter, closing it into the loop of delayed feedback; time lag is here necessary in order to divide the pulses, which completed different number of passages through the nonlinear element, between themselves.

Page 344.

The pulse generator with delayed feedback, called otherwise recirculator, is constructed according to this principle.

Generator with delayed feedback differs from other feedback oscillators in terms of fact that instead of wide-band linear quadrupole for target of feedback (rheostat-capacitance circuit or transformer) it contains delay line.

That that feedback loop in such generators possesses large delay, it is in principle important. The presence of delay excludes the possibility of the development of avalanche-like processes in the recirculators. In contrast to the relaxation oscillators, in which the steep pulse edges are obtained due to the avalanche-like build-up/growth of current in the tube, in the recirculator the steep pulse edges are obtained due to the repeated nonlinear conversion of pulses. By the target of positive feedback in the recirculator is not the creation of conditions for the development of avalanche-like process, but providing repeated conversion of pulse nonlinear element - amplifier-limiter.

In order to clarify difference between relaxation oscillators and recirculators, let us turn to block diagram, shown in Fig. 6.22 and which differs from diagram, given in Fig. 5.1, by presence of delay line into feedback loop. With $t_з$=0 this diagram will be relaxation oscillator, while with sufficiently large $t_з$ - recirculator. Voltage on the input of K-circuit according to Fig. 6.22

$$u_{вх}(t) = u_0(t) + u(t - t_з). \qquad (6.5)$$

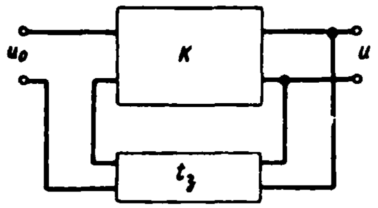

Fig. 6.22. Block diagram of recirculator.

Page 345.

In turn, as it was shown earlier in fifth chapter,

$$u(t)=\int_0^t u_{вх}(t-\xi)\,dK(\xi), \tag{6.6}$$

where K(t) - transient response of K-circuit.

Substituting (6.6) in (6.5), we obtain integral equation of Volterra of 2nd order with delaying nucleus:

$$u_{вх}(t)-\int_0^{t-t_з} u_{вх}(t-t_з-\xi)\,dK(\xi)=u_0(t),$$

solution of which takes form

$$u_{вх}(t)=\sum_{n=1}^{\infty} u_{n-1}[t-(n-1)t_з], \tag{6.7}$$

where $u_{n-1}(t)$ is oscillation, which completed n-1 passage on K-circuit.

As it follows from formula (6.7), with $t_з$=0 voltage on input of K-circuit is sum of infinite number of components, each of which begins at moment of time t=0. This fact generates the very rapid, avalanche-like increase of voltage on the input of K-circuit at the initial moments of time, characteristic for the recirculator. With

$t_3 \neq 0$ all components, from which stores/adds up input oscillation, are shifted on the time. If the converted oscillation $u_0(t)$ has short duration, then voltage on the input of K-circuit of recirculator will represent the sequence of pulses, which is the result one-, two-, triple and so forth of the conversion of input pulse by K-circuit. Thus, the mechanism of the work of recirculator and relaxation oscillator is entirely various.

6.7. Analysis of the work of recirculator.

Pulse generator of recirculator type can be represented in the form of functional diagram, shown in Fig. 6.23.

Page 346.

This diagram differs from that given by preceding/previous figure in that into it special element, which considers nonlinear properties of tube of amplifier is introduced (or special tube, worker in nonlinear section of characteristic and called expander).

Nonlinear element is characterized by fact that voltage/stress on its output is connected with voltage on input with nonlinear dependence

$$u_1(t) = \Phi[u_{\text{вх}}(t)].$$

Repeating the same operations, that also for linearized system, let us arrive at equation, comprised relative to voltage on input of nonlinear element of recirculator:

$$u_{вх}(t) - \int_0^s \Psi[u_{вх}(t - t_з - \xi)\, dK(\xi) = u_0(t).$$

Here K(t) - transient response of amplifier.

Given equation is nonlinear integral equation. For the brevity let us record it in the operational form

$$u_{вх}(t) - Au_{вх}(t) = u_0(t),$$

where A - certain nonlinear operator.

Nonlinear operational equation can be solved by method of consecutive integration. Let us break entire time interval into segments $[(n-1)t_3,\ nt_3]$, n=1, 2, 3, ...

Page 347.

Then in the first interval of time $[0,\ t_3]$ the solution of integral equation will take the form

$$u_{вх}(t) = u_0(t) = A_0 u_0(t),$$

in the second section/segment $[t_3,\ 2t_3]$

$$u_{вх}(t) = Au_0(t) = A_1 u_0(t),$$

in the third section/segment $[2t_3,\ 3t_3]$

$$u_{вх}(t) = AAu_0(t) = A_2 u_0(t) \text{ (1) и т. д.}$$

Key: (1). and i.e.

Imposing for function $u_{вх}(t)$ requirement of equality to zero beyond interval of time $[(n-1)t_3,\ nt_3]$, we obtain solution of operational equation in the form

$$u_{вх}(t) = \sum_{n=1}^{\infty} A_{n-1} u_0(t),$$

where the subscript in operator indicates, what number of times is taken this operator.

If in latter/last expression operation of temporary displacement is recorded explicitly, then

$$u_{вх}(t) = \sum_{n=1}^{\infty} A'_{n-1} u_0[t-(n-1)t_з], \qquad (6.8)$$

where A' - operator, who differs from A in that in it is omitted the operation of temporary displacement.

Expression (6.8) describes transient mode in diagram of a recirculator, consecutively/serially presenting stage of conversion of pulse $u_0(t)$, $A'_1u_0(t)$, $A'_2u_0(t)$ and so forth. In steady state (if such there is a voltage on the input (and at the output) of the recirculator is a periodic pulse train. With sufficiently large n

$$A'_{n-1} u_0(t) = A'_n u_0(t) = u^*(t),$$

where $u^*(t)$ describes the shape of pulse in steady state.

Value $u^*(t)$ is solution of operational equation

$$u(t) - Au(t) = 0$$

or, in expanded/scanned form, nonlinear ineteral equation

$$u(t) - \int_0^{t-t_з} \Phi[u(t-t_з-\xi)]\, dK(\xi) = 0. \qquad (6.9)$$

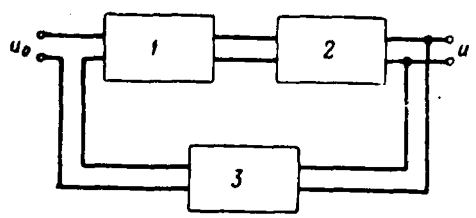

Fig. 6.23. Functional diagram of recirculator; 1-nonlinear element; 2-filter; 3-delay line.

Page 348.

Recirculator With Ideal Limiter.

Solution of nonlinear integral equations, given above, in general case very complicatedly, and therefore for determining form of oscillations/vibrations at output of recirculator one resorts to those or other idealizations. It is possible, for example, to proceed from the fact that the switch time of recirculator in steady state is negligibly small. In this case the nature of nonlinear element can be acquired in the form of the step function, shown in Fig. 6.24. Nonlinear element with this characteristic is called ideal limiter. Its special feature is the fact that when a pulse of any form is supplied to the input of the limiter, a pulse of perfectly rectangular form is obtained at the output. This substantially facilitates the determination of the distortions of those undergone with pulse in transit through the amplifier and filter.

For describing processes, which occur in diagram with ideal limiter, it is convenient to use graph/curve, given in Fig. 6.25. Let us assume that at the input of nonlinear element at a certain moment of time t_0 arrived pulse u'_2 (Fig. 6.25a). According to the characteristic of nonlinear element the voltage/stress on its output will be equal to zero until voltage on the input achieves value Δ. At this moment output potential of nonlinear element abruptly rises to the value, to conditionally equal unit (Fig. 6.25b). Voltage/stress

u', will remain equal to this value until the level of input voltage is lowered to value Δ. Then output potential of limiter falls to zero.

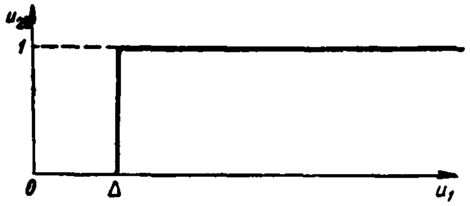

Fig. 6.24. Characteristic of ideal limiter.

Page 349.

After traversing the filter, square pulse will be distorted, as shown in Fig. 6.25c, while after traversing the delay line, it will be shifted along the time axis to the right value t_3 (Fig. 6.25d).

Since adder and amplifier rely by ideal, i.e., contributing none distortion, then after time $t_3+\theta$ pulse u''_2 again will appear at input of limiter. T_3 here indicates the delay of oscillation/vibration in the delay line, and θ - delay of functioning limiter, caused by the fact that the voltage on the input of limiter spends a certain time in order to achieve the level of limitation Δ. Since the amplifier gain $K_0>1$, then the amplitude of pulse u''_2 has large value, than the pulse amplitude at the output of delay line.

At output of limiter again appears square pulse of single amplitude, whose duration is determined by difference in moments of time $t''_{\text{к}}$ and $t''_{\text{н}}$, during which input signal passes through level Δ.

Let us designate through K(t) transient response of amplifier,

and through $t_{\text{н}}^{n}$ and $t_{\text{к}}^{n}$ - moments of time, which correspond to beginning and end/lead of n pulse at output of limiter [1], then

$$K\left(t_{\text{н}}^{n}-t_{\text{н}}^{n-1}-t_{\text{з}}\right)=K(\theta)=\Delta.$$

FOOTNOTE [1]. The following analysis of the work of recirculator is borrowed from the article of Yu. I. Neymark, Yu. K. Maklakov and L. P. Yelkins [105]. ENDFOOTNOTE.

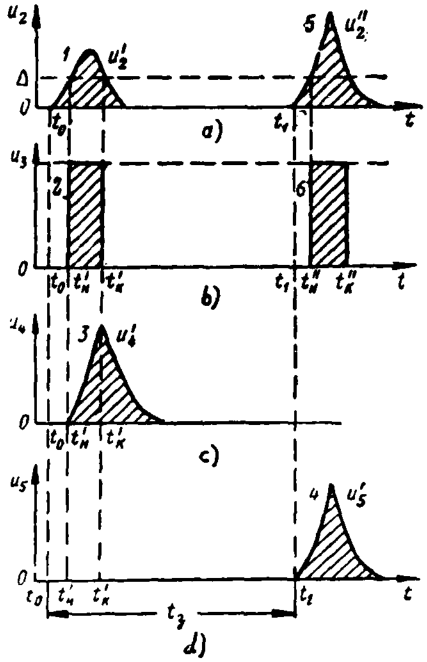

Fig. 6.25. Performance record of recirculator.

Page 350.

Here $t_{\text{и}}^{n} - t_{\text{и}}^{n-1}$ indicates difference between moments of time, at which pass fronts of the n-th and (n- 1)-th pulses θ - mentioned above effective time lag of n pulse with respect to (n-1)-th pulse, caused by combined action of filter and nonlinear element.

Further it is possible to write that

$$K(t_{\text{к}}^{n} - t_{\text{к}}^{n-1} - t_3) = K(t_{\text{и}}^{n} - t_{\text{и}\,n-1}^{n-1} - t_3) = \Delta$$

or

$$K(t_{\text{и}}^{n} + \theta) - K(t_{\text{и}}^{n} - t_{\text{и}}^{n-1} + \theta) = \Delta, \qquad (6.10)$$

where $t_{\text{и}}^{n}$ - duration of n pulse.

Latter/last relationship/ratio can be recorded in the form

$$t_{\text{и}}^{n} = \psi(t_{\text{и}}^{n-1}), \qquad (6.11)$$

expressing dependence of duration of n pulse from duration of (n-1)-th pulse. If the duration of initial pulse $t_{\text{и}}^{0}$ is assigned, then by equation (6.10) will be determined the series/row of the durations of pulses $t_{\text{и}}^{1}, t_{\text{и}}^{2}, t_{\text{и}}^{3} \ldots$ In steady state, i.e., when $n \to \infty$, $t_{\text{и}}^{n-1} = t_{\text{и}}^{n}$, equation (6.11) takes the form

$$t^{*}_{\text{и}} = \psi(t^{*}_{\text{и}}). \qquad (6.12)$$

This solution is stable, if

$$|\psi'(t^{*}_{\text{и}})| < 1.$$

In case in question equation (6.12) can be recorded in the form

$$K(\theta + t^{*}_{\text{и}}) = 2\Delta \qquad (6.13)$$

[we assume/set in formula (6.10) $t_{\text{и}}^{n} = t_{\text{и}}^{n-1}$, $t_{\text{и}}^{n} = t^{*}_{\text{и}}$].

Page 351.

Equation (6.13) physically means that circulation of pulses in system is possible only when maximum value of pulse at input of linear element is twice more than as threshold of functioning limiter. Stability condition for the case takes the form

$$H(\theta + t^{*}_{\text{и}}) < 0, \qquad (6.14)$$

where H(t) - the pulse transient function of filter.

It can satisfy equation (6.13) series/row of durations of pulses $t_{n1}, t_{n2}, t_{n3}, \ldots$ Stable of them will be only those, for which is fulfilled requirement (6.14). Obviously, so that in the system could exist the pulses at least of one duration the transient response of filter it must not be the monotonically increasing function.

Calculation of recirculator with the ideal limiter.

Calculation of recirculator in steady state can be performed on the basis of assumption about the fact that tube is ideal limiter. Let us give the order of calculation of recirculator on the assumption that it is carried out on the base of single-stage resistance-coupled amplifier. The transient response of the amplifier for the region of short times takes the form

$$K(t) = K_0 (1 - e^{-t/\tau_a}), \qquad (6.15)$$

where τ_a - time constant of anode circuit.

For region of long times

$$K(t) = K_0 e^{-t/\tau_{cn}}, \qquad (6.16)$$

where τ_{cn} - time constant of transient circuit.

Calculation of recirculator can be performed in following order. On the basis of the formula

$$K(\theta)=\Delta, \quad (6.17)$$

we determine the effective time lag of pulse in transit through the filter and nonlinear element.

Page 352.

Since the time lag of pulses is caused by the limitedness of the filter pass band in the region of higher frequencies, then into formula (6.17) it is necessary to substitute value of K(t), determined by expression (6.13),

$$K_0(1-e^{-\theta/\tau_a})=\Delta,$$

whence

$$\theta=-\tau_a \ln\left(1-\frac{\Delta}{K_0}\right).$$

Effective time lag of pulses is determined by time constant of anode circuit and depends on ratio of threshold of functioning limiter Δ to factor of amplification K_0. The greater K_0, the less the effective time lag; with $K_0 \to \infty$ effective time lag is equal to zero. Pulse repetition period

$$T=t_s+\theta.$$

For determining pulse duration we will use formula

$$K(\theta+t_u)=2\Delta,$$

into which should be substituted expression (6.16), since pulse

duration is determined by time constant of circuit, which causes limitation of passband in region of lower frequencies:

$$K_0 e^{-\frac{t_и+\theta}{\tau_{сп}}} = 2\Delta,$$

whence

$$t_и = -\tau_{сп} \ln \frac{2\Delta}{K_0} - \theta$$

or

$$t_и = -\tau_{сп} \ln \frac{2\Delta}{K_0} + \tau_н \ln \left(1 - \frac{\Delta}{K_0}\right).$$

At output of nonlinear element pulse has ideal rectangular form. At the output of the filter

$$u(t) = K(t) \overset{(1)}{\text{при}}\ 0 < t < t_и,$$
$$u(t) = K(t) - K(t - t_и) \overset{(1)}{\text{при}}\ t > t_и.$$

Key: (1). with.

In these formulas it is necessary to substitute complete expression for transient response

$$K(t) = K_0 (e^{-t/\tau_{сп}} - e^{-t/\tau_н}).$$

Page 353.

Refinement of the form of the frontal part of the pulse.

Since pulse at output of ideal limiter has rectangular form, then

after passage through amplifier frontal part of pulse will be described by transient response of amplifier for region of short times. The time of the establishment of pulse in this case will comprise $2{,}3\tau_{a}$ (speech it goes about the resistance-coupled amplifier). Since for the circuits of nanosecond pulse technique there is greatest interest precisely in a question about the duration of the pulse edges, then it is desirable to conduct the refinement of the form of the frontal part of the pulse in order to consider the effect on it of the real properties of nonlinear element.

Let us assume that characteristic of nonlinear element takes form, depicted in Fig. 6.26. The dependence between $u_1(t)$ and $u_{\text{вх}}(t)$ in this case is described by the equation

$$u_1(t)=[u_{\text{вх}}(t)]^{\gamma},\quad \gamma<1.$$

As can be seen from Fig. 6.26, when $u_{\text{вх}}<1$ value $u_1>u_{\text{вх}}$ and nonlinear element amplifies oscillation/vibration, and when $u_{\text{вх}}>1$ value $u_1<u_{\text{вх}}$ and nonlinear element attenuates oscillation. This means that in hunting system with this characteristic of nonlinear element the steady-state oscillations can be established/installed. Let us note that with γ=1 the characteristic of nonlinear element coincides with the bisector of right angle, and with γ=0 accepts the form of unit function. Thus, with the change γ from 1 to 0 nonlinear element passes from the circuit with the linear characteristic to the ideal limiter.

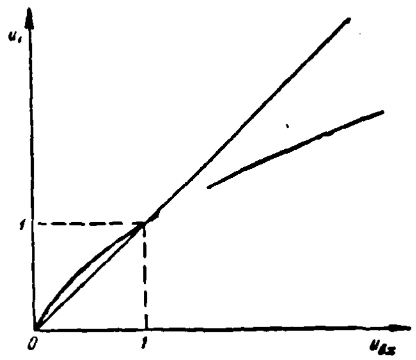

Fig. 6.26. Characteristic of nonlinear element.

Page 354.

Thus, let us assume that characteristic of nonlinear element is described by exponential function, and transient response of amplifier for region of short times it takes form (6.15). Substituting these expressions into nonlinear integral equation (6.8), we will have

$$u(x) - \int_0^{x-x_3} [u(x - x_3 - \xi)]^\gamma e^{-\xi} d\xi = 0, \qquad (6.18)$$

where $x = t/\tau_a$, $x_3 = t_3/\tau_a$.

For determining form of frontal part of pulse there is no need for considering temporary displacement between pulses; therefore it is possible to write

$$u(x) - \int_0^x u^\gamma (x - \xi) e^{-\xi} d\xi = 0. \qquad (6.19)$$

We differentiate this equation for x:

$$u'(x) + \int_0^x u^\gamma (x - \xi) e^{-\xi} d\xi - [u^\gamma (x) - e^{-x} u^\gamma (0)] = 0$$

or

$$u'(x)+u(x)=u^{\gamma}(x), \qquad (6.20)$$

since $u^{\gamma}(0)=0$, and the integral, which stands in the next-to-last expression, is equal to u(x) on the basis (6.19).

Equation (6.20) is nonlinear Bernoulli differential equation, which easily is reduced to linear. Let us divide right and left of the part of the equation on $u^{\gamma}(x)$:

$$u^{-\gamma}(x)u'(x)+u^{1-\gamma}(x)=1.$$

Let us designate

$$u^{1-\gamma}(x)=Z(x),$$

then

$$(1-\gamma)u^{-\gamma}(x)u'(x)=Z'(x).$$

Multiplying by $(1-\gamma)$ and making substitution, we come to linear differential equation

$$Z'(x)+(1-\gamma)Z(x)=1-\gamma.$$

Page 355.

Solving this equation and returning with initial variable u(x), we obtain

$$u(x) = [1 - e^{-(1-\gamma)x}]^{\frac{1}{1-\gamma}}. \qquad (6.21)$$

This is refined formula, which describes frontal part of pulse. In the diagram with the ideal limiter γ=0 and $u(x) = 1 - e^{-x}$, the frontal part of the pulse takes the same form, as the transient response of amplifier. With the percentage distortion γ, different from zero, occurs, in the first place, as if increase in the time constant τ_a

$$\tau_{a\,oe} = \frac{\tau_a}{1-\gamma},$$

in the second place, the form of the frontal part of the pulse changes; it is described no longer by exponential, but more complex function.

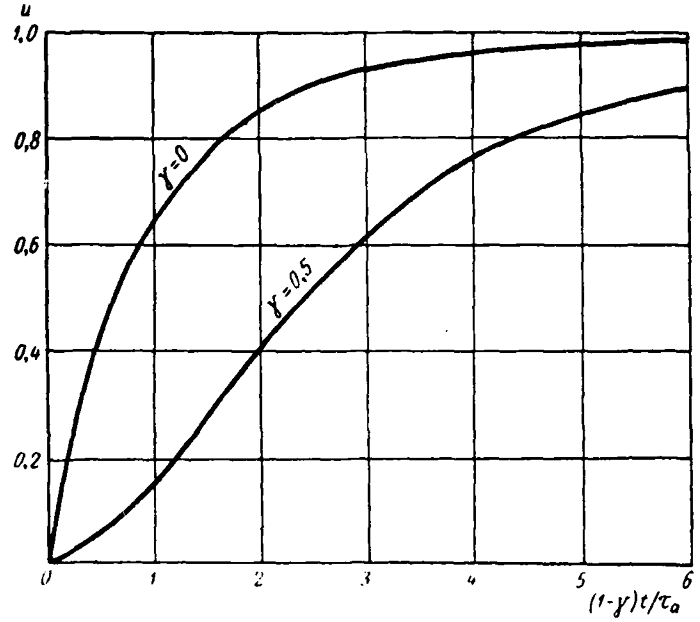

Fig. 6.27. Frontal part of pulses in schematic of recirculator..

Page 356.

Fig. 6.27 gives curves, which show law of change in pulse edge for cases $\gamma=0$ and $\gamma=0.5$. It is well noticeable that with $\gamma=0.5$ is developed a certain time lag in the build-up/growth of the frontal part of the pulse.

Let us determine duration of pulse edge, on the basis of condition that for this time output potential increases to 0.9 of steady-state value. Since according to (6.19) the steady-state value of the pulse amplitude is equal to one, the time of the establishment

$$t_y = \frac{2.3}{1-\gamma}\tau_u.$$

When $\gamma=0$ $t_y=2.3\tau_a$; with increase γ it grows/rises and time of establishment, approaching infinity with $\gamma=1$ (linear system).

6.8. SOME SCHEMATICS OF RECIRCULATORS.

Before examining specific schematics of recirculators, let us make some observations of physical processes relatively occurring in them. Recirculators are hunting systems with delayed feedback, in which is possible the prolonged circulation of pulses. The fluctuating overshoot of voltage on the input of amplifier is trigger pulse in self-contained hunting system (or other section of diagram). This overshoot is amplified by amplifier, also, due to unavoidable stray capacitances (which together with output resistance of amplifier form the integrating component/link), it is expanded. The expanded pulse is supplied through the delay line to the nonlinear element, designation/purpose of which is pulse clipping in the amplitude, which provides establishment in the diagram of the stationary amplitude of oscillations.

In diagram, which contains only enumerated elements, stationary pulse duration cannot be established/installed, since neither nonlinear element nor amplifier block unlimited pulse widening with multiple traversal through integrating component/link.

Page 357.

In order to avoid this expansion, in the schematic of recirculator the shortening (differentiating) circuit must be contained. Transient capacity/capacitance and leakage resistance in the circuit of tube usually serves as this circuit. The time constant of this circuit, as it was shown in the preceding/previous section, determines the duration of the generatable pulses. The presence of the differentiating circuit makes the transient response of the filter of nonmonotonic, the need what has already been discussed earlier.

Let us now move on and to examination of schematics of recirculators. Fig. 6.28 gives the schematic of recirculator, described into [106]. The first tube in this diagram is delivered into such mode, during which its characteristic is utilized on the lower bend. This tube is expander. Filter is formed by output resistance of the first tube and by referred to it stray capacitance of diagram (limitation in the region of higher frequencies), and also by the elements of transient circuit C_{cB1} and R_{c1} (limitation in the region of lower frequencies). Amplifier is carried out on the second tube. The output stage does not affect the passband of the diagram in the region of higher frequencies, since it is loaded to the low-resistance input of the resistor/resistance of cable. The load resistance/resistor in the grid circuit of expander is equal to the wave impedance of cable. In the region of lower frequencies filter attenuation band defines chain/network $C_{cB1}R_{c1}$, as has already been mentioned above, but not chain/network $C_{cB2}R_{c2}$, since the latter has considerably slow response. The delay time of pulse is determined in essence by the time of its passage on the cable.

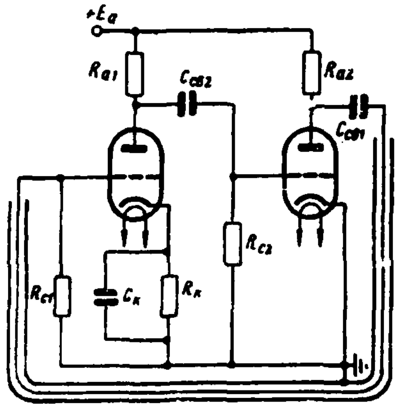

Fig. 6.28. Schematic of recirculator on two tubes.

Page 358.

Experimental research on the schemes of recirculator, described into [106], showed that this diagram can generate pulses by duration to 7 ns at the level with attenuation of 1 Np with the repetition frequency 20 MHz. The amplitude of generatable pulses was 3 V. The cable with a wave impedance of 150 ohms was utilized as the delay line. The author notes that the diagram easily was synchronized from the external signal with an amplitude 0.01 V, applied to the grid of the tube of expander. the shape of pulse is close to the bell-shaped.

In work [107] are given results of study of regenerative pulse generator on tube EFP-60 with secondary emission. This diagram generated the pulses, whose duration was 5 ns, and repetition frequency 50 MHz. Diagram and data of generator are cited in Fig. 6.29. Positive feedback in the diagram was achieved by application of voltage from the anode circuit into the cathode. For the delay of

feedback to this circuit the section/segment of coaxial cable with a length of 5 m was connected. The starting voltage/stress was supplied to control electrode of tube, and output pulse was removed/taken from the load into the circuit of dynode. The amplitude of output pulse was the units of volts.

In [108] description of recirculator on tube with secondary emission, which generated pulses is given by duration of 5 ns with repetition frequency to 170 MHz. The amplitude of the oscillations on the load of 37.5 ohms reached 120 V. Pulses were generated by series with duration into hundreds of microseconds. The schematic of this recirculator is given in Fig. 6.30. Its basic part - strictly recirculator - it is carried out on L_2 - tetrode with secondary emission of patronymic production. The voltage/stress of feedback is supplied from the anode L_2 into the cathode through cable RK-3. Chain/network C_1R_K realizes the automatic gain control, excluding the possibility of the appearance of supplementary pulses in the gaps/intervals between the bases and it shortens and it peaks trigger pulse. Tube L_1 serves for an improvement in form and increase in the slope/transconductance of trigger pulses.

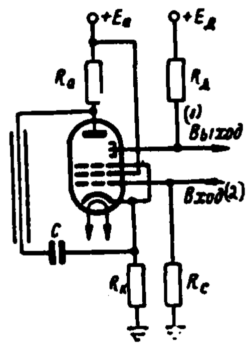

Fig. 6.29. Schematic of recirculator on tube with secondary emission. Key: (1). Output. (2). Input.

Page 359.

During the supplying to the input of the tube L_1 of trigger pulse the first of diagram develops the standard trigger pulse, under action of which the generator on the tube L_2 develops pulse train. The repetition period of these pulses is determined by the delay time of pulse in the cable and differs from it by several nanoseconds, spent by electrons with the flight/span through the tube. The amplitude of oscillations was determined by the saturation current of tube L_2.

Study of recirculator on transistors is carried out into [109]. Fig. 6.31 depicts oscillator circuits: a - on transistors P411 ($E_к = -5$ V) and b - on transistor P403 ($E_к = -5$ V). The transformer of this diagram has following data:

$Tp1 - w_1 : w_2 : w_3 = 21:21:7,\ D = 12$ мм, $S = 17$ мм^2, $\mu_\Delta = 100$.

In first diagram for provoding positive sign of feedback was

utilized supplementary transistor, and second - transformer. Automatic control was realized by means of chain/network $R_{31}C_{31}$, included in the emitter of transistor.

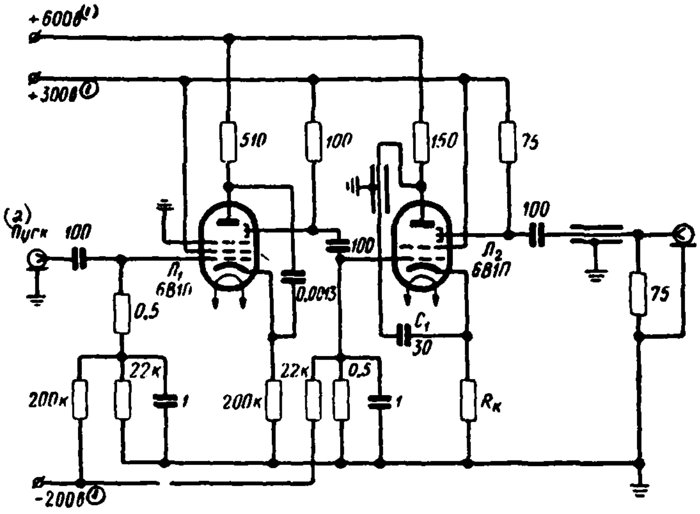

Fig. 6.30. Schematic of recirculator on tetrode with secondary emission.

Key: (1). V. (2). Launching/starting.

Page 360.

Fig. 6.32a gives the voltage oscillogram on the collector/receptacle of transistor (Fig. 6.31a), and in Fig. 6.32b - on load $R_н$ of diagram in Fig. 6.31b. In the diagram as delay unit was utilized cable RS-400-7-12. The pulse repetition frequency in the first diagram was 8 MHz.

In [110] is investigated schematic of recirculator, to feedback loop of which was connected delay line, with nonlinear amplitude characteristic.

Oscillator circuit is given in Fig. 6.33. Generator is carried

out on the tubes 6V1P, connected according to the schematic of the distributed amplifier for the purpose of the expansion of the passband of diagram. The voltage/stress of feedback is supplied from the dynode circuit into the grid through cable RK-3 and chain line, which consists of 20 filter sections of the type M with the nonlinear inductances. The cable segment is included/switched on for an increase in the pulse repetition period.

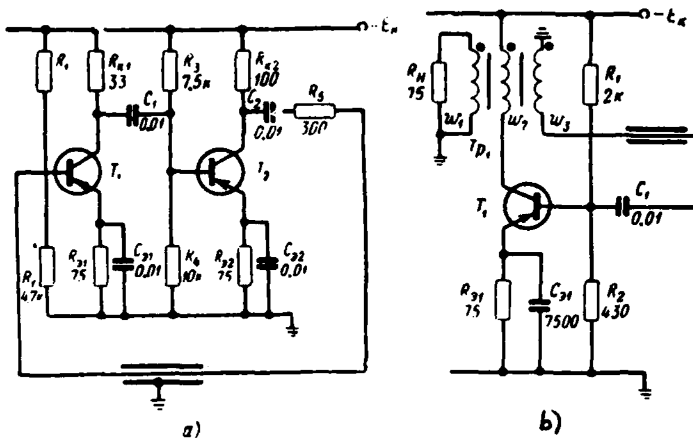

Fig. 6.31. Schematics of recirculators on transistors.

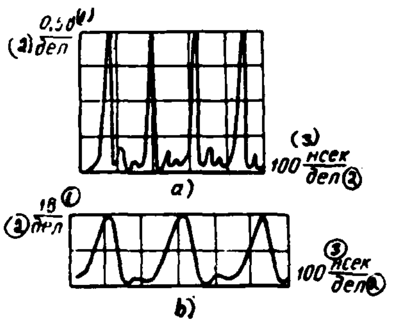

Fig. 6.32. Voltage oscillograms in schematic of recirculator on transistors.

Key: (1). V. (2). div. (3). ns.

Page 361.

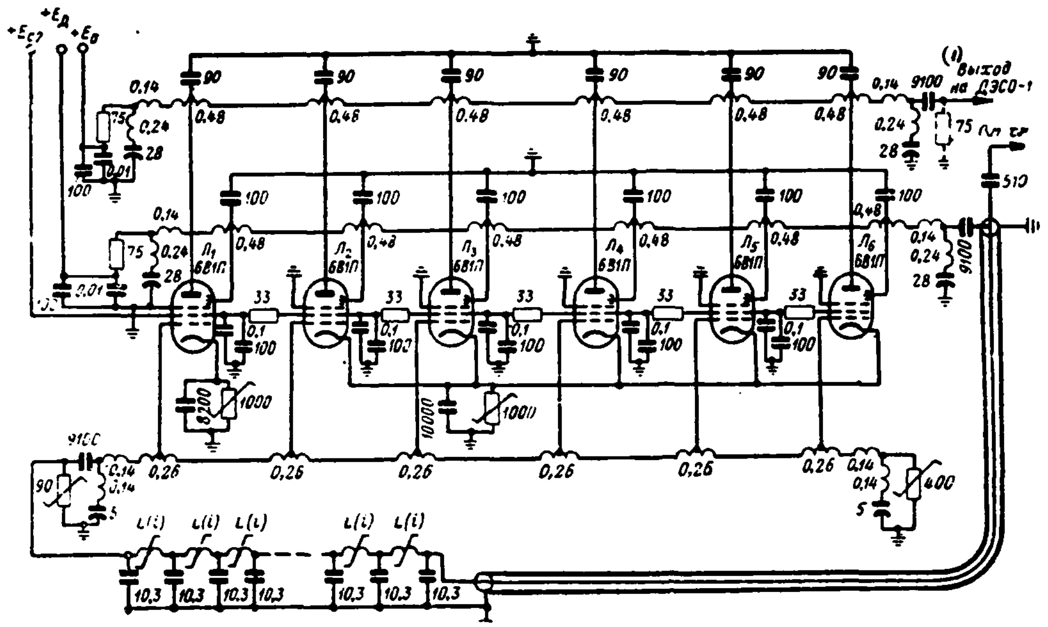

Fig. 6.33. Schematic of recirculator with nonlinear delay line (inductance in microhenry).

Key: (1). output to DESO-1.

Page 362.

The coils of filters were coiled around the ferrite cores of brand VT-6. Output voltage/stress was removed/taken from the load resistor/resistance of 75 ohms. The switching on/inclusion of nonlinear chain/network led to the decrease of the duration of pulses and duration of their fronts, and also to an increase in the pulse amplitude, i.e., it led to the compression of pulses. In particular the pulse edge in the anode circuit decreased from 70 to 20 ns, and amplitude grew/rose from 35 to 50 V. The even better results gave application of capacities/capacitances of p-n junctions in the

feedback loop as the nonlinear elements. The minimum duration of front in this case was 4 ns with the amplitude of pulses of 30 V.

Page 363.

Chapter Seven.

PULSING IN SOLID-STATE ELEMENT CIRCUITS WITH NEGATIVE RESISTANCE.

In recent years in pulse technique of microsecond range had extensive application diverse semiconductor devices, mainly transistors, which successfully replace electron tubes. On the transistors are fulfilled all possible oscillator circuits - multivibrators, blocking oscillators, trigger circuits, they are used for amplifying of pulses, limitation, fixation of level and the like [111]. The large inertness of the processes of moving the charge carriers, which did not make it possible to obtain steep edges in the voltage/stress or current, high pulse repetition frequencies or high counting rate blocked transistorization in the nanosecond pulse technique. Therefore until recently nanosecond pulse technique to a certain degree lagged behind the pulse technique of microsecond range in the part of the application of such promising elements as semiconductor devices.

Situation substantially changed after were opened and developed new types of semiconductor devices - instruments with negative resistance, in particular tunnel diode. The use of such instruments not only made it possible to replace electron tubes in the series/row of diagrams and devices/equipment, but also to make the large step forward by means of increasing the speed of impulse circuits. A real

possibility for the mastery/adoption of the subnanosecond range of the pulse durations was provided.

Page 364.

The tunnel diode, whose work is based on the quantum-mechanical effect - the tunnel passage of the electrons through the potential threshold - possesses the unique properties, which make with its irreplaceable in the diagrams, in which is realized the transmission or the conversion of oscillations with the very wide spectrum. Tunnel diode is the super wide-band active element (i.e. by the element, which possesses negative resistance in the very broadband). Furthermore, it is the element, whose nonlinear properties are retained to the very high frequencies.

Tunnel diodes had extensive application in different areas of technology. In the computers on them are fulfilled the high speed switching elements, logic circuits, memory elements, etc. The application of tunnel diodes in these devices/equipment made it possible to substantially decrease their overall dimensions and to raise speed. Tunnel diode has a switch time of less than 1 ns; the access time, provided by memory units on the tunnel diodes, is obtained less than 10 ns, which is considerably less than the access time of memory units on the ferrites or cathode-ray tubes [112-120].

Great interest cause tunnel diodes in microwave technology. Tunnel diodes permit implemention of a generation of the oscillations

of virtually any frequencies, up to the submillimeter range. Just as effectively work tunnel diodes, also, in the diagrams of the amplification of superhigh frequencies. Tunnel diode amplifiers differ in terms of very small noise level (although exceeding the noise level of molecular or parametric amplifier). The fact that the tunnel diode retains its nonlinear properties to the very high frequencies, are opened/disclosed prospects for its use in detectors and converters of microwave oscillations [121-125].

In nanosecond pulse technique tunnel diodes are utilized as pulse generators with very high repetition frequency, pulse generators of subnanosecond duration, high-speed relays, peakers of pulses. They are suitable also for amplifying the pulses of short duration.

Page 365.

Tunnel diode according to the principle of its action is the inertialess device (since the tunnel passage of the electrons through the potential threshold does not require the expenditure of time) and therefore it is of extreme interest for nanosecond pulse technique [126].

Together with tunnel diode in pulse technique found use and other semiconductor devices with negative resistance. Negative resistance possess point-contact germanium diodes of the type DG- Ts4-DG-Ts12 (section of negative resistance it is located they have on the reverse/inverse branch of characteristic), avalanche-type diodes of

the type p-n-p, four-layer diodes p-n-p-n, etc. [127]. There are also semiconductor three-electrode devices with negative resistance [128]. These instruments (in particular, two-electrode and three-electrode instruments of the type p-n-p-n), are of interest for the nanosecond pulse technique because they are the high-current and relatively high-voltage instruments (in comparison with the tunnel diode, which it works on the very low stress levels). The application of these instruments makes it possible to obtain the powerful/thick current pulses, the duration of fronts of which is the units of nanoseconds [129].

7.1. OPERATING PRINCIPLE OF TUNNEL DIODE.

Tunnel diode was discovered by L. Ezaki in 1957 [130, 131]. Studying the phenomenon of the internal autoelectric emission of electrons in the thin germanium p-n junctions, Ezaki detected the anomalous course of the volt-ampere characteristic of diodes with the high concentration of admixtures/impurities in the crystal (with the concentration of acceptors $N_{акц} = 1{,}6 \cdot 10^{19}$ cm^{-3} and concentration of donors $N_{дон} \approx 10^{19}$ cm^{-3}). The special feature of volt-ampere characteristic was the presence of the maximum in the region of the positive values of voltage/stress (approximately with 0.035 V. Furthermore, this diode possessed larger back conductance, than in the straight line. The form of the volt-ampere characteristic of diode is shown in Fig. 7.1. As can be seen from figure, diode had falling/incident section of volt-ampere characteristic, i.e., in

specific range of change in voltage/stress on it it had negative differential internal resistor/resistance [132, 133].

Page 366.

As has already been indicated above, crystals from which diodes were manufactured, had very high concentration of impurities. With this concentration of impurities, thickness of p-n junction was only 100-150 Å. Therefore electric intensity on the transition/junction due to a contact potential difference reached value on the order of 100 kV/cm. Both these facts (large field strength and the small thickness of transition/junction) lead to the fact that a certain part of the electrons can pass through the potential threshold in p-n layer due to the tunnel effect.

Tunnel effect is quantum-mechanical phenomenon. Its essence consists in the fact that the particle, which has total energy W_1, the lower altitude of potential threshold W_2, has different from zero probabilities to penetrate through the barrier without a change in its energy. This reveals the wave properties of material not observed in classical mechanics. Probability that the particle will pass the potential threshold, depends on the width of potential threshold and its height. In the usual diodes the thickness of junction is such, that the probability of the passage of electrons by tunnel effect is negligibly small; noticeable tunnel current is observed only then when the thickness of transition/junction it decreases to 150-200 Å. The significant role plays the value of the field strength on the

transition/junction, which affects the height of the potential threshold, decreasing it, and also decreasing its width.

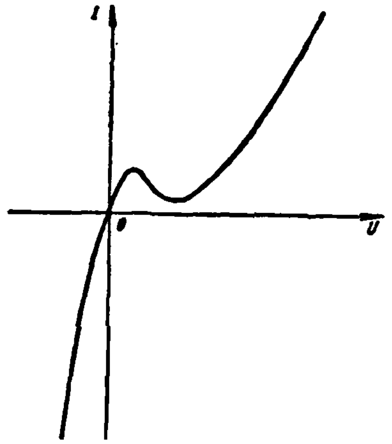

Fig. 7.1. Volt-ampere characteristic of tunnel diode.

Page 367.

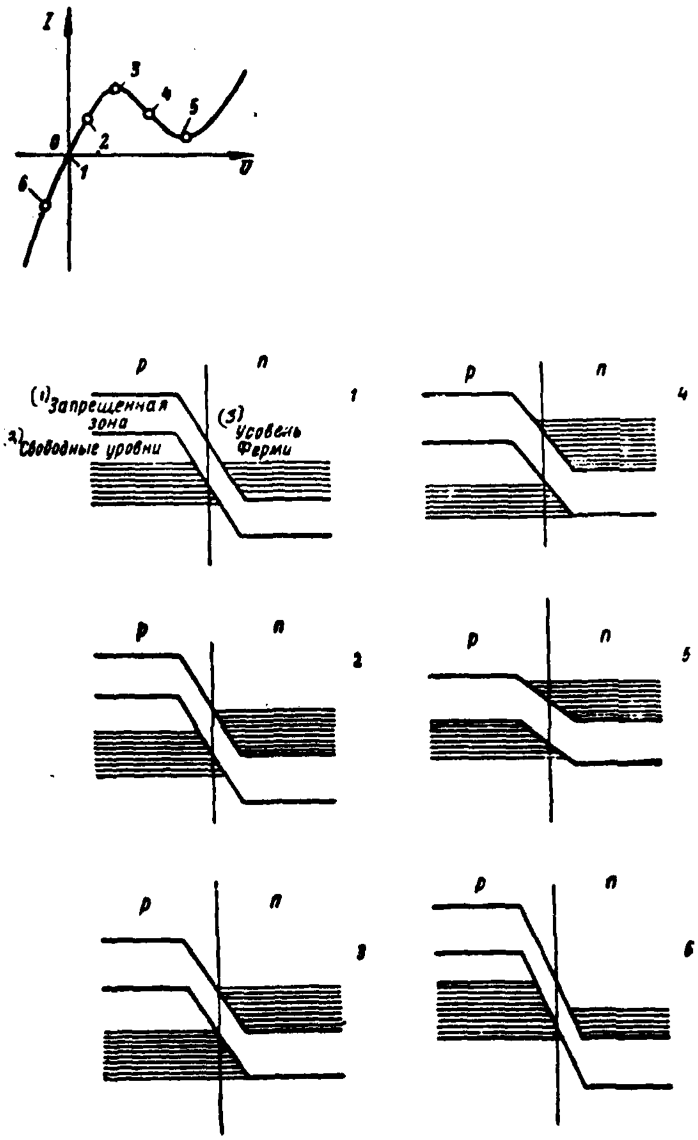

Fig. 7.2. Characteristic and diagram of zones for tunnel diode (each diagram with numeral it corresponds to position of operating point on characteristic of diode).

Key: (1). Forbidden band. (2). Free levels. (3). Fermi level.

Page 368.

In order to explain course of volt-ampere characteristic of tunnel diode, let us turn to simple zone diagram. Let us note preliminarily that the tunnel passage of electrons is feasible only when semiconductor is degenerate. In the degenerate n-type semiconductor the Fermi level is located in conduction band, while in the degenerate p-type semiconductor - in the valence band. As a result the levels in the valence band of p-region higher than the Fermi level turn out not to be filled with electrons, while in the n-region the levels of conduction band, which lie below the Fermi level, prove to be filled. The forbidden bands in this case will be strongly shifted relative to each other.

With zero voltage on diode current, formed by electrons, which pass due to tunnel effect from valence band on free levels of conduction band, is equal to current of electrons, which pass from conduction band to free levels of valence band, and therefore resulting current through diode is equal to zero (Fig. 7.2.1).

If we exert to tunnel diode voltage in forward direction, then Fermi levels in p- and n-regions will be displaced and current of electrons will from right to left be more than current in opposite direction, as a result of which resulting current will be different from zero. The position of zones for this case is shown in Fig. 7.2.2. From the figure one can see that against some of the levels, filled with electrons in the n-region, some of the free levels of p-region are located, whereas against some of the levels, filled with

electrons in the p-region, the forbidden band is located. Shift of Fermi levels will increase the electron current from the n-region into the p-region will rise in proportion to further increase in the voltage on the diode. Fig. 7.2.3 shows the position of zones in the case, when tunnel current reaches maximum.

With further increase in voltage (Fig. 7.3.4) it will seem that against some of levels, filled with electrons in n-region, forbidden band will be located. Tunnel current decreases. When voltage on the diode reaches that value, at which against the filled levels of n-region the forbidden band will be located, tunnel current will become zero (Fig. 7.3.5). Approximately with the same values of voltage in the diode appears the usual (diffusion) current, which rapidly increases with an increase in the applied voltage.

Page 369.

When bias voltage is applied in opposite direction, electrons which pass from p-region into n-region and creating tunnel current of reverse/inverse branch characteristics have preferred position. The position of zones in Fig. 7.2.6 corresponds to this case. As it follows from the figure, with an increase in the voltage/stress inverse current continuously increases, so for of the increasing part of the electrons, that are located in the p-region, appear the free levels in the n-region.

7.2. THE VOLT-AMPERE CHARACTERISTIC OF TUNNEL DIODE AND ITS

APPROXIMATION.

Volt-ampere characteristic of tunnel diode relates to characteristics of N-type (or first class). The manager of variable in instruments with such characteristics is voltage (Fig. 7.3a). At the same time there are instruments, which possess the volt-ampere characteristic of S-type (or the second class). An example of this characteristic is shown in Fig. 7.3b . Current is the controllable of variable in such instruments. They include, for example, four-layer diodes, examined/considered further.

Fig. 7.4a gives graph/diagram of dependence of internal differential resistor/resistance of tunnel diode on value of bias voltage. As can be seen from this graph/curve, with voltages less than U_1, the internal resistor/resistance of diode is positive.

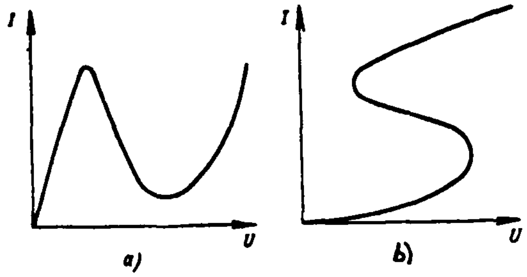

Fig. 7.3. Volt-ampere characteristics of elements with negative resistance of N-type (a) and S-type (b).

Page 370.

With $U=U_1$ the resistor/resistance of diode goes to infinity and with further increase in the voltage becomes negative. The value of negative resistance of tunnel diode is not constant. With a certain value of voltage/stress corresponding to the maximum speed of a change in the current, it has minimum value, and then it begins to increase, being turned with infinity with $U=U_2$. At high values of voltage the internal differential resistance of diode becomes positive.

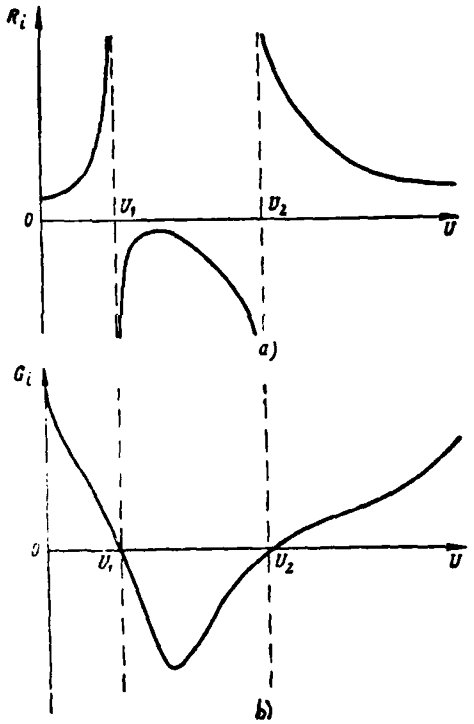

Fig. 7.4. Dependence of differential resistor/resistance (a) and differential conductivity of tunnel diode (b) on bias voltage.

Page 371.

The internal resistor/resistance of tunnel diode is positive with the negative values of voltage. It is characteristic that for the tunnel diode its resistor/resistance at negative values of voltage is less than at positive values. Thereby tunnel diode is not unipolar (or directed) element like usual diodes. The explanation to this special feature of tunnel diode is easy to obtain from the examination of zone diagram. Fig. 7.4b gives the dependence of the internal differential conductivity of tunnel diode on the bias voltage.

Together with internal differential resistor/resistance of tunnel diode it is possible to examine its direct-current resistance $R_{п}$. This resistor/resistance is equal to the ratio of voltage/stress to the current at any point of volt-ampere characteristic. The resistor/resistance of tunnel diode to direct current is the resistor/resistance, which it exerts power supply. In Fig. 7.5 is given the dependence of direct-current resistance of tunnel diode on the voltage on the tunnel diode. From the figure one can see that in section U_1-U_2, within of which tunnel diode possesses negative differential resistance, its direct-current resistance sharply grows/rises.

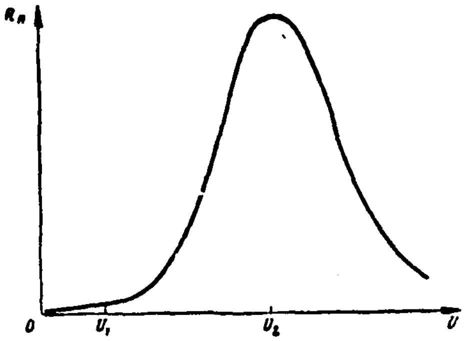

Fig. 7.5. Dependence of resistor/resistance of tunnel diode to direct current on bias voltage.

Page 372.

Resistance R_n is always positive, since with respect to the power supply tunnel diode is always the user of energy.

Need of obtaining analytical expression for volt-ampere characteristic of diodes appears during research on the schemes on tunnel diodes.

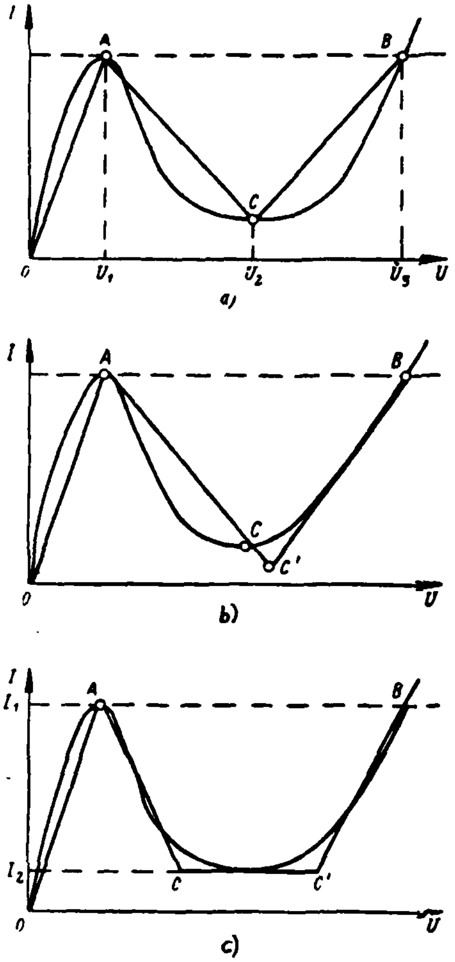

Fig. 7.6. Approximation of volt-ampere characteristic of tunnel diode by dog-leg functions.

Page 373.

By the easiest method of the approximation of characteristic is the replacement of objective parameter polygonal function - the so-called dog-leg approximation.

Fig. 7.6a shows example to approximation of characteristic by

three segments of lines, carried out according to following rule. The first straight line connects points O and A, the second of point A and C and the third of point C and B. The inclination/slope of these straight lines gives the averaged differential resistor/resistance of diode in section [0, U_1], which let us designate $R_{д1}$, in the section [U_1, U_2] - R_0 and in the section [U_2, U_3] let us designate $R_{д2}$. Using another method of the approximation of characteristic the third straight line, given in Fig. 7.6b, it is carried out as tangent to the ascending branch of characteristic at point B. Asymmetry of the volt-ampere characteristic of tunnel diode gives in certain cases to the need for resorting to the approximation with its four line segments, as shown in Fig. 7.6c. In this case the second and fourth sections/segments are conducted as tangents to the linear sections of the descending and ascending branches of characteristic before the intersection with the third section/segment, which is conducted in parallel to the axis of abscissas at level $I=I_2$.

Sharply pronounced nonlinear characteristic of tunnel diode makes dog-leg approximation little effective. Actually, with this approximation the dependence of the resistor/resistance of tunnel diode on the voltage/stress is represented by the step function, shown in Fig. 7.7, and very distant from the real dependence, represented in Fig. 7.4a.

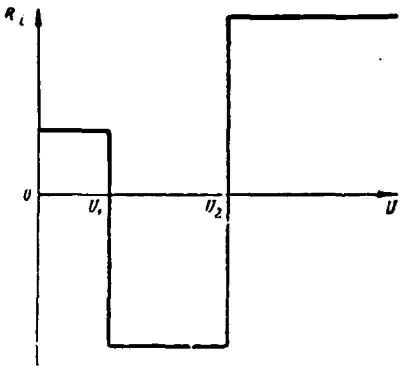

Fig. 7.7. Dependence of internal resistor/resistance of tunnel diode on voltage/stress with approximation of volt-ampere characteristic by dog-leg function (see Fig. 7.6a).

Page 374.

At the same time, as this will be evidently from the following, during the calculation of diagrams on the tunnel diodes, in particular relaxation oscillators, the basic value, which determines the pulse duration or repetition period, is the value of the resistor/resistance of diode in sections [0, U_1] and [U_2, U_3]. It is not surprising that the essential disagreements between the theory and the experiment are obtained with this approximation. Different results due to the different methods of conducting the approximating sections/segments are obtained, moreover, from calculations carried out according to the methods of different authors. It is necessary also to keep in mind that the dog-leg approximation does not make it possible to judge a precise form of the generatable oscillations (in more detail this question it is examined below).

In connection with this in number of cases attempts to approximate volt-ampere characteristic are made using functions of another form. Thus, B. N. Kononov and A. S. Sidorov [134] propose to approximate characteristic by the piecewise-exponential function:

$$I = I_1\left[1 - \left(1 - \frac{U}{U_1}\right)^2\right] \text{при}^{(1)} \; -U_1 \leqslant U \leqslant U_1 \qquad (7.1a)$$

Key: (1). with.

and

$$I = (I_1 - I_2)\left|\frac{U - U_2}{U_1 - U_2}\right|^{\gamma} + I_2 \; \text{при}^{(1)} \; U_1 \leqslant U \leqslant U_2. \qquad (7.1b)$$

Key: (1). with.

Here γ is determined experimentally. For the diodes tested by the authors it was within the limits of 2.6-2.8.

Calculation of diagrams on tunnel diodes, whose volt-ampere characteristic cannot be represented as dog-leg, is very complicated operation.

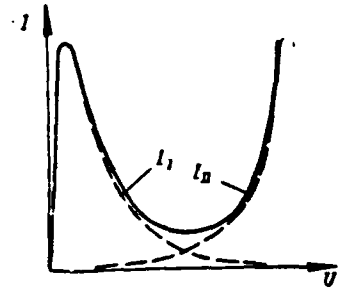

Fig. 7.8. Method of approximation of volt-ampere characteristic of tunnel diode.

Pagė 375.

However, the application of computer technology makes it possible to perform similar calculations and poses the problem of finding this flat approximating function, which in a comparatively simple form by the best about would at once describe volt-ampere characteristic. One of such methods consists in the replacement of real volt-ampere characteristic by polynomial, in this case for the sufficiently good representation of the properties of characteristic it is necessary to take the polynomial of fifth degree.

Another approximation method of volt-ampere characteristic of tunnel diode consisted of following [135]. It was established that in the region of negative resistance the curve, which expresses dependence ln (I/V) in the function of the applied voltage/stress, is straight line. In connection with this it was proposed to approximate the characteristic of tunnel diode by the function

$$I = I_{\text{I}} + I_{\text{II}} = AUe^{-aU} + B[e^{bU} - 1].$$

In this expression I_{I} represents tunnel current, and I_{II} - diffusion current. In Fig. 7.8 solid line showed the volt-ampere characteristic of tunnel diode, and dotted line - components of full current according to the given formula.

If $U<U_2$, then second term can be disregarded/neglected and then $I_{\text{I}} = AUe^{-aU}$ or $\ln(I_{\text{I}}/U) = \ln A - aU$. After constructing dependence $\ln(I_{\text{I}}/U)$ on U, which is straight line, is easy to find a as the angular coefficient of straight line, and ln A - as the section/segment, intercepted/detached by it on the axis of ordinates. With $U>U_2$ it is possible to disregard the first term and to count $I = I_{\text{II}} = B[e^{bU} - 1]$ or $\ln I_{\text{II}} = \ln B + bU$. After constructing straight line $\ln I_{\text{I}} = f(U)$, it is possible to determine values b and ln B. The authors indicate that the accuracy of a similar approximation is better than ±10%.

7.3. EQUIVALENT DIAGRAM OF TUNNEL DIODE.

Equivalent schematic of tunnel diode for small amplitudes (and when operating point it is located in falling/incident section of volt-ampere characteristic) is given in Fig. 7.9.

Page 376.

In this figure the part of the diagram, encircled by dotted line, represents the equivalent diagram of p-n junction; - R_0 is negative

resistance of tunnel diode at the operating point, and C_0 - transition capacitance. R_s is the so-called resistor/resistance of spreading. This is a resistor/resistance of the mass of semiconductor. Inductance L_s is the inductance of loadings of tunnel diode. Values R_0, C_0, R_s and L_s are the parameters of tunnel diode.

As it was possible to see in given earlier Fig. 7.4a, negative resistance of tunnel diode is not constant value, but to a great degree it depends on voltage/stress applied to tunnel diode. Therefore depending on the position of operating point on the volt-ampere characteristic the value of negative resistance will be different. This fact should be considered during the analysis of diagrams on the tunnel diodes (in particular, during the analysis of stability of amplifier circuits). Transition capacitance so is the value, voltage-sensitive on the diode. However, with a change in the voltage on the diode within the limits from 0.1 to 0.5 to a change in the capacity/capacitance do not exceed 15-20% and therefore in the majority of the cases capacitance value of transition/junction in the equivalent diagram is counted constant and equal capacity/capacitance with $U=U_2$.

Three parameters of tunnel diode: L_s, C_0 and R_s, are parasitic, and their values as far as possible they try to decrease. Actually, as it follows from the equivalent diagram (Fig. 7.9), the tunnel diode between the external terminals/grippers is not purely active inertia-free negative resistance - R_0 and certain impedance $Z_{вх}$.

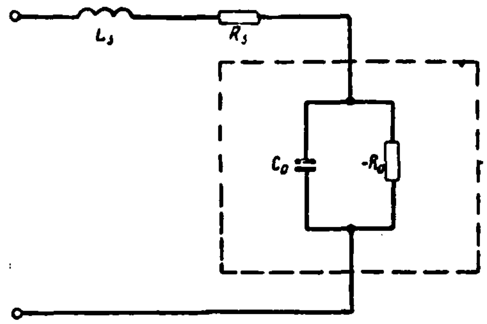

Fig. 7.9. Equivalent schematic of tunnel diode for small amplitudes.

Page 377.

The presence of the scattering resistance R_s decreases the value of negative resistance (in terms of the absolute value). Capacitance of C_0 shunts negative resistance; the presence of this capacitance does not make it possible for voltage on the tunnel diode to change abruptly. The presence of inductance L_s in exactly the same manner and gives to tunnel diode inertial properties, without allowing/assuming an abrupt change in the current through the diode. The parasitic parameters substantially worsen/impair the high-frequency properties of tunnel diode.

For examination of effect of parasitic parameters on high-frequency properties of tunnel diode let us turn to its equivalent diagram.

Its input resistance

$$\bar{Z}_{\text{вх}} = R_s + j\omega L_s + \bar{Z}, \qquad (7.2)$$

where $\bar{Z}$ - resistance of junction, equal to

$$\bar{Z} = -\frac{R_0}{1 - j\omega C_0 R_0} \qquad (7.2a)$$

is one of most important values, which characterize properties of tunnel diode.

Substituting (7.2a) in (7.2), we obtain

$$\bar{Z}_{BX} = \left(R_s - \frac{R_0}{1 + \omega^2 C_0^2 R_0^2}\right) + j\left(\omega L_s - \frac{\omega C_0 R_0^2}{1 + \omega^2 C_0^2 R_0^2}\right). \qquad (7.3)$$

The active part of the input resistance of tunnel diode can be both the positive and negative depending on the relationship/ratio between the circuit parameters. At the frequency, equal to zero, real part $\bar{Z}_{BX}$ will be negative, if $R_0 > R_s$; with other all frequencies the condition of negativity $\mathrm{Re}\,\bar{Z}_{BX}$ is recorded then

$$R_s < \frac{R_0}{1 + \omega^2 C_0^2 R_0^2}. \qquad (7.4)$$

It follows from this formula that with increase in frequency satisfaction of condition $\mathrm{Re}\,\bar{Z}_{BX} < 0$ becomes complicated, since it requires smallness of values R_s and C_0.

Page 378.

Inequality (7.4) can be resolved relative to frequency. The frequency, at which the active part of the input resistance of tunnel diode becomes zero, it is called the cut-off frequency:

$$f_{\text{гр}} = \frac{1}{2\pi R_0 C_0} \sqrt{\frac{R_0}{R_s} - 1}. \quad (7.5)$$

When $R_0 = R_s$ $f_{\text{гр}} = 0$ and diode not at what frequencies possesses negative resistance. Cut-off frequency defines, to what limits (in the frequency) tunnel diode taking into account its parasitic parameters behaves as negative resistance.

Analysis of formula (7.5) shows that input resistance of tunnel diode is negative in a wider frequency band, the less its parameters R_s and C_0. It follows from the formula that the cut-off frequency grows/rises with the decrease of negative resistance proportional to root from R_0.

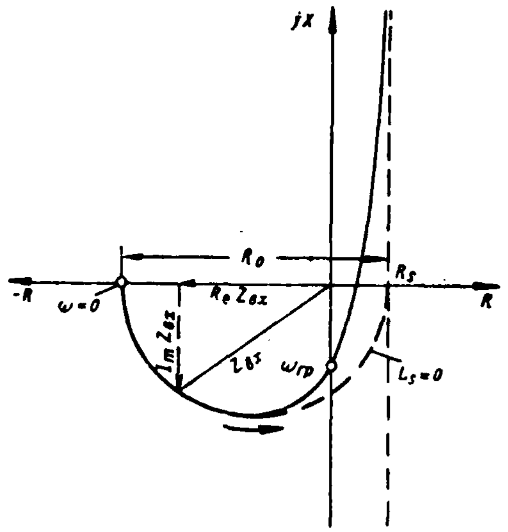

Fig. 7.10. Graph of input resistance of tunnel diode.

Page 379.

Active component of input resistance and cut-off frequency do not depend on inductance L_s.

Upon inclusion of tunnel diode in diagram it is necessary to keep in mind that its parameters change due to effect of network elements. Parameters L_s and R_s grow/rise due to inductance and capacitance of jumpers (or due to the inductance coils and resistor/resistance specially included in diagram). The presence of unavoidable backs-out resistor leads to increase in R_0. All these reasons lead to the fact that the critical frequency of tunnel diode in the diagram is obtained below its natural critical frequency.

Cut-off frequency is one of fundamental indices of suitability of

tunnel diodes for work as super wide-band device/equipment (generator, amplifier).

Input resistance of tunnel diode $Z_{вх}(\omega)$ can be represented on plane (R, jX) in the form of curve, shown in Fig. 7.10. If inductance L_s was equal to zero, then curve would take the form of semicircumference. At the frequency, equal to zero, the representative point lies/rests to the left of the axis of ordinates and has coordinates $[R_s - R_0, 0]$. At the infinite frequency when $L_s=0$ the representative point lies/rests to the right of the axis of ordinates and has coordinates $[R_s, 0]$. The presence of inductance changes the shape of the curve, giving to it the form, shown in the figure by solid line. Point of intersection with curve with the axis of ordinates gives cut-off frequency, i.e., that frequency, at which the active part of the input resistance becomes zero. The frequency, at which it is turned into zero reactive parts of the input resistance of tunnel diode, it is called the resonance frequency of tunnel diode. It is easy to obtain from formula (7.3) that

$$f_{рез} = \frac{1}{2\pi}\sqrt{\frac{1}{L_s C_0}\left(1 - \frac{L_s}{C_0 R_0^2}\right)}. \qquad (7.6)$$

Equivalent schematic of tunnel diode, given earlier, is mixed series-parallel diagram.

Page 380.

In a number of cases it is desirable to have either purely consecutive

or purely parallel equivalent circuit. Series circuit of the substitution of tunnel diode is depicted in Fig. 7.11. In this diagram

$$R'_0 = \frac{R_0}{1 + \omega^2 C_0^2 R_0^2}, \quad C'_0 = \frac{1 + \omega^2 C_0^2 R_0^2}{\omega^2 C_0 R_0^2}.$$

In other cases to more conveniently use the parallel equivalent circuit, shown in Fig. 7.12. In the parallel diagram

$$L'_s = \frac{R_s^2 + \omega^2 L_s^2}{\omega^2 L_s}, \quad R'_s = \frac{R_s^2 + \omega^2 L_s^2}{R_s}.$$

Diagrams given above were valid for the small signal level. During the analysis of the processes, which occur in the diagrams on the tunnel diodes, when the amplitude of oscillations cannot be considered small, it is necessary to take the schematic of the substitution of tunnel diode in the form, represented in Fig. 7.13. On this diagram the p-n junction is substituted by capacitance C_0 and nonlinear element N, the current through which is connected with the voltage applied to it with dependence $I=\varphi(U)$, where $\varphi(U)$ - equation of the volt-ampere characteristic of tunnel diode.

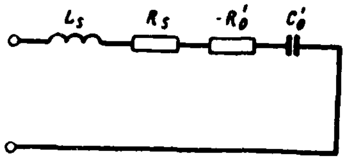

Fig. 7.11.

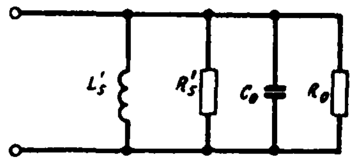

Fig. 7.12.

Fig. 7.11. Series circuit of substitution of tunnel diode.

Fig. 7.12. Parallel schematic of substitution of tunnel diode.

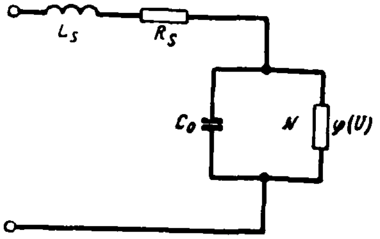

Fig. 7.13. Schematic of substitution of tunnel diode for large amplitudes.

Page 381.

7.4. PARAMETERS OF TUNNEL DIODES.

Let us become acquainted now with parameters of tunnel diodes, entering its equivalent diagram, but so with some properties of tunnel diodes about which it was not mentioned earlier.

Tunnel diodes, as has already been spoken, differ from usual diodes in terms of very high concentration of admixtures/impurities. Therefore the properties of tunnel diodes, their parameters and characteristics first of all depend on impurity content. Described in

[136] is the experiment, which showed that, by changing the degree of the alloying of semiconductor, it is possible consecutively/serially to switch over from typical tunnel diode to usual semiconductor diode. The falling/incident section on the volt-ampere characteristic of tunnel diode is formed only if concentration of admixtures/impurities in such semiconductors as germanium or silicon, has a value of approximately 10^{19} cm^{-3}. With this concentration germanium (or silicon) is the degenerate semiconductor and in the diode the tunnel passage of electrons can be observed. The value of negative resistance of diode is inversely proportional to the probability of the tunnel passage of electrons. In turn the probability of tunnel passage depends substantially on thickness of p-n junction, i.e., from the width of the potential threshold. The higher the concentration of admixtures/impurities, the less the thickness of transition/junction and, therefore, the less the value of negative resistance.

Table, which shows dependence of value of negative resistance and time constant of tunnel diode from electron concentration in n-region for some specimen tunnel diodes, is given to [126].

Increase of concentration of admixtures/impurities in semiconductors for decreasing negative resistance of tunnel diodes is limited to solubility of elements in germanium or silicon.

Table 7.1.

$n_{д+н}$, $см^{-3}$	R_0, ом (1)	R_0C_0, нсек (2)
2,4 10^{19}	90	4,5
3,6 10^{19}	4,5	0,9
4,8 10^{19}	1	0,05

Key: (1). ... ohm. (2). ... ns.

Page 382.

Thus, critical solubility in germanium of n-type comprises for P(>10^{20} cm^{-3}), As($1.8 \cdot 10^{20}$ cm^{-3}), in germanium of p-type for Ga($5 \cdot 10^{20}$ cm^{-3}), for Al($4 \cdot 10^{20}$ cm^{-3}). Besides germanium and silicon for producing the tunnel diodes are utilized also SiC, InSb, GaAs. Tunnel diodes from gallium arsenide cause the greatest interest at present.

Second fundamental parameter of tunnel diode is capacitance of p-n junction. This capacitance is greater, the higher the concentration of admixtures/impurities in the semiconductor. Increase in the concentration of admixtures/impurities, which thereby leads to the decrease of negative resistance, gives undesirable effect in the form of an increase in the transition capacitance. From Table 7.1 it is evident, however, that the decrease of negative resistance occurs more rapidly than an increase in the transition capacitance, so that the time constant of tunnel diode decreases with the increase of the concentration of admixtures/impurities. Value C_0R_0, as we shall see further on, determines the high-frequency properties of tunnel diodes. As already mentioned earlier, thickness of p-n junction in the tunnel

diodes composes 100-150 Å. With this thickness the transition capacitance reaches the very significant magnitude of 5 $\mu F/cm^2$. With the diameter of transition/junction 38 μ its capacitance will be 100 pF [126]. Therefore for obtaining the very small transition capacitances it is necessary to substantially decrease the area of transition/junction. In this case respectively increases negative resistance of diode. As it will be shown below, there are tunnel diodes, whose capacitance comprises fractions of picofarads [137].

Resistor/resistance of spreading R_s for tunnel diodes ranges from portions to units of ohms (in certain cases value R_s it can be and more). Inductance L_s is determined by the construction/design of tunnel diode. Usually it is portions or units of nanohenry.

Besides parameters enumerated above tunnel diodes are rated/estimated so by value of maximum value of tunnel current, by position of maximum, "solution/opening" of characteristic and by some other indices.

Although penetration probability of electrons through potential threshold due to tunnel effect is sufficiently small, strength of tunnel current through transition/junction can be very considerable. The density of tunnel current is 10^3 A/cm^2 [126].

Page 383.

Therefore in the sufficiently large area of transition/junction the

strength of maximum current in the tunnel diode can reach the units of amperes [136]. However, in this case respectively grows/rises transition capacitance.

For high-frequency tunnel diodes strength of maximum current I_1 is portions or units of milliamperes. The strength of maximum current increases with an increase in the concentration of admixtures/impurities. In this case an increase in the degree of the alloying of n-region increases the maximum value of tunnel current, without changing the position of maximum, but an increase in the degree of the alloying of p-region it increases the maximum of current it displaces its position into the region of the high values of voltage.

One of characteristics of tunnel diodes is value of ratio of maximum current I_1 to minimum current I_2. The greater this relation, the sharper the drop in the volt-ampere characteristic of tunnel diode in the region of negative slope/transconductance. The value of ratio I_1/I_2 is determined in by material, from which is manufactured the diode. It comprises 3-4 for Si and 40-70 for GaAs. It follows from given data that from the point of view of obtaining the larger value I_1/I_2 the best material is gallium arsenide, and worst - silicon. They are interested also in the voltage at which is reached current I_1, i.e., by value U_1 of the component of 30-50 mV for GaSb and 90-120 mV - for GaAs.

By "opening" of volt-ampere characteristic of tunnel diode is understood voltage difference ΔU between two points of characteristics, current in which is equal to I_1 (see Fig. 7.6). The greater this value, the greater, in particular, the drop in the voltage removed from the tunnel diode in the mode of switching. It is approximately 200 mV for GaSb and 600 mV for GaAs. More detailed data for different materials are cited further in table 7.2.

With work of tunnel diode as switching element together with time constant $\tau = C_0 R_0$ (it it is equivalent to reciprocal value of quality of tube) are interested in value ratios I/C_0, which does not depend on area of transition/junction, but it depends only on concentration of admixtures/impurities.

Page 384.

For germanium I_1/C_0 is 0.3-1 mA/pf, for silicon - approximately 0.5 mA/pf and for gallium arsenide of 10-15 mA/pf. In this respect gallium arsenide is also the most promising material for producing the tunnel diodes.

Parameters of tunnel diodes enumerated above are given in Table 7.2 [138] and 7.3 [137].

It follows from Table 7.2 that the smallest time constant, equal to $0.5 \cdot 10^{-11}$ s, is possessed by tunnel diodes from indium antimonide. Such tunnel diodes can successfully be used in the high speed

electronic computers; however, they have the deficiency, that they can work only at low temperatures. Table 7.3 gives data of the special superhigh-frequency tunnel diodes, which have very small transition capacitance. In the last column of table the critical frequency of tunnel diodes is given.

Let us pause now at dependence of parameters of tunnel diodes on environmental factors, such, as temperature, emission, etc. As is known, the parameters of transistors and usual semiconductor diodes strongly depend on temperature. Temperature effect on the properties of tunnel diode is characterized by a certain peculiarity.

Table 7.2.

(1) Материал	(2) U_1, мв	(2) U_2, мв	(2) ΔU, мв	I_1/I_2	(3) R_0C_0, сек
InSb	—	—	—	7—10	0,5 10^{-11}
Ge	40—70	270—350	280	10—15	0,5 10^{-9}
GaSb	30—50	200—250	200	15—20	0,1 10^{-9}
Si	80—110	400—500	400	3—4	0,2 10^{-9}
GaAs	90—120	450—700	580	40—70	0,1 10^{-9}

Key: (1). Material. (2). ... mV. (3). ... s.

Table 7.3.

(1) Материал	(2) R_0, ом	(2) R_s, ом	(3) C_0, пф	(4) $f_{гр}$, Ггц
N-Ge	190	6	0,24	18,5
P-Ge	116	4,5	0,13	52,5
P-GaAs	220	40	0,04	38
N-GaAs	350	20	0,027	70

Key: (1). Material. (2). ... ohm. (3). ... pF. (4). ... GHz.

Page 385.

Tunnel diodes on the strength of the fact that the semiconductor in them is degenerate and Fermi level remains in conduction band or in the valence band for regions n- and p-type respectively even at very low temperatures, they can work even at a temperature of liquid helium. It is shown in [136] that a change in the temperature of diode from -193 to +200°C does not lead to a change in position U of the maximum of tunnel current; very current strength is changed in this case not more than by 20%.

With an increase in temperature of tunnel diode increase in

diffusion current begins. The minimum current of diode I_2 increases because of this and value I_1/I_2 decreases. The size/dimension of the falling/incident section of volt-ampere characteristic is decreased and at a certain temperature entirely disappears. The maximum temperature, at which tunnel diode still retains its properties, is equal to +250°C for Ge, +400°C for Si and +600°C for GaAs [136]. Thus, tunnel diodes differ from other semiconductor devices considerably in terms of the broader band of operating temperatures.

Tunnel diodes are characterized by also high permissible intensity of radioactivity. The characteristics of silicic and germanium tunnel diodes noticeably deteriorate during irradiation by their fast neutrons with a density of 10^{17} neutrons/cm^2 or by electrons with the energy 7 MeV at the density of flow 10^{17}0e/cm^2. As a result of irradiation the strong increase in the minimum current, which leads to the disappearance of the section of characteristic with the negative slope/transconductance, occurs.

Speaking about advantages of tunnel diodes, it should be pointed out that they consume power, approximately by an order smaller than transistors, and they are also characterized by small overall dimensions and weight.

At conclusion of present section let us pause at some questions of measurement of parameters of tunnel diodes.

Removal/taking volt-ampere characteristic of tunnel diodes can be realized with the aid of automatic voltampere recorder, whose schematic diagram is shown in Fig. 7.14 [139]. It is the bridge, one of arms of which consists of tunnel diode TD and resistor/resistance R_2.

Page 386.

Resistor/resistance R_2 must be lower than the minimum (on the modulus/module) value of negative resistance of tunnel diode for guaranteeing the stable operation of diagram. Special attention should be given the inductance of the holder and the resistors/resistances would be being brought to the minimum. The alternating voltage from the generator of low frequency is introduced in the diagonal of bridge.

Before removal/taking of volt-ampere characteristic bridge is balanced with off diode. After the switching on of tunnel diode voltage u_i will vary in proportion to the current through the tunnel diode, and u_e will be voltage on the tunnel diode. Amplifying voltages u_i and u_e and supplying the first of them to the those the vertically deflecting, and the second - to the horizontal deflectors of oscillograph, we will obtain on the screen/shield the curve, which expresses the dependence of the current through the diode on the voltage on it, i.e., the volt-ampere characteristic of tunnel diode.

With the aid of system described above it is possible to conduct

measurement of differential resistor/resistance of tunnel diode in any section of characteristic [139]. For this purpose into the diagonal of bridge is introduced the source of bias voltage and the source of alternating voltage $\mathcal{E}$ of low frequency (so that it would be possible to disregard/neglect the reactive/jet circuit parameters). The amplitude of alternating voltage must comprise not more than the units of millivolts on the tunnel diode.

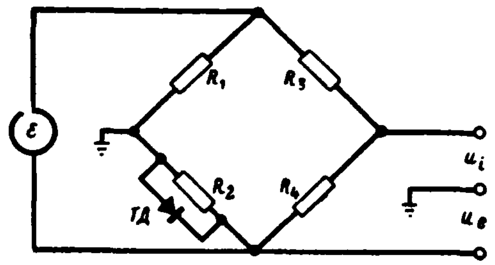

Fig. 7.14. Diagram for removing/taking volt-ampere characteristic of tunnel diode.

Page 387.

Balancing bridge on alternating current, is found the resistor/resistance of the arm, in which the diode is included:

$$R_{обш} = \frac{R_2 R'}{R' + R_2},$$

whence $R' = -\frac{R_{обш} R_2}{R_{обш} - R_2}$, where $R' = R_д + R_s$, R_s - resistor/resistance of spreading, and $R_д$ - resistor/resistance of diode. In the falling/incident section of characteristic $R_д < 0$.

7.5. Stability of the diagrams, which contain tunnel diodes.

Since diagrams, which contain elements with negative resistance, are potentially inclined to self-excitation, let us examine question about stability of diagrams on tunnel diodes. In § 7.4 there were established concepts of the cut-off frequency of tunnel diode $f_{гр}$, at which it is turned into zero active parts of its input resistance, and resonance frequency $f_{рез}$, at which it is turned into zero reactive parts of the input resistance.

It is obvious that if cut-off frequency

$$f_{rp}=\frac{1}{2\pi C_0 R_0}\sqrt{\frac{R_0}{R_s}-1}$$

will be equal to resonance

$$f_{рез}=\frac{1}{2\pi}\sqrt{\frac{1}{L_s C_0}\left(1-\frac{L_s}{C_0 R_0^2}\right)},$$

the at frequency $f_{рез}$ the resistance of the circuit, formed by parasitic parameters of tunnel diode, will be equal to zero. Tunnel diode will be unstable, i.e., will spontaneously generate sinusoidal oscillations. Equality f_{rp} and $f_{рез}$ means that

$$R_s=\frac{L_s}{R_0 C_0}.$$

So that tunnel diode would be stable it is necessary that $f_{рез}>f_{rp}$ or $R_s>L_s/R_0C_0$. But if $f_{рез}\leqslant f_{rp}$ or $R_s\leqslant\frac{L_s}{R_0C_0}$, then tunnel diode will be unstable.

Page 388.

If external elements of network (inductance, effective resistance) are connected to tunnel diode in the manner that it is shown in Fig. 7.15, then it will be the stability condition of diagram

$$R>\frac{L}{R_0 C_0},$$

where

$$R = R_s + R_{вн};\ L = L_s + L_{вн}.$$

It follows from this formula that switching on/inclusion of inductance raises danger of self-excitation of diagram on tunnel diode. Therefore during the construction of diagrams on the tunnel diodes it is necessary to take special measures for decreasing the inductance of the jumpers and other parts.

Let us turn again to diagram, represented in Fig. 7.15. The processes, which occur in this diagram, can be described by the differential equations

$$i = C_0 \frac{du}{dt} + \varphi(u),\quad L\frac{di}{dt} + Ri + u = E.$$

Here i - current of duct/contour; u - voltage on tunnel diode; φ(u) - equation of volt-ampere characteristic of tunnel diode.

In state of equilibrium, when alternating voltage components and current will be absent,

$$i = \varphi(u),\ Ri + u = E.$$

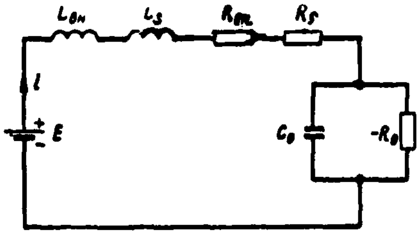

Fig. 7.15. Circuit diagram of elements of external circuit.

Page 389.

These equations determine points of intersection with load straight line with volt-ampere characteristic of diode. Equation of the load straight line

$$i = -\frac{1}{R}u + \frac{E}{R}.$$

It is obvious that depending on value of load resistor/resistance and voltage of source of bias/displacement position of load straight line with respect to volt-ampere characteristic of diode can be different. Fig. 7.16a shows the case, when load straight line intersects volt-ampere characteristic in the falling/incident section, moreover so that the inclination/slope of full-load saturation curve is more than the inclination/slope of volt-ampere characteristic. Fig. 7.16b shows the case, when the value of bias voltage is undertaken either small or large, so that full-load saturation curve intersects volt-ampere characteristic only at one point in the section with the positive slope/transconductance.

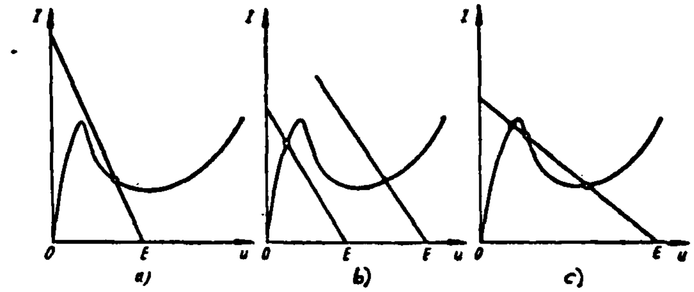

Fig. 7.16. Position of load straight line with respect to volt-ampere characteristic of tunnel diode.

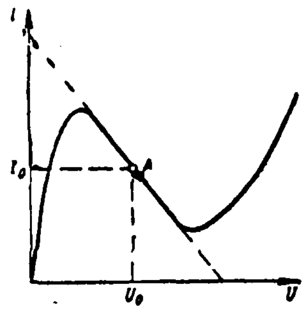

Fig. 7.17. Approximation of section of volt-ampere characteristic of tunnel diode.

Page 390.

Finally, Fig. 7.16c gives the case, when load straight line intersects volt-ampere characteristic at three points. These points indicate the position of equilibrium of system. It is known for [84] that if the load straight line has one point of intersection with the volt-ampere characteristic, then the state of equilibrium is stable, and if three points of intersection, then end states are stable, and average - unstable.

We linearize volt-ampere characteristic of tunnel diode in section with negative slope/transconductance (Fig. 7.17), after assuming

$$i = i_0 - \frac{u - u_0}{R_0}.$$

Then the system of equations, which describes processes in the diagram, will take the form:

$$\begin{gathered} i = C_0 \frac{du}{dt} - \frac{u}{R} + \left(i_0 + \frac{u_0}{R_0}\right); \\ L \frac{di}{dt} + Ri + u = E. \end{gathered}$$

Substituting second equation into the first and converting, we obtain

$$\begin{gathered} -L\frac{d^2 i}{dt^2} + \left(\frac{L}{R_0 C_0} - R\right)\frac{di}{dt} + \frac{R - R_0}{RC_0}\, i = \\ = \frac{1}{R_0 C_0}(u_0 - E + R_0 i_0). \end{gathered}$$

General solution of this equation takes form

$$i = A_1 e^{\lambda_1 t} + A_2 e^{\lambda_2 t} + \frac{E - u_0 - R_0 i}{R - R_0},$$

where

$$\lambda_{1,2} = \frac{1}{2}\left(\frac{1}{R_0 C_0} - \frac{R}{L}\right) \pm j\sqrt{\frac{1}{LC_0}\left(1 - \frac{R}{R_0}\right) - \frac{1}{4}\left(\frac{R}{L} - \frac{1}{R_0 C_0}\right)^2}.$$

Assuming/setting

$$\omega = \frac{1}{\sqrt{LC_0}}, \quad \delta = \omega R_0 C_0, \quad \eta = \frac{R}{R_0},$$

we obtain

$$\frac{\lambda_{1,2}}{\omega}=\frac{1}{2\delta}(1-\eta\delta^2)\pm j\sqrt{(1-\eta)-\frac{1}{4\delta^2}(1-\eta\delta^2)^2}.$$

Page 391.

Fig. 7.18 depicts diagram of stability, which has four zones. If the circuit parameters are such that the values η and δ corresponding to them fall to zone I, then in the diagram the excitation of sinusoidal oscillations will be observed. The sinusoidal damping of oscillations corresponds to the parameters which fall into zone II. Zone III is a zone of exponential damping of oscillations, while zone IV - the zone of an exponential increase in the oscillations. This zone is of greatest interest from the point of view of the generation of relaxation oscillations.

Let us assume that relation $\frac{R}{R_0}=0{,}5$, and let us explain effect of parameter δ on processes, which occur in diagram with tunnel diode. With the change δ from 0 to 0.52 (to these values of the parameter δ at those fixed/recorded R_0 and C_0 it corresponds the greatest value of inductance L) in the diagram occurs aperiodic instability, i.e., diagram can work as switch or as relaxation oscillator.

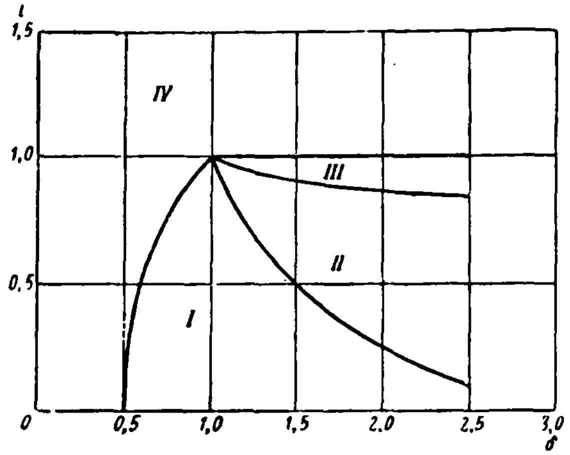

Fig. 7.18. Diagram of zones of stability and instability of diagrams on tunnel diode.

Page 392.

With a decrease of inductance (δ>0.52), the equilibrium in the diagram remains unstable, but the form of the generatable oscillations acquires sinusoidal nature. With an even smaller value of inductance (δ>1.5) the state of equilibrium becomes stable and the randomly emergent in the diagram oscillations attenuate. With this relationship/ratio of the parameters the diagrams on the tunnel diodes are utilized for amplifying the oscillations.

Thus, from diagram examined it follows that with $R>R_0$ state of equilibrium of diagram is unstable with any relationships/ratios of parameters. With $R<R_0$ the state of equilibrium can be both the stable and unstable depending on the value of inductance L. Let us note that the equation curved, dividing zones I and II, takes the form

$\eta=\frac{1}{\delta^2}$ (1) или $R=\frac{L}{C_0R_0}$.

Key: (1). or.

This curve is boundary, which divides zones of stability and instability. So that the diagram would be stable it is necessary that $R>\frac{L}{C_0R_0}$. This conclusion was already obtained earlier of the simple physical considerations. The examination of the zones of stability and instability shows that the range of a change in value R, in which the diagram remains stable, lies/rests within the limits

$$R_0>R>\frac{L}{C_0R_0}.$$

7.6. BISTABLE FLIP-FLOP ON THE TUNNEL DIODE.

Bistable flip-flop is diagram on tunnel diode, for which must be carried out condition $R>R_0$. To the mode of the work of bistable flip-flop corresponds such position of full-load saturation curve with respect to the volt-ampere characteristic, in which they intersect at three points. Bistable flip-flop is utilized for converting the oscillations of sinusoidal or other form into the sequence of steep-sided pulses.

Simplest schematic of bistable flip-flop is given on Fig. 7.19 and consists of tunnel diode TD and resistance R (power supply is not

shown).

Page 393.

With the work of tunnel diode as the switching element should be distinguished the mode of switching current, which occurs with the load resistance/resistor, close to negative resistance of diode at operating point R_0, and the mode of switching voltage, which occurs with $R>>R_0$. In the first case a considerable change in the current through the tunnel diode occurs, and flip-flop has high sensitivity to the input voltage; however, the amplitude of output voltage is comparatively small. In the second case a change of the current is small, the sensitivity of flip-flop proves to be low, but the amplitude of output voltage has the significant magnitude. Usually in the impulse circuits the mode of switching voltage is utilized.

Process of impulse shaping from sine voltage is shown on Fig. 7.20. As can be seen from the figure, the steep-sided pulses are obtained at the output of diagram, although their form strongly differs from rectangular. A negative drop/jump in the pulses is less than the positive.

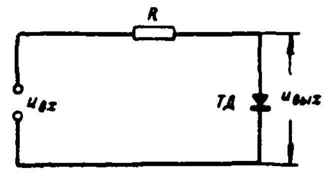

Fig. 7.19. Diagram of bistable flip-flop.

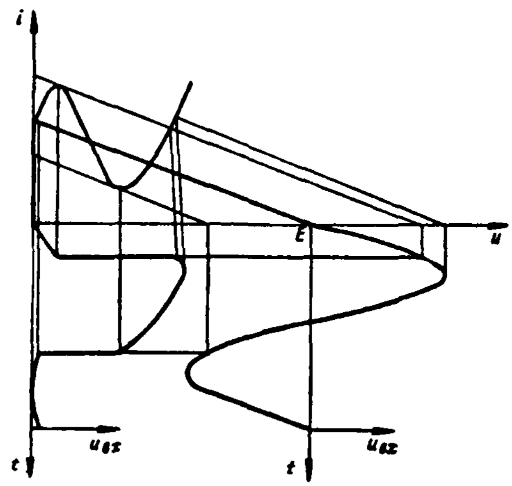

Fig. 7.20. Process of impulse shaping in bistable flip-flop.

Page 394.

The pulse duration at the output of the diagram is determined by the frequency of sine voltage, and amplitude - by characteristic of tunnel diode.

From point of view of possibility of obtaining maximally narrow pulses via their subsequent formation from pulses, developed by flip-flop, there is greatest interest in determination of duration of fronts. The switch time of flip-flop on the tunnel diode is determined only by the elements of its network, since the tunneling

junction of the electrons through the potential threshold can be considered inertia-free. This property of tunnel diodes differ significantly them from other semiconductor devices. In the mode of switching voltage in the form of the smallness of a change in the current it is possible to disregard the effect of its own inductance of tunnel diode; therefore switch time will depend only on transition capacitance.

During analysis of work of bistable flip-flop the fundamental question is the determination of switch time of tunnel diode, which assigns steepness of pulse edges at output, and also operating speed of flip-flop, i.e., frequency of switchings.

Above has already been indicated that tunnel passage of electrons through potential threshold does not require expenditures of time; therefore switch time of tunnel diode is completely determined by its parasitic parameters. In the case, when tunnel diode works in the mode of bistable flip-flop, its full-load saturation curve is arranged/located with respect to the volt-ampere characteristic in the manner that it is shown in Fig. 7.21.

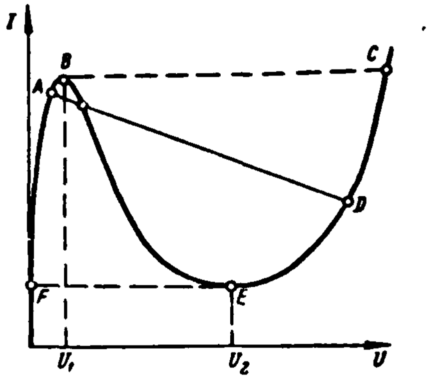

Fig. 7.21. To explanation of process of switching flip-flop.

Page 395.

(Let us note that here for convenience in the graphing there is undertaken the mode of switching current; everything said completely relates below also to the mode of switching voltage). Operating point in initial state is in position A. Then to the diode is supplied the slowly increasing voltage, under the action of which the operating point passes from A to B. From this time on diagram it considers to itself given. Since position B is unstable, then the operating point abruptly passes from B to C. The formation of the front of output pulse occurs at this moment of time. If diagram did not contain reactive/jet elements, then the transition from position B to position C would be completed instantly. Under the actual conditions to this transition/junction the time, called the time of straight/direct switching, is required.

After operating point fell into position C, it spontaneously is

moved to position D. This state of equilibrium is stable, and in it diagram can be found the unlimited time. In computer technology the first stable position of flip-flop (point A) is counted for zero, and the second stable position (point D) - for one. In order to transfer flip-flop from the state, characterized by position D, into the state, characterized by position A, it is necessary to decrease the voltage on the diode, so that the operating point could pass to position E. Hence it spontaneously abruptly will pass to position F, and then in A. The time required for the transition/junction of operating point from E to F is called the time of reconnection of diode.

For realization of reconnection of diode it is necessary that converted voltage would decrease so that voltage on diode would become less than U_2. In the computers for this purpose the negative dumping pulses are supplied.

Let us examine in more detail process of straight/direct switching. In the mode of switching the voltage of point C and D they lie/rest very closely to each other, and therefore we will not take into consideration transit time from C to D. Therefore, it is assumed that the current through the diode virtually is not changed during the switching.

Page 396.

At the moment of time t=0, which corresponds to the beginning of switching diode, the operating point is located in position B and

entire current, developed by source, is the current of diode I_1. Let us note that the voltage of source in the case, when diagram works in the mode of switching voltage, is sufficiently great; it is equal to the voltage, which corresponds to the point of intersection with the straight line AD and axis of abscissas.

Voltage on diode and, therefore, on capacitance of C_0 is equal U_1. As soon as voltage on the diode it will exceed value U_1, begins the charge of capacitance of C_0. The charge of capacitance of C_0 becomes possible because with an increase in the voltage on the tunnel diode its current decreases. Therefore appears certain spill current $i_C=i_1-i_A$, which goes to the charge of capacitance.

Process of charge of capacitance is developed avalanche-like. As soon as small the charging current begins to flow through the capacitance, voltage on the capacitance grows/rises. The increase of voltage causes reduction in current through the diode and increase in the current through the capacitance. Voltage/stress on the capacitance begins still more rapid, which leads to an even larger increase of charging current, etc. The avalanche-like increase of voltage on the capacitance (and, therefore, on the tunnel diode) occurs until with an increase in the voltage on the capacitance grows/rises the current of charge, i.e., until the voltage achieves value U_2. In other words, the avalanche-like process in the diagram on the tunnel diode lasts until tunnel diode is negative resistance.

After the voltage on diode achieved value U_2, voltage on capacitance continues to increase, since through it current of charge continues leak. However, the strength of current of charge now no longer increases, and it decreases with an increase in the voltage, and therefore rate of voltage rise on the capacitance falls.

It is easy to see, that rate of voltage rise on capacitance or, that it is more clearly, time, required for increase of voltage on one volt, is different for different sections of curve. At point the V current of the charge of capacitance is equal to zero; therefore if at the moment of time t=0 input voltage does not exceed the value of voltage U_1, then operating point will be unlimitedly for long located in this position (on the assumption that in the diagram they are absent are electrical fluctuations).

Page 397.

In order to displace operating point from this position, it is necessary that the starting voltage would exceed value U_1.

Fig. 7.22 shows time characteristics of tunnel diode [140]. Depending on the value of the overvoltage (i.e. the values, which show, to how much voltage of starting/launching it exceeds value U_1) the retention time of operating point in the vicinities of point B is different. This time is called the delay time of functioning, and it is the greater, the less the value of overvoltage. However, as far as very switch time is concerned, it barely depends on the value of

overvoltage.

It is not difficult to explain the course of these graphs/curves. As has already been said earlier (chapter 5), avalanche-like processes are characterized by the fact that at the initial moments of the time, when the changing value of voltage is low, its change occurs with the very low speed and for achievement with this value of any level long time is required. After the changing value achieved certain, sufficient large, value, it begins to grow/rise at a very high speed. Supply to the diode of the starting voltage, which exceeds voltage U_1, is necessary for an increase in the voltage of up to the level, on which the speed of its change would be sufficient large.

Let us now move on to timing of switching [134].

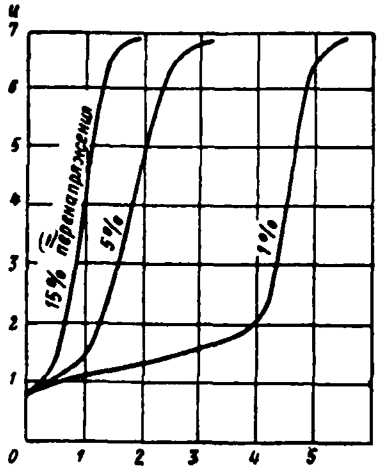

Fig. 7.22. Form of frontal part of voltage pulses on tunnel diode with different values of value of overvoltage.

Key: (1). overvoltage.

Page 398.

At the moment of time t>0 the current of the charge of capacitance (Fig. 7.23)

$$i_C = \frac{E-u}{R} - i_{д},$$

where E - value of voltage, which corresponds to the point of intersection with the straight line AD and axis of abscissas. Rate of the increase of voltage on the capacitance

$$\frac{du}{dt} = \frac{i_C}{C}.$$

The time, during which this voltage will change from value U_1 to U_3, is equal

$$t_2 - t_1 = C\int_{U_1}^{U_2} \frac{du}{i_C}.$$

Let us designate through ΔU difference $U_2 - U_1$ and we will consider that pulse edge is formed/shaped in period, required for changing voltage on capacitance from value $U_1 + 0.1\Delta U$ to value $U_2 - 0.1\Delta U$. Then

$$t_\Phi = C\int_{U_1+0.1\Delta U}^{U_2-0.1\Delta U} \frac{du}{i_C}.$$

Let us consider that $I_C = I_1 - i_д$, where $i_д$ is approximated by function (7.1a).

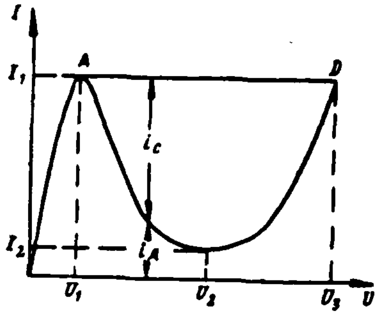

Fig. 7.23.

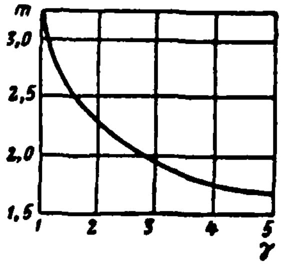

Fig. 7.24.

Fig. 7.23. Determination of switch time.

Fig. 7.24. Dependence of m on γ.

Page 399.

After substituting this expression into the formula for t_Φ, we will obtain

$$t_\Phi = C \int_{U_1+0.1\Delta U}^{U_3-0.1\Delta U} \frac{du}{(I_1 - I_2)\left[1 - \left|\frac{u - U_2}{U_3 - U_2}\right|^{\gamma}\right]} = m(\gamma) R_0 C_0,$$

where m(γ) is certain coefficient. The graph/diagram of dependence of m on γ is given in Fig. 7.24. With γ=3.6-2.8m=2, whence the duration of the front of the positive drop/jump

$$t_\Phi = 2C_0R_0.$$

To analogous results come other authors [126, 141].

Work [140] gives graph/curve, which shows so they are called

switching characteristics of germanium tunnel diodes (Fig. 7.25). It is to the right plotted along the axis of ordinates: N - carrier concentration in the semiconductor of the type n and ρ - resistor/resistance of a semiconductor of the type n. Along the axis of abscissas is plotted the strength of maximum current of diode I_1 and the maximum power P, scattered by diode. To the left along the axis of ordinates is plotted the ratio of the maximum current i_1 to capacitance of C_0 and constant

$$\tau = C_0 \frac{\Delta U}{I_1} \approx 2C_0 R_0,$$

representing the switch time of diode.

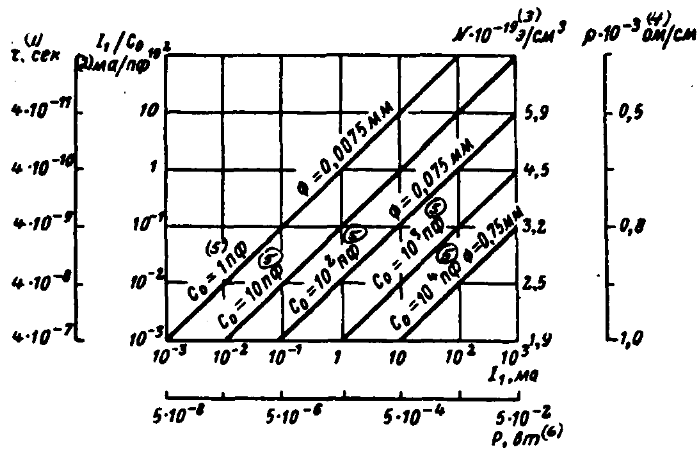

Fig. 7.25. Nomogram for determining parameters of tunnel diode.

Key: (1). s. (2). mA/pF. (3). Oe/cm^3 (4). Ω/cm. (5). pF. (6). W.

Page 400.

The dependences between the values indicated are expressed by the lines, constructed for the different values of the diameter of transition (or capacitance C_0). It follows from Fig. 7.25 that with the capacitance of diode C_0=10 pF and I_1=50 mA the switch time is equal to 0.1 ns.

7.7. MONOSTABLE FLIP-FLOP ON THE TUNNEL DIODE.

Monostable flip-flop on tunnel diode represents system, which possesses by one stable and one by unsteady states of equilibrium. In initial state the diagram is in the steady state; trigger pulse moves it into unsteady state, from which it under the action of external

reasons comes again into the steady state. For the monostable flip-flop on the tunnel diode is characteristic the fact that the full-load saturation curve intersects volt-ampere characteristic only at one point (see Fig. 7.16b).

Let us examine processes, which occur in diagram (Fig. 7.26) in the case, when full-load saturation curve intersects volt-ampere characteristic of tunnel diode at point A (Fig. 7.27). In this state on the tunnel diode operates voltage U_a and through it flows current I_a. Under the action of external voltage (trigger pulse), the full-load saturation curve is moved to the right; operating point passes from position A to position B, and then rapidly jumps to position C. Inductance L_1 supports the constancy of current at the moment of switching. After migration/jump the operating point begins slowly to be moved from position C to position D. At this time the energy, accumulated in the inductance coil, gradually is scattered on the effective resistance of diagram and the current through the inductance decreases.

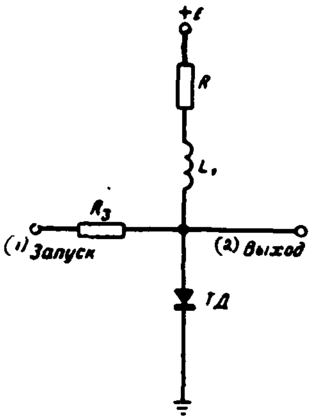

Fig. 7.26. Schematic diagram of monostable flip-flop.

Key: (1). Starting/launching. (2). output.

Page 401.

When operating point falls into position D, it abruptly passes to left branch of volt-ampere characteristic to position E. At this moment of time begins the increase of the current through the tunnel diode and, therefore, through inductance L_1. Magnetic energy of inductance coil begins to grow/rise; the battery, which feeds diagram, is its source. Operating point is moved from E to A. The last position of operating point is stable, and in it it is found until trigger pulse again enters the diagram.

Process, which occurs in monostable flip-flop, can be broken into four stages. The first, during which operating point jumps from position B to position C, is a stage of the formation of the pulse edge or straight/direct switching. The second stage, during which the operating point passes from position C into D, is a stage of shaping of pulse apex. Third stage - the migration/jump of operating point from position D into E - the stage of the formation of the shear/section of pulse or reconnection (jettisoning). Finally, the fourth stage, which corresponds to the transition/junction of operating point from position E into A, the stage of restoration/reduction.

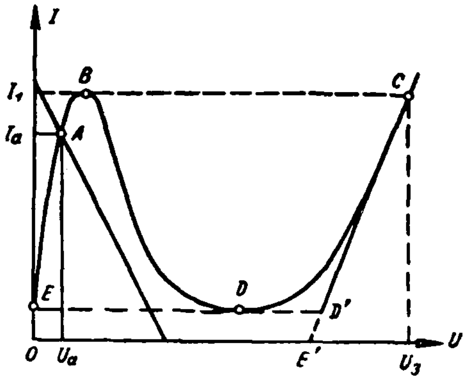

Fig. 7.27. Determination of recovery time t_3 and duration of pulse $t_и$.

Page 402.

Process of switching diagram on tunnel diode has already been examined earlier; therefore let us now pause only at determination of time, required for shaping of apex/vertex (and approximately equal to duration of pulse $t_и$), and recovery time $t_в$. We linearize the volt-ampere characteristic of tunnel diode in the manner that it is shown in Fig. 7.27. Then the tunnel diode in section CD' can be represented as the source of voltage E_1, which possesses internal resistor/resistance $R_{д2}$, shunted by capacitance of C_0 (Fig. 7.28). Equivalent oscillator circuit will contain also supply of power E, inductance L_1 and resistor/resistance R. Since the process of the displacement of operating point from B in C is comparatively slow, in the examination of it it is possible to eliminate the effect of transition capacitance C_0.

Equation, which is used for determining the pulse duration, i.e., transit time of operating point for section CD', in operational form takes form [142, 143]

$$(pL+R_{з})\,I(p)=\frac{U_{з}-E_1}{p}+I_1L_1,$$

since at moment of time, which corresponds to determination of operating point in position C, current $I_0=I_1$. Here $R_{з}=R+R_{дз}$.

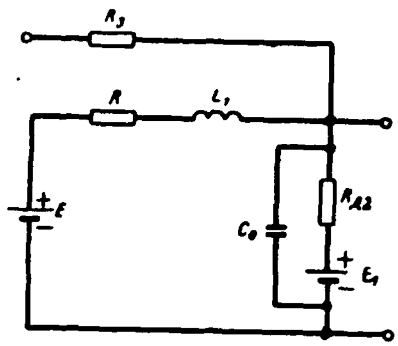

Fig. 7.28. Equivalent schematic of monostable flip-flop for stage of shaping of pulse apex.

Page 403.

The solution of this equation takes the form

$$I(p)=\frac{U_2-E_1}{L_1}\frac{1}{p\left(p+\frac{R_2}{L_1}\right)}+\frac{I_2}{p+\frac{R_2}{L_1}}$$

or in another recording

$$i(t)=\left(I_2+\frac{E_1-U_2}{R_2}\right)e^{-t/\tau_2}+\frac{U_2-E_1}{R_2},$$

and voltage on the diode

$$u(t)=i(t)R_{Д2}+E_1=$$
$$=R_{Д2}\left[\left(I_2+\frac{E_1-U_2}{R_2}\right)e^{-t/\tau_2}+\frac{U_2-E_1}{R_2}\right]+E_1,$$

where $\tau_2=L_1/R_2$.

Assuming $u(t_и)=U_2$ and solving equation relatively $t_и$, we will have

$$t_{\text{и}} = \tau_2 \ln \frac{I_2 + \frac{E_1 - U_2}{R_2}}{\frac{U_2 - E_1}{R_{\text{д}2}} - \frac{E_1 - U_2}{R_2}};$$

Analogously can be determined recovery time of diagram on tunnel diode. Equation for this interval of time according to the equivalent diagram, shown in Fig. 7.29, will be recorded as follows:

$$(pL_1 + R_1) I(p) = \frac{1}{p} E + I_0 pL_1.$$

Here $R_1 = R + R_{\text{д}1}$, where $R_{\text{д}1}$ - resistor/resistance of tunnel diode in section EA; I_0 - current, determined by initial conditions.

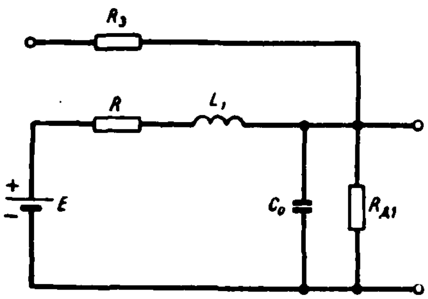

Fig. 7.29. Equivalent schematic of monostable flip-flop for stage of restoration/reduction.

Page 404.

Solution of equation takes form

$$I(p) = \frac{E}{pL\left(p + \frac{R_1}{L_1}\right)} + \frac{I_0}{p + \frac{R_1}{L_1}}.$$

After first cycle of oscillations $I_0 = I_1$ and expression for current as function of time will be recorded in the form

$$i(t) = \left(I_1 - \frac{E}{R_1}\right) e^{-t/\tau_1} + \frac{E}{R_1},$$

where $\tau_1 = \frac{L_1}{R_1}$.

Output potential of diagram

$$u(t) = i(t) R_{\text{Д}1} = \left[\left(I_1 - \frac{E}{R_1}\right) e^{-t/\tau_1} + \frac{E}{R_1}\right] R_{\text{Д}1}.$$

For determining the duration of the restoration/reduction of diagram let us place $u(t_{\text{В}}) = U_1$ and mode equation relatively $t_{\text{В}}$:

$$t_{\text{В}} = \tau_1 \ln \frac{E - I_1 R_1}{E - U_1 R_1 \, R_{\text{Д}1}}.$$

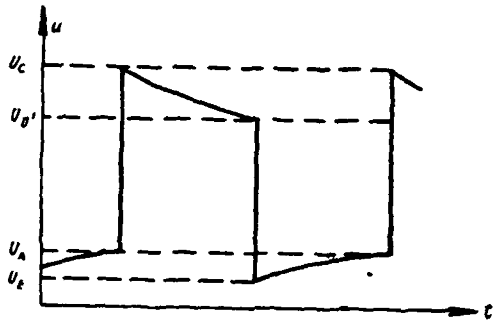

Fig. 7.30. Shape of pulse at the output of monostable flip-flop.

Page 405.

Into this formula enters value $R_{Д1}$ which is determined according to characteristic of diode as follows:

$$R_{Д1} = U_1/I_2,$$

then

$$t_в = \tau_1 \ln \frac{E - I_1 R_1}{E - I_2 R_1}.$$

Shape of pulse at output of monostable flip-flop is shown in Fig. 7.30.

Oscillatory period, which corresponds to maximally possible frequency of work of flip-flop, will be defined as sum of time, spent on shaping of apex/vertex, and time, spent on restoration/reduction of diagram, whence

$$F_{макс} = \frac{1}{t_и + t_в}.$$

Above was examined case, when full-load saturation curve intersected left branch of volt-ampere characteristic of tunnel diode. Is feasible such operating mode, during which the full-load saturation curve intersects right branch. The direction of the motion of operating point for this case is shown in Fig. 7.31, and the form of the obtained voltage - on Fig. 7.32. Trigger pulse must have negative polarity.

Above has already been indicated that approximation of volt-ampere characteristic of tunnel diode by line segments cannot be considered satisfactory on high level of signal, which occurs in generators. Therefore the conclusions, made on the base of this approximation, are very approximate; furthermore, they do not give a correct representation about the form of the generatable oscillations.

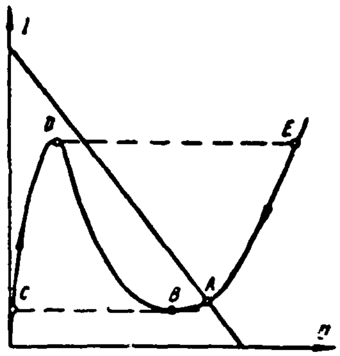

Fig. 7.31. Motion of operating point according to volt-ampere characteristic of tunnel diode.

Page 406.

Data of calculation in the machine of the form of oscillations for the monostable flip-flop taking into account the objective parameter of tunnel diode are cited in [144]. Two curves, which present the dependence of voltage on the tunnel diode from the time with the different values of inductance, are given in Fig. 7.33a and b. As is evident, the form of these oscillations is distant from that, which is shown in Fig. 7.30.

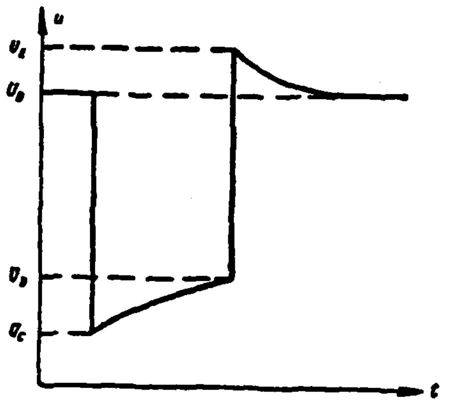

Fig. 7.32. Shape of pulse at the output of monostable flip-flop with change in position of initial operating point.

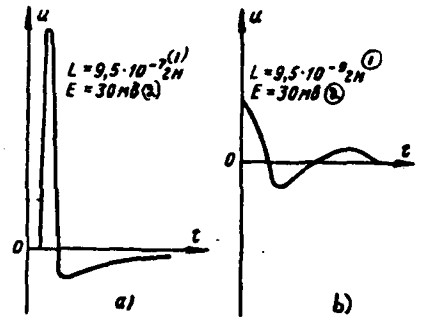

Fig. 7.33. Form of output potential of monostable flip-flop upon consideration of real form of volt-ampere characteristic of tunnel diode.

Key: (1). H. (2). mV.

Page 407. .

7.8. SELF-EXCITED OSCILLATOR ON A TUNNEL DIODE. SOME DIAGRAMS OF FLIP-FLOPS AND GENERATORS.

Self-excited oscillator on tunnel diode differs from flip- flops in terms of fact that full-load saturation curve for it intersects volt-ampere characteristic in section with negative slope/transconductance. Thus, resistor/resistance $R<R_0$; however, the inductance of diagram it is undertaken such value, with which the state of equilibrium in the diagram is unstable. The equivalent diagram of self-excited oscillator with the necessary designations is given in fig. 7.34.

This diagram can be described by system of nonlinear differential equations:

$$\begin{aligned} u &= u_1 + IR, \\ i &= C_0 \frac{du_1}{dt} + i_1(u_1), \\ u &= E + L\frac{di}{dt}. \end{aligned} \tag{7.7}$$

Here $i_1(u_1)$ - equation of the volt-ampere characteristic of tunnel diode.

Allowing/assuming dog-leg approximation of volt-ampere characteristic, it is possible to obtain already known earlier than linear equations, which describe behavior of system into process of shaping of apex/vertex or in reduction process. The results of solving these equations, given in S 7.9, can be used also for determining the period of oscillations and duration of the pulses formed with self-excited oscillator.

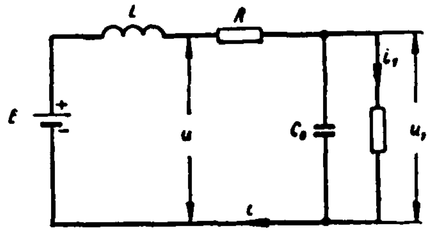

Fig. 7.34. Equivalent diagram of self-excited oscillator on tunnel diode.

Page 408.

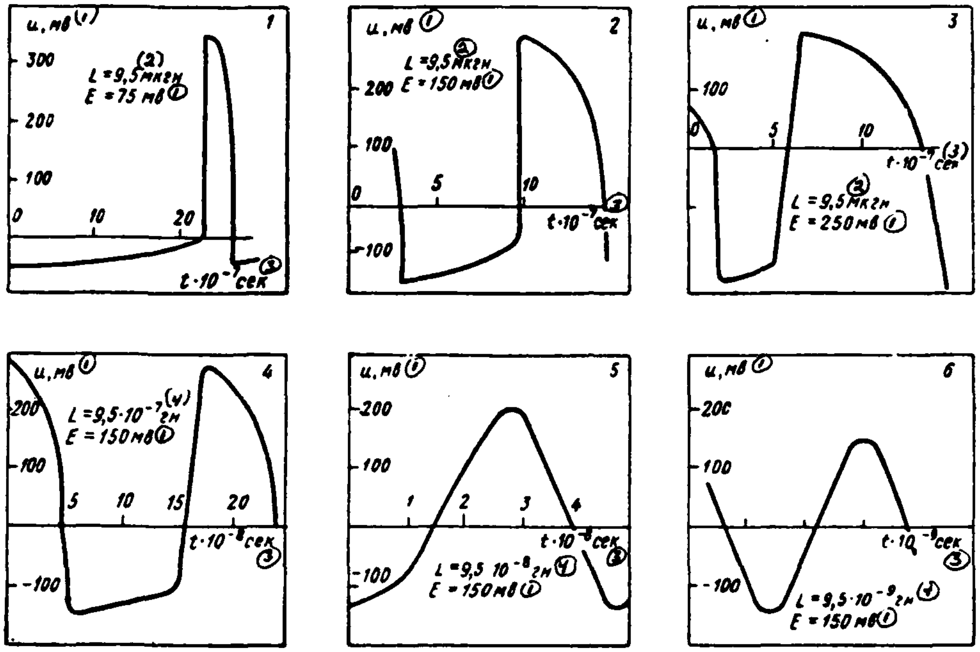

Fig. 7.35. Shapes of pulses, generated by diagram on tunnel diode, depending on position of operating point on volt-ampere characteristic (upper row) and in dependence on value of inductance (lower row).

Key: (1). mV. (2). μH. (3). s. (4). H.

Page 409.

Therefore, without stopping at the analysis of generator with the linearized characteristic, let us give the results of solving the system of equations (7.7) in digital computer [144] and it is expressed them in the form of graphs/curves (Fig. 7.35). In the upper row the diagrams of voltage on the diode in the dependence on the characteristic of point on the characteristic of diode, shown in Fig. 7.36 (on the characteristic of the position of operating point they are designated by the numerals, which correspond to the number of

figure in the upper series/row), are given, whence it follows that the displacement of the position of operating point over the characteristic leads to a noticeable change in period and pulse duration. This fact cannot be discovered by the theory, which is based of a piecewise-broken approximation of the volt-ampere characteristic of diode. In the lower row of curves (Fig. 7.35) the diagrams of voltage on the diode in the dependence on value L are given. With a decrease in the value of inductance the frequency rises, and their form approaches sinusoidal.

Results given above show that form of oscillations in generators on tunnel diodes depends substantially on position of operating point on characteristic and relationship/ratio of parameters of diode and external circuit. This fact indicates that to the conclusions, made on the base of the piecewise-broken approximation of the characteristic of diode, it is necessary to relate with the precaution.

In [145] is described schematic of monostable flip-flop on tunnel diode from gallium arsenide with germanium diode of connection/communication. In the diagram (Fig. 7.37) was utilized the tunnel diode IN3118 and germanium diode ID3-050.

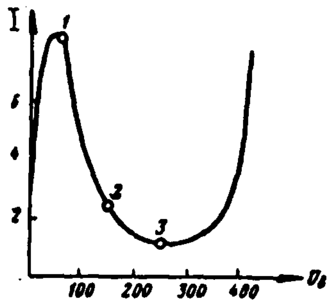

Fig. 7.36. Positions of operating point on volt-ampere characteristic of tunnel diode.

Page 410.

Full-load saturation curve (resistance/resistor of the load of 13 ohms) crossed the volt-ampere characteristic of diode at point somewhat more left than the maximum of current, i.e., diagram worked approximately in the same mode, as the monostable flip-flop, the diagrams of voltage for which were given in Fig. 7.33. This diagram made it possible to form/shape the pulses of the pointed form, which closely coincides with the calculated form, shown in Fig. 7.33a. The pulse duration was determined by inductance L. With L=0.33 μH it was approximately 4 ns, also, with L=0.68 μH - approximately 8 ns. The authors gave the graph/curve, from which it followed that the pulse duration in the sufficiently broad band of a change in the inductance is the linear function of inductance.

Besides diagrams on one tunnel diode are utilized two or more tunnel diodes. Fig. 7.38 shows two schematics of bistable flip-flops

- the first with the inductive, and the second and with capacitive coupling [146]. In the diagram with the inductive coupling supply voltage is taken by such, that one of the diodes is opened when the other diode is closed. A difference in the currents of two diodes passes through inductance. In state of rest the voltage on the inductance is equal to zero. When the input voltage changes over diode, opening it, the voltage which closes the second (open) diode, appears on the inductance.

Systems described above were pulse generator circuits with lumped parameters. Tunnel diodes make it possible to perform generators, also, with the distributed circuits, since they are coupled well with the distributed systems, for example with the strip lines.

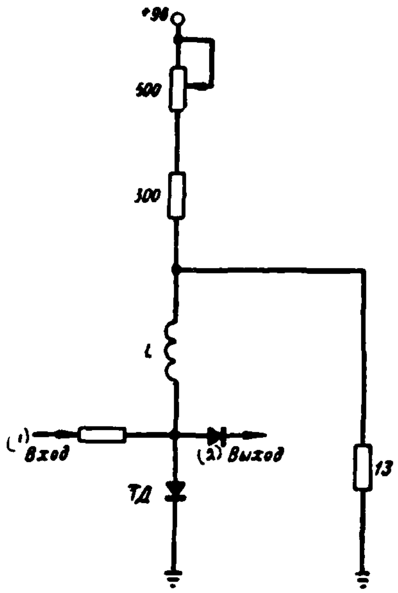

Fig. 7.37. Schematic of monostable flip-flop on tunnel diode. Key: (1). Input. (2). Output.

Page 411.

Theoretically question about excitation of long line by negative resistance was examined by A. Witt as early as 1936 [147]. The method given was used [148] for the analysis of generator with the tunnel diode. The diagram investigated by it was the section of long line, at one end/lead of which were connected they will short circuit the diode and supply of power, and the other is short-circuited.

If the operating point was established/installed in section of characteristic of tunnel diode with negative slope/transconductance, then in the diagram oscillations were excited. In the general case the voltage and current in the generator have very complex stepped

form. The simplest forms of oscillations - square pulses of voltage, were obtained with the low wave impedance; with an increase in the wave shape drag of oscillations became complicated and with $\rho\to\infty$ took the form, which reminds the form of oscillations in the generator with the lumped parameters.

Oscillatory period in simplest case, when form of oscillations is rectangular, has minimum value, equal to $4t_3$ (where t_3 - delay time of oscillation with passage along line). Are possible also oscillations, also, with the considerably larger period. For practical purposes the greatest interest they will represent, apparently, the simplest types of oscillations.

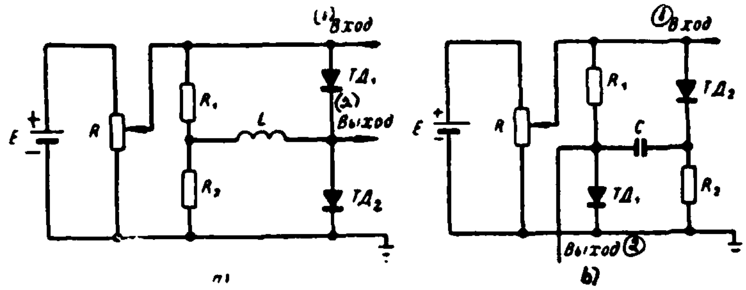

Fig. 7.38. Pulse generator circuits on two tunnel diodes: a) with inductive; b) with capacitive coupling.

Key: (1). Input. (2). Output.

Page 412.

The authors conducted experimental research, which confirmed the forecast theoretically complicated vibration modes. In the line with a wave impedance of 75 ohms were obtained the pulses of pointed form by duration on the foundation of approximately 50 ns and with an amplitude 0.25-0.3 V.

From point of view of nanosecond pulse technique these results cannot consider good; but authors did not set as their goal to obtain maximally narrow pulses. In the diagrams the considerably best results can be obtained, especially if we replace cable with strip line with the low wave impedance.

Fig. 7.39 gives two practical oscillator circuits of pulses, which use cable as time-assigning element [141]. Diagrams on the tunnel diodes, using elements with the lumped parameters, are

characterized by very low frequency stability. The frequency of the vibrations of such generators depends very greatly on a change in supply voltage.

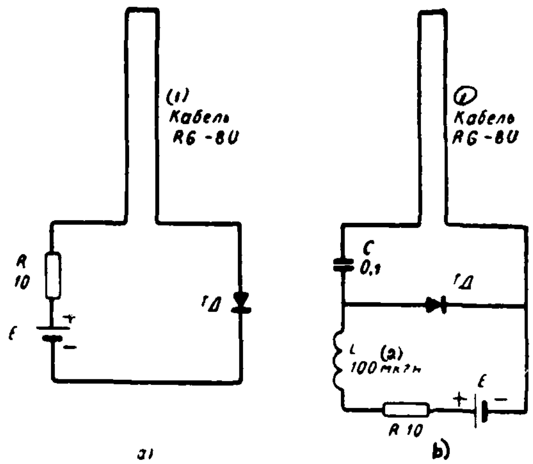

Fig. 7.39. Oscillator circuits, which use cable as time- assigning element: a) consecutive; b) parallel connection of network elements. Key: (1). Cable. (2). µH.

Page 413.

In the oscillator circuits, which use long lines, the oscillatory period is determined by time of landing run of signal along the line and virtually it does not depend on a change in supply voltage. In the first diagram tunnel diode, supply of power and short-circuited cable are connected in series, and secondly - in parallel.

Fig. 7.40 gives oscillograms of output potentials of first diagram taken for three values of bias voltage: 0.12; 0.18; 0.26 V. As can be seen from figure, the oscillatory period virtually does not depend on bias voltage. (In the absence of line oscillator frequency with this change in supply voltage it is changed approximately two times). The duration of the pulse edges is approximately 10 ns, but

it can be reduced during an improvement in the construction/design of generator.

7.9. IMPULSE CIRCUITS ON SEMICONDUCTOR SWITCHES.

Semiconductor switches consist of three series-connected p-ns junction as this shown in Fig. 7.41. Devices/equipment with this structure possess the specific volt-ampere characteristic, represented in Fig. 7.42. During the supplying to the diode of positive voltage to the p-emitter and negative to the n-emitter, in it there begins to flow the current, as in the usual diode.

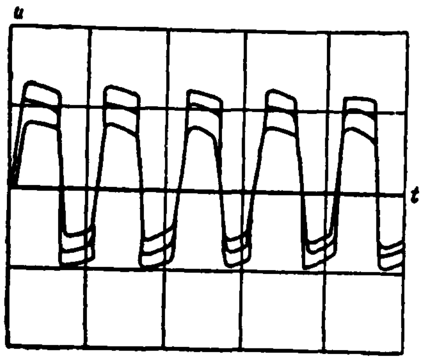

Fig. 7.40. Oscillograms of output potential of generator at different values of bias voltage.

Page 414.

Differential resistor/resistance of diode with this is very great and composes hundreds of megohms. The current grows with an increase in the voltage and at the voltage $U_{пер}$ there occurs breakdown After breakdown the voltage on the diode falls, and the current rises. The section with the negative differential resistance appears on the characteristic. When current reaches value $I_{выкл}$, on the diode operates voltage $U_{ост}$. During the supplying to the changing over diode of voltage $u>U_{пер}$ the instrument is changed over into the conducting state. The input resistance of the open diode is 0.5-1 ohms.

Data of some samples of semiconductor switches [149] let us give in Table 7.4.

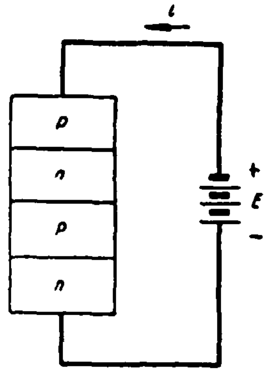

Fig. 7.41 circuit diagram of four-layer diode into external circuit.

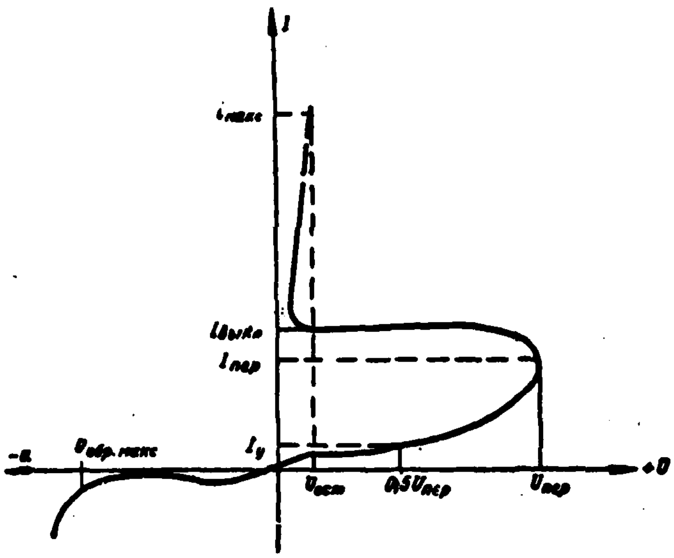

Fig. 7.42. Volt-ampere characteristic of four-layer diode.

Page 415.

Simplest example of diagram on changing over diode is generator of powerful current pulses Fig. 7.43a. Supply voltage E must be more than the voltage of switching diode. Resistance R must be such so that the current limited to it would not exceed the value of the

current of disconnection. With the closed changing over diode capacitor/condenser C is charged through resistances R and R_{n}.

Table 7.4.

(1) Параметры диодов	2N20D — 2N200D (Si)	WX806 (Ge)
(2) Напряжение переключения	20—200 (3) в	25—250 (3) в
(4) Ток переключения	0—0,2 (5) ма	1—10 ма (5)
(6) Остаточное напряжение	0,9 в (3)	0,5—1 в (3)
(7) Номинальный ток	50 ма (5)	500 ма (5)

Key: (1). Parameters of diodes. (2). Voltage of switching. (3). in. (4). Current of switching. (5). mA. (6). Residual voltage. (7). Rated current.

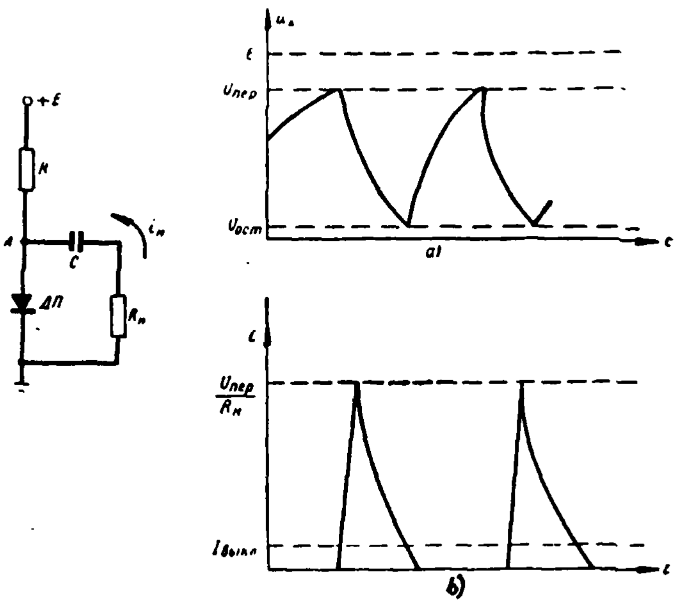

Fig. 7.43. Oscillator circuit of powerful current pulses, voltage oscillogram on diode (a) and current through changing over diode (b).

Page 416.

When potential at point A reaches the value, which corresponds to the voltage of switching, the changing over diode is opened. The capacitor is discharged on the resistance/resistor of load $R_н$ and the changing

over diode. In this case the current in the load virtually is determined by value $R_н$. Capacitor discharge continues until the current through the changing over diode drops to value $I_{выкл}$. At this point the changing over diode returns to the initial state, and cycle is repeated. The diagrams of voltages and currents in the diagram are given on Fig. 7.43b. A similar oscillator circuit makes it possible to obtain with the low resistance/resistors of load (to 100 ohms) current pulses with an amplitude to several amperes with the duration of front of less than 10 ns.

Fig. 7.44 shows schematic of monostable flip-flop with high input resistance. High input resistance is provided by the start of usual diode, as shown in Fig. 7.44. Starting/launching is conducted by pulses of reversed polarity. Fig. 7.45 gives the schematic of bistable flip-flop on two changing over diodes. The circuit parameters are selected so that

$$\frac{E_1}{R_н} > I_{выкл}, \quad \frac{E_1}{R_н} < I_{выкл}, \quad U_{пер} > E_2 > E_1.$$

Let us assume that in initial state changing over diode DP_2 was in conducting state. During the supplying to the input of the diagram of negative pulse occurs the triggering/opening of the changing over diode DP_1. Capacitor C begins to be recharged. During the arrival of the following negative pulse DP_2 remains in the conducting state, and DP_1 is cut off. Switch time and off time are the important parameters of the changing over diode (Fig. 7.46).

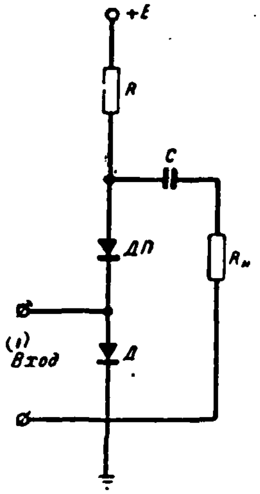

Fig. 7.44. Diagram of monostable flip-flop on four- layer diode.

Key: (1). Input.

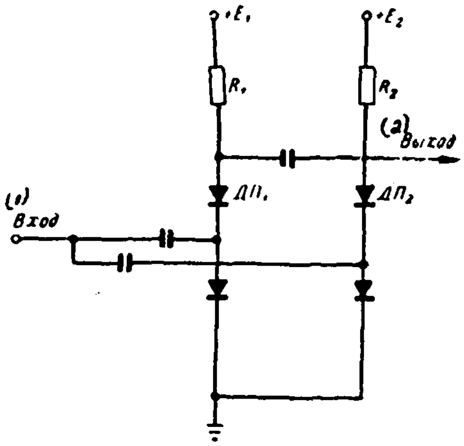

Fig. 7.45. Diagram of bistable flip-flop on four-layer diode.

Key: (1). Input. (2). Output.

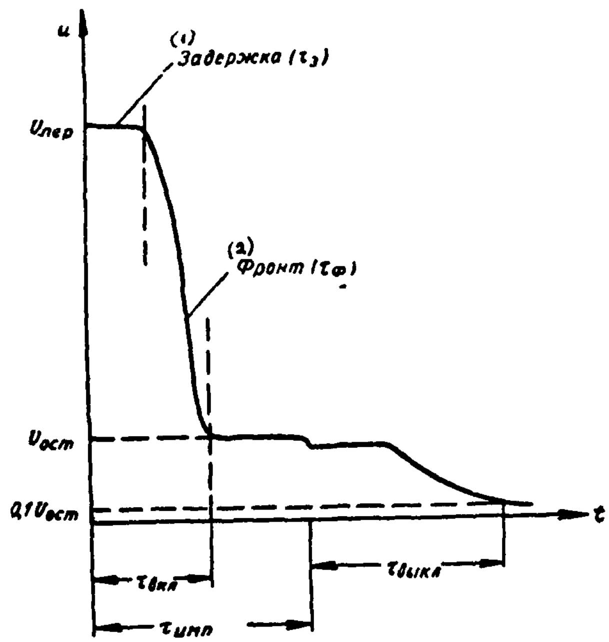

Fig. 7.46. Time characteristics of four-layer diode.

Key: (1). Delay. (2). Front.

Page 418.

This figure gives the oscillogram of a change in the pulse. The time of switching on consists of the delay time and time of front. According to data [149] time of switching on of 200 ns. For the germanium diodes this value composes only of 10 ns, which makes with their interesting for the application in the nanosecond pulse technique. Their high stability to the overloadings with respect to the current is a valuable property of the changing over diodes.

Page 419.

CHAPTER EIGHT.

OTHER METHODS OF IMPULSE SHAPING.

8.1. Impulse shaping in circuits with nonlinear inductance.

In pulse technique recently ever wider application find methods of impulse shaping with nonlinear inductances, which make it possible to obtain "tubeless" oscillator circuits [1].

In forming circuits with nonlinear inductance are utilized properties of nonlinear dependence $B=B(H)$ of ferromagnetic materials (Fig. 8.1). Inductance coils with the ferromagnetic cores in these circuits either are the commutating element during the discharge of the accumulator/storage of energy or the functions of the fundamental forming element are fulfilled.

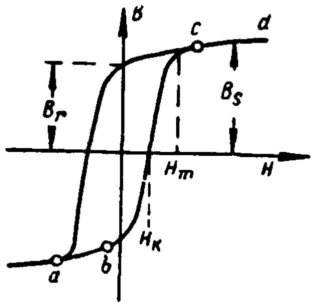

Fig. 8.1.

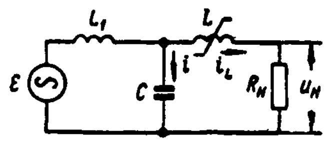

Fig. 8.2.

Fig. 8.1. Hysteresis loop of material of core.

Fig. 8.2. Pulse-shaping circuit with nonlinear inductance.

Page 420.

Fig. 8.2 gives pulse-shaping circuit with nonlinear inductance, which performs role of commutating element. If the core of inductance coil L is made from ferromagnetic square-loop material of hysteresis, i.e., if B_r/B_s is close to unity, then in the process of changing the current strength in the coil its inductive reactance will sharply change from the very low value (when $\mu \approx 1$) to very large (when μ great) and vice versa. Consequently, this inductance coil can be a good commutating element. In the diagram in Fig. 8.2 reservoir capacitor C is charged through choke/throttle L_1 from the source of alternating voltage $\mathcal{E}$. With the aid of the constant magnetic biasing the core of coil L in initial state is in the mode, which corresponds to point b in Fig. 8.1.

Current i_L, which increases strength of field H in core of this

coil, flows/occurs during a charge of capacitor C in coil L. Therefore grows/rises magnetic permeability of core μ and, consequently, also value of inductance L. If condition $L \gg l_1$ is satisfied, then current i_L is small and capacitor/condenser C virtually is charged only through coil L_1. It is possible to fit the parameters of circuit so that the process of charge of capacitor will occur in the oscillatory mode in the presence of the resonance of circuit with a frequency of f of external power supply. Voltage across capacitor in this case changes according to the law

$$u = -UQ(1 - e^{-\alpha t})\cos 2\pi f t,$$

where U - amplitude of the source of alternating voltage;

Q - energy factor of charging circuit;

α - attenuation factor.

Examining only one oscillatory period, it is possible with sufficiently high energy factor of duct/contour to record

$$u = -UQ\alpha t \cos 2\pi f t.$$

For half of oscillatory period voltage across capacitor attains maximum value $u_{макс} = \pi U/2$. and current toward the end of half-period becomes equal to zero.

Page 421.

With a change in direction of flow the capacitor/condenser begins to be discharged, and then to be recharged and to the termination of the

oscillatory period the voltage on it attains the maximum value (in the absolute value), equal to πU. The commutation of circuit must be realized at this moment and capacitor discharge will begin. When capacitor C was charged, current i_L through the commutating coil first increased, reaching maximum to half of the period of oscillations T/2. To the strength of maximum current $i_{макс}$ must correspond the intensity/strength of magnetic field H_m (fig. 8.1). Then for second half-period of current variations i_L, decreasing up to moment/torque t=T, will have small negative value, with which will be created in core field strength, which corresponds to intensity/strength at point b in curve B(H) (fig. 8.1). In this case sharply falls value of magnetic permeability μ and, therefore, inductance L, i.e., commutator operates/wears. From this point on, there begins the capacitor discharge through the effective resistance of load $R_н$, on which is formed/shaped the output pulse. The pulse duration is approximately equal to

$$t_и \approx 0{,}7 R_и C.$$

For obtaining pulse of nanosecond duration time constant of discharge circuit must be small. Furthermore, with the formation of nanosecond pulse the time of commutation must compose a total of several nanoseconds. This is determined by the properties of the material of the core of coil L, i.e., by the form of its hysteresis loop in lower curvature.

In this diagram is formed/shaped pulse, on form which differs

from rectangular. During the replacement of capacitor/condenser on the forming line it is possible to form/shape the pulses, close to the rectangular. Pulse repetition rate can be considerable, but porosity is virtually not more than hundred.

Fig. 8.3 give diagram of formation of nanosecond pulses with coil of nonlinear inductance as commutating element, differing somewhat from preceding/previous [150]. Here the core of coil is prepared also from the ferromagnetic material, characterized by the hysteresis loop, represented in Fig. 8.1.

Page 422.

Sine voltage or trigger pulses with sufficiently steep front can be used as a source of starting voltage. Capacitance value C_1 and inductance L_1 is selected from the condition of obtaining the resonance of circuit with the frequency of external source. With an increase in current i_L, taking place through coil L, grows/rises the intensity/strength of magnetic field in the core of this coil. With an increase in field H the core proves to be in the mode, which corresponds to section bc (Fig. 8.1) hysteresis loop. In this case sharply grows/rises the inductance of coil L and voltage on it $u_L = L di_L/dt$, voltage on circuit CR_n. When field H reaches the value of the saturation of core, further increase in the current does not lead to an increase in the voltage on coil L, but on the contrary, due to the sharp decrease of value L it falls. From this point on, the commutator closes discharge circuit and begins the discharge of the

small capacitance of C through the load resistance/resistor and the low value of inductance $L_{\text{мпп}}$. The shape of the obtained pulse corresponds to the picture of the discharge of the capacitance through inductance $L_{\text{мпп}}$ and resistor/resistance $R_{\text{н}}$. It is desirable so that the value $R_{\text{н}}$ would be close to the critical resistor/resistance of circuit.

Approximate computations of this circuit make it possible to find dependences for evaluation/estimate of pulse duration in different parameters of circuit (Fig. 8.4) [150]. Voltage/stress on load $u_{\text{н}}$ is determined by the expression

$$u_{\text{н}} = -U_C \frac{2}{\sqrt{4k-1}} e^{-t/2kRC} \sin \frac{\sqrt{4k-1}}{2k} \frac{t}{RC},$$

where $k = L_{\text{мпп}}/R^2C$; U_C - voltage across capacitor.

Fig. 8.3. Pulse-shaping circuit with commutating nonlinear inductance.

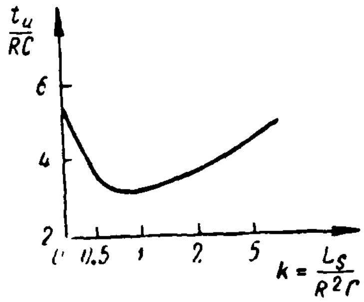

Fig. 8.4. Dependence of pulse duration from parameters of circuit.

Page 423.

For obtaining the pulse of larger slope/transconductance, it is expedient to take value k by equal to one, then, after assigning duration of pulse $t_{и}$, it is possible to find constant value of time $R_{н}C$.

If hysteresis loop noticeably differs from rectangular, then to a different value of saturation current $i_{L\,макс}$ will correspond different value $L_{мин}$, and, consequently, to a certain degree will change duration of formed/shaped pulse with constant value $R_{н}C$.

With impulse shaping of nanosecond duration in this circuit it is

desirable to realize starting/launching of diagram by steep-sided pulse and small duration, for example, obtained from blocking oscillator. Depending on the parameters of circuit and properties of ferromagnetic core the duration of the formed/shaped pulse can be from several ten nanoseconds (or more) to several nanoseconds. The impulse shaping of smaller duration requires the application of the distributed systems, which remove the parasitic circuit parameters, and also the use of considerable circuital currents.

For the normal operation of diagram examined its elements must satisfy following requirements:

a) trigger generator must have high resistor/resistance;

b) starting velocity must be considerable;

c) capacitor/condenser C must have small capacitance in order to have time to be loaded to considerable voltage, but simultaneously sufficiently large so as to ensure necessary power during its discharge, when pulse is formed/shaped.

In similar diagrams as cores of commutating inductance coils can be utilized ferrites with right-angle hysteresis loop, whose data are cited in Table 4.1.

Besides functions of commutating element nonlinear inductance can perform role of forming element. In this case the properties of the material of the ferromagnetic core of coil determine not only triggering time of device/equipment, but also shape of pulse.

Page 424.

Fig. 8.5 gives the diagram of the formation of the nanosecond pulses of high voltage with the spark discharger as commutator [151].

Capacitor C is charged through resistor/resistance of R from dc power supply E. The breakdown occurs after the admission of trigger pulse to the radial deflection terminal of spark discharger P and capacitor/condenser is closed to the discharge circuit. In the lower position of switches the capacitor/condenser proves to be locked directly to the ferrite element. The conductor of the considerable section (with diameter to 20 mm) with a length of about 40 mm with the ferrite rings put on to it is ferrite element. During the capacitor discharge through the conductor of ferrite element is passed current as value on the order of 100 a., which creates the magnetic field, which saturates ferrite, and its permeability μ proves to be close to one. However, magnetic permeability of ferrite is great with the low values of current in the process of its build-up/growth and is great the inductance of ferrite element. Therefore, on the inductance the voltage pulse by value

$$U_L = L_0 \mu(t) \frac{di}{dt},$$

where L_0 - inductance of ferrite element with the saturated ferrite, appears.

Depending on type of ferrite time of its switching with assigned impulse steepness of current is different.

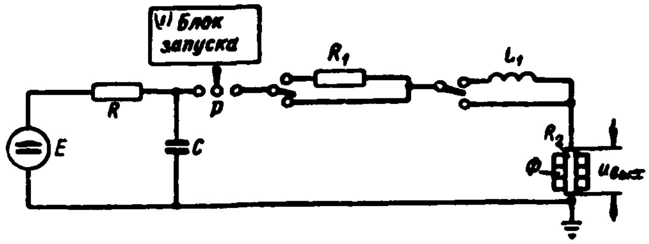

Fig. 8.5. Pulse-shaping circuit with ferrite element and spark discharger.

Key: (1). Unit of starting.

Page 425.

Therefore the duration of the formed/shaped pulse with the different ferrites proves to be different. For removal/taking and recording the voltage pulse in parallel to ferrite element is switched on the ohmic divider R_2.

If into the discharge circuit supplementary inductance L is introduced besides ferrite element, then is obtained series of bipolar pulses with decreasing amplitude, following with natural vibration frequency discharge circuit of capacitor/condenser. Capacitance value C exerts a small effect on the duration and the pulse amplitude, but, changing it, it is possible to regulate the pulse repetition rate and their number in the series. Introduction to the discharge circuit of the supplementary resistor/resistance R_1 makes it possible to obtain single pulses.

Change in supply voltage leads to change in amplitude of pulses and their duration. With an increase in the voltage the pulse amplitude increases, and their duration decreases, since ferrite reverses magnetism more rapidly.

For impulse shaping with duration of order of one nanosecond similar diagram must be free from parasitic parameters of circuit, which requires its appropriate design.

In diagram with spark discharger it is impossible to obtain periodically following pulses of sufficient stability. With its aid single pulses or burst of pulses can be obtained.

Fig. 8.6 gives pulse-shaping circuit of high voltage with thyratron as commutating element and nonlinear inductance. This diagram can form/shape the periodically following pulses of large power [152].

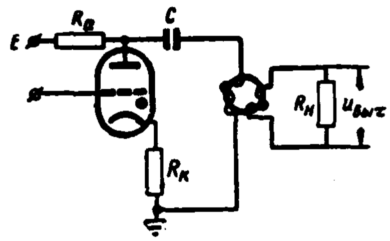

Fig. 8.6. Pulse-shaping circuit with nonlinear inductance and thyratron.

Page 426.

The capacitor/condenser of small amount of capacitance C (about 100 pF) in the initial state is charged/loaded through resistor/resistance R_a from the dc power supply E. The thyratron is triggered after the admission of trigger pulse and capacitor/condenser C is discharged through the coil of the nonlinear inductance, the thyratron and resistor/resistance $R_к$.

Coil of nonlinear inductance is winding, plotted/applied to toroidal core from ferromagnetic material (supermalloy). On the same core is arranged/located the second - output winding, connected with the resistance/resistor of load $R_н$.

Current, which creates in core magnetic field, which rapidly leads it to saturation, flows during capacitor discharge through powerful thyratron over coil of nonlinear inductance. For rise time of current in the coil and magnetic field in the core magnetic

permeability of the latter varies from the value, close to one, to high value and then upon the saturation of core it falls to the value, close to one. The inductance of output coil for this time also varies from low value to large and again takes low value upon the saturation of core.

As a result of this on output winding pulse of approximately triangular form is formed/shaped. The pulse duration depends on the rate of the magnetic reversal of core, which in turn depends on rate of change in magnetic field dH/dt. Depending on the ionization time of thyratron, on the strength of its current and value of the parasitic parameters of discharge circuit rate of change in the current and, consequently, also magnetic fields will be different.

Use of a powerful thyratron makes it possible to obtain pulses at output of diagram by duration about 5 ns with amplitude of 10 kV.

Accurate fulfillment of mounting (for eliminating parasitic circuit parameters), selection of core and thyratron make it possible to form/shape in this diagram pulses of high voltage with duration of front of less than nanosecond.

If in diagrams with linear forming lines and by thyratron does not succeed in obtaining pulse edge of less than ionization time of thyratron, then in this diagram pulse edge due to nonlinear inductance can be less than ionization time of thyratron almost to whole order.

Page 427.

Calculation of such diagrams is complex, since it must consider series/row of nonlinear dependences (nonlinear inductance, nonlinear resistance of thyratron), and also process of magnetic reversal of core. However, the selection of the optimum mode of operation of diagram does not cause experimentally special difficulties.

Pulse repetition rate in this diagram is determined by thyratron. The stability of the sequence of pulses is determined also by thyratron and to a certain extent can depend on the core of nonlinear coil.

8.2. Electronic methods of impulse shaping.

For the formation of nanosecond pulses with very high repetition frequency, measured by hundred megahertz, electronic methods are used. These methods consist in the fact that from the continuous electron stream in the special vacuum devices/equipment form/shape the "packets" of electrons, the being short-term current pulses. Current pulses, flowing through the load connected to the collector/receptacle, isolate on it the voltage pulses.

There are several methods of formation of short-term bundles of electrons; so-called klystron method is most known of them. The high-frequency oscillations of the sinusoidal form, created by special generator, are supplied to the modulator of vacuum-tube instrument.

Electron stream, passing through the modulator, periodically is braked or is accelerated by the field of high-frequency oscillator, are formed electronic clusters. These clusters are recovered by collector/receptacle and create on termination of instrument the voltage pulses.

A pulse generator of klystron type (it would be it is more accurately speak about klystron type shaper) differs from klystron oscillator in terms of shf by the absence of feedback, and also in terms of fact that instead of output resonator aperiodic system serves as its load (cable). From the description of the operating principle of instrument it is evident that the pulse repetition frequency is determined by the frequency of the sinusoidal vibrations, supplied to the modulator, and can be obtained by very high.

Page 428.

Thereby there is obtained the short duration of the formed/shaped pulses, which composes part of the oscillatory period. However, as far as the amplitude of formed/shaped pulses is concerned, it depends on the current strength in the ray/beam of vacuum-tube instrument.

One of klystron type oscillators is schematically depicted in Fig. 8.7 [153]. Sine voltage with a frequency of 210 MHz is supplied from high-frequency oscillator 1 of resonator 2. This resonator is connected to two grids of electric vacuum tube 3 and creates a potential difference 400 V between them. Electron beam, passing

through the field between the grids, is modulated on the rate. In drift space (length of which is equal to 400 mm) occurs electron bunching on the density. The formed electronic clusters are recovered by the collector/receptacle, which is the continuation of the internal core of a 70-ohm cable 4. The external conductor of cable terminates by grid, which is located before the collector/receptacle. The described diagram made it possible to obtain pulses by the duration of 0.2 ns. The pulse amplitude, measured by indirect methods, comprised the portions of volt.

Another sample of pulse generator of klystron type was described into [154]. Its construction/design took approximately the same form, as represented in Fig. 8.7. To the resonator was fed/conducted the voltage from the oscillator with an shf frequency of 100 MHz. The voltage between the resonator grids was 3000 V; power of approximately 150 W was fed for maintaining this voltage to the resonator. For the heat removal from the collector/receptacle the forced cooling was used.

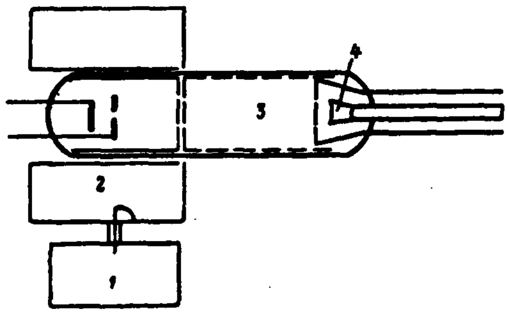

Fig. 8.7. Klystron type electronic shaper.

Page 429.

The 50-ohm cable serves as a load of oscillator. As experimental investigations showed, in this device/equipment is possible the impulse shaping with the duration of 0.3 ns (at the level of half amplitude). The time of the establishment of pulses (on level 0.1-0.9) was 0.1 ns. The pulse amplitude at the output was equal to 15 V, which considerably exceeds the amplitude of pulses, obtained in the preceding/previous oscillator.

For the formation of very narrow pulses tubes with transverse beam deflection can be utilized besides klystron type oscillators. The principle of the work of this oscillator consists of the following. The electron beam is passed between the deflector plates, to which is fed/conducted the voltage from the oscillator of shf (Fig. 8.8). Under the action of this voltage the electron beam completes oscillations, passing twice during the period of high-frequency oscillation along electrode 3. On the electrode there is a special

slot through which they pass the electrons, recovered then by collector/receptacle 1, as which the internal conductor of coaxial cable can serve.

Duration of pulses, generated by tube with transverse beam deflection, can be calculated by formula

$$t_{\text{и}} = \frac{\arcsin \frac{E}{2U}}{\pi f},$$

where E - deflecting voltage, necessary for change-over of ray/beam;

U - amplitude of radio frequency voltage;

f - its frequency.

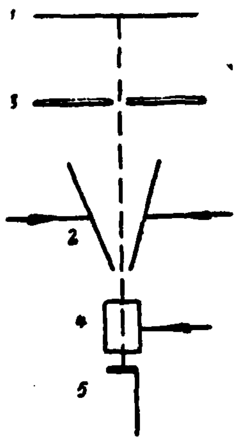

Fig. 8.8. Electronic shaper with beam deflection: 1 - collector/receptacle; 2 - deflector plates; 3 - diaphragm; 4 - control electrode; 5 - cathode.

Page 430.

In particular, for sample of tube, in which E=40 V with U=500 in and f=10 MHz, pulse duration is obtained equal to 1 ns. Oscillators of such type make it possible to comparatively easily obtain pulses by the duration of the units of nanoseconds. A small amplitude of output pulses, which moreover, decreases in proportion to the decrease of the pulse duration, is its deficiency. One of the samples of oscillator on a 100-ohm load made it possible to obtain pulses with an amplitude 0.3-0.5 V for the duration of pulse 1 ns.

8.3. Impulse shaping by limitation and differentiation.

Method of obtaining pulses of short duration by consecutive

limitation and differentiation widely is used in pulse technique of microsecond range; the same method can find to itself and limited application in nanosecond pulse technique.

Let us examine first question about pulse clipping of nanosecond duration. Since pulse clipping on the maximum presents the greatest difficulty, let us pause in essence on this problem. The electron-tube diodes of usual types in the majority of the cases are unsuitable for limiting the nanosecond pulses, since they possess a comparatively high internal resistor/resistance and large stray capacitance. Therefore for pulse clipping in the nanosecond technology are utilized either the semiconductor diodes or the three-electrode and multielectrode tubes, which possess the large ratio of current I_0 to stray capacitance C_0.

L. V. Gorachev [155] conducted research on the schemes of consecutive diode limiter on semiconductor diodes of type DGTs. Limiter circuit is given in Fig. 8.9. Pulses enter the limiter on the cable, loaded to the effective resistance, equal to wave. At the initial moment the diode conducts current, since the voltage of positive polarity from source E is applied to it. Limitation level is determined by the value of the voltage of source E. Resistance plays an important role in this diagram R_a.

Page 431.

This resistance, which is the load resistance/resistor, is the

resistor/resistance of the limitation of the current, which flows through the diode, at the same time. It cannot be less than the value of the ratio of the voltage of limitation E to the maximum permissible current through the diode. However, as far as the capacitance C_0 is concerned, it is the parasitic input capacitance of the subsequent cascade/stage of diagram.

Equivalent limiter circuit in general case takes form, shown in Fig. 8.10a, where $R_д$ and $C_д$ indicate respectively internal resistor/resistance and transfer capacitance of diode. Before the arrival of pulse the diode is opened, and since $R_н \gg R_д + \rho$ and $C_0 \gg C_д$, then equivalent diagram takes the form, depicted in Fig. 8.10b. The voltage

$$E' = E \frac{\rho + R_д}{\rho + R_д + R_н}.$$

is established in the absence of pulse at the output of diagram.

When to the input of diagram pulse there comes a pulse of rectangular shape, the diode will cease to conduct current, then equivalent diagram will take form, shown in Fig. 8.10c.

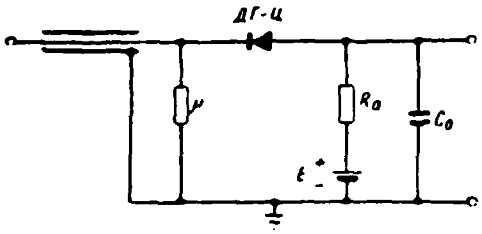

Fig. 8.9. Diagram of consecutive limiter on semiconductor diode.

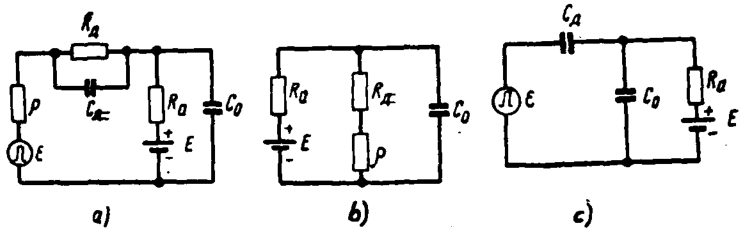

Fig. 8.10. Equivalent limiter circuits.

Page 432.

A drop in the voltage due to the passage of the signal through the capacitance of the diode

$$U_2 = U_1 \frac{C_д}{C_0 + C_д} \approx U_1 \frac{C_д}{C_0},$$

will appear at the initial moment of time at the output of diagram since $C_0 \gg C_д$. Under the ideal conditions during pulse advancing at the output of limiter must operate the voltage of limitation E. Actually, so that this voltage would be established/installed, for a while, determined by product $R_a C_0$ is required·Output potential of limiter will increase according to the law

$$u_{вых}(t) = E\left(1 - e^{-\frac{t}{C_0 R_a}}\right)$$

and the time of its establishment will comprise $2{,}2C_0R_a$.

It is not difficult to conduct timing of establishment of pulses at output of limiter. After taking, for example, E=20 in and after selecting diode DG-Ts7, let us accept the maximum current through the diode 15 mA, which will determine the value of the resistance/resistor of load $R_a = 1340$ ohms. Assuming/setting input capacitance C_0=15 pF, we obtain the time of establishment 44 ns. including four diodes in parallel to each other, we increase the current-carrying capacity in the circuit and obtain $t_y = 11$ ns.

Considerably best results gives application of junction diodes of type DG-Ts23, DG-Ts24, DG-Ts26. Although the diodes of these types possess considerable capacitance; however, the negligibly low resistor/resistance in the straight/direct passage of current is their advantage. As the experiment shows, the limiter on the junction diode virtually does not worsen/impair the pulse edge, but only increases decay in its flat/plane part.

Fig. 8.11. Shape of pulses at the input (a) and output (b) of the limiter.

Page 433.

Fig. 8.11a shows the input pulse with a duration of 45 ns on half of the amplitude, with a duration of the front of 5 ns and amplitudes of 110 V. Fig. 8.11b gives the oscillogram of output pulse on different levels of limitation. As can be seen from oscillogram, the pulse edge virtually is not distorted.

Considerably wider application for limitation find vacuum-tube circuits, carried out on triodes, pentodes and tubes with secondary emission. The suitability of tubes for pulse clipping of nanosecond duration naturally escapes/ensues from their suitability for pulsing. A limiter-amplifier is formed from the relaxation oscillator during interrupting of feedback loop.

Amplifier-limiters of larger partly are used in output stages of pulse generators, in which application of feedback is frequently inexpediently due to presence of effective time lag. In the oscillator of nanosecond pulses, described into [102], the output

stage was limiter on the tube with the secondary emission; its diagram was given earlier in Fig. 6.16. N. Ye. Butorin [3] conducted research of the amplifier-limiter with the transformer; the diagram of this limiter was given in Fig. 8.12. During the use of a tube 6N15P (both triodes they are connected in parallel) to its grid was supplied the pulse of bell-shaped form with the duration of 45 ns at level 0.1 and with an amplitude of 120 V. Pulse $t_и=30$ ns with the same amplitude, but with the plane vertex with a duration of 10 ns was created at the output. During the use of a tube 6S3P in the same diagram was supplied pulse $t_и=20$ ns with an amplitude of 110 V.

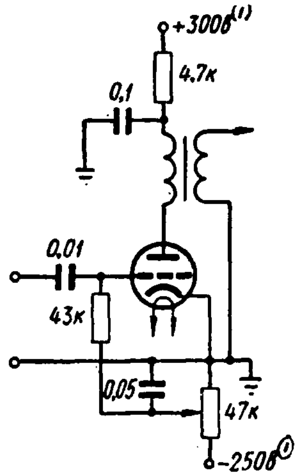

Fig. 8.12. Diagram of amplifier-limiter.

Key: (1). V.

Page 434.

At the output of the diagram there was obtained the pulse of the same duration, but with an amplitude of 90 V. The pulse edge was 4-6 ns. The pulse of the same duration and amplitude was obtained during the supplying to this diagram of pulse $t_{и}=8$ ns with an amplitude of 80 V at the output, but it had a plane vertex with a duration of 4 ns. During the supplying to the diagram of flat-topped pulses, it shortened front and shear/section of pulses.

Amplifier-limiters can effectively be utilized for obtaining pulses of short duration with high repetition frequency from sine voltage. Sinusoidal oscillation consecutively/serially several times is limited and is shortened for this (it is differentiated). Pulse generator of similar type is described into [156]. This oscillator

made it possible to obtain the pulses of nanosecond duration with the repetition frequency several megahertz and an amplitude of hundreds of volts. In the output stages of similar oscillators one should utilize tubes 6P9, 6P13S, GU-29. In more detail about the schematic of this oscillator it will be said below in connection with a question about pulse shortening.

Interesting diagram with nonlinear amplifiers, which makes it possible to obtain pulses with very steep fronts, was described into [157]. The schematic diagram of the basic building block of oscillator is given on Fig. 8.13 and 8.14 they are given the diagrams of voltages/stresses, which elucidate the operating principle of diagram. To the input of transformer and amplifier is supplied a negative drop in the voltage with a relatively steep section (Fig. 8.14a and b).

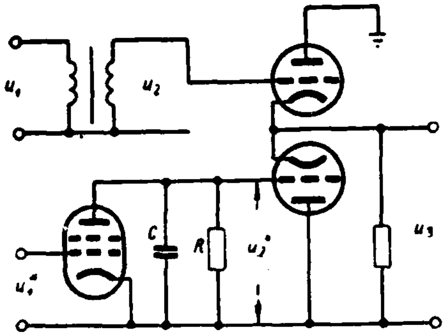

Fig. 8.13. Schematic diagram of nonlinear shaper.

Page 435.

The positive drop in the voltage (d), which has the large duration of front due to the integrating action of the network RC, is obtained at the output of amplifier. At the output of transformer a drop/jump in the voltage is converted into the pulse of exponential form (c) (as a result of the smallness of the primary inductance of transformer). This pulse enters the input of tube L_2, whereas a positive drop in the voltage enters the input of tube L_3; both these tubes are connected in series. As a result on the plate load a positive drop in the voltage with the steep front is obtained (e).

Experimental sample of oscillator was assembled on tubes EL 34 (L_1) and PL 81 (L_2, L_3). Transformer contained 4 turns each in the primary and secondary windings.

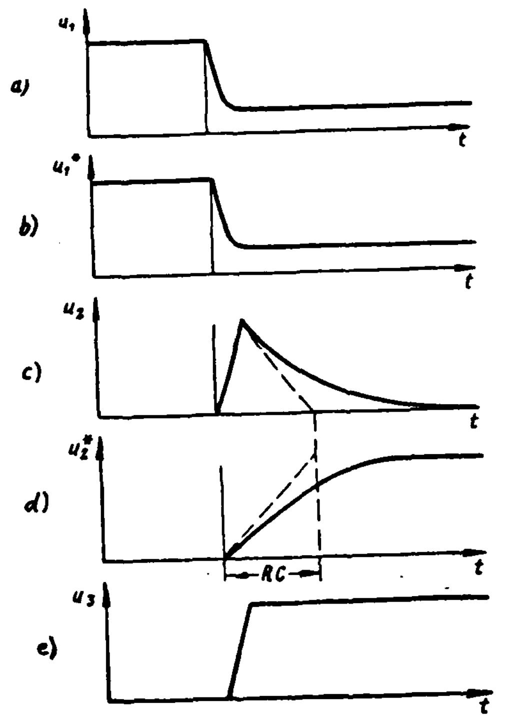

Fig. 8.14. Diagrams of voltages on elements of the shaper.

Page 436.

The core was a ferrite ring with a diameter of 23 mm and μ_0=1300. The diagram made it possible to form/shape drops in the voltage with the very steep fronts; it would have been possible to obtain pulses with the duration in the foundation 3 ns and with an amplitude of 50 V by the subsequent.

Let us pause now at question of shortening of pulse duration.

Simplest shortening circuit is capacitive differentiating circuit, depicted in Fig. 8.15 and which consists of a capacitor of small amount of capacitance C and resistor/resistance R. During the supplying to its input of ideal square pulse with drop/jump E at the output of the circuits are obtained two exponential pulses, whose spread/scope is also equal to E, and the duration, measured at level 5%, comprises 3RC (Fig. 8.16).

For obtaining pulses of short duration it is necessary to take low parameters of differentiating circuit. Thus, for obtaining the pulse with a duration of 6 ns it is necessary to take time constants, equal to 2 ns; this it is possible to obtain with C=40 pF and R=50 ohm. Such values of the parameters are virtually completely acceptable; however, in this case for obtaining the pulses of a sufficient value the output tube, which works to the differentiating circuit, must provide the high strength of output current.

Under actual conditions obtaining very narrow pulses is complicated by two facts: with final rate of build-up/growth of input signal and by presence of parasitic parameters in diagram of differentiating circuit.

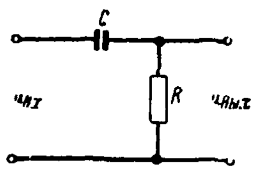

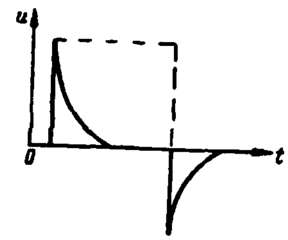

Fig. 8.15. Fig. 8.16.

Fig. 8.15. Capacitive differentiating circuit.

Fig. 8.16. Pulses at the output of the differentiating circuit.

Page 437.

Assuming that the input voltage increases exponentially

$$u_{вх}(t)=E\left(1-e^{-\frac{t}{\eta}}\right),$$

where E - conservative value of input signal, and η - the value which characterizes the slope of growth of the signal, it is possible to find the waveform at the output from known transient response of differentiating circuit. This characteristic takes the form

$$A(t)=e^{-\frac{t}{\tau}},$$

where τ=RC. With the aid of the superposition integral it is easy to determine the output signal, which is expressed equation [2]

$$u_{вых}(t)=E\frac{\tau}{\eta-\tau}\left(e^{-\frac{t}{\eta}}-e^{-\frac{t}{\tau}}\right).$$

Waveform at output of differentiating circuit differs from exponential pulse, examined earlier, by fact that it has final

duration of front and smaller amplitude.

Duration of front of output pulse, if we define it on time of reaching/achievement of maximum, will be expressed as

$$t_{\psi}=\frac{\tau\eta}{\tau-\eta}\ln\frac{\tau}{\eta},$$

and amplitude of pulse

$$U_{\text{вых}}=E\,\frac{\tau}{\eta-\tau}\left[\left(\frac{\eta}{\tau}\right)^{-\frac{\tau}{\eta-\tau}}-\left(\frac{\eta}{\tau}\right)^{-\frac{\tau}{\eta-\tau}}\right].$$

It follows from given formulas that for obtaining narrow pulses with sufficiently large amplitude it is necessary to supply on input of differentiating circuit pulses, equivalent time constant of which η several times of less than time constant of differentiating circuit.

Besides the effect of final rate of build- up/growth of input signal on shape of pulses at output of differentiating circuit, essential effect have parasitic circuit parameters. The complete equivalent diagram of the differentiating circuit taking into account the parasitic parameters is given in Fig. 8.17.

Page 438.

On this figure E - the source of input voltage; R_0 - its output resistance, C_{01} - the input capacitance of source; C_{02} - capacitance of load (for example, the input capacitance of the following tube); C and R - parameters of the differentiating circuit.

Transient processes in differentiating circuit taking into account parasitic parameters were investigated by L. A. Meyerovich [2], who obtained expression for transient response of this circuit:

$$A(t)=EM\left({}^{-\frac{t}{\tau_2}}-e^{-\frac{t}{\tau_1}}\right),$$

where

$$M=\frac{1}{R_0C_2}\,\frac{\tau_1\tau_2}{\tau_2-\tau_1}.$$

In expressions τ_1 and τ_2 written above - time constants, which can be determined according to approximation formulas,

$$\tau_1\approx R_0C_2\frac{1}{1+\frac{R_0}{R}+\frac{C_2}{C'}},$$

$$\tau_2\approx RC'\left(1+\frac{R_0}{R}+\frac{C^2}{C'}\right),$$

where

$$C'=\frac{C^2}{C+C_{01}},$$

$$C_2=C_{02}+\frac{C_{01}C}{C_{01}+C}.$$

An error in these formulas is less than 10% in such a case, when any of the ratios R_0/R or C_2/C' will be less than 0.5.

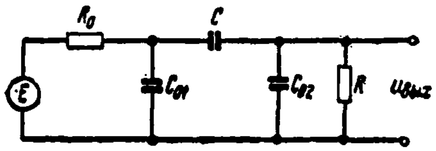

Fig. 8.17. Equivalent diagram of differentiating circuit.

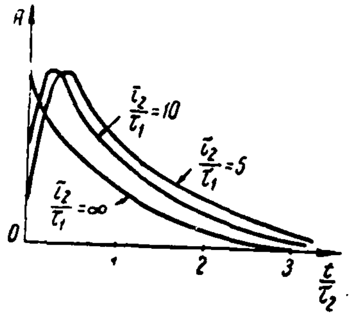

Fig. 8.18. Transient responses of real differentiating circuit.

Page 439.

Form of transient response of differentiating circuit taking into account parasitic parameters is given in Fig. 8.18 at three values of relation τ_2/τ_1 [2]. The maximum value of pulse at the output of the differentiating circuit can be determined according to the approximation formula

$$U_{вых} \approx \frac{EZ_{макс}}{1+\frac{R_0}{R}+\frac{C_2}{C'}},$$

where value $Z_{макс}$ is depicted graphically in Fig. 8.19.

Inductive differentiating circuit is another form of shortening circuit. During the supplying into this circuit of ideal square pulse not its output are obtained the same pulses, as at the output of the

capacitive differentiating circuit. However, upon consideration of the parasitic parameters the inductive differentiating circuit possesses a number of special features.

In practical diagrams, one of which is given in Fig. 8.20, the inductance of the differentiating circuit together with stray capacitance forms oscillatory circuit. For obtaining the narrow pulses, the critical behavior of the work of the circuit is frequently utilized.

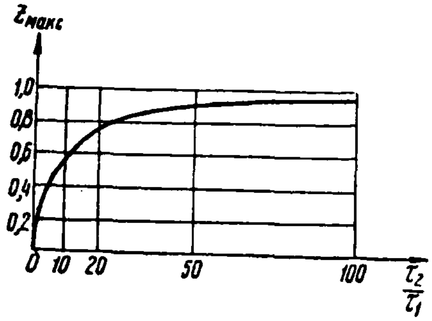

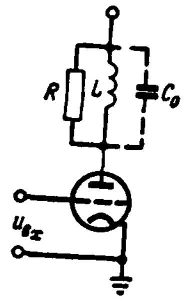

Fig. 8.19. Fig. 8.20.

Fig. 8.19. Dependence of coefficient $z_{\text{макс}}$ on ratio τ_2/τ_1.

Fig. 8.20. Diagram of inductive differentiating circuit.

Page 440.

In this case edge voltage changes according to the law

$$u(t)=\frac{I}{C_0}\,e^{-\alpha t}\,t,$$

where I - value of current taper in the circuit equal to the short-circuit current of tube;

C_0 - stray capacitance;

$\alpha=\frac{R}{2L}$ (R— impedance of ohmic losses in the duct/contour).

Form of edge stress is shown in Fig. 8.21. Maximum output potential of circuit with

$$t_1=\sqrt{LC_0}$$

acquires importance

$$U_{\text{макс}}\approx 0{,}74\,I\sqrt{\frac{L}{C_0}}.$$

Inductive differentiating circuit has series/row of advantages in comparison with capacitive. It makes it possible to obtain the pulses of the sufficiently large amplitude, even which exceeds the value of supply voltage.

The inductive differentiating circuit was theoretically investigated in [156], where differentiation of current taper with final duration of front is examined.

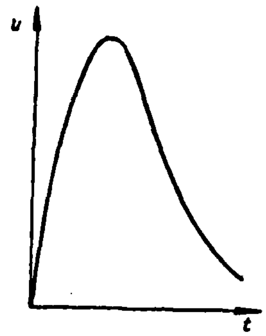

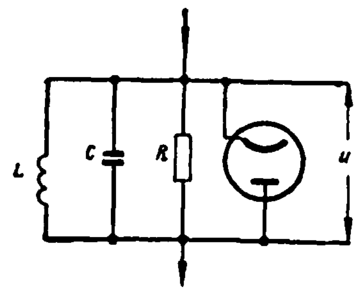

Fig. 8.21. Fig. 8.22.

Fig. 8.21 form of edge stress.

Fig. 8.22. Diagram of inductive differentiating circuit with diode.

Page 441.

It is recommended here to utilize the oscillatory mode of the circuit; the optimum value of the energy factor of duct/contour Q=4, and the optimum value of the ratio of a drop/jump in the natural oscillations T_0 to the duration of the front of current taper t_0=2.7. In this case edge stress

$$U_{макс}=0,1\frac{I_0T_0}{C},$$

where I_0 - value of current taper;

C - capacitance of the circuit.

For suppression of oscillations after first overshoot differentiating circuit can be shunted by diode, since it is shown in Fig. 8.22. As the differentiating transformer it is possible to utilize ouncer transformer on the ferrite ring (diameter of ring 15-30)

mm; the number of turns 10-20 depending on the pulse duration). One of the diagrams of amplifier-limiter with the differentiating transformer is given in Fig. 8.23. Resistor/resistance R serves for guaranteeing the required (small) energy factor of duct/contour.

8.4. GENERATION OF RADIO PULSES OF LOW POWER.

Generation of radio pulses of nanosecond duration in the range of superhigh frequencies can be carried out, when period of carrying oscillations comprises portions of nanosecond.

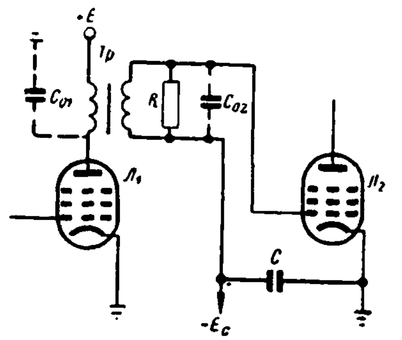

Fig. 8.23. Schematic diagram of a limiter-amplifier with a differentiating transformer.

Page 442.

Therefore as oscillators of the carrier frequency are utilized klystrons, travelling-wave tubes, magnetrons. Magnetrons are utilized usually during the generation of powerful/thick nanosecond radio pulses.

Radio pulses of nanosecond duration of small power initially found use because of need for study of plumbing. For the generation of such pulses, klystrons and LBV were utilized [158-161].

In particular, [158, 159] is proposed and experimentally investigated diagram, which works according to following principle. From klystron oscillator of the carrier frequency they come the input of amplifier on LBV. The amplification of signal occurs only at the moments of acting of front and shear/section of the voltage pulse, supplied to the spiral LBV from the pulse generator. This is caused

by the fact that the amplitude of pulse, supplied to the spiral, corresponds to the interval of accelerating voltage, in limits of which LBV can amplify. Thus, the duration of output radio pulse depends on the jump steepness in the voltage of the nanosecond modulating video pulse. However, with this method of generation noticeable frequency modulation occurs.

Another method of generation of radio pulses with the aid of LBV is based on sufficiently effective and reliable method of modulation on focusing electrode of LBV [160]. Fig. 8.24 gives the dependence of power output of LBV on the voltage on focusing electrode $U_{\text{ф}}$ and is also shown nanosecond video pulse and selection of its value relative to the value of voltage $U_{\text{ф}}$. Travelling-wave tube here works in the mode of the amplification of the oscillations of the carrier frequency.

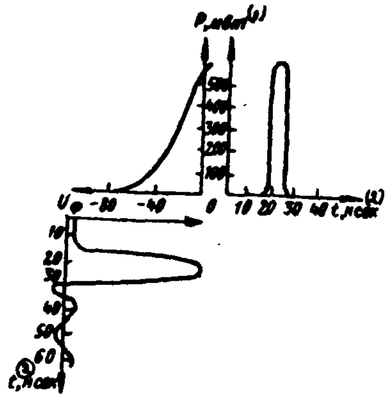

Fig. 8.24. Dependence of power output of LBV on voltage on focusing electrode.

Key: (1). mW. (2). ns.

Page 443.

A large part of the time of LBV is closed due to the negative bias/displacement on the focusing electrode and is triggered after the admission to the modulator of the video pulse of positive polarity. The duration of the generatable radio pulse is determined by the duration of the upper part of the video pulse (Fig. 8.24).

Fundamental oscillator circuit is given in Fig. 8.25. Modulator consists of the input stage of starting (half of L_1), three blocking oscillators (half of L_1 and L_2, L_3), which form the video pulse via its consecutive peaking, and the output stage in the form of amplifier with the transformer output L_4. Video pulse has a duration of 10-15 ns (on the foundation) and an amplitude to 200 V. The oscillations of the carrier frequency from klystron oscillator L_5 come on LBV of

special design [160]. Under the influence of the modulating pulse on the focusing electrode of the LBV the radio pulse generates by the duration of 6 ns (at level 0.5 of amplitude) and by the power of 600 mW.

There is possibility of direct obtaining of nanosecond radio pulses with the aid of LBV and modulator [162]. In this case the need for separate oscillator of the carrier frequency is eliminated. Travelling-wave tube with the self-feedback can oscillate of different types (the discrete spectrum of frequencies). To each type of oscillations corresponds the interval of accelerating voltage, in which this type of oscillations is excited. However, a change in accelerating voltage within the limits of this interval very weakly affects the frequency of the corresponding type of oscillations. Since the interval of the values of accelerating voltage, in limits of which the LBV generates the specific type of oscillations, depends on the strength of the magnetic field of focusing, then, selecting the appropriate intensity/strength of magnetic field, it is possible to establish/install the necessary width of the interval of accelerating voltage.

Fig. 8.26a gives graphs/curves, which elucidate possibility of using dependence of wavelength of oscillations on accelerating voltage for generation of nanosecond radio pulses. With a subject on the accelerating electrode voltage less than U_1, the LBV does not generate.

Page 444.

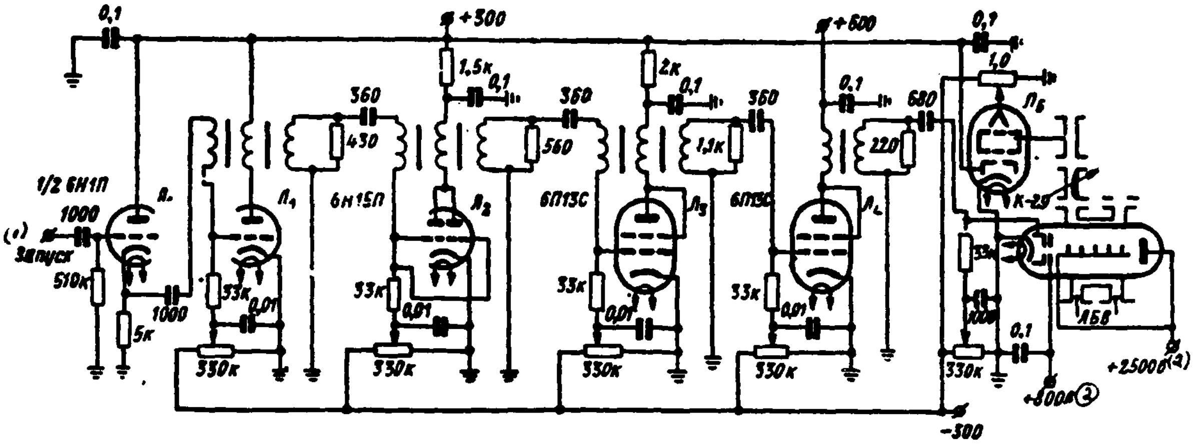

Fig. 8.25. Oscillator circuit of nanosecond radio pulses.

Key: (1). Starting. (2). in.

Page 445.

With an increase in the steep front of accelerating voltage it reaches consecutively levels of U_1 and U_2. The LBV is excited to period t_{u}. for which there occurs a change in the voltage from U_1 to U_2. The form of generated thus radio pulse must they will be determined by the character of the dependence of the generatable power on a change in accelerating voltage within the limits of the range of the excitation of LBV from U_1 to U_2 (Fig. 8.26b).

Duration of generatable pulses can be regulated by change in steepness of edge of pulse of accelerating voltage.

For obtaining nanosecond radio pulses in millimeter wave band is proposed method, in which are utilized reflections of oscillations,

which occur in special shf circuit [163].

Fig. 8.27 gives diagram, which elucidates principle of shaping of radio pulses of millimeter wave band of small power. Radio pulses are obtained with modulation of the continuous oscillations, created by klystron. Energy of fundamental type continuous oscillations, created by klystron 1, enters the input of rectangular waveguide 2, which goes around cone-shaped waveguide expansions, then it passes through the section with ferrite 3, where occurs the rotation of the plane of polarization at angle of 45° and finally it is absorbed by semiconductor diode 4, whose resistor/resistance presents the matched load.

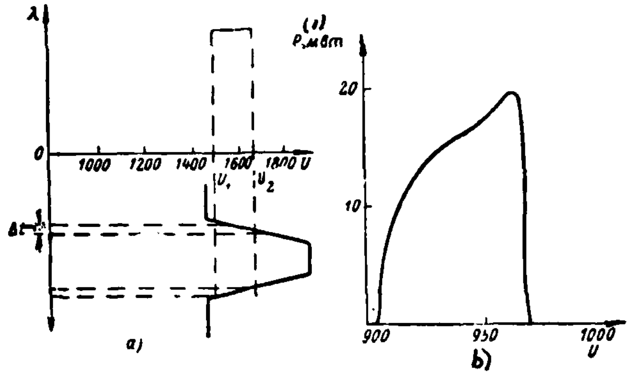

Fig. 8.26. Dependence of wavelength of shhf oscillations on the accelerating voltage of LBV (a) and dependence of power of oscillations on voltage (b).

Key: (1). mW.

Page 446.

During the action fed to the diode of the short-term pulse of bias voltage by 5, there occurs the disagreement/mismatch of diode and therefore the reflection from it of shf oscillations appears. The supplementary rotation of the plane of polarization on 45° occurs with the secondary passage of the oscillations through the ferrite, after which the signal through output 6 enters the waveguide, which leads to the load.

In this diagram semiconductor diode is modulating element. After the admission of shf oscillations (55 GHz) to the diode, loaded to the resistance of 75 ohms, through it the current, which considerably reduces the high-impedance resistor/resistance of diode, flows/occurs.

Therefore it is possible to match the circuit of diode with the circuit of signal and wave reflections it does not occur. However, after the admission to the diode besides this pulse of the bias voltage of negative polarity with an amplitude of about 5 V occurs an increase in the resistor/resistance of the circuit of diode, i.e., disagreement/mismatch conditions are created. Thus, for the time of action of displacing output potential of diagram is isolated radio pulse.

Pulse-shaping circuit of bias/displacement is given in Fig. 8.28. Oscillations with frequency of 100 kHz and to amplitude of approximately 300 V enter nonlinear inductance coil. Upon the saturation of the core of this coil occurs the drop in the voltage, which after differentiation is converted into the sharp pulse of considerable amplitude, which enters the grid of tube. Due to the negative bias/displacement on the grid of tube occurs the limitation of this pulse from below.

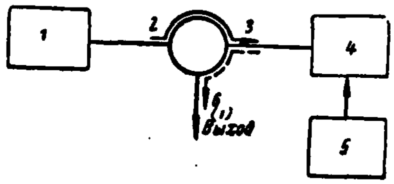

Fig. 8.27. Block diagram of a device for the generation of radio pulses in the range of millimeter waves.

Key: (1). Output.

Page 447.

Therefore, on the load with a resistance of about 75 ohms is formed/shaped pulse with the duration of 3 ns (on the foundation) with an amplitude of about 3 V. Thus, the duration of radio pulses proves to be also 3 ns.

For obtaining nanosecond radio pulses of millimeter range can be used another version of modulation [163]. It is possible to utilize two waveguide resonators, been connected in series, each of which is cut off at the same frequency and is shunted by sharpened silicon diode. The resistances of the diodes are great. With a certain bias voltage and the total energy losses with the work of resonators are approximately 4 dB. With the bias voltage of another polarity of loss they grow/rise to 40 dB. Therefore, using constant bias voltage on one side and nanosecond video pulses of the proper polarity on the other, it is possible to carry out modulation of the shf oscillations, which enter from the klystron. This type of modulator does not require a precise agreement and therefore little it is sensitive to

the insignificant frequency drift of klystron.

With the application of high-speed semiconductor devices there can be obtained other sufficiently simple circuits of modulation for formation of low- power nanosecond radio pulses [164, 165]. Radio pulses are formed/shaped, for example, with the aid of highest harmonic components of a steep edge in the modulating voltage, obtained due to the rapid switching of diffusion silicon diode [164].

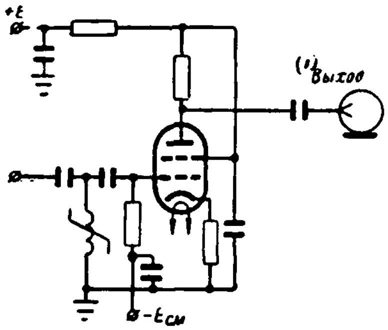

Fig. 8.28. Pulse-shaping circuit of bias voltage.

Key: (1). Output.

Page 448.

For this the diode is assembled in the waveguide (Fig. 8.29) and is changed over during the supplying of the voltage of frequency to 10 or 20 MHz.

In the waveguide oscillations only of very high frequency (8-11 GHz), which appear at moment of sharp drop in voltage during switching of diode into states of direct and reverse conductivities, are propagated. From the secondary winding of transformer, which is located in the anode circuit of tube, to the diode sinusoidal oscillation and bias voltage is supplied. Capacitance C (at the input into the waveguide) together with secondary winding of transformer forms resonance circuit. The isolated with waveguide radio pulses have a duration of approximately 1 ns at the peak power of 0.01 mW and the repetition frequency 10 and 20 MHz.

In the other version of this device/equipment into waveguide tunnel diode, which has very short switch time [165], is placed. As a result succeed in obtaining the radio pulses of the millimeter range with a duration of about 2 ns.

At present methods of generation of nanosecond radio pulses of small power continuously are improved. Besides different installations for the investigation of the circuits of shf and circuits of electronic devices such pulses already successfully are utilized in the electronic computers with increased speed [166, 167].

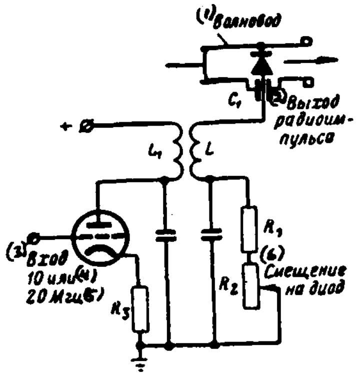

Fig. 8.29. Pulse-shaping circuit with waveguide and high speed diode. Key: (1). Waveguide. (2). Output of radio pulse. (3). Input. (4). or. (5). MHz. (6). Bias on diode.

Page 449.

8.5. GENERATION OF POWERFUL RADIO PULSES.

Magnetron oscillators usually are utilized as a source of powerful radio pulses of SHF band.With the formation of the modulating video pulses of microsecond duration are used the modulator circuits on the electron tubes or diagrams with the forming lines and the thyratron as the commutator, and which frequently are utilized peak transformers. Circuits with the forming artificial lines and peak transformers are most simple. In this case the shape of the pulse, supplied to the magnetron, is determined by the characteristics of the peak transformer, which agrees on impedance of the circuit, which forms pulses, with the magnetron.

Peak transformers, utilized in powerful/thick modulators, have insufficient broad-band character and cannot be used with impulse shaping by duration considerably of less than 0.1 ms. Application in the modulator of the forming circuit without the peak transformer leads to the need for having high charging voltage on the line and, furthermore, appear considerable difficulties with the agreement of circuit with the resistor/resistance of magnetron.

In Chapter 3 were examined forming circuits, which contain non-uniforms circuit of transmission, with the aid of which it is possible to lower charging voltage of line and to match modulator with oscillator of high-frequency oscillations.

However, during development of modulators of magnetron oscillators, intended for generation of nanosecond radio pulses, together with requirements of broad-band character it is necessary to consider specific character of excitation of oscillations in magnetrons. The requirement of the limited rate of the build-up/growth of the modulating voltage on the magnetron is one of the special features of the work of magnetrons. Establishment of the mode, type π different from the oscillations is the final result of too rapid a increase of voltage on the magnetron.

Page 450.

Limited rate of voltage rise, caused on application of magnetron, increases minimum pulse duration, which can be obtained in the case of

applying usual type modulators.

During the generation of nanosecond radio pulses of considerable power the so-called pedestal method of modulation of the magnetron [39], which removes difficulties, found use. Fig. 8.30 gives the shape of the complicated modulating pulse. Pulse consists of pedestal $U_{п}$ and test section $U_{р}$. The pulse of pedestal has relatively small steepness of front, sufficient for the establishment in the magnetron of oscillations of the type π. Due to the pedestal, whose amplitude composes 0.6-0.8 of amplitude of entire pulse, magnetron generates the power of order 5-10% of the nominal power of magnetron.

After the mode of oscillation point is established/installed with the aid of pedestal part of pulse in magnetron, to magnetron there is fed a test section of pulse (operating pulse) of nanosecond duration, which converts magnetron into mode of generation already at nominal power. Since up to the moment/torque of acting the operating pulse magnetron oscillates normal type, the rise time of the current of magnetron and high-frequency power will be, in essence, limited to the parasitic parameters of input circuits of magnetron and to its plate capacitance - cathode. This time composes a total of several nanoseconds.

During generation of radio pulses with duration in several ten nanoseconds required shape of modulating pulse and necessary agreement of modulator with magnetron they can be achieved/reached in modulator

circuit with stepped line. In Fig. 8.31 is given the diagram of pedestal modulator on artificial lines [39]. The here forming line consists of four separate artificial lines with different wave impedance.

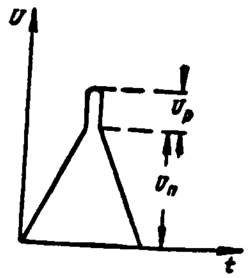

Fig. 8.30. Oscillogram of complicated modulating video pulse.

Page 451.

Three lines are included as quadrupoles, and the latter as two-terminal network. The first line, which forms first stage, has the smallest wave impedance, and in the subsequent stages it grows with an increase in the number of stages. This heterogeneous stepped line is intended for the formation of working nanosecond pulse and impedance matching of circuit with the resistor/resistance of magnetron L_2. This non-uniform circuit is simultaneously a voltage transformer. For the impulse shaping of the pedestal the simplest single-section LC-chain is utilized.

Comparatively long pulse of pedestal through peak transformer is supplied to magnetron. The delay time of stepped line must be such so that it would correspond to rise time of pedestal pulse to its maximum value. At this time the magnetron begins to oscillate fundamental type and its dynamic resistance it is reduced and it proves to be that corresponding to output resistance of stepped line. The entering the magnetron nanosecond operating pulse converts him into the mode of the

generation of total power. As the commutating element in the circuit of the impulse shaping of pedestal and in the circuit of nanosecond pulse is used one thyratron L_1.

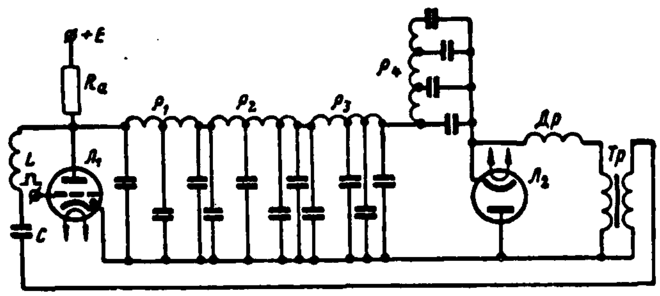

Fig. 8.31. Modulator circuit with stepped forming line.

Page 452.

Fig. 8.32a gives an equivalent schematic diagram of stepped forming line, while Fig. 8.32b shows diagrams of voltage into lines, which occur with shaping of nanosecond pulse. Stepped line is comprised from (n-1) quadrupoles and one two-terminal network. All artificial long lines, which make up the stepped line, must have identical delay time $t_и/2$, where $t_и$ — duration of nanosecond pulse, and also identical frequency-phase characteristics.

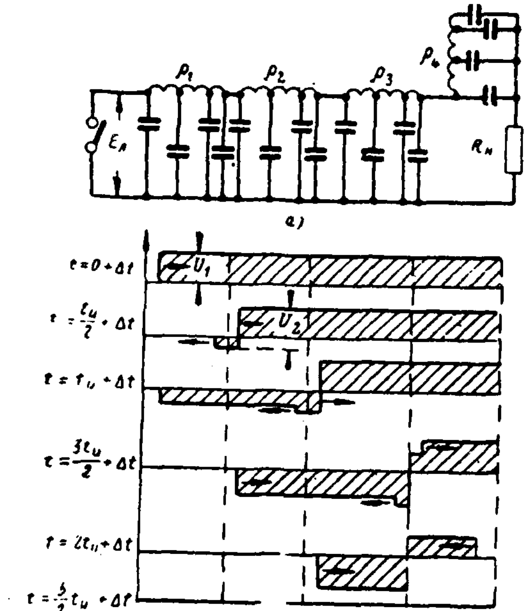

Fig. 8.32. Equivalent diagram of stepped forming line (a); diagram of voltage in this line (b).

Page 453.

Impedances of all artificial lines must satisfy the relationships/ratios

$$\rho_k = \frac{k(k+1)}{n^2} R_{\text{н}}, \quad \rho_n = \frac{R_{\text{н}}}{n},$$

where k - ordinal number of line, k=1, 2, 3, ..., (n-1).

During propagation of wave of voltage along non-uniform circuit of transmission at points, where occur for heterogeneity they appear reflections, and wave amplitude of voltage, which is propagated in forward direction, undergoes change.

When thyratron ignites, appears wave of voltage U_1, opposite on its polarity to voltage $E_л$ of initial charge of line. In this case $|U_1|=|E_л|$. This wave is propagated along the first line with a wave impedance of ρ_1. At junction of the first and second line, that have wave impedance ρ_2 (moreover, $\rho_2>\rho_1$), appear two waves of the voltage: one is propagated along the second line (U_2), and the second (reflected) it is propagated back to the side of the first line (Fig. 8.31b).

Voltage of direct wave can be recorded in the form

$$U_2=2U_1\frac{\rho_2}{\rho_1+\rho_2}.$$

Voltage of wave reflected, which is propagated in first line, will be

$$U'_1=2U_1\frac{\rho_1}{\rho_1+\rho_2}.$$

These waves, being propagated, create new straight/direct and reflected waves (Fig. 8.32b).

Voltage of direct wave, which is propogated through stepped line, grows/rises as a result of gradual increase in wave impedance of separate steps/stages. Therefore the resulting voltage of pulse proves to be in n/2 times of more than the initial voltage of the charged/loaded line. It is possible to conclude from the given

diagrams of voltage (Fig. 8.32b) that the delay time of stepped line is equal

$$t_3 = (n-1)\frac{t_u}{2}$$

or in this case $t_3 = 3/2 \cdot t_u$.

Page 454.

Thus, with the aid of diagram in question it is possible to satisfactorily coordinate circuit of formation with resistor/resistance of magnetron both in initial and in completing stage of excitation of oscillations. Furthermore, the application of non-uniform circuit makes it possible to reduce initial charging voltage of the forming line.

Pedestal method of modulation of powerful/thick magnetrons is convenient in one more sense. Usually after in the process of modulation anode voltage on the magnetron will become close to the nominal, a change in the voltage sharply affects the value of anode current. Therefore in the simple diagrams of modulation it is necessary to remove changes of the voltage on the apex/vertex of the modulating pulse. Obtaining flat-topped pulse with high voltages is difficult. However, in the pedestal method due to the presence of the pulse of pedestal the amplitude of working nanosecond pulse is considerably lower than the total nominal voltage of magnetron. In other words, with a comparatively noticeable nonuniformity of the apex/vertex of operating pulse the relative nonuniformity of the apex/vertex of entire modulating pulse proves to be very small.

Described diagram with stepped line, which consists of artificial delay lines, is insufficiently wide-band, for impulse shaping with duration on the order of 10 ns. However, at present appears ever larger need for powerful/thick radio pulses with duration on the order of 10 ns and even it is less.

For a certain increase in broad-band character of forming circuit as individual lines can be used sections/segments of coaxial cables with different wave impedance. It is possible also stepped line to replace with the appropriate heterogeneous distributed-parameter line.

However, at present there are oscillators of nanosecond pulses of high voltage, not susceptible to value of load. Such diagrams make it possible to easily obtain the reliable agreement of the forming circuit with the resistor/resistance of magnetron even under the condition for a considerable change of the load resistance/resistor in the process of exciting the magnetron.

Thus, as an oscillator of working nanosecond pulse there can be used the diagram proposed by Yu. V. Vvedenskiy (Fig. 3.30b).

Page 455.

In this case the impulse shaping of pedestal and operating pulse must be realized by different diagrams. Both pulses in the specific time-sequential routine must be folded with the aid of appropriate

adding circuit. The block diagram of this modulator is represented in Fig. 8.33.

Thyratron can be used as commutating element in each diagram. If we consider the great possibilities of diagrams with the commutating inductance, used also in the devices/equipment, designed for obtaining of powerful pulses, then can prove to be permissible the replacement of thyratrons by these inductance, which will considerably raise the reliability of entire device/equipment.

Besides method of obtaining radio pulses examined via modulation of the shf oscillator, there is proposed a new method of formation of powerful nanosecond pulses [168]. This method is based on the use of an effect of the build-up/growth of energy in the circular resonator, connected by couplers with the waveguide, on which is propagated the shf energy from the continous wave oscillator. Into the circular resonator the energy enters from the fundamental waveguide and gradually it increases. If the energy of shf oscillations with the aid of the high speed commutator accumulated in the circular resonator is derived to the load, then radio pulse is formed on it. The peak pulse power depends on the energy accumulated in the circular resonator; and its duration is equal to the length of ring, divided into the group velocity of the waves, which are propagated in the ring.

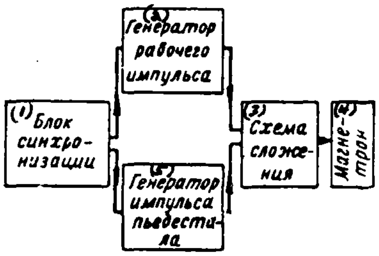

Fig. 8.33. Block diagram of modulator.

Key: (1). Oscillator of operating pulse. (2). Synchronizing unit. (3). Adding circuit. (4). Magnetron. (5). Pulse generator of pedestal.

Page 456.

For usual rectangular waveguide, which works in the relation of critical wavelength to the worker, equal to 1.4 or 1.5 pulse duration into one nanosecond corresponds to the length of ring in 25.4 cm. The duration of the front of radio pulse is determined in essence by triggering time of the commutating element. The specially developed gas-discharge instrument, controlled by external trigger pulse, is utilized as the commutating element. Time of commutation of approximately 2-3 ns. By this method were obtained radio pulses by duration about 10 ns with a peak power of 1 MW.

Page 457.

CHAPTER NINE.

AMPLIFICATION OF PULSES.

The amplification of pulse oscillations is one of the most complex problems of nanosecond pulse technique. As is known, the possibilities of electron tubes in the gain ratio of oscillations with the wide spectrum are rated/estimated by the cut-off frequency of tube in the schematic of the resistance-coupled amplifier

$$f_{rp}=\frac{1}{2\pi}\frac{S}{C_0}, \qquad (9.1)$$

where S - mutual conductance of tube at the operating point;

C_0 - stray capacitance, which is folded from the input and output capacitances of tubes.

Cut-off frequency of tube is that frequency, at which amplification of resistance-coupled amplifier becomes equal to one. It is necessary to keep in mind which under actual conditions f_{rp} is less than the calculated due to supplementary stray capacitance, which appears during the installation of tube into the diagram.

Amplifier can fulfill its functions only if upper cut-off frequency of spectrum of amplified oscillations $f_0<f_{rp}$. Otherwise of component the oscillations, whose frequency is above f_{rp}, will be not amplified but attenuated. All amplifiers utilized in the amplifier

technique of microsecond range work under condition $f_{в}<f_{гр}$. The special feature of the amplification of oscillations in the nanosecond pulse technique is the fact that in the majority of the cases the higher frequency of the spectrum of the amplified oscillations is more than the cut-off frequency of tubes.

Page 458.

This fact led to the need for the creation of the special methods of amplifying the oscillations of nanosecond duration.

However, not only effect of stray capacitance impedes amplification of oscillations with very wide spectrum. At very high frequencies a sharp drop in their input resistance due to the effect of the inductance of introductions/inputs and final rate of the flight/span of electrons is a very essential deficiency in the tubes. The incidence/drop in the input resistance of triple-grids amplifier with the high slope/transconductance causes the need for the replacement by their triodes of shf, which are characterized by high input resistance, and so the use of special circuit diagrams.

In recent years for amplifying pulse fluctuations of small amplitude they began to widely use semiconductor devices, in particular, tunnel diodes.

9.1. Operation of the tube in the super wide-band amplifiers.

In order to rate/estimate behavior of tube in the range of very high frequencies, which seizes pulse spectrum of nanosecond duration, in its equivalent diagram it is necessary to consider not only stray capacitances, but also stray inductances of introductions/inputs.

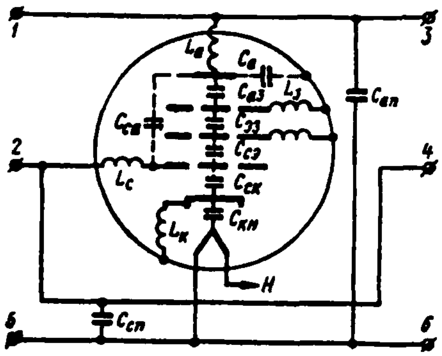

Fig. 9.1. Equivalent diagram of pentode.

Page 459.

Fig. 9.1 gives the equivalent diagram of pentode, comprised for the range of superhigh frequencies [169]. $C_{ап}$ and $C_{сп}$ designate the capacities/capacitances between the anode and the tube panel and the grid and the panel; remaining elements are designated in the figure. It is necessary to note that for the very narrow pulses the tube already cannot be considered as a lumped system; therefore the diagram given in Fig. 9.1 is insufficient strict.

As the theory and experiment show, greatest effect on input admittance of tube exerts inductance of cathode introduction/input $L_к$. Equivalent amplifier circuit taking into account cathode introduction/input is given in Fig. 9.2; diagram is comprised for alternating current. At the very low frequencies, at which it is possible to disregard $L_к$, the input impedance of a tube carries purely reactive/jet (capacitive) character. The input current $\bar{I}_{вх}$ leads the input voltage $\bar{U}_{вх}$ on the phase on 180°. At the higher frequencies

presence L_K leads to the fact that the phase angle between I_{BX} and U_{BX} decreases. This means that the input impedance of a tube is no longer purely reactive/jet, and it contains active component.

Input impedance of a tube at high frequencies can be represented in the form of parallel-connected of input capacitance C_{BX} and input admittance G_{BX} (or R_{BX}) (Fig. 9.3).

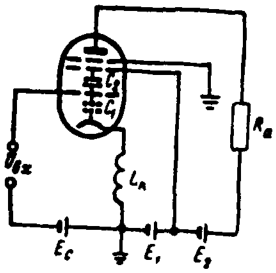

Fig. 9.2.

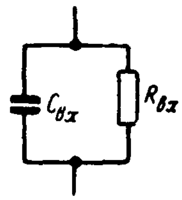

Fig. 9.3.

Fig. 9.2. Equivalent amplifier circuit taking into account inductance of cathode introduction/input.

Fig. 9.3. Diagram of substitution of input circuit of tube.

Page 460.

V. I. Siforov [170] showed that these values can be expressed as follows:

$$C_{вх} = C_1 + C_2, \quad G_{вх} = C_1 L_к S_к \omega^2,$$

where C_1 - grid capacitance - cathode;

C_2 - capacitance control electrode - screen of stack;

$S_к$ - mutual conductance of cathode current.

As it follows from formula, value of active input admittance grows/rises proportional to second degree of frequency, i.e., it is more rapid than capacity susceptance. Therefore for the very high frequencies the negative effect of the increase of active input admittance is manifested more strongly than the effect of capacity susceptance.

Expression for active input admittance can be represented also in the form

$$G_{\text{вх}} = Af^2,$$

where $A = 4\pi^2 C_1 L_{\text{к}} S_{\text{к}}$ — parameter, which characterizes tube.

Taking into account also inductance of introduction/input of screen grid $L_{\text{э}}$, it is possible to obtain that [170]

$$G_{\text{вх}} = (S_{\text{к}} C_1 L_{\text{к}} - S_{\text{э}} C_2 L_{\text{э}})\,\omega^2,$$

where $S_{\text{э}}$ -- mutual conductance of screen current.

As it follows from this formula, presence of inductance in circuit of screen grid decreases active input admittance. Installing additionally inductance into the screen circuit, it is possible to in effect 2-3 times decrease input admittance.

Final rate of electron motion leads to the fact that at very high frequencies in tube appears supplementary input admittance, which can be determined according to formula [170]

$$G_{\text{вх}} = kS_{\text{к}} \tau_c^2 \omega^2,$$

where k - coefficient, which considers geometry of tube;

τ_c — electron transit time from cathode to control electrode.

During design of pulse amplifiers of nanosecond duration with band into hundreds of megahertz it is necessary to compulsorily

consider incidence/drop in active input lamp resistance. Value $R_{вх}$ is given usually in the manuals; for triple-grids amplifier with the high slope/transconductance in the range 100-200 MHz it composes hundreds of ohms.

Page 461.

9.2. Traveling-wave amplifier the principle of operation of amplifier.

As already was mentioned above, in the case, when higher frequency of spectrum of signal $f_{в}$ exceeds cut-off frequency of tube $f_{гр}$, amplification of oscillations in usual diagrams becomes impossible. The parallel connection of tubes does not change position, since it does not lead to an increase in $f_{гр}$, and the series connection of stages gives a negative result. In order to obtain sufficiently high amplification factor in the case, when the factor of amplification of separate cascades/stages is lower than one, it is necessary to carry out an addition of the output voltages/stresses (or the same as the addition of the factors of amplification of separate cascades/stages).

To carry out addition of output voltages/stresses is possible with the aid of building-up principle. Building-up principle consists in the addition of the pulses, which arrive at different moments of time. So that any device could accumulate pulses, it must possess the ability to memorize them, and then to summarize. Pulse oscillation at

the input of storage device/equipment is usually series from the N pulses of identical form, which follow after each other with quasi period T; the delay time of the memory element of storage device/equipment is selected by equal T. As a result of the process of accumulation the output pulse will be in N of times more than input and it will retard with respect to the first input pulse on the period (N-1)T. This time is called storage time. Building-up principle widely is utilized for amplifying the oscillations of the shf in the so-called circular resonators. Let us note that an increase in the amplitude of voltage on the reactive/jet elements of series circuit in the presence of the resonance is also based on the use of building-up principle.

Building-up principle can be realized with the aid of many systems, one of which is subdivided delay line, loaded on rings to effective resistance, equal to its wave. Line consists of N-1 sections, each of which possesses delay time, equal T.

Page 462.

The first of the input pulses is fed to the input of entire line, the second - to the input of the second section, the third - to the input of the third section and so on up to the latter, which is supplied for the load. As a result of this distribution of the feed ends of pulses each of them is delayed in the line accurately by this time interval, on what it anticipates/leads latter/last pulse in the series. As a result of this all pulses come for the load, which is located at the

end of the line, simultaneously and store/add up on it.

In a description of the work of storage device/equipment given above discussion dealt with pulse train, which follow through specific time interval. Under the actual conditions the amplifier must amplify pulses with the most varied repetition periods, including single pulses. In order in these cases to realize building-up principle, the schematic of accumulator/storage must be supplemented with the diagram of multiplier. Multiplier is the device/equipment, which converts single pulse into the series from the n pulses, which follow one after others with quasi period T.

Simplest multiplier can be subdivided delay line, which consists of N-1 sections and loaded to wave impedance for eliminating reflections. From the beginning of line and end/lead of each section the removals/outlets, whose total number is equal to N, are taken; the delay time of pulse T in each section is equal.

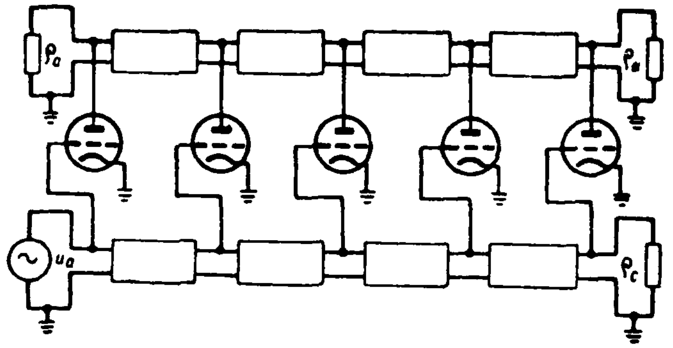

Fig. 9.4. Diagrammatic representation of traveling-wave amplifier.

Page 463.

Passing along the line, input pulse consecutively/serially appears at the end of each section after time T, i.e., is formed the quasi-periodic sequence of pulses.

Traveling-wave amplifier is schematically depicted in Fig. 9.4. It is the combination of the multiplier, whose role performs grid line, and the accumulator/storage, whose role performs plate line. The conclusions/outputs of grid line are connected to the appropriate points of the plate line through the tubes. During the supplying to the input of this system of single pulse it is propagated along the grid line, consecutively/serially appears at the grids of tubes, is amplified by them, it is isolated in the anode circuits of tubes and moves further to the right and to the left along the plate line. The pulses multiplied in the grid circuit come to the right end of plate line simultaneously, and to the left end - with the retardation to 2T one with respect to another. As a result on the load, which consists

on the right end of the line, all pulses are stored, up, which is equivalent to the addition of the factors of amplification of tubes.

Thus, system as a whole first converts one pulse into series of N pulses, amplifies each of them separately and then it summarizes intensive pulses. Above has already been indicated that the amplification is possible when the cut-off frequency of tube f_{rp} is more than the higher frequency of the spectrum of amplified oscillation f_{rp}. If $f_{n}>f_{rp}$, then with the permissible nonuniformity of the amplitude-frequency characteristic of amplifier its amplification is less than one. The use of building-up principle makes it possible to carry out amplification of oscillations, also, in this case, since the resulting factor of amplification of the diagram

$$K_{\Sigma}=NK_{0},$$

where K_0 - factor of amplification of tube in the diagram.

Since load of tube is equal to $\frac{1}{2}\rho_{a}$, where ρ_{a}— wave impedance of plate line of delay (coefficient of 1/2 is caused by the fact that line is connected to tube to the right and to the left), then factor of amplification of tube in diagram $K_{0}=\frac{S\rho_{a}}{2}$, and amplifier gain

$$K_{\Sigma}=\frac{N}{2}S\rho_{a}. \qquad (9.2)$$

Page 464.

In the reasonings given above there was a clear role of the value

of time lag T in one section of line. The response to this question can be given only after the examination of the fundamental amplifier circuits of the traveling wave, which are performed on the networks of low-pass filters, and also in the sections of long lines.

9.3. Traveling-wave amplifiers on the chains/networks of filters.

Initially traveling-wave amplifiers were performed on chains/networks of filters [40]. The schematic diagram of this amplifier is shown in Fig. 9.5. Specially switched on inductance L_c form together with input capacitances of tubes of C_c the chain/network of the filters, which represent the equivalent of long line. The analogous equivalent of long line is formed in the anode circuit by inductance L_a and output capacitances of tubes C_a. These chains/networks of filters play the role of the subdivided delay lines in block diagram of traveling-wave amplifier described above.

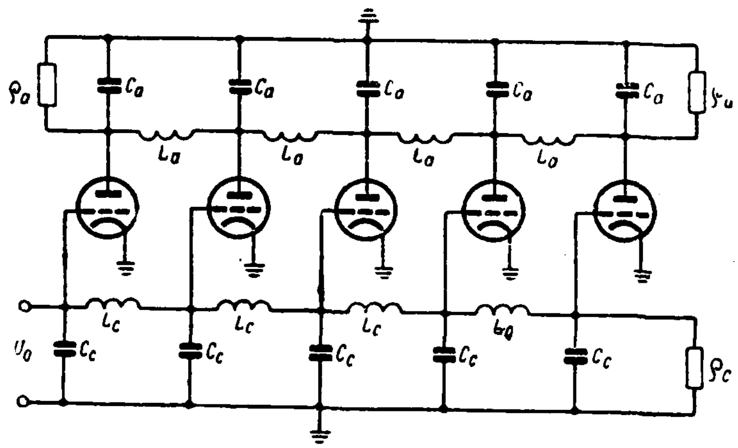

Fig. 9.5. Fundamental amplifier circuit of traveling wave, made on chains/networks of filters.

Page 465.

Fundamental special feature of this amplifier circuit is the fact that parasitic elements (capacities/capacitances of tube) perform role of capacities/capacitances of filters, i.e., are utilized as elements schematics of equivalent long line. In this an essential difference in the amplifier of that running on the chains/networks of filters from the amplifier in the sections of long line. In the traveling-wave amplifier on the chains/networks of filters is utilized such diagram of connection of tubes, in which their slope/transconductance is summarized, and the capacitances are not stored up.

The possibilities of such amplifiers, which ensure the undistorted amplification of pulse signals, are determined by type of

filters used in them. In the diagram given on Fig. 9.5 the simplest constant K filters are used. Cutoff frequency in these filters $\omega_{\text{кр}}=\frac{2}{\sqrt{LC}}$. Since capacitance value C is the given one (it it is equal to stray capacitance of tube), then for an increase in the cutoff frequency, and thereby of the passband of amplifier, it is necessary to decrease the value of inductance L. However, the decrease of inductance leads to the decrease of characteristic impedance $\rho=\sqrt{\frac{L}{C}}$ and thereby to the decrease of the amplifier gain K_0 [formula (9.2)]. After considering that with the assigned magnitude of distortions the passband of amplifier $\Delta F=\alpha F_{\text{кр}}$, where α - certain coefficient (α<1), and after using formula (9.2), let us determine cut-off frequency or, that also, the area of the amplifier gain of the traveling wave:

$$f_{\text{гр}}=K_0\Delta F=\frac{N}{2}S\sqrt{\frac{L_a}{C_a}}\frac{\alpha}{\pi\sqrt{L_aC_a}}=\frac{N}{2\pi}\frac{S}{C_0}\frac{\alpha}{k}, \quad (9.3)$$

where

$$C_0=C_a+C_c,\ k=C_a/C_0.$$

This expression differs from the expression for cut-off frequency of tube (9.1) given earlier, in the first place, in terms of presence of coefficient k<1, which indicates that in this diagram input and output capacitances of tubes are divided and that cut-off frequency due to this is raised, in the second place, by presence of coefficient α<1, of characterizing properties filter and degree of distortions of pulses.

Page 466.

Since α<1, then this coefficient decreases the cut-off frequency.

Most important difference, however, is the fact that the cut-off frequency of diagram is directly proportional to the number of tubes N. This means that by an increase in the number of tubes the cut-off frequency of amplifier can be made as to high as desired (formula on considers the special features of the work of tube at the superhigh frequencies and the ohmic losses in the filters, which establish/install the limit of increase $f_{гр}$).

As it follows from (9.3), for increase in cut-off frequency, which characterizes area of amplifier gain, it is desirable to increase coefficient α. This coefficient shows what part of the filter transmission band is accepted as suitable for the undistorted transmission of pulse oscillations. As is known, the transmission factor of a constant K filter is constant in the range of frequencies from 0 to $F_{кр}$ only when the filter is loaded to the characteristic impedance, which has fairly complicated dependence on the frequency. Only in the range of frequencies $f \ll F_{кр}$ it is possible to consider that the characteristic impedance of filter is equal to $\rho=\sqrt{L/C}$.

Fig. 9.6, borrowed from [33], gives dependences of modulus of complex transmission factor of constant K filter on frequency with different values of load resistance/resistor. As can be seen from the figure, with n=1, i.e., when $Z_н=\rho$, the amplitude-frequency characteristic of filter is far from ideal and for the undistorted transmission its only initial section can be utilized.

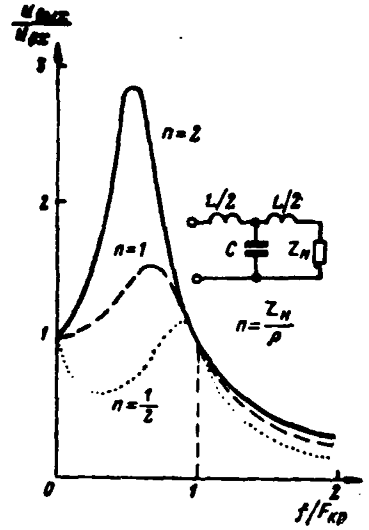

Fig. 9.6. Dependence of transmission factor of filter section of type K on frequency with different values of load resistance.

Page 467.

With an increase in the number of filters of distortion they grow/rise and passband respectively becomes narrow. Therefore the value of coefficient α for the constant K filters is very small. Because of this, the traveling-wave amplifiers on the constant K filters are barely suitable for the application in the nanosecond pulse technique.

Considerably best results are obtained during application in traveling-wave amplifiers by M-derived filter. These filters differ from constant K filters in terms of the fact that the inductance of consecutive branch increases in m of times, so that $L_m = mL_K$, and in parallel branch there is included inductance $L_{m0} = \frac{1-m^2}{4m} L_K$; the capacitance of parallel branch so it increases in m of times (Fig.

9.7a). Virtually a M- derived filter is performed in the form, shown in Fig. 9.7b. Between the coils, which stand in the consecutive branch, the inductive coupling with the mutual inductance factor M is established/installed. The parameters of second circuit are expressed as the parameters of the first as follows:

$$L_1 = L_K \frac{m^2+1}{4m}, \quad M = L_K \frac{m^2-1}{4m}, \quad C = C_K m.$$

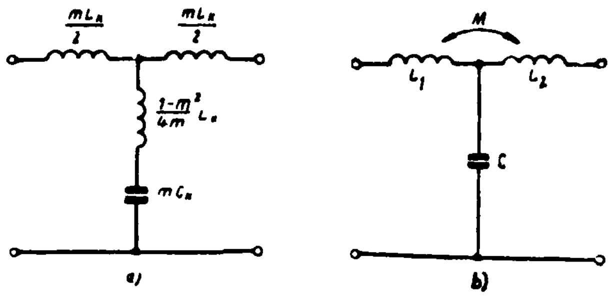

Fig. 9.7. Filter section of type m: a) equivalent diagram; b) practical fulfillment of diagram.

Page 468.

Since the network of filters in the traveling-wave amplifier is equivalent of long line, the quality of filters is convenient to rate/estimate by dependence of time lag of oscillation, passing through filter, on frequency. Fig. 9.8 gives the dependence of time lag on value $x=\frac{\omega}{\omega_{кр}}$ [171]. It follows from the graph that the greatest constancy of delay time, i.e., the smallest dispersion, is possessee by the filter with m=1.27. A filter of the type K(m=1) possesses substantially greater dispersion. Therefore in the traveling-wave amplifiers usually are utilized the chains/networks of filters with m=1.27. For the equalization of the frequency characteristic of the chain/network of filters in the beginning and at the end of the line usually are placed the half-sections with m=0.6.

Theoretical analysis of processes, which occur in traveling-wave amplifiers on chains/networks of filters, is very complex and little it is suitable for engineering. For the amplifiers, which contain

from 3 to 30 sections, the time of the establishment of transient response can be determined according to empirical formula [171]

$$t_{y} = \frac{\sqrt{n}}{\omega'_{\text{кр}}},$$

where $\omega'_{\text{кр}} = 2m\,(L_{K}C_{K})^{-1/2}$.

Overshoot of transient response composes approximately 15-25%.

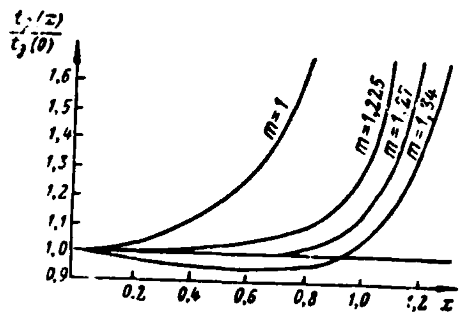

Fig. 9.8. Dependence of time lag on x for different values of parameter m.

Page 469.

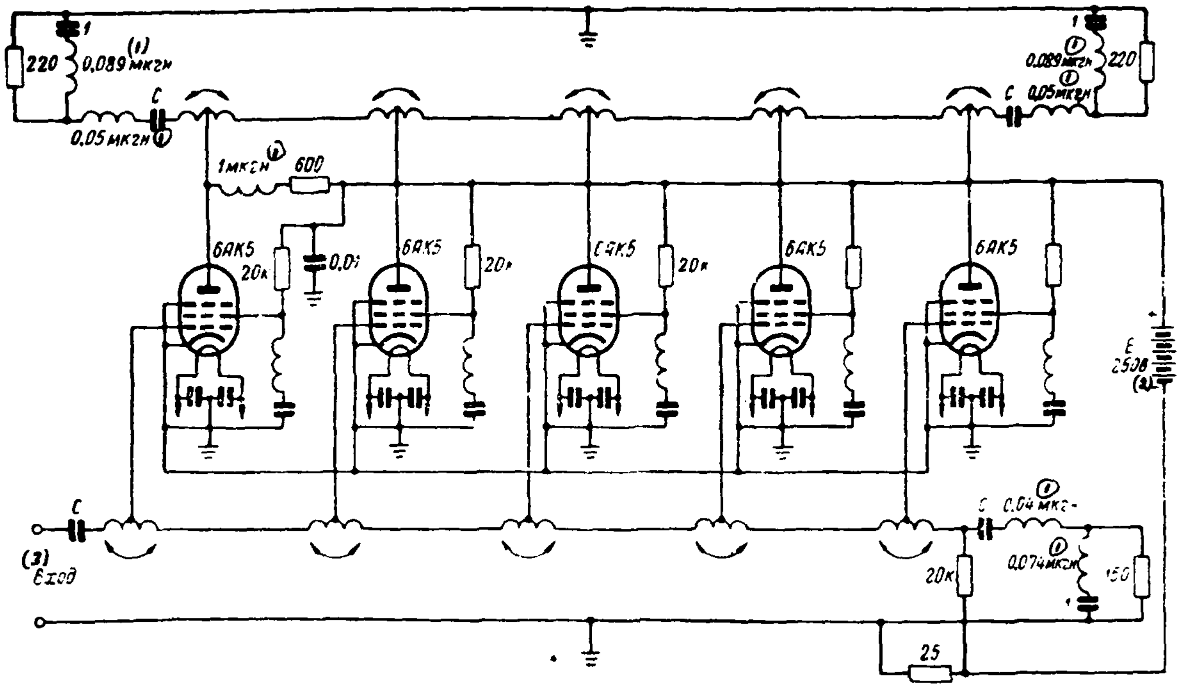

Fig. 9.9. Amplifier circuit of traveling wave on chains/networks of M-derived filters.

Key: (1). μH. (2). V. (3). Input.

Page 470.

Amplifier circuits of the traveling wave on chains/networks of M-derived filters repeatedly were described in the literature; into [40] there is table of reference data on amplifiers. Therefore as the illustration let us give only the one amplifier circuit, shown in Fig. 9.9. It provides the amplification, equal to 2.8 in the frequency band to 400 MHz. The characteristic impedance of the anodic filter equally to 150 ohms (inductance of each half of coil 0.049 μH, mutual inductance factor between the sections 0.020 μH). The input impedance

of a tube increased due to the inclusion of inductance in the screen circuits of tube (which was formed due to the wires of bypass capacitor). The time of the establishment of the transient response of amplifier was less than 2 ns.

The drop in input resistance of the receiver-amplifier tubes at superhigh frequencies leads to need for utilizing, instead of them, the shf triodes, which possess considerably high input resistance. The direct switching on/inclusion of triodes instead of the pentodes is impossible, since it leads to the onset of feedback between the anodic and grid lines due to the transfer capacitance. Therefore triodes in the traveling-wave amplifiers are switched on, for example, in the manner that it is shown in Fig. 9.10. This diagram makes it possible to substantially decrease the capacitive coupling between the anodic and grid lines.

9.4. Traveling-wave amplifiers in the sections of long lines.

Traveling-wave amplifiers on chains/networks of filters have the deficiency, that passband of their is determined by critical frequency of filter.

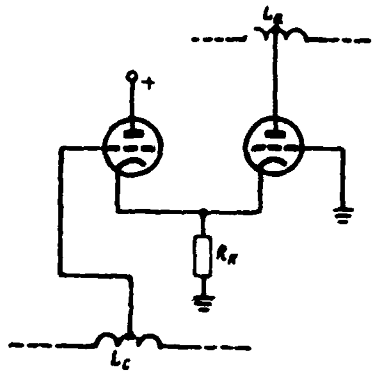

Fig. 9.10. Method of switching on/inclusion of shf triodes for the purpose of a decrease in the effect of transfer capacitance.

Page 471.

In this case virtually, since the chain/network of filters is loaded not on the characteristic impedance, but on the constant effective resistance, the upper band edge of the transmission of filter is considerably less than the critical frequency of filter. This fact leads to the fact that for amplifying the signals with the very wide spectrum it is necessary to proceed from other principles of the construction of amplifiers.

One of methods virtually, of completely removing effect transmitting systems from passband of amplifier, is replacement of filters in anode and grid circuits sections of long line. The long line, loaded on the wave impedance, makes it possible to carry out the undistorted transmission of oscillations with the very wide spectrum. All distortions, which can arise in this amplifier, depend on the

presence of tubes and they will depend on their parameters input and output capacitances, input resistance, etc.).

Structurally the amplifier in sections of long lines appears in the manner that it is shown in Fig. 9.11.

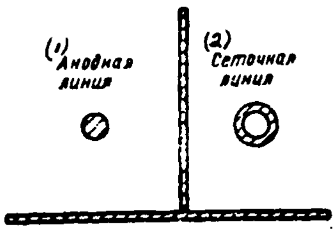

Fig. 9.11. Arrangement of anodic and grid lines in traveling-wave amplifier.

Key: (1). Plate line. (2). Grid line.

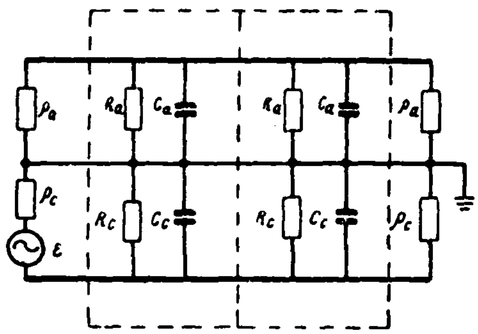

Fig. 9.12. Equivalent amplifier circuit of traveling wave in sections of long lines.

Page 472.

The transmission lines are formed by straight/direct wire or tube and corner screen/shield. The anode and the grid of tube are connected to the appropriate lines, and cathode - to the corner screen. This system, besides the increased electrical indices, possesses still advantages in a design sense.

The traveling-wave amplifier is a distributed system with

discrete/digital heterogeneities (Fig. 9.12). Let us designate the number of tubes through N. In this figure the tubes are replaced with their input and output resistance and capacities/capacitances. The pulse which is propagated on the grid circuit is passed to it through n heterogeneities, which are the integrating components/links, and then it passes through m integrating components/links to anode circuit; it is easy to see that n+m=N+1.

Let us accept at first, that delay time of one section is more than half of pulse duration, then action of each heterogeneity can be examined independently. Let also the pulse have rectangular form and in section/segment $[0, t_n]$ be described by unit function 1(t), whose spectrum exists 1/jω. Pulse spectrum after passage n of the heterogeneities

$$\overline{F}_n(\omega) = \frac{1}{j\omega}(1+\overline{p})^n e^{-j\omega n t_3},$$

where the reflection coefficient from the heterogeneity

$$\overline{p} = \frac{\overline{Z}_c - \rho_c}{\overline{Z}_c + \rho_c},$$

and $\overline{Z}_c$ is the parallel connection of the resistors/resistances of input capacitance C_c, input resistance R_c and input resistance of the right side of the line, i.e., ρ_c. Let us assume that $R_c \gg \frac{1}{2}\rho_c$, then

$$\overline{Z}_c = \rho_c/(1+j\omega\tau_c),$$

where

$$\tau_c = \frac{\rho_c C_c}{2}.$$

Substituting this expression into formula for reflection coefficient and further into formula for $\bar{F}_n(\omega)$, we obtain

$$\bar{F}_n(\omega)=\frac{1}{j\omega}\left[\frac{e^{-j\omega t_3}}{1+j\omega\tau_c}\right]^n,$$

Page 473.

Assuming that time constant of heterogeneity in plate line is equal to time constant of heterogeneity in grid line, then immediately it is possible to write expression for pulse spectrum, which passed through amplifier,

$$\bar{F}_{N+1}(\omega)=\frac{1}{j\omega}\left[\frac{e^{-j\omega t_3}}{1+j\omega\tau_c}\right]^{N+1}.$$

Shape of this pulse, which coincides with form of transient response of amplifier in section/segment $[0.2t_3]$, will be located by computing integral

$$A(t)=\frac{1}{2\pi}\int_{-\infty}^{\infty}\bar{F}_{N+1}(\omega)e^{j\omega t}d\omega,$$

whence

$$A(t)=\frac{1}{N!}\Gamma[N+1,\ x-(N+1)x_3], \qquad (9.4)$$

where

$$x=\frac{t}{\tau_c},\quad x_3=\frac{t_3}{\tau_c}.$$

Transient response of traveling-wave amplifier in sections of

long lines with t≈2t, coincides with transient response of resistance-coupled amplifier, which contains N+1 cascades/stages. Let us note that when deriving the equation of transient response were examined only the distortions, created by heterogeneities, but the amplifier effect of tubes was not considered. If we consider the amplifier effect of tubes, then the steady-state value of transient response must be multiplied on

$$K_0 = \frac{1}{2} NS\rho_a.$$

Time of establishment of transient response of traveling-wave amplifier

$$t_y = 2{,}2\tau\sqrt{N+1} = 1{,}1\rho_a C_a\sqrt{N+1},$$

whence the area of amplification

$$Q = K_0\frac{1}{t_y} = \frac{0{,}5S\rho_a N}{1{,}1\rho_a C_a\sqrt{N+1}} \approx 0{,}46\frac{S}{C_a}\sqrt{N}. \qquad (9.5)$$

Page 474.

It follows from the formula that the area of amplifier gain of traveling wave in sections of long lines is proportional to root from number of tubes. Of this consists a difference in this amplifier from the traveling-wave amplifier on the chains/networks of the filters, for which the area of amplification is proportional to first degree of N. However, this advantage of amplifiers on the chains/networks of filters is retained only in relatively small of frequencies, for which the transmission factor of chain/network can be considered constant, whereas for the amplifier in the sections of long lines relationship/ratio (9.5) remains valid for the very broadband.

Formulas written above did not consider the phenomenon of reflection from heterogeneities. After a lapse of time $2t_3$ to the output of amplifier there will arrive the oscillations reflected from the heterogeneities, i.e., the pulses, which completed besides the passage through N-1 the section of line another cycle on the ring, formed by any of the sections (sections) of line and by two heterogeneities. If we are distracted from the fact that in the plate line the pulses go not only in the direction of load, but also into the opposite I will move that are caused supplementary reflections, then it will be immediately evident that the spectrum of the first signal

$$\bar{F}_{1отр}(\omega) = \frac{K_\Sigma}{j\omega}(N-1)(1+\bar{p})^{N+1}\bar{p}^2 e^{-j\omega(N+2)t_3}$$

reflected.

Under actual conditions in plate line supplementary reflections appear. By examining the process of forming these reflections, it is possible to obtain their expression for the spectrum of the first echo pulse

$$\overline{F}_{1\text{отр}}(\omega)=\frac{K_\Sigma}{j\omega}\Big\{(N-1)(1+\overline{p})^{N+1}\overline{p}^2+ +2\,\frac{N-1}{N}(1+\overline{p})^{N+2}\overline{p}\Big\}\,e^{-j\omega(N+2)t_3},$$

taking into account

Page 475.

Since

$$\overline{p}=\frac{j\omega'}{1+j\omega'},\quad 1+\overline{p}=\frac{1}{1+j\omega'},$$

where $\omega'=\omega\tau$, then

$$\overline{F}_{1\text{отр}}(\omega')=K_\Sigma\tau\,\frac{N-1}{(1+j\omega)^{N+3}}\times \times\Big[(j\omega')^2+j\omega'+\frac{2}{N}\Big]\,e^{-j\omega'(N+2)\frac{t_3}{\tau}}.$$

Realizing the inverse transformation of Fourier, we obtain

$$u_{1\text{отр}}=K_\Sigma e^{-\frac{t-(N+2)t_3}{\tau}}\times \times\left(\frac{t-(N+2)t_3}{\tau}\right)^{N+1}\frac{N-1}{(N+1)!}\left(1-\frac{1}{N}\,\frac{t-(N+2)t_3}{\tau}\right). \quad (9.6)$$

Resulting transient response of traveling- wave amplifier

$$A_\Sigma(t)=A(t)+u_{1\text{отр}}(t),$$

where A(t) is determined by formula (9.4), and $u_{1\text{отр}}(t)$ - by formula (9.6).

Let us exclude from these formulas shift/shear to period $(N-1)t_3$, then

$$A_2(t)=K_2\left[\frac{\Gamma\left(N+1,\frac{t}{\tau}\right)}{N!}+\right.$$
$$\left.+\frac{N-1}{(N+1)!}e^{-\frac{t-2t_3}{\tau}}\left(\frac{t-2t_3}{\tau}\right)^{N+1}\left(1-\frac{1}{N}\frac{t-2t_3}{\tau}\right)\right].$$

Form of transient response depends substantially on value t_3. Fig. 9.13a shows the transient responses of amplifier for N=5, 6, 7 without taking into account the first reflection, while in Fig. 9.13b - the first reflection for the same cases. Time lag $2t_3$ in the latter/last figure is not shown. The resulting transient response is equal to the sum of these curves, displaced by time $2t_3$.

Fig. 9.13c gives example of transient response for N=6 with certain time lag $2t_3$, selected in such a way that transient response would be best.

Page 476.

The obtained transient response has nevertheless very large nonuniformity of apex/vertex, what is the deficiency, characteristic to the traveling-wave amplifiers of such types.

Fig. 9.14 gives amplifier circuit of traveling wave in sections of long lines [172]. Plate line in it is formed by copper wire and

screen/shield, and grid - by tube and by the screen/shield (grid line it must have smaller wave impedance). Amplifier has a passband from 10 to 400 MHz with the nonuniformity of frequency characteristic ±3 dB. Amplification consists of 15 dB and an output resistance of 50 ohms. The form of the frequency characteristic of amplifier is given in Fig. 9.15.

Traveling-wave amplifier on transistors is described into [173]. The diagram of one section of amplifier, input and output circuits is given in Fig. 9.16.

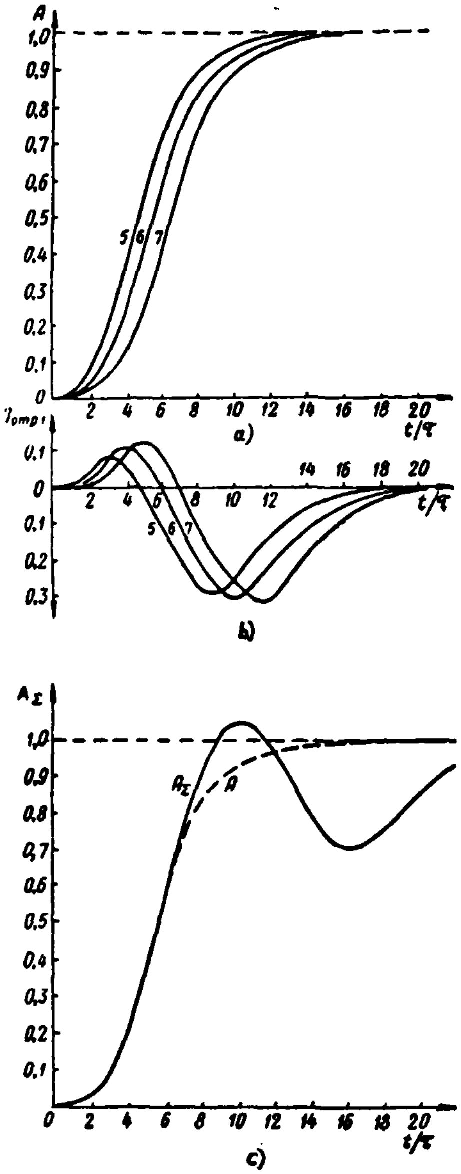

Fig. 9.13. Components, which present transient response of amplifier.

Page 477.

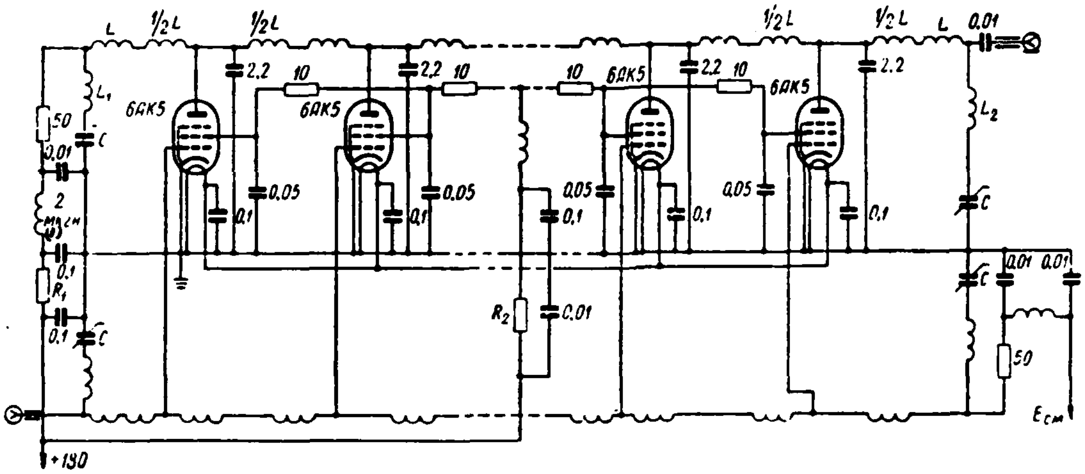

Fig. 9.14. Amplifier circuit of traveling wave on tubes 6AK5.
Key: (1). μH.

Page 478.

Amplifier consists of four sections and gives amplification at 5.1 dB. The passband of amplifier is equal to 290 MHz, the resistance of the load is 43.4 ohms. In the amplifier were utilized the transistors 1N1143. the input and output capacitances of transistors were $C_i = C_0 = 5$ pF. Input resistance of transistor on alternating current $R_i \approx 500$ of ohms, and output R_e=280 kilohms. (At a frequency of 200 MHz of value R_i and R_e they are reduced to 150 and 300 ohms respectively). Amplifier is assembled according to common-emitter connection which it

has the best characteristics, than common-base circuit.

9.5. PULSE AMPLIFIERS ON TUNNEL DIODES. OPERATING PRINCIPLE.

Elements of amplifier possessing negative resistance as, for example, tunnel diodes, can be utilized not only for generation of oscillations, but also for their amplification. The amplifiers, made on the elements with negative resistance, differ from usual amplifiers by tubes or transistors in terms of the fact that the effect of amplification in them it is reached due to the action of self-feedback. Therefore amplifiers on the elements with negative resistance are the regenerated (or regenerative) amplifiers or, in other words, by the underexcited oscillators.

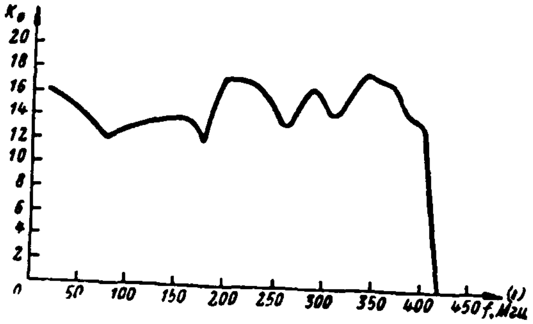

Fig. 9.15. Frequency characteristic of traveling-wave amplifier.

Key: (1). MHz.

Page 479.

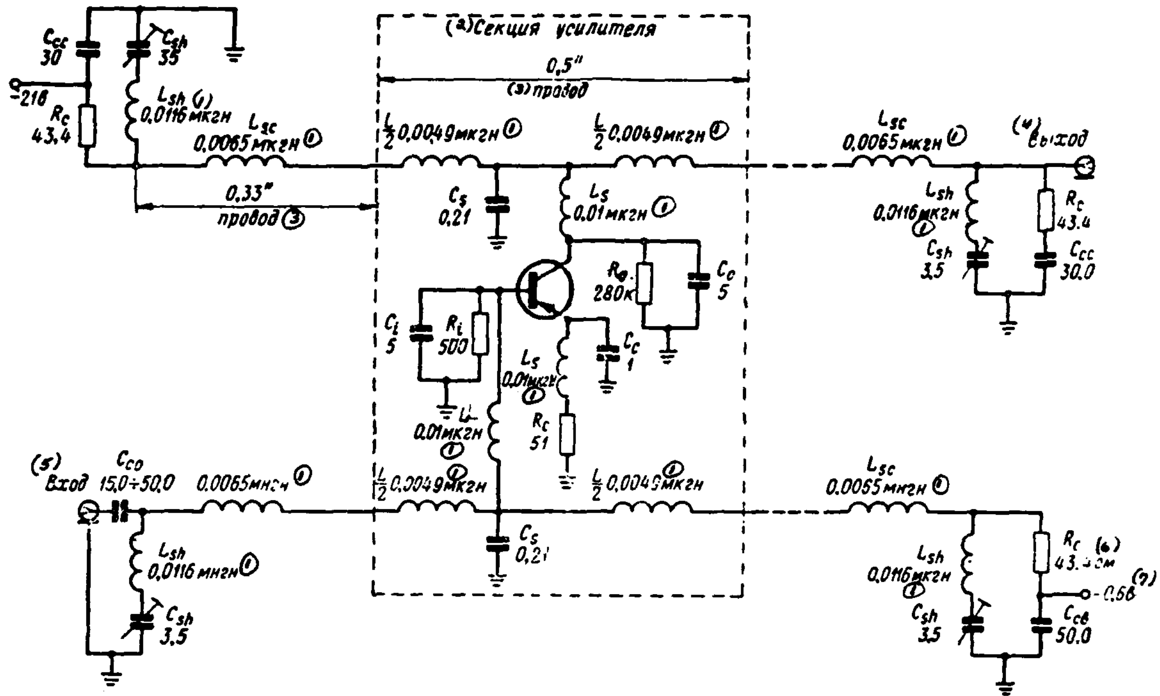

Fig. 9.16. Amplifier circuit of traveling wave, made on transistors.

Key: (1). μH. (2). Section of amplifier. (3). wire. (4). output. (5). input. (6). ohm. (7). V.

Page 480.

Simplest amplifier circuit, made on tunnel diode, is given in Fig. 9.17a. It consists of tunnel diode TD, source of signal and resistor/resistance R. Let us examine the operating principle of this diagram, after being restricted at first to the region of the low frequencies, which does not affect the action of the reactive/jet parameters of circuit and tunnel diode. Equivalent amplifier circuit for this case is depicted in Fig. 9.17b. The resistor/resistance of spreading is included here in the resistance/resistor of load R. Feed

circuits in the figure are not shown.

It is necessary for steady state of equilibrium of this diagram (as this was shown in Chapter 7) so that resistance/resistor of load R would be lower than modulus/module of negative resistance R_0. Therefore load straight line will cross the volt-ampere characteristic of tunnel diode (Fig. 9.18). The angle of the slope of full-load saturation curve ϵ will be more than the angle of the slope γ of the falling/incident section of the linearized volt-ampere characteristic. The point of intersection of full-load saturation curve with the axis of abscissas will indicate the value of voltage of supply source $\mathcal{E}$.

Under the action of source of alternating voltage $\mathcal{E}$, load straight line will be moved in parallel to itself to value U_0 - amplitude of amplified voltage (this value it is counted off along axis of abscissas). Because of this the operating point will be moved according to the volt-ampere characteristic of tunnel diode in section BC. In this case the amplitude of alternating voltage on the tunnel diode U, as can be seen from Fig. 9.18, there will be more than the amplitude of applied voltage.

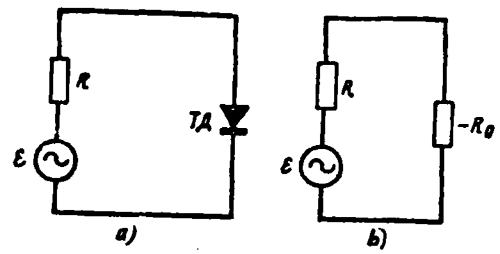

Fig. 9.17. Simplest amplifier circuit, made on tunnel diode.

Page 481.

It is not difficult to see also that at the sharper the angle will intersect the full-load saturation curve the falling/incident section of volt-ampere characteristic, the greater the amplitude of the output voltage U will be. In other words, for obtaining the high amplification factor it is necessary that the resistance/resistor of load R would be close to the modulus/module of negative resistance of tunnel diode.

As can be seen from equivalent diagram, tunnel diode amplifier is potentiometer, which consists of resistors/resistances of $R-R_0$, to which is conducted/supplied voltage υ_0. The transmission factor of this potentiometer

$$K_0=\frac{-R_0}{R-R_0}=\frac{1}{1-R/R_0}$$

is more than one, because one of its arms has negative resistance.

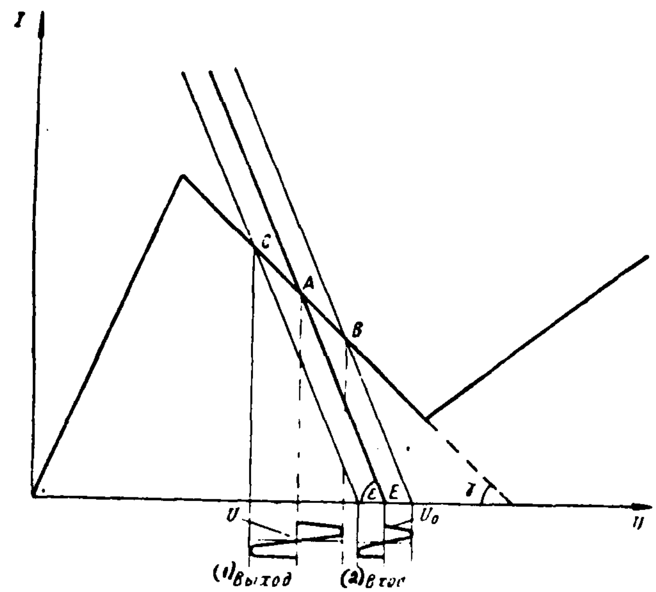

Fig. 9.18. To explanation of operating principle of amplifier.
Key: (1). output. (2). input.

Page 482.

Approaching the ratio R/R_0 to one, it is possible to obtain any value of amplification factor from the diagram. However, in proportion to approximation/approach R/R_0 to one sharply grows/rises the danger of the self-excitation of diagram. Therefore, it is virtually difficult to obtain from one cascade/stage of tunnel diode amplifier amplification factor more than 10.

Tunnel diode amplifier detects much in common with re-generative amplifiers. As is known, the amplifier gain with the positive feedback

$$K_{o6} = \frac{K}{1-m},$$

where K - amplifier gain without the feedback, and m - factor of feedback.

Value 1/(1-m) is gain in amplification factor, attained due to introduction to positive feedback, i.e. due to regeneration. The amplifier gain unlimitedly grows with m⁻1, while amplifier is self-excited with m=1.

Similar pattern is observed also in tunnel diode amplifier. In this simplest diagram value R/R_0 plays the role of the factor of feedback. Therefore entire/all value of the factor of amplification of this type of amplifier is determined only by gain due to the regeneration.

Let us consider now action of transition capacitance and let us depict equivalent amplifier circuit on tunnel diode in the form of Fig. 9.19.

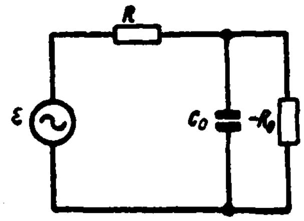

Fig. 9.19. Equivalent amplifier circuit on tunnel diode.

Page 483.

Complex transmission factor of this circuit

$$\overline{K}(\omega)=\frac{\frac{1}{1-R/R_0}}{1+j\omega C_0 R\frac{1}{1-R/R_0}}=\frac{1}{(1-R/R_0)(1+j\omega\tau_{0e})},$$

where $\tau_{0e}=\frac{C_0 R}{1-R/R_0}$.

Passband of amplifier with this characteristic at level $1/\sqrt{2}$.

$$\Delta F=\frac{1}{2\pi\tau_{0e}}=\frac{1-R/R_0}{2\pi C_0 R},$$

and the area of amplification

$$Q=K_0\Delta F=\frac{1}{1-R/R_0}\cdot\frac{1-R/R_0}{2\pi C_0 R}=\frac{1}{2\pi C_0 R}.$$

As is known, introduction to positive feedback to amplifier, time constant of which is equal to τ, it increases it in 1/(1-m) times, which leads to decrease in so many once of passband of amplifier. The area of amplifier gain in this case remains constant/invariable. It is evident from that presented that the amplifiers on the elements

with negative resistance possess all properties of re-generative amplifiers. This is completely natural, since the elements with negative resistance are to circuit with the internal positive feedback.

For transient response of RC-circuit on tunnel diode it is possible to write following expression:

$$A(t) = K_{0e}(1 - e^{-t/\tau_{0e}}),$$

where

$$K_{0e} = \frac{k}{1-m}, \quad \tau_{0e} = \frac{\tau}{1-m}, \quad k = \frac{R_0}{R+R_0},$$

$$m = \frac{2R}{R+R_0}, \quad \tau = C_0 R', \quad R' = \frac{RR_0}{R+R_0}.$$

With m>1 diagram on tunnel diode is bistable flip-flop, while when m<1 - a resistance-coupled amplifier.

Page 484.

9.6. AMPLIFIER CIRCUITS ON THE TUNNEL DIODES.

Simplest amplifier circuit on tunnel diode, given in Fig. 9.17, always cannot be realized for following reasons. For the stabilization of amplification resistor/resistance R must be less than R_0. As it was already said, the resistor/resistance of spreading tunnel diode R_s enters into value R.Furthermore, into it enters the internal resistor/resistance of the source of signal R_i. In a number

of cases even in the absence of the supplementary resistor/resistance R_1 sum R_s+R_i is more than the modulus/module of negative resistance of the tunnel diode R_0.

Therefore in order to ensure stable work of amplifier, it is necessary to modify its diagram, for example, in the manner that it is shown in Fig. 9.20a. This diagram is characterized by from the preceding/previous fact that in parallel to tunnel diode in it stands back-out resistor $R_{\text{ш}}$. Fig. 9.20b shows the equivalent schematic of this amplifier.

In order to clarify action of shunt on properties of tunnel diode, let us turn to figure 9.21, in which are shown volt-ampere characteristics of tunnel diode, shunted by resistor/resistance $R_{\text{ш}}$. Lower curve corresponds to case $R_{\text{ш}}=\infty$, i.e. presents the initial volt-ampere characteristic of tunnel diode. Upon the inclusion of resistor/resistance $R_{\text{ш}}>R_0$ the form of volt-ampere characteristic changes.

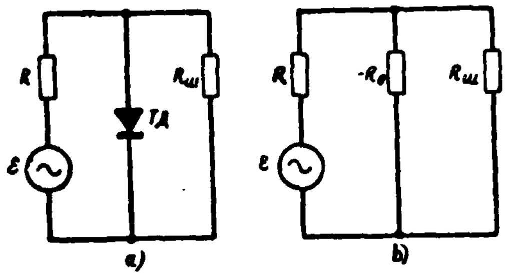

Fig. 9.20. Parallel amplifier circuit on tunnel diode.

Page 485.

First, it entire/all passes above, since the conductivity of circuit tunnel diode - shunt is more; in the second place, the slope/transconductance of the feeding section of characteristic it decreases, which indicates an increase in negative resistance of tunnel diode. The latter is easy to explain, on the basis of the fact that the total resistance of circuit tunnel diode - shunt in the section with the negative slope/transconductance

$$-R'_0 = \frac{-R_0 R_ш}{-R_0 + R_ш}$$

on the modulus/module is more R_0.

With further decrease of resistor/resistance of shunt sets in such situation, when total resistance of tunnel diode and shunt goes to infinity (in this case $R_ш = R_0$). The middle section of volt-ampere characteristic goes in parallel to the axis of abscissas. In this section impedance of tunnel diode is approximately equal to the resistor/resistance of transition capacitance how they sometimes use

for measuring this capacity/capacitance. If $R_{m}<R_{0}$, then on the volt-ampere characteristic of diode middle section acquires positive inclination/slope.

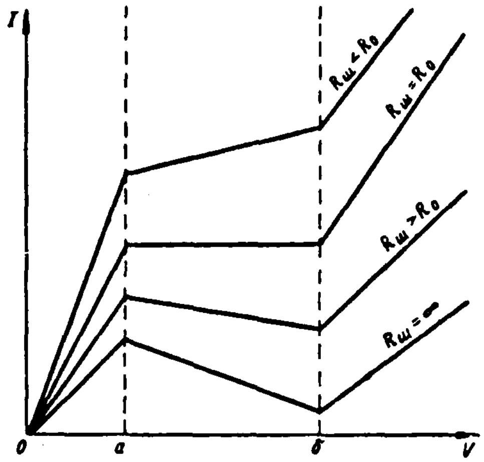

Fig. 9.21. Effect of back-out resistor on characteristics of tunnel diode.

Page 486.

Thus, shunting of tunnel diode, used in amplifier circuit, increases negative resistance of diode and stability of diagram provides thereby. This diagram during the investigation can be brought to the diagram, examined in the preceding/previous section, if we replace in it the resistor/resistance of tunnel diode $-R_0$ on $-R'_0$.

System described above is called parallel. Together with it finds use series circuit of amplifier (Fig. 9.22a). In this to diagram the source of signal, tunnel diode and load resistance/resistor are connected in series. The equivalent schematic of this amplifier is shown in Fig. 9.22b. For guaranteeing the stable operation of this diagram it is necessary that the total resistance R_i+R_n would be less than R_0. This fact to a certain degree limits the

application of series circuit, which, however, has a series/row of advantages in comparison with the parallel diagram (with the work in the compound configurations with the transistors, with the cascade inclusion, etc.).

Transmission factor of amplifier (here it is examined region of low frequencies)

$$K_0 = \frac{R_{11}}{R_1 + R_{11} - R_0}$$

unlimitedly grows/rises in proportion to approximation/approach of sum of positive resistors/resistances $R_i + R_{11}$ to R_0. The characteristics of consecutive amplifier are similar to the characteristics of the amplifier, assembled according to parallel diagram.

Fundamental amplifier circuit with series connection of diode is given in Fig. 9.23a.

( )

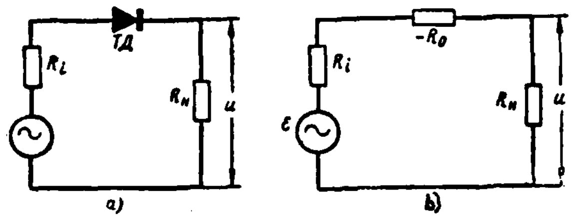

Fig. 9.22. Series circuit of tunnel diode amplifier.

Page 487.

Another feed circuit of diode and transient circuit, which connects amplifier with the subsequent cascade/stage, are shown on this diagram besides the source of signal, tunnel diode and load. Here C_{01} - output capacitance of the source of signal, and C_{02} - the input capacitance of amplifier is given in Fig. 9.23b. On it the tunnel diode is replaced with resistor $-R_0$ and capacitance C_0 (it is assumed that $R_s \ll R_0$).

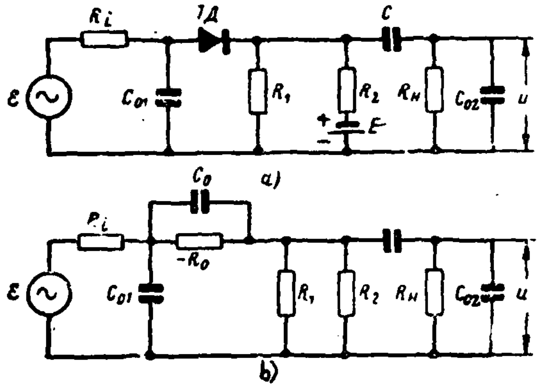

Fig. 9.23. Complete electrical circuit of consecutive tunnel diode amplifier.

Page 488. To [174] is given the calculation of this diagram and the following expressions for its frequency and phase response:

$$K_{\text{в}}(\omega) = K_0 \sqrt{\frac{1+\omega^2\tau^2}{(1+\omega^2\tau_{\text{а}}^2)(1+\omega^2\tau_{\text{б}}^2)}},$$

$$\varphi_{\text{в}}(\omega) = -\operatorname{arctg}\omega\tau_{\text{а}} - \operatorname{arctg}\omega\tau_{\text{б}} - \operatorname{arctg}\omega\tau,$$

and for the region of the lower frequencies

$$K_{\text{н}}(\omega) = \frac{1}{\sqrt{1+\frac{1}{\omega^2\tau_{\text{н}}^2}}},$$

$$\varphi_{\text{н}}(\omega) = \operatorname{arctg}\frac{1}{\omega\tau_{\text{н}}},$$

$$K_0 = \frac{R_{\text{эн}}}{R_i + R_{\text{эн}} - R_0},$$

where

$$R_{\text{эн}} = \frac{R_{\text{н}}R_{\text{п}}}{R_{\text{н}}+R_{\text{п}}},\quad R_{\text{п}} = \frac{R_1R_2}{R_1+R_2},\quad R_{\text{э}i} = \frac{R_{\text{п}}(R_0-R_i)}{R_0-R_{\text{п}}-R_i},$$

$$\tau_{\text{а,б}} = \frac{2\tau_1^2}{\tau_2 \mp \sqrt{\tau_2^2 - 4\frac{\tau_1^2}{|K_0|}}};$$

$$\tau_1^2 = \tau\tau_i + \tau\tau_{\text{эн}}\frac{R_i}{R_{\text{эн}}} + \tau_i\tau_{\text{эн}}\frac{R_0}{R_{\text{эн}}},$$

$$\tau_2 = \tau_i\left(1 - \frac{R_0}{R_{эн}}\right) + \tau_{эн}\left(\frac{R_i}{R_{эн}} - \frac{R_0}{R_{эн}}\right) - \tau\left(1 - \frac{R_i}{R_{эн}}\right),$$
$$\tau = R_0 C_0,\quad \tau_i = R_i C_{0i},\quad \tau_{эн} = C_{02} R_{эн},\quad \tau_н = C(R_{эi} + R_н).$$

Upper and lower cut-off frequencies of amplifier are determined as follows:

$$F_в = \frac{1}{2\pi\tau_э}\sqrt{\sqrt{1 + \frac{\tau_э^4}{\tau_1^2 K_0^2}} - 1},\quad F_н = \frac{1}{2\pi\tau_н},$$

where

$$\tau_э = \frac{\tau_1^2}{\sqrt{\tau_2^2 - 2\frac{\tau_1^2}{|K_0|}\left(1 - \frac{\tau_2}{\tau_1^2}\right)}}.$$

Fundamental amplifier circuit with parallel connection of tunnel diode is given in Fig. 9.24.

Page 489.

The equations of its frequency and phase responses will be recorded as follows: for the region of the higher frequencies

$$K_в(\omega) = \frac{K_0}{\sqrt{1 + \omega^2\tau_в^2}},$$
$$\varphi_в(\omega) = -\operatorname{arc\,tg}\,\omega\tau_в;$$

for the region of the lower frequencies

$$K_н(\omega) = \frac{K_0}{\sqrt{1 + \frac{1}{\omega^2\tau_н^2}}},$$
$$\varphi_н(\omega) = \operatorname{arc\,tg}\frac{1}{\omega\tau_н},$$

where

$$K_0 = \frac{G_a}{G_0 + G_{\text{н}э} - \frac{1}{R_0}},$$

$$G_i = \frac{1}{R_i},\ G_{\text{н}} = \frac{1}{R_{\text{н}}},\ G_{\text{н}э} = G_{\text{н}} + G_{\text{н}},\ G_{\text{н}} = \frac{1}{R_{\text{н}}},$$

$$\tau_{\text{в}} = \frac{C_0 + C_{01} + C_{02}}{G_i + G_{\text{н}э} - \frac{1}{R_0}},\ \tau_{\text{н}} = C\left(R_{\text{н}} + \frac{R_0}{G_i R_0 + G_{\text{н}} R_0 - 1}\right).$$

Upper and lower band edges of transmission

$$F_{\text{в}} = \frac{1}{2\pi\tau_{\text{в}}},\ F_{\text{н}} = \frac{1}{2\pi\tau_{\text{н}}}.$$

According to formulas given above it is possible to perform calculation of amplifiers.

9.7. DISTRIBUTED TUNNEL DIODE AMPLIFIERS.

In the case when amplification of one cascade/stage is insufficient there appears the need for series connection of cascades/stages. In connection with diagrams on the tunnel diodes this question cannot be examined as simply as in the case of applying the tube, since tunnel diode is two-terminal network; therefore it is necessary to resort to some special procedures. Fig. 9.25a shows amplifier circuit on the tunnel diode. Capacity/capacitance of C and inductance L in the frequency band in question are received as so/such large that their effect can be disregarded/neglected.

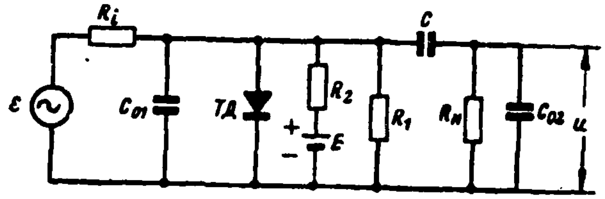

Fig. 9.24. Complete electrical schematic of parallel tunnel diode amplifier.

Page 490.

Then equivalent amplifier circuit will take the form, shown in Fig. 9.25b. Since further examination is conducted only for the relatively low frequencies, then capacitance C_0 of diode is not shown. Amplification of this cascade/stage

$$K_1 = \frac{R}{R - R_0}.$$

So that it would be possible to connect in series cascade/stage, is required to add into diagram one additional tunnel diode, whose presence does not change value of factor of amplification of diagram [175]. This cascade/stage is shown in Fig. 9.26a, and its equivalent diagram in Fig. 9.26b. The factor of amplification of this diagram is the same. The input resistance of the first diagram (Fig. 9.25)

$$R_{вх} = R - R_0,$$

and of the second (Fig. 9.26)

$$R'_{вх} = \frac{-R_{01}(R - R_0)}{R - R_0 - R_{01}}.$$

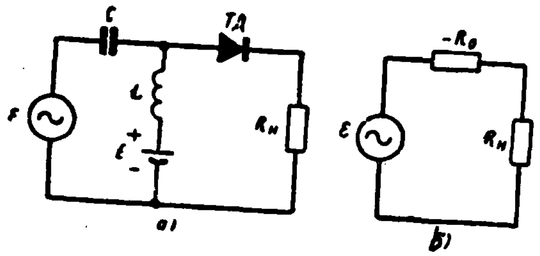

Fig. 9.25. Amplifier circuit on tunnel diode.

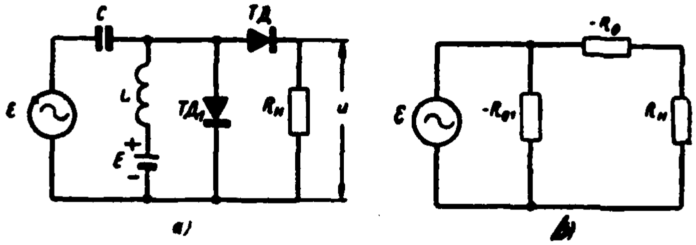

Fig. 9.26. Amplifier circuit with supplementary tunnel diode.

Page 491.

It is possible to select $-R_{01}$ such that in order to $R'_{ex}=R$, then

$$-R_{01}=\frac{R(R-R_0)}{-R_0}.$$

The input resistance of this diagram is equal to load resistance/resistor. This means that the second diagram can be utilized as load for the first diagram.

Schematic of multistage amplifier is shown in Fig. 9.27. The amplification of this diagram is equal K_1K^2, where

$$K_1=\frac{R}{R+R_1+R_0}.$$

This diagram can be considered as a transmission line, which connects the oscillator with a load. Since it consists of elements with negative resistance, then it creates amplification, but not loss. Diagram described here can be considered as one of the versions of the distributed tunnel diode amplifier.

Another type of traveling-wave amplifier [176] (Fig. 9.28) is the network of filters, which consists of N sections.

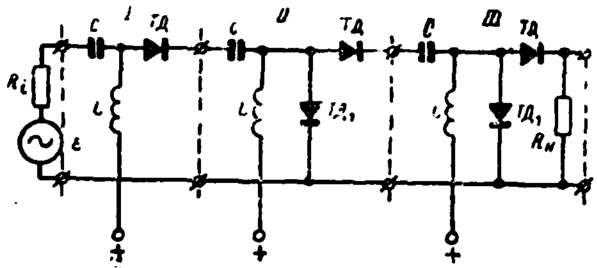

Fig. 9.27. Schematic diagram of multistage tunnel diode amplifier.

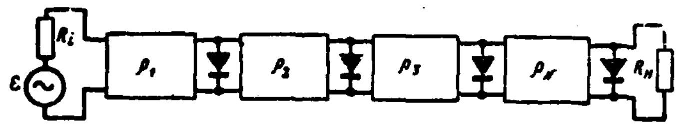

Fig. 9.28. Amplifier circuit of traveling wave on tunnel diodes.

Page 492.

Each of the sections is equivalent to the section of the long line, at end/lead of which is included/switched on tunnel diode, i.e., the parallel connection of negative resistance. $-R_0$ and capacitance C_0. Let the section of long line with the wave impedance ρ be loaded to the parallel connection of resistances $-R_0$ and $R_н$. In this case total resistance at the end/lead of the line

$$R=\frac{R_н R_0}{R_0+R_н}.$$

If $R=\rho$, then the line will be matched. In this case for satisfaction of matching conditions it is necessary that $R_н$ would be less ρ.

In order to attain agreement in presence of capacity/capacitance, it is necessary from section of long line to pass to its equivalent, since this is shown in Fig. 9.29. In this case the capacity/capacitance of the tunnel diode C_0 must be equal to capacity/capacitance of C/2, which loads line. The critical frequency of line $F_{кр}$ and capacity/capacitance of C_0 determine the characteristic impedance

$$\rho=\sqrt{\frac{L}{C}}\quad\left(f_{кр}=\frac{1}{\pi\sqrt{LC}}\right),$$

whence

$$\rho=\frac{1}{\pi C f_{кр}}.$$

Resistance/resistor of load $R_н$ can be input resistance of second cascade/stage ρ_2. The wave impedance of the second cascade/stage must be lower than the characteristic impedance of the first cascade/stage so that the condition for agreement would be satisfied. Analogously still several cascades/stages can be added to the diagram.

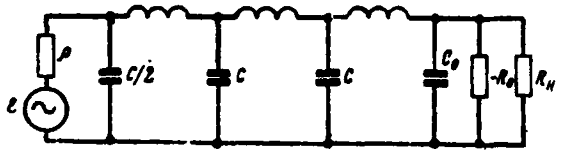

Fig. 9.29. Equivalent schematic diagram of section of traveling-wave amplifier on tunnel diodes.

Page 493.

The latter of them is loaded to the resistance/resistor of load $R_н$. The Nth cascade proves to be loaded on its characteristic impedance, if

$$\frac{1}{R_н}=\frac{1}{\rho_1}+\frac{N}{R_0}.$$

Critical frequency of line

$$f_{кр}=\frac{1}{\pi\sqrt{L_1C_1}}=\frac{1}{\pi\sqrt{L_2C_2}}=\ldots=\frac{1}{\pi\sqrt{L_NC_N}}.$$

Since line will agree in limits of passband, voltage amplification factor is equal to one. However, the power gain of more than one due to the decrease of resistor/resistance is determined by the relationship/ratio

$$G=\frac{\rho_1}{R_н}=1+\frac{N\rho_1}{R_0}.$$

Is described also traveling-wave amplifier [177] with narrow

track diode, arranged/located along axis of strip line, and with two absorbing loads at certain distance the it (Fig. 9.30).

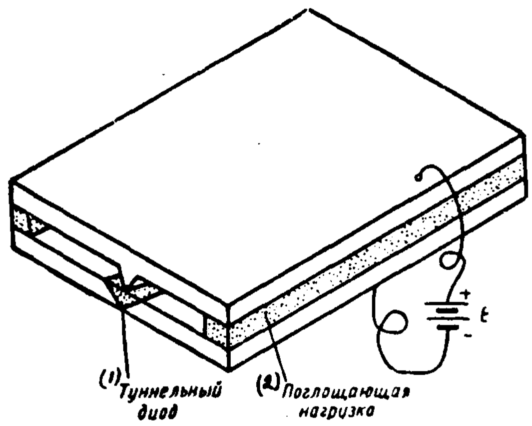

Fig. 9.30. Diagrammatic representation of traveling-wave amplifier, made on distributed tunnel diode.

Key: (1). Tunnel diode. (2). Absorbing load.

Page 494.

In this system are propagated the waves of the type TE, whose phase rate is lower than the speed of light as a result of the capacitive load of track tunnel diode. For these waves magnetic and electric fields in the direction, perpendicular to the band, attenuate exponentially and proportional to frequency. Therefore two absorbing loads have considerable conductivity for all low-frequency oscillations (including for the direct current), without exerting a substantial influence on the high-frequency fields. The difficulty of the realization of this system consists in the fact that it amplifies in both directions. Weak mismatches in the line are the sources of standing waves and if amplification is great, generation begins. On the strength of the fact that negative resistance operates at all

frequencies, the problem of the agreement of the input and output over a wide range of frequencies virtually hardly it is feasible.

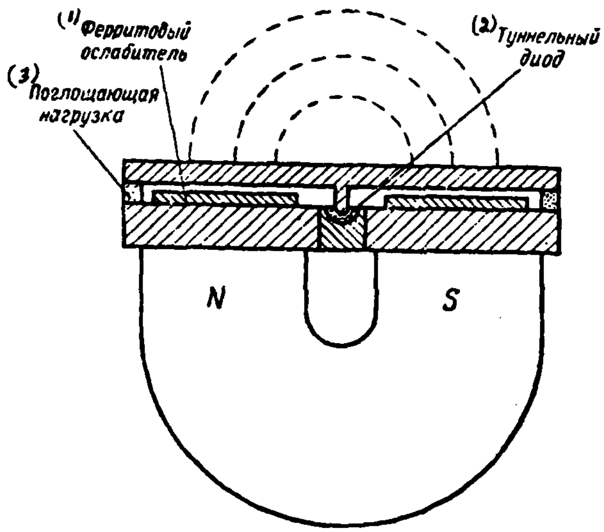

Fig. 9.31. Design of traveling-wave amplifier on distributed tunnel diode.

Key: (1). Ferrite attenuator. (2). Tunnel diode. (3). Absorbing load.

Page 495.

For eliminating generation in the traveling-wave amplifier combined system, which includes distributed tunnel diode and nonreciprocal ferrite attenuator [177], was proposed. This system amplifies the signals which pass in one direction, weakening/attenuating them in the other direction. In the device/equipment there are thin ferrite plates located along both sides from the narrow track diode. The permanent magnet, on which is arranged/located this device/equipment, creates in the ferrite nonuniform field, strong near the axis and weaker on the edges of strip line. Therefore the frequency of ferromagnetic resonance

decreases in proportion to removal/distance from the axis, which retains the nonreciprocal properties of ferrite medium in the very broadband (Fig. 9.31).

9.8. Amplification of pulses in the diagrams on the tubes with the secondary emission. Pulse feed of amplifiers.

Let us examine possibilities of use for amplifying pulses of short duration of usual diagrams on tubes with secondary emission and pulse feed of amplifiers.

One of amplifier circuits on tube with secondary emission is given in Fig. 9.32 [40].

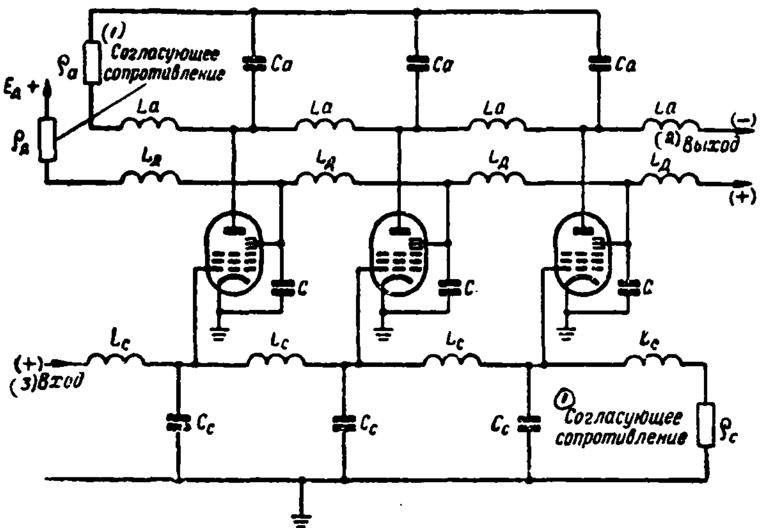

Fig. 9.32. Amplifier circuit of traveling wave on tubes with secondary emission.

Key: (1). Matching resistance. (2). Output. (3). Input.

Page 496.

Amplifier was made on tubes EFP-60, whose cut-off frequency, determined only taking into account interelectrode capacitances, was equal to 225 MHz. The intertube connection was the low-pass filter, formed by elements L and C. The role of capacitances C/2 was fulfilled by the input and output capacitances of the tubes. Resistors R_1 were equal to the characteristic impedance of filter $\rho=\sqrt{\frac{L}{C}}$. In this case the quadrupole in the sufficiently wide frequency band presented for the anode circuit of tube resistor/resistance $\frac{\rho}{2}=\frac{R_1}{2}$. In the anode circuit of tube was switched on resistor/resistance R and sufficiently large inductance L_0. Four cascades/stages of this amplifier gave the voltage amplification,

equal to 500 (i.e. on 4.7 to the cascade/stage). The passband of amplifier was from 10 kHz to 50 MHz, which corresponded to the cut-off frequency of one cascade/stage, equal to 240 MHz. (This value is somewhat higher than the cut-off frequency of the tube because the action of interelectrode capacitances is partially compensated by the action of the inductance of filter).

In certain cases, for increasing the mutual conductance of tubes pulse feed is used. The increase of anode current makes it possible to obtain the large amplitude of output voltage with the same resistor/resistance of plate load. The schematics of such amplifiers are given in Fig. 9.33 and 9.34 [178]. In these amplifiers were utilized tubes 6Zh22P and 6V1P with mutual conductance in the usual mode of approximately 30 mA/V. With the pulse feed of tube 6Zh22P ($E_a=E_э=450$ V, voltage on the space-charge grid is 150 V) its transconductance grew to 80-90 mA/V. With the pulse feed of tube 6V1P ($E_a=1000$ V, $E_э=800$ V, $E_n=250$ V) the slope/transconductance of tube reached 100-120 mA/V. In both cases the cutoff voltage of tube was 5-6 V. The pulse responses of tubes 6Zh22P and 6V1P are given in Fig. 9.35. The application of tubes with the secondary emission is convenient when on the output there must be symmetrical voltage; in this case output signal is removed/taken from anode and diode of tube.

Page 497.

Increase in anode current and slope/transconductance of grid characteristic made it possible to obtain high amplification factor

with diphenyl chloride low resistance/resistors of load (30-150 ohms) which provided required broad-band character of amplification.

In amplifier, whose schematic is given in Fig. 9.33, voltages/stresses on anodes and screen grids of tubes are constant and are equal to 450 V. In the absence of voltage on the space-charge grid of tube 6Zh22P its anode current is virtually equal to zero. Operating conditions of tube is installed by supply to the space-charge grid of positive pulse with a duration of 0.6 μs and with an amplitude of 150 V. This pulse is removed/taken from the cathode follower L_3. With the opening of one of the tubes of amplifier on its plate load there is isolated negative pulse - pedestal, which corresponds to the pulse of feed. The amplitude of pedestal can reach 100 V.

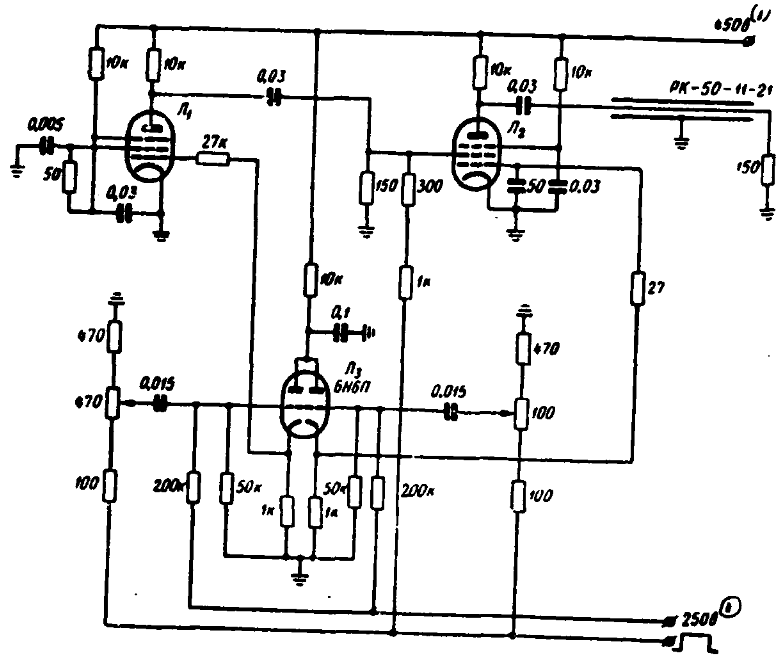

Fig. 9.33. First amplifier circuit with pulse feed.
Key: (1). V.

Page 498.

With the series connection of several amplifier stages the compensation for the pedestal, which enters together with the signal the grid of the following tube, is necessary. Compensation is realized by supply from the adjustable divider of the part of the positive voltage, which enters the space-charge grid.

Circuit of compensating divider with resulting value of resistor/resistance of 75 ohms is the load of the first cascade/stage. The output stage is loaded to coaxial cable with a wave impedance of 150 ohms. Amplifier has a factor of amplification by 60 and a time of

the establishment of transient response 3 ns. Maximum signal amplitude at the output is 50 V.

In the second amplifier (Fig. 9.34) the circuit of divider with cathode follower is load of first tube.

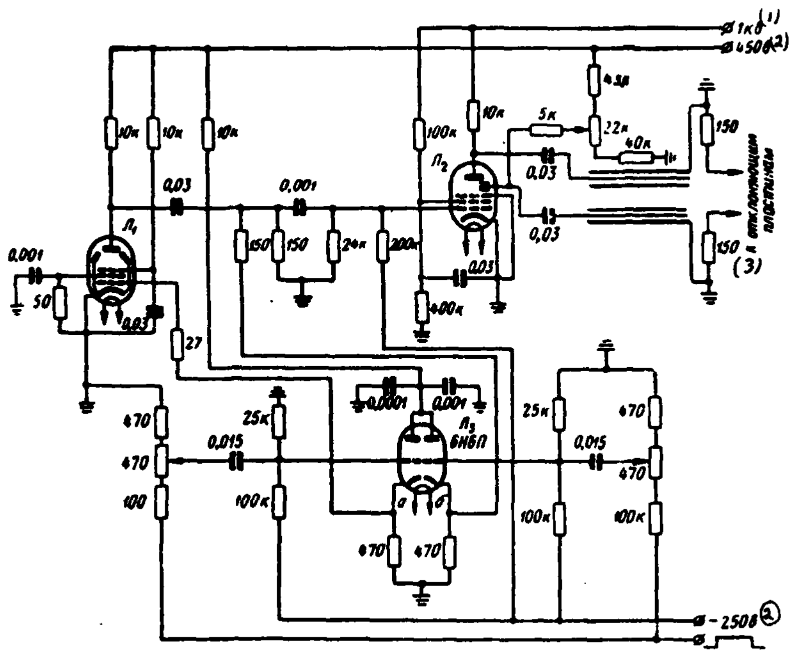

Fig. 9.34. Second amplifier circuit with pulse feed.

Key: (1). kV. (2). V. (3). to deflector plates.

Page 499.

Simultaneously this circuit fulfills the following functions: 1) triggers that preliminarily closed on control electrode of tube L_2; 2) compensate the negative pedestal, which enters from the anode of tube L_1 the grid of tube L_2; 3) realize a selection of operating point on the grid of tube L_2 in accordance with the polarity of the amplified signal.

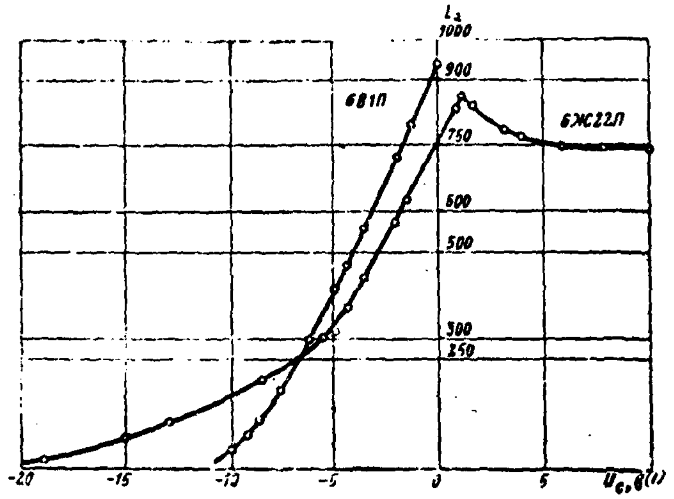

Fig. 9.35. Pulse responses of tubes 6V1P and 6Zh22P.

Key: (1). V.

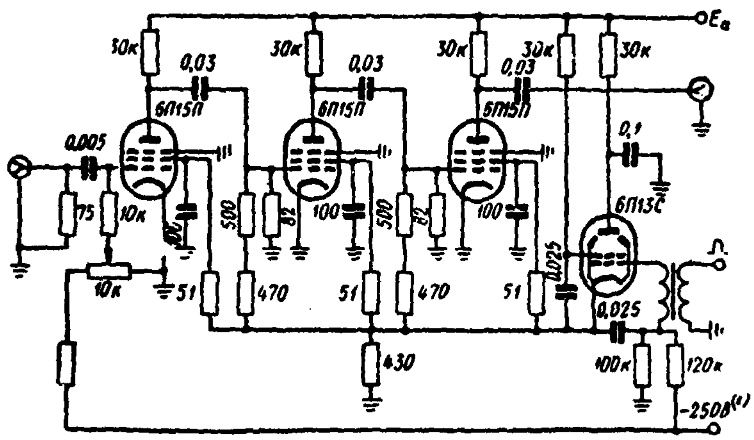

Fig. 9.36. Amplifier circuit with pulse feed as an attachment to oscillograph.

Key: (1). V.

Page 500.

The equivalent load resistor/resistance of this circuit with respect

to the tube L_1 is equal to 100 ohms. The factor of amplification of diagram is equal to 150 with the maximum voltage 160 V. Amplifiers worked stably and stably at the pulse repetition rate with 1 kHz.

Amplifier circuit with pulse feed on tubes 6P15P is shown in Fig. 9.36 [179]. One amplifier stage on this tube during the supplying to its grid of the voltage pulses with an amplitude of 800 V with $E_a = 1$ kV gives amplification factor by 3.2, allotting on the load, to the equal to 75 ohms, pulses with the amplitude of 50 V. The time of the establishment of pulses is approximately 2 ns. The three-stage amplifier given in the figure has an amplification factor equal to 30, with the time of the establishment of pulses, which does not exceed 3 ns, when $R_n = 75$ ohm the amplitude of output voltage is 50 V, but when $R_n = 150$ ohm amplitude rises to 90-100 V. In the second case the amplification factor attains 55-60, and the time of establishment increases to 4 ns.

Amplifiers, intended as attachments to oscillographs, were described also into [180]. With the amplification factor by 10-15 these amplifiers provided output voltage into several hundred volts in the band to 200 MHz. In the amplifiers the tubes with the space-charge grid, with the secondary emission in the pulsed operation of feed were utilized.

Thus, application of pulse feed of tubes with large slope/transconductance makes it possible to carry out necessary

undistorted amplification of pulses sufficiently short duration. Amplifier circuits with the pulse feed contain, as a rule, fewer tubes than the amplifier circuits of the traveling wave, and require less than the power from power supplies; however, one overall serious deficiency is inherent in these diagrams: they cannot work at the very high pulse repetition rate, since this leads to the excessive boosting of the mode of tubes.

Page 501.

CHAPTER TEN.

OSCILLOGRAPHY OF PULSES.

10.1. Specific character and methods of oscillography of nanosecond pulses.

Oscillography of nanosecond pulses has series/row of specific moments characteristic for general problem of precise measurement of time and investigation of processes of very short duration. The problem of the investigation of single short-term processes is most difficult. The methods of the solution of this problem are examined by the so-called temporary/time microscopy (high-speed/high-velocity oscillography, super high-speed cinemotagraphy, optical and electron-optic chronography).

Time microscopy in its improvement is encountered with existence of fundamental limit of time resolution, which under practical conditions for analysis of single processes is 10^{-14} s [181]. The presence of the limit of physical time resolution corresponds to the known quantum-mechanical uncertainty principle. During the investigation of the periodically repeating short-term processes in a number of cases it is possible to achieve the higher threshold of time resolution.

In the case of high-speed/high- velocity oscillography presence

of limit of time resolution is caused mainly by fact that all real systems, intended for transmission of fast signal and its time sweep, have limited passband of frequencies. It is known from the spectral analysis that for the system with the frequency of transmission Δf the time resolution cannot be better than Δt, determined by the ratio $\Delta f \Delta t = const$.

Page 502.

This constraint of temporary/time resolution is associated with distortions in circuit of signal of oscillographs. Furthermore in the oscillographs of nanosecond range occur other reasons for the limitation of resolution. Supplementary limitations in the resolution, connected with the difficulties of obtaining the sufficiently bright image on the screen/shield of oscilloscope tube, appear with the oscillography of single pulses. During recording of periodic pulses in connection with very high scanning speeds, in turn, it is necessary to surmount difficulty, connected with obtaining of the high stability of the temporary situation of pulse on tube face.

Oscillography of nanosecond pulses is at present realized by two methods. The first method (high-speed/high-velocity oscillography) is used already long ago during recording of single very short-term processes of [182]. Here with the aid of the wide-band cathode-ray tube of low sensitivity and high-speed scanning there is observed the oscillogram of the phenomenon being investigated.

With the development of nanosecond pulse technology high- speed oscillographs with higher sensitivity with wide passband were required. The application of new oscilloscope tubes and wideband amplifiers became necessary. Since it was necessary to record short-term phenomena both single and periodically repeating, then the need for the development of high-speed scannings with high stability of the parameters arose.

With oscillography of pulses with small amplitudes in the case of application for this of amplifiers of circuit of signal, it is necessary to simultaneously ensure their broad-band character with high amplification factor. However, the greatest broad-band character is usually reached by the value·of gain reduction. Therefore for observing the pulses by the duration of the order of nanosecond are used high-speed/high-velocity oscillographs without the amplifiers, but the using special oscilloscope tubes with the deflection system of the type of the traveling wave (TBV).

Page 503.

Such tubes are sufficiently wide-band (to 3-5 GHz) and have the increased sensitivity (from 0.5 V to 0.05 V to the line of ray/beam). Recording nanosecond pulses with an amplitude less than 0.1 V with the aid of the high-speed/high-velocity oscillographs proves to be still impossible due to the absence of qualitative amplifiers. In these cases another method of oscillography is used.

Second method of oscillography of nanosecond pulses is based on stroboscopic principle of observation of periodic processes of [183]. On the screen/shield of usual oscilloscope tube is here observed not most process being investigated directly, but its image formed by the individual sections (points) of its oscillogram. In such oscillographs with the aid of the special strobe pulses of very short duration and schematic of converter periodically are examined/scanned the individual sections of the pulse being investigated. The sections of the pulse chosen after converter are expanded and through the amplifier enter the oscilloscope tube, where, being arranged/located in the specific sequence and at the necessary level, the image of pulse is formed.

Since here pulses of nanosecond duration, which have very small amplitude, first are converted, and then only after expansion are amplified, then passband of amplifier can be narrow, but amplification factor by large. As a result the sensitivity of stroboscopic oscillographs proves to be high (to 1 mV/cm) with a sufficient effective passband of instrument. However, stroboscopic method is applicable to the investigations of periodic processes, but it does not make it possible to record single pulses.

As is evident, both methods supplement each other, expanding possibilities of oscillography of nanosecond pulses.

Page 504.

10.2. Special features of high-speed oscillography Resolution. Block diagram of oscillograph.

Block diagram of oscillograph is given in Fig. 10.1. Scanning of the oscillograph here is preliminarily started, and then enters the pulse being investigated directly on the deflection system of tube. Starting system provides the synchronization of the moments/torques of the beginning of scanning/sweep, illumination of the ray/beam of oscilloscope tube and signal arrival from the calibrator. During recording of single pulses appears the need for the starting of scanning by the same pulse (input key in position 2). Pulse supplies to the deflection system of the tube through the cable of delay. Delay factor is determined by triggering time of the trigger circuit and scanning/sweep.

For obtaining of high temporary/time resolution in high-speed/high-velocity oscillographs are utilized transmission systems of pulses, cathode-ray tubes, which are characterized by large broad-band character, and scannings/sweeps, characterized by high rate and high stability of parameters.

At high scanning speed, which reaches in contemporary oscillographs $2\cdot10^{10}$ cm/s, problem of synchronization of work of separate units of oscillograph, which especially records periodic pulses, proves to be fairly complicated. Thus, the requirements of high scanning speed, broad-band character of the circuit of signal and

very rigid synchronization of the work of units are characteristic for the high-speed/high-velocity oscillographs.

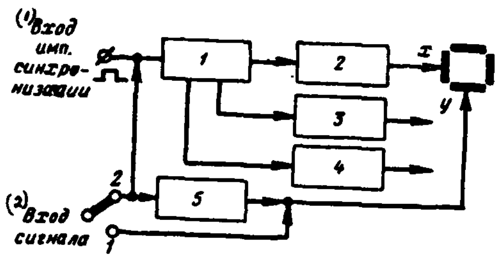

Fig. 10.1. Block diagram of oscillograph: 1 - trigger circuit; 2 - sweep oscillator; 3 - diagram of illumination of ray/beam; 4 - calibrator; 5 - cable of delay.

Key: (1). the input pulse of synchronization. (2). input of signal.

Page 505.

Graphic beam velocity.

High scanning speed, i.e., rate of displacement of electron beam over horizontal, together with considerable rate of change in value of signal, leads to very high graphic rate.

Graphic beam velocity, understood as linear velocity of displacement of ray/beam during recording of process being investigated, in this case can reach values, close to speed of light.

In the case of recording harmonic oscillation

$$y = A \sin 2\pi f t;$$

maximum speed of change in value y is determined by expression

$$v_{y\,\text{макс}} = \frac{dy}{dt}\bigg|_{t=0} = 2A\pi f.$$

Maximum graphic rate $v_{г\,\text{макс}}$ is estimated by the expression which considers also horizontal speed (scanning speed)

$$v_{г\,\text{макс}} = \sqrt{v_x^2 + v_{y\,\text{макс}}^2}.$$

Recording (under condition of sufficient intensity of the glow of tube face) oscillations with frequency of more than 3000 MHz is possible at the above-indicated scanning speed. If in this case the amplitude of oscillations on the screen/shield is more than 1 cm, then the graphic rate is close to the speed of light.

In the case of recording video pulse graphic rate is determined by expression

$$v_г = \sqrt{v_x^2 + v_y^2},$$

where v_x and v_y— respectively rate of displacement of ray/beam over horizontal and vertical axes.

This expression it is possible to record in more detail, if we obtain value for rate v_y.

Page 506.

Let σ - sensitivity of cathode-ray tube

$$\sigma = \frac{\Delta y}{\Delta U_y} \left[\frac{cm}{v}\right],$$

where Δy - path, passed by ray/beam in direction of y axis with change in voltage of pulse on value ΔU_y.

Then for rate v_y we obtain

$$v_y = \frac{\Delta y}{\Delta t} = \sigma \frac{\Delta U_y}{\Delta t}.$$

If Δt→0, then relation $\Delta U_y/\Delta t$ represents differential value of slope/transconductance of building-up S_u at the particular point (at the given instant on the tube face. Then rate v_y will be

$$v_y = \sigma S_u.$$

Graphic rate in the case of recording video pulse will be expressed

$$v_r = \sqrt{v_x^2 + \sigma^2 S_u^2}.$$

Maximum graphic rate will occur at points, which correspond to front and shear/section of recorded pulse, when slope/transconductance reaches maximum.

However, due to insufficient broad-band character of deflection system it is necessary to consider time of establishment of transient processes in it. This reduces graphic rate and, consequently, also the resolution of oscillograph. Knowing the slope/transconductance of

the transient response of the circuit of signal $S_т$, let us find impulse steepness on the screen/shield of oscilloscope tube $S_{вых}$, if the slope/transconductance of the pulse $S_и$ being investigated.

Page 507.

Using the known relationship/ratio between the slope/transconductance of input and output pulses for linear system [184]

$$S_{вых}(t)=\int_0^t S_и(\xi)\, S_т(t-\xi)\, d\xi,$$

we will obtain for the actual value of graphic rate the expression

$$v_г=[v_x^2+\sigma^2(\int_0^t S_и(\xi)\, S_т(t-\xi)\, d\xi)^2]^{1/2}, \qquad (10.1)$$

where $S_и$ and $S_т$ they are examined for current time

$$0<\xi<t;$$

here t - time, for which is determined the value of graphic rate.

Increase in recording speed is conjugated/combined with sharp reduction in the brightness of glow of tube face. During recording of the intermittent processes it is necessary to use measures for an increase in image brightness due to an increase in accelerating voltage in the cathode-ray tube. However, from an increase in accelerating voltage considerably falls the sensitivity of tube, which, in turn, requires the appropriate increase in the voltage of signal and scanning/sweep. To a certain extent to an improvement in the sensitivity contributes the application in the tubes of supplementary accelerating voltage, which affects the electron beam

after it will pass the deflection system (postacceleration). Tubes with the system of postacceleration give the possibility to record periodic pulses with the duration of the order of nanosecond at a small repetition frequency and single - with the increased voltage of postacceleration.

Passband of the circuit of signal.

Graphic beam velocity and resolution of oscillograph, as noted, are limited to insufficient broad-band character of circuit of signal. If we in the oscillograph use tubes with the usual deflection systems in the form of plates, then for an increase in the broad-band character the dimensions of the plates, and also capacitance value and inductance of introductions/inputs must be lowered to the minimum. The equivalent circuit, which corresponds to the deflection system of usual type tube, is given in Fig. 10.2.. Here R is the total external resistance, including the sweep oscillator.

Page 508.

If to the deflector plates there is fed pulse in the form of a drop in the voltage with an amplitude of U, then voltage on the plates can be represented in the following form (with R<2ρ, where ρ - circuit characteristic impedance):

$$u = U\left[1 - e^{-\alpha t}\left(\frac{\alpha}{\delta}\sin\delta t + \cos\delta t\right)\right],$$

where α=R/2L and $\delta = (1/LC - R^2/4L^2)^{1/2}$.

In practical cases value R is selected by such that voltage on deflector plates would have shortest rise time without noticeable overshoots at pulse apex in comparison with input pulse. This condition satisfies ratio α/δ=1, in this case the overshoot comprises not more than 4% [3]. For the resistance we have

$$R = \sqrt{2L/C}.$$

Using the expression for frequencies in this circuit, let us record that resistance

$$R = \frac{1}{\sqrt{2}\pi C f_0} = \frac{0.22}{f_0 C}. \qquad (10.2)$$

This relation makes it possible to determine value of resistor/resistance R at known capacitance C and frequency f_0, found for the specific cathode-ray tube. Using the selected attenuation length, it is possible to find the voltage on the plates

$$u = U\left[1 - e^{-t/RC}(\cos t/RC + \sin t/RC)\right],$$

since the equality

$$a = \delta = R/2L = 1/RC$$

is fulfilled in this case.At the moment/torque, when u=U occurs the relationship/ratio

$$\cos t/RC + \sin t/RC = 0$$

and, therefore,

$$t = \frac{3\pi}{4} RC = 2{,}3RC. \qquad (10.3)$$

Page 509.

Thus, it is possible to rate/estimate duration of pulse edge on tube face, which depends on parameter of circuit of deflection system.

Even in the case, when tube has outputs of deflection system, installed directly into glass of flask/bulb (which reduces parasitic parameters), passband of deflection system is limited by frequency on the order of 150-200 MHz. The deflection system, made in the form of the simplest line of transmission is wider-band (Fig. 10.3).

Investigated pulse through cable with matched load is fed/conducted from the input side to line, and on the other side line it is closed on the effective resistance, equal to line characteristic. This deflection system have tubes of the type 13L0101M, 10L0101M, which found use in high- speed/high-velocity oscillographs [185, 186]. With a good agreement of the deflection

system with the load its passband proves to be about 1000 MHz.

Wider-band is coaxial type deflection system (Fig. 10.4) [187]. In the external conductor of line is opening/aperture, also, above it a comparatively narrow cross connection. Between this cross connection and opening/aperture in the external conductor is passed the electron beam, on which there acts the field of signal. The cable is connected at the input and output of the line. The end/lead of the output cable is loaded to the effective resistance, equal to the wave impedance of cable.

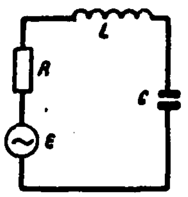

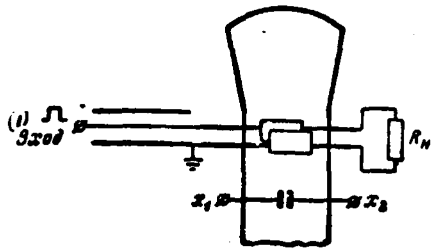

Fig. 10.2. Fig. 10.3.

Fig. 10.2. Equivalent schematic of condenser/capacitor type simplest deflection system.

Fig. 10.3. Deflection system in the form of two-wire circuit.

Key: (1). Input.

Page 510.

This design is advisable with the oscillography of the high- voltage pulses, when the low sensitivity of system is necessary. Broad-band character is here limited to a certain heterogeneity of the field of coaxial system in the area of opening/aperture, and also to possible reflections at junction of cable, which supplies pulse, with the deflection system. The passband of entire system can reach several gigahertz.

Widest-band deflection system for high-voltage oscillographs can be system, formed by coaxial cable (Fig. 10.5). Here the coaxial cable, which supplies the pulse, is simultaneously the coaxial deflection system. For this it passes through the special opening/aperture to the neck of oscilloscope tube. In the center

section of the tube the external conductor of cable has opening/aperture and metallic cross connection above it. Cross connection is arranged/located within the tube, but has contact with the external conductor of cable. As in the preceding/previous system electron beam is passed under the cross connection above the opening/aperture to the external conductor of cable. The broad-band character of this system, apparently, can be close to 10 GHz, since heterogeneities at the input of the system are here excluded.

In oscillographs of increased sensitivity are utilized cathode-ray tubes with deflection system of type of traveling wave (TBV).

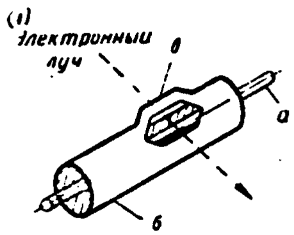

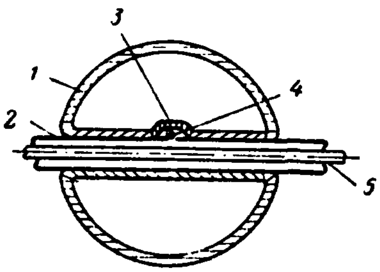

Fig. 10.4. Fig. 10.5.

Fig. 10.4. Coaxial type deflection system.

Key: (1). Electron beam.

Fig. 10.5. Deflection system with coaxial cable: 1 - flask; 2 - external conductor; 3 - cross connection; 4- electron beam; 5 - internal conductor.

Page 511.

In this system (Fig. 10.6) the electron beam is passed between the grounded plate and the deflecting element, as which is utilized the spiral, prepared from the metallic tape and which has the semicircular form (with the flat/plane side). Spiral is surrounded by the screen/shield of the same form, the flat/plane side of screen/shield playing the role of the grounded plate. Spiral has constant width, the distance between the spiral and the screen/shield is also constant; this deflection system operates as the line of distributed type transmission. The sizes/dimensions of spiral are selected by such, that the phase signal velocity along its axis is equal to the rate of electron beam and remains constant.

In high-speed/high-velocity oscillographs widely is used Soviet tube of type 13L0102M, bandwidth of which is more than 3 GHz [186]. The broad-band character of system of TBV is limited to the dispersive properties of helix and to the heterogeneities of transition/junction from the spiral to coaxial cable.

For increasing the sensitivity of tubes of such type double-helix systems [188] are utilized. The signal through the wide-band phase splitter (phase inverter) being investigated in the antiphase is supplied simultaneously to two identical deflection systems of the type of the traveling wave. As a result of paraphase divergence the sensitivity of tube grows/rises two times. These tubes have a sensitivity to 0.03 V to the line.

In wide-band oscilloscope tubes with deflection system of coaxial type and TBV resulting passband of circuit of signal affect heterogeneities of circuit.

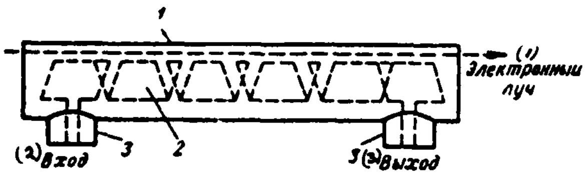

Fig. 10.6. Deflection system of type of traveling wave: 1 - plate of screen/shield; 2 - strip/tape spiral; 3 - coaxial output.

Key: (1). Electron beam. (2). input. (3). output.

Page 512.

These heterogeneities occur in coaxial pairs and in the places of transition/junction from the helix to the coaxial (for TBV). As it was noted in chapter 1 and 2, in the presence of heterogeneity in the line is created a certain reactance, which limits the broad-band character of system, which causes the distortion of the pulses being investigated. In connection with this important value the construction/design and the quality of the execution of coaxial pairs have at the input of the deflection system of tube. The difficulty of obtaining qualitative coaxial pairs usually appears at frequencies of 3-5 GHz.

Deflection systems of coaxial type and TBV must be coordinated on wave impedance with their termination. Poor agreement also leads to the distortion of the signal being investigated. These distortions are noticeable with the oscillography of comparatively long pulses and especially during the investigation of stationary processes (for example, oscillations of SBCh).

With the oscillography of very short-term pulses with use of very high speed scannings/sweeps signals reflected from load can appear after termination of pulse being investigated, without having distorted its form, or prove to be entirely out of interval of scanning/sweep. Therefore to rate/estimate the broad-band character of such tubes with the aid of the frequency characteristics of the deflection systems, taken/removed under the conditions of steady state, is inexpedient. This evaluation/estimate must be conducted according to the pulse transient responses, taken/removed with the aid of the very short-term sounding pulses (see Chapter 11).

Resulting broad-band character of circuit of signal is determined not only passband of deflection system of tube, but also by broad-band character of cable, which supplies pulse being investigated. In a number of cases the length of this cable proves to be considerable. In the oscillographs, intended for recording the single pulses, the onset of which cannot be synchronized since the beginning of the starting/launching of sweep oscillator, it is necessary to use the cable of delay (Fig. 10.1). The length of the cable segment in this case reaches several ten meters.

Page 513.

In Chapter 1 the transient and frequency characteristics of coaxial cable are examined. On them it is possible to rate/estimate the broad-band character of the segment of the cable of the assigned

length and to determine the time of the establishment of transient processes in it.

Effect of the electron transit time.

Second reason for distortion of form of pulse being investigated and limitation of resolution of high-speed/high-velocity oscillograph is transit time effect of electrons in field of deflection system of tube.

If it is electronic during electron transit time along deflector plates of usual - beam/radiation tube voltage on plates substantially changes, then phenomenon being investigated will be distorted on tube face. With the oscillography of the pulses, which have the duration of the order of several nanoseconds, the deflecting voltage on the plates changes for the time of 10^{-9}-10^{-10} s. In the usual cathode-ray tubes, used in the oscillographs for the investigation of microsecond pulses, the electron transit time through the deflection system is 10^{-9}-10^{-8} s. Consequently, such cathode-ray tubes cannot reproduce the pulses of nanosecond range without distortions.

Let us examine the character of distortion of sine voltage of high frequency, caused by effect of electron transit time. For the electron in the uniform field of the plates of the deflection system (Fig. 10.7) occurs the equation

$$m\frac{d^2x}{dt^2}=e\frac{u}{a},$$

where m, e - mass and electron charge;

a - distance between the plates.

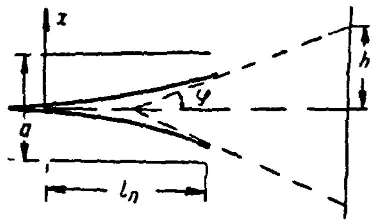

Fig. 10.7. Graph of displacement of the beam by deflector plates.

Page 514.

Then for the rate at which there are deflected electrons under the action of field u/a, where u - voltage on deflector plates, we obtain expression

$$v = \frac{dx}{dt} = \int_0^{t_n} \frac{eu}{am}\, dt, \qquad (10.4)$$

where t_n - electron transit time through deflection system.

With small divergences of electrons, replacing tangent of angle of deflection of ray/beam directly with value of angle itself, we will obtain following expression for amount of deflection:

$$\varphi_0 = \int_0^{t_n} \frac{eu}{amv_0}\, dt, \qquad (10.5)$$

where v_0 - longitudinal velocity of electron, determined by value of accelerating voltage of cathode-ray tube.

With sinusoidal deflecting voltage u=U sin ωt expression (10.5) takes form [182, 184]

$$\varphi_0 = \sigma U \sin\omega\left(t+\frac{t_n}{2}\right)\left[\frac{\sin\frac{\omega t_n}{2}}{\omega t_n/2}\right], \qquad (10.6)$$

where σ - coefficient, which determines static sensibility of cathode-ray tube, which is equal to

$$\sigma = \frac{e l_n}{m a v_0^2};$$

here l_n - length of deflector plates.

The relation which stands in brackets (10.6), depends on frequency of recorded vibrations, sizes/dimensions of plates and rate of electrons $v_0 = \frac{l_0}{t_n}$.

Page 515.

It determines the degree of the distortion of the amplitude of the recorded oscillations under the given conditions. Therefore let us introduce the value of the dynamic sensitiveness

$$\sigma_d = \sigma\frac{\sin\omega\frac{t_n}{2}}{\omega t_n/2}. \qquad (10.7)$$

With values $\frac{\omega t_n}{2} = 2n\pi$ (where n - whole number) dynamic sensitiveness of oscillograph is equal to zero, while at frequencies

$$f = \frac{2n+1}{\pi}$$

it reaches maximums. In addition to this, as can be seen from (10.6), appears supplementary phase displacement to value $\omega t_n/2$. As a result amplitude and phase distortions appear. In other words, the

limitation of the effective passband of the circuit of the signal of oscillograph occurs due to the effect of the electron transit time. If we count off passband at level 3 dB, then from (10.7) we will obtain

$$\frac{\sin\frac{\omega t_{\text{п}}}{2}}{\omega t_{\text{п}}/2} = 0{,}707,$$

whence for the passband we have

$$\Delta f = \frac{0{,}45}{t_{\text{п}}}. \qquad (10.8)$$

If deflecting voltage takes form of ideal drop/jump with amplitude of U, then formula (10.5) of signs form

$$\varphi_0 = \frac{eUt}{mav_0} = \varepsilon U\frac{t}{t_{\text{п}}}, \qquad (10.9)$$

i.e., beam deflection grows/rises in the course of time and pulse edge is linearly made by flat. At the moment of time $t = t_{\text{п}}$, when electrons emerge from space between the deflector plates, their divergence is equal

$$\varphi_{\text{п}} = \varepsilon U,$$

but the time of drop is final and is equal to $t_{\text{п}}$ (Fig. 10.8).

Page 516.

If voltage, subject on plates, linearly increase, i.e.,

$$u(t) = kt,$$

the beam deflection is proportional

$$\varphi_0 = \frac{k\sigma t^2}{2t_n}, \qquad (10.10)$$

where $0<t<t_n$.

Character of distortion of form of voltage in this case is shown on Fig. 10.9. Of up to moment t' the voltage increases according to the parabolic law, and then changes according to the linear, corresponding law of a change in the subject to the plates of sweep voltage. The value of error in the beam deflection is proportional to rate of voltage rise. At the moment of the output of electrons from the space between the deflector plates a difference in the assigned and recorded voltage will be equal to $\sigma k/2$.

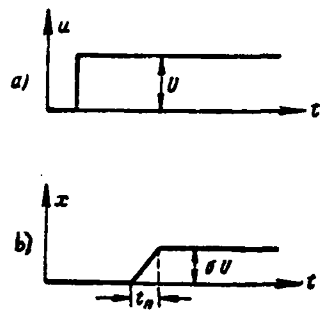

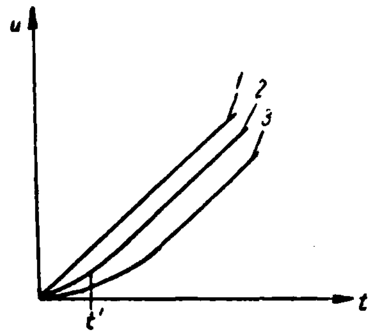

Fig. 10.8. Fig. 10.9.

Fig. 10.8. Ideal drop in voltage (a) and caused by it displacement of the beam taking into account the effect of electron transit time (b).

Fig. 10.9. Distortions of linearly increasing voltage: 1 - voltage on input; 2 - recorded voltage taking into account effect of electron transit time; 3 - recorded voltage taking into account limitation of passband of deflection system and effect of electron transit time.

Page 517.

With an increase in the accelerating voltage used in the cathode-ray tube, there increases longitudinal velocity of electrons in beam v_0, and, consequently, electron transit time $t_п$ decreases. Thus, with an increase in accelerating voltage increases the frequency of the vibrations, recorded with error σ_d/σ. If at the input of usual type deflection system operates the linearly changing voltage

$$u=0 \overset{(1)}{\text{при}}\ t<0$$

Key: (1). with.

and

$$u = kt \overset{(1)}{\text{при}}\ t \geqslant 0,$$

Key: (1). with.

that, using the equivalent circuit diagram of the deflection system of tube (Fig. 10.2), it is possible to obtain the following expression for the voltage, which operates on the deflector plates:

$$u = k\left[t - RC + e^{-\alpha t}\left(\frac{R^2C/2L - 1}{\sigma}\sin\delta t + RC\cos\delta t\right)\right].$$

If value R is selected close to critical resistor/resistance, then the expression for voltage takes form

$$u = k\left[t - RC\left(1 - e^{-t/RC}\cos t/RC\right)\right]. \qquad (10.11)$$

In order to consider action of transit time effect of electrons through deflection system, it is necessary to use expression (10.5). After substituting value of u from expression (10.11) into formula (10.5) and after producing integration, we will obtain for diverging the electron beam

$$\varphi_0 = \frac{ke}{amv_0}\left[\frac{t^2}{2} - RCt + \frac{1}{2}R^2C^2e^{-t/RC}\left(\sin\frac{t}{RC} - \cos t/RC\right)\right]_0^{t_n}.$$

Form of voltage on screen/shield of oscilloscope tube for the present instance is depicted as curve 3 in Fig. 10.9.

For decreasing the electron transit time in tubes with usual deflection systems are used plates of small length and high rate of

electron motion (accelerating voltage several kilovolts). In this case simultaneously grows/rises the broad-band character of tube due to the decrease of the capacity/capacitance of plates and decrease of the inductance of the introductions/inputs, which are derived/concluded through the glass of flask/bulb.

Page 518.

The sensitivity of such tubes is small. This deficiency to the certain degree is removed due to the decrease of the diameter of electron beam to such size/dimension, that on tube face is obtained the spot by the width only about 0.01 mm [189]. The image of the oscillogram on the screen/shield proves to be very small and it is necessary to examine it with the aid of the special microscope.

In oscilloscope tubes with coaxial deflection system of low sensitivity electron transit time is determined by width of cross connection (Fig. 10.4) and by velocity of electrons. Time of flight here decreases to the value of 0.05-0.01 ns by applying of high accelerating voltages and decrease of sizes of the powered phases of the deflection systems.

In oscilloscope tubes of type of traveling wave dynamic sensitiveness is determined by expression [186]

$$\sigma_d = \sigma \frac{\sin\left[\frac{\omega l}{2}\left(\frac{1}{v_0} - \frac{1}{v_\Phi}\right)\right]}{\frac{\omega l}{2}\left(\frac{1}{v_0} - \frac{1}{v_\Phi}\right)}, \qquad (10.12)$$

where σ - static sensibility, l - length of circuit, v_0 - velocity of electrons, v_Φ - phase signal velocity in circuit. Under condition $v_0=v_\Phi$ this sensitivity is maximum and does not depend on frequency. However, the real circuits have a dispersion and therefore condition $v_0=v_\Phi$ can be made only at one frequency ω_0. At other frequencies the sensitivity σ_d is somewhat lower, i.e., the action of the effect of the flight of the electrons is developed, and, true, here it is many times less than in the standard tubes.

Therefore, for tubes of TBV important is the selection of such accelerating voltage when the condition $v_0=v_\Phi$ is satisfied at that frequency, at which passband of tube proves to be greatest.

Page 519.

The broad-band character of system TBV, determined by the effect of the flight/span of electrons, is evaluated according to cut-off frequency $\omega_{\Gamma P}$, at which $\sigma_d(\omega_{\Gamma P})=0,707$, and the time of establishment is approximately equal to $t_y \approx \frac{2,2}{\omega_{\Gamma P}}$. Thus, knowing the dispersive characteristic of circuit $v_\Phi(\omega)$ and using formula (10.12), it is possible to find $\omega_{\Gamma P}$ and then t_y.

Resolution of oscillograph and minimally permissible duration of the pulse being investigated.

If we are not concerned about distortions in circuit of signal, then the time resolution of oscillograph can be determined through

scanning speed v_x and width of line of electron beam on screen/shield d:

$$\Delta t_1 = \frac{d}{v_x}.$$

This potential temporary/time resolution with contemporary cathode-ray tubes with high-quality focusing systems, which make it possible to obtain beam width d of less than 0.1 mm, and at scanning speed, close to speed of light, proves to be order 10^{-12}-10^{-13} s. However, with the oscillography of the repeating pulses, the observed on the screen/shield (dynamic) beam width is determined not only by the construction/design of cathode-ray tube and by the quality of the focusing system. At scanning speeds, close to the speed of light, even the very small temporary/time instability of the oscillograms of the repeating pulses leads to a considerable increase in the width of the line of ray/beam on the screen/shield (chattering of image) [190, 191].

If temporary/time instability of scanning/sweep is equal to Δt_2, then dynamic beam width on screen/shield, expressed in units of time, will be

$$\Delta t_n = \Delta t_1 + \Delta t_2.$$

Furthermore, most important reason, which decreases temporary/time resolution of oscillograph, is finite time of establishment of transient processes in circuit of signal of

oscillograph.

Page 520.

In the general case it is possible to rate/estimate the resulting time of the establishment of the circuit of the signal of high-speed/high-velocity oscillograph if known the time of establishment in coaxial cable, which supplies the pulse t_{y1}, being investigated the time of the establishment of voltage in the deflection system of oscilloscope tube t_{y2} and the electron transit time in the field of deflection system $t_{п}$. Since all enumerated factors affect the period of establishment in the circuit of signal independently, the resulting time of establishment can be evaluated by the expression

$$t_y = \sqrt{t^2_{y_1} + t^2_{y_2} + t^2_{п}}.$$

Knowing time of establishment of circuit of signal and dynamic beam width, it is possible to rate/estimate minimum duration of image of pulse on oscilloscope face. Thus, in the case of the oscillography of square pulse with the gradual decrease of its duration the form of the obtained on the screen/shield image will increasingly more differ from rectangular, approaching a pulse of the type front - through, to close one in the form to the triangular. The duration of this pulse, measured at the level of half of its amplitude and equal to

$$\Delta t = t_y + \Delta t_{л}, \quad (10.13)$$

can characterize the resolution of oscillograph.

For increasing time resolution, thus, it is necessary to decrease time of establishment of transient processes of circuit of signal t_y and to raise stability of scanning/sweep, i.e., to decrease Δt_2.

For decreasing time of establishment t_y it is necessary to utilize small sections/segments of most adequate/approaching coaxial cables (see Chapter 1), to use oscilloscope tubes with very wide-band deflection systems (coaxial type and TBV) and with minimum electron transit time. The time of establishment t_y in the cable with a length of 1 m can be 0.02 ns. Coaxial type widest-band deflection systems and best samples of systems of TBV have the time of establishment of 0.025-0.08 ns. The electron transit time succeeds in decreasing to 0.05-0.02 ns.

Page 521.

The value of the instability of the channel of scanning/sweep Δt_2 in the developed very high speed oscillographs is reduced to the value of 0.015 ns [187, 191]. Therefore in the best cases value Δt proves to be approximately equal to 0.06 ns.

With oscillography of single pulses is eliminated need for considering instability of scanning/sweep, i.e., $\Delta t_2=0$ and therefore $\Delta t_{:1}=\Delta t_1=10^{-4}$ ns. However, in this case in the circuit of signal usually it is necessary to use the cable of delay with a length of 10 m and more. Therefore, value t_{y1} proves to be more than 0.15 ns that

the resolution of oscillograph is decreased.

Evaluation/estimate of minimum permissible duration of pulse, which can be reproduced on oscillograph with accuracy assigned in duration is of interest. Due to finite time of the establishment of the circuit of signal the duration of the front of the signal being investigated, which has at the input duration $t_{ф1}$, increases by value

$$\Delta t_{ф}=\sqrt{t_{ф_1}^2+t_y^2}-t_{ф1}.$$

For right-angled pulse $t_{ф1}=0$ and $\Delta t_{ф}=t_y$. Total increment in the duration of square pulse $t_и$ is equal to $\Delta t_и=\Delta t=t_y+\Delta t_з$. If the permissible error in the reproduction of pulse in the duration ν, expressed in the percentages is assigned, then

$$\frac{\Delta t}{t_и}100\leqslant\nu.$$

Permissible minimum duration of square pulse, reproduced by oscillograph with accuracy in duration ν

$$t_{и\,мин}\geqslant\frac{\Delta t}{\nu}100$$

hence there is determined.

Consequently, an increase in the time resolution of high-speed oscillographs is connected not only with expansion of passband of circuit of signal, but also with increase in stability of functioning electronic circuits of channel of scanning/sweep.

Page 522.

During development of high-speed/high-velocity oscillographs selection of type of cathode-ray tube and minimum sweep length is determined by assigned temporary/time resolution and sensitivity of oscillograph. However, if it turned out that the tube was given and the bandwidth of its deflection system was known, then it remains to select optimum scanning speed. This rate must ensure the best time resolution and not be excessive with large. Actually, if known is the value of the time of the establishment of the circuit of signal t_y and the width of the line of ray/beam on the temporary/time scale Δt_1, i.e., is given $\Delta t = t_y + \Delta t_1$, then it is expedient to select scanning speed $v_p = l/\Delta t$. This rate must be such that the interval of time Δt would correspond on the screen/shield to the length l, sufficient for the clear observation and recording the pulse. Higher scanning speed only will complicate it will only complicate obtaining the stable work of diagram.

10.3. OSCILLATORS OF HIGH-SPEED SCANNINGS.

Fundamental requirements and characteristics.

For oscillography of pulses with duration from 0.1 ns to tens of nanoseconds are required scannings/sweeps with duration from one to hundreds of nanoseconds. Depending on the sensitivity of tube rate of change of sweep voltage must be from 10^9 to 10^{12} v/s.

For obtaining high-speed scannings there are utilized a linear

generator analogous to sweep oscillators of microsecond range, and specific oscillator circuits of nanosecond scannings/sweeps.

Sweep oscillators are characterized by following parameters:

- with value of working drop in voltage $u_р$;
- with sweep length $T_р$;
- with duration of sweep retrace (recovery time) $T_в$;
- by percentage distortion

$$\gamma=\frac{|u'(t)|_{макс}-|u'(t)|_{мин}}{|u'(t)|_{макс}}, \qquad (10.14)$$

where $u'=\frac{du(t)}{dt}$.

Page 523.

If for the sweep voltage there is utilized the initial section of charge or capacitor discharge through the effective resistance, then

$$\gamma=\frac{I_н-I_к}{I_н}\approx\frac{u_р}{E_m}, \qquad (10.15)$$

where E_m - the steady-state value of voltage across capacitor;

$I_н$ and $I_к$ - initial and finite quantity of the current of the charge (or discharge) of capacitor;

- by effectiveness of sweep oscillator, evaluated by the voltage efficiency, i.e., by the attitude of operating voltage to supply voltage E:

$$\xi=\frac{u_р}{E}; \qquad (10.16)$$

- with the delay time of the starting/launching of the oscillator

of the waiting scanning/sweep t_3;

-by stability of the delay time of the starting/launching of sweep oscillator $\Delta t_3/t_3$.

At maximum speeds of scanning/sweep causes difficulty, both obtaining given speed and guaranteeing of proper linearity and stability of scanning/sweep. If in the sweep oscillator the diagram of charge or discharge of capacitance C through the effective resistance is utilized, then for obtaining high scanning speed it is necessary to ensure the considerable current through the capacitor/condenser

$$i = C\frac{du_C}{dt}.$$

At rate of change in voltage of order of 10^{11}-10^{12} v/s and smallest possible capacitances of capacitor, equal taking into account stray capacitances of diagram, for example, 20 pF, current takes value of 2-20 a. During the use of usual oscilloscope tubes with the deflection systems in the form of plates it is necessary to also consider the effect of capacitive coupling between the plates of the systems of horizontal and vertical deflections. The capacity/capacitance between the adjacent systems of deflector plates is the part of capacitor voltage divider, whose second arm is formed by stray capacitance between the deflector plates and earth/ground.

Page 524.

With a decrease in this capacitance the interconnection between the systems of the horizontal and vertical deflection of ray/beam grows/rises. For decreasing this connection/communication they sometimes specially increase the capacity/capacitance of deflector plates relative to the earth/ground. This entails an increase of the charging current in sweep circuit. Thus, the capacity/capacitance of deflector plates and the parasitic wiring capacitance of diagram present very noticeable load at the output of sweep oscillator. Therefore, in the diagram the tube, which has a sufficient pulse power, must be used.

In high-speed/high-velocity oscillograph are utilized cathode-ray tubes with high voltage of acceleration, which decreases sensitivity of deflection system and leads to need for using sweep voltage on the order of hundreds of volts.

The indicated requirements to pulse generators of sweep voltage of high-speed/high-velocity oscillographs can be most simply satisfied in thyratron diagrams. In such diagrams it is easy to ensure considerable current with the relatively low supply voltage. With the thyratrons, designed for higher voltage, very fast sweeps can be obtained, since current pulses in them reach several ten amperes.

However, as noted in chapter 3, majority of thyratrons works at repetition frequency not more than 5-30 kHz, but ignition time lag of thyratron relative to moment/torque of its starting/launching can be

more than 100 ns. Furthermore, some thyratrons have the low stability of ignition. Therefore, for obtaining the scanning/sweep with a duration it is less than 10 ns, when the increased stability of starting/launching has already been required, it is expedient to utilize diagrams on vacuum lamps. Thus, depending on the designation/purpose of oscillograph and required scanning speeds can be used sweep oscillators on thyratron or vacuum lamps.

For obtaining photographs of pulse from tube face of oscillograph it is desirable so that electron beam would cause glow of screen/shield only into moment/torque, which directly precedes appearance of sweep voltage on deflector plates.

Page 525.

After the passage of ray/beam along the screen/shield it must be extinguished and the glow of screen/shield is ended. For this in the oscillograph is used the diagram, which creates the pulses of illumination, supplied either to the cathode or to control electrode of tube. The pulses of illumination must be short-term with the very steep front and it is rigidly synchronized with the scanning/sweep, which is necessary for the timely and very rapid illumination of the ray/beam of tube. Therefore the stages of starting or preliminary formation of high-speed scanning simultaneously are utilized for the impulse shaping of illumination.

Methods of obtaining the high-speed scannings.

In the case of construction of sweep oscillator on vacuum lamps requirement of large pulse currents is fundamental during selection of sweep circuit and tube itself. At the same time the scanning/sweep must be sufficient linear, and the duration sweep retrace, i.e., recovery time of diagram is small.

These requirements can be satisfied in simple sweep circuit, which works on principle of charge or capacitor discharge. For retaining/maintaining the linearity of scanning/sweep the circuital current of capacitor/condenser must be supported constant value. The current-stabilizing element relies on high currents. The value of output resistance of sweep oscillator must satisfy the condition for the smallest distortion of the form of sweep voltage (as it is indicated in S 10.1).

Application in sweep oscillator of vacuum lamp as commutating element is connected; however, with possibility of distortion of initial part of scanning/sweep due to effect of form of trigger pulse. Actually, if the pulse edge lasts the time interval, commensurate with the sweep length, then sweep voltage together with the parameters of charging circuit will be determined by the character of the build-up/growth of the front of trigger pulse.

Page 526.

Let the front of trigger pulse increase according to the linear law,

then the current of charge of capacitor in the sweep circuit also increases according to the linear law

$$i = kt$$

and voltage across capacitor will be

$$u_C = \frac{1}{C}\int_0^{t_\Phi} i\,dt = \frac{kt^2}{2C}\Big|_0^{t_\Phi},$$

where t_Φ - duration of the front of trigger pulse.

Voltage across capacitor for rise time of trigger pulse changes in time according to parabolic law. Therefore it is desirable so that the trigger pulse would have the large steepness of front and relatively flat/plane apex/vertex. This is all the more important, the more the scanning speed increases. The different methods of increasing the linearity of scanning/sweep are used for maintaining the constancy of scanning speed. Are known the oscillator circuits of scanning/sweep of microsecond the range, where is utilized charge or capacitor discharge, with the application of the current-stabilizing two-terminal network (Fig. 10.10).

In the case of charge of capacitor voltage on it changes according to the law

$$u(t) = (E + E_э)\left(1 - e^{-\frac{t}{R_э C}}\right),$$

where $E_э$ and $R_э$ - equivalent voltage and resistor/resistance of current-stabilizing two-terminal network.

In this case percentage distortion

$$\gamma = \frac{u_p}{E + E_э} \approx \frac{u_p}{E_э},$$

since usually $E_э \gg E$.

As simple current-stabilizing two-terminal network is utilized pentode, for which equivalent voltage $E_э$ attains several kilovolts. Sweep circuit with the pentode can be used also for the high-speed/high-velocity oscillograph, if required scanning speeds are provided with the currents, permitted for the pentodes.

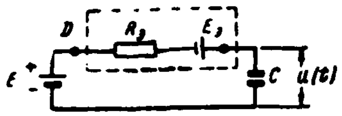

Fig. 10.10. Equivalent sweep circuit with current-stabilizing two-terminal network.

Page 527. 97 The more compound circuits of the current-stabilizing two-terminal networks contain feedback loop on the current. Thus, in the microsecond range for obtaining increased scanning speeds with the satisfactory linearity is found use of the diagrams, in which is utilized the charge of capacitor in the presence so-called compensating emf. (Fig. 10.11) [1].

Here with the aid of capacitor/condenser of considerable capacity/capacitance of C_0>>C and cathode follower L_2 there is formed the current-stabilizing circuit, which supports current i of constant value during charge of capacity/capacitance of C, i.e., with formation of linearly changing sweep voltage u_C. The charging current

$$i = \frac{E - u_C(t) + e_k(t)}{R},$$

where $e_k(t)$ - compensating emf, which ensures the compensation for a change in voltage across capacitor $u_C(t)$ so that the strength of current i remains capacitor/condenser it presents the series connection of the source of equivalent emf $E_э$, resistor/resistance R and equivalent capacity/capacitance $C_э$

$$C_э = \frac{C}{1-K},$$

where K - transmission factor of the cathode follower

$$K = \frac{SR_1}{1 + SR_1}$$

and

$$R_1 = \frac{R_k R_i}{R_k + R_i}.$$

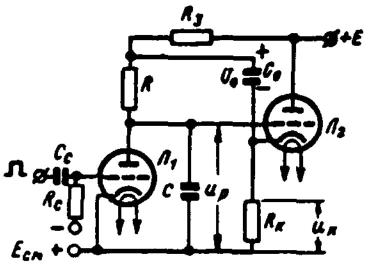

Fig. 10.11. Sweep circuit with current-stabilizing circuits.

Page 528.

Equivalent voltage

$$E_э = \frac{E - Ku_1}{1 - K},$$

here u_1 - residual voltage across capacitor C at initial moment of its charge.

Percentage distortion

$$\gamma = \frac{u_p}{E_э - u_1} = \frac{u_p (1 - K)}{E - u_1} \approx \frac{u_p (1 + R_i/R_к)}{(E - u_1)\mu}, \quad (10.17)$$

where μ - factor of amplification of tube L_2.

In the case of applying this diagram for obtaining scanning/sweep with duration several of ten nanoseconds are required tubes, designed for considerable current which with minimum for this diagram capacity/capacitance of 20-30 pF and sweep voltage with amplitude about kilovolt it reaches value more than ampere. For obtaining the high current necessary to decrease charging resistor of R (less than 1

kilohms), and this impedes the selection of tube L_1, since its internal resistance must be considerably lower than the resistor/resistance of R, since this tube is intended for the capacitor discharge C in the period of the restoration/reduction of diagram. If this condition is not satisfied, then the residual voltage across capacitor u_1 grows/rises and the voltage efficiency ξ proves to be very small. Furthermore, the low value of resistor/resistance R_1 worsens/impairs the mode of operation of cathode follower [1].

Therefore in high-speed/high-velocity oscillographs during scanning/sweep with duration several of ten nanoseconds (minimally to 10 ns) car be used modified schematic of this oscillator (Fig. 10.12) [192]. The here commutating tube L_1 is connected in series with capacitor/condenser C. Resistor/resistance R_0 of small value is intended for the capacitor discharge C in the period of the restoration/reduction of diagram. Tube L_2 is designed for the high current.

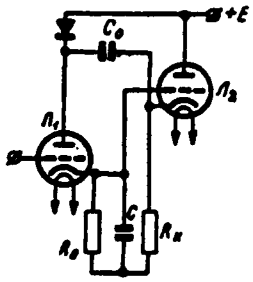

Fig. 10.12. Sweep circuit of nanosecond s-band current-stabilizing circuit.

Page 529.

In this case, if we do not consider the effect of the current-stabilizing two-terminal network (C_0 and L_2 they are disconnected), for the circuit we will obtain the equation of charge of capacitor C

$$E = iR_i + u_C,$$
$$i = \frac{u_C}{R} + C\frac{du_C}{dt},$$

where i - current of conducting tube L_1, $R_i = \text{const}$ - its resistance.

Voltage across capacitor C in this case changes according to the law

$$u_C = \frac{R_0 E}{R_0 + R_i}\left(1 - e^{-\frac{t}{\tau}}\right),$$

where

$$\tau = C\frac{R_0 R_i}{R_0 + R_i}.$$

If we now consider effect of current-stabilizing two-terminal network, just as this done for diagram in Fig. 10.11, then for percentage distortion we will obtain

$$\gamma = \frac{u_p}{E_0} \approx \frac{u_p(1-K)}{R_0 E/(R_0 + R_i)}. \qquad (10.18)$$

Value of percentage distortion in this diagram is not more than 10%. Working sweep voltage attains the value

$$\frac{R_0 E}{R_0 + R_i} < u_p < E.$$

In this case voltage efficiency ξ proves to be equal to 0.8-0.9 even at high scanning speeds. In the case of high-speed scannings/sweeps the percentage distortion is sometimes permitted order 10-15%, since in the diagrams the calibrator of sweep length commonly is used. This makes it possible to utilize simpler methods of the linearization of scanning/sweep. Such methods, in particular, include the charge of the capacity/capacitance through RL-network. The use of the corrective inductance L, connected in series with capacitor/condenser C and effective resistance R, makes it possible to support the constancy of the charging current i, since current i induces in coil L of emf, which counteracts to a change in the current.

Page 530.

If circuit is found in oscillatory mode, then voltage across capacitor

$$u_C = E + \frac{E}{\omega R} e^{-\alpha t} \sin(\omega t - \varphi).$$

Initial part of oscillogram of voltage u_C will be more linear, the higher energy factor of duct/contour. The value of operating voltage u_C here can be more than supply voltage, i.e., the voltage efficiency ξ>1.

With formation of voltage of high-speed scanning similar diagram finds use as circuit, which converts the drop in voltage into linearly changing voltage of assigned slope/transconductance (Fig. 10.13).

Let us assume that at the input of the circuit an ideal drop in voltage operates. For the voltage and the circuital current we have expressions

$$u_C = U\left[1 - \frac{1}{\beta_1 - \beta_2}(\beta_1 e^{\beta_2 t} - \beta_2 e^{\beta_1 t})\right],$$
$$i = \frac{UC}{\beta_1 - \beta_2}(\beta_1^2 e^{\beta_1 t} - \beta_2^2 e^{\beta_2 t}),$$

where

$$\beta_{1,2} = \frac{-L \pm \sqrt{L^2 - 4R^2LC}}{2RLC},$$

$U = E - U_T$; here U_T - a voltage drop across the commutating element.

Change in voltage across capacitor is close to linear dependence, if circuit is found in oscillatory mode.

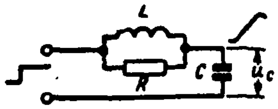

Fig. 10.13. Forming circuit for obtaining voltage of high-speed scanning.

Page 531.

Expressions for the current and the voltage in this case take the form

$$u_C = U\left\{1 - \frac{e^{-\alpha t}}{\sqrt{\omega^2-\alpha^2}}\left[\sqrt{\omega^2-\alpha^2}\cos\sqrt{\omega^2-\alpha^2}\,t - \right.\right.$$
$$\left.\left. - \alpha\sin\sqrt{\omega^2-\alpha^2}\,t\right]\right\};$$
$$i_C = UC\cdot e^{-\alpha t}\left[2\alpha\cos\sqrt{\omega^2-\alpha^2}\,t + \right.$$
$$\left. + \left(\sqrt{\omega^2-\alpha^2} - \frac{\alpha^2}{\sqrt{\omega^2-\alpha^2}}\right)\sin\sqrt{\omega^2-\alpha^2}\,t\right],$$

where

$$\alpha = \frac{1}{2RC}, \quad \omega^2 = \frac{1}{LC}.$$

Percentage distortion for voltage across capacitor is determined by relation

$$\gamma = \frac{i_{t_1} - i_{t_2}}{i_{t_1}}.$$

Counting $t_1=0$, we will obtain for percentage distortion following expression:

$$\gamma = 1 - RCe^{-\alpha t_2}\left[2\alpha\cos\sqrt{\omega^2-\alpha^2}t_2 + \right.$$
$$\left. + \left(\sqrt{\omega^2-\alpha^2} - \frac{\alpha^2}{\sqrt{\omega^2-\alpha^2}}\right)\sin\sqrt{\omega^2-\alpha^2}t_2\right]. \quad (10.19)$$

Condition of minimum value of percentage distortion is equality

$$\sqrt{\omega^2-\alpha^2} = 2\alpha$$

or

$$L = 0{,}8R^2C. \quad (10.20)$$

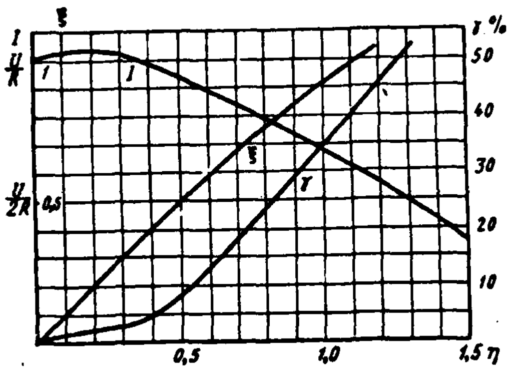

Fig. 10.14. Dependences of current and voltage from scanning time and percentage distortion from voltage for circuit design of scanning/sweep.

Page 532.

Fig. 10.14 depicts dependences of current and voltage from scanning time, and also percentage distortion from value of change in voltage across capacitor, used for scanning/sweep. In the figure there is denoted

$$\xi=\frac{u_C}{U},\ \eta=t_p/RC.$$

It follows from Fig. 10.14 that during the use for scanning/sweeping only the part of voltage across capacitor, it is possible to obtain the sufficiently linear dependence of voltage from the time. With η=0.18 the current has maximum value and is equal to

$$I_{\text{макс}}=1{,}02\frac{U}{R},$$

whence percentage distortion can be determined according to the

formulas

$$\gamma=\frac{I-I_0}{I_0} \overset{(1)}{\text{при}}\ \eta<0,18$$

Key: (1). with.

and

$$\gamma=\frac{I_{\text{макс}}-I}{I_{\text{макс}}}+\gamma_0 \overset{(1)}{\text{при}}\ \eta\geqslant 0,18,$$

Key: (1). with.

where

$$\gamma_0=\frac{I_{\text{макс}}-I_0}{I_0}.$$

Here I_0 - initial sweep current, i.e., $I_0=\frac{U}{R}$ with $\eta=0$.

Utilizing time interval, limited by value $\eta=0.5$, it is possible to obtain sweep voltage with amplitude U/2 with percentage distortion of order 5-7%. If in sweep circuit were utilized the integrating circuits of the type RC, then with the same sweep amplitude percentage distortion would attain approximately 50%.

Values of percentage distortion, found according to above-indicated relationships/ratios and Fig. 10.14, are valid only at ideal drop in voltage, supplied to the input of integrating circuits. In the real diagram the nonlinearity increases because a drop in the voltage has a certain final duration of front.

Page 533.

In practice the value of percentage distortion does not exceed 10%. A

deficiency in this method of the formation of scanning/sweep is considerable recovery time of diagram, which limits sweep frequency.

High-speed vapor phase scanning/sweep can be obtained in diagram with power tetrod as commutating tube (Fig. 10.15).

Advantage of application of tetrode over triode consists in the fact that it has smaller input capacitance and, furthermore, potential change on screen grid of tetrode to the same value, as on cathode, is not caused change in anode current. This fact is very important for obtaining the sufficiently line voltage of scanning/sweep. The capacitor/condenser of the corresponding capacitance of C_3 is included for this purpose between the screen grid and the cathode of tetrode. With the triggering/opening of tube by positive pulse, supplied to control electrode, capacitor/condenser C_1 is discharged by the anode current of tube, and capacitor C_2 is charged by anode and screen current. Because of the action of capacitor/condenser C_3 the currents of charge and discharge remain approximately constant value during the duration of steering impulse. In the period of the restoration/reduction of diagram capacitor/condenser C_1 is charged through resistor/resistance R_a, and capacitor/condenser C_2 is discharged through resistor R_2.

Power tetrodes provide current, which makes it possible to obtain scanning speed on the order of 10^9 cm/s with percentage distortion not more than 10%. For the formation of the high-speed scannings of

different duration it is possible to utilize an electron tube simultaneously as the amplifier of the linearly changing voltage and as the source of a steep edge in the voltage for the integrating circuits (Fig. 10.16).

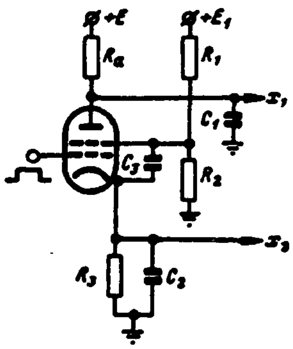

Fig. 10.15. Diagram of high-speed vapor phase scanning/sweep on a tetrode.

Page 534.

Its amplification by high- power tube occurs after admission to control electrode of preliminarily formed linearly changing voltage. For obtaining the scanning/sweep with the maximum speed (on the order of 10' cm/s) the linearly changing voltage is removed/taken from the anode of tube and is supplied directly to the deflection system of tube. The linearity of scanning/sweep is determined by the shape of pulse at the input of tube and by the possible distortions due to the parasitic parameters of tube and anode circuit of diagram. In obtaining of scannings/sweeps with the lower speeds a drop in the voltage from the anode of tube is supplied to the integrating circuits, with the aid of which are formed/shaped the necessary scannings/sweeps. The linearity of these scannings/sweeps is determined in essence by the character of the integrating circuits and by the slope/transconductance of an initial drop in the voltage. For increasing the linearity of scanning/sweep can be used LCR the

integrating circuits, described above.

If requirements for stability of starting of scanning are not very rigid, then as a commutating element it is expedient to utilize a thyratron. Thyratron diagram is more economical. With the aid of the thyratron easy to obtain considerable currents with the voltage on its anode of approximately 1 kV, while for the power tetrods is required the voltage into several kilovolts. During the use of a thyratron it is easy to obtain the initial drop in the voltage of large slope/transconductance, which then can be supplied to integrating LCR-chain.

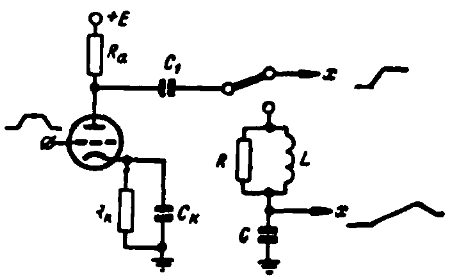

Fig. 10.16. Oscillator circuit of scanning/sweep with forming circuit.

Page 535.

High scanning speed can be obtained by simple method, if we utilize properties of characteristic of ionization of thyratron (Fig. 10.17a). As the sweep voltage here is utilized the voltage drop across the equal in magnitude resistors/resistances of R_1 and R_2, which is created due to the discharge of capacitor C_1. With sufficiently great capacity C_1, i.e., if $C_1R_{11} \gg t_p$ $(R_{11}=R_T+R_1+R_2)$, voltage on resistors/resistances of R_1 and R_2 follows the form of the characteristic of ionization (Fig. 10.17b).

For scanning/sweep is utilized only section of linear build-up of characteristic of ionization. The linearity of scanning/sweep is determined by the properties of thyratron, and percentage distortion does not usually exceed 15-20%. Changing supply voltage, it is possible to obtain different scanning speeds (continuously variable control). The linear section of the characteristic of ionization has a duration from 2 to 10 ns, which depends on the type of thyratron and

value of anode voltage. In this case the sweep voltage can reach hundreds of volts even with the low-power thyratrons. Consequently, this diagram can be used for obtaining high scanning speeds, which reach 3·10’ cm/s.

To deficiencies in generators with thyratrons it is necessary to relate difficulty of achieving stable work of diagram, comparatively long delay time of starting of generator and low maximum sweep frequency, equal to 5-10 kHz.

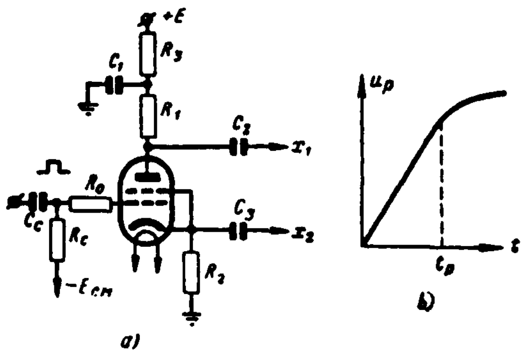

Fig. 10.17. Diagram of high-speed scanning/sweep (a), in which is utilized process of ionization of thyratron and sweep voltage (b).

Page 536.

Factors, which determine operational stability of diagram with thyratrons, are examined in Chapter 3. During the correct selection of the type of thyratron and with the observance of the proper working conditions for its in the diagram of high-speed scanning, as investigations showed, the stability of the starting can be led to the tenths of nanosecond (0.2-0.1 ns) [3]. This high stability is especially necessary with the oscillography of repetitive pulses with the duration in all into several nanoseconds.

Considerable delay of starting of thyratron sweep circuit (reaching 100 ns and more) has value during recording of single pulses. In the case of recording the repeating pulses delay factor of starting does not play the significant role, since in the diagram it is always possible to provide synchronization of the moment of the starting of scanning relative to the moment/torque of the arrival of

the pulse being investigated. In sweep circuit on the thyratrons it is possible to carry out continuously variable control of delay time by changing the bias voltage on control electrode.

Methods of formation of linearly changing voltage examined do not make it possible to obtain very high speed scannings/sweeps, for which is necessary rate of change in voltage of order of 10^{10} v/s. The need for such rates of change in the voltage appears in the very high speed oscillographs. In such oscillographs it is necessary to use high accelerating voltage, which, however, decreases the sensitivity of the horizontally deflection system. In these cases is necessary working the sweep voltage on the order of 1 kV. The sweep length of such oscillographs is sometimes less than 1 ns, which can correspond to scanning speed, close to $3 \cdot 10^{10}$ cm/s.

This high rate of change in voltage is easily achieved by use of ferrite forming lines, where shock electromagnetic wave is formed. In Chapter 4 the description and the calculation of such lines is given. The oscillator circuit of scanning/sweep with the nonlinear forming line on the ferrites is given in Fig. 10.18 [187].

Page 537.

Linearity of this scanning/sweep (i.e. form of front of obtained drop/jump) is determined in essence by quality of forming line and by parasitic parameters of mounting of diagram. The correct identification of the parameters of the cells of the forming line and

their sufficient number makes it possible to form a drop in the voltage, the nonlinearity of working section of which does not exceed 10-15%. The application of a constant magnetic biasing of ferrites of line makes it possible to obtain continuously variable control of the delay time of line, which is substantial for the synchronization of the moment/torque of the beginning of scanning/sweep and arrival of the pulse being investigated.

Reasons for the instability of scanning/sweep.

At high scanning speeds appears difficulty in obtaining of stable position of pulse on time axis of oscillograph being investigated, reason for which can be insufficient stability of parameters of linearly changing sweep voltage. If during the observation of repetitive pulses change the delay time of scanning/sweep, the value of the initial level of the working section of scanning/sweep and the average speed of working section, then the temporary situation of pulse will be unstable, and its form is distorted.

Let in the sweep circuit a charge occur or capacitor discharge is utilized linear section of change in voltage

$$u(t) = U_1 \pm k(t - t_1),$$

where U_1 - initial level of working section of scanning/sweep; t_1 - moment/torque of beginning of straight/direct trace of a scan; k - slope/transconductance of change in voltage.

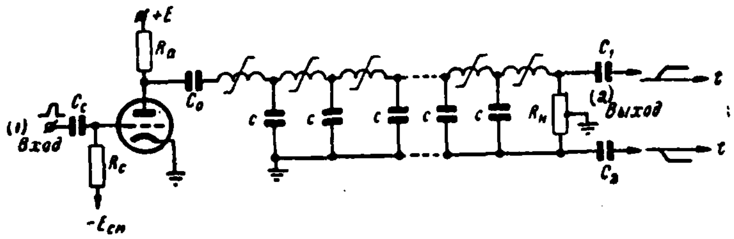

Fig. 10.18. Oscillator circuit of scanning/sweep with nonlinear forming line on ferrites.

Key: (1). Input. (2). Output.

Page 538.

Let there be at moment $t=t_p$ a linearly increasing sweep voltage $u(t)=u_p$, then for scanning time t_p

$$t_p = t_1 + \frac{u_p - U_1}{k}.$$

If we do not consider nonlinearity of scanning/sweep, then value of the time error in scanning/sweep depends on effect of parameters t_1, U_1 and k. Magnitude of error of scanning time due to a change in the delay of the starting of sweep oscillator is equal to an error in this delay:

$$\frac{\Delta t_{p1}}{t_p} = \frac{\Delta t_1}{t_1}.$$

Error due to change in rate of working section of scanning/sweep

$$\frac{\Delta t_{p2}}{t_p} = \frac{\Delta k}{k}$$

and error due to change in initial stress level of scanning/sweep

$$\frac{\Delta t_{p3}}{t_p}=\frac{\Delta U_1}{kt_p}=\frac{\Delta U_1}{u_p}.$$

Change in scanning speed Δk/k and initial stress level $\Delta U_1/u_p$ depends on stability of source of anode voltage. A change in the value of the anode voltage of tube can lead to a change in the value of voltage across capacitor residual after the restoration/reduction of diagram. The value of this error depends on the type of diagram and characteristic of tube. The same reason produces a change in the strength of current of the charge (or discharge) of capacitor/condenser and leads to the error in the rate of the working section of scanning/sweep. Both these errors are usually small under the condition of a good stabilization of power supply.

Instability of moment of triggering of sweep oscillator of high-speed/high- velocity oscillograph plays significant role.

Page 539.

In the channel of the starting of high-speed scanning several cascades/stages on the electron tubes, which work in the waiting mode and intended for a consecutive increase in the steepness of the front of the trigger pulse of sweep oscillator, commonly are used.

Let us examine reasons for instability of starting with any of cascade/stage (pulse amplifier or relaxation oscillator in waiting

mode), which is located in trigger circuit of sweep oscillator. Usually the tube of this cascade/stage in the initial state is closed by bias voltage E_{cm} (Fig. 10.19). From the preceding/previous cascade/stage the grid of tube comes trigger pulse $u_{вх}(t)$. during the build-up/growth of front of which occurs the triggering/opening of the tube of the cascade/stage in question. The beginning of the starting of the cascade corresponds to moment/torque t_1, when $u_{вх}(t)=E_1$.

Moment of triggering of tube will be unstable, if changes value $E_1=E_{cm}-E_{\text{п}}$ and steepness of front of trigger pulse $(du_{вх}(t)/dt)_{t=t_1}$. With the aid of Fig. 10.19 it is possible to rate/estimate the value of the instability of the moment of triggering of tube [193]. Representing small changes in the values by differentiation, for changing the moment of the triggering of tube we will obtain

$$\Delta t_1 \approx \frac{dE_1}{(du_{вх}(t)/dt)_{t=t_1}}. \qquad (10.21)$$

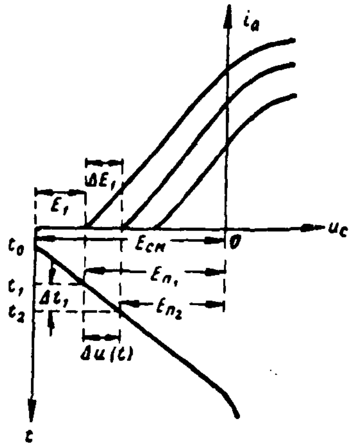

Fig. 10.19. Graph which elucidates triggering/opening of tube by linearly increasing voltage.

Page 540.

Since change in potential of closing of tube depends on change in anode voltage and filament voltage, i.e., $E_п = f(E_a, u_н)$, the

$$dE_1 = dE_{см} + \frac{\partial f}{\partial E_a} dE_a + \frac{\partial f}{\partial u_н} du_н = dE_{см} + A dE_a + B du_н,$$

where A and B - proportionality factors.

According to (10.21) for Δt_1 we will obtain

$$\Delta t_1 \approx \frac{1}{\left(\frac{du_{вх}(t)}{dt}\right)_{t=t_1}} (dE_{см} + A dE_a + B du_н).$$

If trigger pulse enters with certain instability Δt_0, then resulting instability of starting of cascade

$$\Delta t = \Delta t_1 + \Delta t_0.$$

In the particular case if the front of trigger pulse is linearly increasing function,

$$u_{\text{вх}}(t) = \frac{U}{t_\Phi}(t - t_0),$$

where U - amplitude, and t_Φ - duration of front of trigger pulse, then delay of starting of cascade is determined by expression

$$t_3 = t_1 - t_0 = u_{\text{вх}}(t_1)\frac{t_\Phi}{U} = \frac{t_\Phi}{U}(E_{\text{см}} - E_{\text{п}}) = \frac{t_\Phi}{U}E_1$$

or

$$dt_1 = \frac{t_\Phi}{U}\,dE_1 + \frac{E_1}{U}\,dt_\Phi - \frac{E_1 t_\Phi}{U^2}\,dU.$$

Passing to increases in value, we will obtain for instability of starting of cascade

$$\Delta t_1 \approx \frac{E_1}{U} t_\Phi \left(\frac{\Delta E_1}{E_1} + \frac{\Delta t_\Phi}{t_\Phi} - \frac{\Delta U}{U}\right). \qquad (10.22)$$

If the front of trigger pulse increases exponentially:

$$u_{\text{вх}}(t) = U(1 - e^{-t/\tau}),$$

that instability of triggering of cascade will be initial sector of the front of pulse [193]

$$\Delta t_1 = \Delta\tau \ln\frac{U}{U - E_1} + \frac{E_1\tau}{U - E_1}\left(\frac{\Delta E_1}{E_1} - \frac{\Delta U}{U}\right). \qquad (10.23)$$

Page 541.

And (10.23) it is evident from expressions (10.22) that with increase in bias voltage E_{cM} (i.e., with an increase in E_1) increases instability of starting Δt_1, which depends on change in voltage E_1 and steepness of front of trigger pulse. As is evident, with the linearly increasing front of trigger pulse instability Δt_1 depends on value $\Delta E_1/E_1$, and during the exponential build-up/growth of front the instability in all cases depends to a considerable degree on value E_1, which it is desirable to take as small as possible.

To instability of starting of cascade besides instability of supplies of power (technical instability) and instability of parameters of trigger pulse factors, connected with presence of fluctuations, caused by noise of resistors/resistances of diagram and tube, will also affect (natural instability). Therefore in the general case the problem about the instability of the moment of the triggering of start-up circuit is a statistical problem. Are at present indicated the solutions of this problem only in general form [194, 195]. Thus, the total instability of the moment of operation of electronic relay, including natural fluctuations, is determined by expression [195]

$$\Delta t_1 = -\frac{\xi(t)}{\left[\frac{du_{nx}(t)}{dt}\right]_{t=t_1}} + \frac{\xi(t)\xi'(t)}{\left[\frac{du_{nx}(t)}{dt}\right]^2_{t=t_1}} - \frac{\left[\frac{du_{nx}(t)}{dt}\right]_{t=t_1}\xi^2(t)}{2\left[\frac{du_{nx}(t)}{dt}\right]^3_{t=t_1}} + \ldots,$$

where $\xi(t)$ - total small fluctuation enumerated in input circuit of cascade/stage.

However, in available literature there is no evaluation/estimate of natural instability in waiting diagrams, and therefore, without knowing value $\xi(t)$, even in the case of linear approximation/approach it is impossible to calculate value Δt_1.

In developed samples of very high speed oscillographs [187, 191] experimentally was determined instability of triggering time of trigger circuits and sweep oscillators. Thus, the total instability of entire channel of scanning/sweep can have a value $\pm(1-2)\times10^{-11}$ s. With further decrease of this value, apparently, is necessary reduction in noise in the cascades/stages of diagram.

Page 542.

10.4. IMPULSE SHAPING FOR THE STARTING OF SWEEP OSCILLATORS. Requirements for the trigger circuits.

Pulses for starting of generators of high-speed scanning must have a very steep front, sufficient amplitude and high stability of their parameters. The parameters of pulses are determined by the oscillator circuit of scanning/sweep.

For the starting of sweep oscillators, which work on electron tubes, pulse must have large steepness of front and flat vertex. In the commutating tube of sweep oscillator increases insufficiently rapidly with small steepness of the front of the starting current pulse and therefore the initial section of scanning/sweep proves to be nonlinear. This especially is developed at very high scanning speeds. The duration of the front of trigger pulse must be considerably less than the sweep length (with exception of those cases, when the build-up/growth of the front of trigger pulse it is utilized further as the scanning/sweep). The presence of oscillations and overshoots at the pulse apex also leads to an increase in the percentage distortion of scanning/sweep, since the change of the current strength in the tube, which appears in this case, distorts the form of sweep voltage. Trigger pulse wave in these diagrams is determined by the duration of straight/direct trace of a scan and it is desirable so that it would be regulated.

During starting of sweep oscillators, which work on thyratrons, requirement for trigger pulse less rigid. The pulse duration here must not be very small and is determined not by the duration of straight/direct trace of a scan, but by the conditions of the stable starting of thyratron. Therefore the duration of trigger pulse lies/rests within the limits of several microseconds.

In thyratron oscillator circuit of scanning/sweep front of trigger pulse does not have direct effect on degree of linearity of

scanning/sweep, as it takes place in diagrams on vacuum lamps, since current strength in thyratron after its ignition is no longer determined by trigger pulse.

Page 543.

The front of trigger pulse must be selected from the condition of the stable starting of thyratron. The steepness of the pulse edge is necessary the order of 10' v/s.

It is desirable so that output circuits of trigger circuit of thyratron would be low-resistance. The diagrams, which form trigger pulses, must have short delay time, which is especially important with the oscillography of single short-term processes.

In designs of high-speed oscillographs rigid synchronization of moments of beginning of scanning/sweep and illumination of straight/direct course of ray of oscilloscope tube and moment of supplying temporary/time markers for calibrating scanning/sweep is important. Therefore pulses for the starting of sweep oscillator, pulse-shaping circuit of illumination and modulator of high- frequency mark generator are formed/shaped in the single trigger circuit of oscillograph.

At high scanning speeds all trigger pulses indicated must have steep front and be characterized by stability. Furthermore, in the trigger circuits of oscillograph it is desirable to provide impulse

shaping for the starting of external diagrams, since oscillograph can work both in trigger conditions from the external diagram and in the mode of its own starting. In the second case the starting of the diagrams being investigated is conducted from the oscillograph. Pulse repetition rate of starting must be regulated in the considerable limits.

Generator of driving pulses is fundamental synchronizing circuit of starting system of oscillograph. The pulses developed by it must be formed into the trigger pulses of the necessary amplitude and duration with the high steepness of front. Blocking oscillator is the most adequate relaxation diagram for the impulse shaping with the steep front with their large porosity. Therefore in starting system they had extensive application of a diagram of the blocking oscillators of microsecond and nanosecond ranges.

For starting of the generator of high-speed/high-velocity scanning/sweep is usually necessary pulse into several hundred volts with front with duration about 10 ns. Such pulses are formed/shaped by an increase in the steepness of the edge of pulse of the master oscillator with the aid of the sequence of the diagrams of blocking oscillators and amplifier-limiters, in latter/last cascades/stages of which are utilized the high-power tubes.

Page 544.

For impulse shaping of illumination of ray/beam and starting of

modulator of block of calibrator blocking oscillators also frequently are utilized. With the consecutive peaking of trigger pulse one of the cascades/stages of starting system simultaneously is utilized also for the impulse shaping of illumination.

Possible version of system block diagram of starting of high-speed oscillograph is given in Fig. 10.20.

Necessary adjustment of moment/torque of beginning of scanning/sweep can be realized by change in bias voltage on control electrode of tube of one of cascades/stages of starting system. However, this is not desirable at high scanning speeds, since a change in the grid voltage of tube can supply cascade/stage in the mode, during which is not provided a sufficient stability of the time of its starting. Therefore for the adjustment of the delay time of the starting of scanning/sweep it is desirable to provide either the diagram of electronic delay or the special circuit of the continuously adjustable delay.

Question of operational stability of starting system is very important. Just as in the case of sweep oscillator, which operates in the waiting mode, the operational stability of cascades of starting is determined by error $\frac{\Delta t_0}{t_0}$ due to a change in the starting time of diagram and due to a change in the steepness of the front of trigger pulses $\frac{\Delta k}{k}$, formed/shaped from one cascade/stage to the next.

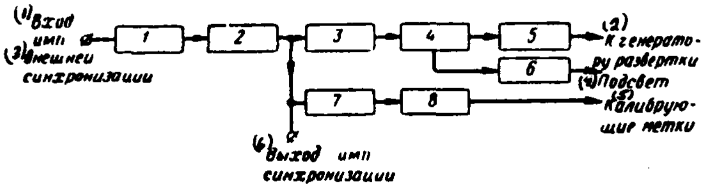

Fig. 10.20. System block diagram of starting of oscillograph: 1 - input circuits; 2 - pulse generator of starting; 3 - cascade/stage of delay; 4 - amplifier-peaker; 5 - pulse amplifier; 6 - diagram of illumination; 7 - amplifier-limiter; 8 - calibrator.

Key: (1). Input pulse. (2). To sweep oscillator. (3). External synchronization. (4). Illumination. (5). Calibrating markers. (6). Output of pulse of synchronization.

Page 545.

The main reason for error proves to be a change in the value of supply voltage, which ensures bias/displacement on control electrode of cascade/stage and in the smaller measure a change in the voltage of the source of anodic feed.

Since in trigger circuits blocking oscillators frequently are utilized, then the explanation of stability of time of their functioning is of interest. In the very high speed oscillographs for obtaining temporary/time resolution on the order of 0.05 ns the instability of triggering time of the separate cascade/stage of starting system must be less than 0.01 ns. The stability of triggering time of a diagram of the type of blocking oscillator in

this case, apparently has already been determined not only by the stability of the parameters of trigger pulse and supplies of power of diagram, but also by the noise level of diagram.

As can be seen from system block diagram of starting (Fig. 10.20), for obtaining parameters of trigger pulse of scanning/sweep necessary for high-speed/high-velocity oscillograph it is necessary to use a series of cascades, which are found in waiting mode. This leads to the significant magnitude of the total delay time of the starting of scanning, which reaches 50-200 ns.

High scanning speed sometimes is not required, but necessary is the minimum delay time of starting of scanning, which is important for oscillographs, intended for recording single process, in circuit of signal of which cable of delay is used; its length (and broad-band character) is determined by required delay time of starting of the scanning. In these cases the number of cascades/stages must be minimal, and the rate of their functioning is great. Therefore the application of diagrams on the tubes with the secondary emission is expedient. At low scanning speeds the total delay time of starting can be reduced to the value of 15-20 ns [196].

If sweep oscillator works on thyratron, then trigger circuit is more simple. In this case for the starting of the scannings it suffices to use a blocking oscillator and cathode follower, which form/shape pulse with the the amplitude 200-300 V for the duration of

front of approximately 0.1 μs.

Page 546.

Schematics of starting systems and generators of high-speed/high-velocity and very high speed scannings/sweeps.

Simplified circuits of units of starting and scanning/sweeping some contemporary high-speed oscillographs are given as examples of pulse-shaping circuits of starting and sweep oscillators.

Fig. 10.21 gives trigger circuit of high- speed/high-velocity oscillograph [197], constructed on blocking oscillators, sweep circuit, assembled on tetrode, and diagram of calibrator.

Here assigning blocking oscillator L_1 works in mode of external synchronization. Pulse from its output enters the amplifier L_2, cathode load of which is the circuit, which consists of the divider of voltage and delay lines. The circuit indicated provides the necessary value of the pulse amplitudes, which start the separate cascades/stages of diagram and the correct sequence of their work in the time.

After line of pulse delay enters second blocking oscillator L_3, intended for peaking of formed/shaped pulse. Bias on control electrode of tube $L_{3,1}$ it is possible to change and with the aid of this to smoothly change the moment of the starting of sweep

oscillator. The pulse shaped in the cascade/stage $L_{3,2}$ has a duration 50 or 200 ns, which is determined by capacitance value of capacitor/condenser, which is located in the grid circuit of tube. Then this pulse is amplified and is limited in the cascade/stage on the tube L_4. On secondary winding of transformer Tp_3 is formed the pulse with an amplitude of 120 V for the duration of front 7 ns. Formed thus pulse starts sweep oscillator L_5. From the third winding of the same transformer the pulse of the illumination of straight/direct trace of a scan is removed/taken.

Sweep oscillator is assembled according to fundamental diagram in Fig. 10.15. The use of a tetrode makes it possible to obtain scanning/sweep with the maximum speed of 10^9 cm/s. Sweep length is regulated by switching capacitors/condensers in the circuit of anode and cathode of tube L_5.

Trigger pulse from amplifier L_2 enters modulator of calibrator L_6. For obtaining the calibration markers are two sine wave oscillators (L_7 and L_8, L_9). Working oscillator frequency 200 and 500 MHz, which corresponds to the duration of oscillogram time marks 5 and 2 ns.

As example of trigger circuit and sweep oscillator on thyratron let us examine unit of starting and scanning high-speed pulse oscillograph [185].

Page 547.

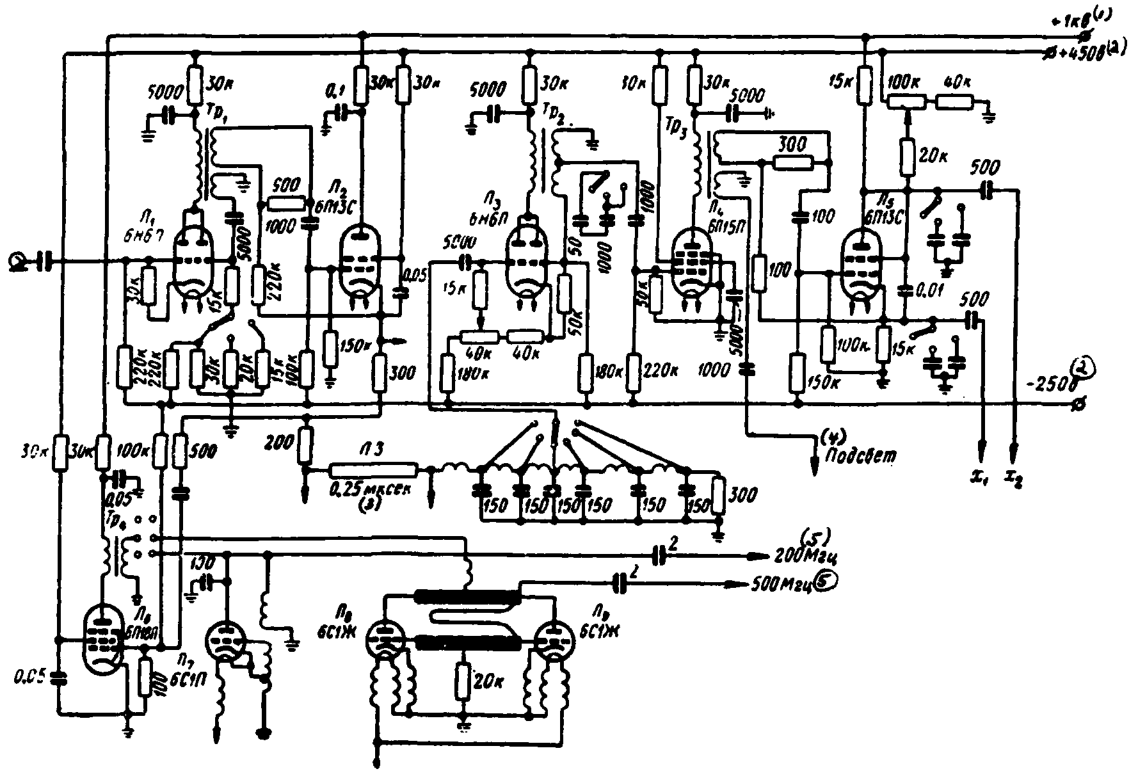

Fig. 10.21. Schematic of high-speed/high-velocity oscillograph.

Key: (1). kV. (2). in. (3). μs. (4). Illumination. (5). MHz.

Page 548.

Fig. 10.22 gives the simplified circuit of the scan unit and calibrator of oscillograph.

Here starting system consists of amplifier of external trigger pulses L_{11}, blocking oscillator L_{12}, which operates in waiting or auto-oscillating modes, and cathode followers L_2. Cathode follower L_{22} serves for the starting of thyratron L_3. Cathode follower L_{21} and delay line serve as the channel of synchronizing pulses for the

starting from the oscillograph of the external pulse generators, which work both on the thyratrons, and on the hard tubes. From the same the helmet yes is taken the trigger pulse of thyratron L_4.

Scanning/sweep pulses are formed/shaped in two cascades/stages, which work on finger thyratrons of type TGI1-3/1. Cascade/stage on the thyratron L_3 is intended for obtaining the scanning/sweep with duration of 15.50 and 100 ns and impulse shaping of the illumination of the straight/direct course of ray of oscilloscope tube. The linearly changing sweep voltage is formed/shaped with the aid of integrating LCR-networks (S 10.3), to the input of which is supplied a drop in the voltage with the steep front. a drop in the voltage is removed/taken from the peak transformer, which is located in the cathode circuit of thyratron. The forming cable, connected to the anode circuit of thyratron, is charged through the choke/throttle and the effective resistance. It ignites after the admission of trigger pulse on the grid of thyratron and cable is discharged through the resistor/resistance, equal to the wave impedance of the cable:

$$\rho = R_T + R',$$

where R_T - resistor/resistance of the open thyratron; R' - cathode load of the thyratron

$$R' = \frac{RR_K}{n_1^2 n_2^2 (R\, n_1^2 + R_K\, n_2^2)};$$

here $n_1 = w_2/w_1$, $n_2 = w'_2/w_1$ - the transformation ratios of pulse wide-band transformer relative to output on the integrating circuits and relative to output to cathode resistor/resistance R_K of the circuit of

illumination, w_1, w_2, w'_2 - number of turns in primary and secondary windings, R - effective resistance of the integrating circuits.

Page 549.

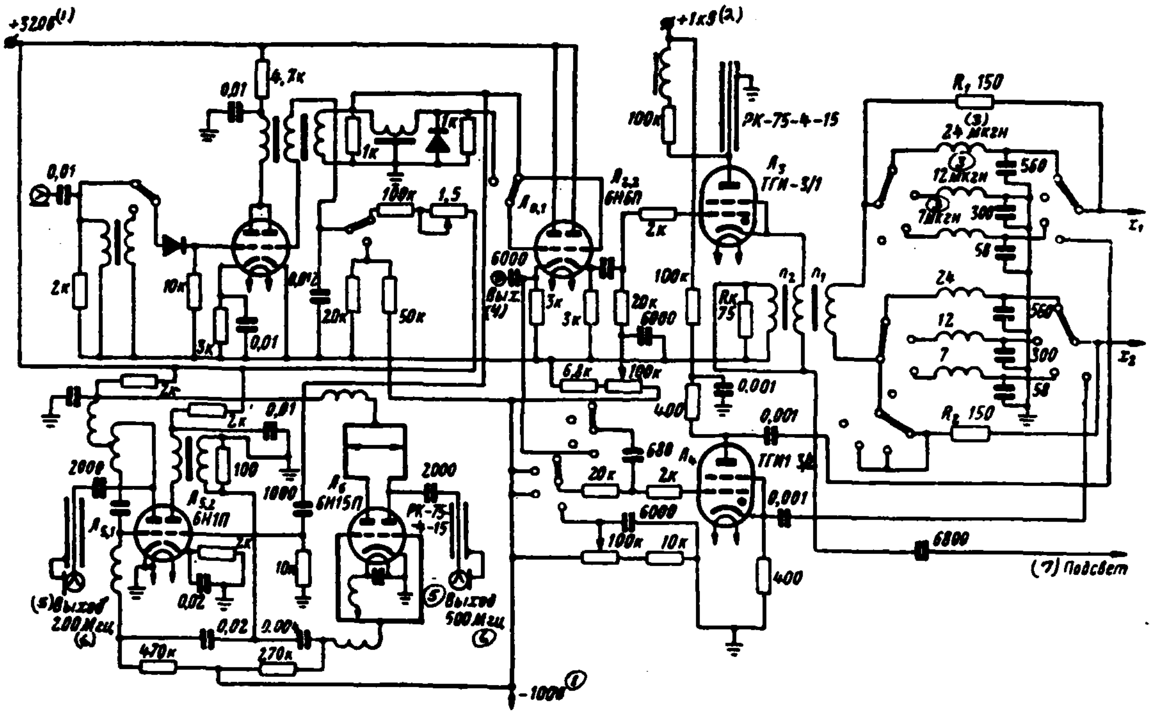

Fig. 10.22. Schematic diagram of an oscillograph with thyratron sweep oscillators.

Key: (1). in. (2). kV. (3). µH. (4). Output. (5). Output. (6). MHz. (7). Illumination.

Page 550.

Value of drop in output potential of integrating circuit will be

$$U = (E - U_T)\frac{R' n_1}{\rho + R' + R_T},$$

where E - voltage of anodic supply;

U_T - voltage drop across open thyratron.

Transformation ratios is expedient to take as equal to $n_1>1$ and $n_2<1$. The identification of the parameters of the integrating circuits is conducted taking into account expression (10.20) in the assigned sweep length t_p. For this it is necessary to assign the value of resistor/resistance of $R=R_1+R_2$, where R_1 and R_2 - resistors/resistances in each arm of scanning/sweep. The value of resistor/resistance R for any sweep length remains constant/invariable. During the calculation of the integrating circuits for the minimum sweep length (10-15 ns) should be increased time t_p by the value of the ionization time of the thyratron, used in the diagram.

A change in scanning speed is conducted by switching integrating circuits. In this case it is simultaneously necessary to change the length of the forming cable for changing the duration of the pulse of the illumination, which from the second output of peak transformer enters control electrode of oscilloscope tube. In gap/interval $0<t<t_{\text{ион}}$, where $t_{\text{ион}}$ - ionization time of thyratron, scanning/sweep has the nonlinear section, which must not be utilized. In this diagram

this section of scanning/sweep is not illuminated, since the pulse of illumination has rise time of front, the approximately equal to the ionization time of thyratron.

Relatively low maximum sweep frequency is the main disadvantage in diagram on thyratron. The application of a choke in charging circuit of cable provides the stable operation of diagram (without the repeated ignitions of thyratron) to the frequency of 10 kHz. The adjustment of sweep frequency during the internal starting is conducted by changing the frequency of blocking oscillator. The synchronization of blocking oscillator in the mode of frequency division is possible during the external starting of oscillograph. As a result of this it is possible to investigate the pulses, which follow with a frequency of up to 100 kHz, on the oscillograph.

Page 551.

For obtaining high-speed scanning, which reaches a rate of 2 cm/ns, (i.e., 4 ns to diameter of tube face 10LO101M), there is used a second thyratron cascade/stage L_4, assembled according to the schematic diagram given in Fig. 10.17. The pulse synchronization of illumination and high-speed scanning is achieved by the adjustment of grid bias on both thyratrons.

Unit of calibrator of oscillograph consists of pulse amplifier L_{52} and sine wave oscillators with frequency of 200 MHz (on L_{51}) and 500 MHz (on tube L_6).

As is evident, a diagram of the scan unit on the thyratron is sufficiently simple, since starting system has only one blocking oscillator and cathode follower, and pulse generator of illumination and sweep oscillator are combined in one cascade/stage on thyratron. the oscillography of pulses by duration on the order of 0.1 ns and less thyratron diagram they are not applicable due to the insufficient stability of triggering time. In this case the more compound circuits of starting system and sweep oscillator, carried out on the electron tubes, are used. Fig. 10.23 gives the simplified circuit of the unit of starting system and sweep oscillator of very high speed pulse oscillograph [187], intended for the investigation of the repetitive pulses of high voltage with a duration on the order of 10^{-10} s.

Generator of starting is assigning blocking oscillator L_2. It can work in the mode of auto-oscillations or in the mode of external pulse sinchronization of both polarities. With the external synchronization is utilized input cascade L_1. The operating mode is selected depending on the special features of the diagrams being investigated and their triggering time. Positive pulses of the master oscillator enter the cathode followers L_3, from the output of which there are taken the trigger pulses of the diagrams being investigated and positive pulse, supplied to the input of the cascade/stage of electronic delay L_4. The cascade of the continuously adjustable delay is necessary for the coincidence in the time of the pulse being investigated and scanning/sweep. To achieve this with the aid of a

change in the bias voltage on the subsequent cascades of starting is impossible, since the noticeable instability of triggering time of diagram can arise.

Page 552.

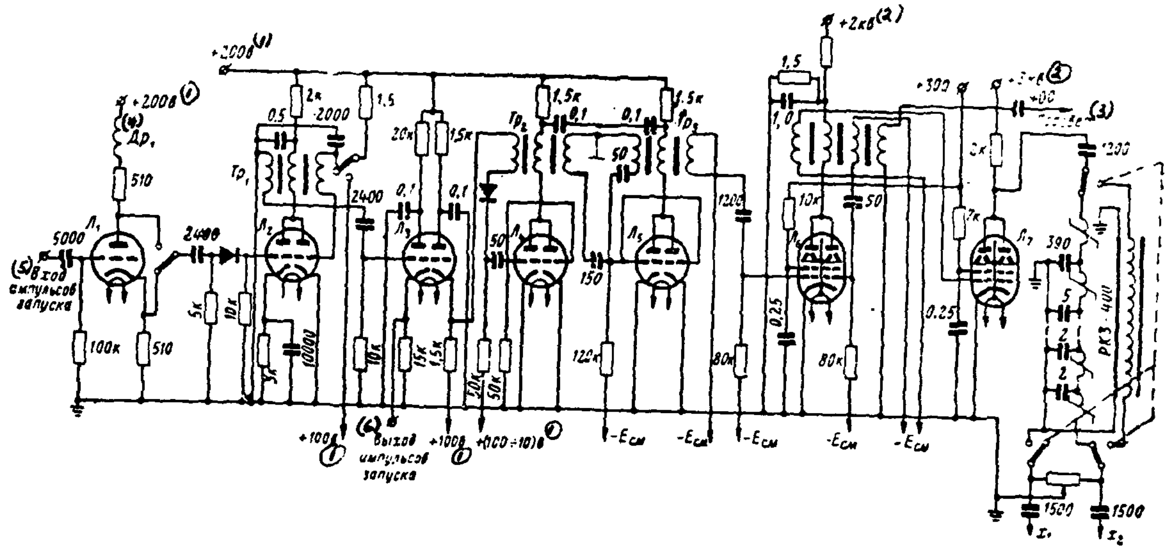

Fig. 10.23. Schematic of starting system and sweep oscillator of very high speed pulse oscillograph.

Key: (1). V. (2). kV. (3). Illumination. (4). Choke. (5). Input of trigger pulses. (6). Output of trigger pulses.

Page 553.

The grid biases of tubes of the cascades of starting must be thoroughly selected and fixed.

Subsequent two cascades L_3 and L_4 - two blocking oscillators, are intended for consecutive increase in steepness of front of trigger pulse. On half of tube L_4 is assembled the buffer stage, which unties blocking oscillators. From the output of the second blocking oscillator is removed/taken the pulse by the duration of 50 ns with the front with the duration of 15 ns. This pulse enters the modulating electrode of oscilloscope tube for the illumination of

ray/beam and the input of power amplifier L,. From the plate load of power amplifier the pulse of negative polarity with an amplitude of 3 kV and a duration of the front of 15 ns enters the input of the nonlinear forming line or the cable of delay.

For obtaining high-speed scanning with a duration of 5 ns from output of cable of delay linearly changing voltage due to frontal part of pulse is removed/taken. In this case for the scanning/sweep is isolated the linear part of the pulse edge.

For obtaining very high speed scanning/sweep with duration of 0.5-1 ns nonlinear forming line with ferrite, connected according to diagram, given in Fig. 10.18, is used. In the line is formed/shaped the stationary shock electromagnetic wave with the front with a duration of 1-2 ns and with an amplitude of about 2 kV. The steepness of front changes in the dependence on the number of utilized cells of the forming artificial line. For the scanning part of the shock wave front (linear) is utilized, which is provided with the aid of the controlled delay of the starting of diagram, the displacement of scanning along the axis X and the proper illumination of the beam. As a result from the load of the forming line is removed/taken paraphase scanning/sweep by the duration of 1-0.5 ns. Delay time of the forming lines is equal the delay time of the segment of cable RKZ-400, utilized in obtaining of scanning/sweep with a duration of 5 ns.

Forming line is artificial delay line, which consists of

LC-cells, inductance coils of which are wound around ferrite rings of type VT-5 with outer diameter of 3 mm. The calculation of this line is conducted, as it is indicated into § 4.3.

Page 554.

In trigger circuit of oscillograph several cascades work in mode of external starting. For guaranteeing the temporary/time stability of the starting of diagram it is necessary to select in each cascade/stage such value of bias voltage, with which the tube is opened to steepest sectors of the front of trigger pulse. Furthermore, supplies of power (especially grid bias) must have the high quality of stabilization. In the described oscillograph is obtained the temporary/time instability of the beginning of scanning/sweep not more than $\pm 1.5 \cdot 10^{-11}$ s.

10.5 Stroboscopic method of oscillography.

Stroboscopic method of oscillography is based on obtaining of image of oscillogram of repeating signal by consecutive isolation/liberation of its separate sections with the aid of very short-term strobe pulses and transformation circuit. The essence of method is explained with the aid of the oscillograms Fig. 10.24 and simplest block diagram of oscillograph (Fig. 10.25). The periodic sequence of the pulses being investigated enters the input of converter.

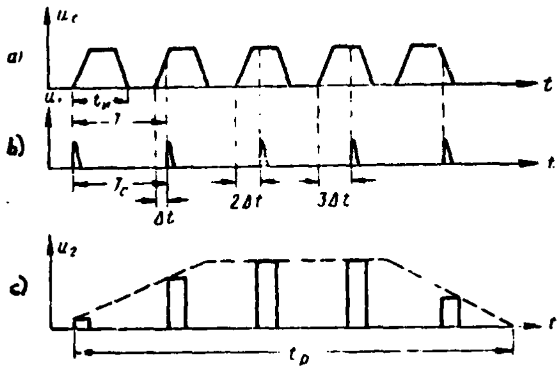

Fig. 10.24. Voltage oscillograms: a) pulse being investigated; b) strobe pulse; c) pulse at output of circuit of converter.

Page 555.

Simultaneously entering into the converter are auxiliary so-called strobe pulses (gate pulses) of very short duration t_c, occurs inequality $t_c \ll t_u$. The repetition period of gate pulses T_c differs somewhat from the repetition period of the pulse T being investigated. If the first gate pulse is synchronized since the beginning of the signal being investigated, then each following gate pulse is shifted/sheared in the time relative to signal to the interval of time Δt, called the step/pitch of reading. In this case occurs inequality Δt<<T.

Generally speaking, repetition frequency of gate pulses F_c can into whole number of times differ from repetition frequency of signal F. It is necessary only so that the repetition period of gate pulses would be more than the duration of signal t_u, so that with each of the

repeating signals one gate pulse would coincide.

As a result of effect of signal and gate pulse on converter at its output is formed a pulse only at the moment of coinciding of signal and gate pulse. The value of output pulse proves to be proportional to the instantaneous value of signal at the moment of the admission of gate pulse. In the interval of time t_p (Fig. 10.24c), equal to nT_c, will be isolated with n of the pulses, whose amplitude corresponds to the value of signal at different points in entire interval of its duration t_n. This process is repeated periodically. Pulses at the output of the converter are expanded and then are amplified.

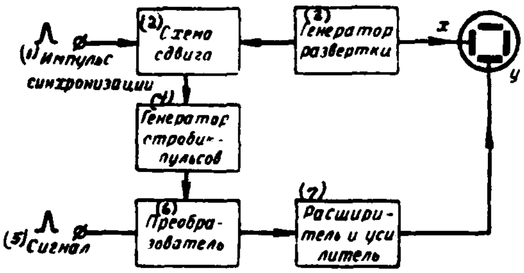

Fig. 10.25. Simplified block diagram of stroboscopic oscillograph. Key: (1). Synchronizing pulse. (2). Shift circuit. (3). Sweep oscillator. (4). Gate generator. (5). Signal. (6). Converter. (7). Expander and amplifier.

Page 556.

If we synchronize the scanning of the beam of oscilloscope tube synchronize with the onset of an initial gate pulse and to ensure the illumination of ray/beam only at the apex/vertex of the expanded pulses, then the points which form the image of the oscillogram of signal will be observed on the screen/shield of oscilloscope tube.

Thus, in the oscillograph it is necessary, in the first place, to synchronize scanning of the beam with that investigated of signals and to make its duration of equal to nT; in the second place, to synchronize since beginning of scanning/sweep first gate pulse and to ensure with the aid of circuit of automatic shift synchronous with scanning/sweep change in delay of gate pulse; thirdly, with the aid of converter to obtain output pulses, whose amplitude is proportional to instantaneous values of signal corresponding to them in time. Then on

the oscilloscope face is observed the signal being investigated, transformed in the time with the coefficient

$$m=\frac{t_{\text{p}}}{t_{\text{u}}}=\frac{nT}{n\Delta t}=\frac{1}{F\Delta t}.$$

Consequently, signal, reproduced on tube face on points, is dilated/extended in time into m of times and in so many once decreases rate of change in value of signal, and this means that in so many once decreases upper cut-off frequency of active width of spectrum of signal.

Since phenomena of expansion of signal and decrease of cut-off frequency of its spectrum are mutually dependent, then for obtaining the image, which corresponds to a waveform, in stroboscopic oscillograph after converter it is possible to use low-pass filter with cutoff frequency of F/2. For the same it is possible to use the storage device/equipment, which increases the duration of output pulses, since considerable time $T=\frac{1}{F}$. is passed between the moments/torques of the reproduction of the adjacent sections of signal. The second method is more preferable, since here there are no distortions, connected with the overlap of spectral components of serrated signal at the output of converter, which prove to be in the filter pass band.

Usual narrow-band linear amplifiers are used after expander of pulses.

Page 557.

The latter have a small inherent noise level, which makes it possible with the appropriate amplification factor to observe low in the signal amplitude. As a result the sensitivity of stroboscopic oscillograph proves to be the high with a sufficient effective bandwidth.

Quality of reproduction of waveform is determined to a considerable degree by number of points (sections), from which is comprised image. For the reproduction of the larger possible number of the harmonic components of the spectrum of the signal being investigated necessarily that the oscillogram would be represented by the largest possible number of points. For this it is desirable to have the high repetition frequency of signal and the low sweep frequency of ray/beam, in other words, the step/pitch of reading Δt it must be small. If the repetition frequency of signal is small, for example, it is equal to hundreds of hertz, then the sweep frequency of ray/beam must be equal to several hertz. Therefore for obtaining the possibility of observing the signals with the small repetition frequency oscilloscope tube must have a screen/shield with the long afterglow, otherwise the initial part of the image will already prove to be indistinguishable.

10.6. Quality of reproduction and the resolution of stroboscopic oscillograph.

It follows from an examination of the stroboscopic method of

oscillography that for qualitative signal reproduction it is necessary to, first of all, convert it without distortions. Therefore the schematic of converter must be sufficient wide-band and not introduce noticeable nonlinear distortions. Furthermore the gate length and the step/pitch of reading must be found in the dependence on the assigned range of the durations of the signals being investigated.

Depending on the required broad-band character of oscillograph schematics of converters can be constructed on electron tubes or semiconductor diodes. Fig. 10.26a gives the schematic of converter and its equivalent diagrams (Fig. 10.26b and c), which correspond to the moment/torque of reading and to period after the supply of gate pulse [198]. Signal is supplied to control electrode, and the gate pulse of negative polarity - to the cathode.

Page 558.

In the case of applying the semiconductor diode the signal and gate pulse are supplied to its input.

For the moment of reading according to the equivalent diagram (Fig. 10.26b) we have

$$u(t) = \frac{1}{C}\int i(t)\,dt,$$

$$i(t) = S(t)\cdot u_c(t) - \frac{u(t)}{R_1},$$

$$R_1 = \frac{R_i R}{R_i + R},$$

whence we obtain differential equation of converter

$$u(t) = \frac{1}{C}\int_0^t \left[S(t)\cdot u_c(t) - \frac{u(t)}{R_1}\right]dt \ \overset{(1)}{\text{при}}\ 0 \leq t \leq t_c. \quad (10.24)$$

Key: (1). with.

Converter is nonlinear diagram; however, frequently mode of its operation proves to be by such that it is possible to count conversion diagram of linear, so forth S(t)=S=const.

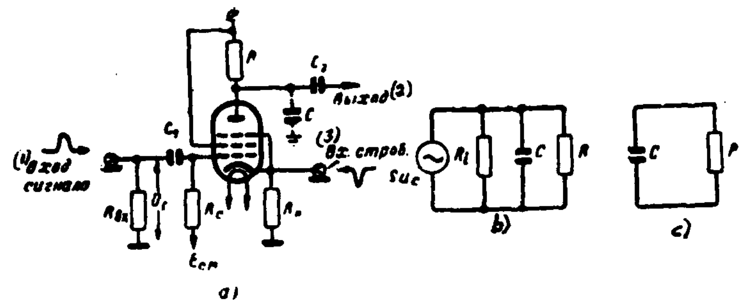

Fig. 10.26. Schematic diagram of converter (a); its equivalent diagram corresponding to moment of reading (b) and to moment after reading (c).

Key: (1). Input of signal. (2). Output. (3). Input of strobing.

Page 559.

Actually, if the signal being investigated is small, and gate pulse is selected such value, that at the moment of reading the tube works in the linear conditions, then in general form expression for output potential of converter for the time of action of gate pulse will be

$$u(t_1)=\frac{S}{C}\int\limits_{t_1-t_c/2}^{t_1+t_c/2} f(t)dt, \qquad (10.25)$$

here moment/torque t_1 corresponds to the center section of the gate pulse.

For evaluation/estimate of quality of reproduction on stroboscopic oscillograph of periodic signal of arbitrary form it is necessary to establish/install, with what accuracy function $u(t_1)$ will correspond to signal being investigated, assigned by function $u_c=f(t)$.

If we do not consider the effect of the transformation of time and to consider that the circuit of signal after converter does not introduce distortions into the shape of pulse, then the image of signal is determined by the shape of the envelope of pulses at the output of converter. Expanding in expression (10.25) integrand f(t) into the Taylor series and producing conversions, it is possible to obtain [199]

$$u(t_1) \approx \frac{St_c}{2}\left[f(t_1)+\left(\frac{t_c}{2}\right)^2\frac{f''(t')}{3!}\right],$$

where $(t_1-t_c/2)\leqslant t'\leqslant(t_1+t_c/2)$.

Absolute error in reproduction of any point (section) of function f(t) can be approximately determined in value of this second addend expression, i.e.

$$\gamma=\frac{St_c}{2}\left(\frac{t_c}{2}\right)^2\frac{f'(t')}{3!}.$$

Page 560.

For evaluation/estimate of distortion of shape of pulse being investigated it is more expedient to use ratio of absolute error to amplitude of output pulse (or to peak-to-peak), i.e., by expression

$$\nu=\frac{\gamma}{\frac{St_c}{2}[f(t_{\text{макс}})-f(t_{\text{мин}})]}=\left(\frac{t_c}{2}\right)^2\frac{f''(t'_{\text{макс}})}{6[f(t_{\text{макс}})-f(t_{\text{мин}})]}, \quad (10.26)$$

where $t_{\text{макс}}$ - moment of time, which corresponds to maximum voltage of pulse;

$t_{мин}$ - moment of time, which corresponds to minimum voltage of pulse;

$t'_{макс}$ -moment of time, which corresponds to maximum value second derivative shape of pulse.

Using formula (10.26), it is possible with assigned shape of pulse f(t) being investigated to find necessary gate length, in which distortions of reproduction of shape of pulse correspond to assigned error ν. Thus, if the video pulse being investigated has bell-shaped form $f(t)=Ae^{-at^2}$, then it is easy to show that $f''(t'_{макс})=4Aae^{-\frac{3}{2}}$. Then, after assigning the accuracy of reproduction of pulse in 10% i.e. ν=0.1 we find

$$\nu=0,1=\left(\frac{t_c}{2}\right)^2\frac{4Aae^{-\frac{3}{2}}}{5,4A}.$$

The hence required gate length must be not more

$$t_c-\sqrt{\frac{2,42}{a}}.$$

Besides selection of gate length it is necessary for qualitative signal reproduction to have sufficient number of points, from which is composed image, i.e. to select step/pitch of reading. Obviously, representation about the signal there will be the more complete, the greater the points we on it count. In connection with this it is necessary to check, is it possible to decrease the step/pitch of reading to any value convenient to us. It is shown [199] that the decrease of the step/pitch of reading in comparison with the gate

length is limited to following inequality:

$$\frac{\Delta t}{t_c} \geqslant \left| \frac{\left(\frac{t_c}{2}\right)^2 f'''(\xi)/6}{f'(\xi) - (t_c/2)^2 f'''(\xi)/12} \right|, \qquad (10.27)$$

where $(t_1 - t_c/2) \leqslant \xi \leqslant (t_1 + \Delta t + t_c/2)$.

Page 561.

Determination of minimum step/pitch of reading according to this formula is impossible, since usually is not previously known form of signal being investigated. But for the series/row of radio signals it is possible to previously establish/install some limiting values of derivatives and to use formula (10.27). The obtained oscillogram shows, what class includes the signal being investigated. Virtually it proves to be completely sufficient, if the number of points of reading will be about hundred or even it is equal to several ten.

As has already been indicated above, quality of work of stroboscopic oscillograph is determined to a considerable degree by operational stability of its fundamental nodes. Is required the sufficiently rigid synchronization of the onset of the first gate pulse since the beginning of scanning/sweep of electron beam and the beginning of the signal being investigated. Furthermore, is necessary the stable shift/shear of gate pulse (synchronization of the step/pitch of reading).

The signal itself being investigated sometimes is the fundamental synchronizing pulse. In this case the signal is supplied to the

converter through the cable of delay. The delay time of cable is determined by triggering time of the cascades/stages of the formation of gate pulse. However, the application of a cable in the circuit of signal leads to signal distortion, i.e., worsens/impairs time resolution. Furthermore, the presence of the drive circuits in the channel of the formation of gate pulse, which include several cascades/stages, is connected with the limitation of the rigidity of synchronization due to the instability of triggering time of the waiting electronic circuits, whose reason has already been examined during the analysis of the methods of obtaining the high-speed scannings (S 10.3).

Time resolution of stroboscopic oscillograph affects also finite time of establishment of transient processes in converter. Examining the case of effect on the signal-data converter in the form of a drop in voltage of low value U_c and gate pulse of triangular form by duration on foundation t_c (Fig. 10.27), we will consider that the diagram works in the linear conditions, i.e., S(t)=S=const. Furthermore, is not considered the effect of the form of gate pulse and in the changed its duration with a change signal amplitude.

Page 562.

Then, as it was shown above, for output potential of converter we have

$$u(t) = \frac{S}{C} \int_{t_1 - t_c/2}^{t_1 + t_c/2} U_c dt.$$

If a drop in voltage enters the input of converter at moment t_0 so that

$$\left(t_1-\frac{t_c}{2}\right)<t_0<\left(t_1+\frac{t_c}{2}\right),$$

$$u(t_1)=\frac{S}{C}\int\limits_{t_0}^{t_1+t_c/2} U_c dt=\frac{U_c S t_c}{C}\left(\frac{1}{2}+\frac{t_1-t_0}{t_c}\right).$$

For case

$$t_0<\left(t_1-\frac{t_c}{2}\right)$$

we have

$$u(t_1)=\frac{S}{C}\int\limits_{t_1-t_c/2}^{t_1+t_c/2} U_c dt=\frac{U_c S t_c}{C}. \qquad (10.28)$$

Thus, in the case of linear conditions of work of converter time of establishment of transient response of diagram cannot be more than gate length.

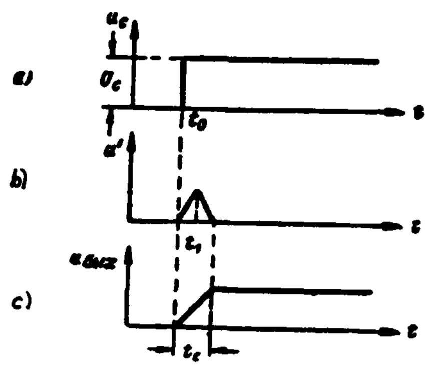

Fig. 10.27. Oscillograms: a) drop in voltage at input of converter; b) strobe pulse u'; c) drop in output potential of converter.

Page 563.

Since in the general case the converter is nonlinear system, then for the evaluation/estimate of the time of the establishment of diagram with the large signals already it is not possible to use the transient response of diagram and the method of imposition. However, it is possible to consider for the low signals in a number of cases that the diagram works in the linear conditions, and then the evaluation/estimate of the frequency properties of diagram [198] is of interest.

Let us assume that being fed to the input of diagram is a harmonic signal of small amplitude. Let us find the ratio of the value of output potential of converter at a certain frequency ω to the value of output voltage at the low frequency. If to the input linear (S=const) converter there is fed a sine voltage $u_c = U_c \sin \omega t$, then output potential for the time of action of the gate pulse

$$u(t_1)=\frac{U_c S}{C}\int\limits_{t_1-t_c/2}^{t_1+t_c/2}\sin\omega t\,dt=\frac{2U_c S}{\omega C}\sin\frac{\omega t_c}{2}\sin\omega t_1; \qquad (10.29)$$

here moment/torque t_1 corresponds to the center section of the gate pulse, whose form it is expedient to assume triangular. The divergence of electron beam of oscilloscope tube there will be to the proportionally obtained value of output voltage. Since the beam deflection at the low frequency Y(0) according to (10.29) proves to be proportional to value $SU_c t_c/C$, the ratio of the deflection of the beam of tube $Y(\omega)$ at the frequency ω to divergence of Y(0) will be

$$\frac{Y(\omega)}{Y(0)}=\frac{\sin\omega t_c/2}{\omega t_c/2}. \qquad (10.30)$$

Hence it is apparent that if we take as the cut-off frequency of passband the frequency, which corresponds to the level at 3 dB, then for the case of linear conditions of the work of converter according to (10.30) we obtain

$$\frac{\sin\omega_{rp}t_c/2}{\omega_{rp}t_c/2}=0{,}707$$

or

$$f_{rp}=0{,}45/t_c.$$

Page 564.

(Although, strictly speaking, this system nonlinear) they sometimes characterize broad-band character of converter by value calling its effective passband [198].

It is necessary to note that it is assumed in all given computations that linear input circuits of converter are sufficiently wide-band and do not introduce distortions into signal during its transmission being investigated. Knowing the time of the establishment of transient processes in converter t_{y1}, the time of the establishment of input circuits (including the cable of the delay, when it is) t_{y2}, it is possible to estimate the resulting time of the establishment

$$t_y = \sqrt{t_{y_1}^2 + t_{y_2}^2}.$$

Temporary/time resolution of stroboscopic oscillograph will be determined by value t_y, and also by absolute value of instability of triggering time of channel of formation of gate pulse. Thus, just as in the case of high-speed oscillographs, an increase in the time resolution of stroboscopic oscillograph is connected not only with the decrease of the time of establishment in the circuits, but also with an increase in the stability of functioning diagrams on the electron tubes or the semiconductor devices.

10.7. Designs of converters.

Converter and gate generator are the fundamental nodes of stroboscopic oscillograph.

As converter can be used cascades/stages on electron tubes and semiconductor diodes, structurally fulfilled in the form of extension caps.

Diagrams on electron tubes are distinguished depending on method of supplying strobe pulse - on anode, cathode or third grid of tube. The widest use found the diagram, in which the gate pulse of negative polarity is supplied to the cathode of tube (Fig. 10.26). In this circuit the diagrams of gate pulse and output circuit of converter are divided. Diagram has a low-resistance input, coordinated with coaxial cable, on which is supplied the signal being investigated. Gate pulse also on coaxial cable enters the low-resistance cathode load.

Page 565.

In initial state tube is closed. Bias voltage and amplitude of gate pulse are selected by such that with the maximum value of the voltage of gate pulse the working section of the characteristic of tube would be approximately linear. The amplitude of the signal being investigated must not be great. The signal and gate pulse simultaneously operate at the moment of reading on the tube, and at the output of diagram are formed the pulses, modulated in the amplitude by the signal being investigated. In the anode circuit of tube is a parasitic or specially introduced capacitance of C, which forms with resistor/resistance R the integrating circuit, as a result of acting which increases the duration of output pulse. Thus occurs preliminary pulse widening, which then enter the cascade/stage of

expansion and the amplifier.

Application in such schematics of radio-frequency pentodes and special wide-band tubes makes it possible to obtain converters, which have time of establishment 1-3 ns. Obtaining diagrams with the higher time resolution is possible only with the aid of the inverter stage, carried out in the form of coaxial construction/design on the semiconductor diode. In fig. 10.28 is given the schematic of converter on the semiconductor diode and the characteristic of diode. Gate pulse must have a sufficient amplitude in order to derive signal on the middle of the working section of the volt-ampere characteristic of diode.

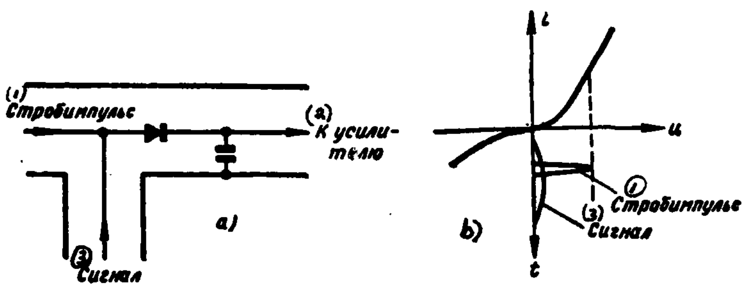

Fig. 10.28. Schematic of converter on diode (a); characteristic of diode and oscillogram of pulses (b).

Key: (1). Gate pulse. (2). To amplifier. (3). Signal.

Page 566.

Thus, at the moment of reading a change of the voltage on the capacity/capacitance is proportional to the algebraic sum of the voltage of signal at the moment of strobing/gating and amplitude of gate pulse. After the termination of gate pulse the restoration/reduction of initial voltage on capacity/capacitance of C occurs with the time constant, determined by capacity/capacitance C and by high resistor/resistance of the closed diode, i.e., is realized preliminary pulse widening at the output of converter.

However, diodes have finite time of transition from the open state to the closed. Therefore capacitance C loses the part of its charge, being discharged by inverse current of the slowly locking diode. Moreover, inverse current of diode is proportional to the value of release voltage (in the transient mode), and, thus, this current is determined by a change in the signal after the termination

of gate pulse, which leads to the distortion of the process of conversion. so the high speed diode 1N263 utilized in the foreign stroboscopic oscillographs has a reverse recovery time of approximately 2 ns. True, under the influence of very short-term gate pulse ($t_c = 0{,}2 \div 0{,}3$ ns) the base of diode does not manage to be filled up with minority carriers and the reverse recovery time, apparently, proves to be considerably less than 2 ns.

For eliminating deficiency in converter indicated sometimes is used diffusion diode with breakdown section of reverse/inverse branch of volt-ampere characteristic (Fig. 10.29) [201]. The switch time (decay in inverse current) of this diode is rated/estimated by the expression

$$t_п = \frac{2{,}4\tau_1}{1 - \left(\frac{U_{см}}{U_в}\right)^6},$$

where $\tau_1 = (1-2) \cdot 10^{-11}$ s - time of the retention/maintaining current in the region of the multiplication of carriers;

$U_в$ - voltage of the breakdown of diode;

$U_{см}$ - bias voltage.

Page 567.

Value $t_п$ can be less than 0.1 ns. Is desirable bias voltage $U_{см}$ to take considerably less than the voltage $U_в$, and the amplitude of gate pulse - sufficient for the work in the linear section of characteristic in the region of the electrical reversible breakdown. The amplitude of the signal being investigated must be less than the

amplitude of gate pulse, so as to signal could not itself discover diode or derive it from the mode, which corresponds to linear section.

After termination of gate pulse capacity/capacitance slowly is discharged through diode and resistor/resistance R and output pulse proves to be expanded to duration into several microseconds.

During more detailed analysis of work of converter it is necessary besides switch time of diode to consider nonlinear distortions. The nonlinear distortions, introduced by converter (especially with the work on the straight/direct branch of the characteristic of diode) can be considerable. The appearing distortions are connected with the fact that the capacitance of converter C for the length of gate (if $t_c<1$ ns) it does not manage to be loaded to the peak value, which leads to a change in the time of the charge of capacity/capacitance with a change in the voltage of signal. Counting the form of the gate pulse of triangular and its active duration of equal to t_{ca}, duration on the level, which corresponds to the triggering/opening of diode (to corresponding beginning of the linear section of characteristic), and the steepness of its front equal k, it is possible to calculate amplitude conversion diagram [201].

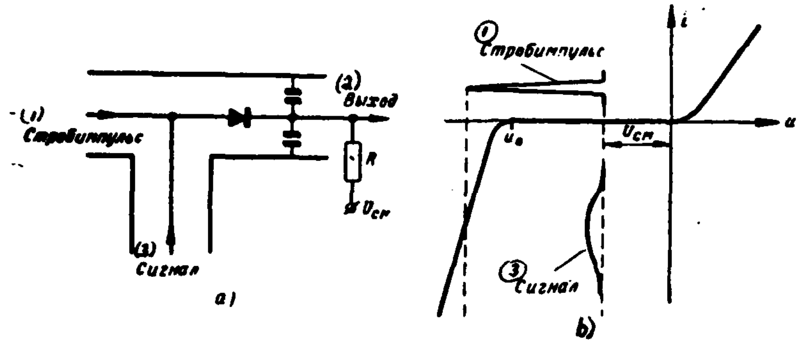

Fig. 10.29. Schematic of converter (a); characteristic of diode and oscillogram of pulses (b).

Key: (1). Gate pulse. (2). Output. (3). Signal.

Page 568.

This characteristic can be described by the expression

$$u_{вых} = k\left[t_{сд}/2 - \tau \ln\left(2 - e^{-\frac{t_{сд}}{2\tau}}\right)\right],$$

where the time constant of the circuit of the charge of capacity/capacitance $\tau=(R_{д}+R_{л})\cdot C$; $R_{д}$ - the resistor/resistance of diode; $R_{л}$ - the line impedance of transmission at the entrance point to the converter.

Converter with semiconductor diode will have linear amplitude characteristic when $\tau \ll t_{сд}$. to carry out this inequality in practice is difficult. The use of a diffusion diode in the operating mode proves to be most favorable on the reverse/inverse branch of volt-ampere characteristic. This diode has a small transfer capacitance (about 0.3 pF) and therefore resulting capacity/capacitance of C', formed by

the series connection of passage C_n and fundamental C of capacities/capacitances, it decreases to 10 pF. There cannot be considerably decreased the fundamental capacitance, since capacitive voltage-divider is formed, as a result of which the signal is transmitted to the output and in the absence of gate pulse.

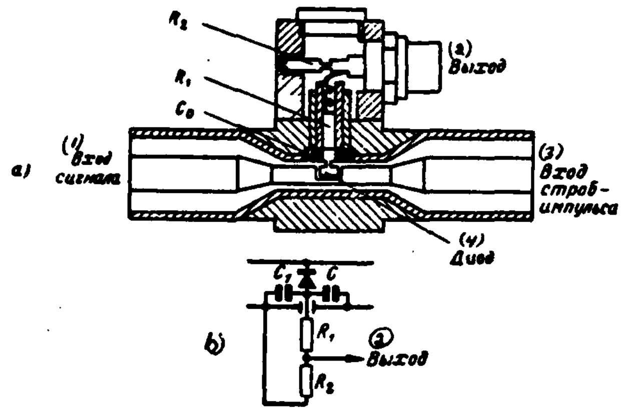

Fig. 10.30. Device of converter (a) and its equivalent diagram (b). Key: (1). Input of signal. (2). Output. (3). Input of gate pulse. (4). Diode.

Page 569.

Structurally the converter is fulfilled in the form of coaxial system, matched at the input and output. Fig. 10.30 gives diagrammatic representation of converter with point type special semiconductor diode from gallium arsenide [200]. Diode is installed between the internal and external conductors of the coaxial line, which has the wave impedance of 50 ohms. The decrease of the inside diameter of line in the point of connection of diode serves for its best agreement with the line.

In this converter, which works are somewhat unique, small capacitance of C_0, which is formed between housing of the diode and external conductor, simplest low-frequency filter is created together with resistor/resistance at output of converter. The application of a

filter of RC-type and mode of direct detection on the capacity/capacitance of converter makes it possible to considerably raise the time resolution of oscillograph.

For realization this reading of signal it is obtained due to difference in repetition periods of signal and gate pulse ΔT, which is very stable. This is reached by applying two generators with the quartz-crystal control, which synchronize the work of gate generator and generator of the signal being investigated. The time constant of the RC network of converter is selected in such a way as to remove high- frequency pulsations, but not to distort the pulse edge. This is fulfilled, since value ΔT is more than to two orders of less than the resolution of oscillograph. Fig. 10.31 shows the oscillogram of voltage u_1 on the capacity/capacitance of converter and voltage of gate pulse u_2.

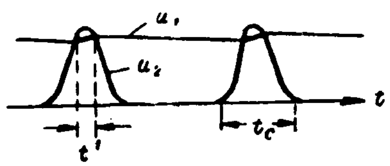

Fig. 10.31. Oscillograms of voltage u_1 on capacity/capacitance and of gate pulse u_2.

Page 570.

As can be seen from figure, the operating time of converter t' is much less than the length of gate t_c, since capacity/capacitance of C_0 only insignificantly is discharged from one pulse to the next. Because of this mode of the work of converter the time resolution reaches the value of 0.06 ns [200].

However, this method of oscillography has essential deficiency, which consists in the fact that to investigate it is possible signal only with completely specific strictly fixed/recorded frequency, which must be sufficiently high moreover, (not less than 10 MHz). In the case of another repetition frequency of signal the new clock frequency of gate generator is necessary, i.e., the new pair of generators with the quartz-crystal control is necessary.

Stroboscopic oscillograph can be used and, also, for observing pulse envelope and their high-frequency filling. The carrier frequency of the radio pulses of nanosecond duration reaches tens of gigahertz and therefore converter is fulfilled in the form of

waveguide section. Fig. 10.32 gives the drawing of this converter [202]. Converter consists of the germanium diode, installed into the waveguide so that it is arranged/located perpendicularly to the direction of propagation of waves in the waveguide. Diode is connected with the umbilical connectors, fastened/strengthened to the walls of waveguide. Gate pulse is fed/conducted along the cable to the cathode of diode. The anode of diode is connected with the cable, on which the pulse from the output of converter proceeds to the amplifier of usual oscillograph.

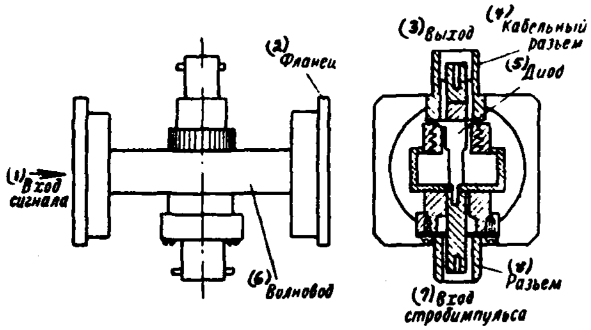

Fig. 10.32. Device/equipment of converter in the form of waveguide with semiconductor diode.

Key: (1). Input of signal. (2). Collar. (3). Output. (4). Cable connector. (5). Diode. (6). Waveguide. (7). Input of gate pulse. (8). Coupling.

Page 571.

Pulse signal is introduced through collar of waveguide and is propagated along latter. The load of waveguide is placed at another end/lead and serves for absorbing the signal, which passed through the section with the diode toward the end of the waveguide section. Signal does not enter cable, but gate pulse - into the waveguide, since the critical value of the frequency of waveguide and cable does not make it possible for signal to be propagated in the cable, but to pulse - in the waveguide. The time constant of output circuit of converter of approximately 1 μs is determined by the parameters parallel-connected capacity/capacitance of output cable, back resistance of diode and by input resistance of amplifier, which is located on the output of converter. Time constant is great in

comparison with the repetition period of pulses and is low in comparison with the period of scanning/sweep of oscillograph. Therefore possible to utilize this circuit for the accumulation of information from one section of the reading of oscillogram to another.

10.8. Generators of strobe pulses.

As noted above, quality of reproduction time resolution of stroboscopic oscillograph together with broad-band character of circuits of converter is determined, mainly, by gate length. Therefore depending on requirements for the resolution it is necessary to select the appropriate oscillator circuit of gate pulse. If instrument is designed for the band to several hundred megahertz, then there can be used the vacuum-tube circuits of gate generators, which make it possible to obtain pulses by the duration of the order of nanosecond and somewhat less. The amplitude of gate pulse usually comprises the units of volts or the tenths of volt.

Therefore as gate generator it is possible to utilize diagrams of formation of nanosecond pulses on tubes of secondary emission and blocking oscillators with consecutive peaking. The diagrams, which contain limiters and differentiating circuits on the coaxial lines, are frequently the output stages of the diagram of the formation of gate pulses.

Page 572.

With operation of the oscillograph at high repetition frequencies in number of cases master oscillators with quartz-crystal control and diagrams of frequency multiplication are used. The formation of gate pulses then is realized with the aid of the sufficiently simple vacuum-tube circuits or the diagrams on the semiconductor diodes.

Sufficiently simple diagrams of formation of gate pulses can be obtained in the case of using sinusoidal oscillation as starting voltage. Fig. 10.33 gives the diagram of the formation of gate pulse from the sinusoidal oscillation with the aid of two cascades/stages [202]. Sine voltage is supplied to the forming cascade/stage (L_1) with the grounded grid, which works on lighthouse type triode, which has small anodic and cathode capacities/capacitances. After limitation the voltage enters the differentiating circuit, in which is utilized that short-circuited at the end/lead of severings of cable. The obtained pulse further enters the cathode of miniature type triode, on which is assembled the amplifier- limiter. After peaking the gate pulse with duration about 0.5 ns enters on coaxial cable the converter. The input and output of the last cascade have a resistor/resistance of 50 ohms.

If stroboscopic oscillograph is designed for effective passband of more than 1 GHz, then the gate length must be considerably less than 1 ns. Such pulses usually are formed/shaped into two stages.

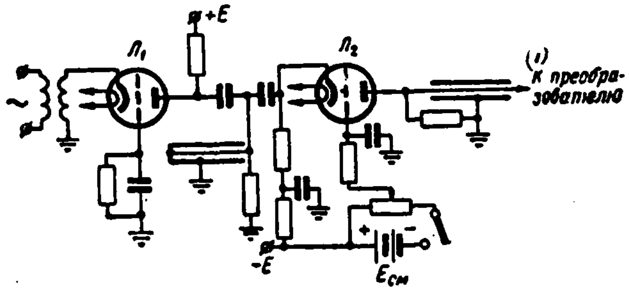

Fig. 10.33. Diagram of formation of gate pulse from sinusoidal oscillation.

Key: (1). To the converter.

Page 573.

During the first stage the blocking oscillators or amplifier-limiters are shaping circuits, while in the second stage the diagrams of pulse shortening in the form of distributed type differentiating circuits are utilized or the high speed semiconductor diodes, assembled in the coaxial systems, are utilized. During the first stage are formed/shaped the pulses of considerable amplitude with the steep front (to 10^{11}-10^{12} V/s). Frequently at the output of the diagram of the first stage of formation are utilized pencil type miniature tubes, which are assembled in the coaxial holder.

Fig. 10.34 gives diagram of second stage of formation of gate pulse [203]. The output tube of the diagram of the first stage of the formation of gate pulse and the coaxial shortening circuit is shown here. Output tube is pencil type triode 5675 (analogous in the construction/design to Soviet tube 6S13D). In the anode of this tube

is used right-angled junction with the arms, which have the delay time of pulse, equal to t_1. For the pulse which is propagated from the anode of tube into the line, this system is the short-circuited section/segment, as a result of which first pulse shortening occurs. After attenuator the pulse undergoes secondary shortening due to the presence of short-circuited stub with the delay time t_2. After passing the second attenuator gate pulse it enters the converter.

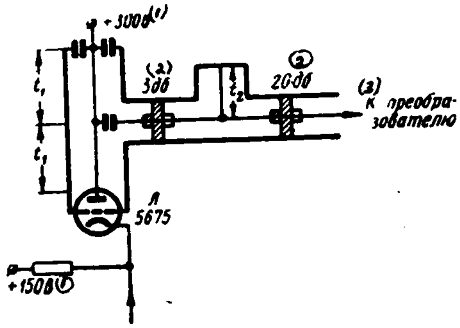

Fig. 10.34. Schematic diagram of output stages of gate generator.
Key: (1). V. (2). dB. (3). To converter.

Page 574.

Fig. 10.35 gives somewhat different design of the device for diagram of formation of second stage [205]. Here in contrast to the preceding/previous NOT circuit second short-circuited line and attenuator, and is added the diode, which cuts the foundation of gate pulse. In the single coaxial system the diagram of the second stage of the formation of gate pulse and converter on the semiconductor diode is assembled. To the left to the input of coaxial line from the cascades/stages of the diagram of the first stage of the formation of gate pulse enter pulses with the duration of the order of several nanoseconds.

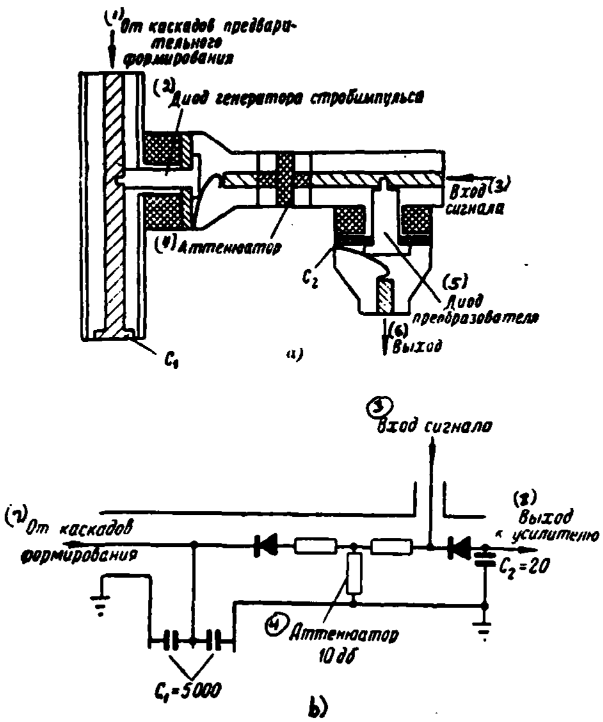

Fig. 10.35. Device/equipment of coaxial system with output stage of gate generator and converter (a); equivalent diagram (b).

Key: (1). From cascades of preliminary formation. (2). Diode of gate generator. (3). Input of signal. (4). Attenuator. (5). Diode of converter. (6). Output. (7). From cascades of formation. (8). Output to amplifier.

Page 575.

Further pulse is differentiated by the circuit, which consists of the section of the line, locked the capacity/capacitance, and enters the peaking diode-limiter. The obtained pulse with a duration of less than a nanosecond through the attenuator enters the diode converter. Simultaneously to the converter along the coaxial line comes the pulse

being investigated. From the output of coaxial system the converted and preliminarily expanded pulses fall on amplifier.

Fig. 10.36 shows device/equipment of second stage of formation of gate pulse on high speed semiconductor diode [204]. The diode, to cathode of which is biased in the forward direction, it is assembled between the internal and external conductors of coaxial line. During the supplying to the input of the system of pulse from the cascades/stages of preliminary formation the diode, which shunts line, passes for the very small time interval into the nonconducting state, as a result of which the drop in voltage, which is propagated along the line, is formed. This drop in the voltage then is differentiated with the aid of the short-circuited coaxial loop of the corresponding length. As a result at the output of coaxial line is obtained the pulse by the duration of 0.2 ns with the the amplitude 0.5 V.

Section of coaxial line with diode and by short-circuited stub is isolated from diagram of shaping of first stage, on one hand, and from termination, on the other hand, by two attenuators. Thus is reached the decoupling of line by cascades/stages at its input and output.

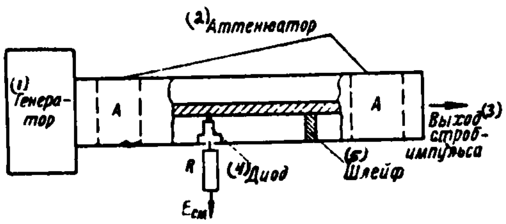

Fig. 10.36. Schematic diagram of design of gate generator.
Key: (1). Generator. (2). Attenuator. (3). Output of gate pulse. (4). Diode. (5). Loop.

Page 576.

As is noted, the converter and gate generator are fundamental wide- band nodes of stroboscopic oscillograph. The remaining cascades/stages of the schematic of oscillograph are assembled according to the usual diagrams, widely utilized in the pulse technique. As an example let us examine block diagram and designation/purpose of the fundamental nodes of the series sample of the stroboscopic oscillograph, which has effective passband 900 MHz and sensitivity 3 mV/cm [206].

Fig. 10.37 gives block diagram of oscillograph. In the diagram for guaranteeing the synchronization of the starting of units is provided besides the input of the pulse being investigated also the input of trigger pulse. Converter 3 enters the pulse from the input being investigated and the strobe pulse from the generator of strobe pulses 2. From the output of pulse converter through amplifier 4 enters the expander of pulse 5 and then the vertical deflectors of

oscilloscope tube 7.

So that moment of reading of signal would change, being displaced along time axis to value of step/pitch of reading, the generator of strobe pulses must put out pulses at strictly defined moments of time. For this there is a unit of the generator of rapid linearly increasing voltage 1 and a unit 6, in which is formed/shaped the step voltage and the sweep voltage of oscilloscope tube.

After starting of oscillator circuit of step voltage 6 develops voltage, whose amplitude grows/rises by steps/stages, whose value can be regulated. Negative voltage from the output of this generator enters the input cascade of the generator of strobe pulses. Simultaneously the linearly increasing voltage from generator 1 comes the same cascade/stage.

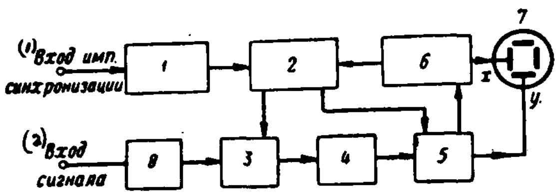

Fig. 10.37. Block diagram of stroboscopic oscillograph.

Key: (1). Input of pulse of synchronization. (2). Input of signal.

Page 577.

When the values of these voltages become equal, generator 2 puts out strobe pulse and in the converter it occurs the reading of the fixed point of signal. With an increase of negative step voltage the delay time of the delivery of strobe pulse increases and, thus, is realized bias/displacement along the time axis of the moment of the reading of signal.

Moment/torque of formation of step voltage in turn by timed pulses, which come from expander of pulses 5. Consequently, the moment of the subsequent reading is synchronized with the moment of the preceding/previous reading. The greater interval of reading (i.e. the points of reading for the scanning time the less), the greater the amplitude of steps/stages, installed with the aid of the appropriate switch in the unit of the generator of step voltage.

Unit of generator of rapidly linearly increasing voltage contains cascade/stage of switching polarity and amplification of trigger

pulses, the cascade of starting and generator, assembled according to the diagram similar to sweep circuits (Fig. 10.12). The starting of generator and its work must be characterized by high stability. The stability of the temporary situation of the linearly increasing voltage must be not worse than 10^{-10} s.

Unit of generator of strobe pulses includes cascade/stage of comparison, input of which enters negative step voltage and linearly increasing voltage. At the moment of the equality of these voltages/stresses from the output of cascade/stage enters the pulse to the generator of strobe pulses, which generates pulse with the amplitude into several volts and a duration of 0.5 ns at the level of half of amplitude value.

Converter is fulfilled in the form of coaxial system, into which is installed semiconductor diode of converter. In the same system the latter/last cascade/stage of the generator of strobe pulses, which works on the semiconductor diode is assembled (diagram of peaking). A preliminary increase in the pulse duration occurs at the output of converter. Then pulse enters amplifier 4. Amplifier has an amplification factor, equal to 3000. for the sufficiently precise measurements the stability of amplification is necessary to 0.5-1%.

Page 578.

After pulse amplifier enters expander. The expander of pulses works on the principle of charge of capacitor by the current of tube

during the action of pulse. The capacitor/condenser is discharged through the time interval with a duration of 1 ms with the aid of the special discharge lamp. Thus, from the output of expander is removed/taken pulse by the duration of the order of millisecond. The discharge lamp of the diagram of expander is controlled by the pulse, which comes from the generator of strobe pulses. Pulse from the output of expander is supplied to backplates of oscilloscope tube and simultaneously on the unit of the generator of step voltage.

Unit of generator of step voltage consists of diagram of formation of step voltage with storage capacity/capacitance, pulse-shaping circuit of illumination of straight/direct course of ray of oscilloscope tube and switch of capacities/capacitances, with the aid of which changes amplitude of steps of step voltage. For scanning the beam of oscilloscope tube the step voltage, supplied to the deflector plates of the tube through the appropriate regulator and the phase inverter in the form of vapor phase voltage, is utilized.

Resulting time resolution of this oscillograph is determined by effective passband of system, which depends to a considerable degree on gate length, passband of cable of delay 8, located on input circuit of signal, and operational stability of basic sets of instruments. In the described oscillograph the resolution is not worse than 0.5 ns.

Considerable attention to developments of stroboscopic oscillographs of nanosecond range is paid recently. The large number

of investigations, in particular in the region of semiconductors (especially tunnel diodes), is connected with the measurement of the very short-term voltages/stresses of low value [201]. The construction of the stroboscopic oscillographs, which make it possible to record the very low-power radio pulses of nanosecond duration, even more greatly will expand the field of application of a stroboscopic oscillography.

Page 579.

Chapter Eleven.

MEASUREMENTS OF PARAMETERS OF PULSES.

Use of pulses of nanosecond duration causes need of measuring parameters of these pulses, i.e. their amplitude, duration, repetition frequency or porosity.

Development of high-speed/high-velocity and stroboscopic oscillography makes it possible increasingly to raise accuracy of the determination of form of nanosecond pulses and measurement of their parameters. However, there is a range of values of the parameters of the pulses, whose measurement with the aid of the oscillographs it is hindered/hampered or it is impossible. In particular, the difficulties of the measurement of the parameters of the nanosecond pulses of a small amplitude are caused, especially if they are not periodically repeating. Furthermore, there is considerable practical interest in the possibility of measuring the parameters of such pulses with the aid of the directly indicating instruments (voltmeters, the meters of small time intervals, etc.), which make it possible to take a direct reading of value, also, with the larger accuracy than this can be carried out with the oscillograph.

11.1. SPECIFIC CHARACTER OF THE MEASUREMENT OF NANOSECOND PULSES.

Measuring meters, intended for work in nanosecond range of pulse durations, must have nodes, which are characterized by considerable broad-band character.

Page 580.

Therefore, the greatest difficulties are caused by measurements of pulses of a small amplitude, when for guaranteeing the high instrument sensitivity appears the need of amplifying the measured pulses, what by itself is insufficient the nanosecond pulse technique solved by problem. In connection with this new methods must be developed or the old methods of pulse radio meterings are improved.

In the measurement of parameters of pulses of nanosecond duration methods, based on preliminary increase in duration of pulses [found use 207, 208, 209]. In this case input circuits of the instrument and diagram of the expander of pulses must satisfy specific requirements. Other units do not differ from those used in different radio gage devices/equipment. In such instruments are realized also the methods of measurement with the aid of compensative and autocompensational voltmeters [40, 210], which make it possible to measure the pulses with a minimum duration of 10-100 ns.

Wide-band diagrams with high-frequency diodes in fundamental measuring units are very frequently used. However, the use, for example, of peak diode voltmeters makes it possible to measure the pulses with the amplitude, that exceeds 5-10 V. In this case in

entire scale range of voltmeter there is no dependence of its readings/indications on duration and shape of pulses, since the characteristic of diode can be considered linear. But if the pulse amplitudes decrease to values less than 5-10 V, then the need for the account of the special features of the real volt-ampere characteristic of diode appears. With the low values of anode current the characteristic of diode differs significantly from linear function. This leads to the need for the account of both the form and the duration (or porosity) of pulses, which complicates work with the instrument and noticeably reduces the accuracy of measurements. Use in the schematics of such voltmeters of wideband amplifiers does not make it possible to measure pulses with the duration of less than 3-5 ns due to the insufficiency of the broad-band character of amplifiers with the considerable amplification factor.

Page 581.

For eliminating deficiencies in voltmeters, connected with special features of nonlinear characteristic of diodes, are proposed methods of measuring nanosecond pulses with small amplitude, when properties of nonlinear elements with different volt-ampere characteristics are utilized. In this case the dependence of the results of measurements from the pulse duration is eliminated, and, furthermore, there is the possibility to measure the pulse duration together with the measurement of its amplitude, moreover to measure it is possible both periodically repeating and single pulses [211, 212]. For measuring only the repetitive pulses of nanosecond duration are

developed other methods [213, 214].

Appear specific special features, also, in measurement of parameters of nanosecond pulses of high voltage. The need of applying the voltage dividers in many instances encountered here limits the minimum duration of the measured pulses due to the insufficient broad-band character of dividers. Therefore for pulse measurements in the nanosecond range the development of the corresponding attenuators acquires essential vital importance.

Lines of transmission of pulses are utilized in all cases of measuring parameters of nanosecond pulses in measuring circuit. The methods of characteristic measurement of entire transmitting circuit of measuring unit and therefore are of considerable interest. The attention to the development of the devices/equipment, which make it possible to measure the pulse responses of the transmission lines, to rate/estimate character and value of heterogeneities in them and to find other parameters of measuring systems is paid recently.

11.2. METHODS OF MEASURING THE PARAMETERS OF PULSES BASED ON AN INCREASE IN THEIR DURATION.

Difficulties which appear in the measurement of duration and amplitude of nanosecond pulses are to a certain extent removed if preliminary increase in their duration is realized. Actually, in this case those preceding the unit of the expander of pulses must satisfy

the requirement of considerable broad-band character only input circuits of measuring device.

Page 582.

The expander of pulses must ensure the completely specific and stable increase in the duration of the measured pulses, and the subsequent cascades/stages of measuring device are the usual diagrams, widely utilized in the radio gage technology.

Fig. 11.1a gives block diagram of device/equipment for measuring duration of pulses [207]. Here the pulse of the nanosecond duration through the sufficiently broadly tuned circuits enters the expander of pulses 1, which realizes linear magnification in the pulse duration. Pulse from the output of expander enters the controlled generator of harmonic oscillations 2; the number of oscillations, obtained from the generator, for the pulse action time, is counted off by electronic counter 3 and is recorded by appropriate indicator 4. Fig. 11.1b gives the diagram of the simplest expander of pulses. In the absence of pulses voltage across capacitor C is close to zero, since the resistor/resistance of diode D_2 in the conducting state is small in comparison with resistor/resistance R_2.

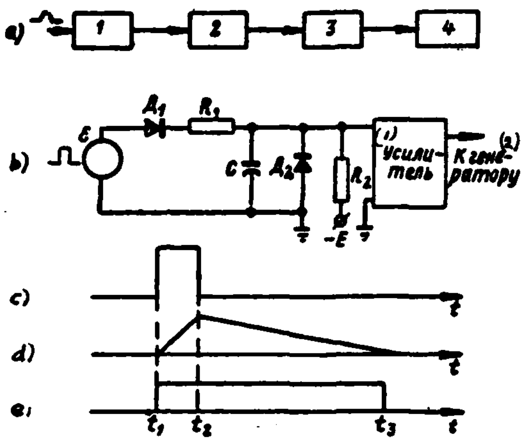

Fig. 11.1. Block diagram of device/equipment for measuring duration of pulses (a), diagram of expander of pulses (b), measured pulse (c), pulse at output of expander (d), pulse at output of amplifier (e). Key: (1). Amplifier. (2). To generator.

Page 583.

During the action of positive pulse the diode D_1 works as the peak detector, which makes it possible for capacitor/condenser C to be charged through resistor/resistance of R_1, which is considerably lower than the resistor/resistance of R_2. An increase in voltage across capacitor changes the polarity of voltage on the diode D_2. Up to moment of time t_2, which corresponds to the termination of the action of pulse, both diodes are not conducted and capacitor/condenser C is discharged through the high resistor/resistance of R_2. The capacitor discharge ceases up to moment t_3. Pulse of the increased duration, which has the triangular form (Fig. 11.1d), enters the amplifier, which works also in the mode of the limitation of amplitude.

Therefore from the output of amplifier is removed/taken the pulse of approximately rectangular form (Fig. 11.1e), which controls generator.

Duration of triangular pulse, measured on its foundation, linearly depends on duration of measured pulse. Proportionality factor depends on the relation of resistors/resistances R_1 and R_2, and also on the value of the voltage of the measured pulse and bias voltage E. The coefficient of expansion does not depend on capacitance value of capacitor/condenser C over a wide range. Capacitance value C is selected for the specific range of the duration of the measured pulse so that the charge of capacitor C would be realized according to the linear law. The linear law of the increase of voltage across capacitor C more easily is fulfilled for the pulses of short durations. For an increase in the range of durations of the measured pulses a change in capacitance value C can be provided. For an increase in the interval of the measured durations with constant/invariable capacitance value C inductance L, back-out resistor of R_1, can be used. The calculations of such a LRC-chain, utilized also for the linear scanning/sweep in the oscillographs, are given in § 10.3.

Usually expander relies on increase of duration of measured pulse 100 times and works in the range of change in initial durations to 10 times with divergence from linear law of expansion not more than 1-5%. For decreasing the error of measurement the frequency of the vibrations of controlled generator 2 must be sufficient high, since

electronic counter records each half-period of oscillations. In the measurement by such impulse-momentum method with the duration several of ten nanoseconds resultant error is approximately 5%.

Page 584.

M. I. Gryaznov proposed methods of measurement of amplitude and durations of nanosecond pulses, based on increase in duration of part or entire pulse, that make it possible to lower error of measurement for pulse duration up to units of nanoseconds [208, 209]. Fig. 11.2 gives the diagram, elucidating the method of measurement indicated and intended for measuring the amplitude of nanosecond pulses of the positive polarity (analogous diagram it can be constructed, also, for measuring the negative pulses). The expander of the apex/vertex of the measured pulse in combination with the compensative pulse voltmeter here is used.

When voltage of pulse exceeds compensating voltage across capacitor C_0, occurs charge of capacitor C through the resistor/resistance of open diode $R_д$, moreover $R_д \ll R$. Time constant of the charge

$$\tau_з = \tau_д (1 + C/C_д), \qquad (11.1)$$

where $\tau_д = C_д R_д$,

$C_д$ - the transfer capacitance of diode.

After termination of pulse capacitor/condenser is discharged through resistor/resistance R to capacitor/condenser C_0>>C up to

voltage U_0 with time constant $\tau_p = CR$. Fig. 11.3 gives the oscillogram of pulse at the output of expander.

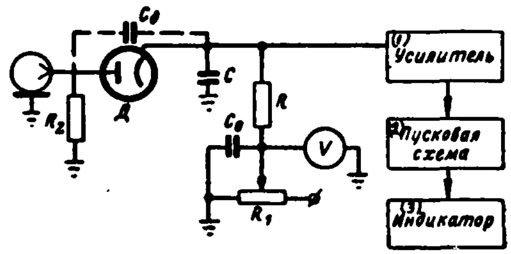

Fig. 11.2. Diagram for measuring amplitude of nanosecond pulses.

Key: (1). Amplifier. (2). Start-up circuit. (3). Indicator.

Page 585.

On resistor/resistance of R is formed the pulse of exponential form, whose amplitude U_p is proportional to the excess of the surge voltage above that compensating for and it is inversely proportional to the duration of the measured pulse (when $t_{и}<\tau_{з}$). This pulse is the expanded apex/vertex of the measured pulse. The bellying of the measured pulse is amplified and then this pulse enters the start-up circuit, starting it; functioning this diagram is recorded by indicator. Changing the value of the compensating voltage with the aid of potentiometer R_1 it is possible to draw nearer the compensating voltage the amplitude value of the measured pulse so that will be discontinued functioning start-up circuit. The value of the compensating voltage U_0, which corresponds to the threshold of functioning start-up circuit, is measured by voltmeter. The accuracy of measurements is rated/estimated by the relationship/ratio

$$\xi=1-\frac{U_0}{U}, \qquad (11.2)$$

where U - amplitude of measured pulse.

At moment of cessation/discontinuation of functioning start-up circuit occurs equality $U_п = KU_p$, where $U_п$ - voltage of threshold of functioning start-up circuit; K - amplifier gain. If values U and U_0 are constant, then with a decrease in the duration of pulses $(t_и < \tau_з)$ the amplitude of the bellying of pulse U_p decreases, which causes need (for guaranteeing the given value $U_п$) in the decrease of value U_0. However, the decrease of voltage U_0 according to (11.2) leads to an increase in the error of measurement.

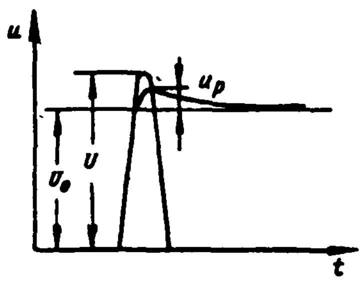

Fig. 11.3. Pulse at output of expander.

Page 586.

Therefore, with a decrease in the pulse duration, in order to decrease an error of measurement, it is necessary to increase factor of amplification K.

Thus, expansion of apex/vertex of measured pulse makes it possible to measure its amplitude for short pulse duration, since application of narrow-band amplifier becomes possible. However, the duration of the expanded pulse must be less than the pulse repetition period. This means that the passband of amplifier is determined only by the maximum repetition frequency of the measured pulses.

The expansion of pulse apex, furthermore, contributes to the elimination of effect of transfer capacitance of diode $C_д$, measured pulse through capacity/capacitance of diode (if $t_и \ll \tau_p$) evinced by straight/direct passage. The amplitude of this pulse is equal to

$$U_д = \frac{U}{1 + C/C_д} \quad (11.3)$$

and it does not depend on the compensating voltage. For eliminating the undesirable effect of straight/direct pulse advancing it is necessary that the amplification of this pulse would be insignificant, i.e., amplification factor would satisfy the inequality

$$K_д < \frac{U_и (1 + C/C_д)}{U}. \quad (11.4)$$

If this condition is not satisfied, then a false response of

start-up circuit appears. Since amplifier has narrow passband, the inequality (11.4) is fulfilled for the pulses of the nanosecond duration, when $t_и \ll \tau_p$. If necessary to measure the amplitudes of pulses, whose duration is more than τ_p, it is necessary to reduce amplification factor or to introduce the diagram of the compensation for straight/direct pulse advancing through the diode. Such diagrams, which include inverter cascade/stage or bridge circuit, complicate the construction/design of measuring meter.

As has already been indicated, in measurement of pulse amplitude with smallest duration of ($t_и \ll t_э$) for reduction in error of measurement it is necessary to increase factor of amplification K.

Page 587.

For the same purpose to desirably reduce time constant $\tau_з = \tau_д(1 + C/C_д)$, for which should be used the diodes with the minimum value of time constant $\tau_д = C_д R_д$. However, the selection of the low value of relation $C/C_д$ is undesirable, since this can lead to the unstable work of instrument and an increase in the error of measurement. It is necessary to note that with the estimation of error in the measurement of the pulse amplitude the value of the resistor/resistance of open diode $R_д$ is considered constant. However, the volt-ampere characteristic of diode, is especially in its initial part substantially nonlinear. Therefore the expressions given above are valid only in the measurement of pulses with the sufficiently large amplitude. A total error of measurement of the pulse amplitudes with

a duration of about 1 ns composes 1-5%, and for the pulse duration of more than 20 ns error compose a total of about 0.5% with the pulse amplitude of approximately 100 V.

Fig. 11.4 gives another diagram with expander of pulses [209], which makes it possible to measure pulse duration at its assigned level E. The here measured pulse enters the balance detector, assembled on the diodes and which is used for a preliminary increase in the pulse duration.

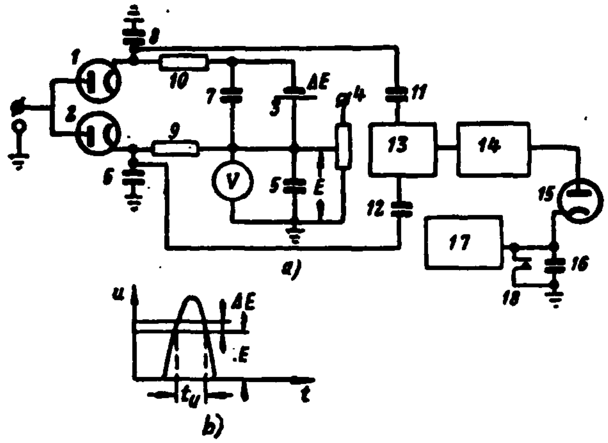

Fig. 11.4. Diagram for measuring pulse duration at assigned level (a), oscillogram of pulse (b).

Page 588.

The reference-voltage source 3 is included in one arm of the detector, and in the second arm reference voltage is created by the source, connected to terminals 4. When the voltage of the measured pulse exceeds voltage across capacitor 5, occurs charge of capacitor 6 through diode 2. However, in the case of the excess of the voltage of the pulse above total voltage across capacitors 5 and 7 the charge of capacitor 8 through diode 1 is realized. The capacitor discharge 6 through resistor/resistance to 9 occurs after the termination of pulse, while that of capacitor/condenser 8 - through resistor/resistance to 10. Thus, on resistances to 9 and 10 there are formed the expanded pulses of approximately triangular form, but with the different amplitude. These pulses through capacitors/condensers 11 and 12 enter subtraction scheme 13. The pulse, obtained as a

result of the subtraction of two pulses indicated, will have an amplitude, proportional to the duration of the measured pulse at the assigned level (fig. 11.4b). Differential pulse after amplifier 14 through diode 15 enters capacitor/condenser 16, which is connected with electrometric diagram 17. This diagram measures voltage across capacitor 16, which corresponds to the duration of the measured pulse at the assigned level. Key 18 serves for stress relieving from capacitor/condenser 16.

11.3. METHOD OF MEASURING THE PARAMETERS OF THE PULSES OF KNOWN FORM AND BY THE JETTY OF AMPLITUDE.

Methods of measurement of parameters of nanosecond pulses described above are suitable, if pulse amplitude is considerable, i.e. when its value exceeds value of nonlinear section of volt-ampere characteristic of diode. In the measurement of the parameters of the periodic pulses of a small amplitude stroboscopic methods can be used, whereas the measurements of single pulses with a small amplitude and the duration are very difficult.

M. I. Gryaznov proposed method of simultaneous measurement of amplitude and duration of nanosecond pulses of known form and small amplitude, based on use of two nonlinear elements with different volt-ampere characteristics [211, 212].

Page 589.

In the measurement of such pulses, which have the large porosity (more than 10^3), is realized the conversion of nanosecond pulses with the aid of the nonlinear circuit into the longer pulses, amplitude whose measurement is easy to carry out.

Simplest diagram of expander of pulses with nonlinear element is given in Fig. 11.5. During the action of the pulse of voltage u_1 occurs the charge (or the discharge in the dependence on the pulse polarity) of capacitor/condenser C. After the termination of pulse this capacitor/condenser is discharged (it is charged) to the initial voltage through resistor/resistance of R and internal resistor/resistance of nonlinear element. For pulse widening the proper relationship/ratio of the time of charge and capacitor discharge C is selected.

Let us examine dependence of amplitude of expanded pulse on parameters of measured pulse. For the majority of the nonlinear elements, utilized in the diagram of the expander of pulses, the volt-ampere characteristic is represented by the expression

$$i = F(u_1 - Du_2), \qquad (11.5)$$

where D - permeability of nonlinear element (in the case of diode D=1). Process in the diagram is described by nonlinear equation [212]

$$F[u_1(t) - Du_2(t)] = C\left[\frac{du_2(t)}{dt} + \frac{1}{RC}u_2(t)\right], \qquad (11.6)$$

where $u_1(t) = u_1 - u_{10}$; $u_2(t) = u_2 - u_{20}$; u_{10} and u_{20} - initial constant voltages on input and output of nonlinear element, its determining mode works.

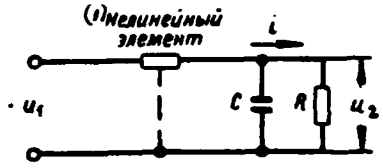

Fig. 11.5. Diagram of expander of pulses with nonlinear element.
Key: (1). Nonlinear element.

Page 590.

If the discharge time of capacitance C is considerably more than the duration of measured pulse $t_p \gg t_{\text{и}0}$ ($t_{\text{и}0}$ - the pulse duration, measured on its foundation), then

$$\frac{1}{RC}u_2(t) \ll \frac{du_2(t)}{dt},$$
$$Du_2(t) \ll u_1(t).$$

Then equation (11.6) takes form

$$F[u_1(t)] = C\frac{du_2(t)}{dt}, \qquad (11.7)$$

from which it is located amplitude of expanded pulse

$$U_2 = \frac{1}{C}\int_0^{t_{\text{и}0}} F[u_1(t)]\,dt. \qquad (11.8)$$

If expression of input pulse is recorded in the form

$$u_1(t) = Uq(t_0), \qquad (11.9)$$

where U - pulse amplitude; $q(t_0)$ - function of shape of pulse; $t_0 = t/t_{\text{и}}$; $t_{\text{и}}$ - pulse duration at certain level, then

$$U_{2}=\frac{t_{\text{и}}}{C}\int_{0}^{Q}F\,[Uq\,(t_{0})]\,dt_{0}, \qquad (11.10)$$

where $Q=\frac{T}{t_{\text{и}}}$ - porosity.

If we take $t_{\text{и}}=t_{\text{и0}}$, then

$$U_{2}=\frac{t_{\text{и0}}}{C}\int_{0}^{1}F\,[Uq(t_{0})]\,dt_{0}. \qquad (11.11)$$

Thus, amplitude of expanded pulse is linear function of duration and nonlinear function of amplitude of measured pulse.

Page 591.

If pulse is supplied to the input of two expanders with nonlinear elements, which have different characteristics $F_{a}(u)$ and $F_{b}(u)$, then at their outputs there will be those expanded of pulse with amplitudes of

$$U_{2a}=\frac{t_{\text{и}}}{C_{a}}\int_{0}^{Q}F_{a}\,[Uq\,(t_{0})]dt_{0},$$
$$U_{2b}=\frac{t_{\text{и}}}{C_{b}}\int_{0}^{Q}F_{b}\,[Uq\,(t_{0})]\,dt_{0}. \qquad (11.12)$$

Counting $C_{a}=C_{b}$, is examined relation

$$h_{q}\,(U)=\frac{U_{2a}}{U_{2b}}=\frac{\int_{0}^{Q}F_{a}\,[Uq(t_{0})]dt_{0}}{\int_{0}^{Q}F_{b}\,[Uq\,(t_{0})]dt_{0}}. \qquad (11.13)$$

This relation does not depend on pulse duration and is only function of amplitude of pulse U, assuming that shape of pulse is known. Obviously, $h_q(U) \neq \text{const}$, if functions $F_a(u)$ and $F_b(u)$ are linearly independent in the operating range of voltages/stresses.

Thus, determination of amplitude of pulses of known form is reduced to measurement of amplitudes of expanded pulses U_{2a} and U_{2b} and determination of their relations, and then on their relation and known dependence $h_q(U)$ for assigned shape of pulses is located their amplitude. Measuring device to more simply develop when is known not $h_q(U)$ for any given shape of pulse, but relation for the square pulses

$$h_r(U) = \frac{F_a(U)}{F_b(U)},$$

which proves to be simplest (here $q(t_0)=1$ with $0<t_0<1$ and $q(t_0)=0$ with $1<t_0<Q$). Then on this dependence and on the known shape of the measured pulse the result of measurements is recounted by simple method.

Page 592.

This conversion can be realized with the aid of the graph or simply with the aid of the calibrated dial faces, which records relation $h_r(U)$ for the different shapes of pulses.

It is possible to show [211, 212] which for graphing of translation is conveniently relation $h_q(U)$ represented in the form of

series/row according to degrees of value U with coefficients

$$K_n = \frac{\int_0^Q q^{n+1}(t_0)\,dt_0}{\int_0^Q q^n(t_0)\,dt_0}, \qquad (11.14)$$

which are determined exclusively by shape of pulse and are called factors of form of pulses of n order. In the general case the factors of the form of the pulses of the n order can be expressed through the factor of first-order form as functions $K_n(K_1)$. In this case for the most widely used forms of video pulses these functions differ little from each other.

Table 11.1 gives values of coefficient K_n for some shapes of pulses [211, 212].

When nonlinear element has volt-ampere characteristic, expressed by quadratic dependence, then above- indicated series/row has only one member with factor of form K_1. In this case the measurement of the pulse amplitude is reduced to the determination of the value of relation $h_q(U)$, and then according to graph/curve (Fig. 11.6) is determined value $K_1U=U_0$. Knowing pulse and, consequently, also K_1, it is possible to find U. Virtually it is expedient determine value $h_q(U)$ with the aid of the logometer. If the output meter of logometer is graduated directly in values $U_0=K_1U$, then it is possible to directly count off the amplitudes of measured pulses.

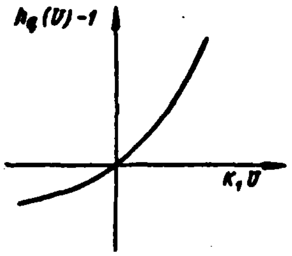

Fig. 11.6. Dependence of function $h_q(U)$ on K_1U.

Page 593.

Table 11.1.

(1) Название импульса	(2) Форма импульса	$q(t_0)$	K_1	K_n	(3) Уровень отсчета длительности	(4) Примечание
(5) Прямоугольный		$1;\ 0<t_0<1$ $0;\ 1<t_0<Q$	1	1		
(6) Трапецеидальный		$\frac{t_0}{a};\ 0<t_0<a$ $1;\ a<t_0<1$ $0;\ 1<t_0<Q$	$\frac{2}{3}\cdot\frac{3-2a}{2-a}$	$\frac{2}{n+2}\times$ $\times\frac{(n+2)(1-a)+a}{2-a}$	$\frac{1}{2}$	$a=\frac{t_ф+t_{cp}}{t_0}$ (7) a-1 для треугольной формы
(8) Прямоугольный со скошенной вершиной	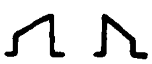	$a+(1-a)t_0;$ $0<t_0<1$ $0;\ 1<t_0<1$	$\frac{2}{3}\times$ $\times\left(a+\frac{1}{1+a}\right)$	$\frac{2}{n+2}\ \frac{1-a^{n+2}}{1-a^2}$		(9) a—относительная величина спада вершины
(10) Экспоненциальный		$e^{-t_0};\ 0<t_0<Q$	$\frac{1}{2}$	$\frac{1}{n+1}$	$\frac{1}{e}$	

Key: (1). Name of pulse. (2). Shape of pulse. (3). Reference level of duration. (4). Note. (5). Rectangular. (6). Trapezoidal. (7). a-1 for triangular form. (8). Rectangular with chamfered vertex. (9). a - relative value of decay in apex/vertex. (10). Exponential.

Page 594.

Continuation Table 11.1.

(1) Прямоугольный с экспоненциальным срезом		1; $0<t_0<1$; $e^{-a(t_0-1)}$; $1<t_0<Q$	$\frac{2a+1}{2(a+1)}$	$\frac{a(n+1)+1}{(a+1)(n+1)}$	$\frac{1}{e}$	$a=\frac{t_и}{\tau_{ср}}$ (2) ($\tau_{ср}$—постоянная времени среза)
(3) Треугольный с экспоненциальным срезом		$\frac{t_0}{a}$; $0<t_0<a$; e^{a-t_0}; $a<t_0<Q$	$\frac{2a+3}{(a+2)\cdot 3}$	$2\frac{a(n+1)+n+2}{(a+2)(n+1)(n+2)}$	(4) от $\frac{1}{3}$ до $\frac{1}{e}$	$a=\frac{t_ф}{\tau_{ср}}$
(5) Косинусоидальный		$\cos\frac{\pi t_0}{2}$; $0<t_0<1$; 0; $1<t_0<Q$	$\frac{\pi}{4}$	$K_2=\frac{2}{3}$	0,54	
(6) Косинусквадратный		$\cos^2\left(\frac{\pi t_0}{2}\right)$; $0<t_0<1$; 0; $1<t_0<Q$	$\frac{3}{4}$	$\frac{2}{2^{2(n+1)}}\binom{2n+2}{n+1}$	$\frac{1}{2}$	
(7) Колоколообразный		$e^{-t_0^2}$; $-Q<t_0<Q$	$\frac{1}{\sqrt{2}}$	$\frac{1}{\sqrt{n+1}}$	0,456	

Key: (1). Rectangular with the exponential shear/section. (2). ... time constant of section). (3). Triangular with exponential section. (4). from ... to .... (5). Cosinusoidal. (6). Cosine-squared. (7). Bell-shaped.

Page 595.

With the more complicated volt-ampere characteristics for determining the pulse amplitude besides coefficient of K_1 in the form of correction it is necessary to consider the factors of the form of higher order, expressed through coefficient of K_1. However, in the measurement of pulses with small amplitudes and in these cases with a sufficient degree of accuracy it is possible to use the graph/curve, analogous to that given in Fig. 11.6, or to calibrate the scale of

output meter directly in values U_0.

If pulse amplitude is measured, then according to (11.11) in value U_2 it is possible to determine pulse duration expedient to t_u. For measuring the pulse duration is more expedient to select this mode of nonlinear element, with which in working amplitude range of measured pulses his volt-ampere characteristic it would be possible to consider linear, i.e., F(u)=Su, where S - mutual conductance. Then instead of (11.11) it is possible to record

$$U_2 = \frac{t_u}{C} SU \int_0^Q q(t_0)\, dt_0$$

or the duration of the pulse

$$t_u = \frac{U_2 C}{SU \int_0^Q q(t_0)\, dt_0}. \qquad (11.15)$$

It is convenient to select reference level of pulse duration by such, in order to

$$\int_0^Q q(t_0)\, dt_0 = 1,$$

then pulse duration, measured under this condition,

$$t_u = \frac{U_2 C}{US}. \qquad (11.16)$$

It is virtually convenient at output of meter of value U_2 to place divider of voltage (potentiometer), with the aid of which in measured pulse amplitude it is possible to establish/install

coefficient of division, proportional 1/U.

Page 596.

Then readings/indications of meter (millivoltmeter) are proportional to the duration of pulse $t_{\text{и}}$ and, consequently, its scale can be graduated in the values of the pulse duration.

Described method of measuring of amplitude and duration of nanosecond pulses of small amplitude (less than 1 V can be used for measuring parameters both of periodically of repeating and single pulses. In the latter case for measuring the amplitude of expanded pulses, whose duration can be led to hundreds of microseconds, should be used the peak memory/memorizing pulse millivoltmeters.

The possibility of measuring parameters of single nanosecond pulses considerably raises value of method in question since similar measurements with the aid of high-speed/high-velocity oscillographs are very hindered/hampered, and - it is generally impossible with the aid of stroboscopic.

Accuracy of measurement of parameters of pulses with amplitude considerably smaller of 1 V, it is determined by selection of characteristic of nonlinear elements, by stability of mode and by accuracy of preliminary calibration of scales. In spite of the relative complexity of the method examined, can be obtained the satisfactory accuracy of the measurements of the parameters of the

nanosecond pulses, whose amplitude is approximately to two orders lower than permitted in the oscillographic measurements of pulses, especially single.

Method in the case of applying of three or more number of nonlinear elements indicated makes it possible to determine coefficients, which characterize form of video pulse [211, 212]. Thus, during the application of three nonlinear elements becomes possible the development of the instrument, which measures simultaneously three parameters of pulse.

11.4. MEASUREMENT OF THE PARAMETERS OF THE REPEATING PULSES BY THE METHOD OF COMPARISON.

For determining time parameters of repetitive pulses duration of order of tenths and units of nanoseconds into [213] proposed method of measurements, based on comparison of two identical pulses.

Page 597.

This method is similar to the stroboscopic method (see § 10.6), but here the role of strobe pulse fulfills the pulse being investigated, and at the output of meter instead of the image of the pulse being investigated is obtained the graph/curve, from which are determined the time parameters of pulse - the duration of front, shear/section and pulse apex.

Fig. 11.7a gives block diagram of meter. The pulse being investigated enters the coaxial splitter both through coaxial line 1, which has constant length and also through coaxial line 2, whose length can be regulated, it is supplied to the wide-band comparison circuit of 3. Voltage u_0 at the output of comparison circuit is noted by indicator 4. Changing the length of line 2, it is possible to note the different values of the output voltage u_0, which correspond to selected time difference of the delay τ of the second line relative to the first. From the obtained graph/curve $u_0=f(\tau)$ are determined the parameters of pulse. In Fig. 11.7b is given comparison circuit. After coaxial splitter identical pulses enter the diagrams (points b and c).

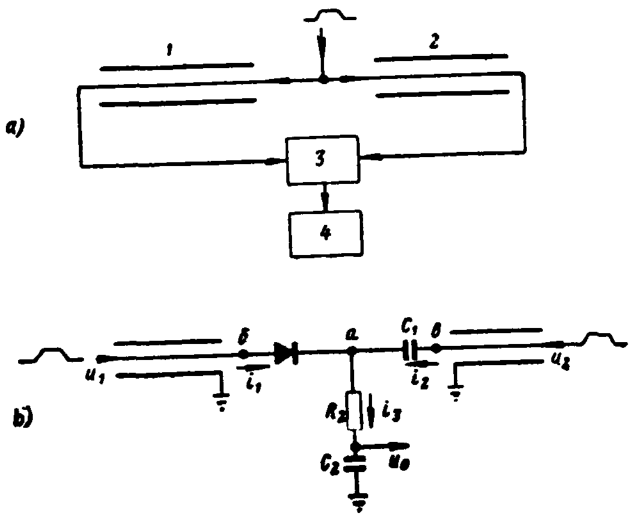

Fig. 11.7. Block diagram of installation for measuring duration of pulses (a), comparison circuit (b).

Page 598.

The coaxial line, connected to point c, has a variable length. Comparison circuit consists of a high-frequency diode, resistor/resistance R_2 and capacities/capacitances of C_1 and C_2.

Let us examine case of trapezoidal shape of measured pulse. Fig. 11.8 gives the oscillograms of pulse u_1, which enters point b pulse u_2, which enters the point that delaying to the period τ relative to pulse u_1. At point a of diagram voltage u_a is created. Depending on the instantaneous values of pulses u_1 and u_2 the diode proves to be in the state of straight/direct or reverse/inverse conductivity. Fig. 11.9 gives the equivalent diagrams, which correspond to the comparison circuit in the case of the straight/direct (Fig. 11.9a) and

reverse/inverse (Fig. 11.9b) conductivities of diode. Here φ - the line characteristic, R_1 and R_3 - respectively the resistor/resistance of diode with the straight/direct and reverse/inverse conductivity. Since resistor/resistance R_2 is considerably more than resistors/resistances of R_1 and R_3, then current i_3 is less than currents i_1 and i_2. Determining first voltage at point a, equal to u_a, then it is possible to find voltage on capacity/capacitance of C_2, i.e. the output voltage u_0. If the volt-ampere characteristic of diode is approximated by piecewise-linear function, then for voltage u_a it is possible to obtain [213] following expressions:

$$u_a \approx 2u_1 - \frac{2(R_1+\rho)}{R_1+2\rho}(u_1-u_2) \overset{(1)}{\text{при}}\ t \leqslant (t_1+\tau) \quad (11.17)$$

Key: (1). with

and

$$u_a \approx 2u_2 - u_{C_1}(t_1+\tau)\, e^{-\frac{t}{(R_3+2\rho)C}} \overset{(1)}{\text{при}}\ t > (t_1+\tau). \quad (11.18)$$

Key: (1). with.

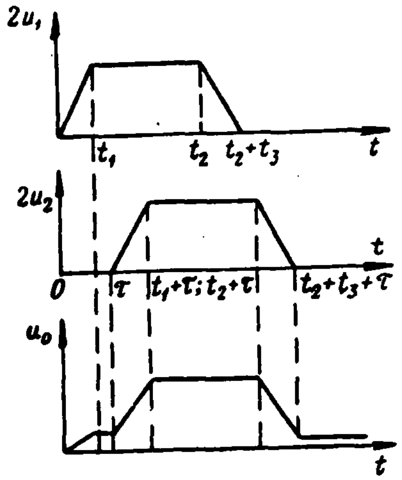

Fig. 11.8. Oscillograms of pulses in comparison circuit.

Page 599.

Amplitude of output potential of comparison circuit is determined from formula

$$U_{0}=\frac{1}{R_{1}C_{2}}\int_{0}^{\infty}u_{a}dt. \qquad (11.19)$$

Knowing value of voltage U_0 for different values of delay time τ, it is possible to construct graph/curve $U_0=f(\tau)$. In the case of the linear approximation of the characteristic of diode from this graph/curve it is possible to find two characteristics of the pulse: the sum of the durations of front and the shear/section of pulse and the duration of flat/plane pulse apex (Fig. 11.10a).

If we consider that with direct conductivity of diode its volt-ampere characteristic is approximated by square-law characteristic, and with reverse conductivity - by the linear function, then it is possible to determine by the method indicated three time parameters of pulse. For the interval of time $t>(t_1+\tau)$ occurs the reverse/inverse conductivity of diode and voltage u_a is determined by expression (11.18). With $0<t<(t_1+\tau)$ voltage u_a is nonlinear function from u_1, u_2, t_1 and τ and can be determined by graphic method. Designed thus dependence $U_0+f(\tau)$ is represented in the form of graph/curve in Fig. 11.10b.

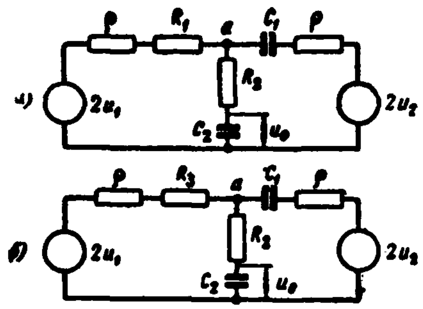

Fig. 11.9. Equivalent diagrams which correspond to comparison circuit in the case of direct conductivity of diode (a), reverse/inverse conductivity of diode (b).

Page 600.

With the aid of this graph/curve are determined three time parameters of pulse - the duration of front, shear/section and flat/plane pulse apex.

In measurement of parameters of pulse error will be the less, the more precise carried out precomputation by curve $U_0=f(\tau)$ for this type of diode and the wider-band comparison circuit, which is fulfilled in the form of coaxial system similarly to converter in stroboscopic oscillograph. For various forms of the pulses being investigated it is necessary to previously have calculated graph/diagrams of dependence $U_0=f(\tau)$. Experimental investigations show that it is possible to construct a comparison circuits with the passband of approximately 5 GHz and to carry out measurements of pulses with the front with duration on the order 0.1 ns [213].

Method of determining parameters of pulses with self-strobing can be different [214]. Let the diode which operates in the comparison circuit have the quadratic volt-ampere characteristic $i=ku^2$. Both pulses enter directly the diode indicated. Depending on delay factor of the pulse, which passes variable delay line, overlapping of the pulses, which come the diode, will be different (Fig. 11.11), therefore, will be different and output potential of comparison circuit

$$u(t)=k[u_1^2(t)+u_2^2(t)+2u_1(t)u_2(t)].$$

Value of the product $u_1(t)u_2(t)$ can give information about parameters of pulse being investigated.

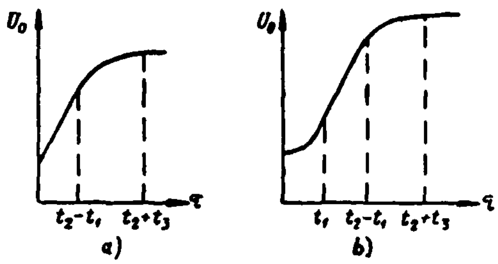

Fig. 11.10. Dependence $U_0=f(\tau)$: a) for case of linear characteristic of diode; b) for case of square-law characteristic of diode.

Page 601.

If pulses do not overlap, then this product will be equal to zero. Let us examine expression for the value of impulse flashing over of trapezoidal form and rate of change in this overlap as the functions of relative pulse delay τ. Using the designations of Fig. 11.11 we have in the interval of delay $0<\tau<(t_ф+t_{cp})$ a height/altitude

$$h=\tau\frac{\sin\alpha\sin\beta}{\sin(\alpha+\beta)}=\frac{\tau}{\operatorname{ctg}\alpha+\operatorname{ctg}\beta}=\frac{\tau U}{t_ф+t_{cp}}.$$

Area of impulse flashing over

$$S=\frac{\tau h}{2}=\frac{\tau^2 U}{2(t_ф+t_{cp})}.$$

Rate of change in area of overlap

$$\frac{dS}{d\tau}=\frac{U\tau}{t_ф+t_{cp}}.$$

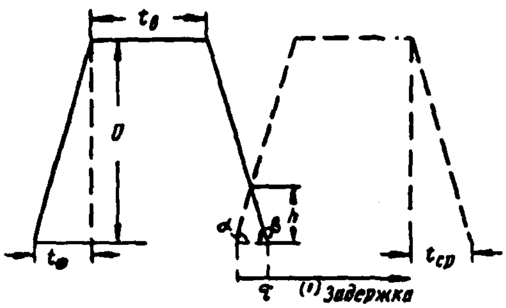

Fig. 11.11. Graphs of pulse overlap with self-strobing.
Key: (1). Delay.

Page 602.

Analogously for interval of delay $(t_{\Phi}+t_{cp})<\tau<(t_{\Phi}+t_{cp}+t_{B})$ we will obtain $dS/d\tau=U$; for interval of delay $(t_{\Phi}+t_{B}+t_{cp})<\tau<(t_{\Phi}+2t_{B}+t_{cp})$ we have $dS/d\tau=-U$; for interval of delay $(t_{\Phi}+t_{cp}+2t_{B})<\tau<(2t_{\Phi}+2t_{B}+2t_{cp})$ this rate of change $\frac{dS}{d\tau}=-\frac{U\tau}{t_{\Phi}+t_{cp}}$,

where t_{Φ}, t_{cp}, t_{B} - respectively duration of front, shear/section and flat/plane pulse apex; U - amplitude of voltage.

For different intervals of the variation of delay factor τ dependence of area S on τ is differently and represented either by parabolic or linear function with different inclination/slope. Observing slope deviation the crown of curve for different intervals of delay τ it is possible to obtain information about the sum of the durations of front and shear/section $(t_{\Phi}+t_{cp})$, the corresponding to parabolic section curve, about the duration of pulse apex t_{B}, by the corresponding to linear section curve, and about amplitude U, which

corresponds to the slope of the linear section of curve. The obtained relationships/ratios are valid for the quadratic dependence of the volt-ampere characteristic of diode, which occurs with the work with the low value of signal.

In contrast to stroboscopic method of oscillography, where time resolution is determined not only by broad-band character of converter, but in essence with gate length, here plays role only broad-band character of comparison circuit. Furthermore, in the measurements by the method examined there is practically eliminated the effect of the factor of the instability of the temporary situation of the gate pulse of that of relatively investigated.

11.5. Dividers of the voltage of nanosecond pulses.

During the investigation of nanosecond pulses of high voltage and in measurement of their parameters voltage dividers frequently are utilized, since in majority of cases high-speed oscillographs, pulse voltmeters and other instruments of nanosecond range are not designed for work with high voltage.

The fundamental requirement for different attenuators, which are utilized in nanosecond range of durations, is the requirement of considerable broad-band character. Therefore, such devices are built mainly in the form of systems with distributed parameters.

Page 603.

When the required passband does not exceed hundreds of megahertz, there can be utilized dividers in the form of circuits with the lumped parameters. Dividers with the lumped parameters are capacitive or from the effective resistance. Capacitive voltage- dividers must be arranged/located directly about termination in order to avoid the stray inductances of coupling conductors. The transmission of pulse from the output of divider to the load with the aid of the cable is here excluded due to the impossibility of the agreement of capacitive voltage-divider with the wave impedance of cable. During the proper construction/design of capacitive voltage-divider with its aid it is possible to divide the voltage of pulses with a minimum duration of front of up to 0.5-1 ns.

So that dividers from effective resistance would not have noticeable parasite inductances and capacitances, the effective resistances are fulfilled in the form of special carbonic coatings, applied to ceramic rods, cylinders or washer. The resistor/resistance of the high-voltage arm of divider does not usually exceed 1 kilohms, since with the high value of resistor/resistance there is manifested the shunting effect of longitudinal capacity/capacitance. However, the resistance of the output arm of divider there must not be too little, otherwise is manifested the effect of stray inductance. The output arm of divider from the effective resistance can be coordinated with the wave impedance of the cable, utilized sometimes for the transmission of pulse from the divider to the load. Dividers from the

effective resistance sometimes are placed into the coaxial systems. Thus, during the use T - the figurative circuit of divider is obtained the simple construction/design of the divider of the voltage, which has the low parasitic parameters (Fig. 11.12) [215]. Central rod from the ceramics is located within the cylindrical external conductor. As resistor units R_1 (sequential branch of divider) there are used the resistors/resistances from the carbonic coatings on the ceramic stream, while as the element of resistor R_2 (parallel branch of divider) - layer, applied to the ceramic disk, which has contact with the central rod and the external conductor. Carbonic layer will be deposited to one side of disk in order to avoid supplementary stray capacitance. For eliminating eddy-current effect on the value of resistor/resistance at different frequencies the thickness of carbonic layer is taken by very small.

Page 604.

Divider of this construction/design can be used for work with pulses, duration of front of which approximately one nanosecond.

As dividers of voltage of nanosecond pulses find use dividers, which are simultaneously load resistors/resistances usable in technology of superhigh frequencies.

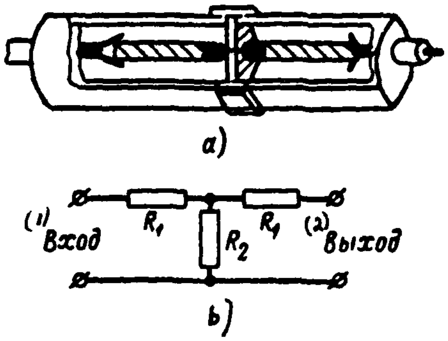

Fig. 11.12. Diagrammatic representation of construction/design of divider of voltage (a), schematic of divider (b).

Key: (1). Input. (2). Output.

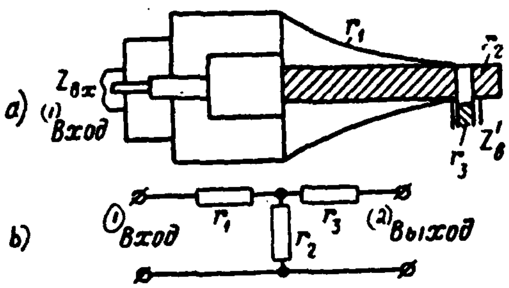

Fig. 11.13. Diagrammatic representation of construction/design of divider of type NS-1 (a), diagram of divider (b).

Key: (1). Input. (2). Output.

Page 605.

Thus, for instance, utilized are series load resistors/resistances, which are simultaneously dividers, of the type SN-1, ESN-100, designed for different power with the coefficients of the division of voltage 10 and 25, and also other dividers. Fig. 11.13 gives diagrammatic representation of the construction/design of a divider of the type

NS-1. Here cylindrical resistor/resistance of the type of UNU is made in the form of carbon coating, applied onto a ceramic rod. Resistor/resistance is placed into aluminum shield of the variable/alternating section, whose diameter changes exponentially. Stepped transition/junction provides the matching of input resistance of divider with coaxial cable (of type RK-75-4-15), which has the wave impedance of 75 ohms. In the design the removal/outlet of divider, designed for the weakening 20 dB at the power to 10 W, is provided. Output resistance of the divider of 75 ohms. The broad-band character of divider is affected the quality of transitions/junctions and on properties of carbonic coating. The latter has a layer, whose thickness is small, and it is possible to disregard the effect of surface effect to the frequencies, which exceed 1 GHz. Such dividers can be utilized with the work with the pulses, which have the duration of front of approximately 0.5 ns and more.

Fig. 11.14 depicts divider in the form of distributed system, developed by Fletcher [216]. At the base of divider lies/rests the simplest dividing circuit (Fig. 11.14a), where consecutive and parallel resistor elements R_1 and R_2 are formed by the input resistances of two concentrically arranged/located coaxial lines (Fig. 11.14b). Internal line with a wave impedance of 5 ohms (resistor/resistance R_1) has polyethylene insulation. In the external line as the insulation is used rutile (TiO_2), whose relative dielectric permeability is equal to 85 and does not depend on frequency up to 30 GHz. The internal and external surface of rutile is covered with silver.

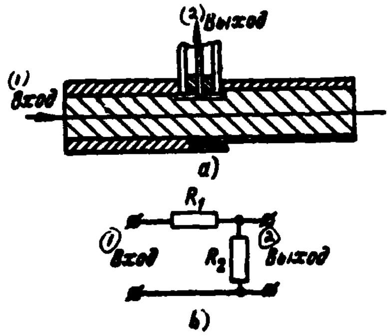

Fig. 11.14. Diagrammatic representation of coaxial divider of voltage (a), schematic of divider (b).

Key: (1). Input. (2). Output.

Page 606.

The wave impedance of the second line (resistor/resistance R_2) is equal to 0.5 ohms. Thus, the coefficient of the division of voltage is equal to 100. The output removal/outlet of divider is taken from the internal conductor of the second line through the opening/aperture in the ceramics. Tapping point is selected so that the corresponding sections of line would be agreed on. The distortions of pulse during its division do not exceed 10% for the duration of front 0.3-0.4 ns.

When continuously variable control of coefficient of division is required, can be used construction/design of divider, carried out in the form of non-uniform circuit of transmission, whose length of center conductor is regulated. With a change in the length of center conductor the resistor/resistance of one branch of divider changes, and consequently, changes the coefficient of division. However, it is

necessary to bear in mind, that during the transmission of pulses along non-uniform circuit appear some distortions of pulse, as this follows from the examination of the transient responses of non-uniforms circuit of transmission (S 1.8).

11.6. Measurement of the pulse responses of the transmission lines.

In measurement of parameters of nanosecond pulses high value has quality of lines of transmission of measuring circuit. The transmission lines must not distort the pulses, applied to the input of the measuring instrument or transmitted from one unit of measuring device to another. Transmission lines must be sufficiently wide-band and not have noticeable heterogeneities.

During transmission of pulses of nanosecond duration it is frequently indicated that the time of propagation of the pulse along the line is considerably longer than its duration. The presence of heterogeneities in the line causes appearance of the echo pulses, which are propagated in the form of incidental and counterflows.

Page 607.

However, in the form of the short duration of main impulses and with their considerable porosity the echo pulses do not introduce such noticeable distortions of fundamental pulses, as this could be with the longer pulses or in the case of the transmission of continuous oscillations. Therefore during the transmission of nanosecond pulses

the evaluation/estimate of the quality of the transmission lines according to their frequency characteristics, taken/removed in steady state, can be erroneous. Instead of the widespread in the technology of shf method of the evaluation/estimate of lines with the aid of the standing-wave ratio, measured in steady state, for the nanosecond pulse technique is frequently desirable the measurement of the transient or pulse responses of lines. The latter, in particular, make it possible to reveal and to rate/estimate the heterogeneities, available in the transmission line.

Thus, for evaluation/estimate of heterogeneities in two-wire circuits and waveguides already sufficiently widely is used method of measurements with the aid of pulses of very short duration, based on principle of radar [217-220]. Fig. 11.15 gives the block diagram of the measuring device, intended for the evaluation/estimate of heterogeneities and removal/taking of the pulse responses of line. The master oscillator 1 shapes the trigger pulse, which enters the generator of sounding pulses 2, and also shapes the calibration pulse, which enters pulse oscillograph 6 through a certain time interval, whose value is regulated. The generator of sounding pulses forms/shapes either video pulses or radio pulses in the dependence on the type of the circuit (cable or waveguide) being investigated and its designation/purpose. Sounding pulses very by the jetty of duration and the pulses, reflected from the heterogeneities of measured line 3, come detector 4 and after it to the attenuator or amplifier 5 oscillograph.

All these pulses are observed on the oscillograph and intervals between them are measured with the aid of calibration device/equipment.

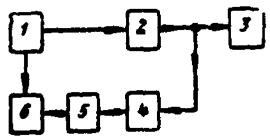

Fig. 11.15. Block diagram of device/equipment for measuring heterogeneities of the channel of transmission of pulses.

Page 608.

Realizing preliminary calibration of the circuit of the signal of oscillograph, it is possible to measure the voltage of the echo pulses and to rate/estimate the value of heterogeneities along the line being investigated. Depending on the required resolution of instrument as the sounding pulse are utilized the pulses by a duration from fractions of a microsecond to fractions of a nanosecond. During the selection of the duration of sounding pulse is considered both the necessary time resolution and the reliability of the determination of the coefficient of reflection of waves from the heterogeneities. Therefore, a certain optimum value of the duration of sounding pulses [158] is selected.

During investigation of waveguides, furthermore, it is necessary to consider optimum value of pulse duration in connection with increase in duration of radio pulses during their propagation on waveguide due to dispersion, whose effect on increase in pulse duration depends on length of waveguide being investigated (see § 1.7). For rectangular waveguides the optimal duration of the sounding

radio pulse is within the limits of 2-5 ns.

During investigation of nanosecond pulses by means of an oscillograph, which contains a tube with a deflecting system of type of traveling wave (TBV), it is very desirable to know characteristics of tube and, in particular, value of heterogeneities at the input and output of the deflection system and along its spiral. Such measurements can be carried out according to the method in question. If we in the measuring unit use the stroboscopic unit, which makes it possible within large limits to change the value of the amplification of pulses after their conversion, then the sensitivity of entire installation considerably increases. Therefore it proves to be possible with a sufficient degree of accuracy to investigate the heterogeneities of the deflection system of the TBV and, consequently, also to estimate its pulse response.

Fig. 11.16 gives simplified block diagram of installation, intended for investigation of circuits of travelling-wave tube and TBV [221]. The unit of pulse generator 1 forms/shapes the sounding radio pulses, which enter the TBV 2 being investigated, and it also shapes the synchronizing pulses, which pass to the generator of strobe pulses 3.

Page 609.

The pulses, reflected from the heterogeneities of the tube being investigated, with the aid of directional coupler 4 are

separated/liberated from launched pulse and are fed to the converter 5 of the stroboscopic unit, to which simultaneously come the strobe pulses. After amplification with the aid of the travelling-wave tube 6 converted radio pulses enter detector 7. After detector the pulses through low-frequency filter 8 fall on usual oscillograph 9, which has amplifier in the circuit of signal. The spacings between pulses are measured on the oscillograph and their amplitude is determined. After this, the pulse response can be constructed.

There is great interest in the possibility with the aid of method in question to determine the nature of heterogeneities in the line, and to also measure the value of wave impedance along the line [220]. The application of a stroboscopic oscillograph for indication and measuring the pulses allows in the series/row with the sounding pulse to measure the echo pulses of a small amplitude. The ratio of the amplitudes of the sounding and reflected pulse can be 1000, and the measured distances between the heterogeneities in the cable can be the order of centimeters.

For determining the nature of the reactance, created in line by heterogeneity, a comparison of signals reflected from investigated and known heterogeneities is conducted. Fig. 11.17 shows the oscillograms of the signals, reflected from the purely inductive (a), capacitive (b) and active (c) heterogeneities [220].

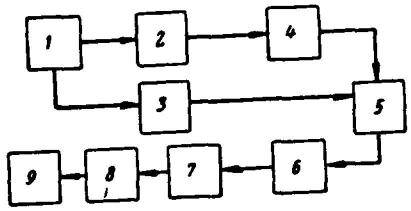

Fig. 11.16. Block diagram of installation for investigation of delaying systems.

Page 610.

When heterogeneity is effective resistance, it is possible to take its measurement with an accuracy to hundredths of an ohm. For this instrument it is calibrated on the standard resistance.

With the aid of such instrument, duration of sounding pulse of which is equal to 0.5 ns, were investigated coaxial cables, heterogeneities were determined and change in wave impedance of cable along its length was measured. This made it possible to coordinate the electrical length of the cable with an accuracy to several millimeters.

Further improvement of described methods of characteristic measurement of lines of transmission and wide-band deflection systems of oscilloscope tubes will make it possible to improve evaluation/estimate of the quality of the systems and, thus, to ensure proper checking during development of new pulsers of nanosecond range.

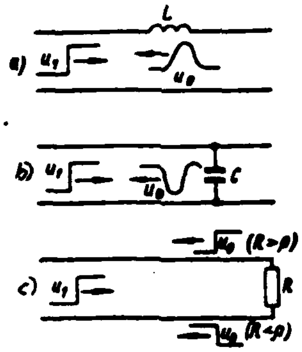

Fig. 11.17. Oscillograms of input and echo pulses during a study of a line with heterogeneity of inductive (a), capacitive (b) and active (c) character.

DOC = 88076735

Page 1009

REFERENCES.

1. Ицхоки Я. С Импульсные устройства. Изд-во «Советское радио», 1959.

2. Меерович Л. А., Зеличенко Л. Г. Импульсная техника. Изд-во «Советское радио», 1953.

3. Глебович Г. В., Моругин Л. А. Формирование импульсов наносекундной длительности. Изд-во «Советское радио», 1958.

4. Белоруссов Н. И., Гроднев И. И. Радиочастотные кабели Госэнергоиздат, 1959.

5. Глебович Г. В. Переходные характеристики коаксиальных кабелей с учетом потерь в проводниках и диэлектрике. «Электросвязь», 1961, т. 15, № 5, стр. 73.

6. Жекулин Л. А. Неустановившиеся процессы в коаксиальном кабеле «Известия АН СССР» ОТН, 1946, № 9, стр. 1243.

7. Солодовников В. В., Топчиев Ю. И. и Крутиков Г. В. Частотный метод построения переходных процессов с приложением таблиц и номограмм. Гостехиздат, 1955.

8. Глебович Г. В. Переходные процессы в однородных линиях передачи импульсов «Труды Горьковского политехнического института». 1964, т. 20, вып. 2.

9. Глебович Г. В. Искажения наносекундных импульсов при прохождении по коаксиальному кабелю. «Радиотехника», 1963, т. 18, № 10, стр. 54.

10. Глебович Г. В. Переходные процессы в распределенных системах при передаче и формировании наносекундных импульсов. «Известия вузов». Радиотехника, 1964, т. 6, № 1, стр. 42.

11. Nahman N. S., Gooch G. M. Proc. IRE, 1960, v. 48, № 11, p. 1852.

12. Cohn S. B. Trans. IRE, v. MTT-2, 1954, № 2, p. 52.

13. Глебович Г. В. Переходные характеристики полосковых линий передачи. «Радиотехника и электроника», 1963, т. 8, № 2, стр. 337.

14. Whinnery J. R., Jameison H. W. Proc. IRE, 1944, v. 32, № 1, p. 98.

15. Whinnery J. R., Jameison H. W., Robbins T. E. Proc. IRE, 1944, v. 32, № 9, p. 695.

16. Seitzer D. Arch. El. Übertragung, 1961, B. 15, № 7, S. 303.

17. Лошаков Л. Н., Ольдерогге Е. В. К теории коаксиальной спиральной линии. «Радиотехника», 1948, т. 2, № 3, стр. 11.

Doc =88076735

page 1010

18. Blewett J., Rubel J. Proc. IRE, 1947, v. 35, № 12, p. 1580

19. Lewis I. Proc. IEE, 1951, v. 98, pt. III, p. 312.

20. Kallmann H. Proc. IRE, 1946, v. 34, № 9, p. 646.

21. Ditoro M. Conv. Rec. IRE, Circ. Theory, 1953, pt. 5, p. 64.

22. Белозеров Ю. С. Экспериментальное исследование спирального трансформатора импульсов наносекундной длительности. «Известия вузов», Радиотехника, 1962, т. 5, № 1, стр. 58.

23. Белозеров Ю. С. Искажения радиоимпульсов в спиральной линии задержки. «Радиотехника и электроника», 1964, № 2, стр. 234.

24. Karbowiak A. E. Proc. IEE, 1957, v. 104, pt. C(6), p. 339.

25. Forrer M. P. Proc. IRE, 1958, v. 46, XI, № 11, p. 1830.

26. Ильин В. А. Длинные линии с изменяющимися по длине параметрами. «Электричество», 1950, № 2, стр. 42.

27. Фельдштейн А. Л. Неоднородные линии. «Радиотехника», 1951, т. 6, № 5, стр. 38

28. Литвиненко О. Н., Сошников В. И. Принцип построения формирующих схем с неоднородными линиями. «Радиотехника и электроника», 1959, т. 4, № 2, стр. 1448

29. Нейман М. С. Экспоненциальная линия «Известия электропромышленности слабого тока», 1938, № 4, стр. 420.

30. Литвиненко О. Н. Синтез неоднородных линий по входному сопротивлению, заданному в виде дробно-рациональной функции частоты. «Радиотехника и электроника», 1961, т. 6, № 11, стр. 1825.

31. Stapelfelds R., Joung F. Trans. IRE, 1961, MTT-9, № 1, p. 290

32. Нейман М. С. Автоматические процессы и явления. Изд-во «Советское радио», 1958

33. Харкевич А. А. Теоретические основы радиосвязи. Гостехиздат, 1957.

34. Евтянов С. И. Переходные процессы в приемно-усилительных схемах. Связьиздат, 1948

35. Seitzer D. Archiv Elektr. Übertragung, 1962, B. 16, № 6, S. 263

36. Ицхоки Я. С. Импульсная техника. Изд-во «Советское радио», 1949

37. Kukel J., Williams E. Conv. Rec. IRE, 1953, C. T. p. 81.

38. Хиршман И. И., Уиддер Д. В. Преобразование типа свертки. Изд-во иностранной литературы, 1958

39. Parker I. J. Conv. Rec. IRE., 1955, pt. 5, p. 142.

40. Lewis I. A., Wells F. H. Millimicrosecond Pulse Techniques. Perg. Press London, 1959

41. Колотов О. С., Лабанов Ю. Н., Шильберский З. Генератор наносекундных импульсов с плавной регулировкой длительности. «*Приборы и техника эксперимента*», 1961, № 3, стр. 87

42. Winnigstad G. N. IRE Trans. N. S., 1959, № 3, p. 26.

43. Введенский Ю. В. Генератор наносекундных импульсов. Авторское свидетельство № 122823, 1959.

Doc=88076735 Page 1011

44. Введенский Ю. В. Тиратронный генератор наносекундных импульсов с универсальным выходом. «Известия вузов», Радиотехника, 1959, т. 2, № 2, стр. 249.
45. Литвиненко О. Н., Сошников В. Н. Расчет формирующих линий. Гостехиздат УССР, Киев, 1962.
46. Wheler H. Proc. IRE, 1939, v. 27, № 1, p. 65.
47. Schatz E., Williams E. Proc. IRE, 1950, v. 38, № 12, p. 1208.
48. Грановский В. Л., Деионизация разряженного газа. «Труды ВЭИ», Электронные приборы, 1941, стр. 98.
49. Драбкин Д. С., Слуцкин Е. Х. Разработка методики определения деионизационных параметров и предельной частоты работы тиратронов в импульсном режиме. Сборник материалов по вакуумной технике, вып. 5. Госэнергоиздат, 1954.
50. Ворончев Т. А. Импульсные тиратроны. Изд-во «Советское радио», 1958.
51. Глебович Г. В., Грязнов М. И., Птицын К. Н. Исследование некоторых схем формирования коротких импульсов. «Радиотехника и электроника», 1958, № 4, стр. 562.
52. Горячев Л. В. Некоторые вопросы формирования наносекундных импульсов в тиратронных схемах. «Труды Горьковского политехнического института»; 1964, т. 20, вып. 2.
53. Глебович Г. В. Тиратронный генератор наносекундных импульсов с применением магнитного поля. «Известия вузов», Радиотехника, 1959, т. 2, № 1, стр. 111.
54. Птицын К. Н., Грязнов М. И. Некоторые вопросы генерирования коротких импульсов в схемах с тиратронами. «Труды Горьковского политехнического института», 1957, т. 13, вып. 1, стр. 84.
55. Витенберг М. И. Расчет электромагнитных реле для аппаратуры автоматики и связи. Госэнергоиздат, 1956.
56. Brown J., Pollard C. Electrical Eng., 1947, v. 66, № 11, p. 1106.
57. Селезнев П. С., Тюльников Л. Н., Моисеев А. В. Авторское свидетельство № 107469, 1956.
58. Тюльников Л. Н., Генератор импульсов. Авторское свидетельство № 126919, «Бюллетень изобретений», 1960, № 6.
59. McQueen J. Electronic Eng., 1959, v. 24, № 296, p. 436.
60. Прозоровский Ю. Н. Генератор треугольных импульсов. «Радиотехника», 1958, т. 13, № 9, стр. 47.
61. Стекольников И. С. О работе трехэлектродного реле. «Бюллетень ВЭИ», 1935, № 2.
62. Fletcher R. Phys. Rev., 1949, v. 76, № 12, p. 1501.
63. Rompe R., Weizel W. Ztschr. Phys., 1944, № 1, S. 122.
64. Месяц Г. А., Усов Ю. П. Влияние давления в искровом промежутке разрядника на параметры фронта высоковольтного импульса. «Известия вузов», Энергетика, 1961, т. 4, № 12, стр. 68.
65. Воробьев Г. А., Месяц Г. А. Техника формирования высоковольтных наносекундных импульсов. Госатомиздат, 1963.
66. Воробьев А. А., Воробьев Г. А., Месяц Г. А., Голынский А. И. Генератор высоковольтных импульсов наносекунд-

Doc=88076735 Page 1012

ной длительности. «Приборы и техника эксперимента», 1962, т. 7, № 1, стр. 96.

67. Fletcher R. Rev. Scient. Instrum., 1949, v. 20, № 12, p. 861.

68. Аделендер В. Л., Ильин О. Г., Шендерович А. М. Формирование импульсов тока регулируемой длительности. «Приборы и техника эксперимента», 1962, т. 7, № 3, стр. 81.

69. Катаев И. Г. Устройство для формирования импульсов с крутым фронтом. Авторское свидетельство № 118859, 1958.

70. Гапонов А. В., Фрейдман Г. И., Об ударных электромагнитных волнах в ферритах. ЖЭТФ, 1959, т. 36, № 3, стр. 957.

71. Гапонов А. В, Фрейдман Г. И. К теории ударных электромагнитных волн в нелинейных средах. «Известия вузов», Радиофизика, 1960, т. 3, № 1, стр. 79.

72. Катаев И. Г. Ударные электромагнитные волны. Изд-во «Советское радио», 1963.

73. Островский Л. А. Образование и развитие ударных электромагнитных волн в линиях передачи с ненасыщенным ферритом. ЖТФ, 1963, т. 33, № 9, стр. 1080.

74. Богатырев Ю. К. Стационарные волны в нелинейной дискретной линии передачи. «Известия вузов», Радиофизика, 1961, т. 4, № 4, стр. 680.

75 Богатырев Ю. К. Ударные электромагнитные волны в нелинейной линии с сосредоточенными параметрами. «Известия вузов», Радиофизика, 1962, т. 5, № 6, стр. 1130.

76. Белянцев А. М., Богатырев Ю. К. Формирование ударных электромагнитных волн с двумя разрывами. «Известия вузов». Радиофизика, 1962, т. 5, № 1, стр. 116.

77. Хохлов Р. В. К теории ударных радиоволн в нелинейных линиях. «Радиотехника и электроника», 1961, т. 6, № 6, стр. 917.

78. Белянцев А. М., Богатырев Ю. К., Соловьева Л. И Формирование ударных электромагнитных волн в линиях передачи с ненасыщенным ферритом. «Известия вузов», Радиофизика, 1963, т. 6, № 3, стр. 551.

79. Белянцев А. М., Богатырев Ю. К, Соловьева Л. И. Стационарные ударные электромагнитные волны в линиях передачи с ненасыщенным ферритом. «Известия вузов», Радиофизика, 1963, т. 6, № 3, стр. 561.

80. Белянцев А. М., Богатырев Ю. К. Расчет нелинейных формирующих линий. «Известия вузов», Радиотехника (в печати).

81. Богатырев Ю. К. Расчет нелинейной формирующей линии с сосредоточенными параметрами. «Известия вузов», Радиотехника (в печати).

82. Шамаев Ю. М., Пирогов А. И., Лисицын Г. Ф. Методика и результаты экспериментального исследования динамических характеристик импульсного перемагничивания ферритов. В сб. статей «Ферриты». Изд-во АН БССР, 1959, стр. 409.

83. Белянцев А. М., Островский Л. А. Распространение импульсов в линиях передачи с полупроводниковыми диодами. «Известия вузов», Радиофизика, 1962, т. 5, № 1, стр. 183.

84. Андронов А. А, Витт А. А., Хайкин С. Э. Теория колебаний. Физматгиз, 1959.

DOC=88076735 Page 1013

85. Лукин В. Ф. Переходные процессы в линейных элементах радиотехнических устройств. Оборонгиз, 1950.
86. Меерович Л. А., Зеличенко Л. Г. Метод расчета скорости опрокидывания спусковых и релаксационных устройств. «Радиотехника», 1953, т. 8, № 1, стр. 42.
87. «Генерирование электрических колебаний специальной формы». Пер. с англ. Изд-во «Советское радио», 1951.
88. Мюнц Т. Интегральные уравнения, ОНТИ, 1934.
89. Железнов Н. А. Радиотехнические устройства управляющих колебаний. Изд-во ЛКВВИА, 1949.
90. Кризе С. Н. Усилители напряжения низкой частоты. Госэнергоиздат, 1953.
91. Narud J. A. Trans. IRE, EC-9, 1960, № 4, p. 439.
92. Moody N. F., Mc Lusky G. J. R. and Deighton M. O. Electronic Eng., 1952, № 291, p. 241; № 292, p. 287; № 293, p. 330.
93. Wells F. H. Nucleonics, 1952, april, p. 28.
94. Бартенев Л. С. Импульсный генератор с нелинейной обратной связью. «Известия вузов», Радиотехника, 1961, т. 4, № 2, стр. 222.
95. Kroebel W. Ztschr. anqew. Phys., 1954, № 7, S. 293.
96. Rumsninkel K. E. Ztschr. anqew. Phys., 1954, № 12, S. 551.
97. Bay Z. and Grisamore N. T. Trans. IRE, EC-5, 1956, № 3, p. 121.
98. Gruhle W. Elektronik, 1957, № 9, S. 261.
99. Мельников Ю. П., Шац С. Я. Миллимикросекундный блокинг-генератор. «Радиотехника», 1960, т. 15, № 6, стр. 36.
100. Мельников Ю. П., Шац С. Я. Миллимикросекундный блокинг-генератор при малой рабочей емкости. «Радиотехника», 1960, т. 15, № 11, стр. 34.
101. Чиликин В. С. Генератор миллимикросекундных импульсов ГМИ-23. «Электросвязь», 1960, № 1, стр. 40.
102. Удалов В. В., Тумин Ю. И. Генератор групп импульсов наносекундной длительности. «Приборы и техника эксперимента», 1960, т. 5, № 6, стр. 62.
103. Формирование импульсов с высокой частотой следования. «Экспресс-информация», ВТ-132, 1959, вып. 33.
104. Mac Donald Smit J. El. Eng., 1957, № 4, p. 184
105. Неймарк Ю. Н., Маклаков Ю. К. и Елкина Л. П. Циркуляция импульсов в сильно нелинейной среде, обладающей дисперсией. «Радиотехника и электроника», 1958, т. 3, стр. 1348.
106. Cutler C. C. Proc. IRE, 1955, v. 43, № 1, p. 196.
107. Rosenhein and Anderson A. G. Proc. IRE, 1957, v. 45, № 2, p. 212.
108. Горбачев В. М., Королев В. Н., Уваров Н. А. Генератор наносекундных импульсов. «Приборы и техника эксперимента», 1962, т. 7, № 6, стр. 81.
109. Распутный В. Н. Транзисторные регенеративные импульсные генераторы с запаздывающей обратной связью. «Известия вузов», Радиотехника, 1962, т. 5, № 2, стр. 171.
110. Богатырев Ю. К. Генератор наносекундных импульсов с нелинейной запаздывающей обратной связью. «Известия вузов», Радиотехника, 1962, т. 5, № 3, стр. 399.

Doc= 88076735

Page 1014

111. Фролкин В. Т Импульсная техника. Изд-во «Советское радио», 1960.
112. Магуайр Т. Вычислительное устройство для работы на частоте 1 000 *Мгц*. В сб. «Туннельные диоды». Изд-во иностранной литературы, 1961.
113. Ешимура Т. Быстродействующее электронное вычислительное устройство на туннельных диодах. В сб. «Туннельные диоды». Изд-во иностранной литературы, 1961.
114. Bergman B. H. Trans. IRE, EC-9, 1960, № 4, p. 430.
115. Sarrafian G. P. IRE Internat. Conv. Rec., 1961, № 2, p. 871.
116. Vzonoglu V. Proc. IRE, 1961, № 9, p. 1440.
117. Whetstone A. L. Proc. IRE, 1961, № 9, p. 1444.
118. Guckel H. Proc. IRE, 1961, № 11, p. 1685.
119. Corneretto A. Electronic Design, 1962, № 3, p. 4.
120. Aleksander I. and Scarr P. W. A. J. Brit. IRE, 1962, III, p. 177.
121. Соммерс Х. и др. Применение туннельных диодов для усиления с малыми шумами. В сб. «Туннельные диоды». Изд-во иностранной литературы, 1961.
122. Гершензон Е. М., Селиваненко Н. Е., Эткин В. С. О применении туннельных диодов в радиотехнических схемах. «Электросвязь», 1961, т. 15, № 8, стр. 11.
123. Tranburulo R. F., Burrus C. A. Proc. IRE, 1960, № 10, p. 1776.
124. Burrus C. A. Proc. IRE, 1960, № 12, p. 2024.
125. Chang K. K. N., Heilmeier, Prager, Proc. IRE, 1960, № 5.
126. Соммерс Х. Использование туннельных диодов в качестве высокочастотных приборов. В сб. «Туннельные диоды». Изд-во иностранной литературы, 1961.
127. Берг М. А., Горяинов С. А. Полупроводниковые приборы с отрицательным сопротивлением. «Электросвязь», 1961, № 3, стр. 31.
128. Ашимов Н. М. Свойства и применения *p-n-p-n* приборов. «Радиотехника», 1962, т. 17, № 12, стр. 69.
129. Доброхотов Н. Г. Полупроводниковые *p-n-p-n* переключатели. В сб. «Полупроводниковые приборы и их применение», вып. 7. Изд-во «Советское радио», 1961.
130. Эзаки Л. Новые явления в тонких германиевых *p-n* переходах. В сб. «Туннельные диоды». Изд-во иностранной литературы, 1961.
131. Эзаки Л. Свойства высоколегированного германия и тонких *p-n* переходов. В сб. «Туннельные диоды». Изд-во иностранной литературы, 1961.
132. Lesk I. A., Suran J. J. Electronic Eng. 1960, № 4, p. 270.
133. Roberts G. W. Electronic technology, 1960, № 6, p. 222.
134. Кононов Б. Н., Сидоров А. С. Туннельные диоды и их применение. В сб. «Полупроводниковые приборы и их применение», вып. 7, Изд-во «Советское радио», 1961, стр. 340.
135. Ferendeci A., Kow H. Proc. IRE, 1961, № 8, p. 1898.
136. Леск Д. и др. Германиевый и кремниевый туннельные диоды. В сб. «Туннельные диоды». Изд-во иностранной литературы, 1961.

DOC= 88076735 Page 1015

137. Dickens L. S. Microwave J. 1962, № 7, p. 70.

138. Фистуль В. И., Шварц Н. З. «Туннельные диоды», УФН, 1962, т. LXXVII, вып. 1, стр. 129.

139. Воронцов Ю. И., Петров В. М., Ржевкин К. С. Измерение параметров туннельных диодов. В сб. «Полупроводниковые приборы и их применение», вып. 7. Изд-во «Советское радио», 1961, стр. 115.

140. Herzog G. B. Onde électr., 1961, № 409, p. 370.

141. Dalley E. J. Electronic Design, 1961, April, p. 36.

142. Todd C. D. Semiconductor Products, 1960, dec. p. 27.

143. Wen-Hsing Ko Electronics, 1961, № 6, p. 68.

144. Shuller M., Gärtner W. W. Proc. IRE, 1961, № 8, p. 1482.

145. Wrestone A. and Konnosu S. Rev. Seient. Instr., 1962, № 4, p. 422.

146. Перуджини М., Линдгрен Н. Некоторые применения туннельных диодов. В сб. «Туннельные диоды». Изд-во иностранной литературы, 1961.

147. Витт А. А. К теории скрипичной струны. ЖТФ, 1936, № 1.

148. Nagumo J., Schimura M. Proc. IRE, 1961, № 8, p. 1494.

149. «Полупроводниковые приборы с отрицательным сопротивлением». Госэнергоиздат, 1962.

150. Hussey L. W. Proc. IRE, 1950, v. 38, № 1, p. 40.

151. Андреев С. И., Ванюков М. П., Серебренов В. А. Применение ферритов для генерирования мощных импульсов высокого напряжения наносекундной длительности. «Приборы и техника эксперимента», 1962, т. 7, № 3, стр. 89.

152. Kult K. Slaboproudy Obzor, 1958, № 5, p. 292.

153. Капорский А. С., Чернецкий Л. В., Коротких Н. В., Вознесенский В. И. Электронные методы генерации сверхкоротких импульсов. УФН, 1957, т. 63, № 4, стр. 801.

154. Cornetet N. H., Josenhans J. G. Trans. IRE, v. ED-8, 1961, № 6, p. 464.

155. Горячев Л. В. Применение кристаллических диодов в схемах ограничения наносекундных импульсов. «Труды Горьковского политехнического института», 1958, вып. 1.

156. Мамырин Б. А. Генерирование миллимикросекундных импульсов с высокой частотой следования. Радиотехника, 1958, т. 13, № 11, стр. 27.

157. Kohn G. Arch. Electr. Übertragung, 1958, № 3, S. 109.

158. Beck A. C. Bell Syst. Tech. J., 1956, v. 35, p. 35.

159. Beck A. C. Trans. IRE, MTT-3, 1955, № 6, p. 48.

160. Догадкин А. В. Аппаратура для исследования неоднородностей в волноводах наносекундными импульсами. «Радиотехника и электроника», 1959, т. 4, № 5, стр. 894.

161. Догадкин А. Б. Метод оценки кратчайшей длительности радиоимпульсов в устройствах сверхвысоких частот. «Электросвязь», 1963, № 2, стр. 11.

162. Венеровский Д. Н., Пурто В. М. К вопросу о возбуждении наносекундных импульсов при помощи генераторной ЛБВ. «Радиотехника и электроника», 1958, т. 3, № 11, стр. 1404.

DOC = 88076735

Page 1016

163. Burrus C. A. Rev. Scient. Instr., 1957, v. 28, № 12, p. 1062.

164. Dietrich A. F. Proc. IRE, 1961, v. 49, № 5, p. 972.

165. Kibler L. V. Proc. IRE, 1961, v. 49, № 7, p. 1204.

166. Sterzer F. Trans. IRE. EC-8, 1959, № 3, p. 1.

167. Eckhardt W., Sterzer F. Proc. IRE, 1962, v. 50, № 2, p. 148.

168. Schwarzkopf D. B. Microwave J. 1962, v. 5, № 10, p. 172.

169. Прозоровский Ю. Н. Усилитель с распределенными постоянными как система многополюсников. «Радиотехника и электроника», 1957, вып. 1, стр. 57.

170. Сифоров В. И. Радиоприемные устройства. Воениздат, 1954.

171. Мамонкин И. Г. Импульсные усилители. Госэнергоиздат, 1958.

172. Erchholr J. J., Nelson C. E., Weiss G. T. Rev. Scient. Instr., 1959, № 1, p. 1.

173. MacMullen. Rev. Scient. Instr., 1959, № 4.

174. Симонов Ю. Л. К теории RC-усилителей на туннельных диодах. «Радиотехника», 1962, т. 17, № 12, стр. 52.

175. Chirlian P. M. Proc. IRE, 1960, № 6, p. 1156.

176. Moody N. F., Wacker A. G. Proc. IRE, 1961, № 4, p. 835.

177. Hines M. Bell Syst. Tech. J., 1960, № 3, p. 477.

178. Колотов О. С., Никитина Т. Н. Усиление наносекундных импульсов. «Известия АН СССР», серия физическая, 1961, № 5, стр. 624.

179. Колотов О. С., Лабанов Ю. Н. Усиление коротких импульсов при импульсном питании ламп усилителя. «Приборы и техника эксперимента», 1961, т. 6, № 2, стр. 94.

180. Веретенников А. И., Аверченков В. Я., Егоров А. Г., Спехов Ю. А. Усилительная приставка для фотографирования коротких импульсов. «Приборы и техника эксперимента», 1961, т. 6, № 1, стр. 104.

181. Фанченко С. Д. Проблемы точного измерения времени и исследования процессов сверхмалой длительности. «Приборы и техника эксперимента», 1961, т. 6, № 1, стр. 5.

182. Стекольников И. С. Осциллографирование со скоростью записи, близкой к скорости света. «Доклады АН СССР», 1946, т. 54, № 6, стр. 499.

183. Jonnson J. Philips Techn. Rev., 1950, v. 12, № 2, p. 52.

184. Теумин И. И. Экспериментальный анализ переходных процессов в линейных электрических цепях. Изд-во «Советское радио», 1956.

185. Бартенев Л. С., Глебович Г. В., Горячев Л. В., Шаров Ю. А. Импульсный скоростной осциллограф. «Приборы и техника эксперимента», 1958, т. 3, № 4, стр. 60.

186. Букин А. Н., Филлипов М. М., Исаев А. Э. Осциллографирование колебаний сверхвысоких частот. Изд-во Ленинградского университета, 1963.

Doc = 88076735 Page 1017

187. Бартенев Л. С., Глебович Г. В., Птицын К. Н. Сверхскоростной импульсный осциллограф. «Приборы и техника эксперимента», 1961, т. 6, № 6, стр. 80.

188. Cathode ray Tube «KR-3», J. Seient. Instr., 1958, v. 35, № 3, p. XIX.

189. Ardenne M. Hochfrequenztechnik und Electroakustik, 1939, B. 54, № 6, S. 181.

190. Глебович Г. В. О временной разрешающей способности скоростных и стробоскопических осциллографов. «Измерительная техника» (в печати).

191. Бартенев Л. С., Глебович Г. В., Птицын К. Н. Особенности разработки сверхскоростных осциллографов. «Труды Горьковского политехнического института», 1964, т. 20, вып. 2.

192. Леонов А. М. Генератор развертки для скоростного осциллографа. «Известия вузов», Радиотехника, 1961, т. 4, № 3, стр. 335.

193. Баринов К. В. О стабильности момента запуска блокинг-генератора. «Труды Московского авиационного института», 1960, вып. 126, стр. 83.

194. Тихонов В. И. Воздействие малых флюктуаций на электронное реле. «Вестник МГУ», серия физико-математическая, 1956, № 5, стр. 31.

195. Стратанович Р. Л. Избранные вопросы теории флюктуаций в радиотехнике. Изд-во «Советское радио», 1961.

196. Уваров Н. А. Генератор развертки с малым временем задержки. «Приборы и техника эксперимента», 1961, т. 6, № 5, стр. 178.

197. Колотов О. С., Санин А. А., Шильберский З. Прибор для наладки импульсной аппаратуры наносекундного диапазона. «Приборы и техника эксперимента», 1961, т. 6, № 5, стр. 82.

198. Вол В. А. К теории стробоскопического осциллографа. Радиотехника, 1958, т. 13, № 8, стр. 63.

199. Вол В. А. О воспроизведении стробоскопическим осциллографом периодических сигналов произвольной формы. «Радиотехника», 1959, т. 14, № 3, стр. 69.

200. Goodall W. M., Dietrich A. F. Proc. IRE, 1960, v. 48, № 9, p. 1591.

201. Маранц В. Г. Применение стробоскопического метода для измерения переходных процессов полупроводниковых приборов. В сб. «Полупроводниковые приборы и их применение», вып. 8. Изд-во «Советское радио», 1962, стр. 137.

202. Farber A. S. Rev. Scient. Instr., 1960, v. 31, № 1, p. 15.

203. Louis H. P. Elektron. Rundschau, 1960, B. 4, № 4, S. 137.

204. Dietrich A. F., Goodall W. M. Proc. IRE, 1960, v. 48, № 4, p. 791.

205. Sugerman K. Rev. Scient. Instr., 1957, v. 28, № 11, p. 933.

206. Starke L. Elektronik, 1961, B. 10, № 12, S. 812.

207. Rarity J., Roberts H., Saporta L. Proc. Nation. Electron Conf., Chicago, 1958, v. 13.

208. Грязнов М. И. Устройство для измерения длительности импульсов. Авторское свидетельство № 136792. «Бюллетень изобретений», 1961, № 6.

DISTRIBUTION LIST

DISTRIBUTION DIRECT TO RECIPIENT

ORGANIZATION	MICROFICHE
A205 DMAHTC	1
A210 DMAAC	1
C509 BALLISTIC RES LAB	1
C510 R&T LABS/AVEADCOM	1
C513 ARRADCOM	1
C535 AVRADCOM/TSARCOM	1
C539 TRASANA	1
C591 FSTC	4
C619 MIA REDSTONE	1
D008 MISC	1
E053 HQ USAF/INET	1
E404 AEDC/DOF	1
E408 AFWL	1
E410 AD/IND	1
E429 SD/IND	1
P005 DOE/ISA/DDI	1
P050 CIA/OCR/ADD/SD	2
AFIT/LDE	1
FTD	
CCV	1
MIA/PHS	1
LLYL/CODE L-389	1
NASA/NST-44	1
NSA/T513/TDL	2
ASD/FTD/TQIA	1
FSL/NIX-3	1

DOC=88076735

Page 1018

209. Грязнов М. И. Измерение амплитуды коротких импульсов. Сборник докладов научной сессии НТО РиЭ им. А. С. Попова, М., 1959.

210. Harbert J., Fresser D. Wireless Eng. 1955, v. 32, № 7, p. 187.

211. Грязнов М. И. Интегральные методы измерения некоторых параметров наносекундных импульсов малой амплитуды. Доклады пятой Всесоюзной конференции по автоматике и электрометрии. Сибирское отделение АН СССР, 1963.

212. Грязнов М. И. Способ измерения амплитуды и длительности наносекундных импульсов малой амплитуды. Доклады 19-й Всесоюзной научной сессии, посвященной Дню радио, Радиоизмерения, 1963, стр. 7.

213. Gaddy O. L. Trans. IRE, 1960, I-9, № 3, p. 326.

214. Agouridis D. C. Rev. Scient Instr., 1962, v. 33, № 12, p. 1396.

215. Elliott J. Bell Labor. Rec. 1949, v. 27, № 3, p. 221.

216. Fletcher R. Rev. Scient. Instr., 1949, v. 20, № 12, p. 861.

217. Herreng P., Ville J. Cables et Transmission, 1948, № 4, 111.

218. Miller S. E. Proc. IRE, 1953, № 3, p. 240.

219. Чернушенко А. М. Установка для исследования высокочастотных трактов и замедляющих систем наносекундными импульсами. Сборник докладов научной сессии НТО РиЭ им. А. С. Попова, М., 1959, стр. 99.

220. Halverson H. Electronics, 1961, v. 34, № 26, p. 28.

221. Melrog D. O., Closson H. T. Proc. IRE, 1960, v. 48, № 2, p. 165.